Cold Fusion Source Book

Belarusian State University
Minsk, Belarus
May 25-26, 1994

COLD FUSION SOURCE BOOK

Edited by Hal Fox

Editor-in-Chief, *Fusion Facts*

Proceedings of the
International Symposium on Cold Fusion and Advanced Energy Sources

held at the Belarusian State University

Minsk, Belarus, May 24-26, 1994

Published by
FUSION INFORMATION CENTER
University of Utah Research Park
P.O. Box 58639
Salt Lake City, Utah 84158-0639

COLD FUSION SOURCE BOOK
Edited by Hal Fox

Proceedings of the International Symposium on Cold Fusion and Advanced Energy Sources.

Published and distributed by

Fusion Information Center, Inc.
P.O. Box 58639
Salt Lake City, Utah 84158

Price: $100 postpaid airmail to any country
Book includes a diskette with 1,500 references together with INFOFIND, a search and retrieval program. Enter any word to recover resource information on authors, title, journals, etc.

First Edition.

ISBN

Printed in the U.S.A.

The monthly scientific newsletter *Fusion Facts*™, and the monthly newsletter *New Energy News*™ are also available through this address, or call for information (801) 583-6232, Fax (801) 583-2963.

DEDICATION

This book is dedicated to three classes of people:

1. To those international scientists, engineers, and inventors that have diligently pursued the truth; who have trusted the integrity of other scientists who reported on their new discoveries; who have replicated, improved, and, in turn, reported on this new science of cold nuclear fusion and other enhanced energy devices.

2. To the new scientists, engineers, inventors, and scholars who now can follow in the footsteps of those who have led and become leaders of others. You will be the individuals and the generation who will develop, install, and use the new non-polluting, inexpensive energy systems that will help improve our homes, our countries, and our world.

3. To the Children of Chernobyl.

ACKNOWLEDGEMENTS

As editor, I wish to thank those many people that helped produce this book: Ben Filimonov for his work in gathering and translating many Russian papers; Tamara Grinevich for her superb skills in interpreting and translating; to Eva Call, Dineh Torres, and Robyn Gillen, the staff at the Fusion Information Center, who do such a superb job. Finally, forgive me for errors made and please send corrections.

Hal Fox, Editor
Salt Lake City, Utah
May 7, 1994

Cold Fusion Source Book

ADDITIONAL COPIES OF THIS BOOK
MAY BE OBTAINED FROM:

FUSION INFORMATION CENTER
P.O. BOX 58639
SALT LAKE CITY, UTAH 84158 USA

1 801 583 6232 FAX 1 801 583 2963

TABLE OF CONTENTS

FOREWORD

We are always harvesting what others have planted. Each new graduate uses tools fashioned by his predecessors. All of us enter our selected (or imposed) professions and build on the past. If we are clever, we add to knowledge, build new tools, and pass on that small or large contribution to the stream of mankind who will harvest where we have planted.

This book is, in large part, an invited contribution of technical reports about cold nuclear fusion and a few other enhanced energy systems. Mainly this book presents the early harvest from the pursuit of truth as introduced by Stanley Pons and Martin Fleischmann.

It has been over five years since Pons and Fleischmann were requested by the University of Utah administrative staff to announce their discovery of "cold fusion" at a press conference on March 23, 1989. The press conference was called in response to many phone calls to the University of Utah about the rumors of a new discovery. These phone calls were the result of the failure of the peer-review system that allowed copies of the paper by Pons, Fleischmann, and Hawkins to be privately circulated prior to publication.

The flurry of excitement that greeted the announcement of cold fusion was soon followed by a barrage of attacks upon this new discovery and even by accusations of fraud against Pons and Fleischmann. The many successes of cold fusion replication, improvement, and of new discoveries is the story presented in this book. This book is a partial report on the efforts of many that has stilled the strident voices of the pathological skeptics.

The terms "cold fusion" and "cold nuclear fusion" may not accurately describe the rich phenomena that has been discovered by those seekers of truth who have followed Pons and Fleischmann. These reports of replication and new discoveries have also engendered many new findings and new theories. A few selected theory papers have been included in this volume.

This volume of selected papers does not include all of the reports that we would like to have published. It is a beginning. To the many new investigators, this book is meant to serve as a starting place. The bibliography (available on the diskette that accompanies this book) is, we believe, the most complete listing available of papers on cold fusion and associated reports.

It is expected that what we have planted, you will cultivate, and the world will harvest. Here are some tools -- till well.

ABOUT THE EDITOR

Hal Fox was the director of the first research laboratory at the University of Utah Research Park. He claims that the cold fusion announcement by Pons and Fleischmann was responsible for him not becoming famous. He had just retired and was going to take up tap dancing. Hal was the principal founder of the Fusion Information Center, Inc. He was also co-founder of Fusion Resources, Inc. and Future Energy Applied Technology (FEAT) and served as CEO and Chairman of FEAT until shortly before Fusion Resources and FEAT were merged and named ENECO, Inc. (a Utah corporation).

Hal Fox is the editor of *Fusion Facts*, a monthly technical newsletter designed to keep its subscribers informed of the latest developments in cold fusion research and development. Hal is also editor of *New Energy News*, a monthly newsletter provided to members of the **Institute for New Energy** and to other subscribers. Hal is also author of **Cold Fusion Impact in the Enhanced Energy Age**.

TO THE CHILDREN OF CHERNOBYL

When I first learned of the devastation to Belarus (and parts of Ukraine) from the Chernobyl nuclear power plant disaster, I was strongly distressed at the intense penalty that was imposed on a nation, its people, and especially its children. I determined to do something for the "Children of Chernobyl." I desire to express my commendations to those who risked their lives to tell the world about the silent killer in their land and all of us express our thanks to the concerned citizens from many nations that are trying to help. There is no nation on earth that is in a better location for an international conference on new energy than Belarus. There is no nation on earth that deserves and needs a new non-polluting source of energy more than Belarus. That is why I am here with you at this conference.

I am pleased to be the editor of the English version of the proceedings of this important international conference. Early this year I wrote to over 50 cold fusion scientists, whom I call my friends, and asked them to provide reports on their work. Each one was asked to write an article which would become a part of a "Cold Fusion Source Book". In addition, my friend Ben Filimonov of Belarus invited papers from leading scientists from his part of the world who had been successful in the development of this exciting new technology of cold nuclear fusion. With the help of excellent translators, especially Ms. Tamara Grinevich, those papers, mainly from CIS (Commonwealth of Independent States), have been included in this publication. In addition, we have also included some invited papers that deal with some other *enhanced energy systems* (new energy systems that provide more energy out than used as input or driving energy).

The first article in the Cold Fusion Source Book is mine and is meant to set the stage for the articles that follow by providing a review of the many new methods, in addition to the original Pons-Fleischmann cold fusion cells, by which nuclear reactions and/or excess thermal energy can be produced in relatively simple "table-top" experiments. The second paper is by Dr. Ben Filimonov, who categorizes the many phenomena of cold nuclear fusion and provides us with a new way of looking at this rich phenomena.

To the attendees of this conference and to those who will read of our work: we challenge you to make use of this knowledge, improve what we have done, and solve the energy problems so that there will never again be any more "Children of Chernobyl".

It is intended that this **pre-proceedings** of the International Symposium on Could Fusion and Advanced Energy Sources be distributed with a diskette which contains over 1500 bibliographic materials on cold nuclear fusion and associated scientific phenomena. The Fusion Information Center, who has published this English version, believe that it has compiled the world's most complete collection of positive reports on this new science. We know that our collection is not complete and we ask our readers to send us copies of positive papers that are not included in our bibliography. We have chosen not to catalog all of the negative papers that have been written. In general, the negative papers merely summarize ways in which cold fusion does not work. Except to illustrate specific incorrect procedures that have been attempted, these papers have little scientific value. In addition, out of our great respect for well-meaning scientists who have been misled in their conclusions that cold fusion is somehow contrary to respectable science, we have not catalogued their temporary errors. We are sure that most of them will soon join the many scientists from over 30 countries who have been successful in the development of this exciting new science.

COLD NUCLEAR FUSION, SPACE ENERGY DEVICES & COMMERCIALIZATION

Hal Fox
Editor-in-Chief, *Fusion Facts*; Editor, *New Energy News*
President, Fusion Information Center, Inc.
P.O. Box 58639, Salt Lake City, UT 84158

ABSTRACT

After nearly five years of reporting on cold fusion (*Fusion Facts*) and one year editing and publishing *New Energy News* about other enhanced energy devices, a bibliography of over 1500 entries has been compiled from papers gathered and reviewed from over 30 countries. This paper presents a five-year retrospective report on nine different methods by which nuclear reactions are produced and controlled. The emphasis is on demonstrated devices having commercial potential. A similar review is provided concerning a longer history of experiments and devices that are apparently dependent on space energy (an energetic ether) for their operation. Although there exist unexplained experimental reports that are about one century old, this paper examines devices that are currently being developed and replicated. Through the efforts of the **Institute for New Energy**, several candidate enhanced energy devices that appear to have immediate application to solving the world's energy problems have been identified and are discussed. These devices include the dePalma N-machine, the Adams magnetic motor, and the Shoulders' Effect. There are other **unreplicated** devices that appear to have commercial potential within the next few months. All of the devices cited have been reported in either *Fusion Facts*, *New Energy News*, or in both.

INTRODUCTION

The reward received from collecting, reading, reviewing, and publishing information about enhanced energy devices has been the privilege of becoming friends with a large number of dedicated international scientists and engineers who have risked their scientific reputations to investigate and report on new science. Chief among these scientists are Dr. Martin Fleischmann and Dr. Stanley Pons whose once-in-a-lifetime discovery of cold nuclear fusion has now been replicated in over 30 countries and which is approaching commercialization. Also among new friends are included many scientists from Italy, Japan, China, and from several countries of the Commonwealth of Independent States. Thanks to all of you for your loyalty to science and truth. In addition, my newer friends include scientists and engineers who have risked their reputations by their decades of insistence that space itself, all around us, contains a source of energy that can be and should be used. To those of you who read this paper and this publication, you are especially urged to discard the two major fallacies of yesterday's science: **That there is not an energetic ether and that the Coulomb barrier prevents nuclear reactions in/on a metal lattice.**

COLD NUCLEAR FUSION DEVICES

A variety of anomalous phenomena have been rediscovered, remembered, or newly discovered since the announcement by Pons and Fleischmann of apparent nuclear reactions from the Pons-Fleischmann Effect (PFE). This section briefly describes eight of those experimental findings, cites the literature, and speculates on the commercial potential of such devices.

1. Heavy-Water Electrochemical Cells

The original Pons-Fleischmann discovery involves electrochemical cells using heavy water, a palladium cathode, usually a platinum anode, and lithium in the electrolyte [1]. Many research groups were unable to replicate the Pons-Fleischmann effect and some became instant critics, even to the extent of accusing Pons and Fleischmann of fraud. However, positive results have been obtained by research groups in more than 30 countries in replicating the P-F effect [2]. There has been little cold fusion research among the Ivy-League colleges in eastern U.S. and, except for Italy, only a few cold fusion papers from Western Europe. Several groups in Eastern Europe and Russia have helped to develop a better understanding of the cold fusion technology [3]. However, no group has **fully resolved** the problems associated with the preparation of the palladium metal, the loading of the palladium cathodes, and the "turning on" of the excess heat reactions. See Fig. 1.

A heavy-water cell operated at atmospheric pressure can be expected to produce low-level excess heat, whenever the palladium cathode is loaded with deuterium such that the D/Pd atomic ratio is greater than 0.85 and provided other now well-known protocols are followed. Pressurized heavy-water cells are now being tested that are expected to produce higher levels of heat and lead to commercial applications. The maximum temperature at which pressurized electrochemical cells can operate is in the range of 700°F. At higher temperatures there is no definite demarkation between liquid and gas regardless of the pressure and it is believed that standard electrochemistry would not function above this critical temperature. Therefore, this factor limits the range of commercial applications to industrial and domestic processes requiring temperatures of less than 700°F.

2. Light-Water Electrochemical Cells and Nuclear Transmutations

Although the Pons-Fleischmann patent applications anticipated the use of light-water (as an addition to heavy water) in cold-fusion electrochemical cells, and Matsumoto (Japan) measured nuclear byproducts using light water [4], it was Randell Mills (Lancaster, Penn.) who first showed that light-water electrochemical cells using some alkali-metal carbonates could produce excess heat [5]. The Mills theory of the functioning of light-water electrochemical cells is still being carefully evaluated. Drs. Bush and Eagleton (Cal-Poly, Pomona, California) have extended the light-water cold-fusion experimental work and Dr. Bush has modified his Transmission Resonance Model (TRM) to explain both the heavy-water and the light-water results as being alkali-metal-hydrogen fusion [6]. See Fig. 2. More recently Bush and Eagleton have demonstrated that there are definite transmutations of alkali elements by fusion with hydrogen (in the light-water electrochemical experiments) [7] to produce elements with an added proton in the nucleus.

Experimental results from Bush and Eagleton and later several groups at BARC, Trombay, India [8], Dr. Reiko Notoya at Hokkaido University [9], and Drs. Ohmori and Enyo at Hokkaido University [10] have shown that the light-water electrochemical cells are highly reproducible; usually produce 20 to 70% and occasionally up to 300% excess heat; and function with all of the alkali metals (usually as carbonates). The cathodes used are nickel, gold, silver, and tin and range from wire and plate to porous materials (such as the porous nickel used in Nickel-Cadmium batteries.)

There has been some evidence, especially in small-scale light-water electrochemical cells, that excess heat considerably higher than 300% has already been achieved. Therefore, by definition, this technology qualifies for potential commercialization. It is expected that the newer experimental discoveries in light-water electrochemical cells will certainly lead to a better understanding of the **overcoming of the**

Coulomb barrier, of the basic structure of matter, the control of nuclear reactions in/on a metal lattice, and possibly stabilizing radioactive nuclides. These are important reasons for accelerating funding for further experimental investigations into both heavy- and light-water cold fusion reactors.

3. Molten Salts Electrochemistry

Drs. Liaw and Liebert of the University of Hawaii invented and demonstrated the use of molten salts to provide relatively high temperatures in an electrochemical cold-fusion cell [11]. Their work showed that as much as 1500% excess heat could be achieved using palladium as the anode and using an eutectic mixture of salts in an aluminum container. See Fig. 3. It has been found that there are some serious materials problems to be resolved in working at these higher temperatures. The replication of this work has been difficult. Only a few other groups have replicated the Liaw-Liebert molten salt work [12]. However these problems are expected to be resolved and the molten salts "cold fusion" devices become an important part of future enhanced energy systems. The high level of heat achieved does mark this technology as eligible for commercialization after the materials problems are solved. The applications for molten-salts cold-fusion devices are obviously destined for systems where higher temperatures are desired or required, such as in the manufacturing and/or processing of many glasses and metals. Recently, Liaw has reported some successes with the use of a nickel cathode in a molten salt reactor [13].

4. Gas Plasma Devices

One U.S. inventor (John Marshall of Surface Solutions in Boulder, Colorado) has filed a patent for a gas-plasma device which is expected to produce excess heat. Some excellent work using gas-plasma devices has also been performed in Russia by Drs. Kucherov, Karabut, and Savvatimova [14]. Other gas plasma replication has been accomplished by Romodanov in Russia [15] and by scientists in the People's Republic of China [16]. This Kucherov et al. device uses deuterium gas at relatively low pressures and in the presence of moderately-high voltages (about 500 volts). See Fig. 4. The cathode is palladium. A variety of nuclear reactions have been identified in the glow-discharge, gas-plasma devices.

It is projected that the development of this gas-plasma device will produce enhanced-energy systems that operate at high temperatures and in aerospace environments. (Neither heavy-water nor light-water electrochemical cells are deemed suitable for either high-temperature or aerospace use.) The best results that have been achieved with gas-plasma devices (over 500% excess heat) appears to make this type of cold fusion device a candidate for future commercialization.

5. Capillary Fusion

Some types of metal crystals can be made in which small diameter, long tubes or capillaries are created. Under appropriate conditions it has been experimentally shown that fusion of hydrogen can be achieved in this type of device. See Fig. 5. Dr. Graneau [17] has described unusual longitudinal electrical forces in wires, and Dr. Vigier [18] has described the observation of capillary cold fusion in metal wires using high amperage. After initial successes, work is being continued by Baraboshkin and Samgin in Russia to investigate this approach to the development of excess heat [19]. The Vigier article and other articles about the role of Ampère forces in nuclear fusion [20] suggest that devices using the right combination of capillaries, hydrogen (or deuterium) gas and appropriate treatment with high-amperage electrical current may develop sufficient excess heat to be subject to commercialization. Recently, Peter Graneau [21] presented a concept for a capillary fusion reactor. Graneau believes that it will take some expert materials engineering to produce this type of reactor because of the relatively large internal forces that are expected

to be produced. However, Graneau's approach is a serious proposal for a device that would lead to commercialization of capillary fusion.

6. The Yamaguchi Pd sandwich.

Eiichi Yamaguchi and Takahashi Nishioka [22] have shown that palladium plates that are gold-plated on one side (to prevent migration of deuterium) and plated with MnO on the opposite side (to slow down rate of deuterium diffusion) can produce nuclear reactions. The plates, see Fig. 6, are exposed first to a vacuum then to deuterium gas. Being again exposed to vacuum and triggered with an electrical pulse, tritium, neutrons, and alpha particles (^{4}He nuclei) are produced together with considerable heat. As Yamaguchi and Nishioka reported in the third annual cold fusion conference, "We have for the first time succeeded in detecting ^{4}He production ***in situ*** and with high reproducibility. Our ***in vacuo*** method gives the first definite evidence for the reality of **cold nuclear fusion** in solids."

This work has been of great importance to demonstrate the rich phenomena involved in the production of nuclear reactions in or on the surface of a metal lattice. It is not easy to predict the degree of commercialization that can be achieved by use of the Pd sandwiches, however, the reproducibility is important for studying the parameters that are involved with the production of nuclear byproducts. Because of the production of neutrons, this device may find applications where a neutron flux is desired.

7. Proton Conductors

Two very important papers were presented at the Hawaiian ICCF-4 about the use of proton conductors in the investigation of cold fusion. The paper by Samgin et al. [23] describes the types of solid-state materials that show promise for the production and control of nuclear reactions. The paper by Mizuno et al. [24] details an experiment in which a small layered proton conductor provided excess power over a 20-hour time period in which the excess heat exceeded several thousand times the input power.

8. Sparking Devices

Dr. J. Dufour [25], working in France, has designed, tested, proven, and reported on a technique by which electrical discharges are used to create nuclear reactions. The object of the work was to obtain excess energy of a significant amount over a significant time period and then to identify nuclear byproducts. Dufour's conclusions incudes the following: A fully-reproducible and stable system has been designed and tested; excess heat is achieved over long time periods; and a possible explanation is an hypothetical class of nuclear reactions based on virtual neutron transfer.

9. New nickel phenomena

A recent (February, 1994) report from three Italian scientists (F. Piantelli from Siena, S. Focardi from Bologna, and R. Habel from Cagliari) describes the use of a nickel electrode producing 40 watts of excess heat. This new discovery used a nickel bar (1 sq. cm. in cross section and 9 cm. long) in a hydrogen atmosphere and heated to about 350 degrees C. After a proprietary electromagnetic stimulation, the system generated about 40 watts of excess heat. The results are reported to be highly reproducible.

Summary

These are exciting times in the study of the new science of cold fusion. Every conference reports on new

experimental findings that serve to advance the understanding of the phenomena of the catalysis of nuclear reactions in/on a metal lattice. It can now be reasonably predicted that there will be a number of commercial applications derived from the rich phenomena that has been discovered in cold nuclear fusion.

ROTATING DEVICES THAT CONVERT SPACE ENERGY

1. Introduction

There are a variety of experiments that can be more easily understood if the existence of an energetic ether is acknowledged. No one should depend on the misinterpretation of the Michelson-Morley experiment as proof of the non-existence of an energetic ether. A 15-year-old young man has provided a didactic paper showing that the Michelson-Morley experiment **could not measure the effect for which the experiment was designed** [26]. Michelson, himself, was not convinced of the truth of his **null experiment**. Later he and Gale set up a 2 million sq. ft. interference loop in Illinois in the winter of 1923-24 to measure changes in the speed of light and obtained different results. See Hayden et al., "If Michelson-Morley, Why not Sagnac and Michelson-Gale?", (*Galilean Electrodynamics*, vol 1, **1990**). It is claimed that Einstein's theory of relativity is based on the mistaken interpretation of the Michelson-Morley experiment so that the mathematical development was constrained by not allowing the existence of an energetic ether. The following are a few of the experiments that can best be understood if one accepts the existence of space energy:

a. Electrical induction (Faraday): When a conductor is moved through a volume of space in which a magnetic field is present, current flow is induced in the conductor. Note that this statement says nothing about "cutting lines of force."

b. Magnetic Field (Faraday): When a direct current flows in a coil a magnetic field appears in the center of the coil and the orientation of the magnetic polarity can be determined if the direction of the current is known.

c. Magnetic Materials (Faraday): Some atomic and/or molecular structures can sustain temporarily or exhibit permanently, strong magnetic fields, especially when such a magnetic material is placed within an electric coil in which current is flowing.

d. Levitation with Conducting Sphere (George S. Piggot, 1904, as reported by William F. Hamilton): When a conducting spherical electrode is rotated and high-voltage electricity is applied, it was shown that small metal balls, cork, and wood could be supported against gravity.

e. Gravity & High Voltage (Dr. Francis Nipher, St. Louis, Missouri, 1916-17): When a mass is connected to high-voltage, gravitational attraction was affected.

f. Gravity & Gyroscope (dePalma): When a spinning gyroscope falls along its axis of rotation, the rate of fall in an earth's gravity field is slowed.

g. Gravity & Magnets/Coils (Kelly, 1993-4): When non-inductive coils are wound around magnets, and the coils are energized, then the rate of fall is decreased. [On May 15, 1994, Kelly demonstrated this phenomena to about 100 people attending the 1994 International Symposium on New Energy, Denver, CO. See Proceedings.]

h. N-Machines (dePalma, Tewari, Inomata): When layers of magnets and conductors are rotated, electricity is produced (as in an N-machine.) This is a specific embodiment of example **a**.

i. N-Machine & Back Torque (Tewari, Inomata): When an N-machine is operated in a no-load condition, the input torque is measured. When the N-machine output is switched to a full-load condition, the input torque is not directly proportional to the load. This is a dramatic difference between N-machines and classical electric motors/generators. See also examples **a and h**.

j. Force by High Voltage (T. Townsend Brown): When high-voltage is applied to an air foil, mechanical forces are produced.

k. Energy Stored in Magnetic Field (Aspden, 1993): Under certain conditions, magnets can store energy in space and that energy can be recaptured and used. This is believed to be the phenomena used in the Adams magnetic motor.

l. Electron Charge Clusters (Shoulders, 1985): When a high-density electron charge cluster is produced it travels at about 0.1 the speed of light in the electric field between cathode and anode. Under certain conditions, more energy can be extracted from the moving high-density charge cluster than required to produce the charge cluster. This is the Shoulders' Effect as shown in U.S. Patent 5,018,180.

m. Electric Generator & Levitation (Searl 1970): When magnetic forces are produced at right angles in the presence of rotary motion, high voltage electricity is generated, the temperature is reduced, and gravity is reduced. This effect is reported to have been demonstrated by the Searl "levitating disks".

n. Space Energy is not Isotropic (Christian Monstein, Freienbach, Switzerland, 1993-4): When rotating a cylindrical magnet on its axis the time for slowing down is different depending on the direction of rotation. Note: This may be an effect of interaction with earth's magnetic field. Marinov (in his book Divine Electromagnetism) describes experiments that definitely show that space energy is not the same in every direction.

o. Electric Generator, Cermet (Lambertson, 1993-4): When electric current flows in "an accelerated fashion" in ceramic-metal semiconductor devices (cermets), a circulating current can be produced that provides excess energy to a tank circuit.

There are many other examples of patented "over-unity" machines that appear to depend on an energetic ether for the machines to operate as claimed. However, the above examples should be sufficient to indicate that there is at least a 75-year history of experimental evidence for space energy. The following describes a few of these devices that have been replicated and where the development of the machine or system is still being pursued.

2. The N-Machines

This author has not, as yet, mastered the three-decade history of the development of rotating machines that produce excess power (also known as over-unity machines). The basic device is the homo-polar electrical generator discovered by Michael Faraday in December, 1831. (We have replicated Faraday's homo-polar generator in our laboratory). Bruce DePalma is one of the proponents and successful experimenters with machines that appear to obtain excess power by using magnets and conductors rotating together on a shaft (often driven by an electric motor.) These electrical generating machines are characterized by the

following: (1) the demonstrated ability to produce more electrical power than used to rotate the machines; (2) an electrical output of low voltage but high current; (3) power produced without **cutting lines of force;** (4) the dynamic characteristic that requires relatively high rotational speeds to produce over-unity power; (5) the apparent lack of increasing counter-torque on the generator shaft as high output is achieved, and (6) the requirement for relatively high magnetic field strengths [27, 28, 29].

Recent articles by Bruce dePalma [27] have been published in *New Energy News.* During the past decade (or more) P. Tewari has developed N-machines with the current experimental work being documented in both printed [28] and video media. This report and video presentations depict a machine driven by an electrical motor that is capable of rotating the generator at more than 4,000 rpm while consuming up to about one-kilowatt of input electrical power from the standard electrical mains in India. See Fig. 7. As is shown and described, the generator has produced more output power than is being consumed by the driving motor. The output voltage is less than three volts but with high amperage. The demonstrated over-unity condition is achieved at rotational speeds of about 3,000 to 4,000 rpm.

Shiuji Inomata of the Electrotechnical Laboratory in Ibaraki, Japan has developed and tested a smaller motor/generator which has been shown to produce over-unity power output at high rotational speeds [29]. Recently, Inomata provided *New Energy News* with his latest design which will use superconducting magnets to increase the magnetic field strength [30]. Inomata has derived an equation for the voltage output of the machine showing that the output voltage is directly proportional to rpm and to magnetic strength and proportional to the square of the radius of the rotating copper disks used in his machine. His calculations, based on experimental evidence with the current model (see drawing, Fig. 8) indicates by using superconducting coils to increase the magnetic force, that the output can be increased to provide 10 kW and more from a machine using a 25 cm diameter copper disk.

The biggest disadvantage of the N-machines is their low-voltage output (in the range of 1 to 40 volts). However, the output current can be in thousands of ampères. This combination, together with the requirement that the d.c. output must be taken off a rotating disk, places substantial demands on the development of the electrically-conducting brushes. The second problem is to transform the low-voltage, high-current output into more acceptable electrical power. Both problems have been potentially resolved by modern engineering developments. The use of hundreds of hair-like conducting-metal fibers for the brushes and the use of modern solid-state devices for transforming low-voltage d.c. into high-voltage a.c. are the proposed solutions.

Tewari's goal is to produce a motor-generator plus transforming circuitry so that the generated power can be used to drive the electrical motor and still have excess power delivered to the output load. This demonstration will be, of course, the final proof that such a machine is transferring power from a heretofore unused energy source. That source is "space energy" or ZPE (zero-point energy). We await such demonstration with keen interest.

3. The Adams Magnetic Motor

The Adams magnetic motor (See Fig. 9) has had considerable recent publicity but no peer-reviewed articles have been published. Adams is an inventor without the standard Ph.D. qualifications to be called "scientist". He has made claims for significant over-unity power production. Recent verbal and video reports have been made concerning the replication of the Adams machine. Dr. Harold Aspden has joined forces with Adams for further development of this type of magnetic motor. Dr. Aspden, who has long been an advocate of the existence of an energetic **aether**, has filed for a patent on a similar magnetic

machine [31]. The most interesting report on the Adams Magnetic Motor is that (when properly "tuned") it appears to charge the battery that operates the motor.

SOLID-STATE SPACE-ENERGY DEVICES

1. The high-density electron charge clusters.

Dr. Harold Puthoff is one of the scientists who have written extensively about space energy [32, 33]. He and Kenneth Shoulders have been working in this new field of science for several years. The discovery by Kenneth Shoulders [34] that high-density electron clusters can be produced, maintained, and controlled has laid the groundwork for a new revolution in electronic devices. Of most importance for this paper is Shoulders' demonstration (as reported in the patent discussion [34], prior to the claims) that under certain conditions an EV (Shoulders' name for high-density electron clusters) can produce more than 30 times the amount of energy required to produce the EV. The drawing in Fig. 10 is taken from the patent abstract and illustrates how the EVs are created and how power is obtained. Basically, the EV is produced and launched through a tube or channel which is surrounded by a wire coil. The EV is a traveling bundle of electrons, moves at about 0.1 the speed of light, and induces a surge of electrical power in the coil. The EV is captured by the anode and provides about the same amount of energy that was required to produce the EV. The power from the coil has been measured to be more than 30 times the power required to produce the EV. (In discussions with Shoulders, he reported great difficulties in producing continuous excess power due to induced electrostatic charges caused by the energetic EVs.) Shoulders' latest innovation is expected to overcome the problems and provide for a commercial product.

In the discussion given in the patent, the statement is made (and accepted by the patent examiner) that the source of power "appears to be the zero-point radiation of the vacuum continuum." **It is believed that this is the first U.S. patent that has been granted which claims to tap the energy of space.** The important aspect of the production and use of EVs is that the charge density (in terms of charge per cubic centimeter) is extraordinarily high, perhaps similar to ball lightning or within lightning strokes. It appears that the highly-dynamic nature of the EV actually does tap the energy of space and that a traveling EV is continually giving off energy and having its internal energy restored. There will obviously be an increasing interest in creating, launching, and studying the methods by which the energy of the EV can be coupled to provide useful work.

2. The Lambertson cermet device.

Dr. Wingate Lambertson has invented a device which uses a cermet (ceramic-metal) type of semi-conductor. Under proper conditions, the electrons are accelerated in such a manner that useful excess power can be extracted and delivered to an outside load. Dr. Lambertson describes this device in a March, 1994 article published in *New Energy News* [35]. See Fig. 11.

SUMMARY AND PREDICTIONS

Since March 23, 1989, when Drs. Pons and Fleischmann were directed to make a public announcement of their discovery of cold fusion, the world has changed. As has previously happened with new scientific discoveries, many confirmed skeptics have treated cold fusion with emotional reactions ranging from disdain through false claims of fraud. Serious scientists, especially those who were aware of the reputations of the inventors, have not only replicated the original Pons-Fleischmann work but have also added seven (and growing) new methods by which nuclear reactions (or, at least, excess heat) can be

produced and controlled in a variety of devices.

In an amazing demonstration of near-synchronicity, the recognition of and the commercialization of tapping space energy has emerged from its doldrums and is being recognized for its scientific merit. Now we have several serious concurrent developments of devices and systems that appear to obtain energy from the environment (space) around us. The N-machine, magnetic motors, and some solid-state devices are being developed to help resolve the world's energy problems.

In both cases, of cold fusion and space energy devices, there are corporate efforts involved in the commercialization of new energy devices. Particularly in Japan, there is both academic and corporate development work with the goal of solving the world's energy crisis. In India, there are strong efforts to develop new energy sources, especially at the Bhabha Atomic Research Centre near Bombay. Additional efforts are being made in many other countries, most notably in Russia, China, Taiwan, Italy, Spain, and in the United States. More modest scientific efforts are being pursued in many other nations such as Argentina, Romania, Hungary, and France. The oil-rich nations and the highly industrialized western nations have appeared more reluctant to pursue developments in either cold fusion or in space energy. However, companies such as ENECO, Inc. and Fusion Information Center (both of Salt Lake City, UT); HydroCatalysis Power Corporation (Lancaster, PA); and the Electrical Power Research Institute (Palo Alto, CA) have assets, funds, and personnel working on the development and commercialization of new energy systems.

Japan through its MITI organization plus several major corporations, such as IMRA and Toyota, have committed major funding. It is Japanese funds that have built a new $6 million laboratory for Drs. Pons and Fleischmann near Nice, France where significant progress is being made toward the commercialization of cold fusion.

One of the major developments in the U.S. is the financial assistance of Lynda and Bill Beierwaltes to fund the first and second International Symposia on New Energy. These conferences, plus the activities of the Institute for New Energy (founded in May 1993) are making a dramatic difference in the world's renewed interest in tapping the energy of space.

Therefore, the following is predicted:

1. There will be a continued effort to commercialize both cold fusion and other new energy systems.

2. As soon as successful demonstrations of commercial prototypes are made there will be a strongly accelerated, world-wide interest in developing, manufacturing, and distributing new energy devices and systems.

3. Drs. Fleischmann and Pons will be nominated to receive a Nobel prize.

4. The largest investment and the most new energy products will be made in Japan.

5. The nuclear fission power industry will cease to expand.

6. Finally, the U.S. Department of Energy will officially admit the reality of cold fusion and new energy devices and point with pride to the activities of their own national laboratories in the development of cold fusion.

REFERENCES

[1] Martin Fleischmann, Stanley Pons, and M. Hawkins, "Electrochemically Induced Nuclear Fusion of Deuterium," *J. Electroanal. Chem.*, 1989, vol 261, pp 301-308, and erratum, vol 263, p 187.

[2] Hal Fox, Cold Fusion Impact in the Enhanced Energy Age, published by Fusion Information Center: Salt Lake City, UT, 1993, see the included bibliography diskette, also available in Russian and Spanish.

[3] Vladimir Tsarev (Lebedev Physical Inst.), "Cold Fusion Researches in Russia," in Frontiers of Cold Fusion, Proceedings of the Third International Conference on Cold Fusion, H. Ikegami, Ed., pp 341-351, 30 refs, c1993, Universal Academy Press, Tokyo.

[4] T. Matsumoto, "Cold Fusion Observed with Ordinary Water," *Fusion Technology*, May 1990, vol 17, no 3, pp 490-492, 3 figs, 4 refs.

[5] Randell L. Mills and Steven P. Kneizys, "Excess Heat Production by the Electrolysis of an Aqueous Potassium Carbonate Electrolyte and the Implications for Cold Fusion", *Fusion Technology*, vol 20, Aug 1991, pp 65-81, 10 refs, 9 figs, 2 tables.

[6] Robert T. Bush, "Cold Fusion with Light Water," *Fusion Facts,* December 1991, p 1-2. See also Robert T. Bush, "A Light Water Excess Heat Reaction Suggests that 'Cold Fusion' may be `Alkali-Hydrogen Fusion'," *Fusion Technology*, vol 22, Sept 1992, pp 301-322, 61 refs, 2 figs.

[7] Robert T. Bush (Cal Poly, Pomona, California), "Towards a Solid State Nuclear Physics: The LANT Model (Lattice-Assisted Nuclear Transmutation) for Cold Nucleosynthesis," *Fusion Technology*, 1993, accepted for publication. See also Peter Glück, "Nuclear Catalysis & Cold Fusion - The SURFDYN Model," *Fusion Facts*, June 1992, pp 1-3, also *Fusion Technology*, vol 24, no 2, pp 122-126, 44 refs.

[8] M. Srinivasan, A. Shyam, T.K. Shankarnarayanan, M.B. Bajpai, H. Ramamurthy, U.K. Mukherjee, M.S. Krishnan, M.G. Nayar and Y. Naik (Bhabha Atomic Research Centre, Bombay, India), "Tritium and Excess Heat Generation During Electrolysis of Aqueous Solutions of Alkali Salts with Nickel Cathode," Frontiers of Cold Fusion, Ed. by H. Ikegami, Proceedings of the Third International Conference on Cold Fusion, October 21-25, 1992, Universal Academy Press, Tokyo, pp 123-138, 8 figs, 3 tables, 9 refs.

[9] Reiko Notoya (Hokkaido Univ.), "Cold Fusion by Electrolysis in a Light Water - Potassium Carbonate Solution with a Nickel Electrode," *Fusion Technology,* vol 24, no 2, Sept 93, 4 figs, 5 refs.

[10] Tadayoshi Ohmori & Michio Enyo (Hokkaido University, Catalysis Research Ctr., Kitaku, Sapporo), "Excess Heat Evolution During Electrolysis of H_2O with Nickel, Gold, Silver, and Tin Cathodes," *Fusion Technology*, vol 24, no 3, pp 293-295, 9 refs, 2 figs, 4 tables.

[11] Bor Yann Liaw, Peng-Long Tao, and Bruce E. Liebert* (Hawaii Natural Energy Institute, and *Department of Mechanical Engineering, University of Hawaii), "Recent Progress on Cold Fusion Research Using Molten Salt Techniques," The Science of Cold Fusion, Ed by Bressani, Del Guidice & Preparata, c 1991, Società Italiana di Fisica, Bologna, Italy, pp 55-64, 11 figs, 2 tables, 17 refs.

[12] L.J. Yuan, C.W. Wan, C.Y. Liang and K.S. Chen (National Tsing Hua Univ.), "Neutron Monitoring

on Cold Fusion Experiments," in Frontiers of Cold Fusion, Proceedings of the Third International Conference on Cold Fusion, H. Ikegami, Ed., pp 461-464, 5 figs, 2 refs, c1993, Universal Academy Press, Tokyo.

[13] Bor Yann Liaw, "Some Thermodynamic Aspects Related to Charging Hydrogen Species into Metal Lattice," presented at the Fourth International Conference on Cold Fusion, Maui, Hawaii, December 6-9, 1994.

[14] A.B. Karabut, Ya. R. Kucherov and I.B. Savvatimova, "Nuclear Product Ratio for Glow Discharge in Deuterium," *Phys. Lett. A,* 1992, vol 170, pp 265-272.

[15] Romodanov, Savin, Skuratnik, & Elksnin, "Reproducibility of Tritium Generation from Nuclear Reactions in Condensed Media," paper presented at the Fourth International Conference on Cold Fusion, Hawaii, Dec. 9, 1993.

[16] Xing Zhong Li (Tsinghua Univ. Beijing, China), Personal communication.

[17] Peter Graneau, "First Indication of Ampère Tension in Solid Electric Conductors," *Physics Letters*, vol 97A, no 6, 5 Sept 1983, pp 253-255, 6 refs, 1 fig.

[18] Jean-Pierre Vigier (Univ. P. and M. Curie, Paris), "New Hydrogen Energies in Specially Structured Dense Media: Capillary Chemistry and Capillary Fusion," Preprint courtesy of the author, to be published in *Phys. Lett. A.*

[19] K.A. Kaliev, A.N. Baraboshkin, A.L. Samgin, "Reproducible Nuclear Reactions During Interaction of Deuterium with Oxide Tungsten Bronze," *Phys. Lett. A*, 1993, vol 172, p 199.

[20] Peter Graneau (Center for Electromagnetic Research, Northeastern Univ. Boston, MA), "The Role of Ampère Forces in Nuclear Fusion," *Physics Letters A*, vol 165, 1992, pp 1-13, 10 figs, 29 refs.

[21] Peter Graneau, "Concept of a Capillary Fusion Reactor," in *Proceedings of the International Symposium on New Energy*, April 16-18, 1993, Denver, Colorado, pp 153-168, 2 figs, 11 refs.

[22] Eiichi Yamaguchi & Takahashi Nishioka, "Direct Evidence for Nuclear Fusion Reactions in Deuterated Palladium," in Frontiers of Cold Fusion, Proceedings of the Third International Conference on Cold Fusion, pp 179-188, 5 figs, 12 refs.

[23] A.L. Samgin, A.N. Baraboshkin, I.V. Murigin, S.A. Tsvetkov, V.S. Andreev, G. Varkarin (Inst. of High-Temp. Electrochemistry, Russian Acad. of Science, Ekaterinburg), "The Influence of Conductivity on the Neutron Generation Process in Proton Conducting Solid Electrolytes," presented at the Fourth International Conference on Cold Fusion, Maui, Hawaii, December, 1993. To appear in the Proceedings.

[24] Tadahiko Mizuno, Michio Enyo, Tadashi Akimoto & Kazuhisa Azumi (Hokkaido Univ., Sapporo, Japan), "Proton Conductors during Absorption/Desorption of Deuterium in Alternate Electric Field," presented at the Fourth International Conference on Cold Fusion, Maui, Hawaii, December, 1993. To appear in the Proceedings.

[25] J. Dufour, "Cold Fusion by Sparking in Hydrogen Isotopes," *Fusion Technology*, **1993,** vol 24, p

205ff.

[26] Stefan Marinov (writing about Fritzchen Zungezeige), "Once More on the Herd of the Blind," *Deutsche Physik*, **April-June 1994**, vol 3, no 10, pp 30-34.

[27] Bruce DePalma, "Where Electrical Science Went Wrong," *New Energy News*, vol. 1, no. 5, Sept. 1993, pp 1-4, 5 figs, 3 refs. Also, "On the Nature of Electrical Induction", *New Energy News*, vol 1, no 6, pp 2-8, 5 figs, 14 refs.

[28] Paramahamsa Tewari, "Generation of Cosmic Energy and Matter from Absolute Space (Vacuum)," *Proceedings of International Symposium on New Energy*, Maury Albertson, Ed., Denver, Colorado, April 16-18, 1993, pp 291-303, 6 figs, 8 refs.

[29] Shiuji Inomata & Yoshiyuki Mita, "Small Neodymium Magnet Twin N-Machine," *Proceedings of 28th Intersociety Energy Conversion Engineering Conference*, August 8-13, 1993, Atlanta, Georgia, pp 2.347-2.352, 11 figs, 2 refs.

[30] Shuiji Inomata, "Letter from Shiuji Inomata with Conceptual Design of JPI-II Test Machine," *New Energy News*, vol 1, no 7, pp 7-8, 2 tables, 3 figs.

[31] Harold Aspden, "Open Letter from Harold Aspden," *New Energy News*, vol 1, no. 10, pp 13-14, 1 ref.

[32] Harold E. Puthoff, "The Energetic Vacuum: Implications for Energy Research," *Speculations in Science & Technology*, 1990, vol 13, no 4, pp 247-257, 33 refs.

[33] Hal Fox, "Space Energy - Peer Reviewed," *New Energy News*, Feb 1994, vol 1, no 10, pp 2-6, 8 refs.

[34] Kenneth R. Shoulders, "Energy Conversion Using High Charge Density," U.S. Patent 5,018,180, May 21, 1991, 80 pages, 97 figs, 42 claims.

[35] Win Lambertson, "Electric Power from Space Energy," *New Energy News*, March, 1994, vol 1, no 11, pp 1-4, 4 figs.

COLD FUSION AND SUPERFAST LOW-TEMPERATURE CHEMICAL PROCESSES IN SOLIDS: COMMON BASIS FOR UNDERSTANDING

V.A. Filimonov, V.A. Lishnevskii
Institute of Physicochemical Problems, Belarus State University,
14 Leningradskaya Str., Minsk 220080 Belarus

ABSTRACT

It is obvious that cold nuclear fusion (CF) [1] isn't similar to the thermonuclear "hot" fusion, etc. There are dozens of theoretical models but their abilities to describe CF qualitatively and quantitatively are poor. Even now, five years after the memorable Utah News Conference, it is not clear what CF is similar to. We claim that there are certain analogies between CF, on one hand, and various fast chemical reactions and physico-chemical processes in solids, on the other hand.

In both classes, the processes do not obey the exponential dependence on activation energy/temperature (Arrhenius's law for chemical reactions) and seem to be a similar but more gently sloped function. The most exciting case of solid state chemical processes under consideration is superfast (explosion-like) cryo-chemical reactions in frozen gas mixtures at phase transition temperatures as has been studied by one of us (V.A.L.) during 1968-1978 [2]. Rates of such reactions differ from extrapolated gas phase reaction rates of the same components by 10-10. [sic]

Both the first and second processes are likely to be described by the synergetic activation model [3]. After this consideration, one more type of cold fusion process, namely CF under chemical detonation of solids, is suggested.

THE NATURAL CLASSIFICATION OF COLD FUSION PROCESSES

Since cold nuclear fusion (CF) was announced (Deryagin, et al., 1986 [4], Fleischmann and Pons, 1989 [1]), the kinetic impossibility of intense nuclear reactions having high potential barriers (E.g., Coulomb barrier) that proceed at low temperatures and pressures has been stressed. A complete explanation of this phenomena is one of the main problems in this field. This problem appears as an unprecedented one and together with poor reproducibility of experiments engenders great skepticism in the scientific community to the existence of the phenomenon itself [5].

There is no common acceptable classification of CF types. Using different methods of classification one may obtain up to 10 or more different types of CF [6]. It is likely that under successful development of the field the number of CF versions would be close to the number of elementary particles. For present consideration we neglect certain kinds of CF objects, methods of action, etc., and will limit our categories to the type of processes in solids or on the surface of the solids that produce CF. Therefore, the number of CF types is reduced to four. These are shown in Table 1.

Assignment of known CF systems to one or another of the above types may be not clear, but can be understood after more extensive study of systems noted. First consider some common regularities of or parallels, also taking into account unavoidable differences due to incommensurable activation energy scales. The first concerns mechano-fusion and mechano-chemistry. These phenomena were observed in a variety of systems under different kinds of action: with single deuteride crystals and with D_2O ice

Table 1. Types of CF versus analogous physicochemical processes in solids

1..Destruction of crystal lattice	
Mechano-Fusion: Deryagin et al., 1986	Mechano-Chemistry: Yaroslavskii, 1989
2. Cooperative mass transfer	
Electrochemical fusion in Pd: Fleischmann, Pons, 1989	Conjugated diffusion in Pd: Sokol'skii et al., 1988
3. Phase transition	
Fusion in ferroelectrics: Daryagin et al., 1992	Fast cryochemical reactions: Lishnevskii, 1978
4. Surface dynamics	
Light water fusion on Ni: Mills, 1991 Bush, Eagleton, 1992	Heterogeneous catalysis:
5. Detonation of Solids	
Deto-fusion Free position	Chemical detonation: Yenicolopyan et al., 1991

polycrystals in the case of fusion [4], and a set of inorganic crystalline salts and their mixtures, polymers etc. in the case of chemistry [7]. The type of "trigger" action may be different, such as: shock wave impact to samples, bullet blast, mechanical grinding, pressure plus mechanical action, etc. The result is similar in all cases: nuclear or chemical reaction rates at small or large magnitudes as compared to background rates at the same temperatures without mechanical action. We especially point out that the specified action itself cannot lead to sufficient heating of the reaction materials, and the temperature changes under mechanical action are negligible from the point of view both nuclear fusion and chemical reaction activation. The matter is concerned with not heating of the reaction medium, i.e. enhancing chaotic motion in solid, but with unidirectional action on it.

The second mode concerns the most famous CF version - the Fleischmann-Pons effect [1] and may also include such CF as the following: Ti loading by deuterium gas experiments by De Ninno et al., [8] and Kaliev-Baraboshkin tungsten bronzes - deuterium gas loading experiments [9]. The physicochemical analog is surprising but could be compared with the phenomenon of the high mobility of impurities in palladium and palladium alloys under conjugate transfer of hydrogen isotopes [10]. The acceleration of such a process, using significant activation energy, exceeds expectations by ten orders of magnitude more.

The next comparison concerns the nuclear and chemical anomalies under phase transition in solids. This phenomenon in the nuclear fusion field has been discovered by Deryagin and collaborators in 1992 [11]. We suppose that the same phenomenon is concerned, to some extent, in some other versions of CF, e.g., in above mentioned Ti-loading by deuterium gas with thermal cycling [8] and in Samgin-Baraboshkin's 1993 experiment on electrochemical deuteration of the strontium cerate hydrogen-ion conductor using thermal cycling [12].

THE SUPERFAST CRYOCHEMICAL REACTIONS IN SOLIDS - THE CLOSEST CHEMICAL ANALOG OF COLD FUSION

It is worth mentioning that the physicochemical analogy to CF is the most exciting one. It was studied by one of us (V.A.L.) during 1968-1978 in Minsk [2]. Fast exothermic cryochemical reactions may proceed in some electronic, protonic, and other donor-acceptor molecular systems having strong cooperative interactions. We especially note that most of the chemical reactions of the same components, in a gas phase, do not proceed at significant rates in ambient and moderate temperatures due to the relatively high activation energies of valence-saturated molecular reactions. Temperature dependencies of the noted reaction rates are significantly non-Arrhenius's ones, and the rates themselves are high and even explosion-like down to liquid nitrogen temperature - 77°K.

Usually the reaction mixtures for noted process - gas compositions having stoichiometric donor-to-accepter ratio fixed at 77°K are non-equilibrium processes for their structures and compositions. When treated by slow precipitation (freezing) at 77°K, the reaction activity of these mixtures proceeds rapidly and entirely at the temperatures some (3° to 20°K) below the phase transition points (including intermediate complexes and eutectics) such as melting points or structure transitions. Acceleration of the cryochemical reactions under phase transitions in solids appears to be up to 30 or even 60 orders of magnitude higher than expected by Arrhenius's rates for the same components in a gas phase or at high or enhanced temperatures as extrapolated down to the temperature of relevant phase transition (see Fig. 1). In all cases, both gas phase and solid state reactions, only the reactions carried out in full darkness are taken into account.

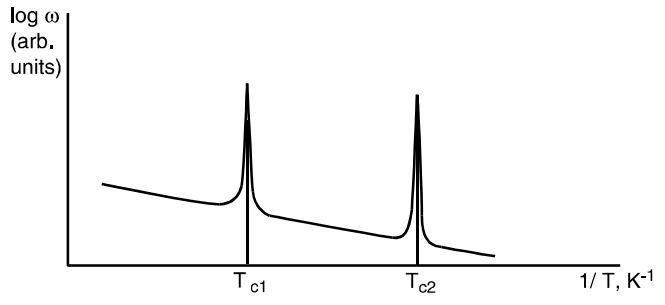

Fig. 1. The common view of temperature dependence of fast cryochemical reaction rate ω. $T_{c1,2}$ are phase transition temperatures [2].

It is especially noted that the features (mentioned above) are not mainly produced by the quantum phenomena because the upper temperature of quantum tunneling T of particles through potential barrier E for low-temperature chemical reactions is given by the following equation derived by Goldanskii [7]:

$$T_t = \frac{h}{k\pi\sqrt{2d}} \cdot \sqrt{\frac{E}{m}} \qquad (1)$$

(where h is the Plank's constant, k is the Boltzmann constant, d is the hopping length, m is the mass of the particle). The resulting temperature is 50°K for protons and correspondingly lower for particles having larger masses whereas the reported reactions proceed at more temperatures. Moreover, quantum tunneling, in this case, must exhibit a constant reaction rate below T as compared with its rate as temperatures are deceased. The observed enormous increasing value of the reaction at fixed temperature points is not expected.

It is also noted that at relatively low temperatures in solid state materials even small changes of entropy due to formation of complexes or cooperative effects in clusters sharply exhibit macro-effects of superfast cryochemical processes without the introduction of foreign matter, such as a catalyzer, although thermal energies of the molecules at the same temperatures are far lower than the quantum zero vibration energy level or Van der Waals intermolecular interaction energy.

One more analogy - compare the light water-nickel CF system by Mills, Bush-Eagleton and their followers with the surface dynamics of hydrogen and various heterogeneous catalysts. This effect is proposed and considered in detail by Glück [13].

THE SYNERGETIC ACTIVATION MODEL - A COMMON BASIS FOR COLD FUSION AND FAST CHEMICAL REACTIONS IN SOLIDS

It's easily seen that there are clear similarities in the horizontal rows of Table 1. Now let's consider similarities in the vertical columns that aren't so evident. There seem to be similar or common points between different types of CF as is observed between different kinds of chemical reactions and/or transport phenomena in solids. But it's not so.

The concept connecting different cells in the right column of the table is, in our opinion, the common nature of cooperative processes which proceed in accordance with synergetic activation (SA) model. This model dramatically distinguishes unidirectional cooperative action from thermal, chaotic actions. The main points of the SA model are as follows:

1. SA model is more gently sloped than is the exponential distribution of atoms or molecules by energy - namely quasi-power one:

$$P_n^{/} \approx (E_n / E_0)^{-\lambda} \qquad (2)$$

(where P is the probability of obtaining the energy packet E by the atom, E is the average energy per atom, e.g. the thermal one, $l > 1$ and its value depends on the structure of excited energy levels of the system). This combination makes overcoming potential barriers by the system easier. Thus, this effect is possible in highly non-equilibrium, self-organizing systems. The results is a sequel to nondirect but multi-stage excitation of atoms (molecules etc.) up to higher excitation levels in some kinds of dissipative structures (see, for example, [14]).

2. Such distribution is realized in spatiotemporal limits of shock or detonation wave (SW and DW correspondingly) fronts that are therefore considered as dynamic, dissipative structures.

3. These shock waves may be introduced into solids from outside but a self-generation of SW (DW) and self-focusing of the same waves can then promote accumulation of energy in focal zones (such as are possible under mechanical action upon crystals with the resulting destruction of the lattice, phase transition implementation in the same or intense heat and mass transfer (e.g. intense hydrogen or deuterium transport) in perfect crystalline solids or on their surfaces in vicinity of phase separation region. As for the self-generation of shock waves, a phase transition and flawless crystal patterns are the conventional conditions to produce shock waves - owing to nonlinear acoustics.

The synergetic activation model is suitable for the understanding of a wide range of processes in highly non-equilibrium systems. The model is able to predict some important criteria for the implementation of high-excitation phenomena in such systems concerning both the possibility of shock wave-type nonlinear wave formation under appropriate conditions (such as phase transition, cooperative mass transfer etc.) and ensuring easy propagation of the waves in solids (such as low enough extended defects content in a crystal lattice).

Therefore, we suppose that significant and enormous acceleration of different physicochemical processes may be caused not by quantum phenomena but cooperative, synergetic processes.

We suppose also that the left column i.e. CF area may also be described within the framework of the synergetic activation model. Moreover, certain criteria of reproducible CF implementation proposed by the SA model are in accordance with published experimental data, as we've stated recently. It is unfortunate, but quite natural, that most of published papers do not record and publish data allowing one to ascertain the real crystal structure of the samples used in CF experiments. However, the minor part of the papers concerning relevant data, exhibit certain positive correlations with the main SA criterion - lattice perfectness - and the distinct correlation of the type "necessary, but not sufficient" with the second one - highly non-equilibrium state of the system under action, as we've reported recently.

So we have to claim once more that CF phenomena are caused mainly not by quantum but by synergetic phenomena. In addition to distinct criteria of CF reproducibility, the SA model is able to predict some new CF types, as is shown below:

PREDICTION OF ONE MORE COLD FUSION PROCESS TYPE

Turning back to the right column of Table 1 - physicochemical analogies of CF types - we must add one more cell. This cell is to be occupied by chemical reactions of detonation of solids. Similar to other members of this group, these exothermic processes initiated by some type of shocking action to some solids. These reactions are characterized by their superhigh rates at ambient and moderate temperatures in strange contradiction with low rates of the usual combustion of the same crystal substances when ignited. The differences between volume rates may consist up to 20 orders of magnitude. Similar to other mentioned processes, the detonation of solids and the dependency on temperature do not obey the Arrhenius's law. This fact allowed Yenikolopyan, et al., [15] to propose that chemical detonation is implemented in non-kinetic but so-called "dynamic" regime and its rate is not dependent on temperature. The latter report may not be correct, however some structural aspects of the model fit experimental data and are acceptable. Worthy of mention is that the chemical detonation of solids may be best described by SA model. Subsequent application of the SA model to detonation of solids [16] allowed us to derive the analytical expression of detonation rate v, dependencies on temperature T, activation energy E, and heat release DE of the reaction:

$$v_{dw} = A \cdot \frac{(kT)^{\lambda}}{E_n^{\lambda-1/2}} \cdot \sqrt{1 + \frac{\Delta E}{E_n}} \qquad (3)$$

This equation is in satisfactory agreement with experimental data. As one can see, the corresponding cell on the CF side of the table is empty. Now we can predict that it must be filled by corresponding kind of CF phenomenon. What kind of a process might it be?

We are convinced that the chemical detonation of solids must be accompanied by nuclear fusion with a probability that differs from zero. Moreover, deto-fusion must be more intense than other CF types because the average energy per atom (molecule) in the detonation wave front is higher than typical thermal energies or energies of phase transitions (E in the formula 2).

It may be said that similar to heavy water and light water fusion, the predicted deto-fusion is possible in both deuterium-containing solids and in their protium equivalents. The important point to be stressed is

that the deto-fusion rates/intensities in deuterated solid substances are expected to be similar to CF rates but the reaction products are expected to be similar to "hot" fusion reactions due to destruction of crystal lattices. It is suggested that it will be impossible to stabilize the He reactions in such a reaction. One more important point is a prime criterion of SA model: the specimen used for the reaction must be perfect crystal with low (down to 10 per square centimeter) content of extended defects.

If one understands the above mentioned parameters for the predicted deto-fusion, the discovery of the effect appears to be quite easy. We have shown the deto-fusion cell as empty in Table 1 and challenge any of our interested colleagues to find the predicted effect to fill this cell.

REFERENCES

[1] M. Fleischmann, S. Pons, and M. Hawkins, *J. Electroanal. Chem.*, vol 261, no 5, pp 301-308 (1989).

[2] V.A. Lishnevskii, *J. Phys. Chem.* (Russ.), vol 52, no 1, pp 1-14 (1978).

[3] V.A. Filimonov, *J. Radioanal. Nucl. Chem.* (Articles), vol 162, no 1, pp 99-109 (1992); *Russ. JTP.* vol 62, no 6, pp 221-224 (1992); *Russ. JTP Letters.* vol 16, no 19, pp 42-46 (1990); *Ibid.*, vol 16, no 20, pp 29-34 (1990).

[4] B.V. Deryagin, V.A.Klyuev, A.G.Lipson, Yu.P.Toporov, *Kolloidnyi Zhurnal*, vol 48, no 1, pp 12-14 (1986).

[5] D. Morrison, presented at the Fourth Int. Conf. on Cold Fusion, Maui, Hawaii, USA, December 1993.

[6] H. Fox., Proc. Int. Conf. "Possibilities of Ecologically Clean Energy Production and Energy Conservation", Minsk, Belarus, 25-27 May, 1993.

[7] V.I. Goldanskii, *Uspekhi Khimii*, vol 44, no 12, pp 2121-2149 (1975).

[8] A. De Ninno et al., *Europhysics Letters*, vol 9, pp 221-224 (1989).

[9] K.A. Kaliev, A.N. Baraboshkin, A.L. Samgin et al., *DAN (Repts. Russ. Acad. Sci*), vol 330, no 2, pp 214-216 (1993).

[10] D.V. Sokol'skii, N.N. Gudeleva, B.Yu. Nogerbekov, *Elektrokhimiya*, vol 24, pp 990-992 (1988).

[11] A.G. Lipson, B.V.Deryagin et al., *Russ. JTP Letters*, vol 18, no 16, pp 90-95 (1992).

[12] A.L. Samgin, A.N. Baraboshkin et al., presented at the Fourth Int. Conf. on Cold Fusion, Maui, Hawaii, USA, December 1993.

[13] P. Glück, Proceedings of the Minsk International Cold Fusion and Energy Conference.

[14] P. Glansdorff, I. Prigogine, Thermodynamic Theory of Structure, Stability and Fluctuations. Wiley-Interscience, London & New York, 1971.

[15] N.S. Yenikilopyan, L.I. Manevich, V.V. Smirnov, *Khimicheskaya Fizika*, vol 10, no3, pp 389-398 (1991).

[16] V.A. Filimonov, E.N. Naumovich, Proc. 2nd Int. Workshop "Self- organization in Complex Systems", Polotsk, Belarus (February 1993), pp 81-88.

ACKNOWLEDGEMENTS

One of us (V.A. F.) acknowledges Belarus Fundamental Researches Foundation for financial support within Grant No F54-144/1.

Fusion Facts

This monthly scientific publication is devoted to ***Cold Fusion Systems.*** *Contributing authors and researchers from around the world supply articles for this informative publication. The publisher, Fusion Information Center, Inc. has become the world's center for information on cold fusion and other energy systems. This monthly publication is a MUST for ALL who are engaged in cold fusion reseach and those who want to stay on the leading edge of new knowledge about this expanding science. A subscription for 12 months is US$300.00 which will be mailed first class or air mail to all countries.*

Send your order to:

Fusion Information Center, Inc.

P.O. Box 58639, Salt Lake City, Utah 84158 USA

1 801 583 6232 / FAX 1 801 583 2963

INTRODUCTION TO COLD FUSION THEORY PAPERS

At a recent conference on cold fusion one of the few remaining pathological skeptics announced that because there were more than 20 cold fusion theories that were supporting evidence for his contention that cold fusion was not real! If the same logic were applied to superconductivity, then all work on superconductivity should be abandoned. So, too, should all work on chemical catalysis be abandoned because we still do not have a comprehensive theory to fully explain chemical catalysis.

It is the editor's judgement that the technical area of cold fusion is so rich in new phenomena that **no one theory can explain all of the experimental findings.** I hope I am wrong. I believe that *Fusion Facts* was the first to write about "nuclear catalysis" and "proton capture". While these are just words, it is suggested that the concepts help to solidify our understanding of some of the phenomena of cold fusion and the theories than are presented.

The following theory papers present a few of the theories on cold fusion and its phenomena. The first is a new paper by Dr. Robert Bass. He willingly admits that he has drawn on the work of others to present his theory based on fundamental, accepted, (and peer-reviewed) principles of physics. Bass asks for your critical examination of this theory and your comments on its weaknesses and strengths. I'm sure that the other writers of theory will also be pleased with comments and **most important of all, your experimental data.**

LINT:
A SEMI-CLASSICAL QUANTIZED THEORY OF LATTICE INDUCED NUCLEAR TRANSMUTATIONS

Robert W. Bass
Scientific Advisory Board, ENECO, Inc.
391-B Chipeta Way, Salt Lake City, UT 84108

ABSTRACT

In a frozen supersaturated or fully deuterated ("beta phase") $Pd{\cdot}D_{[1.0]}$ crystal lattice, an incoming deuteron of energy 5.1 eV [above the elsewhere-estimated zero-point energy level of 6.257 eV] will collide with a zero-point energy level E_0 = 0.052 eV [+ 6.257 = 6.31 eV] bound deuteron, losing 18 of its 31 quanta of linear momentum as measured by Duane's Rule (for Inelastic Collisions between a particle and a lattice), and knocking the bound deuteron, approximated as a quantized harmonic oscillator, into its 40th bound energy level above ground state E_1 = 0.156 eV [+ 6.257 eV = 6.41 Ev], i.e. E_{40} = 4.2 eV [+ 6.3 = 10.5 Ev] which, in the present admittedly over-simplified theory, ALSO coincides with a Resonant Transmission energy level, as in the Turner-Bush theory of transmission resonance, in which the de Broglie wavelength of an excited particle is in resonance with the lattice period. Elsewhere the WKB Approximation is used more realistically with a Madelung-Coulomb lattice potential to compute 88 Resonant Transmission energy levels for excited bound deuterons of energies between 6.32 eV and 13.74 eV, but no mechanism for exciting zero-point (or room-temperature!) deuterons to these resonant energy levels has been suggested. The present semi-classical scattering calculation exhibits an explicit quantal mechanism for exciting the bound deuterons and introduces two new integral quantum numbers (*J,K*) in terms of which all possible such resonant *scattering* scenarios may be enumerated.

INTRODUCTION

The theoretical analysis of high-energy $D + D$ collisional interactions in a near vacuum (e.g. a low-density fusion plasma made from deuterium gas) predicts two principal reactions, namely [with $D = {}_1{}^2H, T = {}_1{}^3H$]

$$D + D \rightarrow {}^3He + n + 3.27 \text{ MeV}, \tag{1}$$

$$D + D \rightarrow T + H + 4.03 \text{ MeV}. \tag{2}$$

Theory and experiment (cf. Miley [1]) predict and confirm that these two reactions occur with approximately equal probabilities, the ratio of which is the *branching ratio*. A third possibility, usually ignored because its branching ratio, in comparison to either of the preceding reactions, is about 10^{-7} times smaller, is

$$D + D \rightarrow {}^4He + \gamma + 23.85 \text{ MeV}, \tag{3}$$

where the excess energy appears in the form of a gamma-ray photon γ.

The usual explanation for the rarity of (3) is that when one high-energy (say about 10 keV) D-nucleus approaches another high-energy *D*-nucleus the three-dimensional orientations and linear and angular

momenta of the colliding nuclei are quite *asymmetrical*; the nucleon farthest from the system's center of mass escapes the strong nuclear force and is torn from its original partner, while the remaining nearest three particles coalesce.

But (recalling *Bloch's Theorem* that a solution of Schrödinger's equation inside of a periodic lattice is not valid unless its logarithmic derivative is a *spatially periodic function* of the same period) it is pure unreflective dogmatic incompetence to *assume* [in the absence of experimental evidence] that at low energies, and inside of a *PERIODIC* lattice, the established high-energy, near-vacuum branching ratio remains unaltered. In the prophetic words of Nobel Laureate Julian Schwinger [2A], the question demands "study, not fiat."

In particular, if two bound *D*-nuclei forming a harmonic-oscillator pair inside a lattice approach each other when the energy level of the oscillator is excited, their momenta and orientations could be relatively symmetrical, leading by tunneling to their transitory conjunction as an excited α-particle (or ^4He* nucleus). Could such an excited ^4He* somehow shed its excess energy and drop into its unexcited ground state ^4He?

According to Schwinger [2B], quantum electrodynamic (QED) selection rules now "forbid" the emission of a photon -- apparently (Park [3A]) because two S-state, spin 1 boson *D*-nuclei can only produce a ^4He* of spin 0 or 1 or 2, but there are no photons of spin 0 or spin 2, and because parity must change in an allowed transition from the spin 1 state ("Laporte's Rule", [3B, p. 364]) there can be no photon emitted in that case either.

Park [3A] doubts that phonons can be emitted, for he expects that purely radial pulsations of the $^4He^*$ would have insufficient amplitude to affect the lattice. However, no one has ever suggested a detailed micro-physical "picture" of how mass is transformed into energy according to $E = m \cdot c^2$, and it has been suggested by R.D. Washburn ([4]) that the excess energy is shed by the two *D*-nuclei in the form of decreasing kinetic energy of angular momentum as they spiral around one another in shrinking orbits while "radiating" millions of phonons and coalescing (to use a classical picture) via the strong force. [Such a 3-dimensional problem is beyond the scope of the present point-particle viewpoint paper.]

At any rate, Hagelstein [5] and Schwinger [2B] have postulated the possibility that the excess 23.85 MeV can somehow be released into the lattice as heat energy via phonon excitations. Schwinger [2B] has assumed that the *D* lattice inside a fully loaded $Pd \cdot D$ or doubly-loaded $Pd \cdot D_2$ lattice absorbs 2.4×10^8 phonons of energy 0.104 eV each.

Some high-energy physicists, such as S.E. Jones [18] have attempted to refute the possibility of such a reaction by the following argument. According to Heisenberg, $\Delta E \cdot \Delta t \cong h$; assuming that photons or phonons or whatever is emitted cannot travel superluminally, and that the distance between nuclei is $L \cong 1$Å, one finds that $\Delta t = L/c = 10^{-8}\text{cm}/(10^{10}\text{cm/sec}) = 10^{-18}\text{sec}$. Thus, from Heisenberg's relationship in the form $\Delta E \cong h/\Delta t = (10^{-15}\text{eV-sec})/10^{-18}\text{sec} = 10^3$ eV = 1 keV, which is vastly less than 23.85 MeV. The incompetence of this argument is exposed by noting that a photon [or phonon] of energy $2h\nu$ can split into two photons [or two phonons] of energy each $h\nu$, and so there is no good reason for simply ASSUMING that the emitted energy has to have the characteristics of a single particle! (Also, in *non-relativistic* quantum mechanics the time-duration of transition of energy levels is treated as if it were either *instantaneous* or (Park [3B]) *non-analyzable*, and so light-cone arguments are irrelevant). Therefore Schwinger's postulate of 2.4×10^8 phonons being released into the *D* lattice merits further serious

consideration.

However, the mean potential energy of a Pd-oscillator in the Pd lattice is only 22.8% of that of a *D*-oscillator in the *D*-lattice (because of the Virial Theorem for quantized harmonic oscillators, and because the phonon energy scale in a *Pd*-lattice is 0.0237 eV).

Accordingly, if the postulated 23.85 MeV release puts the *Pd·D* lattice into its lowest available energy state, the release would be absorbed by the *Pd* lattice rather than the *D* lattice. Consequently the present theory purports to improve and refine Schwinger's NEAL theory by postulating that instead of 2.4×10^8 phonons going into the *D*-lattice, about 1×10^9 phonons of size 0.0237 eV go into the Pd-lattice.

ANALYSIS

In the following theory, we shall borrow from (non-relativistic) quantum mechanics the proposition that *energy* and *linear momentum* are commuting observables, and therefore both can have *simultaneously sharp* observed values. Accordingly we shall assume that it is legitimate to change back and forth between the *kinetic energy E* of a particle of [constant] mass *M* and its *linear momentum p* by the transformations

$$E = p^2/2M, \;\; p = (2M \cdot E)^{1/2} . \tag{4}$$

Also, instead of utilizing quantum mechanics, we shall proceed as did Bohr, applying what Landé [6] calls *quantal postulates* in an *ad hoc* manner to a classical treatment. Note that Landé says that his three *quantal postulates*

$$\text{(PLANCK)} \quad \Delta E = n \cdot (h/T) \equiv n \cdot h\nu, \;\; (\nu = 1/T) , \tag{5a}$$

$$\text{(DUANE)} \quad \Delta p = n \cdot (h/L) \equiv n \cdot h\kappa, \;\; (\kappa = 1/L) , \tag{5b}$$

$$\text{(deBROGLIE, BOHR, SOMMERFELD-WILSON)} \quad \Delta H = n \cdot (h/[2\pi]) \equiv n \cdot \hbar , \tag{5c}$$

(which result from PERIODICITY in *time T*, in *space L*, and in *angular orientation* 2π) are in some sense more fundamental than quantum mechanics, because by simply assuming (5a,b,c) together with some innocuously unobjectionable postulates about *symmetry* and *invariance* in probability theory, Landé derives Schrödinger's equation!

In the following one-dimensional model of a collision between an incoming free D-nucleus and a bound D-nucleus which is half of a bound-oscillator pair, we shall replace (5a,b) *in the present context* by the more appropriate postulates (which can be derived quantum-mechanically from, respectively, the theory of Quantized Harmonic Oscillators and the theory of Transmission Resonance of a free particle in a lattice defined by a periodic potential):

$$E_n = (2n + 1) \cdot E_0, \;\; E_0 = (1/2)(h/T) \equiv (1/2)h\nu , \tag{6a}$$

$$p_m = (2m + 1) \cdot p_0, \;\; p_0 = (1/2)(h/L) \equiv (1/2)h\kappa , \tag{6b}$$

where the factor (½) accounts for the *zero-point* quantum level. The use of Duane's Rule (5b) in the form (6b) is equivalent to the most basic part of the Bush Transmission Resonance Model (TRM) [7], wherein

he developed the concept suggested by Turner [8]; for more details concerning Duane's Rule in the context of quantum mechanics and relativity, see Bush [9]-[10]. The intent of the present paper could be described as an attempt to "combine the best features of the Bush TRM theory and the Schwinger NEAL theory."

In the case of a quantized bound-oscillator, we shall denote the rms oscillation amplitude Λ and rms linear momentum |p| by the symbols

$$\Lambda \equiv \langle x^2 \rangle^{1/2}, \; |p| \equiv \langle p^2 \rangle^{1/2} , \tag{7}$$

where $\langle \cdot \rangle$ denotes the quantum-mechanical expectation operator.

According to Duane's Rule, a free particle in a lattice of period L can only exchange linear momentum with the lattice in *integral* units of (h/L). Thus we have for a free particle of mass M_f and able to exchange linear momentum with a lattice:

$$p_{f,m} = (2m + 1)\cdot p_{f,0}, \quad p_{f,0} = h/(2L) , \tag{8}$$

$$E_{f,m} = (2m + 1)^2 \cdot E_{f,0}, \; E_{l,0} = [h/(2L)]^2/(2M_f) , \tag{9}$$

where (8) is equivalent to Duane's Rule (6b), and (9) follows by (4).

The theory of a quantized harmonic oscillator is well known and will not be repeated here; suffice it to say that Schwinger [2B] is being followed in supposing that the zero-point rms amplitude Λ_0 of a bound particle of mass M_b is known from x-ray measurements, and therefore the energy levels of what in the present context should be called a *Schwinger oscillator* are given by:

$$E_{b,n} = (2n + 1)\cdot E_{b,0}, \quad E_{b,0} = \{h/(2[2\pi\Lambda_0])\}^2/M_b , \tag{10}$$

$$|p_{b,n}| = (2n + 1)^{1/2} \cdot |p_{b,0}| , \quad |p_{b,0}| \equiv (M_b \cdot E_{b,0})^{1/2} = h/(2[2\pi\Lambda_0]) , \tag{11}$$

where (11) follows from (10) by (4), and where in (10) the mass M_b is used instead of $2M_b$ (as for a free particle having kinetic energy only) because of the Virial Theorem's result that the absolute values of the mean kinetic and mean potential energies of a harmonic oscillator are equal (and therefore the mean total energy is twice either one).

Note the analogy, between L in the case of the free particle and $2\pi\Lambda_0$ in the case of the bound particle, disclosed by comparison of (8) and (11). It may be a mere coincidence, but in the two numerical cases where we shall use measured values of L and Λ_0, they exhibit a commensurability to almost four decimal places. Accordingly this question merits further investigation. But we shall assume that it is simply a remarkable coincidence pertaining to the $Pd{\cdot}D$ and $Pd{\cdot}D_2$ lattices that there can always be found an integer n_σ such that a resonance in spatial periods (hence in wave numbers) exists, namely:

$$L = (n_\sigma + [½])\cdot (2\pi\Lambda_0) \equiv (2n_\sigma + 1)\cdot (\pi\Lambda_0) . \tag{12}$$

In the First Example below, $n_\sigma = 4$; but in the Second Example below, $n_\sigma = 1$.

However, (12) alone is insufficient to allow us to derive Diophantine equations for the quantum-transitions

involved in the postulated collision between a free D-nucleus and a bound D-nucleus.

QRT PRINCIPLE

For this purpose we need the *Quantum Resonance Triggering* (QRT) *principle,* which assumes that *certain* energy levels of incoming free particles have ground-state *momenta* which are in resonance with the ground-state rms-momentum of a bound particle, in the sense that there exist *incommensurable* positive integers *(r,s)* such that

$$r\cdot |p_{b,0}| = s\cdot p_{f,0} \ . \tag{13}$$

Now suppose that a free *D*-nucleus of momentum-level *m* collides with a bound D-nucleus which is part of a Schwinger oscillator of energy-level *j*, and that after their interaction the free D-nucleus remains free but has *lost* (*m-k*) quanta of linear momentum, while the oscillator has *gained* (*n-j*) quanta of energy. In an obvious notation,

$$D_{f,m} + D_{b,j} \rightarrow D_{f,k} + D_{b,n} \ . \tag{14}$$

Since conservation of both energy and linear momentum are obeyed in quantum mechanics, we may then conclude that (14) implies that

$$\text{(CONSERVATION OF MOMENTUM)} \quad p_{f,m} + |p_{b,j}| = p_{f,k} + |p_{b,n}| \ , \tag{15a}$$

$$\text{(CONSERVATION OF ENERGY)} \quad E_{f,m} + E_{b,j} = E_{f,k} + E_{b,n} \ . \tag{15b}$$

In order to demonstrate the quantum-level transitions determined by (15a,b), we rearrange them as

$$p_{f,m} - p_{f,k} = |p_{b,n}| - |p_{b,j}| \ , \tag{16a}$$

$$E_{f,m} - E_{f,k} = E_{b,n} - E_{b,j} \ . \tag{16b}$$

Therefore, using (8), (9), (10), (11), we have from (16a,b):

$$p_{f,m} - p_{f,k} \equiv 2(m-k)\cdot p_{f,0} =$$

$$= |p_{b,n}| - |p_{b,j}| \equiv \{(2n+1)^{1/2} - (2j+1)^{1/2}\}\cdot |p_{b,0}| \ , \tag{17a}$$

$$E_{f,m} - E_{f,k} \equiv \{(2m+1)^2 - (2k+1)^2\}\cdot E_{f,0} \equiv 4(m-k)\,(m+k)\cdot E_{f,0} =$$

$$= E_{b,n} - E_{b,j} \equiv 2(n-j)\cdot E_{b,0} \ . \tag{17b}$$

Thus conservation of momentum and energy are equivalent to

$$(2n+1)^{1/2} - (2j+1)^{1/2} = 2(m-k)\cdot\{p_{f,0}/\,|p_{b,0}| \ , \tag{18a}$$

$$n - j = 2(m-k)\,(m+k+1)\cdot\{E_{f,0}/E_{b,0}\} \ . \tag{18b}$$

Recall that, from the **QRT** hypothesis of *momentum resonance* (13), together with the *oscillation-amplitude resonance* "coincidence" [?] (12),

$$r/s = p_{f,0}/\,|p_{b,0}| \equiv (2\pi\Lambda_0)/L = 2/(2n_\sigma + 1), \tag{19}$$

whence, incidentally, there must exist a positive integer n_{QRT} such that

$$r = 2n_{QRT}\ , \tag{20a}$$

$$s = (2n_\sigma + 1)\cdot\, n_{QRT}\ . \tag{20b}$$

Similarly

$$E_{f,0}/E_{b,0} = [M_b/(2M_f)]\cdot\,(r/s)^2\ . \tag{21}$$

Henceforth we shall concentrate on the case (14), in which

$$M_f = M_b\ . \tag{22}$$

PROBLEM STATEMENT

Then the conditions of conservation of momentum and conservation of energy become, after inserting (19) and (21)-(22) into (18a,b),

$$(2n + 1)^{1/2} - (2j + 1)^{1/2} = 2(m - k)\cdot\,(r/s)\ , \tag{23a}$$

$$(n - j) = 2(m - k)\,(m + k + 1)\cdot\,(r/s)^2\ . \tag{23b}$$

These are *Diophantine equations*, in that the only solutions sought are to be in *integers*. Clearly this is impossible unless both $(2n + 1)$ and $(2j + 1)$ are perfect squares, which will emerge in the following. For the moment it is essential to note that even if the left hand side of (23a) were the difference of two integers, the equation has no solutions unless $(m - k)$ is divisible by s. Accordingly we assume that there exists an integer l such that $(m - k) = s\cdot\, l$. Then the conditions of *conservation of momentum, momentum resonance, and conservation of energy* become

$$(2n + 1)^{1/2} = (2j + 1)^{1/2} + 2lr\ , \tag{24a}$$

$$m = k + s\cdot\, l\ , \tag{24b}$$

$$n - j = 2sl(2k + 1 + sl)\cdot\,(r/s)^2 \equiv [(2k + 1)/s]\cdot\, lr^2 + l^2r^2\ . \tag{24c}$$

These three Diophantine equations can be somewhat simplified by squaring both sides of (24a), simplifying, and dividing by 2 to obtain

$$n - j = 2(2j + 1)^{1/2}\cdot\, lr + 2l^2r^2\ . \tag{25}$$

Now equate the right-hand sides of (25) and (24c), simplify, and divide by lr^2 to obtain

$$(2/r)\cdot (2j+1)^{1/2} = [(2k+1)/s] + l\ , \tag{26}$$

which, of course, is equivalent to (24a). Thus, finally, we may conclude that the conditions of *conservation of momentum, momentum resonance, and conservation of energy* are equivalent to the three Diophantine equations

$$l = [(2k+1)/s] - (2/r)\cdot (2j+1)^{1/2}\ , \tag{27a}$$

$$m = k + l\cdot s\ , \tag{27b}$$

$$n = j + [(2k+1)/s]\cdot lr^2 + l^2r^2\ . \tag{27c}$$

The lengthy algebra required in deriving a complete solution of (27a,b,c) will be omitted in favor of specifying the results, which can be verified by substitution to be the *completely general solution* of (27a,b,c), in that they convert these equations into identities.

PROBLEM SOLUTION

Let (J,K) be an arbitrary pair of non-negative integers. Then define

$$n_{\mathrm{QRT}} = 2J + 1 \tag{28a}$$

$$n_J = n_\sigma + (2n_\sigma + 1)\cdot J\ , \tag{28b}$$

$$r = 2(2J+1) \geq 2\ , \tag{28c}$$

$$s = 2n_J + 1 \equiv (2n_\sigma + 1)\,(2J+1)\ , \tag{28d}$$

$$j = 2J(J+1)\ , \tag{28e}$$

$$k = n_J + (2n_J + 1)\,(K+1)\ , \tag{28f}$$

$$l = 2(K+1) \geq 2\ , \tag{28g}$$

$$m = n_J + 3(2n_J + 1)\,(K+1)\ , \tag{28h}$$

$$n = 2J(J+1) + 8(K+1)\,(4K+5)\,(2J+1)^2 \geq 40\ . \tag{28i}$$

Using the definitions (28a-i), and some algebra, it is easy to verify that, also,

$$2j + 1 = (2J+1)^2\ , \tag{29a}$$

$$2n_J + 1 = (2n_\sigma + 1)\,(2J+1)\ , \tag{29b}$$

$$2k + 1 = (2n_\sigma + 1)\,(2J+1)\,(2K+3) \geq 3\ , \tag{29c}$$

$$2m + 1 = (2n_\sigma + 1)\,(2J+1)\,(6K+7) \geq 7\ , \tag{29d}$$

$$2n + 1 = [(2J+1)\,(8K+9)]^2 \geq 81\ , \tag{29e}$$

Now, upon inserting the definitions (29a-i) and identities (29a-e) into the three Diophantine equations (27a,b,c) one finds (after some algebra which is left as an exercise for the reader) *identities* in (J,K). Hint: Use the identity

$$(8K+9)^2 \equiv 1 + 16(4K+5)\cdot (K+1)\ . \tag{30}$$

The *new quantum number J* specifies the level at which the **QRT** scenario begins. The *new quantum number K* specifies the number of quanta which are gained and lost in the transition (14). In fact,

$$p_{f,m} - p_{f,k} = 2n_p \cdot p_{f,0} \,, \tag{31a}$$

$$n_p \equiv m - k = 2(2n_\sigma + 1)\cdot (2J + 1)\cdot (K + 1) \geq 2(2n_\sigma + 1) \geq 2 \,, \tag{31b}$$

which displays the fact that in the collision the free D-nucleus *loses* $n_p \geq 2$ quanta of linear momentum. Likewise, making use of (30), it is not difficult to verify that

$$E_{b,n} - E_{b,j} \equiv 2n_E \cdot E_{b,0} \,, \tag{32a}$$

$$n_E \equiv n - j = 8(K + 1)\,(4K + 5)\,(2J + 1)^2 \geq 40 \,, \tag{32b}$$

which displays the fact that in the collision the bound D-nucleus harmonic oscillator *gains* $n_E \pm 40$ quanta of energy.

In the theory of Schwinger oscillators (Bass [13]) it is proved that

$$E_{b,n} = M_b(\omega\Lambda_n)^2,\ \Lambda_n = (2n + 1)^{1/2}\Lambda_0, \tag{33a}$$

$$\omega = h/\{2M_b\,[2\pi(\Lambda_0)^2]\} \tag{33b}$$

wherein the frequency $\nu \equiv \omega/(2\pi)$ is completely determined by the empirically measured rms oscillation amplitude Λ_0. In his theory of Nuclear Energy in an Atomic Lattice (NEAL), Schwinger [2B] computes that the tunneling between two bound D-nuclei in a harmonic oscillator is such that the fusion rate for reaction (3) is given roughly in the case $n = 0$ by

$$1/T \cong C_n \cdot \exp(-(1/2)\sigma^2_n),\ \ C_0 = 1, \tag{34a}$$

$$\sigma_n \equiv L/\Lambda_n = \sigma_0/(2n + 1)^{1/2},\ \ \sigma_0 \equiv L/\Lambda_0 \tag{34b}$$

where it is appropriate to call σ_0 the *Schwinger Ratio,* inasmuch as he has proved in his NEAL theory ("albeit crudely") that this ratio summarizes the results of ALL of the forces at work in the lattice. (The mistaken conjecture that $C_n \cong C_0$ for $n \geq 1$, which is not correct, is hereinafter called *naive extrapolation*; actually C_n is a function of both n and σ_0 *and* the GLOBAL nature of the potential, and for every bound state above zero-point state of the deuteron in a Madelung-Coulomb potential considered as an isolated potential well, there is a corresponding *Transmission Resonance Transparency* if the well is just one cell of an endless *periodic* linear chain of cells; therefore, in a more realistic model [12]-[15], one would take $C_n = +\infty$ for every $n > 1$.)

Moreover, in the case of the numerical value of the ratio at $n = 0$ for a doubly-loaded $Pd{\cdot}D_2$lattice, Schwinger has shown that if Λ_0 were only 25% bigger than it is in the zero-point state, then the fusion rate (34a) would be large enough to account for the Fleischmann-Pons (FP) Effect's measured excess enthalpy.

The present QRT theory purports to be a refinement and an improvement of Schwinger's NEAL theory,

since it provides a *specific mechanism* for raising the energy level above the zero-point level considered by Schwinger (and so, in consideration of a WKB-based theory presented elsewhere, of *ASSURING* fusion). Moreover the result (32b) shows that even if $j = 0$, after the collision $n \geq 40$ and so $(2n + 1)^{½} \geq 9$, so that instead of being increased by a mere factor of 1.25, the oscillation amplitude Λ_0 is increased *AT LEAST* by a factor of nine! And in a more realistic theory, the deuteron actually finds the Coulomb "barrier" transparent when it is in any excited level above the zero point; this suggests that perhaps a better theory is the wave-mechanical theory of the Chubbs [19] in which the deuteron is regarded as a *delocalized* entity which fills the entire crystal and occupies all cells simultaneously.

Elsewhere I suggested (with a naive extrapolation of Schwinger's zero-point energy level fusion rate calculation which I now perceive as a mistake) that (34a) predicts the availability of 19.7 kW of excess enthalpy per cm^3 of $Pd{\cdot}D_2$ in an *aneutronic, radiationless* reaction (3) if even the first energy level $n = 1$ can be attained. Afterwards Bush & Eagleton [11] measured values of the order of 1 kW/cm^3 in an F-P type of cell using *thin-film Pd* coated on a gold cathode.

The obvious basic explanation for this discrepancy between my now-discarded naive theory and experiment is that the zero-point energy-level fusion rate computed by Schwinger in the case $n = 0$ needs to be redone using the higher-order harmonic-oscillator wave functions with *multiple nodes* to provide $C_n \neq 1$ for $n \geq 1$, in the case of an isolated or *local* potential well; and it needs to be done keeping in mind the known theory of Transmission Resonance (Bohm [20]) in the case of a *globally periodic* well.

An additional obvious contributor to this discrepancy between theory and experiment is simply that the approximation of the equilibrium *D*-nuclei in a *D*-lattice contained in a *Pd*-lattice as being in *quadratic* potential wells is only good for *SMALL* departures from equilibrium. When the *D*-nuclei in a Schwinger oscillator move a significant fraction of the distance between themselves, the electron screening (which had made the *quadratic* potential wells and the *harmonic* oscillators and the theory of the *Schwinger Ratio* a viable theory) is less effective in reducing the Coulomb repulsion between the *D*-nuclei, and a more refined theory of quantized *anharmonic* oscillators based on a Madelung-Coulomb potential (Bass [14]) must be used; however, the preceding theory appears to be qualitatively correct.

Moreover, even if a more accurate form of potential were used, the resultant oscillator could still be quantized, and a theory leading to Diophantine equations similar to those above could still be developed; cf. Bass [12]-[13]-[14]-[15].

Finally, even if the zero-point oscillation amplitude Λ_0 were not raised to the magnitude $\Lambda_n = (2n+1)^{½}{\cdot}\Lambda_0 \geq 9{\cdot}\Lambda_0$ indicated by the quadratic approximation to the potential (which is valid only near equilibrium), it would only have to be increased to a level $\Lambda_{0,NEW} \geq 1.25{\cdot}\Lambda_{0,OLD}$ in order to "explain" the FP Effect quantitatively.

However, the preceding parameter-sensitivity (which Schwinger has aptly characterized as "verging on chaos") is not the most striking result of the present QRT theory. What appears to merit that description is the fact that in the preceding theory the *minimum resonant energy* of an entering *D*-nucleus is independent of the nature of the particular spatial resonance (12) which is available, and depends *ONLY* upon h, Λ_0 and the deuteron mass M_b! To see this, note that

$$E_{res} = E_{f,m} = (2m + 1)^2{\cdot}E_{f,0} = 2n_{res}{\cdot}E_{b,0}\,, \tag{35a}$$

$$n_{res} \equiv [(2m + 1)/(2n_\sigma + 1)]^2 = [(2J + 1)\cdot(6K + 7)]^2 . \quad (35b)$$

Thus

$$E_{res} = 2[(2J + 1)\cdot(6K + 7)]^2\cdot E_{b,0} \geq 98\cdot E_{b.0} , \quad (36)$$

where, as mentioned, $E_{b,0}$ depends *only* upon upon h, Λ_0 and M_b. Whether it is a mere happy coincidence, or whether further research on Schwinger oscillators reveals it to be a universally valid relationship, the established values of Λ_0 for *Pd·D* and for $Pd\cdot D_2$ are almost identical; accordingly the *minimum* resonant triggering energy of $98\cdot E_{b,0}$ will be almost the same in each case!

This seemingly *universally valid minimum resonant triggering energy* (36) will now be estimated in detailed presentations of two specific examples of the QRT theory.

FIRST EXAMPLE

In this example we use values of L and Λ_0 from Chubb [16]. Consider a fully loaded *Pd·D* lattice, in which

$$E_{b,0} = 0.052 \text{ eV},\ L = (3.89/2^{½})\otimes 1.03 \text{ Å},\ \Lambda_0 = 0.1002 \text{ Å},\ \sigma = 9\pi. \quad (37a)$$

Thus, a spatial resonance is available with

$$n_\sigma = 4. \quad (37b)$$

The lowest-order examples of the QRT principle are obtained by taking $J = 0$ and $n_j = 4$ and

$$r = 2,\ s = 9,\ j = 0,\ k = 13 + 9K,\ l = 2(K + 1),\ m = 31 + 27K, \quad (37c)$$

$$n = 8(K + 1)\cdot(4K + 5),\ (K = 0, 1, 2, 3, ...). \quad (37d)$$

The absolutely lowest order example is then at $K = 0$:

$$r = 2,\ s = 9,\ j = 0,\ k = 13,\ l = 2,\ m = 31,\ n = 40, \quad (37e)$$

$$E_{res} = 98\cdot E_{b,0} = 3969\cdot E_{f.0} = 5.1 \text{ eV}. \quad (37f)$$

(To make this example more realistic, one must note that according to the more accurate quantum-mechanical theory (Bass [12]-[15]) the zero-point bound deuterons are at the bottom of Madelung-Coulomb energy wells at about 6.257 eV, and so this should be added to the above over-simplified point-lattice theory of $E_{b,0}$ = 0.052 to give an adjusted zero-point of 6.309 eV, and likewise the energy level E_{res} = 5.1 eV should be replaced by 11.4 eV.)

SECOND EXAMPLE

Here we follow Schwinger [2B] in his theory of Tritium production from a $D + D$ reaction in an (extremely overloaded) doubly-deuterated $Pd\cdot D_2$ lattice, in which, according to Sun and Tomanek [17],

$$E_{b,0} = 0.052 \text{ eV},\ L = 0.94 \text{ Å},\ \Lambda_0 = 0.0997 \text{ Å},\ \sigma = 3\pi. \tag{38a}$$

Thus, a spatial resonance is available with

$$n_\sigma = 1. \tag{38b}$$

As in the preceding example, we have, for $J = 0$ and $n_j = 1$, the results

$$r = 2,\ s = 3,\ j = 0,\ k = 4 + 3K,\ l = 2(K + 1),\ m = 10 + 9K. \tag{38c}$$

Accordingly, the lowest-order example of the QRT principle, for $K = 0$, is now

$$r = 2,\ s = 3,\ j = 0,\ k = 4,\ l = 2,\ m = 10,\ n = 40, \tag{38d}$$

$$E_{res} = 98 \cdot E_{b,0} = 441 \cdot E_{f,0} = 5.1 \text{ eV}. \tag{38e}$$

(As in the previous example, for greater realism this should be adjusted upward by a few eV to account for the fact that the present oversimplified theory treats the bound deuterons as points in a rigid lattice rather than as particles at the bottom of periodic energy wells; however, this case has not yet been computed by the more accurate WKB approximation.)

CONCLUSION

The preceding reasoning seems at least as plausible as that by which Bohr arrived at his model of the hydrogen atom. Accordingly, unless someone who is skeptical of the reality of cold fusion can point out a *specific flaw* in the preceding arguments, it would seem to be mandatory to proceed to an experimental test of the *principal result* derived above, namely that for each deuteron of energy 11.4 eV entering a fully-loaded *Pd·D* lattice perpendicular to a plane of the *D* lattice there will be produced exactly one α-particle which was not previously present.

REFERENCES

[1] G.H. Miley, H. Towner, & N. Ivich, *Fusion Cross-Sections & Reactivities*, Report C00-2218-17, Fusion Studies Labs., Univ. of Illinois, Urbana, 1974.

[2A] Julian Schwinger, "Nuclear Energy in an Atomic Lattice. I," *Zeitschrift für Naturforschung*, vol 45 (1990), pp 221-225.
[2B] Julian Schwinger, "Nuclear Energy in an Atomic Lattice," *Progr. Theor. Phys.,* vol 85 (1991), no 4, pp 711-712.

[3A] David Park, private communication, 1993.

[3B] David Park, Introduction to the Quantum Theory, McGraw Hill, 3rd Ed, 1992.

[4] R.D. Washburn, private communication, 1993.

[5] Peter Hagelstein, "A Simple Model for Coherent DD Fusion in a Lattice," submitted to *Phys. Rev. Lett.* April 5, 1989 (since withdrawn).

[6] Alfred Landé, New Foundations of Quantum Mechanics, Cambridge U. Press, 1965.

[7] Robert T. Bush, "Cold `Fusion': The Transmission Resonance Model Fits Data on Excess Heat, Predicts Optimal Trigger Points, and Suggests Nuclear Reaction Scenarios," *Fusion Technology,* vol 19 (1991), pp 313-356.

[8] Leaf Turner, "Peregrinations on Cold Fusion," *J. Fusion Energy,* vol 9 (1990), pp 447-450; cf. "Thoughts Unbottled by Cold Fusion," Letters to the Editor, *Physics Today,* Sept. 1989, pp 141-142.

[9] Robert T. Bush, "A Theory of Particle Interference Based Upon the Uncertainty Principle," *Lettere Al Nuovo Cimento*, vol 34 (1982), pp 363-369; Part II, "Additional Consequences," *ibid,* vol 36 (1983), pp 241-244.

[10] Robert T. Bush, "The deBroglie Wave Derivation for Material Particle Diffraction Reexamined: A Rederivation Without Matter Waves," *Lettere Al Nuovo Cimento*, vol 44 (1985), p 683.

[11] Robert T. Bush & Robert D. Eagleton, "Calorimetric Evidence in Support of the Transmission Resonance Model," *Fusion Technology*, vol 20 (1991), p 239.

[12] Robert W. Bass, "A Closed Form Expression for a Generic Madelung Series," to be submitted for publication.

[13] Robert W. Bass, "Proof that Madelung Forces Predict the Schwinger Ratio Correctly," to be submitted for publication.

[14] Robert W. Bass, "Proof that Zero-Point Fluctuations of Bound Deuterons in a Supersaturated Palladium Lattice Provide Sufficient Line-Broadening to Permit Low-Energy Resonant Penetration of the Coulomb Barrier," to be submitted for publication.

[15] Robert W. Bass, "Bi-Resonant Transparency of Quadruple Coulomb Barriers in Periodic Triple Potential Wells," to be submitted for publication.

[16] Scott R. Chubb, private communication, 1991.

[17] Z. Sun & D. Tomanek, "Cold Fusion: How Close Can Deuterium Atoms Come Inside Palladium," *Phys. Rev. Lett.*, vol 63 (1989), pp 59-61.

[18] S.E. Jones, private communication, 1991.

[19] Scott R. Chubb & Talbot A. Chubb, "Lattice Induced Nuclear Chemistry," *Proc. Conf. on Anomalous Nuclear Effects in Deuterium/Solid Systems*, BYU, October, 1990, published by American Institute of Physics, 1991.

[19bis] Scott R. Chubb & Talbot A. Chubb, "Ion Band State Fusion: Reactions, Power Density, and the

Quantum Reality Question," *Fusion Technology* (to appear).

[20] David Bohm, Quantum Theory, Dover Publications, 1989.

IS THE COULOMB FUSION-'BARRIER' A RESONANTLY-TRANSPARENT MIRROR? REFUTATION OF THE CONVENTIONAL COLD-FUSION 'QM-IMPOSSIBILITY' "PROOF"

by Robert W. Bass, *Ph.D.*
Registered Patent Agent
Scientific Advisory Board, ENECO, Inc., Salt Lake City, Utah 84108
Technical Advisory Board, F.I.C., Inc., Salt Lake City, Utah 84108

"... information can be made memorable only when it is slightly coloured by prejudice,"
Sir Kenneth Clark, in *All There is to Know,* (ed. A. Coleman), Simon & Schuster, 1994.

The University of Utah announced the millennial advent of a potentially unlimited, cheap, clean, non-polluting new energy source on March 23, 1989. The alleged discovery of a room-temperature electro-chemically induced form of nuclear fusion power by Dr. Martin Fleischmann, *FRS*, and Dr. Stanley Pons stunned the high-energy physics Establishment and the controlled thermonuclear fusion Establishment. Many other scientists and engineers throughout the world were electrified at the startling news. Frantic efforts to duplicate the **FP** Effect were initiated at numerous laboratories, in some cases by reluctant scientists more interested in previous ongoing activities than in their interruption to satisfy demands for confirmation or refutation. After some well-publicized 'failures-to-confirm' at highly reputable, well-equipped laboratories, a discussion panel of the American Physical Society voted 9-to-l that the subject of cold fusion (CF) was 'dead'. Subsequent commentary by Establishment physicists was almost universally dismissive, based on the proposition that "cold fusion *contradicts* the Laws of Physics!" with the obviously mandatory qualification "as those Laws are presently understood" often negligently omitted.

The initial dismissive skepticism, among sincere if possibly hasty or underinformed critics, was based upon two principal objections:

Objection 1. Deuterium fusion (as elucidated for the past half-century in the *H-bomb* and in the international quest for *controlled* civilian thermonuclear power) **either** produces *neutrons* **or** *tritium* in copious amounts with roughly equal probability, or (in extremely rare cases) energetic gamma-ray photons, but neither of these three *SUPPOSEDLY 'DIAGNOSTIC'* SIGNATURES was present in the FP Effect in amounts even remotely proportional to the excess heat allegedly generated.

Objection 2. Deuterons in a palladium lattice are not significantly closer together than in a molecule of deuterium gas, where the amazing but well-established phenomenon of quantum-mechanical '**tunneling**' can bring two positively-charged 'heavy' hydrogen nuclei to overcome their electrostatic repulsion and move near enough for the **strong nuclear force** to bring about their fusion into an excited helium-4 nucleus; but in deuterium gas such an event is never observed.

The second objection is much more fundamental, and the exposure of the fatal fallacy in this *sole* objection is the central purpose of this article, which slights many other important questions in favor of focusing upon a single issue: was the initial *theoretical* skepticism truly justified? (Newcomers to this field will find a well-illustrated tutorial introduction in Fig. 3-1, Fig. 3-2, Fig. 3-3, and Fig. 3-4 on pp. 46-48 of F. David Peat's *Cold Fusion,* Contemporary Books, Chicago, 1990; this should be followed by pp. 19-20, 107, 109, 116-117, 124, 130 & 231 of Eugene F. Mallove's *Fire From Ice,* Wiley, 1991.)

DISCLAIMER (Added 5-7-94): There are a host of issues pertaining to nuclear physics, solid-state physics, material-science practicalities, etc. which are only peripherally mentioned or not addressed here; several readers of a prior draft expected to find an account of a complete theory, which is not my objective. *Added in Proof:* The just-appeared, and hereafter indispensable/invaluable extensive review of CF theories by Chechin, Tsarev, Rabinowitz & Kim [*Int. J. Theor. Phys*., vol. 33 (1994), pp. 617-670, which cites some 173 papers, agrees with the view that the "main difficulty in CF is in surmounting, i.e., tunneling through the Coulomb barrier *V(r)"* (p. 632); while of enormous value, this monumental review fails to cite or discuss what I would choose as the single most seminal paper on the subject [Leaf Turner, "Peregrinations on CF", *J. Fusion Energy,* vol. 9 (1990), pp. 447-450], and errs grievously in finding fatally flawed by "a basic defect" the Turner-Bush Transmission Resonance approach [in my ICCF4 paper I *did include* the nuclear well in a TR model] and in mistakenly concluding that "this approach appears futile" because, echoing Jändel, "the unaddressed and unresolved issue in Bush's theory is that it takes too long for the wave function to become large"; if the present paper does no more than provide a (trivially easy) rebuttal to the unwarranted dismissal of the Turner-Bush approach it will achieve its purpose. My intent was to address the initial skepticism on this point, but the 4-author March, 1994 theory review just cited shows that after 5 years this *initial sticking point* lingers on as a *perennial stumbling block!* (The review, although calling Schwinger's NEAL "the most notable theoretical support for CF," complains that "Schwinger's LV (Lattice Vibration) approach appears applicable only for $\delta V \ll V$", i.e. in the notation used here, only in the quadratic-approximation region of the *bottom* of the potential well *V(r),* near $r = 0$; but in my ICCF4 paper I attempted to extend Schwinger's quantized harmonic oscillator to a *globally* rigorous *anharmonic* quantized oscillator using a *periodic* **Madelung** potential $V(r) \equiv V(-r) \equiv V(r+2L)$ defined firstly on $-L < r < L$, which *predicts* the correct size of the rms vibration amplitude $\Lambda \ll L$ and so the correct value of the *Schwinger Ratio* $[\sigma :\equiv L/\Lambda]$ for the zero-point fluctuations [**ZPF**] near $r = 0$, yet in a global WKB calculation improves his approximate [harmonic-oscillator] **ZPF** tunneling probability $\Theta \simeq exp(-\sigma^2/2)$ by 10^{57} because it is 40% deeper and much *flatter* at the bottom, and therefore *steeper* near the barriers than a naive Coulomb potential well treated as quadratic and extrapolated too far from the classical equilibrium value of $r = 0$.)

Assuming that an excited helium-4 nucleus has been created, there are well-understood physical reasons for the subsequent decay modes of this excited particle, which explain the conventional *branching ratios* observed, as in the first objection, to follow from a three-dimensional collision between two isolated, rotating deuterons in a vacuum; the exposure of the fallacy in jumping to the [false] conclusion that the branching ratios *must be the same* inside of a crystal lattice as in a vacuum was first made soundly by Nobel Laureate, and UCLA Physics Professor Emeritus, Dr. Julian Schwinger as exposited by this peerless theoretician himself in the first issue of *"Cold Fusion"* Magazine (May, 1994). [A brief summary of Schwinger's definitive refutation of Objection 1, including reference to Selection Rules, will be found below in Appendix A.]

Schwinger himself also made a truly giant fundamental step toward refuting Objection 2, in a series of 1989-submitted papers on the subject of Nuclear Energy in an Atomic Lattice (NEAL). However, this basic step needs augmentation by another giant step, first suggested in an eerily prophetic paper presented at the Santa Fe Workshop, May 22-25, 1989 and also in a Letter to the Editor of *Physics Today,* by Los Alamos thermonuclear-fusion plasma researcher Dr. Leaf Turner, and later developed and elaborated into his Transmission Resonance Model (TRM) by Dr. Robert T. Bush of Cal Poly (Pomona); the TRM soon gained incontrovertible but unjustly widely doubted *"fine structure"* experimental evidence in its favor in FP-type experiments by Bush using automated closed-cell calorimetry apparatus constructed by his colleague and (for the past 5 years) cold-fusion collaborator, Dr. Robert D. Eagleton (some of

whose friends distinguish between them in conversation as 'Bob Tritium' and 'Bob Deuterium').

At the request of *Fusion Facts* Editor Hal Fox in a private conversation at ICCF2, Bush advanced the ground-breaking opinion that the 'light water' electrolysis results of Dr. Randall Mills could be better explained by conventional nuclear physics and his TRM than by Mills' novel and revolutionary but controversial *("di-hydrino")* revision of chemistry. This soon led Bush to discover and to establish with experimental evidence (duplicated abroad after dissemination of his preprints) the profound generalization of the FP Effect to Cold Alkali Fusion (CAF) wherein Bush has seemingly incontrovertibly transformed rubidium nuclei into strontium nuclei by means of a proton from ordinary hydrogen (supplied by ordinary or 'light' water) using an FP type of cell but with the palladium cathode replaced by a porous nickel cathode, and the rubidium supplied in the form of rubidium carbonate dissolved in water. (The daughter-product strontium has its isotopic abundance ratio drastically altered from that of natural strontium, precluding contamination-error, but consistent with the isotopic-abundance ratio of the parent rubidium!)

Later, using a patent-pending process of mine entitled Quantum Resonance Triggering (QRT) [explained below], as well as his own TRM, Bush generalized his CAF process to include nearly 350 nuclear-fusion reactions which he predicts can be induced by his far-reaching principle of **Transmission Resonance Induced Nuclear Transmutations** (TRINT). See Fig. 1.

Anyone familiar with Secretary of Energy O'Leary's well-founded dismay at the fact that the Department of Energy (DOE) had to spend more than $12 Billion during the two years preceding her accession to management of the DOE in cleanup of radioactive hazards at various continental atomic installations should call to her attention the fact that (at my urging) Bush labored for many hours to include in his TRINT process the safe reduction to harmlessness of every single known long-lived radioactive element listed in the *Handbook of Chemistry and Physics.*

It was a great personal thrill and one of the supreme satisfactions of my own life that as a licensed practitioner of Intellectual Property Law before the U.S. Patent & Trademark Office (PTO) I had the unique historical privilege of drafting Patent Applications for Bush & Eagleton pertaining to both the CAF process (which Fleischmann has called *'millennial,* if confirmed') and the more general and, admittedly, awesomely portentous TRINT process (originally financed by Proteus Processes & Technology, Inc. a Denver company founded by Mr. Joseph N. Ignat and Mr. Ronald N. Flores, and now under license to ENECO as regards power-generation applications), which I hope will enable us to bequeath to our grandchildren a less radioactively-endangered world.

Unfortunately, Bush's TRM concept was harshly criticized, during and after ICCF2, by Dr. M. Jändel, who published a stinging and seemingly fatal deflation of the TRM in Dr. George Miley's open-minded *Fusion Technology,* a professional journal of the American Nuclear Society (ANS). Briefly, Jändel's apparently devastating criticism is:

Objection 3. Even if the conditions for Resonant Transparency of the Coulomb Barrier could be met, the tunneling of one lattice-bound deuteron through the electrostatic repulsion barrier to the vicinity of an adjacent lattice-bound deuteron is so unlikely that one would have to wait for 'billions of years' for any significant amount of tunneling to occur.

In the forthcoming *Proceedings* of ICCF4, I have presented scientific arguments which I find persuasive (not having yet received any competent criticisms) that Objection 3 also can be overcome, by

use of yet another idea first used in this context by Schwinger, namely the so-called Zero-Point Fluctuations (ZPF) of a lattice at Absolute Zero temperature, which Schwinger wryly calls VCFI (Very Cold Fusion Indeed).

The primary purpose of this article is to provide an accessible overview of what I proffer as decisive refutations of Objections 2 & 3. (Technical details will be found in Appendices B and F below.)

As most readers by now know, *water* contains about one part in 5,000 of *heavy water,* which can be extracted economically by fractional distillation. The *heavy water* can be electrolytically decomposed into Oxygen and Deuterium (Heavy Hydrogen). In an FP cell using an electrolyte consisting of salted heavy water, the deuterium atoms are attracted into the cathode, where each atom becomes ionized (or loses its orbital electron) and becomes a bare deuterium nucleus or *deuteron.* A deuteron consists of one positively charged *proton,* and one electrically neutral *neutron.* (Free neutrons decay in a few minutes into a proton and an electron, and for present purposes can be regarded as the result of collapsing an electron onto a proton.) The proton and neutron are (relatively loosely) bound together by the *strong nuclear force,* which operates only over such short ranges that it is negligible in comparison to electrical and magnetic forces except in the vicinity of a nucleus. So in the present context the essential features of the problem are maintained if one regards deuterons as positively charged particles of Atomic Mass Number Two which can be regarded as 'point particles' that have no properties other than charge and mass when separated by distances typical of atoms, molecules, and basic cells of crystal lattices.

In Fig. 2 the electrostatic potential, also called the *Coulomb potential,* of an isolated *bound* (or lattice-fixed) deuteron is displayed. This potential has the value $V = e/|r|$ at a radial distance r, where $|r|$ denotes the unsigned or *absolute* value of r, and where e is the charge on an electron. In Fig. 2, r is measured in units of the lattice-period length $L = 2.83 \times 10^{-8}$ cm, and V is measured in units of $E_C \equiv e/L$. As is well known, if a second (conceptually *free,* or unbound) deuteron is brought into this picture, it experiences a repulsive force equal to the negative of the slope of the curve (that is, the force is the negative *gradient* of the potential *energy* $e \cdot V$, or $\mathcal{F} = -e^2/|r|^2$). Notice that as the free deuteron gets closer to the bound deuteron, the magnitude of the repulsion increases beyond all limits, i.e. tends to become *infinite.* (In reality, when the free deuteron has reached within a distance of the bound deuteron's *nuclear radius* $r_n = 2.1 \times 10^{-13}$cm, *i.e.* when r satisfies $-r_n \le r \le r_n$, or equivalently when $|r| \le r_n$, then the repulsion is overcome by the strong nuclear force and dwindles to zero and then reverses sign and becomes an attraction -- but this detail is too small for a drawing to scale, because $r_n/L = 7.4 \times 10^{-6} \cong 10^{-5}$.)

Everyone who has heard about *quantum weirdness* knows that on the atomic scale particles behave contrary to what we expect from experience with macroscopic objects, such as charged ping-pong balls. A low-energy deuteron approaching from the right, with an initial velocity whose kinetic energy is measured in *electron volts* (eV) rather than in kilovolts (keV) or megavolts (MeV), must slow down and then reverse course and be reflected back toward its origin with the same final speed as its initial speed, but with the direction of motion reversed. See Fig. 2A and Fig. 2B, which may become clearer in the sequel, upon a second reading. However, even though the *barrier height* is almost infinite, there is a finite chance (computable by quantum mechanics) that instead of being reflected elastically (as might be an ideal ping-pong ball bouncing from an infinitely hard surface), the deuteron will somehow 'tunnel' through the *'energetically-forbidden region'* [of negative kinetic energy and imaginary speed] and be found on the other side of the barrier, moving toward the left with the same ultimate kinetic energy as which it began. To nineteenth-century physicists, this would be an incredible miracle. Neither Einstein nor Schrödinger

ever fully accepted what the co-discoverer of quantum-mechanics in its wave-mechanical version called "this damned quantum jumping!"

A detailed `understanding' of how quantum tunneling can be possible is a highly debatable subject. But patrons of *Radio Shack* who have purchased *tunnel diodes,* or users of any transistor-based solid-state electronic devices (such as modern TVs or computers) are beneficiaries of the fact that *quantum tunneling* is an objectively real phenomenon. Other quantum weirdnesses must be invoked to explain even certain macroscopic phenomena, such as superfluidity and superconductivity. When palladium is saturated with either hydrogen or deuterium, and cryogenically refrigerated, it becomes a superconductor, which cannot be explained by classical physics.

Inside of a palladium lattice, free deuterons typically have energies measured in tenths of an eV, or at most a few eV, as discussed by Dr. Stan Pons at ICCF4. Advanced undergraduates at Princeton who use the recent excellent text on *Quantum Mechanics* by the Einstein Professor of Science, Dr. P.J.E. Peebles, find that after an initial study of the subject of only 52 pages they have learned enough to compute the *tunneling probability* under discussion. It turns out that if the deuteron's energy is less than several hundred eV, the tunneling probability is so *infinitesimally* small that for all practical purposes it is negligible. At the end of his lucid 9-page demonstration of the negligible likelihood of CF's possibility (in the scenario associated with Fig. 2), Dr. Peebles exhibits admirable **intellectual honesty** by musing aloud as to whether or not he could have overlooked some aspect of solid state physics (such as had produced the **unpredicted** discovery of high temperature superconductivity) which could have led to a less pessimistic conclusion. But after rehearsing some qualitative reasons found convincing by unspecified other "people" (presumably including Caltech theorist Dr. Steven Koonin, and University of Illinois authorities Dr. Gordon Baym *et al*., Peebles gives up and moves on.

The purpose of this article is to show readers how important overlooked *tacit assumptions* may be, in the arena of logical arguments, even when advanced by eminently qualified scholars, and to point out *critically important* features of the problem absent from Fig. 2 but very much present in a more realistic model, and which raise the tunneling probability from negligibly small to 100 percent! (The critical expert reader should be patient while the needed improvements are introduced one-at-a-time.)

The first inadequacy of Fig. 2 is that it neglects the other bound deuterons in the lattice. (As a first approximation, the effects of the mobile electrons are ignored.) As a start, and referring to Fig. 3, consider one ("infinitely") rigidly *bound* deuteron on the left at $r = -L$, and another such rigidly bound deuteron on the right at $r = L$. (This perfect rigidity is an oversimplification, but adequate for the present.) Suppose that the free deuteron is initially at a position r on the open interval $-L < r < L$. The electrostatic potential which affects the free deuteron is now the *sum* of the potentials from each rigidly bound deuteron, namely

$$V(r) = \{e/(L + r)\} + \{e/(L - r)\} \equiv 2 \cdot L \cdot e/(L^2 - r^2) \equiv V(-r),$$

where the second, identically equivalent, form requires a bit of high-school algebra to verify. Notice that because $r^2 \equiv |r|^2 \equiv |-r|^2$ it no longer matters whether r is positive or negative, and the potential has *mirror symmetry* when one considers reflection in an imaginary mirror placed along the vertical line erected through the *origin* (at $r = 0$).

Now draw a horizontal line representing the initial kinetic energy $\mathscr{E}$ of a free deuteron in Fig. 2, Fig. 2A and Fig. 2B, when starting 'infinitely' far off to the right and therefore completely uninfluenced

by the potential. When such a particle moves from the right toward the repulsive bound deuteron, it loses kinetic energy but gains potential energy, their sum remaining equal to the initial value $\mathscr{E}$.

Similarly, draw a horizontal line at the same level $\mathscr{E}$ in Fig. 3 and Fig. 3A representing the *total* energy of a free deuteron moving under the influence of the potential of bound positively-charged particles on its left and right. In Fig. 3 and Fig. 3A, if the free but energetically-excited deuteron is started with this total energy at the origin, then according to *classical physics* [neglecting quantum weirdness], this free deuteron gets "trapped in the potential well", and becomes itself bound, but bound at an *'excited energy level',* in the following sense. By a fundamental Law of Physics, to which classical physics knows no exceptions, namely, the *conservation of energy,* the sum of the free deuteron's *kinetic energy* $\underline{K}$ (or energy of motion) and *potential energy* $e \cdot V$ (or energy of position) must remain *constant,* and therefore equal to its initial value $\mathscr{E}$. As discovered by Isaac Newton, and taught in high-school, $\underline{K} = (1/2) \cdot m_D \cdot v$ where v is the *speed* of motion, or rate of change of position r, and M_D is the mass of a deuteron. Thus, in Fig. 2A, Fig. B and Fig. 3A, no matter what the value of position r (and corresponding speed v),

$$\underline{K} + e \cdot V(r) \equiv \mathscr{E}.$$

This simple relationship has profound consequences. In the first place, since $\underline{K} \geq 0$, the position r must be *restricted* to the domain in which $e \cdot V(r) \leq \mathscr{E}$. See Fig. 2A, Fig. B and Fig. 3A to see graphically how this affects allowed values of r.

Next, notice in Fig. 3A that as r increases from $r = 0$, the potential energy $e \cdot V(r)$ increases toward $\mathscr{E}$, and when r reaches a value r_t (called the classical turning point) such that at this point $e \cdot V(r_t) = \mathscr{E}$, then necessarily at this same point $\underline{K} = 0$, i.e. at a turning point, the deuteron's speed $v = 0$. By applying high-school algebra to the last displayed equation for V, set equal to $\mathscr{E}/e$, find $(r_t)^2 = L^2 - (2 \cdot L \cdot e^2/\mathscr{E})$. But again from high school we know that whenever $\mathscr{E} > 2 \cdot (e^2/L)$ this *quadratic equation* has TWO distinct "real" (or non-imaginary) solutions found by taking square roots:

$$r_t = \pm\sqrt{L^2 - (2 \cdot L \cdot e^2/\mathscr{E})} \equiv \pm L \cdot \sqrt{1 - [(2 \cdot e^2/L)/\mathscr{E}]}\,.$$

If for simplicity we define r_t to be the *positive* square root, then $(-r_t)$ is the other solution. This means that the deuteron is "trapped" in the region $-r_t < r < r_t$, as shown in Fig. 3A. As the deuteron moves from right to left, it slows down until the left-hand turning point $(-r_t)$ is reached, at which point its motion has been momentarily brought to a standstill. But then the repulsion from the left-hand bound deuteron, previously overcome by the leftward momentum, encounters zero momentum and so is free to act alone, dominating the weaker repulsion from the more-distant right-hand bound deuteron, and accelerating the free deuteron towards the right. As the deuteron crosses the origin $r = 0$, the repulsion from the deuteron on the right becomes larger than that from the deuteron on the left, and it begins to decelerate. When the deuteron approaches the right-hand turning point r it again slows down completely and then reverses its motion. This cycle is then repeated endlessly.

This back-and-forth motion is similar to the motion of a shallow-angle frictionless *pendulum* under gravity, or that of a lead ball in outer space and attached by an astronaut to *springs* held apart by a rigid frame on its left and right, in which the *restoring force* $-Kr$ is proportional to the displacement r, and the constant of proportionality K is called the *spring constant.* Again according to Isaac Newton, the ball of mass m_D has an *acceleration a* which satisfies his famous equation of motion

$$m_D \cdot a = -Kr.$$

In freshman calculus this differential equation is solved in terms of periodic *trigonometric functions,* such as $\sin(\theta) \equiv \sin(\theta + 2\pi)$, and shown to have the functional form $r = A \cdot \sin(2\pi[t/T])$ as a function of time t. If the position r is plotted against time t, the curve is *sinusoidal,* with a maximum *amplitude* $A = \sqrt{2\mathscr{E}/K}$. This kind of motion is *periodic* in time with a *period* T (measured in seconds), where in freshman physics it is shown that $T = 2\pi \cdot \sqrt{m_D/K}$. Such a motion is called *simple harmonic motion,* and any system which exhibits this behavior is called a *harmonic oscillator*.

For small-amplitude oscillations, i.e. for small initial energies $\mathscr{E}$, the bottom of the potential energy well in Fig. 3 and Fig. 3A can be well-approximated as a *quadratic* function, which defines a parabola:

$$e \cdot V = e \cdot V_{MIN} + (1/2) \cdot K \cdot r^2 + \cdots .$$

In this case, it is easy to show [see Appendix C] that the spring constant is given by $K = 4 \cdot (e^2/L^3)$. For every small value of $\mathscr{E} >$ MINIMUM $\{e \cdot V(r)\} \equiv e \cdot V(0) \equiv 2 \cdot (e^2/L)$, it will be true in classical physics that the free deuteron oscillates in a simple harmonic motion about the origin, as in Fig. 3A.

Physicists have a short-hand picture in which the deuteron is visualized as being trapped on the horizontal line-segment $e \cdot V = \mathscr{E}$ between the points $e \cdot V(-r_t)$ and $e \cdot V(r_t)$, and as sliding back and forth at this *energy level* $\mathscr{E}$ while executing harmonic motion.

In classical physics the energy level $\mathscr{E}$ (so long as it is larger than V_{MIN} as explained already) is completely arbitrary. The top peaks in Fig. 3 would be infinite except that they have been truncated to allow for the strong nuclear force. If the nuclear radius were neglected, then any value of $\mathscr{E}$, no matter how great, would produce a trapped deuteron. More realistically, this occurs only for energy levels between

$$\mathscr{E}_{MIN} = e \cdot V_{MIN} \equiv 2 \cdot (e^2/L), \ \& \ \mathscr{E}_{MAX} = e \cdot V_{MAX} \equiv e \cdot V(L - r_n) \equiv (1/2) \cdot \mathscr{E}_{MIN}/(r_n/L) + \cdots ,$$

where the omitted terms are negligible, so that in comparison $\mathscr{E}_{MAX} \cong 5 \times 10^4 \cdot \mathscr{E}_{MIN}$. Thus in classical physics there is a *continuum* of possible energy levels at which deuterons could be trapped, corresponding to the *continuous infinitude* of values of $\mathscr{E}$ which satisfy $\mathscr{E}_{MIN} \le \mathscr{E} \le \mathscr{E}_{MAX}$.

However, when *quantum weirdness* is taken into account, this picture becomes radically modified, as shown in Fig. 3B. Below any given energy level, there is only a *finite number* of other energy levels which are "permissible", or "allowed by the laws of quantum mechanics as presently understood"! These *discrete* energy levels for excited bound deuterons are determined by a *resonance* condition which will now be explained.

Toward the bottom of the well, where the curve can be closely approximated by the bottom of a parabola, the *only acceptable energy levels* E_n are given by the formula for the energy levels of a *quantized* harmonic oscillator (involving Planck's constant h):

$$E_n = (n + [1/2]) \cdot h/T, \ (\ n = O, 1, 2, 3, \ldots \ ),$$

where T is the harmonic oscillator's *period* defined above, and where n is an arbitrary non-negative *integer*

(or whole number). Another way to express the preceding is to factor out the (1/2) and write:

$$E_n = (2n + 1)\cdot h/(2T), \text{ (n = O, 1, 2, 3, ...).}$$

Note that for every integer n, the integer $(2n + 1)$ is necessarily an *ODD* number; in Fig. 3A, the value of $n = 9$ has been illustrated, so that $2n + 1 = 19$ is an odd number.

This oddness is the key to understanding the physical possibility of CF. In my patent-pending QRT process, which purports to show how the energy level may be raised from the ZPF level $n = 0$ to a value of $n \geq 1$ at which Resonant Transparency becomes sufficiently likely, the user takes the lattice-period *length* L and divides it by the bound particle's root-mean-square *(rms)* amplitude of vibration Λ when the lattice is at Absolute Zero temperature [both of which lengths L and Λ can be determined from x-ray crystallography or well-established theory] and so forms what I call the *Schwinger Ratio* $\sigma = L/\Lambda$ which is a pure number that Schwinger has prophetically identified as summing up ("albeit crudely") all the forces at work in the lattice. Now claim 2 of my pending patent calls for the user to divide the Schwinger Ratio by $\pi = 3.14159...$, and check whether or not the result is an *odd* integer (or near to oddness). If so, the lattice and particle are suitable. If not, my QRT theory claims that there is no way to excite the bound particle (at $n = 0$) to a higher energy level ($n \geq 1$) by collision *inside the lattice* with a similar particle!

In Appendix D (which the reader may not find easy before finishing the paper) I have tested the validity of my Coulomb-Madelung potential by correctly predicting the Schwinger Ratio for $Pd\cdot D_{1.0}$, and then used it to extrapolate to those of some 6 other cases for which I could not find measured data, thus now having results on 7 cases:

$$(Pd\cdot D_{1.0},\ Pd\cdot D_{2.0},\ Pd\cdot H_{1.0},\ Ni\cdot D_{1.0},\ Ni\cdot H_{1.0},\ Ti\cdot D_{2.0},\ Ti\cdot H_{2.0}).$$

Define $\sigma_{QRT} \equiv \sigma/\pi$. Then for the 7 cases my pending QRT patent criterion (filed in June, 1991), when applied *de novo,* predicts:

$$\sigma_{QRT} = (9.00,\ 3.00,\ 7.57,\ 8.74,\ 7.35,\ 3.00,\ 2.52) \cong (9,\ 3,\ 8,\ 9,\ 7,\ 3,\ 2.5),$$

which corresponds *perfectly* to experimental experience in that it predicts that *either* deuterons or protons may work with nickel, and that deuterons (but only marginally protons) may work with titanium, while only deuterons should work with palladium! When I derived the QRT criterion, I used only classical *conservation of energy,* classical *conservation of momentum,* and a single *ad hoc* ("Old QM") quantizing principle *(Duane's Rule,* discussed below), and expressed amazement at the "coincidence" (?) that the criterion succeeded, to almost 4 decimal places, with $Pd\cdot D_{1.0}$ & $Pd\cdot D_{2.0}$; but I failed to test the criterion further. Recently Dr. Mario Rabinowitz of EPRI told me that he doubted that my QRT criterion could possibly be correct, and when I asked why, he said: "replace the deuteron mass m_D by half its value, to give a proton mass, $m_P = m_D/2$, and your theory will still predict CF, in which case you are in **deep trouble**!" So I can now claim that the reader ought to take my work seriously since it has passed 'the Rabinowitz acid test', plus six other *gratuitous* tests, with flying colors! [*cf* App. D]

Returning to Fig. 3 and Fig. 3A, if one uses the methods of the eminent scholars referred to above to compute the probability of tunneling out of the well, for energy levels below a few hundred eV, the answer is once again negligibly small. So what has been gained by going from Fig. 2 to Fig. 3? Not enough, but progress in the right direction is being made.

There are three more modifications in the direction of greater realism that remain to be introduced before the pessimistic tunneling probabilities can be overcome.

The *first* modification is to consider *all* of the bound deuterons in the lattice, not just the two adjacent bound deuterons. It is a time-honored (because successful) approximation to assume that there is an endless array of deuterons to both the left and the right of the original two. These *bound deuterons are* assumed to be *rigidly* fixed (i.e. not to be affected by the free deuteron), and located at the positions

$$r = \pm k \cdot L, \ \ (k = 1, 2, 3, ...).$$

(If the reader balks at infinity, he may imagine k increasing up to $k_{MAX} = 10^{22}$ and then the position at k_{MAX} being conceptually identified with that at $(-k_{MAX})$, i.e. one may conceptually place the bound deuterons on a one-dimensional linear crystal lattice which is gradually bent round in a circle until it joins itself; many successful computations in solid-state physics have been carried out with such an approximation.)

The *second* improvement in the model is to render it, at macroscopic distances away from the lattice, electrically neutral, by placing negative charges $(-e)$ between every pair of positive charges. In reality, the electrons are circulating in their own quantized loci, including "delocalized *band states",* but for present purposes it is adequate to place them *rigidly* in *averaged* positions, and unless the averaged positions fall *half-way* between the bound deuterons, then these idealized rigidly-bound electrons will not be in an equilibrium state. A consideration of the totality of positive and negative bound charges in a lattice was first undertaken fruitfully by Madelung, and so the potential resulting from all of the Coulomb forces, of both signs, everywhere in the lattice, is called a Coulomb-Madelung potential V_M. This potential can be represented in terms of known, almost-divergent but tabulated series called *Digamma Functions* (wherein the divergent harmonic series is asymptotically "summed" by using Euler's famous constant). By using known digamma-identities, Dr. David Park has kindly independently verified my new infinite series expression for V_M (presented to ICCF4) which converges so rapidly that it can be truncated after 44 terms and the remainder rigorously bounded by a simple algebraic formula which shows that the remaining terms, if they had been added up, would not change the numerical value of the answer until past the 17th decimal place.

The *third* significant modification is to notice that my new Coulomb-Madelung potential $V_M(r)$ is now a *periodic* function of distance r from the origin; in fact

$$V_M(r + 2L) \equiv V_M(r) \equiv V_M(-r), \ \ (-\infty < r < +\infty).$$

The first two modifications increase the well-depth by some 40%. This can be seen in Fig. 4, where the bottom of the well is visibly deeper than when only the nearest two deuterons are considered. This is a tangible illustration of a point which Schwinger made very early in the history of FP Effect analyses, namely that the critics were ignoring the attractive forces from the entirety of the lattice. Indeed, if one computes the tunneling probability using only a single isolated (aperiodic) Coulomb-Madelung potential well, as if there were no adjacent wells, then the tunneling probability is improved by a factor of 10^{57}, or, as physicists would say, is enhanced by "57 orders of magnitude!". Nevertheless, the tunneling probability is still so small that not even this gigantic enhancement can affect the pessimistic assessment of Objection 2. (However, the new bottom 40% of the well added by including all of the Madelung forces is what enables *low energy* CF, as will be shown below, which completely justifies the complication of adding the Madelung forces to the Coulomb forces which were the sole forces considered by the

pessimistic scholars quoted above.)

Moreover, the reader is now in a position to understand the enormous *conceptual error* which was committed in the formulation of Objection 2.

This is to note that the wells now form an endless *periodic array* of the form barrier-well-barrier ... Furthermore, in the microphysical domain of *quantum weirdness,* particles have some aspects of waves which cannot be dispensed with. In particular, the *momentum* of a particle can be analyzed as if it were a *plane wave,* travelling from left to right, or *vice versa*.

The reader who has had high-school physics doubtless knows about the distinction between *geometrical optics* (ray-optics) and *physical optics* (concerning *interference* phenomena, such as diffraction and refraction, and variations in light *intensity* which would not be predicted if light consisted strictly of little energy-bullets, or *photons,* which behaved like classical bullets); therefore light unquestionably has some true wave aspects.

However, after Einstein explained the photoelectric effect by making the contrary assumption that light waves of frequency $2\pi/T$ *sometimes* behave like a stream of tiny bullets of individual energies $E = h/T$, where the very small number $h = 10^{15}$ eV-seconds is *Planck's constant,* it was suggested by de Broglie that electrons of momentum p should correspondingly exhibit some wave-like properties, and with a wavelength λ, given by the *de Broglie wavelength* $\lambda = h/p$. This was soon verified by the discovery of electron diffraction in crystals, and used by Bohr to predict the lowest energy level and corresponding smallest allowed radius of an electron orbiting a proton to form a hydrogen atom, by assuming that only an integral number n of de Broglie waves can fit around the circumference of such an orbit. This is the "Old" Quantum Theory. In the "Semi-Classical" Quantum Theory obtainable from the "WKB approximate solution of Schrödinger's Equation" [see below], the arbitrary positive integer n gets improved to $(n + [1/2])$, in order to account for the ZPF at $n = 0$; but often the (1/2) is factored out, leaving an <u>odd</u> number $(2n + 1)$, which accounts for the QRT *oddness* test above. If my QRT test be deemed valid, then CF is a practical method of tapping the ZPF energy!!!

The fact that waves and particles sometimes are measured to have properties that are indisputably those of classical particles and waves has led some popularizers of quantum weirdness to say that matter is composed of *'wavicles'* which are *neither* particles nor waves but are more abstract and non-analyzable entities which exhibit wave properties or particle properties depending upon the design of the measurement apparatus being used. The reader who has heard of the paradox of *Schrödinger's cat* knows that the standard version of Quantum Mechanics (QM) is based upon application of Schrödinger's equation, which is a wave equation. The square of the amplitude of Schrödinger's wave-function ψ was recognized as providing the probability-density required to compute the probability of measurement of an 'observable' quantum-mechanical variable in micro-physics.

Alfred Landé, one of the pioneers of QM, has proposed to derive Schrödinger's equation from three postulates, which he advocates as based upon experimental discoveries. One is that in a temporally *periodic* system of *period T,* changes in energy must be quantized as integral multiples of h/T. A second (used by Bohr), is that in rotationally periodic systems, characterized by having angular *periodicity* of *period* 2π, changes in angular momentum must be quantized as integral multiples of $h/(2\pi)$. The third axiom, which Landé felt had been unjustly ignored, is *Duane's Rule,* that in a spatially *periodic* lattice of *period*-length L, changes in linear momentum must be quantized in integral multiples of h/L. The

original version of the TRM is essentially a corollary of Duane's Rule, which Bush interprets as the condition for a free particle to collide inelastically with a lattice in which it is moving linearly (as well as, paradoxically, providing the condition for a particle to find an array of lattice cells resonantly transparent, prior to a collision). This subject becomes very counter-intuitive, since a successful treatment of the Mössbauer Effect requires consideration of "coherent states" and *phonons* [quanta of sound waves], in which there is a finite (non-zero) probability that the recoil momentum of a nucleus emitting a gamma ray will be taken up by every single atom of the lattice simultaneously; the phonons travel at the speed of sound in the crystal, but according to accepted quantum mechanics they appear in an unanalyzed 'quantum jump' everywhere throughout the lattice all at once! (Feynman warns: to claim to "understand" QM is to deceive oneself!)

In his NEAL theory, Schwinger postulates that if two deuterons so close together that they can be regarded as an *excited* alpha particle (or helium-4 nucleus) shed the excess energy of 23.85 MeV required in order to become a stable ^{4}He-nucleus, they do it by exciting the *deuteron lattice* with 2.4 x 10^8 phonons of energy of size 0.104 eV each. With all due respect to Schwinger, I have modified his hypothesis to: 1 x 10^9 phonons (of energy 0.0237 each) go into the host *palladium lattice* instead, for the following reasons. My work satisfies me that if even a small but fixed fraction of the phonons *always* go into the deuterium lattice embedded in a palladium lattice, then eventually there will be a very slow chain-fusion reaction, which will grow toward a meltdown unless quenched by irregularities in the lattice structure which interrupt the connected chain of lattice cells. But if *all* of the phonons always go into the deuterium lattice, there will be a miniature fusion-bomb explosion. Accordingly, it is the *branching ratio* between these two possible reactions which is the criterion between *a fizzle* and a *meltdown.* According to energy-minimization arguments, the phonons *will* go into the *Pd* lattice, because then the mean potential energy of a *Pd* oscillator is only 22.8% of that of a *D* oscillator.

Since including the preceding predictions in my June, 1991 patent application, I was gratified to learn that in the fall of the same year Schwinger presented a UCLA progress report in which he said: "loading does not proceed with perfect spatial uniformity. ...It may happen that a ... region of the lattice attains ...such uniformity that it can function collectively in absorbing the excess nuclear energy released in an act of fusion. And that energy might initiate a chain reaction as the vibrations of the excited ions bring them into closer proximity. This burst of energy will continue until the increasing number of irregularities in the lattice produce a shut-down. The start up of another burst is an independent affair. It is just such intermittency -- or random turnings on and off -- that characterizes those experiments that lead one to claim the reality of CF."

At this point it is desirable to consider a basic result of QM in periodic lattices which is based upon an approximate solution of Schrödinger's equation called the WKB (Wentzel-Kramers-Brillouin) method [though it was published earlier by H. Jeffreys]. In deriving this result, the wave-picture as well as the particle-picture must be used. Since the momentum p of a deuteron of mass m_D and velocity v is given, according to Newton, by $p = m_D v$, which enables one to re-express the kinetic energy $\underline{K}$ as $K = p^2/(2 \cdot m_D)$, the *total energy* $\mathscr{E} \equiv \underline{K} + e \cdot V$ can be re-expressed as:

$$\mathscr{E} \equiv p^2/(2 \cdot m_D) + e \cdot V(r),$$

which provides an alternative version of the sum of kinetic and potential energies. It is another trivial exercise in high-school algebra to solve this quadratic equation for p; then, for a classically trapped particle, the linear momentum has two possible values:

$$p = \pm\sqrt{2m_D \cdot [\mathscr{E} - e \cdot V(r)]}.$$

Using this formula for p as a function of r, we can *average* p over one complete cycle of the oscillation between the turning points ($-r_t$) and r_t. (The averaging requires elementary integral calculus.) The result depends only on the given energy level $\mathscr{E}$.

Now I shall quote two *Theorems* from the WKB or 'semi-classical' approximation to QM, whose proofs can be found in Bohm's classic *Quantum Theory* at pages 281-286:

Theorem 1. A necessary and sufficient condition for $\mathscr{E} = E_n$ to be a permissible energy level of a bound deuteron in an isolated potential well defined by the potential $V(r)$ is that E_n should satisfy the semi-classical quantization condition:

$$4 \cdot <|p|> = (n + [1/2]) \cdot h/L, \ (n = 0, 1, 2, 3, ...),$$

where by definition the *average* linear momentum $<|p|>$ is given by the definite integral

$$<|p|> \equiv \frac{1}{L}\int_0^{r_t} |p(r)|\, dr \equiv \frac{1}{L}\int_0^{r_t} |\sqrt{2m_D \cdot [\mathscr{E} - e \cdot V(r)]}|\, dr.$$

Corollary: if we define the *mean* de Broglie wavelength $<\lambda>$ of the trapped particle as $<\lambda> \equiv h/<|p|>$, and if we define the *well-width* as $L_w \equiv 2L$ (which is an exaggerated over-estimate of the actual well-width $2r_t$), then the above *quantization* condition can be reformulated as a simple *resonance* condition between the well-width and the quarter-value of the trapped particle's de Broglie wavelength:

$$L_W \equiv 2L \equiv (2n + 1) \cdot (<\lambda>/4),$$

namely the *ratio* of these two lengths should be an *odd integer!* See Fig. 3A.

The reader familiar with elementary integration can check the validity of the preceding theorem in the case of the energy levels of the quantized harmonic oscillator quoted above. [Hint: Redefine $\mathscr{E}$ as $(\mathscr{E} + e \cdot V_{MIN})$ and replace $e \cdot V(r)$ in the conservation of energy as last displayed above by $e \cdot V_{MIN} + (1/2) \cdot K \cdot r^2$ before solving for the turning point; or see Appendix E.] In the case of a quantized *quartic* anharmonic oscillator, the WKB approximation makes an *error* in energy level E_n of 18% in the case $n = 0$ in comparison to the exact QM solution, and then makes errors of less than 1.5% for all other values of n; the higher the value of n, the more accurate is the approximation (see David Park, Introduction to the Quantum Theory, 3rd Ed., McGraw-Hill, 1992, pp. 114-115). For present purposes, we may regard the WKB method as sufficiently accurate for all *positive* integers n.

In order to explain the next result, we must consider the wave picture instead of the particle picture. The physical situation is exactly the same as that in the preceding theorem, with one important exception. The potential well is *NOT* isolated, as in Fig. 3, but is part of a *periodic chain* of barrier-well-barrier cells, as in Fig. 4. Now far from a resonance of the type just defined, an incident wave-function ψ_{inc} gets diminished in amplitude as it passes from left to right through the barrier-well-barrier configuration shown in Fig. 5. But at a resonance, the wave function inside the well is large, and the transmitted wave has the same intensity as the incident wave, as shown in Fig. 6. To quote from Bohm: "...a very intense wave is

trapped in the well, reflecting back and forth between the barriers in such a phase as to continually reinforce itself, and leaking out very slowly ....To a first approximation, the wave inside the barrier resembles a bound-state wave function, because it is large in such a restricted region ....In fact, the metastable states of the well with barriers resemble bound states much more closely than do those of the well without barriers, mainly because their lifetimes are much longer as a result of the very small transmissivities of the barriers."

Theorem 2. (Turner-Bush-Bass). A necessary and sufficient condition for $\mathscr{E} = E_n$ to be the energy level of a free deuteron encountering *resonant transparency* of a periodic linear array of chained barrier-well-barrier cells defined by a spatially *periodic* potential function $V(r) \equiv V(r + 2L)$ is that E_n should satisfy the Transmission Resonance Condition (TRC):

$$L_W \equiv 2L \equiv (2n + 1) \cdot (<\lambda>/4).$$

Note that from a *local* rather than a correct *global* viewpoint, the condition for resonant transparency appears at first glance to be identical with the condition for a particle to be in an excited bound state, which can be seen by comparing Fig. 3B with Fig. 6.

This is the source of the mistaken pessimism of the eminent scholars quoted above, who have mistakenly computed only the local *barrier penetration probability* Θ, rather than the global *resonant transmissivity* $\mathbb{T}$. (Experts should consult Appendix F below.)

In my presentation to ICCF4, I announced the computation of the numerical values of 600 Resonant Transparency energy levels between $E_0 = 6.26$ eV and $E_{600} = 140.96$ eV, with 88 such levels between E_0 and $E_{88} = 13.74$ eV. This WKB-computed Resonant Transparency Spectrum is between 4.5 and 4.8 times more "dense" than the TRM spectrum earlier computed by Bush using a cruder approximation technique than the WKB method. In attempting to correlate Bush's empirical data showing 6 out of an ascending sequence of 16 theoretically-predicted rounded peaks and cusped valleys in relative excess enthalpy as a function of cell current, which should be a parameter that determines free deuteron energy in the deuteron current being dragged past bound deuterons by being dragged through the beta-phase (or "fully loaded") palladium-deuterium lattice, I came to the preliminary, tentative conclusion that to correlate Bush's quantum numbers n_B with my own, I should use $n_B \equiv 1 + k \cong 1 + (27/31) \cdot k$, for $k = 6, 7, ..., 11$ in the Bush TRM and assume his quantum numbers n_B refer to my own spectrum $n = 31 + 27 \cdot (k - 6)$ for the same values of k:

$$\text{BUSH: } n_B = (7, 8, 9, 10, 11, 12) \Longleftrightarrow \text{BASS: } n = (31, 58, 85, 112, 139, 166).$$

Accordingly, the stunning Bush hill-valley TRM experimental data can be cited as additional evidence in favor of the present more refined WKB calculations.[cf Apps. D,G]

An improvement in computational accuracy would be to replace the WKB work in my ICCF4 paper by work based on exact numerical solutions of Schrödinger's equation, in a mathematical approach advocated at ICCF4 by Drs. Yeong Kim and Jin-Hee Yoon of Purdue in a joint paper with Dr. Alexander Zubarev of Hebrew University, Israel and Dr. Mario Rabinowitz of EPRI; however, I predict that unless they use my Madelung potential $V_M(r)$ [rather than tabulated *Coulomb* Wave Functions], and unless they include *periodicity* of the potential in their approach, they will never find the *low-energy* branch of the

Resonant Transparency energy-level spectrum which I disclosed at ICCF4. Further improvements can be obtained by generalization from a one-dimensional lattice to three dimensions, and by considering the screening effects of conduction electrons from the host palladium lattice, using e.g. the Thomas-Fermi-Mott equation as done by R.H. Parmenter & W.E. Lamb, Jr. *(Proc. Nat. Acad. Sci.,* vol. 87 (1990), pp. 8652-8654).

After receiving an earlier draft, one of the world's most knowledgeable experts on CF wrote me on May 1, 1994: "The observations of Dr. Bush which show a [fine] structure in the current *[vs]* excess-heat relationship, although impressive, have not been confirmed by anyone else. Failure of other careful and detailed studies to see this behavior creates great doubt about the existence of his proposed resonance behavior. Would your approach suffer from the same problem?" With all due respect, I cannot agree that any published studies known to me were conducted in a sufficiently short experimental *duration,* over a sufficiently *large* current *range,* with sufficiently *fine* incremental changes in *current,* with calorimetry systems having a sufficiently *short settling time,* at similar *macrophysical* conditions (temperature, pressure, etc.) for me to conclude that there is "great doubt" about the objective reality of the TRM-forecast fine structure. Firstly, my own experience as a practitioner of Patent Law amply confirms the judicial *dicta* distilled from 200 years of intellectual-property case law that "negative results by competitors are to be given no credence." Secondly, if one re-processes the IMRA JAPAN data of Kunimatsu *et al* (ICCF3) so as to display, instead of a vertical scatter-blur, an <u>average value</u> plus an error bar delimiting the scatter-range, on a *linear* rather than a log plot, there emerges what seems to my eyes to be a *cusped valley* reminiscent of one such local-minimum region of the 6 distinct cusped-valleys of the TRM Fine Structure type. Thirdly, the fact that others can have unintentionally violated *any one* of the *many* criteria required in order to observe (or to definitively *rule out)* the TRM predictions can be explained easily if one is aware of the many subtle pitfalls sketched in Appendix G below. Accordingly I judge the alleged *"problem"* to be illusory, and my theory does not *"suffer"* from it, but has its validity <u>enhanced</u> by citation of Bush's TRM data as <u>confirmatory</u> of the QRT principle!

Thus Theorem 2 and the preceding numerically computed and <u>experimentally confirmed</u> Resonant Transparency Spectrum completely refute Objection 2, as promised.

In a 1992 *Fusion Technology* paper, Dr. M. Jändel has pointed out an apparently fatal flaw in the Resonance Transparency arguments, mentioned above as Objection 3. To understand this objection, in a simplified but not misleading form, the reader needs to recall from the domain of quantum weirdness the famous *Heisenberg Uncertainty Principle,* which states that the product of the rms errors in the mean values of certain specifiably "canonically conjugate" *pairs* of physical variables can never be smaller than $h/(4\pi)$. The most famous such pairs are *position & momentum;* however, of equal importance is the pair consisting of *energy & time.* Letting $\hbar \equiv h/(2\pi)$, the Uncertainty Principle for measurements of energy E and time t asserts that if ΔE is the expected root-mean-square (rms) *error* in E, and if Δt is the expected root-mean-square (rms) *error* in t, then their product

$$\Delta E \cdot \Delta t \geq \hbar/2.$$

If we compute the sensitivity of the transmission resonance condition to variations in the value of the energy E near E_n, at which [Appendix F] the *transmissivity* $\mathbb{T} = 1$, and reduce the requirement on $\mathbb{T}$ to merely requiring $\mathbb{T} > 0.5$, then it will be found that E cannot differ from the exact value of E_n by more than a very tiny number, smaller than 10^{-200} eV. Then by Heisenberg's Principle,

$$\Delta t \geq \hbar/(2\Delta E) = (1/2)\ 10^{-15}\ \text{eV-sec} \times 10^{200}\ (\text{eV})^{-1} = 5 \times 10^{184}\ \text{sec}.$$

Therefore the uncertainty in the time at which the resonant-transparency tunneling has taken place, in comparison to 15 x 10^9 years ≅ 5 x 10^{17} sec, is greater than the currently accepted age of the universe!

This objection seems to be so potent that many of the staunchest followers of the Bush TRM work have given up on it, and sought for an alternative approach to eluding the Coulomb barrier. This includes Bush himself, with his "casimir-lattice" approach at ICCF4, though I trust his seeming recantation under fire was only temporary.

Happily, there is an easy refutation of Objection 3, which depends upon the fact that the positions of the bound deuterons to the left and right of the free deuteron are not actually at exactly $r = -L$ and $r = L$, because there is an irreducible quantum weirdness uncertainty in these positions, of expected rms amplitude $\Delta \ll L$. In his theory of **NEAL/VCFI**, Schwinger has provided tunneling calculations ("albeit crude") which indicate that *all* the forces at work in the lattice can be summed up in the ratio $\sigma = L/\Lambda \cong 28$, which I have called the *Schwinger Ratio* in his honor. Also I have tested the validity of my Coulomb-Madelung potential by using it to *predict* the Schwinger Ratio, and (considering that one is trying to approximate a harmonic oscillator by just two terms from 44 terms defining the potential of an intrinsically anharmonic oscillator) obtained the surprisingly "close" estimate that $\sigma \cong 23$. Now in computing my Resonant Transparency Spectrum, I have used the numerical value of L stated above. But upon careful examination, the averaged momentum in the resonance condition is not a function of E only; the Coulomb-Madelung potential, and so the integral used to average the momentum, is also a function of L, whose sensitivity to variations in L may be found by numerical differentiation with respect to L and multiplication of the result by the uncertainty in L, namely $\delta L \cong \Lambda = L/\sigma = L/28$. This provides an *additional uncertainty* in E not considered by Jändel, and at $n = 88$, this *additional* uncertainty δE augments the preceding infinitesimal value of ΔE by a significant amount: $\delta E_{88} = 0.08$ eV. Accordingly the uncertainty in the tunneling time is reduced to a mere

$$\Delta t \geq \hbar/(2\delta E) = 10^{-15} \text{ eV-sec} \times (100/8)\ (\text{eV})^{-1} = 6.25 \times 10^{-15} \text{ sec.}$$

Thus Objection 3 has also been refuted, as promised.

CONCLUSIONS

The experts who have published 'proofs' that according to established QM the FP Effect is vanishingly *improbable* have committed 3 **identifiable errors** in their calculations:

1. Ignoring *periodicity,* they have treated as mathematically *local* a problem in QM which is intrinsically and inherently *global*.

2. They have overlooked the well-developed global theory of Resonant *Transparency* of multiple Coulomb barriers in a barrier-well-barrier chain.

3. They have overlooked unavoidably-present sources of *resonant-line broadening,* such as the ever-present ZPF.

All three errors are a consequence of ignoring the known foundations of solid state physics, including *Bloch's Theorem.* According to NRL solid-state theorist Dr. Scott Chubb, who together with his uncle Dr. Talbot Chubb has published a completely wave-mechanical approach to the FP Effect which they call Lattice Induced Nuclear Chemistry (**LINC**), in a *periodic* lattice Bloch's Theorem implies that

no solution of Schrödinger's equation is relevant unless its logarithmic derivative is periodic of the same period. The Chubbs' theory is somewhat too sophisticated for me to use, but it contains *inter alia* a completely *three-dimensional* version of Duane's Rule, whose elementary one-dimensional application is the basic tool used above, and it incorporates phonon-mediated transfer of momentum from a nucleus to an entire lattice, as in the amazing but well-established Mössbauer Effect.

In the final analysis, the skeptics of the reality of the FP Effect failed because they treated the problem as if it were one regarding the random 3-D collision of isolated rotating particles in a vacuum, rather than one of symmetry and order in a solid-state *periodic* lattice environment.

Those who know Bob Bush personally have observed that his flamboyant personality and strong sense of humor are proportional to his creativity. When Hal Fox and I first heard Bob Bush speak on CF, in December 1989 at the San Francisco *ASME* session on it, he concluded his prescient remarks about the Resonant Transparency of the alleged 'Coulomb barrier' by noting that "CF is just one more startling evidence of the wave-nature of matter", and in parting quipped that "the critics who say that CF is 'all smoke & mirrors' are right about the mirrors!"

ACKNOWLEDGEMENTS

While all opinions and any remaining errors are solely my own, it is a pleasure to thank Dr. Don A. Baker, Dr. Gordon Baym, Mr. Charles Becker, Dr. Roger E. Billings, Dr. John O'M. Bockris, Dr. Robert T. Bush, Dr. George Chambers, Dr. Scott R. Chubb, Dr. B. Gale Dick, Dr. Robert T. Eagleton, Dr. Martin Fleischmann, Mr. Ronald N. Flores, Dr. Hal Fox, Dr. Peter Hagelstein, Dr. B. Kent Harrison, Dr. Nathan Hoffman, Mr. Joseph N. Ignat, Mr. Frederick G. Jaeger, Dr. Caroil D. Johnson, Dr. Steven E. Jones, Dr. Brian D. Josephson, Dr. Steven E. Koonin, Dr. Yan Kucherov, Dr. Bor Y. Liaw, Dr. Eugene F. Mallove, Dr. Michael C.H. McKubre, Dr. George Miley, Dr. David J. Nagel, Dr. David Park, Dr. Robert H. Parmenter, Ms. Evelyn G. Placido, Dr. B. Stanley Pons, Dr. Mario Rabinowitz, Dr. Julian Schwinger, Mr. Gene Scott, Dr. Edmund Storms, Dr. Leaf Turner, Dr. Gale Thorne, Dr. Victor Vurpillat, and Dr. Philip R. Wallace, for valuable information, correspondence, assistance, and/or suggestions and criticisms.

Appendices A through G will be made available in the second edition of this Source Book. They may also be had by writing to the Fusion Information Center, P.O. Box 58639, Salt Lake City, Utah, 84158-0639.

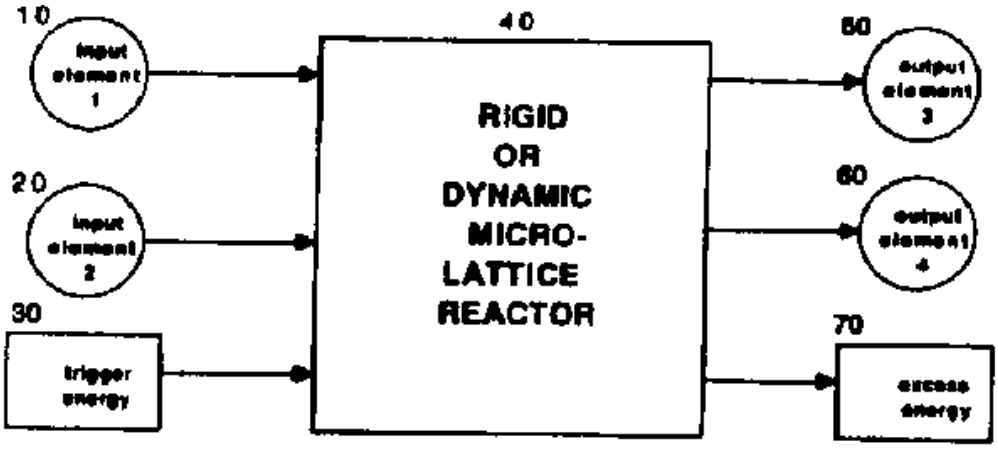

TRINT PROCESS

Transmission Resonance Induced Nuclear Transmutation
(After figure in a Bush-Eagleton Patent Application)

FIG. 1

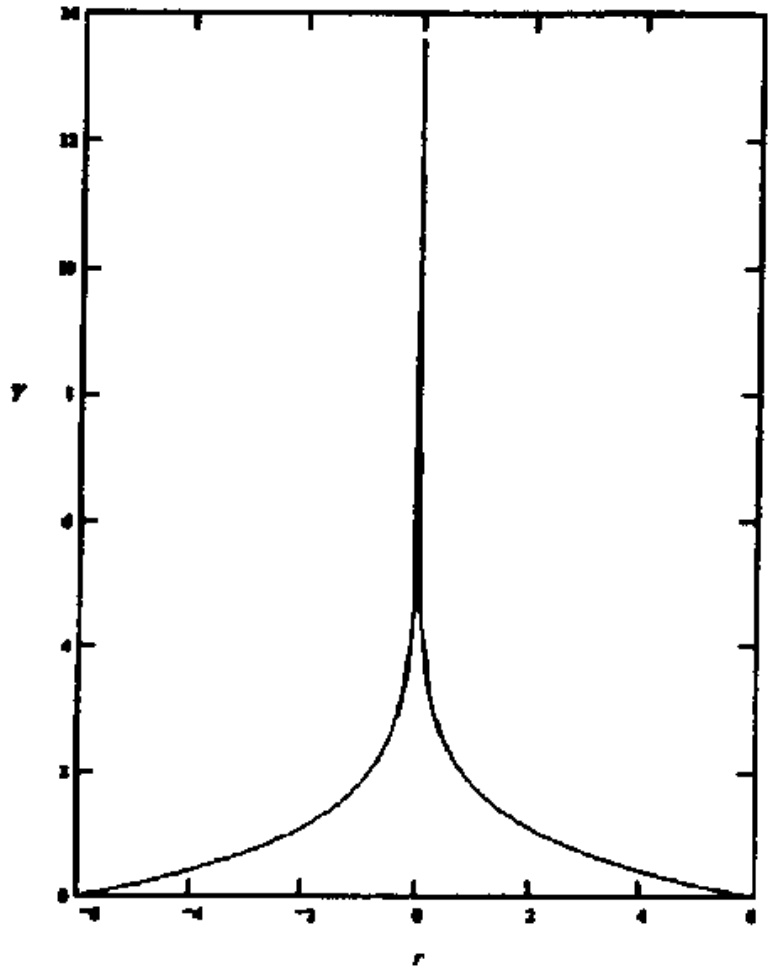

Coulomb Potential of Isolated Charged Particle

FIG. 2

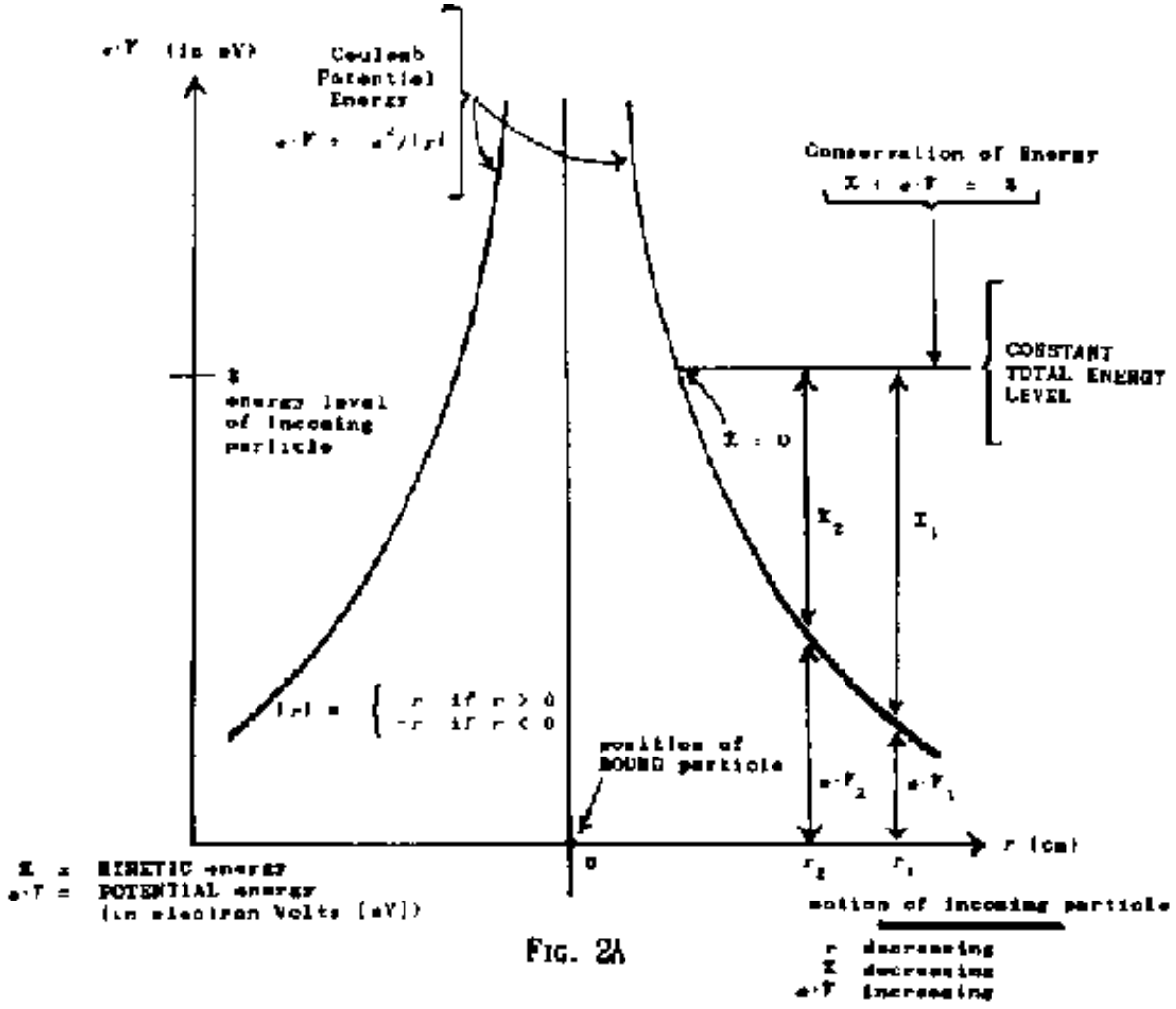
e·V (in eV)
Coulomb Potential Energy
e·V = e²/|r|
Conservation of Energy
T + e·V = E
CONSTANT TOTAL ENERGY LEVEL
E
energy level of incoming particle
T = 0
T₂
T₁
|r| = { r if r > 0 ; -r if r < 0
position of BOUND particle
e·V₂
e·V₁
r (cm)
0
r₂
r₁
T = KINETIC energy
e·V = POTENTIAL energy (in electron Volts [eV])
motion of incoming particle
r decreasing
T decreasing
e·V increasing

FIG. 2A

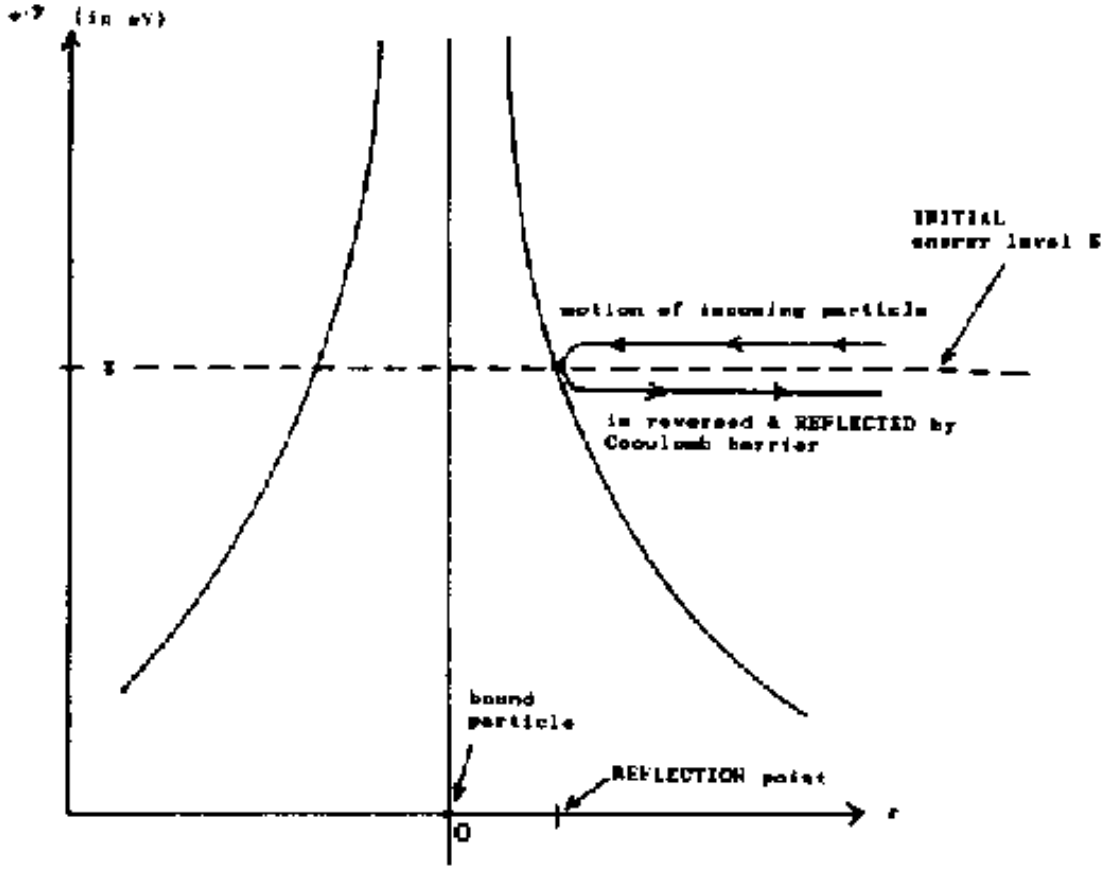
e·V (in eV)
INITIAL energy level E
motion of incoming particle
E
is reversed & REFLECTED by Coulomb barrier
bound particle
REFLECTION point
r
0

FIG. 2B

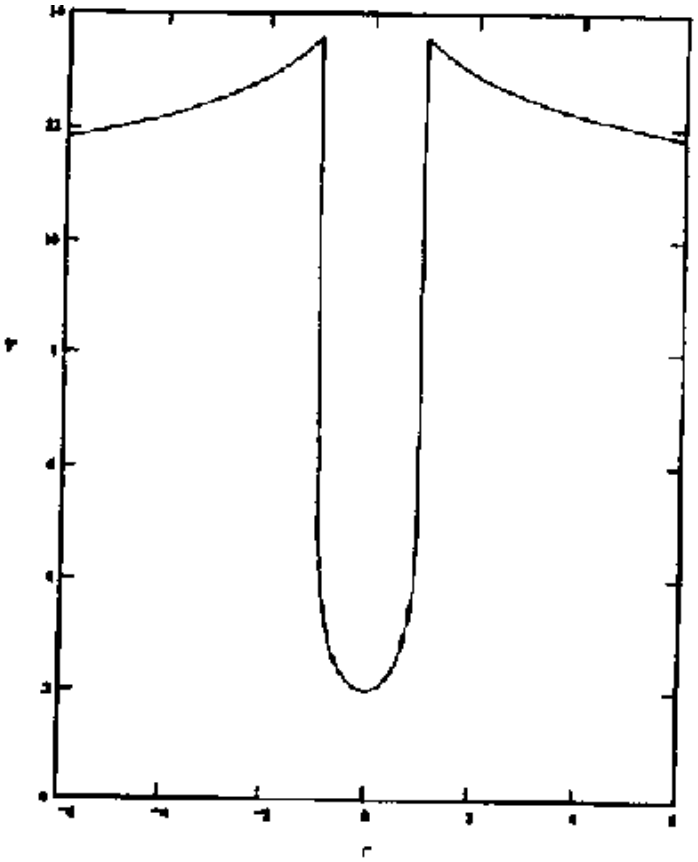

$V = V(r) = 2\cdot(\alpha/L)\cdot(1/(1-(r/L)^2)) = V(-r)$

Coulomb Potential of Two Adjacent But Otherwise Isolated Particles

FIG. 3

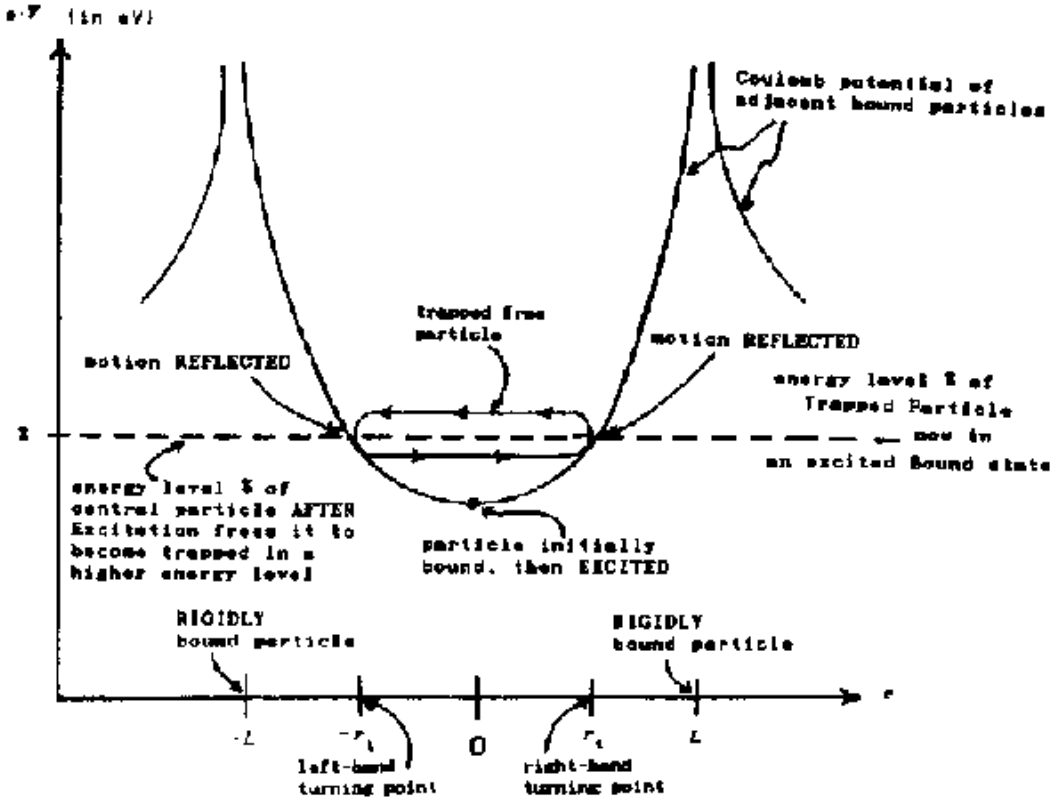

CLASSICAL TRAPPED PARTICLE

Initially in static Equilibrium State, then Excited Bound State

(adjacent particles idealized as bound with "infinite" rigidity)

FIG. 3A

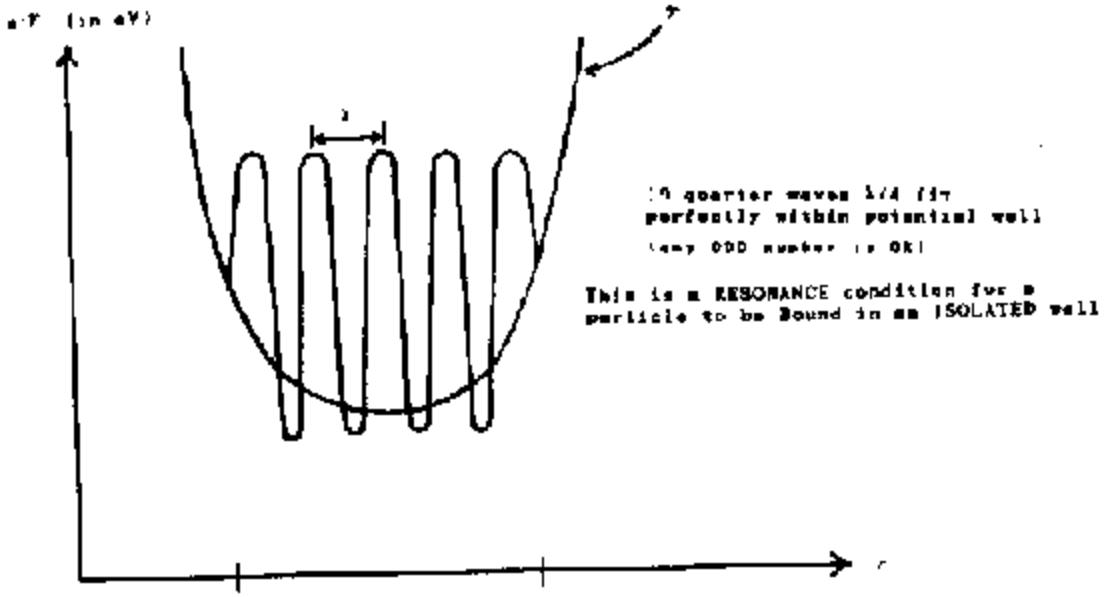

WAVE-MECHANICAL TRAPPED PARTICLE

Free particle is Bound (in an Excited State) when the well-width is an ODD multiple of one-quarter of the particle's de Broglie wavelength

FIG. 3B

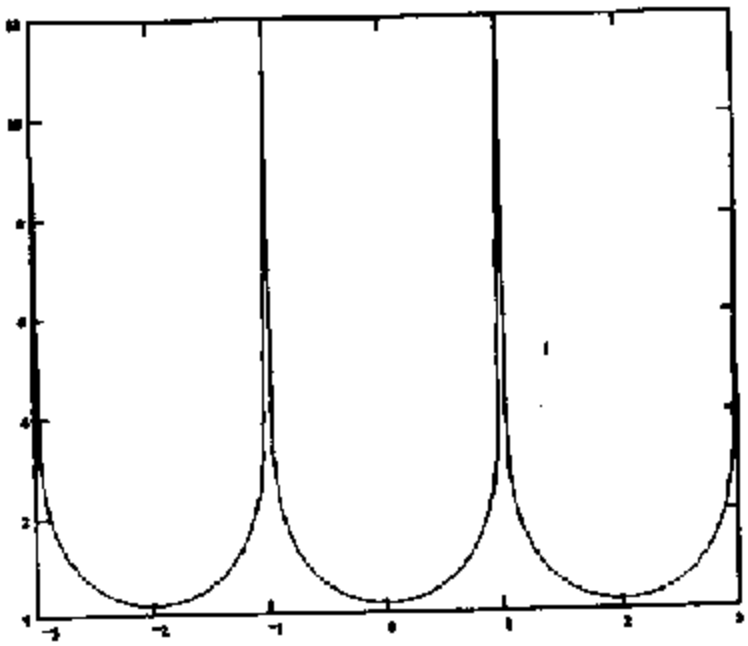

Periodic Coulomb-Madelung Potential of Infinitely Many Positive & Negative Point Charges (of ALTERNATING Signs)

$L_w = 2L = 20 \cdot (\lambda/4)$ (20 is EVEN)

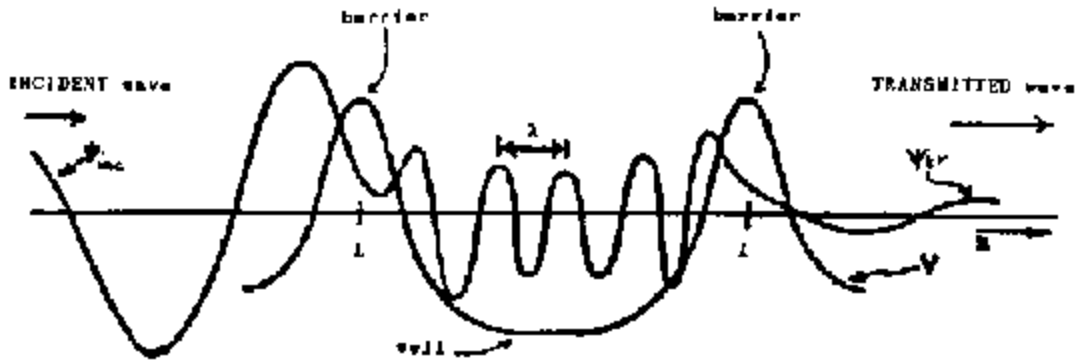

FIG. 5
(after BOHM)

Potential 'BARRIER-WELL-BARRIER' Configuration

WELL-WIDTH L_w = 2L is EVEN multiple of Quarter-Wavelength (λ/4):

NO RESONANCE!

Intensity of Transmitted Wave LESS than Intensity of Incident Wave
(after many transmissions, wave is completely attenuated)

$L_w = 2L = 19 \cdot (\lambda/4)$ (19 is ODD)

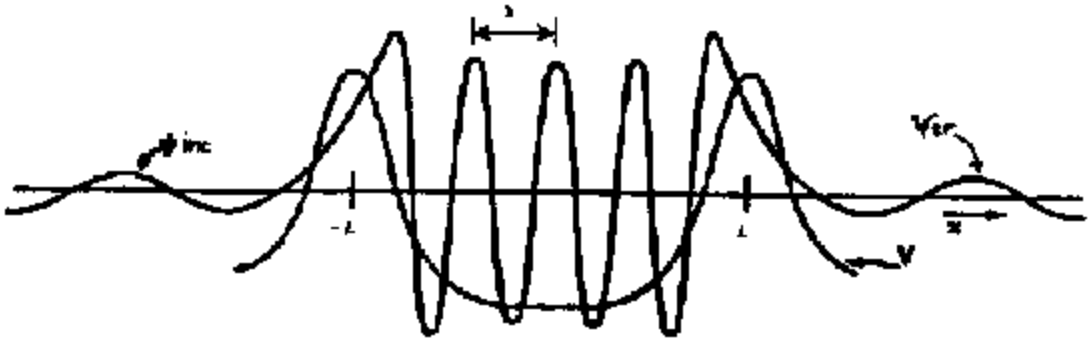

FIG. 6
(after BOHM)

Potential 'BARRIER-WELL-BARRIER' Configuration

WELL WIDTH L_w = 2L is (ODD) multiple of Quarter Wavelength (λ/4):

PERFECT RESONANCE!

Intensity of Transmitted Wave EQUALS Intensity of Incident Wave

Perfect Resonant Transmission = Resonant TRANSPARENCY

(note similarities & differences with FIG 7B)

LITHIUM FISSION TO FUSE DEUTERIUM?

Billings Brown
Salt Lake City, UT 84109

ABSTRACT

The excess enthalpy generated in some Pd/LiOD/D_2O electrochemical cells can be explained by invoking fission of the ^{6}Li followed by T(D,n)α in a chain reaction. Initiation occurs haphazardly by a cosmic ray. Initiation on demand might be accomplished by use of a commercial neutron source. Tritium and neutrons formed are largely utilized in maintaining the chain.

INTRODUCTION

The excess enthalpy generated by some (but not all) Pd/LiOD "cold fusion" experiments has been attributed to classical deuterium fusion:

$$^2H + {}^2H \rightarrow {}^4H^* \begin{matrix} \nearrow {}^3H + n \\ \searrow {}^3H + {}^1H \end{matrix}$$

Often invoked is the assistance of muons, heavy electrons, ion plasma, channeling, crystal fracture, or other exotic physics. This "frontal fusion assault" has not generated any practical solutions.

Science has become splintered and compartmentalized since Plato. In the pursuit of $E = mc^2$ we have chemistry versus physics, hot fusion vs. cold, fission vs. fusion, classical physics vs. exotic. Like the three blind men describing an elephant, each theorist with his or her own narrow training and experience views the problem uniquely. Perhaps a more global, interdisciplinary approach is needed. What follows combines electrochemistry, heterogeneous catalysis, fusion and fission technology and organic chemistry (for the concept of chain reactions).

It is Lithium Fission

Many of the reported experimental results in the Pd/LiOD system can be explained by postulating lithium-6 fission followed by deuterium-tritium fusion. This is a chain reaction set (1,2):

$$^6\text{Li} + \text{n} \rightarrow {}^3\text{H} + {}^4\text{He} + 4.79\ \text{MeV} \quad (1)$$

followed by

$$^3\text{H} + {}^2\text{H} \rightarrow \text{n}\ (14.05\ \text{MeV}) + {}^4\text{He}\ (3.54\ \text{MeV}) \quad (2)$$

Reaction (1) is unique in yielding no gammas [3]. Little tritium from reaction (1) is observed because it is used up in reaction (2). Few neutrons from reaction (2) are observed because they are used up in reaction (1). The deadly radiation hazard predicted by some Pons detractors is much reduced.

The change in the ^{6}Li/^{7}Li ratio would be so slight as to escape measurement. Murphy [4] detected no

change in ^{6}Li or ^{7}Li. Bush [5] however cites Thompson as detecting ^{6}Li depletion.

The thermal cross section for reaction (1) is 945 barns [1] falling to 2.75 barns at 0.258 MeV and to 0.6 barn at 6 MeV. Thermalizing of teh neutrons is no problem in the D_2O solvent. Much enthalpy would be transferred to the solvent in this process.

The reaction cross section for reaction (2) is 5 barns at 0.1 MeV [1], falling to 1 millibar at 0.01 MeV.

Thus reactions (1) and (2) are both probable considering the energy released in each.

Chain Initiation

It is proposed that each of Pons' experiments [14] was initiated by a random cosmic ray (or a bremstrahlung):

$$\gamma\ (2.2\ MeV) + {}^{2}H \rightarrow {}^{1}H + n \qquad (3)$$

Gai [6] measured 1.8 ± 0.4 gamma counts hr^{-1} in his fusion experiments, or one per 10^{3} s.

This suggestion could be readily tested by employing a commercially available neutron source (from the fission industry) to initiate reaction (1). Such sources include ^{252}Cf (2 Mev), Pu-^{9}Be(4 MeV), Po-^{9}Be and ^{241}Am (available from a home smoke alarm?).

Incubation Period

Pons [14] claimed 2 to 3 weeks (10^{6}s) to "charge" or "load" his 4 mm diameter Pd rods with deuterium [7]. Lewis [8] reached "charge" in 0.l22 mm rods in 20 minutes (2 x $l0^{3}$s). These different times are consistent with a diffusion mechanism.

Pons waited 10^{6}s for a reaction to occur. None of his detractors exhibited so much patience. **Their touted negative results are meaningless**.

Neutron Sinks

Neutrons are needed to maintain the chain reaction. But everybody's apparatus contains neutron sinks and leaks. Rolison [11] used SIMS to probe the isotopic composition of Pd. She should have looked also for Ag according to

$$^{108}Pd + n \rightarrow {}^{109}Ag\ (12\ barns\ thermal)$$

DeAngelis [12] has suggested another route to silver

$$^{108}Pd + {}^{2}H \rightarrow {}^{109}Pd + {}^{1}H$$

$$^{109}Pd \rightarrow {}^{109}Ag + {}^{0}e\text{-}$$

Any neutrons leaving the cell would encounter first, the boron in the Pyrex cell wall (750 barns), then second, the bath water where the reverse of reaction (3) occurs

$$^{1}H + n \rightarrow {}^{2}H + \gamma \text{ (2.2 MeV, 0.33 barn)} \quad (4)$$

Perhaps reaction (4) is the source of the disputed gamma spectrum.

If neutrons must be conserved to supply reaction (1), maybe a neutron reflector would be useful.

Brown [13] calculated the neutron mean free path and leakage from Pons' apparatus. Leakage from the 0.0122 cm diameter wires used by Lewis [8] and others would have been 97 percent, and no sustained reaction would have been expected. Leakage from the 0.2 to 0.6 cm diameter Pd rods used by Pons [14], Gai [6] and Weismann [10] would have been 30 to 50 percent. Brown's analysis correlates Pons' data at a cell current density of 8 mA cm^{-2} very well. The data at 64 mA cm^{-2} and 512 mA cm^{-2} fare less well.

Surface or Volume?

If ^{6}Li is a reactant, can Li diffuse into the Pd, or does it need to? Lithium does diffuse into aluminum commercially. The diffusivity of lithium in metals is 10^{-4} that of deuterium.

But not even Pons is certain that the nuclear reaction(s) are internal to the Pd. Nobody has measured the internal (BET/porosity) area of the Pd electrodes.

Pons [14] shows a plot of excess enthalpy per volume (w cm^{-3}) vs current density. But a similar plot of enthalpy electrode area (w cm^{-2}) vs current density correlates his data just as well. Further, the fission/fusion might be occurring in the Bruner-Nernst solvent layer which is also under extreme galvanostatic pressure at the test overpotentials used [8].

REFERENCES

[1] D.B. Hoisington, Nucleonics Fundamentals, McGraw-Hill (1959), p 302.

[2] S. Glasstone, Principles of Nuclear Reactor Engineering, van Nostrand (1955), p 86

[3] R. Stephenson, Introduction to Nuclear Engineering, 2nd ed., McGraw-Hill (1958), pp 218, 230.

[4] J. Murphy, *Chem. & Eng. News*, 16 Apr 1990, p 29.

[5] R .T. Bush, *Fusion Facts*, Mar 1994, p 6.

[6] M. Gai et al., *Nature*, 6 July 1989, p 29.

[7] *Science*, 7 April 1989, p 27.

[8] F.A. Lewis et al., *Surface Technology,* vol 4, 1976, p 89.

[9] N.A. Lewis et al., *Science*, 10 Nov 1989, p 793.

[10] H.W. Wiesmann, *Fusion Technology*, vol 17, Mar 1990, p 350.

[11] D. Rolison, *Chem. & Eng. News*, 16 April 1990, p 30.

[12] A. De Angelis, *Chem. & Eng. News*, 15 May 1989, p 3.

[1]. B.A. Brown, private communication to Pons, 2 June 1989.

[14] S. Pons et al., *J. Electroanalytical Chem.*, (1990) p 293.

ADDENDUM

The Nernst equation [1]

$$E = \frac{RT}{nF} \ln \frac{P_1}{P_2} \quad (1)$$

where E is the open circuit cell voltage, R is the gas constant, T is the absolute temperature, F is Faraday's constant, P_1 and P_2 are related to the thermodynamic ion activity and n relates to the number of electrons transferred. It is the basis for electrochemistry. This equation relates mechanical pressure to electrical pressure or electricity to chemistry.

I cannot find in Pons' publications wherein he has tested his data according to the Nernst equation, although he did discuss its application [2].

The Plot

Pons' data for LiOD with 0.4 cm diameter Pd cathodes are shown platted according to the Nernst equation in the attached Fig. 1. The tacit assumption is made that the excess specific enthalpy generation is proportional to the galvanostatic pressure. Data for other diameter cathodes and/or sulfate anion are more scattered but follow a similar trend. The y-axis of the plot is specific excess power BASED ON Pd ELECTRODE SURFACE AREA computed in w cm^{-2}. The x-axis is the applied voltage to the cell.

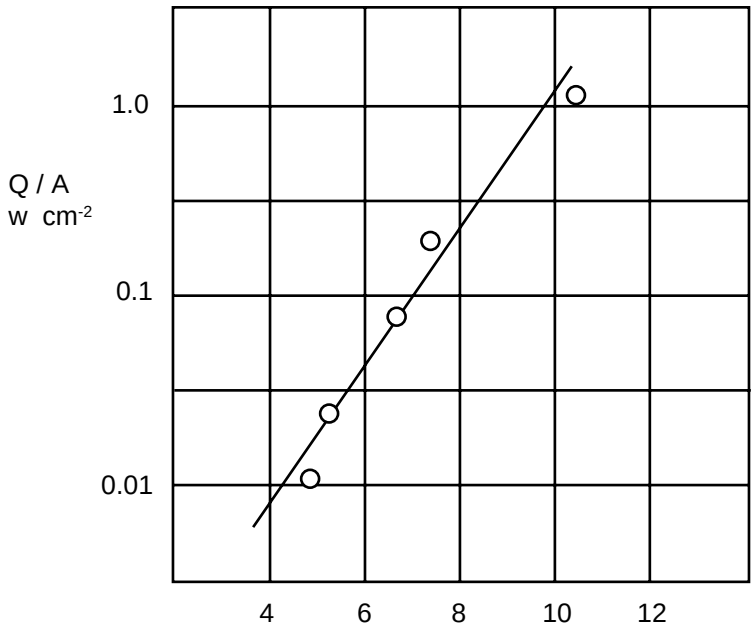

Two conclusions can be drawn from the figure:

· Pons' data are correlated and supported by the classical Nernst equation, and
· Electrode surface area (not volume) is important.

In addition, the assumption of QαP appears valid.

Discussion

If the hypothetical fusion reaction (or its proxies)

$$^{2}D + ^{2}D \rightarrow ^{4}He \quad (2)$$

is to be achieved, the competing chemical reaction

$$D + D \rightarrow D_2 \text{ (gas)} \quad (3)$$

must be minimized.

How might this reduction me accomplished? Reaction (3) is catalyzed by the chemically active (high energy) sites on the Pd surface. It is well known since 1905 [4] that poisoning the Pd surface will reduce or eliminate the catalysis.

Pons has never revealed his "special trick" [5] for achieving nuclear fusion (or fission). Based on his data and hints, his trick must be cathode pre-treatment (Pd poisoning). A gold coating would yield the 0.8 volt overpotential reported by Pons [2]. However, his data [3] reflect an achieved overpotential of 1.2 volts.

An overpotential of 0.8 volt in the Nernst equation is equivalent to a galvanostatic pressure of 10^{14} atmospheres. If Pons can achieve his predicted 2.0 volts, the electrode pressure would be 10^{34} atm.

One significant effect of these pressures is to suppress reaction [3]. But what is the effect of such high confinement pressures on nuclear reactions? Does anybody know?

REFERENCES

[1] C.F. Prutton, S.H. Maron, Fundamental Principles of Physical Chemistry, MacMillan (1944), pp 522, 548.

[2] S. Pons, M. Fleischmann, *J. Electroanal. Chem.*, April 6, 1989.

[3] M. Fleischmann et al., *J. Electroanal. Chem.*, vol 287, 1990, p 293.

[4] Tafel, *Z. Physik Chem.*, vol 50, 1905, p 641.

[5] *Deseret News*, Jan. 8, 1991.

AN INTERPRETATION OF THE PIANTELLI EFFECT BASED UPON THE LANT HYPOTHESIS AND ECFM MODEL FOR COLD FUSION

Robert T. Bush
Physics Department, California State Polytechnic University*
(Pomona)
and
ENECO **
Proteus Processes and Technology, Inc.***

ABSTRACT

The recently announced (January, 1994) Piantelli effect [1] of anomalous heat production in a hydrogen-loaded rod located in a hydrogen-pressurized chamber provides an important challenge for hypotheses and models on "cold fusion." The present author's hypothetical LANT Hypothesi [5] ("Lattice Assisted Nuclear Transmutation"), a generalization of his earlier CAF Model [4] ("Cold Alkali Fusion") and an attempt, like the latter, to unify the heavy water/excess heat effect (Fleischmann/Pons [2]) and the light water excess heat effect (Mill [3]), is applied to the Piantelli Effect [1] hypothesized to be an example of light water "cold fusion." For the Piantelli Effect, LANT predicts which metals should be most effective. A theoretical basis for LANT is hypothesized to be the author's ECFM [6,7,8] ("Electron Catalyzed Fusion Model").

INTRODUCTION

Recently, in a brief note in the January, 1994 issue of Il Nuovo Cimento, entitled "Anomalous Heat production in Ni-H Systems", F. Piantelli of the University of Siena and his collaborators, S. Focardi and R. Habel [1] (Hereafter: F/H/P) announced evidence for the excess heat production of up to 50W in a hydrogen-loaded nickel rod.

Controlled experiments devised to investigate the effect, discovered by Piantelli at the end of 1989, were begun around the end of 1992 at the University of Siena. Briefly, a nickel rod in the form of a solid cylinder of 5 mm diameter, and 90 mm length is heated by a platinum heater coil inside a stainless steel reaction chamber pressurized with hydrogen gas. Hydrogen was initially expected to be relatively neutral, with deuterium gas anticipated to produce the effect. Surprisingly to F/H/P it was found that ordinary hydrogen gas produces the heat anomaly. A stainless steel rod of the same size serves as an excess heat blank. Temperatures as high as about 450 C were employed with typical hydrogen gas pressures around 500 mbar. It will be hypothesized that the Piantelli Effect is closely related to the light water excess heat effect originally achieved by Mills [3] with an electrolytic cell employing a nickel cathode and a light water based potassium carbonate electrolyte. Moreover, it should be pointed out that, apparently unknown to F/H/P, the author and his colleague R. Eagleton at Cal Poly (Pomona) have achieved essentially 100% reproducibility for the light water excess heat effect with gains of 30% or more with closed electrolytic cells (platinum black recombiner utilized) employing nickel mesh cathodes and light water based electrolytes of carbonates and hydroxides of potassium, sodium, rubidium, and cesium [9,10,11,13].

THE LANT HYPOTHESIS

The author's LANT Hypothesis [5] ("Lattice Assisted Nuclear Transmutation") is a generalization of the

author's previous CAF Hypothesis [4] ("Cold Alkali Fusion") seeks to unify the heavy water and light water excess heat effects. According to CAF the excess heat for an electrolytic cell with a nickel cathode and light water based electrolyte of an alkali atom salt of lithium, sodium, potassium, rubidium, or cesium, is essentially the positive Q value for the cold nuclear reaction in which a nucleus for one of the above alkali atoms somehow adds a proton to become a nucleus, respectively, of helium, magnesium, calcium, strontium, or barium. Strong preliminary evidence has been found for the production of both calcium in the case of potassium cells and strontium in the case of rubidium cells [11].

CAF is unifying in that it considers isotopic hydrogen as special cases of alkali atoms. So, it encompasses the D-D reaction to give He-4 and the hypothetical cold nuclear reactions of protons, deuterons, and tritons with other alkali atom nuclei. The LANT Hypothesis generalizes CAF in recognizing that the two reactants could be other than an alkali atom nucleus and a nucleus of isotopic hydrogen, and that there could even be more than two reactants. As in the case of CAF the Laws of Physics may not be broken, and the excess heat is assumed to be essentially the positive Q value given by the difference in the sum of the rest-mass energies of the reactants and that of the products.

A LANT HYPOTHESIS EXPLANATION OF THE PIANTELLI EFFECT

In what follows, three versions are presented, all highly hypothetical. Version A is the simpler of the three attempting to explain effects in terms of cold nuclear reactions that begin with stable nuclides and end with stable nuclides. No attempt is made with regard to the cross-sections of the reactions. Version B is more complex in bringing in hypothetical nuclear cross-sections and treating all nuclides present as potential reactants. Like B, Version C treats all nuclides present as potential reactants. However, like A it is simpler than Version B in leaving out nuclear cross-section considerations. All three versions make predictions of reactivities of materials with ordinary nickel taken as the standard.

Version A

LANT, in the absence of an alkali atom species such as rubidium, implicates the nickel material of the cylindrical rod as a candidate reactant. However, the prime candidate reaction is

$$p + Ni^{62} \rightarrow Cu^{63} \text{ [6.12 MeV]}$$

This is a cold nuclear reaction in which a Ni-62 nucleus adds a proton in a lattice-assisted cold nuclear reaction to become a nucleus of Cu-63. The Q value of 6.12 MeV is assumed to end up essentially as excess heat in the nickel lattice. Note that Ni-64 could not substitute for Ni-62 in the reaction since the Q value is negative. The natural abundance of Ni-62 is 3.66%.

Stainless steel blank comparison: For the iron constituent, the only candidate is Fe-58, with a natural abundance of 0.33%. The reaction adding the proton is then written in analogy to the earlier nickel reaction as $Fe^{58} + p \rightarrow Co^{59}$ [7.37 MeV]. If iron were the only constituent of stainless steel, it should be an excellent heat blank with a ratio of excess power to the nickel cylinder of the same size of about one tenth as seen by the following:

$$(7.37 \text{ MeV}/6.12\text{MeV})(0.33\% / 3.66\%) = O.11$$

However, iron is not the only component of stainless steel. Off-the-shelf stainless steel varies widely in the constituents alloyed with iron. However, the key constituent for excess heat considerations based upon

LANT is manganese. Only Mn-55 is stable (100% abundant) and the relevant reaction is $Mn^{55} + p \rightarrow Fe^{56}$[6.03MeV]. Another constituent is chromium with the relevant reaction $Cr^{54} + p \rightarrow Mn^{55}$ [8.00 MeV]. The stainless steel designated **403 (The double asterisks are part of the designation given in the Handbook of Physics and Chemistry [12], which contains: 86% iron, 13% chromium, and 1% manganese: Multiplying the fractional constituency by the natural abundance fraction and then by the excess energy (i.e., Q value) in MeV and adding these products for iron, chromium, and manganese, yields a "LANT index" for stainless steel **403 of 0.06:

$$(0.86)(0.0033)(7.37) + (0.13)(0.0238)(8.00) + (0.01)(1.00)(6.03)= 0.06.$$

This is to be compared for the LANT index for the nickel cylinder:

$$(1.00)(0.0366)(6.12) = 0.22$$

The ratio is in favor of the nickel. If on the other hand, one uses -202 stainless steel (which is at the high end of manganese content the situation changes drastically: 65% iron, 19% chromium, 6% nickel, and 10% manganese). Now, the LANT index becomes

$$(0.65)(0.0033)(7.37) + (0.19)(0.0238)(8.00) + (0.06)(0.0366)(6.12)+$$

$$0.10)(1.00)(6.03) = 0.66.$$

Which is about 3 times the nickel index. So that now the -202 stainless steel sample would give three times the excess power given by the nickel cylinder. Thus, if Version A of LANT is correct, the excess heat yield for stainless steel cylinders of the same size should depend critically upon the manganese content. And, manganese by itself would do best of all.

LANT index calculations for some other metals with nickel taken as (1.0) are as follows: Mn: (46.3), Rh: (39.5), Cu: (36.1), Sn: (11.8), Pb: (16.6), Ge: (11.3), Pt: (6.6), Zn: (5.5), stainless steel (-202): (3.0), Ti: (1.9), Ni: (1.0), stainless steel (**403): (0.27), and Fe: (0.1).

Possible evidence in favor of LANT, and Version A in particular, involves the high relative LANT index of Cu (36.1), and the low relative index of Fe (0.1). Thus, Bush [9] recently hypothesized that the addition of Cu to the nickel fibrex cathode would improve the excess heat yield for light water cells with nickel cathodes, and Bush and Eagleton [9] have demonstrated this for the cases of potassium, rubidium, and cesium. Corroboration for the case of potassium has come from the Srinivasan et al [15] of BARC (Bombay, India). In addition, Srinivasan et al. [15] have experimental evidence that the addition of Fe to the light water cell with nickel cathode tends to suppress the excess power yield, which would be consistent with the low relative index value (0.1) of iron.

Version B

In this more complex version an attempt is made to allow proton addition in a cold nuclear reaction, i.e. lattice-assisted, to all stable isotopes whether or not the reaction leads directly to another stable isotope or not. An attempt is also made to put in a relative reaction cross-section as a factor in a modified LANT index. Since it is the author's opinion, and based upon his ECFM, that "cold fusion" is genuine cold fusion catalyzed by a collapse of the electron to a ground state orbit very near the nucleus, it was decided to employ the cross-section for the absorption of a thermal neutron as a relative cross-section factor with the

idea that the collapsed proton electron system would very much resemble a neutron on the scale employed. (All of the Q values, abundances, and thermal neutron absorption cross-sections are from Ref. [16].)

Calculation of this modified LANT index with the thermal neutron cross-sections in barns produced the following results: nickel: (32.8), stainless steel **403: (16.9), stainless steel -202: (28.0). Thus, we see that there is still a considerable difference between the two extremes in manganese content of off-the-shelf stainless steel in terms of relative excess heats. However, **403, which should afford the best heat blank of the off-the-shelf stainless steels based upon the manganese content, would give one half the heat of the nickel sample. This seems too large for the heat blank and suggests an advantage of LANT Version A over Version B.

For other representative metals relative to nickel as 1.O, Version B predicts the following modified relative LANT Indices Rh: (38.1), Au: (21.4), Mn: (4.1), Pt: (1.9), Ni: (1.0), Cu: (0.86), stainless steel (-202): (0.85), stainless steel (**403): (0.52), Fe: (0.51), Pb: (0.02), and Sn: (0.008). So, while the two Versions show some similarities, there are enough differences to make a testable distinction. Thus, while Fe (0.51) is still low relative to nickel in Version B, it is much lower in Version A [Fe (O.1)] suggesting a superior excess heat suppressant in the case of A. In addition, Cu (0.86) is lower than nickel on the basis of B, and much higher on A [Cu(36.1)] showing that A supports Cu as a promoting agent for excess power, while B indicates that Cu is slightly suppressive. It is important to bear in mind for purposes of comparison that factors as relative number of interstitial sites and relative affinity of the surface for hydrogen could also be significant.

Version C

Version C is like B except that the thermal neutron cross-sections are left out of the modified relative LANT indices. Ni corresponds in this scheme to an absolute value of 8.49. However, taking Ni as having a relative index of 1.0, one obtains the following values for some representative metals: Mn: (1.20), Rh: (1.02), Ni: (1.00), Pt: (0.93), stainless steel (-202): (0.93), stainless steel (**403): (0.87), Cu: (0.84), Au: (0.84), Fe: (0.74), Sn: (0.44). As was the case for Version B, Version C suffers in comparison with the LANT Version A based upon the consideration of the stainless steel blank, Cu as an excess heat promoter, and Fe as a significant suppressor.

CONCLUSIONS: SUPERIORITY OF LANT VERSION A

It is interesting that all three versions suggest the superiority of manganese (Mn) with respective relative indices of (46.3), (4.1), and (1.20). (Ni taken as 1.00.) Finally, there is some preliminary experimental evidence from the Cal Poly research suggesting the efficacy of tin (Sn) as a promoter of the light water excess heat effect. With the respective LANT index values for Sn of (11.8), (0.008), and (0.44), it is clear that only LANT Version A suggests tin as a promoter. We can conclude, then, that the bulk of the evidence presently available favors Version A of the author's LANT Hypothesis. To summarize the supporting evidence in favor of LANT Version A over B and C: Thus, Version A: {l} Suggests a stainless steel variety that would serve as an effective blank (0.27), whereas neither B (0.52) nor C (0.87) do. {2} Predicts that Cu (36.1), a demonstrated excess heat promoter, is an excess heat promoter, whereas B (0.86) and C (0.84) predict Cu as an excess heat suppressor. {3} Predicts that Fe (0.1), a demonstrated excellent excess heat suppressor, is a suppressor, whereas B (0.51) and C (0.74) predict only slightly suppressant properties for Fe. {4} Predicts that Sn (11.8), for which there is preliminary evidence of being a promoter, is one, whereas B (0.008) and C (0.44) suggest suppressant properties. {5} By leading from a stable reactant to a stable product predicts minimal radiation, which is well-known for "cold fusion," and

measured for the Piantelli Effect [1]. Thus, Version A is preferred.

DOES THE ZERO-POINT ELECTROMAGNETIC FIELD EXPLAIN COLD FUSION?: THE ECFM ("ELECTRON CATALYZED FUSION MODEL") TO EXPLAIN LANT.

The LANT Hypothesis is meaningful only if there is a way of getting through the Coulomb barrier, which is obviously more severe the greater the positive charges of the reactants. In the author's opinion the tunneling rate is significantly enhanced in the condensed matter environment by virtue of a reduced width of the Coulomb barrier achieved in one of two ways: (1) S-electrons spending part of their time inside a proton or deuteron. The delocalization of electrons in the lattice allows them to be much more effective in this role than in the case of a gas. (2) Electron collapse into ground state orbits of small enough radius. The author's ECFM [6,7,8] ("Electron Catalyzed Fusion Model") achieves this by employing the zero-point electromagnetic field. (Note that the "novel chemistry" explanation by Mills [3] to provide nuclear effects cannot explain the Piantelli Effect, since Mills requires potassium carbonate (absent from the F/H/P experiment) in his explanation. However, this problem does not afflict the author's ECFM [6,7,8] in that protons near the nickel surface can provide the "Casimir reflectors" required for the ECFM's more substantial electronic orbital collapse resulting in nuclear effects.)

ACKNOWLEDGEMENTS

H. Fox is thanked for his encouragement. F. Jaeger, President of ENECO (Salt Lake City, UT) and G. Thorne, Vice President of ENECO, are thanked for their information and encouragement. ENECO, Proteus Processes and Technology, Inc., of Denver, CO., J. Ignat, CEO and Ron Flores of Proteus Processes and Technology, Inc., are thanked for their support and encouragement. Thanks to M. Srinivasan (BARC, Trombay, Bombay, India) for alerting me to the F/H/P work. Finally, I am grateful to my colleague, R. Eagleton at Cal Poly (Pomona) for his encouragement and for serving as a sounding board for my ideas.

*3801 West Temple Avenue, Pomona, CA 91768.
**University of Utah Research Park, 391-B Chipeta Way, Salt Lake City, Utah 84108.
*** 1570 Emerson Street, Suite 100, Denver, CO 80218-1450.

REFERENCES

[1] S. Focardi, R. Habel, and F. Piantelli, "Anomalous Heat Production in Ni-H Systems", *Il Nuovo Cimento*, vol 107, p 103, January 1994.

[2] M. Fleischmann and S. Pons, "Electrochemically Induced Nuclear Fusion of Deuterium," *J. Electroanal. Chem.*, 261, 301 (1989).

[3] R. Mills and K. Kneizys, "Excess Heat Production by the Electrolysis of an Aqueous Potassium Carbonate Electrolyte and the Implications for Cold Fusion", *Fusion Technol.*, vol 19 (1991).

[4] R. Bush, "A Light Water Excess Heat Reaction Suggests That 'Cold Fusion' May Be 'Alkali-Hydrogen Fusion', *Fusion Technol.*, 22, 301 (1992).

[5] R. Bush, "Towards a Nuclear Physics of Condensed Matter", accepted for *Fusion Technol.*, under revision.

[6] R. Bush, "An Electron-Catalyzed Fusion Model (ECFM) Suggests a Unification of Heavy- and Light Water Cold Fusion Phenomena", manuscript submitted for publication to *Fusion Technology*.

[7] R. Bush, "A Unifying Model for Cold Fusion," talk delivered at Maui Conference, 4-ICCF, 1993.

[8] R. Bush, "A Unifying Model for Cold Fusion", submitted to the Proceedings of the 4-ICCF.

[9] R. Bush and R. Eagleton, "Calorimetric Studies for Several Light Water Electrolytic Cells With Nickel Fibrex Cathodes and Electrolytes with Alkali Salts of Potassium, Rubidium, and Cesium", submitted to Proc.4-ICCF, (1994).

[10] R. Bush and R. Eagleton, "Experimental Studies Supporting the Transmission Resonance Model for Cold Fusion in Light Water: II. Correlation of X-Ray Emission with Excess Power", Proc. 3-ICCF, 409 (1993).

[11] R. Bush and R. Eagleton, "Strontium Production in Two Electrolytic Cells with Light Water Based Rubidium Carbonate Electrolytes and Nickel Mesh Cathodes," talk delivered at the Maui Conference, 4-ICCF (1993), submitted to the Proceedings.

[12] R. Weast, editor, CRC Handbook of Chemistry and Physics, 61st Edition, CRC Press, Inc., Boca Raton, Florida, 1980-1981.

[13] R. Bush and R. Eagleton, "The Transmission Resonance Model for Cold Fusion in Light Water: I. Correlation of Isotopic and Elemental Evidence with Excess Power", Proc. 3-ICCF, 409 (1993).

[14] R. Bush, "Evidence for an Electrolytically Induced Shift in the Abundance Ratio of Sr88 to Sr86", submitted to the Proceedings of the Minsk Conference, May 1994.

[15] M. Srinivasan, P. Adi Babu, M. Bajpai, D. Gupta, U. Mukherjee, H. Ramamurthy, T. Sankarnarainan, A. Sinha, and H. Shyam, "Excess Heat and Tritium Measurements in Ni-H2O Electrolytic Cells", submitted to Proc. 4-ICCF.

[16] Bureau of Radiological Health, Radiological Health Handbook, January 1970.

THE PHYSICAL-CHEMICAL AND NUCLEAR MULTISTAGE REACTION MECHANISM AND THE MULTISTAGE IGNITION CONDITION ON COLD FUSION

Yi-Fang Chang, Chuan-Zan Yu
Department of Physics, Yunnan University
Kunming, 650091, China

ABSTRACT

Combining the known theories we propose the physical-chemical and nuclear multistage reaction mechanism on cold fusion. Then the multistage ignition condition, which is analogous to the Lawson criterion, and its various forms are obtained, and a concrete threshold value is estimated for the D-Pd system.

Nowadays cold fusion not only has been confirmed by more and more experiments, but also we believe that it is a kind of nuclear reaction. For this purpose we have proposed the multistage nuclear reaction mechanism of cold fusion [1], in which, first D+D→T+p or He^3+n; next p-nuclei reacts; then various nuclei react, etc. Moreover, some results are calculated quantitatively and some predictions are discussed. But the recent theories are unsatisfactory still for cold fusion at very low energy, in which the nuclear reaction probability is too small according to the quantum mechanics, even though the Coulomb screening effect is considered.

So far, the nuclear reaction mechanism of cold fusion is mainly of two types, (1) Deuterons accelerated by an electric field react directly with Pd nuclei or deuterons, etc., on the cathode. The multistage nuclear reaction belongs to this type, and (2) Deuterons accumulate continuously on the cathode, and finally, a plasma is formed. It includes some Coulomb screening theories. But both probabilities at low energy are very small. Therefore, some adhere to the opinion that cold fusion is only a physical or chemical reaction. Of course, they cannot give an explanation for many experimental phenomena of cold fusion.

We combine both mechanisms and extend the multistage nuclear reaction mechanism, then propose the physical-chemical and nuclear multistage reaction mechanism of cold fusion. First, a physical-chemical reaction happens between the cathode material and deuterons, etc., under action of electric current, etc. In this process, on the one hand deuterons accumulate continuously on the cathode, on the other hand the plasma on the cathode is heated. Next, when the time reaches a threshold value, the multistage nuclear reaction may appear.

From the general consideration we propose the ignition condition of cold fusion, which is analogous to the Lawson criterion of thermonuclear fusion [2], and research its various forms.

The total input energy for a system per unit volume

$$E_{in} = E_e + 3n_i kT_i + E_i + E_l \,, \tag{1}$$

where $E_e=IUt/V=\rho Ut/l$ is the input electric energy (ρ is the electric current density, U is the voltage, t is the action time of electric current, l should be the action thickness of the electric current on the cathode),

$3n_ikT_i$ is the initial kinetic energy of plasma formed under action of the electric current, etc., in solution, E_i is other input energy (including heated energy, stirring energy, etc.), E_l is various energy loss (including the radiation loss) of system. The total output energy of the system

$$E_{out} = P_R\tau + P_c\tau' \tag{2}$$

where P_R and τ are power and time of nuclear fusion, P_c and τ' are power and time of physical-chemical reaction on the cathode. Then we obtain a form of the general criterion of cold fusion

$$E_{in} \le E_{out}\,, \tag{3}$$

i.e.
$$\rho UtA^{-1}l^{-1} + 3n_i kT_i + E_i + E_l \le P_R\tau + P_c\tau'. \tag{4}$$

For a concrete installation the produced energy cannot completely transform to a useful gain in energy. Suppose that the transformation efficiency is η, so the ignition condition of cold fusion, which may keep recirculation and derive a beneficial result of energy, i.e., another form of the general criterion is

$$\eta(E_{in} + E_{out}) \ge E_{in}\,, \tag{5}$$

i.e.
$$\eta(P_R\tau + P_c\tau') / (\rho UtA^{-1}l^{-1} + 3n_i kT_i + E_i + E_l) \ge 1-\eta. \tag{6}$$

The above criteria may have various concrete forms for those different reaction mechanisms.

In the different processes there are different forms of criterion for the physical-chemical and nuclear multistage reaction mechanism. In the first stage, suppose that the nuclear reaction may be neglected, the cathode plasma is being heated by the physical-chemical reaction, so eqs. (4) and (6) become the first ignition condition

$$P_c\tau' \ge \rho UtA^{-1}l^{-1} + 3n_i kT_i + E_i + E_l\,, \tag{7}$$

and
$$\eta P_c\tau' / (\rho UtA^{-1}l^{-1} + 3n_i kT_i + E_i + E_l) \ge 1-\eta. \tag{8}$$

In the second stage, the physical-chemical reaction energy is also input for the condition under which the nuclear reaction can be kept, so we obtain the second ignition condition. We assume that the physical-chemical energy heats plasma on the cathode continuously, and finally, the critical temperature T_o of nuclear reaction is reached. In this case, the input energy is $\rho UtA^{-1}l^{-1} + 3n_i kT_i + E_i + E_l$ from (7), while according to the Lawson condition of thermonuclear fusion, the input energy should be $3nkT_o+P_b\tau$. Therefore, suppose that the input electric energy transforms into the physical-chemical energy, which heats the plasma, let the transformation efficiency be η, furthermore, E_i, E_l and $P_b\tau$ are neglected, so

$$3nkT_o = \eta(\rho UtA^{-1}l^{-1} + 3n_i kT_i),$$

i.e.
$$kT_o = \frac{\eta}{3n}(\rho UtA^{-1}l^{-1} + 3n_i kT_i). \tag{9}$$

It is namely an approximate formula of the second ignition condition.

According to the present theory, kT_o should be a limited value, so we may obtain the general conclusion:

the favorable conditions for cold fusion are larger electric current density ρ, higher voltage U, longer time, smaller l and n. It is consistent with our prediction based on the quantum theory [1]. But, because $P_R = RE_R$, and

$$R_{DD} = 2.3 \text{ X } 10^{-14} n_{DD}^{2} (kT)^{2/3} \exp[-18.8/(kT)^{1/3}], \quad (10)$$

which is directly proportional to n^2 for the D+D reaction, the density n cannot be too small.

By using the D-Pd system as an example, a concrete threshold value may be estimated. Since at present the conditions under which cold fusion can happen are [3]: $n_D/n_{Pd} \geq O.9$, $n_D = O.9n_{Pd} = 6.03 \times 10^{22}$ cm^{-3}; the keeping time of electric current t = 300h = $1.08 \times 10^{\delta}$s; ρ 200 mA cm^{-2} and U = 220 V, $kT_o = 1.64(\eta/l)$keV + $\eta(n_i/n)kT_i$. If the second term is neglected, let η = ½ and l = 1mm, so kT_o = 8.2keV. Therefore, the nuclear fusion may be produced under above the conditions from this criterion. We can infer that cold fusion may happen, so long as above threshold values may be reached when the experiments fulfill various conditions. Further, combining new experiments and theories, the criterion condition can be corrected and developed.

REFERENCES

[1] Yi-Fang Chang and Chuan-Zan Yu, *Fusion Facts* (ICCF 4), vol 5, no 7 (1994), p 21.

[2] J.D. Lawson, *Proc. Phys. Soc*., B70 (1957), 6.

[3] Li Xing Zhong, report on Conference on Entropy and Intersecting Science, Kunming, Aug. 1, 1993.

ION BAND STATES: WHAT THEY ARE, AND HOW THEY AFFECT COLD FUSION

Talbot A. Chubb and Scott R. Chubb,
Research Systems, Inc., 5023 N. 38th St.,
Arlington, VA 22207
Feb. 24, 1994

It is not a difficult task to understand why cold fusion takes place. One needs only to think of it more in terms of the way transistors work than vacuum tubes work. We find it easy to visualize the operations of a vacuum tube, in which pointlike electrons are boiled off a hot filament to form a cloud of colliding objects that drift down an electric field onto a plate collector. This flow can be controlled by varying the potential on a negatively charged grid placed between the filament and the plate. But the physics of atoms, molecules, metals, and semiconductors cannot be described realistically with this type of thinking. In a transistor the electrons that are responsible for conductivity more closely resemble stationary waves than moving point particles. The energy of the electrons depends on the direction and amplitude of their wave vectors. The electrons occupy an energy band rather than a single energy state. Moreover, because of the Pauli exclusion principle, the set of electrons can completely fill an allowed band, in which case a semiconductor resembles an insulator. When the band is not quite filled, one has a p-type semiconductor, and when it is overfilled so that a few electrons have been forced to enter an otherwise empty band state, one has an n-type semiconductor. It is this interplay between periodic order, which allows electrons to be wave-like, and periodicity disruption (e.g. trapping sites), which allows electrons to be more particle-like, that controls the flow of current in transistors. Without this interplay and the ability to control electrons in this manner, there would be no modern day computers or solid state electronics.

The physics of Fleischmann and Pons (F and P) type cold fusion[1] differs from the physics of electrons in a solid because it deals with D^+ ions (deuterons), which do not obey the Pauli exclusion principle. These particles, like electrons, can occupy band states, as shown by Casella[2] and a number of other workers[3-5]. The important point is not the fact that band states can be occupied, but that D^+ ions occupying band states resemble stationary waves rather than point particles. Transistor type thinking applies. As in the physics of transistors, it should be possible to control cold fusion by controlling the behavior of the stationary waves that are responsible for the phenomena.

Quantum mechanics provides the means for describing the behavior of particles subject to different environments. The allowed behavior is embedded in the particle system wave function. The type of wave function that describes the behavior of a particle occupying a band state in a periodic solid is called a Bloch function, named after Felix Bloch. Bloch functions have the same spatial distribution in each unit cell of a crystal, with only the wave phase changing with position within the crystal. The active ingredient in F and P type cold fusion is Bloch function D^+, designated D^+_{Bloch}. Deuterium in D^+_{Bloch} form is as different from the interstitial D atoms normally encountered in metal deuterides as ozone O_3 is from molecular oxygen O_2.

An important aspect of cold fusion is that very little D^+_{Bloch} is required to release heat at the power levels observed by F and P, and others[6]. Reaction rate calculations[7] show that only about 10^{-7} D^+_{Bloch} per Pd atom may be required to give 600 W/cc. This reaction rate was calculated using the ordinary rules of quantum mechanics and using a nuclear potential *V* that is zero whenever the reacting D^+_{Bloch} don't occupy the same

volume of space and whenever they don't have antiparallel nuclear spins. When overlap occurs with proper spin cancellation V = -23.8 MeV for the 2 $D^+ \rightarrow {}^4He^{++}$ reaction. Like the D^+, the ${}^4He^{++}$ must be in an overlapping band state. Nuclear physics allows no interaction at a distance, i.e. requires non-zero wave function overlap. Reaction rates are calculated by the Fermi Golden Rule of time-dependent perturbation theory[8]. The requirement for D^+-D+ overlap is the property that forces free particle fusion to occur only at high temperatures. This requirement for overlap also prevents D^+-D^+ fusion in D_2 molecules, and makes futile all attempts to achieve fusion by squeezing D atoms together inside a solid.

So why does D^+_{Bloch} fuse whereas the D_2 molecule is highly stable? The answer to this question goes back to the guiding rules of quantum mechanics as applied to bound state physical systems, i.e. the wave function must minimize energy. Physics says that the correct ground state wave function is the one that minimizes system (kinetic plus potential) energy. If the lowest energy is achieved with wave functions that keep the D^+ separated from each other, there will be no fusion, but if it occurs with the D^+ having overlapping wave functions (finite amplitude when separation distance r_{12}=0), then fusion is allowed. To keep the particles separated, the many-particle wave function has to decrease to zero at each 2-particle zero-separation distance. The deviations in the wave function that are required to do this cause increases in kinetic energy. As a result, in some systems, minimum energy is achieved without full particle avoidance. For example, as shown in Fig. 1, the two electrons of the helium atom have more than 70% overlap[9] (most of the time), hence would undergo fusion if they had the nuclear properties of deuterons. But when the mass of the particle is larger, the kinetic energy increase associated with the same amount of wave function curvature is reduced. Because of the heavier deuteron mass, the D_2 molecule, which has the same order of size as the helium atom, has minimum energy with zero D^+-D^+ overlap.

Fig. 1 Amplitude squared of the helium ground state 2-electron wave function on the surfaces of 2 spheres of constant radius (=s/2). Values have been normalized with respect to the peak values, which occur when the 2 electrons are on opposite sides of the nucleus (θ=180○). Nature uses a cusp (a pointed dimple) when separation r_{12} = 0 to compensate for the infinite electrostatic potential existing at this condition. The amplitude squared at θ=0° measures the degree of electron-electron overlap. The electrons spend most of their time at s<0.5 Bohr radius. If the electrons had the nuclear properties of deuterons, they would fuse.

But what about a metal containing D^+_{Bloch}? Here the answer depends on host crystal size, i.e. the volume V_{xtal} over which the stationary wave description is valid[10]. When the crystal is very microscopic, the system resembles the D_2 molecule. There is no overlap and no fusion. But when the crystal is of the order

of 0.4 micron in size, the overlap is essentially complete and the behavior resembles that of the electrons in the helium atom. This change in overlap in the ground state wave function is a result of the different behavior of the kinetic energy relative to the potential energy when the many-body wave function amplitude goes to a minimum at zero D^+-D^+ separation. The potential energy decrease varies as $1/V_{xtal}^{\ 2}$ whereas the kinetic energy increase varies as $1/V_{xtal}$ for the case where the ion charge is shielded by a neutralizing electron cloud within the volume of one unit cell. For crystals larger than about 0.4 micron, kinetic energy dominates over potential energy and the situation resembles that of the 2 electrons in the helium atom rather than that of the 2 D^+ in the D_2 molecule, i.e. there is D^+-D^+ overlap, hence fusion. The details of electron screening do not affect this general result.

The other big question is: Why is cold fusion radiationless? Here the answer is found in Fermi's Golden Rule of time-dependent perturbation theory[8].

$$w = 2\pi/\hbar^2 \, |\langle k|V|s\rangle|^2 \, \rho_f(E_k^{(O)}) \quad ,$$

where w is the reaction rate (transition probability per unit time), $\langle k|$ and $|s\rangle$ are the final and initial state wave functions of the total system, *V* is the perturbing potential, (in our case the nuclear potential), and $\rho_f(E_k^{(o)})$ is the density of final states of the unperturbed system Hamiltonian when final state energy $E_k^{(0)}$= initial state energy $E_s^{(o)}$. The states $\langle k|$ and $|s\rangle$ include not only the D^+ and $^4He^{++}$ Bloch functions, but also the lattice and its excitation spectrum. The nuclear reaction makes available in each unit cell $23.8/N_{cell}$ MeV energy, which is available for lattice excitation. N_{cell} is the number of unit cells in the crystal, which is typically > 10^9 for a 0.4 micron crystal. The large number of lattice excitation modes available to this energy makes the transition irreversible and prevents the energy from becoming concentrated into a single unit cell, as required for energetic particle emission.

With this background we can identify some of the research requirements for cold fusion. The experimental problem for F and P type cold fusion is: How do you create and contain a D^+ Bloch population within a metal or metal hydride? Fundamental to the ion band state picture is that energy be minimized in an environment in which there is sufficient periodic order. Just as in the case of electrons in transistors, it is the interplay between periodic order and disorder that dictates whether or not a D^+ Bloch population will exist. Previous theory[7] shows that a fully loaded PdD crystallite containing 10^8 unit cells should support cold fusion in which the energy is released in the form of long-wavelength phonons and never becomes concentrated so as to release energetic particles, and in which the product wave-like $^4He^{++}$ is released at the crystallite surface. The work of Storms[11] suggests that occupations of the band state increases with temperature, indicating that thermal excitation played a role in state occupation in his experiment. In the work of McKubre et al.[12] and Hasegawa et al.[13] the bulk D/Pd ratio serves both as a measure of the surface chemical potential achieved in their electrolysis operations and of the chemical uniformity produced in their cathodes. Their D/Pd ratios exceed those of equilibrium chemistry, suggesting that an D^+ ion transmitting polarized layer on their cathode surfaces created a potential barrier against ion escape for the Pd surface. This condition leads to a higher chemical potential within the bulk than would otherwise exist.

A competing approach to cold fusion uses ion implantation. With ion implantation there seems to be a need for full encapsulation of the reactor within a barrier layer that blocks passage of D_{+Bloch}. The D_{+Bloch} can be expected to have vastly different transmission properties than possessed by interstitial hydrogen. A very thick barrier layer, or one that destroys all periodic order, may be required. Ion implantation through this layer would be needed to create and maintain the D_{+Bloch} required for fusion.

REFERENCES

[1] M. Fleischmann and S. Pons, "Electrochemical Induced Nuclear Fusion of Deuterium," *J. Electroanal. Chem*., vol 261, p 301 (1989).

[2] R.G. Casella, "Theory of Excitation Bands of Hydrogen in BCC Metals and of Their Observation by Neutron Scattering", *Phys. Rev. B*, vol 27, p 5943 (1983).

[3] M.J. Puska, R.M. Nieminen, M. Manninen, B. Chakraborty, S. Holloway, and J.K. Norskov, "Quantum Motion of Chemisorbed Hydrogen on Ni Surfaces", *Phys. Rev. Lett*., vol 51, p 1081 (1983).

[4] M.J. Puska and R.M. Nieminen, "Hydrogen Chemisorbed on Nickel Surfaces: a Wave-mechanical Treatment of Proton Motion", *Phys. Rev. B*, vol 29, p 5382 (1985).

[5] C. Astaldi, A. Bianco, S. Modesti, and E. Tosatti, *Phys. Rev. Lett.*, vol 68, p 90 (1992).

[6] B.Y. Liaw, P. Tao, P. Turner, and B.E. Liebert, "Elevated-Temperature Excess Heat Production in a Pd-D System", *J. Electroanal. Chem.*, vol 319, p 161 (1991).

[7] T.A. Chubb and S.R. Chubb, "Cold Fusion as an Interaction between Ion Band States", *Fusion Technology*, vol 20, p 93 (1991).

[8] E. Merzbacher, Quantum Mechanics, p 470, John Wiley & Sons, New York (1964).

[9] F. Seitz, The Modern Theory of Solids, pp 227-234, McGraw-Hill, New York (1940). E.A. Hylleraas, *Zeit. f. Phys*. vol 65, p 347 (1929).

[10] S.R. Chubb and T.A. Chubb, *Fusion Technology*, vol 24, p 403 (1993).

[11] E. Storms, ICCF4 Notebook, vol 1, p C 2.6 (1993).

[12] M.C.H. McKubre et al., ICCF4 Notebook, vol 1, p C 1.5 (1993).

[13] N. Hasegawa, N. Hayakawa, Y. Yamamoto, and K. Kunimatsu, ICCF4 Notebook, vol 1, p C 1.3 (1993).

COLD FUSION - A LOGICAL NETWORK APPROACH

Peter Glück
Institute of Isotopic and Molecular Technology
PO Box 700
3400 Cluj-Napoca, ROMANIA

The great obstacles in the way of general acceptance and rapid development of cold fusion are: the difficult-to-comprehend diversity of systems, phenomena and results; the difficult-to-recognize difference from plasma hot fusion; and the most difficult-to-accept difficulty of both experiment and theory. A strategy, based on the author's surfdyn concept, on a breadth-first approach and on cooperation, is presented. The aim is to stimulate discussions on the subject `strategy' at the Symposium.

INTRODUCTION

During the time elapsed since its discovery, cold fusion has demonstrated three big `D's as follows:

a. DIVERSITY of the systems, phenomena, results - a first source of confusion.
b. DIFFERENCE from the `classical' hot plasma fusion: actually it is an entirely different class of nuclear phenomena,
c. DIFFICULTY both in reproduction of experiments and in finding a theoretical explanation, and further, an almost fatal source of confusion and disappointment.

These D's had a strong divisive effect on the scientific community. However, both the adepts and the adversaries of cold fusion resisted the assimilation of these unexpected facts and ideas. Actually, all these problems are unavoidable pains of birth characteristic for a new science which is much more extensive and novel than it was initially imagined.

Obviously, difficulty is the most difficult to accept and is the greatest drawback for a healthy, dynamic development of the field. To tackle hyperfine, hypercomplex, hypersensitive processes is a strategic task.[l] Therefore, only a synthesis, a prospective view, a breadth-first approach can solve the long range problems, i.e. to find correlation and unity in diversity, reason and vision in difference, explanation and cure for difficulty.

In this paper the author intends to present his offer for a strategy. Full objectivity cannot be warranted given the author's thinking is hypothesis-driven [2], however methodology is more important than any results. This Minsk Congress is (or has to be) an excellent opportunity to discuss seriously cold fusion strategy/alternative strategies and to line out the new paradigm.

It is worth mentioning that J. Dufour [3] has worked out an exemplary strategy for his important system and theory.

UNDERSTANDING DIVERSITY

If we include here the Siena University breakthrough [4] and Reifenschweiler's `ancient' experiment [5], there are at least ten different systems/devices which produced positive results of a kind or another.

For reasons of editorial economy, these won't be listed here, however we want to emphasize the following:

a) both devices with liquid/gas/solid and with gas/solid interfaces have been worked out;
b) all the hydrogen isotopes are active, cold fusion is not a privilege of deuterium.

For reasons of conceptual economy (Occam's razor) we have to admit that one and the same chemical environment opens the `windows of opportunity' for these nuclear reactions. The author, based on his hypothesis regarding the catalytic nature of these phenomena, and using the quasi-entirety of the published data, has arrived at the following conclusion: "The triggering factor in all cases is the contact of a hydrogen isotope with a surface having active sites with high concentration, very high localization, and ultra high mobility of the hydrogen isotopes. To attain this with a high global hydrogen/metal ratio (as e.g. in the Fleischmann-Pons or McKubre et al. cells) is a straightforward solution. However, to attain this without a high global H/Me ratio as in the light water/Ni cells, in the gas discharge, ozonizer-type, protonic conductors-based or sonofusion devices is a creative solution (at least from the point of view of the engineering)."

According to the size, density and activity of these catalytic centers, in a similar manner as for the heterogeneous catalysis, see e.g. [6], a great variety of reactions can be triggered. Understanding, prediction, and control of these processes is only fragmentary and partial yet. However, it is essential to classify them in precursors, primary, secondary, chain reactions. Recent trials to integrate these reactions with a logical taxonomy have been performed by Dufour [3] and Moon [7].

EMPHASIZING DIFFERENCE

The misunderstanding of cold fusion is, for the most part, due to the consequent but apparently useless trials to adapt the new data to the old paradigm of `classical' plasma hot fusion by diverse depth-first approaches. The result: weakness for the adepts, a weapon for the adversaries of cold fusion. Actually, the accumulating data show more and more convincing that the topology, nature, mechanism(s) of the two different categories of nuclear phenomena have little in common. In such circumstances, cold fusion produced excess of heat sometimes, excess of theories all the time (with Moon's words: "the mental barrier was even higher than the Coulomb barrier"). In the case of hot fusion, the latter barrier is violently penetrated, while in the case of cold fusion it is shrewdly (and humanly) bypassed. The mechanisms of these new nuclear reactions are still unknown, however this logical network approach tends to favor neutral-particles-mediated few-body interactions.

EXPLAINING DIFFICULTY

It is difficult to decide what is more damaging for the development of the field: lack of a theory or the difficult-to-reproduce behavior of the experiments. As a US-Russian team of eminent scientists has stated: "The problem of an adequate theoretical model of cold fusion has turned out to be no simpler than the problem of its unambiguous experimental proof" [8]. Is this a symptom of the pathological character of cold fusion? Surprisingly enough, the reverse is true. Our `foraging in neighboring areas'-type actions [1] performed with the aim of gathering inspiring information, have concluded that all the breakthrough fields of solid-state science scarcely have theoretical underpinnings. We refer here to: high-temperature super conductivity, conductive polymers, porous silicon, and heterogeneous catalysis, this last issue being considered by the author as directly bound to cold fusion. (An essay on this theme is generously distributed by ENECO at the Maui conference).

In the author's opinion, difficult reproducibility is inherent to the cold fusion systems in their pre-engineered form and catalysis (with its high sensitivity toward poisons) seems to be the only logical explanation for such a behavior. Catalysis seems to be the unique possibility to realize that positive and negative results are complementary and not contradictory.

In the systems where the three essential conditions (concentration, localization, mobility) are accomplished in a natural way, reproducibility is high. An example: the proton conductor devices, whose prototype was made at Ekaterinburg [9], with their crystalline capillary channels are based on smart nanostructured materials with maximal internal surface of the highest reactivity: these create an unique environment where the functions of the surface are enhanced to an unprecedented level. Therefore such forced-contact devices work well. If we accept the catalytic nature of cold fusion, the problem will become a part of the solution.

EXPLAINING CATALYSIS

The author is well aware that a theory or a hypothesis considering cold fusion as a form of catalysis is not welcomed by either those working in the new science or by the specialists in catalysis. For the former, the surface topology is usually unacceptable (despite the experimental data supporting a surface mechanism!), for the latter, the generation of MeV scaled effects by eV scaled causes seems to be impossible.

The root of the problem is the limited understanding of catalysis and the trend to restrict it only to chemical catalysis. Actually, catalysis is an essential phenomenon in nature and has diverse forms such as: nuclear, physical, chemical, biochemical, biological, intellectual, managerial, social catalysis. Important processes such as life, evolution, thinking, are based on catalysis.

Much beyond its primitive etymology (catalysis means dissolution), it is a cooperative dynamic action with two levels of organization of matter which makes impossible things possible. A recent example [10] shows how the coherent nuclear motions in a membrane protein explain the mechanism of photosynthesis, which is hence a nuclear-biochemical joint business. The `ancient' Philips experiment [5], is perhaps one of the first examples of a cooperative interaction of this type: here electrons and nuclei can work together due to the very small dimensions of the Ti particles which create a catalytic environment.

Catalysis and surface are issues of extreme complexity, therefore catalysis is more an art than a science [11], or in other words, for this discipline, which is over 170 years old, there is "a repeated phase shift of 20-40 years with technology starting first, followed by the evolution of scientific research" [12]. It seems that something analogous will happen to the 5-year old cold fusion. If this really is a catalytic process intimately (and causally) bound to the dynamical properties of the surface and near surface atoms, direct "in situ" and "in tempore" studies of the very mechanisms will be possible only by use of advanced methods as are just-now emerging electrochemical microscopy [13,14]. On the macabre side, any type of post-mortem (ex-situ) analysis will give limited information, given that the dynamic activity is lost.

CONCLUSION

Due to the immense theoretical and experimental problems, the future development of the new science and technology of cold fusion will be based mainly on know-how data and working hypotheses (as our SURFDYN). However, some fundamental theoretical issues as the nature of the reactions have to be explained in the near future. The keyword for this action just as for the essence of catalysis is

cooperation: both international cooperation and cooperation of the theories which have to be considered complementary and not contradictory. For example, the SURFDYN model has a lot in common with Filimonov's synergetic activation model (self-organization) [15] as well as with the catalysis by trapped neutrons of Mizuno [16] and so on... An efficient strategy has to rely on cooperation, in all the three meanings of this word used in this paper.

REFERENCES

[1] Steven H. Kim, Essence of Creativity: a Guide to Tackling Difficult Problems, Oxford University Press, 1990.

[2] P. Glück, "The SURFDYN Concept: an Attempt to Solve (or Rename) the Puzzles of Cold Nuclear Fusion," *Fusion Technology*, vol 24, (1993) p. 122.

[3] J. Dufour, J. Foos, J.P. Millot, "Cold Fusion by Sparking in Hydrogen Isotopes. Energy Balances and Search for Fusion Byproducts. A Strategy to Prove the Reality of Cold Fusion," ICCF-4, preprint N1.6.

[4] F. Piantelli, S. Focardi, R. Habel "Production of Anomalous Heat in a Nickel-Hydrogen System," *Il Nuovo Cimento*, to be published.

[5] O. Reifenschweiler, "Reduced Radioactivity in Small Titanium Particles," *Physics Letters A*, vol 184 (1994), p 149.

[6] G.C. Bond, "Source of the Activation Energy in Heterogeneously Catalyzed Reactions," *Catalysis Today*, vol 17 (1993), p 399.

[7] D. Moon, "A Cold Fusion Theory," preprint, October 1993.

[8] M. Rabinowitz, Y.E. Kim, V.A. Cbechin, V.A. Tsarev, "Opposition and Support for Cold Fusion," ICCF-4, preprint T1.5.

[9] K.A. Kaliev, A.N. Baraboshkin, A.L. Samgin, E.G. Golikov, A.L Shaliapin, V. S. Andreev, P.I. Golubnichiy, "Reproducible Nuclear Reactions during Interaction of Deuterium with Oxide Tungsten Bronze," *Physics Letters A*, vol 172 (1993), p 199.

[10] M.H. Voss, F. Rappaport, J-C. Lambry, J. Breton, J-L. Martin, "Visualization of Coherent Nuclear Motion in a Membrane Protein by Femtosecond Spectroscopy," *Nature*, vol 363, 27 May 1993, p 320.

[11] R. Schloegl, "Heterogeneous Catalysis: Is it Still an Art or Already a Science?" *Angewandte Chemie* vol 105, no 3 (1993), p 402.

[12] G.A. Somorjai, "Heterogeneous Catalysis, Future Opportunities in an Historical Perspective," *Catalysis Today*, vol 18 (1993), p 113.

[13] R. Cassidy, "Liquid-Solid Interfaces: the Birth of Electrochemical Microscopy," *R&D Magazine*, August 1993, p 22.

[14] G. Nunes Jr., M.R. Freeman, "Picosecond Resolution in Scanning Tunneling Microscopy," *Science*, vol 262, 12 Nov. 1993, p 1029.

[15] V.A. Filimonov, "Synergetic Activation Model: Key to Intense and Reproducible Cold Fusion," ICCF-4, preprint T4.13.

[16] H. Kozima, "Trapped Neutron Catalyzed Fusion of Deuterons in Inhomogeneous Solids," ICCF-4, preprint T2.5.

Editor's Comments: This paper carefully explores a possible source of excess heat in certain types of electrochemical cells. As this effect is chemical, not nuclear, the occurence of excess heat together with "nuclear byproduct" would be a confirmation of the occurence of nuclear reactions. The cold fusion experimenter should be aware of the effect that the latent heat of water can have on his/her experiments. Because many papers have reported both excess heat and nuclear byproducts, this paper is not the full explanation of excess heat generation, but it is certainly an excellent contribution to the understanding of the complex phenomena that we have labeled "cold fusion."

JAHN-TELLER SYMMETRY BREAKING AND HYDROGEN ENERGY IN γ-PdD "COLD FUSION" AS STORAGE OF THE LATENT HEAT OF WATER

K.H. Johnson
Massachusetts Institute of Technology
Cambridge, MA 02139

ABSTRACT

In 1989, we proposed a common quantum-chemical basis for superconductivity and anomalous electrochemical properties of palladium loaded with hydrogen and deuterium, derived from H-H/D-D bonding molecular orbitals at the Fermi energy between tetrahedral interstices ("γ-phase" PdD). Symmetry-breaking anharmonic vibrations of the protons/deuterons, induced by the dynamic Jahn-Teller effect, promote superconductivity in PdH/PdD at T_c = 9/10°K, while the large vibronic anharmonicity explains the inverse H/D isotope shift of T_c. The calculated deuteron vibronic amplitude of 0.46Å implies a closest D-D approach of 0.76Å between neighboring tetrahedral sites and fusion rate of only ~10^{-24} per deuteron pair per second in γ-PdD at ambient temperature, much too small to explain reported excess heats. *Ab initio* quantum-chemical computations for γ-PdD further indicate that the "channels" connecting tetrahedral sites provide, via the Jahn-Teller effect, an "orbital pathway" for bulk catalytic recombination of atomic deuterium to rapidly diffusing dideuterium, $4D \rightarrow 2D_2$, the recombination heat equaling 9.4eV per Pd atom per unit diffusion cycle time, equivalent to the storage and release of latent vaporization heat of 2.5 moles of D_2O. While the diffusion cycle time depends on cell conditions, for cycles between 1 and 100 minutes, this process could generate 17 to 1700 watts/cm^3 of stored latent heat in γ-PdD. The inverse isotope effect implies a slower hydrogen reaction, $4H \rightarrow 2H_2$, and diffusion in γ-PdH, leading to negligible latent heat power from Pd-based light-water cells. However, this mechanism could explain reported heat generation in light-water cells using nickel cathodes, where $2H \rightarrow H_2$ catalysis is a rapid (110) surface or near-surface phenomenon.

The Dynamic Jahn-Teller Effect, Superconductivity, and D-D Fusion

An abstract theorem proposed in 1936 by Jahn and Teller[1] laid the foundation for a theory of the static and dynamic coupling of nuclear motions to electronic structure. In a 1983 paper[2] on a "real-space" molecular-orbital basis for superconductivity, we first suggested that Cooper pairing and the inverse isotope shift, T_c = 9/10°K, in PdH/PdD are associated with dynamic Jahn-Teller-induced *anharmonic* vibrations of the protons/deuterons inside Pd. The amplitudes of these vibrations are determined from the formula [2]:

$$\delta = (m/M)^{\beta} d \qquad (1)$$

where M is the atomic mass, *m* is the conduction electron mass, *d* is the interatomic distance, and $0 < ß \leq 1/2$ is the anharmonicity. In the "harmonic limit, ß = 1/2, the dynamic Jahn-Teller-induced vibrations reduce to the "virtual phonons" of the BCS theory of superconductivity. In Ref. 2 it was shown how ß follows directly from the bond overlap of degenerate molecular orbitals at the Fermi energy (E_F). This theory has since been successfully applied to high-T_c oxide and fullerene superconductors.[3,4]

In more recent work,[5] we have confirmed, from density-functional molecular-orbital and *ab-initio* Hartree-Fock calculations, that for high H/D loading in palladium, the sole occupation of octahedral interstices is Jahn-Teller unstable toward migration of H/D's to the tetrahedral interstices, forming the so-called "γ-phase" of PdH/PdD. Spatially extended, degenerate H-H/D-D bonding molecular orbitals at E_F between the tetrahedral sites in γ-PdH/PdD are found to be a precursor to Cooper pairing, superconductivity at $T_c = 9/10°K$, and the inverse isotope effect on T_c. The hydrogen molecular orbitals at and just above E_f are sσ-bonding along and sσ-antibonding in "channels" of opposite phase ψ +, ψ- connecting tetrahedral interstices, as shown schematically for γ-PdD in Fig. 1 and computationally in Fig. 2 as a contour map through a (110) plane. D-D sσ-bond overlap is enhanced by the "compression" effect of significant Pd(4d)-D(ls) antibonding at E_F (Fig. 2). Indeed Pd(4d)-D(ls) antibonding at E_F substantially weakens the effect of *Pd(4d)-D(Is)* bonding states below the Pd d-band, explaining the small heats of formation of PdD, while promoting delocalized D-D sσ-bonding molecular orbitals at E_F. Evidence for hydrogen atoms "banding" together on nickel (110) surfaces, with electron density similar to that shown in Fig. 1, has recently been reported.[6]

In the dynamic Jahn-Teller coupling between interstitial D-D sσ-bonding electrons at E_F and anharmonically vibrating deuterons required for Cooper pairing and superconductivity in PdD for $T_c \leq 10°K$, there is continual symmetry-breaking dynamical interconversion between alternate D-D sσ-bond deformations, δ, along the three crystallographical equivalent directions of the "bonding channels" ψ+ and ψ- shown in Fig. 1 and Fig. 2. These rapid oscillations of the deuterons are equivalent to "anharmonic local optical phonons" of amplitude δ given in Equation (1). For the calculated D-D bond overlap between tetrahedral sites in γ-PdD (Fig. 2), δ = 0.46Å.

Under the influence of the Jahn-Teller effect, the D-D nuclear fusion rate can be calculated from the formula:[5]

$$R = (\hbar\sigma / M\delta^3 d^4) \exp\left[-(2/\hbar)(d-2\delta)\sqrt{2M(V-\hbar^2/2M\delta^2)} \right] \quad (2)$$

where σ is the fusion cross-section extrapolated to ambient temperature and *V* is the Coulomb potential barrier between the γ-PdD tetrahedral sites ("*T*-sites") and the "S-sites" half way between neighboring *T*-sites along the D-D bond direction (Fig. 2). Combining formulas (1) and (2) and using the relationship between anharmonicity ,ß and bond overlap,[2,5] *R* can be plotted as a function of D-D bond overlap, leading to the graph of Fig. 3. For the 20% D-D overlap characteristic of γ-PdD (Fig. 2), this graph gives a value of R = $R_0 \cong 10^{-24}$ fusion per deuteron pair per second, resulting from the Jahn-Teller effect. This value is of the same order of magnitude as that determined from neutron counts in electrochemical experiments on deuterated electrodes by Jones *et al*.[7] Clearly, this very low level of fusion, while fifty orders of magnitude larger than that expected for an isolated D_2 molecule, is not large enough to produce significant amounts of heat under electrochemical conditions in PdD.

It is theoretically possible to enhance the effective D-D bond overlap in γ-PdD to almost 33% via alloying (see below), increasing the D-D fusion rate to a maximum of $R \cong 10^{-21}$ according to Fig. 3, but still too

small for significant heat production.

Symmetry Breaking, D-D Recombination, and Hydrogen Energy in PdD

The D-D potential energy surface in γ-PdD, calculated from *ab initio* Hartree-Fock theory, resembles the "Mexican hat" shown in Fig. 4. The high-symmetry (T_d) coordination of a Pd atom by four D atoms in four of the eight surrounding face-centered-cubic Pd tetrahedral interstitial sites is Jahn-Teller unstable, leading to a central energy minimum of distorted tetrahedral (C_{3v}) symmetry at the "crown of the hat" and a square coplanar (D_{2h}) "broken-symmetry" energy minimum at the "brim of the hat," 9.4eV below T_d symmetry, for an equilibrium D-D distance of 0.76Å. The latter is practically equal to the equilibrium bond distance of a free D_2 molecule. The 9.4eV energy per Pd atom released in the Jahn-Teller distortion of each PdD_4 molecular unit in γ-PdD from T_d to D_{2h} symmetry is likewise remarkably close to the sum of the chemical bond energies of two free D_2 molecules.

Thus, the D-D "bonding channels" connecting tetrahedral sites in γ-PdD provide, via the symmetry-breaking Jahn-Teller effect, an "orbital pathway" for the bulk catalytic recombination, $4D \rightarrow 2D_2$, of rapidly diffusing atomic deuterium to rapidly diffusing dideuterium, the large exothermic chemical heat of recombination equaling 9.4eV per Pd atom. Once a steady state of high electrochemical loading is achieved, this process is likely to be rapid and continuous, facilitated by the Jahn-Teller displacement of diffusing atomic deuterium from octahedral to tetrahedral interstices, forming the "γ-phase," then rapidly diffusing as dideuterium through the γ-PdD "bonding channels" connecting the tetrahedral sites to the cathode surface, where the dideuterium escapes as D_2 gas.

It is impractical to calculate a precise cycle time for this process, because the diffusion depends on the input electrical current, the ambient temperature and pressure, the structural integrity of the Pd lattice, and the surface condition of the Pd cathode. However, if the cycle time for recombination, $4D \rightarrow 2D_2$, is somewhere between 1 and 100 minutes, at 9.4eV per Pd atom per unit time, this process could generate heat at a rate of 17 to 1700 watts/cm^3 palladium. For this power range, the total heat released over ten minutes would be between 10KJ and 1MJ. This is consistent with the wide range of "excess" powers reported in laboratories around the world.

"Cold Fusion" Heat as Chemical "Latent Heat"; "Heat after Death"

This dynamical Jahn-Teller-induced catalytic mechanism is, of course, a chemical process, although an unusual one in that it corresponds to an internal phase change of the deuterium within γ-PdD. Since the energy release is effectively due to an internal cyclic γ-phase change of atomic deuterium to dideuterium, the heat produced may be viewed as "latent heat" produced by repeated formation of the "interstitial sublattice" of D-D bonds between the tetrahedral interstices in γ-PdD, as atomic deuterium diffuses into palladium and dideuterium diffuses out. "Latent heat" of 9.4eV per Pd atom for 6.8×10^{22} Pd atoms/cm^3 adds up to 102KJ/cm^3 palladium. Since the latent heat of vaporization of D_2O is 41.5KJ/mole at 100°C, the "latent heat" of 102KJ produced in one cm^3 of γ-PdD per unit diffusion cycle time is equal to the latent vaporization heat of 2.5 moles of D_2O. <u>In other words, the heat of "cold fusion" appears to be the storage and release of the latent vaporization heat of heavy water</u>. Indeed, if the electric power input is turned off a fully loaded cell, this stored latent heat is sufficient to boil away 2.5 moles of D_2O, the so-called "heat after death" of Pons and Fleischmann.[8]

Equivalence of "Excess" Heat to the Latent Vaporization Heat of Water

Why then is this heat interpreted as "excess heat"? To answer this question, one must first understand the nature of the bonding between H_2O/D_2O molecules in water. It is commonly thought that the breaking of electrostatic or weakly covalent O-H or O-D "hydrogen bonds" between neighboring water molecules accounts for all the latent heat required to take water from the liquid to vapor phase. However, a recent experimental study of the interatomic structure of water at supercritical temperatures, reported in *Nature*,[9] has revealed that breaking of nearest-neighbor O-H and O-D bond correlations in the liquid accounts for only a fraction of the latent vaporization heat. Fig. 1 of Ref. 9 reveals that second- third- and even fourth-neighbor hydrogen-hydrogen (or D-D) bond correlations persist after the nearest-neighbor O-H/O-D and H-H/D-D bonds are broken at supercritical temperatures. These longer range H-H/D-D bond correlations account for the major part of the latent vaporization heat of water.

In the electrolysis of water, only the O-H/O-D bond correlations are broken as H/D penetrates the Pd cathode and O_2 is evolved at the anode. For high loading and the formation of γ-PdD, the D-D bond correlations accounting for a major part of the latent heat of the electrolyte are effectively "stored" cooperatively between the tetrahedral sites of the γ-PdD lattice, as described above and in Fig. 2. The release of the latent heat by the Jahn-Teller-induced bulk catalytic process, $4D \rightarrow 2D_2$, per Pd atom, effectively a cooperative γ-phase transition between interstitial atomic deuterium and dideuterium, thus is interpreted as "excess" heat. Therefore, this mechanism of storage and release of the latent heat of heavy water by palladium is more appropriately viewed as a "new hydrogen energy," the terminology commonly used in Japan instead of "cold fusion."

Light Water Versus Heavy Water

Significant amounts of "excess" heat from Pd-based light-water cells are not observed, most likely because of substantially more sluggish hydrogen diffusion in γ-PdH, compared to deuterium in γ-PdD. Although the mass of D is twice that of H, this inverse isotope effect, comparable to the one discussed above for the superconducting T_c's of PdH and PdD, is probably due to the effectively larger diffusion cross sections of H and H_2 versus those of D and D_2, resulting from the larger amplitude, δ, of dynamic Jahn-Teller-induced anharmonic vibrations for hydrogen versus deuterium, according to Eq. (1). The larger effective radii of H and H_2 in γ-PdH markedly impede hydrogen diffusion and thus lengthen the full $4H \rightarrow 2H_2$ cycle time, as compared to the rapid D and D_2 diffusion, leading to the much faster $4D \rightarrow 2D_2$ catalytic process in γ-PdD.

Nevertheless, this mechanism may explain reported heat production from nickel cathodes in light water cells, where catalytic hydrogen recombination, $2H \rightarrow H_2$, is mainly a rapid (110) surface or near-surface phenomenon. Nickel (110) surfaces harbor the tetrahedral interstices of the bulk crystal. While the solubility of hydrogen in nickel is much lower than in palladium, the latent heat of H-H bond formation between tetrahedral sites close to the (110) surface (the "surface γ-phase" of NiH) could yield substantial heat for high-surface-area nickel, since the diffusion path to the surface is much shorter.

Supporting Experimental Evidence for $4H \rightarrow 2H_2$ Conversion

Experimental evidence for H_2 molecular "excited states" in other transition-metal hydrides has recently been reported by Baker *et al*.[10] from proton spin-lattice relaxation data.

A molecular analogue of the $4H \rightarrow 2H_2$ process has recently been reported by Wisniewski *et al*.[11] in the

form of an $Ir(PR_3)_2ClH_4$ complex, in which the H ligands undergo a rapid dynamical dimerization to the dihydrogen dihydride $Ir(PR_3)_2ClH_2H_2$, as shown in Fig. 5.

The Importance of Lattice Structural Integrity in Palladium

For the γ-PdD lattice to maintain an "interstitial network" of D-D bonds (Fig. 1 and Fig. 2), formed and reformed between rapidly diffusing deuterium at high loading, the structural integrity of the material is crucial. Crack tips and grain boundaries in transition metals can be sites of rapid catalytic hydrogen recombination, which tend to cause metallic decohesion, intergranular embrittlement, and crack propagation.

Enhanced "Cold Fusion" and Superconductivity in γ-$Pd_{0.75}Ag_{0.25}D$

Density-functional molecular-orbital calculations have been performed for a γ-$Pd_{0.75}Ag_{0.25}D$ alloy. Maximum hydrogen solubility near this composition has been reported by Lewis[12]. The pertinent wavefunction contour map for this alloy, showing D-D bonding between the tetrahedral sites at E_F, is displayed in Fig. 6 and may be compared with Fig. 2 for pure γ-PdD. As a result of the increased "compression" effect of Ag(4d)-D(1s) antibonding in γ-$Pd_{0.75}Ag_{0.25}D$ at E_F, the tetrahedral D-D bond overlap in Fig. 6 is enhanced to practically 33%, as compared with 20% in Fig. 2 for γ-PdD. From Fig. 3, this would suggest a possible increase of the D-D nuclear fusion rate from $R \cong 10^{-24}$ in γ-PdD to $R \cong 10^{-21}$ in γ-$Pd_{0.75}Ag_{0.25}D$, which should be detectable by increased neutron emission, provided the $Pd_{0.75}Ag_{0.25}$ alloy can be loaded with deuterium. However, this predicted increase in fusion rate is still too small to generate significant heat on its own.

Tracking this predicted increase in D-D fusion in the Pd-Ag alloy, is the experimental fact uncovered by Stritzker[13] that the superconducting transition temperature is raised from $T_c = 9°K(10°K)$ in PdH(D) to $T_c = 15°K$ in $Pd_{0.75}Ag_{0.25}H$. This is consistent with the dynamic Jahn-Teller anharmonic vibronic mechanism for high-T_c superconductivity discussed above and in Refs. 2-5.

"Cold Fusion" in High-T_c Superconductors

In accord with the above thesis that a dynamic Jahn-Teller anharmonic vibronic mechanism is responsible for both high-T_c superconductivity and "cold-fusion" manifestations is a recent report of low-level neutron production from deuterated high-T_c ceramic superconductor, $YB_{a2}Cu_3O_7$, below the superconducting transition temperature.[14]

CONCLUSION

Latent-Heat-of-Water Storage as Practical "New Hydrogen Energy"

Given the latent heat of vaporization content of a gallon of water, approximately 8MJ or 7,600BTU, its electrochemical storage and release by the process described above could be a viable method of hydrogen energy conversion. Ten gallons of water contain approximately 80 MJ or 76,000BTU of latent heat which, if stored and released electrochemically over one hour, approaches the heating capacity of a modest commercial household furnace. To convert this amount of latent heat from 10 gallons of water, would require an electrochemical cell power output of 22KW. Since one cm^3 of Pd (or the equivalent surface area of Ni) is capable, under ideal conditions, of yielding upwards of 1.7KW of stored latent heat,

this would require approximately 13cm^3 or 156g Pd, or the equivalent amount of much cheaper Ni. A power of 22KW corresponds to 30HP, suggesting the possibility of a "water engine" electrochemically generating both heat and hydrogen for a fuel cell, which could be used to power or partially power an automobile.

ACKNOWLEDGEMENTS

I am very grateful to Dr. Kailash Mishra for performing the *ab initio* quantum chemistry calculations for the D-D potential surfaces in PdD, and for his helpful discussions.

REFERENCES

[1] H. Jahn and E. Teller, "Stability of Degenerate Electronic States in Polyatomic Molecules," *Phys. Rev.*, vol 49, p 874 (1936); see also I.B. Bersuker and V.Z. Polinger, Vibronic Interactions in Molecules and Crystals, Springer-Verlag, New York (1989); M.C.M. O'Brien and C.C. Chancey, "The Jahn-Teller Effect: an Introduction and Current Overview," *Am. J. Phys.* vol 61, p 688 (1993).

[2] K.H. Johnson, "Molecular Orbital Basis for Superconductivity in High and Low Dimensional Metals," *Synth. Metals*, vol 5, p 151 (1983).

[3] K.H. Johnson, D.P. Clougherty, and M.E. McHenry, "Dynamic Jahn-Teller Coupling, Anharmonic Oxygen Vibrations, and High-T_c Superconductivity in Oxides," *Mod. Phys. Lett. B*, vol 3, p 367 (1989).

[4] K.H. Johnson, M.E. McHenry, and D.P. Clougherty, "High- T_c Superconductivity in Potassium-Doped K_xC_{60} via coupled $C_{60}(p\pi)$ Cluster Molecular Orbitals and Dynamic Jahn-Teller Coupling," *Physica C*, vol 183, p 319 (1991).

[5] K.H. Johnson and D.P. Clougherty, "Hydrogen-Hydrogen/Deuterium-Deuterium Bonding in Palladium and the Superconducting/Electrochemical Properties of PdH/PdD," *Mod. Phys. Lett. B*, vol 3, p 795 (1989).

[6] R. Nieminen, "Hydrogen Atoms Band Together," *Nature*, vol 356, p 289 (1992).

[7] S.E. Jones et al., "Observation of Cold Nuclear Fusion in Condensed Matter,'" *Nature*, vol 338, p 737 (1989).

[8] S. Pons and M. Fleischmann, "Heat after Death," paper presented at the Fourth International Conference on Cold Fusion, Maui, December 6, 1993.

[9] P. Posterino et al., "The Interatomic Structure of Water at Supercritical Temperatures," *Nature*, vol 366, p 668 (1993).

[10] D.B. Baker et al., "Evidence for the High-Temperature Spin-Relaxation Anomaly in Metal Hydrides," *Phys. Rev.*, vol 46, p 184 (1992).

[11] L.L. Wisniewski et al., "Mechanism of Hydride Scrambling in a Transition-Metal Dihydrogen Dihydride as Studied by Solid-State Proton NMR," *J. Am. Chem. Soc.*, vol 115, p 7533 (1993).

[12] F.A. Lewis, The Palladium Hydrogen System, p 74, Academic Press, New York (1967).

[13] B. Stritzker, "High Superconducting Transition Temperatures in the Palladium-Noble Metal-Hydrogen System," *Z. Physik*, vol 268, p 261 (1974).

[14] A.G. Lipson et al., "Possible Cold Nuclear Fusion in the Deuterated Ceramic $YBa_2Cu_3O_7$ in the Superconducting State," *Sov. Phys. Dokl.*, vol 38, p 849 (1991).

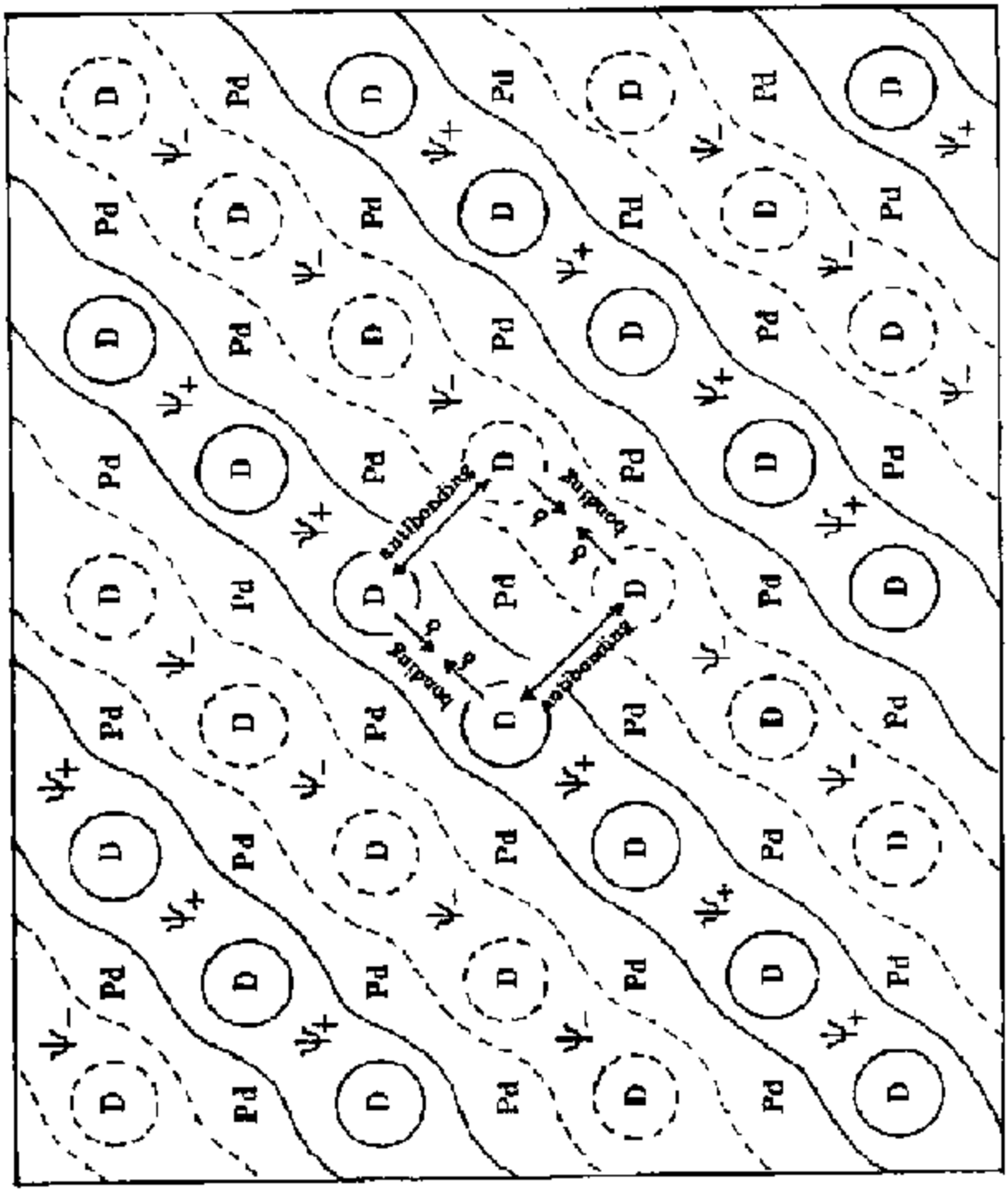

Fig. 1. Schematic representation of D-D bonding "channels" at the Fermi energy (E_F) in γ-PdD. Solid and dashed contours represent positive and negative amplitudes of the wavefunction. The amplitude, δ, of Jahn-Teller-induced D-D vibrations, calculated from Eq. (1), is indicated.

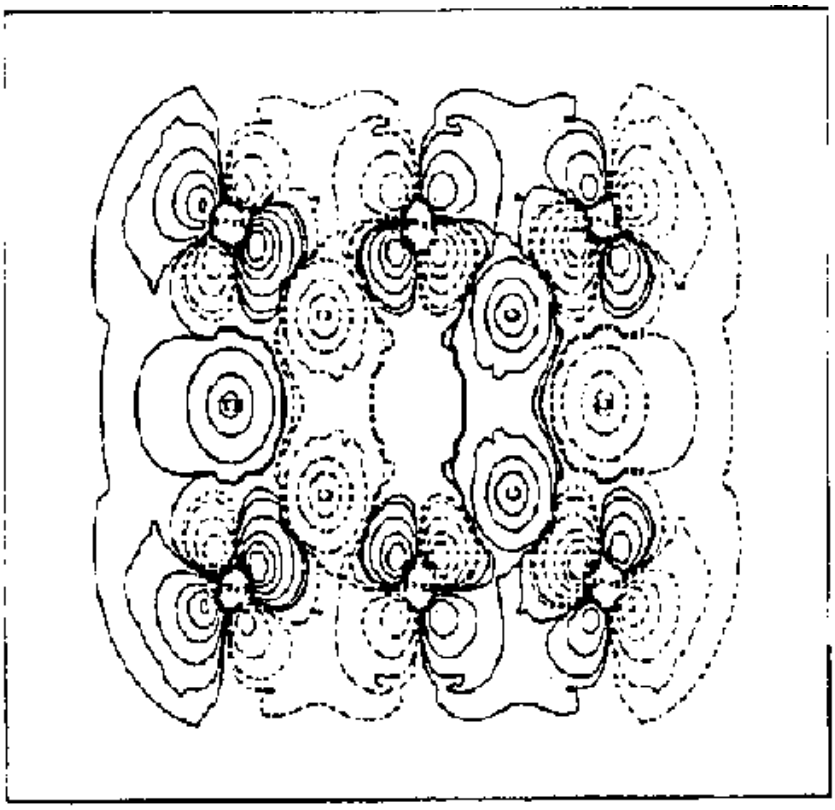

Fig. 2. Density-functional molecular-orbital wavefunction at E_F for γ-PdD plotted in a (110) plane.

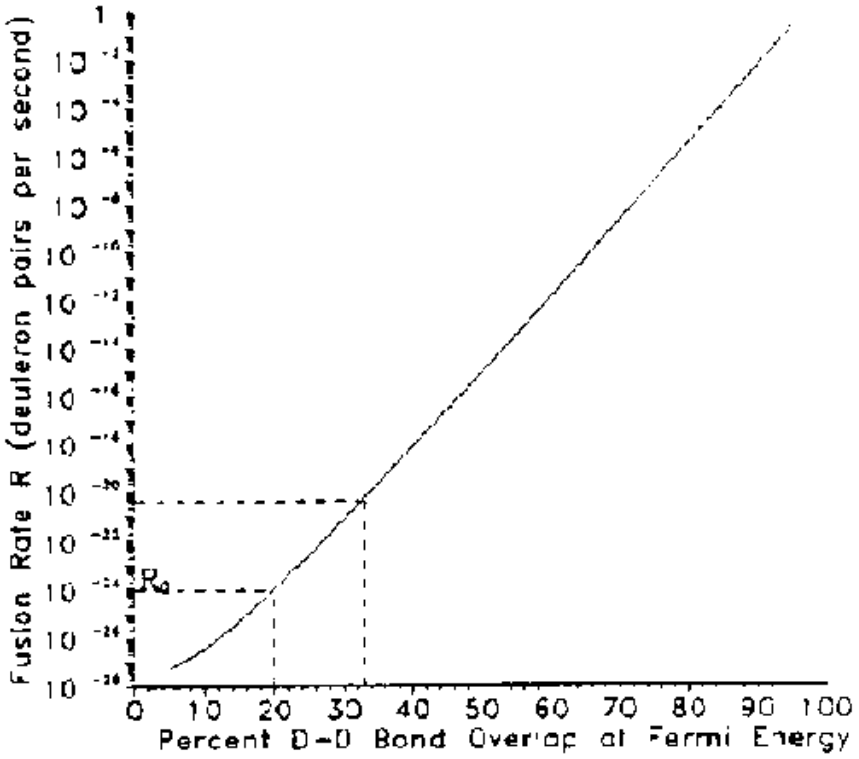

Fig. 3. D-D nuclear fusion rate in γ-PdD induced by the Jahn-Teller effect according to Eq. (2), plotted against D-D bond overlap between tetrahedral sites. The dashed lines bracket the practical limits of fusion.

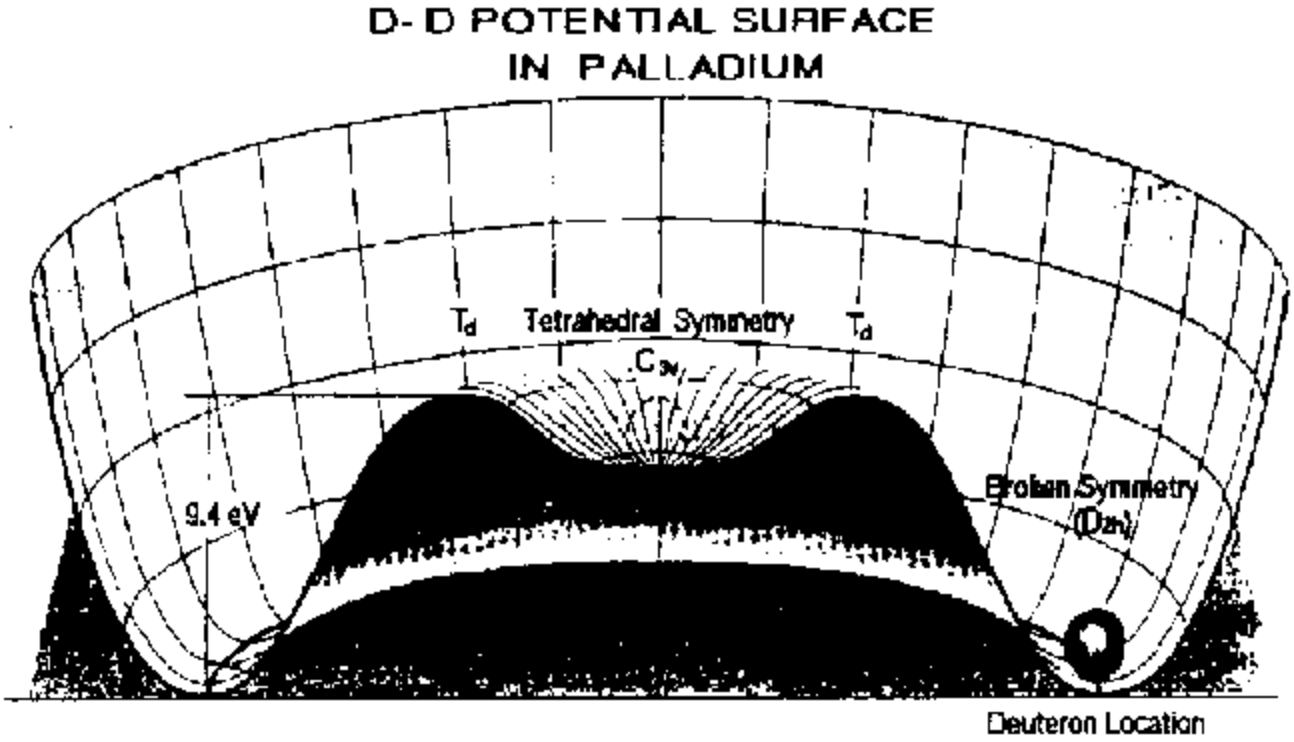

Fig. 4. Schematic "Mexican hat" representation of the D-D potential surface in γ-PdD.

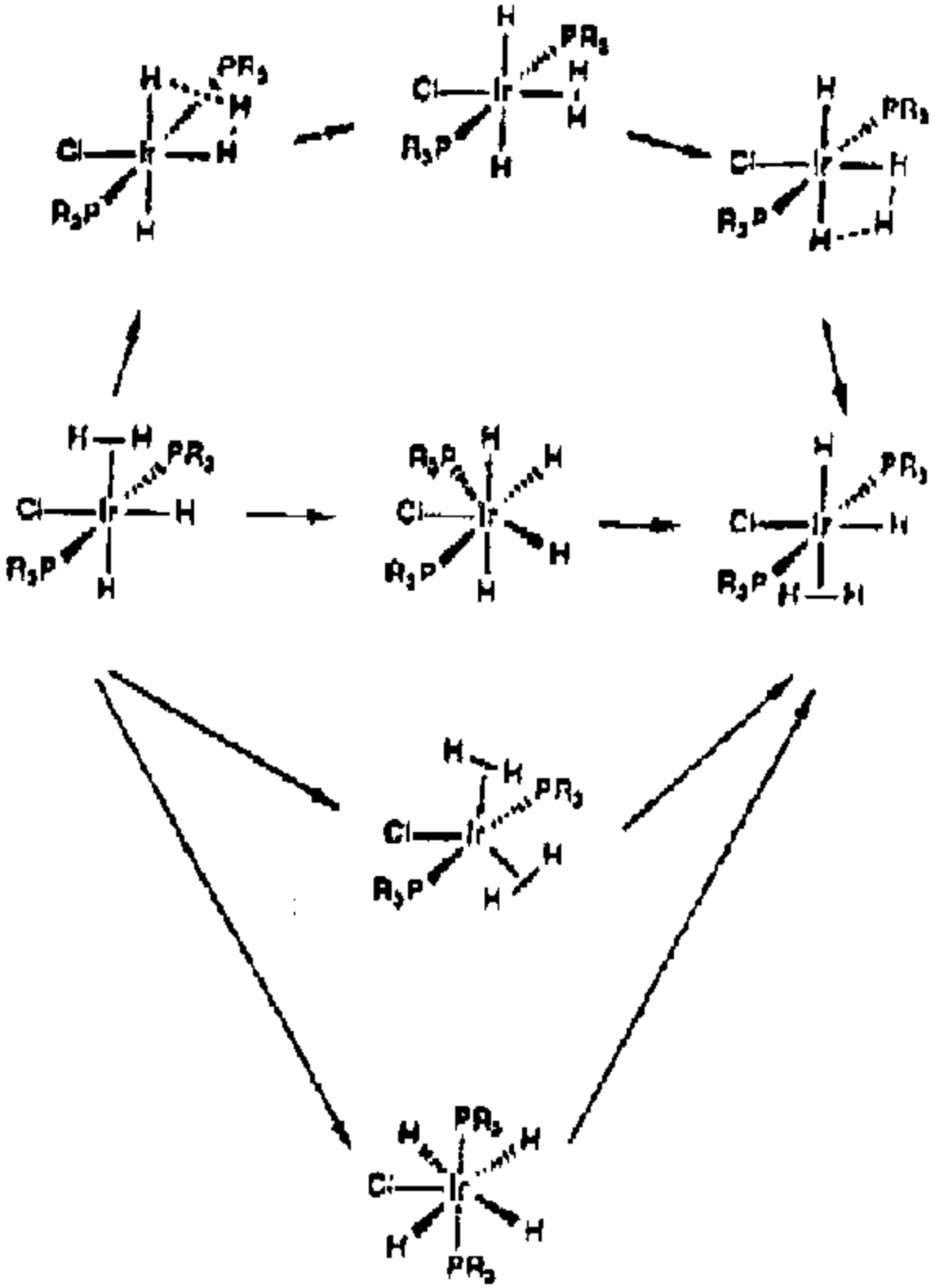

Fig. 5. A molecular analogue of the 4D → 2D$_2$ process in γ-PdD$_2$: the molecular complex Ir(PR$_3$)$_2$ClH$_4$, in which the 4H ligands undergo a rapid dynamical dimerization to the dihydrogen dihydride Ir(PR$_3$)$_2$ClH$_2$H$_2$ (see Ref. 11).

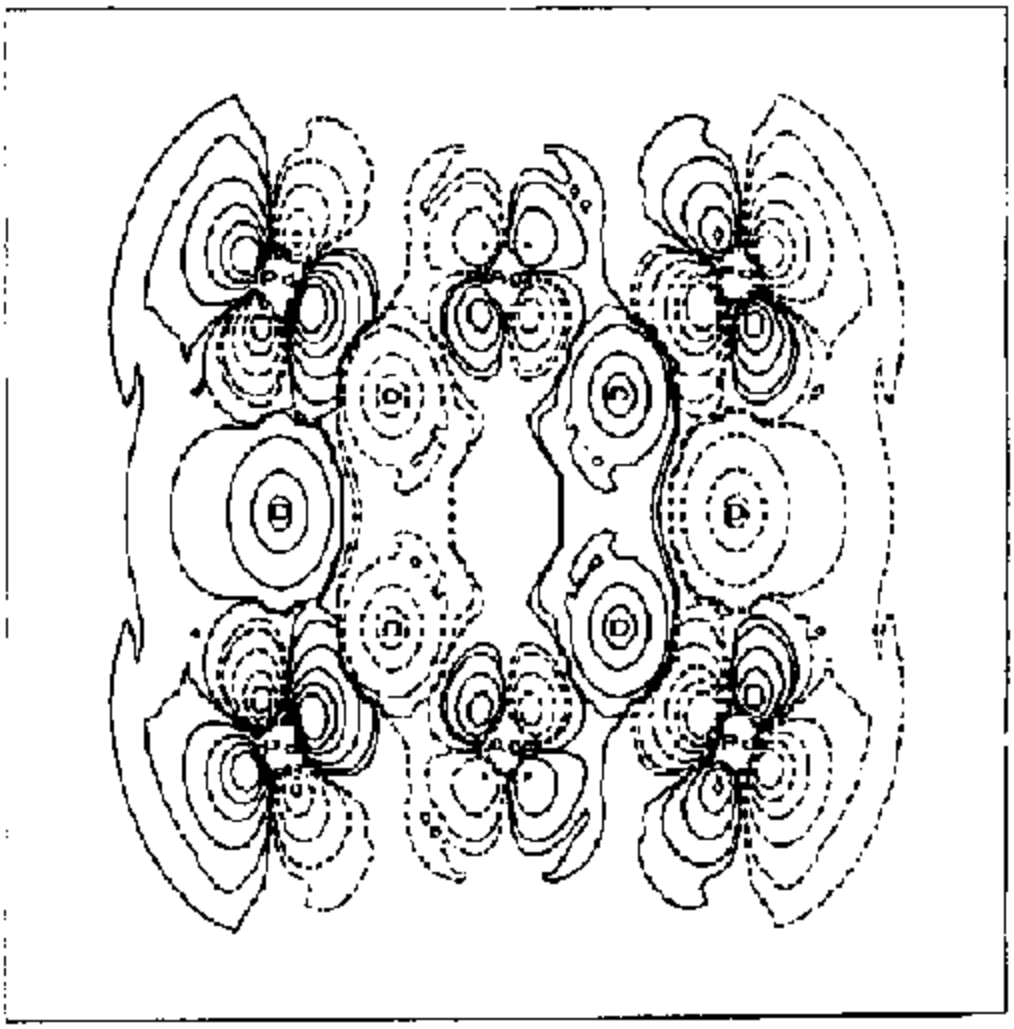

Fig. 6. Density-functional cluster molecular-orbital wavefunction at E_F for γ-$Pd_{0.75}Ag_{0.25}D$ plotted in a (110) plane

I. DEUTERIUM INTERACTION IN UNITARY QUANTUM THEORY

Lev G. Sapogin
Department of Physics, Technical University (MADI)
Leningradsky Prospect 64, A-319, 125829 Moscow, Russia

ABSTRACT

A unitary quantum theory (UQT) with a new perspective on the problem of particle interaction was developed in the author's papers [1-8]. According to this theory any elementary particle is a condensed group of some unitary field traveling in a packet of partial waves. Dispersion and nonlinear nature of the process spreads the wave packet periodically across space and assembles it; the envelope of the process happens to coincide with the de Broglie wave. The formalism of the theory amounts to the relativistically invariant system of 32 non-linear integral-differential equations from which relativistic quantum mechanics in the form of Dirac's equation follows. On the other hand Hamilton-Jacobi's relativistic mechanics follows strictly mathematically from the theory. We can solve this problem in a different way, though for this purpose we must sacrifice part of the ideology of the UQT, (refraining from dividing particles or wave packets). As a matter of fact we can do this [accept this restriction] if the energies are low when the interactions are elastic (though there are exceptions.) This paper will show that despite the roughness of the approach the results may be outstanding. Even when using this approximation the approach can provide outstanding results. The approximate solution of some of the UQT equations [7,8] gives the value of the electric charge together with the value of a fine structure constant; the data being in very good agreement with experimental results. This achievement allows one to give a heuristic description of a moving particle as a charge oscillation with the de Broglie wave frequency. In other words, in all macro experiments the effective value of a charge is measured, the oscillation being unnoticeable.

INTRODUCTION

Newton's equation for a moving mass point with an electric charge q and a modified equation for the electric force acting on the electric charge oscillating at the de Broglie wave frequency in the field with intensity E are suggested as the basic model equations:

$$F - m\ddot{r} = qE\,2\cos^2(\varphi), \quad \varphi = \frac{m\dot{r}^2}{2h}\,t - \frac{m}{h}\,\dot{r}\,r + \varphi_0 \ . \tag{1}$$

where E = -grad V, V(r) is a potential. Such approach is a natural outcome of (8). Further on only spherically symmetrical potentials will be considered. To simplify the non-linear equation given let us introduce scale coefficients for coordinates, time, and velocity: $r = S_r r_s$, $t = S_t t_s$ and $S_v = S_y/S_t$, respectively.

Assuming $mS_r^2 / hS_t = 1$, $k = qmS_r^3 / h^2$ we will obtain the following normalized equation (omitting "s" indices):

$$\ddot{r} = kE\,2\cos^2(\dot{r}^2\,t/2 - \dot{r}\,r + \varphi_o) \tag{2}$$

which despite the apparent simplicity of the initial premises can drive any mathematician to deep despair. As the first scale coefficients relation provided a simplified expression for the phase, the second relation unambiguously describing S and S will be chosen proceeding from the simplified expression for the potential examined. Let us consider the main properties of equations (1) and (2). For simplicity's sake it will be assumed that the particle can move along the axis of r=(x,0,0) in the field of E(r)=(E(x),0,0).

FIXED CHARGE

If x-0, then the electrostatic force is F = *kE 2cos*^{2} φ_0 and $\int_0^{\pi} F d\varphi/\pi = F_{clas}$ is classical electrostatic force.

Averaging a great number of charges results in a force equal to F_{clas}.

UNIFORMLY ACCELERATED MOTION

If E(x)=E>0 is a uniform constant field where a = kE2cos^2 φ_0 and $\int_0^{\pi} a d\frac{\mathbb{C}}{\pi} = T_{clas}$ is classical particle acceleration aligned with the uniform constant field. If the field acts in a D-size range, the accelerated particle kinetic energy is equal to T=maD and $\int_0^{\pi} T d\varphi / \pi = T_{clas}$ is classical kinetic energy.

As $v(\varphi_0) = \sqrt{2sD} = v(0)\ |\cos\varphi_0|$, then at the uniform phase $\varphi_0 = 0 \ldots \pi$ probability density of velocity distribution after acceleration is equal to $2_{\pi}[v(0)^2 - v(\varphi_0)^2]^{1/2}$.

Motion studies at the constant phase of φ_0 = const show that $\dot{x} = (x/t) \pm [(x/t)^2 - 2(\varphi-\varphi_0)/t]^{1/2}$ and the particular solutions will be $x(t) \approx t^2$ (linearly accelerated) and $x(t) \approx \sqrt{t}$ (diffusive).

Within the force field the particle will move uniformly (due to inertia) at f~p/2 accelerating in all other cases. Such nonuniform motion in respect to average values gives rise to relations similar to uncertainly quantum relations.

TUNNELING

If we take up the problem of particle/bell-shaped potential interaction, all known qualitative quantum-mechanical implications will remain valid. This results from the fact that in a potential step considered above and an accelerating part which does not hinder motion. But, unlike quantum mechanics, there is no above barrier reflection in the model at velocities v over a certain threshold value. As an example, we will consider the way the particle passes a symmetrical potential barrier of the Gaussian type $V(x) = \exp[-(x/6)^2]$. The particle motion should meet equation

$$\ddot{x} = 2(x/\delta^2)\ \exp[-(x/\delta)^2\ J\ 2\cos^2(\dot{x}^2\ t/2 - \dot{x}\ x + \varphi_0),$$

with the initial conditions of x(0) = -4, $\dot{x}(0) = v$, $\varphi_0 = 0 \ldots \pi$.

Fig. 1 shows probability P(v) of particles passing through the potential barrier vs. velocity (energy) v and uniform initial phase distribution = 0... p.

Fig. 2 shows probabilities P(s) of a particle passing through potential barrier vs tunneling distance. It can be seen that the curve has resonance peaks at small v_0. An increase in velocity v_0 leads to a threshold effect when all the particles pass through a sufficiently wide barrier without reflection. The regularities observed in passing through a potential barrier are similar to quantum-mechanical predictions. But in quantum mechanics particle passage probability is proportional to its squared wave function modules and is entirely independent of the phase. So one might ask why some particles reflect from the barrier while some others pass through it. Our model answers the question as follows: the probability of a particle passing through the barrier is dependent of the particle phase. If the phase is such that the charge is small, the particle will fly through the barrier without "noticing" it.

PARTICLE IN THE PARABOLIC WELL

Let $V(x) = fx^2$, $E(x) = -2fx$.

We'll assume 2kf=1 and start examining particle behavior in such a potential well. The initial equation is $\ddot{x} = -x\,2\cos^2(t^2/2 - tx + \varphi_0)$, the initial conditions are x(0) = 0, $\dot{x}(0) = v$, $\varphi_0 = 0...\pi$.

The numerical analysis of the equation leads to four solution types:

1) Unstable periodic solutions. When velocity v goes down, oscillation period approaches 2p asymptotically, as is to be expected.

2) Irregular dying particle oscillation in a potential well. For some initial values the amplitude of particle oscillations first goes down and then infinitely up.

3) Irregular oscillations with an infinitely increasing amplitude. For some initial values the amplitude of particle oscillations first goes down and then infinitely up.

4) Diffusion at which the particle can be tunneling through the potential for an indefinitely long time is similar to the particle behavior in the potential step problem. With a limited depth parameter the particle will leave it by all means, though it might spend sufficiently long time doing it. Periodic and irregular oscillation states can be defined as discrete and continuous (blurred) zones, respectively.

ABOVE BARRIER REFLECTION FROM A POTENTIAL WELL

In considering particles flying through the potential well the following phenomena are observed. Unlike quantum mechanics there is a threshold velocity for flying particles, above which all the particles fly over the potential well without reflection. If the initial velocity v0 is under the threshold value, the particle will get into a potential well and will either tunnel through the barrier or start oscillating in the well. It can "jump out" of the well and go on with its motion (reflection or flight through) or form a bound state similar to the one discussed in the parabolic well problem.

DEUTERON INTERACTION

Let's consider two charged particles (deuterons) moving towards each other along an X axis.

Let's choose a starting point on the reference frame in the center of one of the particles with a charge Q. Let the second particle with a charge q and velocity V_0 move from a coordinate point X_0. If opposite beams collide we can arrive at the above-state situation having introduced the normalized mass. The particles are expected to approach each other at a distance of X_{clas} where their velocity will drop down to zero and then start to accelerate again. In accordance with the classic Coulomb's law this distance can be calculated by the expression:

$$X_{clas} = \frac{2QqX_0}{2Qq + m X_0 V_0^2} \tag{3}$$

If the charge q oscillates by the de Broglie wave frequency, the motion equation could be written using the Gauss's system as

$$m \ddot{X} = \frac{2Qq \cos^2 (m \dot{X}^2 t/2h - m \dot{X} X/h + \varphi_0)}{X^2} \tag{4}$$

$$\ddot{X} = -\frac{k}{X^2} \cos^2 \left(\frac{\dot{X}^2}{2} t - X \dot{X} + \varphi_0\right), \text{ where } k = 2Qq \tag{5}$$

THE VALIDITY OF EQUATION

To clarify the physical situation, the digital computation of equation 5 was done by a computer with the initial conditions being provided to make it quicker: with X_0=10, different values were used for the initial velocity and phase variations from 0 to p. It was discovered that the laws of energy and momentum conservation were partially observed. In case of particle reflection at a distance of X0 its velocity ranged about 20-30% higher or lower, respectively. But if we sum up the incident and reflected particles throughout all the phases, the entire energy value will be preserved. As was expected, the effect of particle acceleration occurred at the largest value of the charge.

On the other hand at the last stage of moderating (for a number of values of velocity and phase values) we could observe a fantastic process: the velocity and charge being too small, the repulsive force is also small. This phenomenon can continue for quite a long period of time and the particle has an additional opportunity to penetrate the repulsive potential for an indefinite depth. All that reminds very much of a furtive clandestine penetration upon the enemy territory. This outstanding phenomenon occurs only within some phase range close to p/2 and it can be conveniently called the "phase precipice" as is shown on Fig. 3. The relative depth of the "phase precipice" equals Xmin/Xclas = 10^{-6} to 10^{-9} and is independent of the energy. Under very small energies (0.01 to 1eV) the precipice exists but it is narrow (10^{-10} to 10^{-8}) and not easily traced in terms of digital computation. For instance, the phase change in 10^{-10} may eliminate the precipice. As a matter of fact energy and momentum conservation laws are not observed for an individual particle but they are related by the relations of uncertainty type, though of a different origin.

The regularities observed in passing through the potential barrier are similar to quantum-mechanical predictions. Now the quantum mechanics may be slightly kicked not withstanding its attractiveness. I've never understood why God has not used the phase in any way in his quantum Universe though he hasn't ever been noticed making any surprises before. At least now it is obvious that the phase might be used like that, but nobody has ever guessed it.

REFERENCES

[1] L.G. Sapogin, "Investigation of systems," *Vladivostok*, no 2, p 54, 1973 (in Russian).

[2] L.G. Sapogin, *Il Nuovo Cimento*, vol 53A, no 2, p 251 (1979).

[3] L.G. Sapogin, *Annales de la Fondation Louis de Broglie*, vol 5, no 4, p 285 (1980).

[4] L.G. Sapogin, *Il Nuovo Cimento*, vol 70B, no 1, p 80 (1982).

[5] L.G. Sapogin, *Il Nuovo Cimento*, vol 71B, no 3, p 246 (1982).

[6] V.A. Boichenko, L.G. Sapogin, *Annales de la Fondation Louis de Broglie*, vol 9, no 3, p 221 (1984).

[7] L.G. Sapogin, V.A. Boichenko, *Il Nuovo Cimento*, vol 102B, no 4, p 433 (1988).

[8] L.G. Sapogin, V.A. Boichenko, *Il Nuovo Cimento*, vol 104A, no 10.

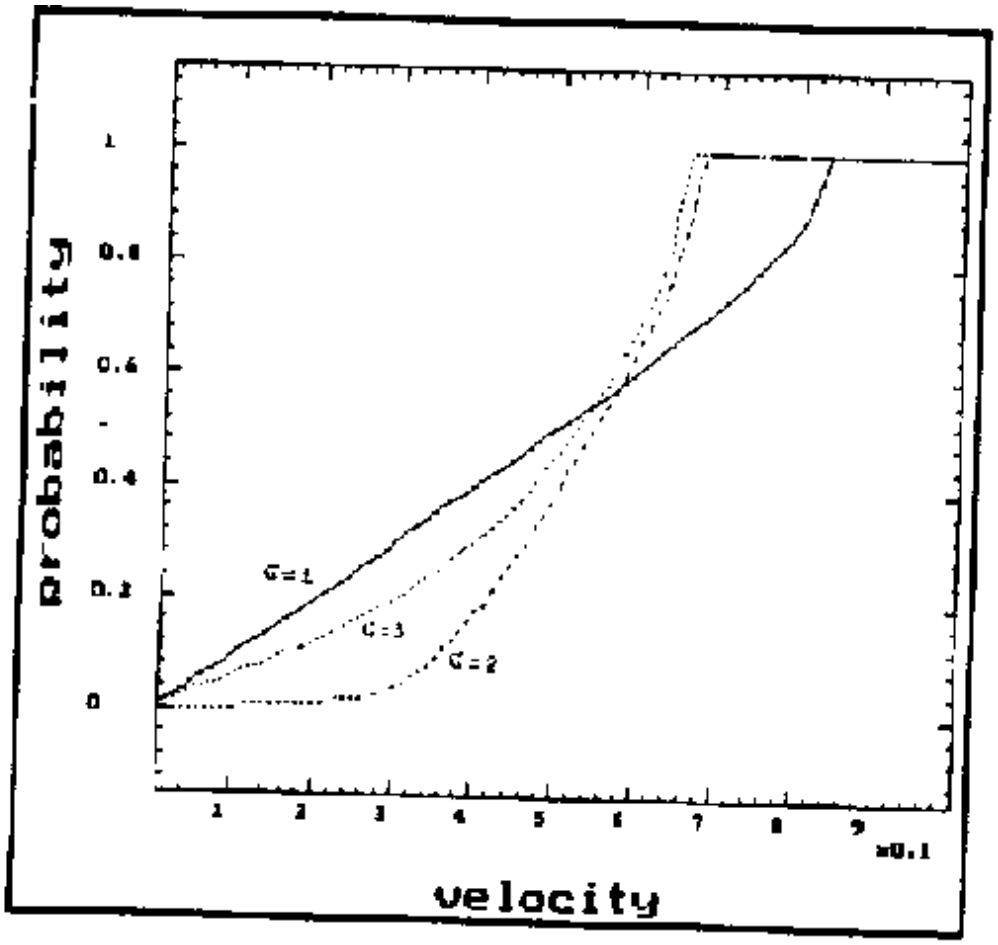
probability
velocity
G=1
G=3
G=2
x0.1

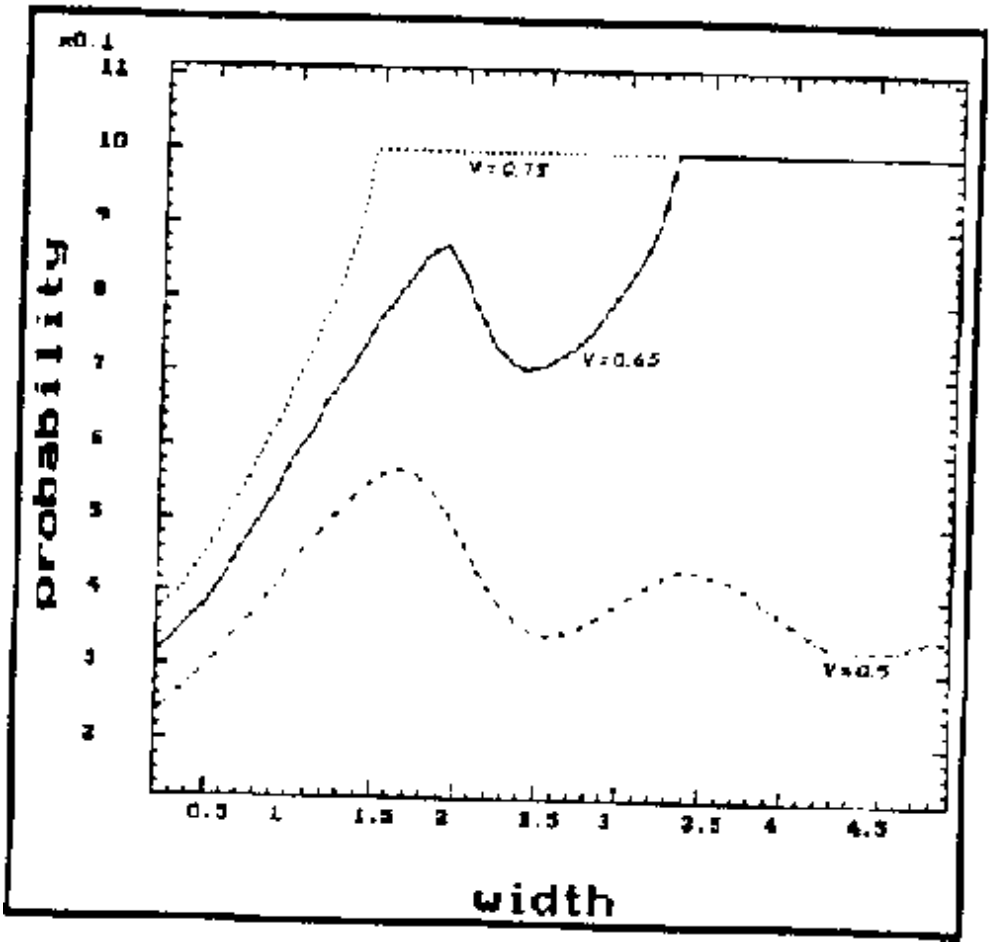
probability
width
V=0.75
V=0.65
V=0.5

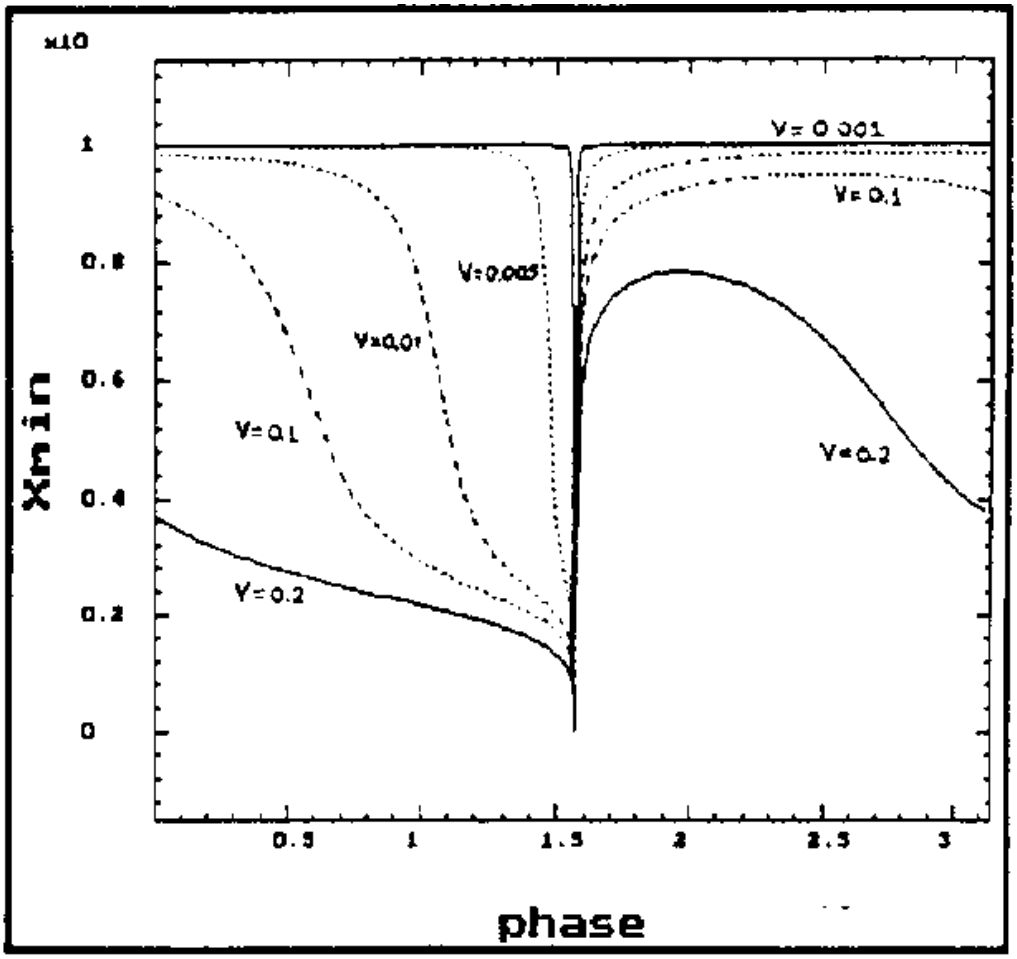
x10
1
0.8
0.6
0.4
0.2
0
Xmin
V= 0.001
V= 0.1
V=0.005
V=0.01
V=0.1
V=0.2
V=0.2
0.5
1
1.5
2
2.5
3
phase

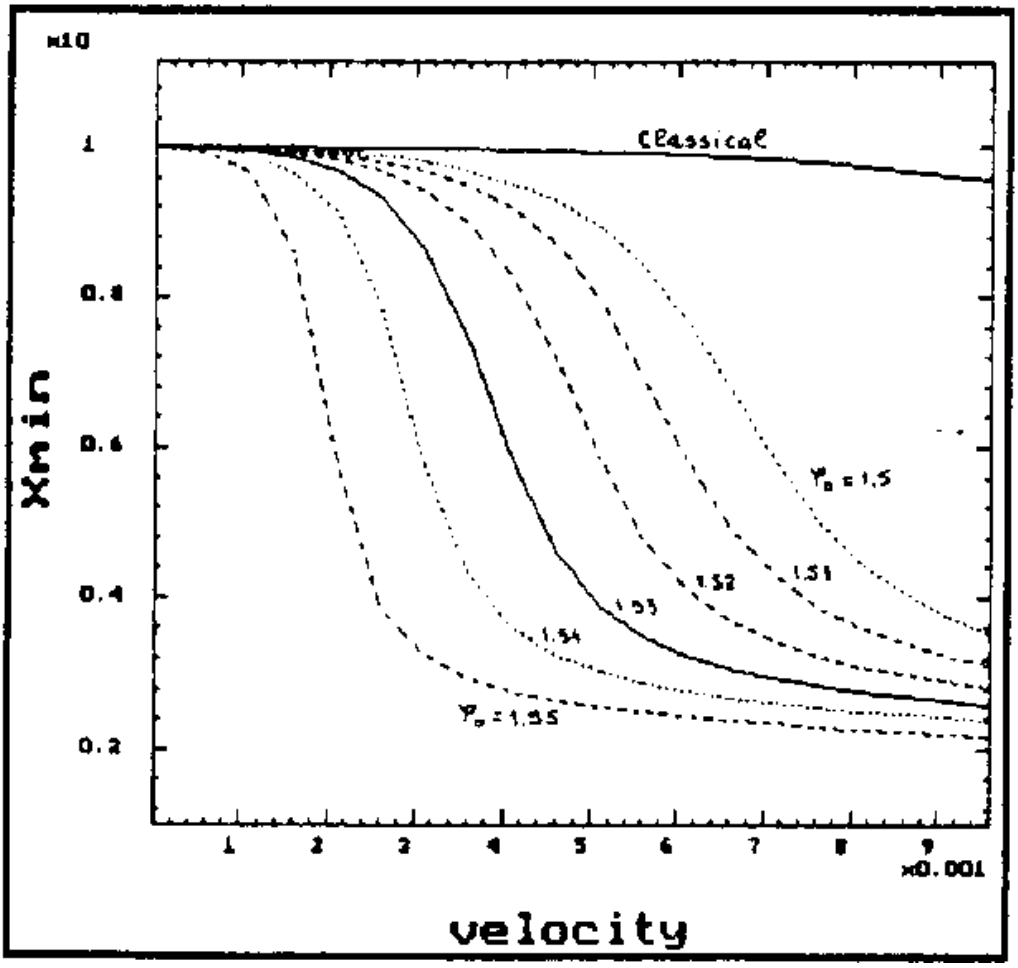
x10
1
0.8
0.6
0.4
0.2
Xmin
Classical
γ_0 = 1.5
1.51
1.52
1.53
1.54
γ_0 = 1.55
1
2
3
4
5
6
7
8
9
x0.001
velocity

II. ON THE MECHANISM OF COLD NUCLEAR FUSION

Lev G. Sapogin
Dept. of Physics, Technical University (MADI)
Leningradsky Ave. 64, A-319, 125829 Moscow, Russia

Let us try to consider from the viewpoint of Jones's the epoch-making experiments of Fleischmann and Pons' group and others. The results of these works can be briefly summarized as follows: the cold nuclear fusion (CNF) phenomenon exists but nobody knows how to explain it. In spite of the fact that the number of fantastic theories explaining CNF mechanisms increases, only a few believe them. Let us give some estimation of these experiments. The minimum classical distance X_{clas}, at which deuteron nuclei may approach each other, equals X_{clas} = [unreadable] = 14(a)/E(eV). The deuteron nucleus size is about $4x10^{-12}$ cm, the nuclear force range is $4x10^{-13}$ cm (deuteron is very friable [sic]). The solution of equation 5 from (1) for these initial conditions X_0 = 3A and [unreadable] = 1.57079632 shows that nuclear reactions can occur with the energy more than 1 eV. If the phase approximates /2 (sic) the energy value may decrease by hundreds of times. Fig. 1 shows the dependence of X_{min} on the energy value in some fixed phases.

One shouldn't think that the phase precipice phenomena causes the nuclear reaction in the wide range of the precipice. The Coulomb's repulsion at this moment may happen to be less than the attraction of the small interaction, but nobody knows when it may happen, because the phase may similarly influence the value of nuclear forces. Besides, sometimes the particle arrives at the turning point X_{min} having "thinned" sufficiently. Will it be able to take part in full-scale nuclear reaction or will it pass through rapidly as an electron usually does when in an S-atom state? But there exist very narrow ranges of the phase, where particle charge increases rapidly and the particle accelerates after stopping. The charge may amount to maximum value in the nuclear force action range. Apparently a narrow phase range is responsible for the cold nuclear fusion. These data are essential for the development of the new-generation nuclear reactors. Interaction D-D takes place in three channels (energy in MeV):

$$D + D \rightarrow T\ (1.01) + p\ (3.03) \quad (1\ \text{channel})$$
$$D + D \rightarrow {}^{3}He\ (0.82) + n\ (2.45) \quad (2\ \text{channel})$$
$$D + D \rightarrow {}^{4}He + \text{gamma}\ (5.5) \quad (3\ \text{channel})$$

All of them are exothermic, have no threshold (now it is clear why) and may occur even at very small relative energies.

For example in D molecule the balance distance between atoms 0.74 Å, in conventional theory the interaction rate being very slow 10^{-64} per sec. But at a distance of 0.1Å this value is sufficient for cold fusion events according to the classical theory.

The rate of reaction ratio for tritium and neutron channels is close to a unity according to classical theory, but in numerous cold fusion experiments [the tritium/neutron ratio is large]. Let us try to explain the cause of the phenomenon. At a small velocity in a phase precipice the nuclear forces of attraction act on neutrons and the electrostatic forces of repulsion act on protons. Two deuterons are turned with the neutron parts facing each other under the influence of these forces. The nuclear forces saturation occurs after the neutrons approach each other. So the proton connections grow weak and because of the

electrostatic repulsion one of them leaves the nuclear system. It is like the Oppenheimer-Philips effect. It is easy to estimate that for E > 10 KeV deuterons have no time for turning, in this case the 2nd and 3rd channel reactions may occur.

The increase of the neutron channel may be due to the secondary neutrons birth in the reaction $T + D \rightarrow {}^{3}He + n$ (14.1 MeV). In the environment rich with deuterons the majority of the emerged tritons are transformed into neutrons by 5 barn cross-section reaction for E = 70 KeV. According to the estimations (3) the number of such secondary neutrons to the unit triton equals 7.9×10^{-12}; 1.7×10^{-9}; 2.7×10^{-6} for E = 10; 20 and 100 KeV respectively. So the predominance of $T/n = 10^{6}$ may only be expected in those reactions, where triton emerges with the energy of E < 40 KeV.

It should be noted that there is still a possibility to explain one of the nuclear physics anomaly, the existence of which nobody seems to notice. For nucleon energy of 1 MeV, $v = 10^{9}$ cm/s, $R_{nuclear} = 10^{-12}$ cm; $t = R/y\text{-}10^{-21}$ sec.; the time range of nuclear disintegration is anomalously large - 10^{-14} sec. Apparently at strong nuclear forces the phase precipice mechanism is working also, i.e. the nucleon is very slowly crawling into the nuclear system.

All the programs for the controllable nuclear fusion are based on heating and squeezing of the reacting material. In spite of the progress achieved in this field Dr. Alan Gibson, the head of the research in England, said that it would take at least 50 years to build the first demonstrative model of the reactor. It should be noted that such a reactor would be extremely sophisticated, expensive, and harmful to ecology. No classic approach to this problem has hitherto given any positive results, and this in spite of the billions of dollars spent and the enormous number of research workers and other personnel employed (physicists, engineers, managers, laboratory staff, etc.). It is only natural that such a huge army of scientific workers should potentially be antagonized by any other alternative project of nuclear fusion. It has been noticed that the "creativity" of any scientific theory stands in direct proportion to the number of researchers employed and the money spent. The reaction itself was experimentally confirmed in 1989 by M. Fleischmann and S. Pons in the US, where the two researchers were met with a strong opposition.

All the programs for controlled thermonuclear fusion are defined by the adjective "controlled", though in reality there is no control as such. For this reason the provided quantity of reaction material is taken extremely small. For instance, a lithium deuteride ball is no more than 1-2 mm in diameter. The direct approach being used at the fusion process is absolutely natural, because there are no means to influence this process in quantum mechanics. UQT provided us with such an opportunity. UQT equations show that the minimum distance to which the deuterons may approach each other depends greatly on the wave function phase. The future of the really controllable nuclear fusion system is not in primitive squeezing and heating of the material, but in collision of small energy nuclei with fine adjustment of wave function phase.

In principle, this can be achieved by applying the external controlling electromagnetic field upon the reacting system that contains quasi-fixed-ordered deuterium atoms and free (unbound) deuterons. The same properties may be also manifested by the special geometry of atomic frames. The diffractional scattering of deuteron flow on such frames will result in deuteron automatic selection in accordance with their energy and phasing. In this case the energy of colliding nuclei may be less than 1 eV.

Analysis of experiments made so far in CNF produces an impression that the reaction is effective only in cases of at least weak phasing, determined by either the inner structure of the environment or applied variable external fields. Apparently, in the course of their electrochemical experimentation M.

Fleischmann and S. Pons discovered this ordered system and observed occasional incomplete phasing that explained the experimental results.

In future reactor models, in contrast with the existing ones, only a very small portion of all deuterons will react simultaneously, their automatic selection being carried out by phase correlations. This will result in discharging small quantities of energy in a prolonged period of time until the reaching light nuclear source is exhausted. It is doubtful that such kind of nuclear fusion could be rightfully defined as "controllable".

Is it possible that the considered Vendee and Austerlitz of the eq. 3 will collide with Waterloo in Bohr-Sommerfeld problem and other cases, moreover taking into consideration my reasonable ignoring of the mass? What happened with the mass under the changing of the wave function phase? I can't give the precise answer. It has been assumed implicitly that the mass is either constant or a specific charge which depends on the phase. An application of the eq. 3, which was done for D-D interaction ad hoc doesn't result in failure of Bohr-Sommerfeld and scattering models. The states with $l > 0$ correspond to the electron trajectory similar to some beautiful flowers of buttercup sort. All results remind very much of the radial wave function, divided by spheric harmonics and can be used for good amusement at the computer during long nights.

If to calculate the electric field intensity E(r) for the spatial charge in term of the equation resolution of the UQT (1) and to observe the problem of the electron, passing through such a field (S-state), so there arise typical pendulum orbits, passing through the nucleus. Those orbits had been excluded in the classic Bohr-Sommerfeld model as absurd. As all of that doesn't contribute any new knowledge to atom physics, but has only art interest; we shall not dwell on it.

Apparently in atomic physics there are some situations when all the above said will not work. It doesn't mean the UQT failure, but means the eq. 3 roughness solely. Anyone can say: "if it is not the truth, it is a good invention". I would be very much surprised if God has ignored the beautiful chance of using the phase. If all that was said above is true it means that the resolving of the nuclear fusion problem is to be dealt with in a quite a different fusion already in 1983 (2) and all that is said above is the development of my old ideas. But the problem of nuclear fusion is the theme for further investigations.

My thanks to Prof. Vladlen S. Barashenkov (Dubna Jinr, Russia), Franz Mair (Innsbruck, MAITRON GmbH, Austria).

REFERENCES

[1] L.G. Sapogin, "I. Deuterium Interaction in Unitary Quantum Theory", Proceedings of the International Symposium on Cold Fusion and Advanced Energy Sources, May 24-26, 1994, Minsk, Belarus.

[2] L.G. Sapogin, "Clear-cut Picture of Micro World," *Technic for the Young*, no 1, p 41, 1983 (in Russian).

[3] G. Shaw, R. Bland, L. Fonda et al., *Il Nuovo Cimento*, vol 102b, no 4, p 1441 (1989).

NEW HYDROGEN (DEUTERIUM) BOHR ORBITS IN QUANTUM CHEMISTRY AND COLD FUSION PROCESSES

Jean-Pierre Vigier
Gravitation et Cosmologie Relativistes
Université Paris VI - CNRS/URA 769
Tour 22 = 4ème étage, Boîte 142
4, place Jussieu, 75005 Paris

ABSTRACT

It is suggested that recent confirmation of the existence in dense matter of very small quantities of fusion "ashes" both in electrolysis and glow-discharge experiments [1], can be heuristically interpreted (within the frame of conventional Quantum Mechanics and Nuclear theory) if one combines screening (i.e. tunneling) and the introduction of spin-spin and spin-orbit couplings with the usual effects of the Coulomb Potential in atoms and molecules.

The new Quantum Chemistry associated with the corresponding new tight Bohr orbits in dense matter explains [2] the observed excess heat [3] (above break even) and predicts the existence of fusion processes which become dominant at high energy current input [4].

As we shall now see, the formation of a new stable tight phase H_2^+ and D_2^+ of H_2^+ and D_2^+ can be justified, within the frame of present quantum theory (i.e. quantum chemistry), as a consequence of the introduction of spin-spin and spin-orbit forces (which always exist but cancel out in free-space due to random spin orientations) when they resonate with the surrounding electron plasma oscillations.

The existence of such new "tight" states is now supported by two facts: The exothermic formation [5] of the corresponding states which could correspond to resonance phenomena within the cathode (such as resonances within the electron clouds in internal regions suggested by Preparata). Their de-exitation (also corresponding to quantum jumps from one new Bohr orbit to another) leads to soft X-ray spectra... and X-rays have been observed in such experiments [1].

The formation of the new "tight" states H_2^+ and D_2^+ is not necessarily tied to the existence of the input current. Even when cut it can be supported by internal (ionization) currents or internal voltage differences carried by the Pd or Nickel... so that one could explain in this way, the existence of the "heat after death" phenomena discovered by Fleischmann and Pons [5]. The excess heat depends on the number of H_2^+ and D_2^+ (in light and heavy water) i.e. on the loading of the capillaries contained in the electrode. It is created only when they are formed, i.e. not necessarily immediately since individual capillary situations change with the metal. The corresponding binding energies have been shown [5] to be of the order of $\approx$50 kev instead of the usual $\approx$5 ev of quantum chemistry. The corresponding heat is $\approx$4 times as big for D_2^+ as for H_2^+.

As first basis for the new phenomena one can add (following a suggestion of Barut [6]) to the Coulomb Potential (utilized in Hydrogen and Deuterium) spin-spin and spin-orbit interactions. Usually neglected, they manifest themselves when $\vec{L},\ \vec{M}_1,\ \vec{M}_2$ are oriented (parallel) by internal electromagnetic interactions when H and D are in various types of electrodes. Indeed for two charged particles e_1, e_2 with magnetic moments $\vec{M}_1$ and $\vec{M}_2$ the usual quantum Schrödinger Hamiltonian is given by

$$H = \frac{1}{2m_1}\left(\vec{P}_1 - e_1\vec{M}_2 \times \frac{(\vec{r}_2 - \vec{r}_1)}{(r_1 - r_2)^3}\right)^2 + \frac{1}{2m_2}\left(\vec{P}_2 - e_2\vec{M}_1 \times \frac{(\vec{r}_2 - \vec{r}_1)}{(r_1 - r_2)^2}\right)^2 + \frac{e_1 e_2}{(r_1 - r_2)} - M_1 \cdot M_2 \cdot S_{12}(r_1 - r_2) \qquad (1)$$

where S_{12} is the usual dipole-dipole interaction tensor* and r their distance, i.e.

$$S_{12}(\vec{r}) = \frac{3\sigma_1 \cdot r_1 \cdot \sigma_2\, r - \sigma_1 \cdot \sigma_2}{r^3} + \frac{8\pi}{3}\vec{\sigma}_1 \cdot \vec{\sigma}_2\, \delta(\vec{r}) \qquad (2)$$

This 2-body problem with magnetic forces is separable, like the 2-body Coulomb problem. With

$$\vec{r} = \vec{r}_1 - \vec{r}_2 \qquad R = \frac{m_2\vec{r}_1 + m_2\vec{r}_2}{M_0} \qquad \vec{p} = \vec{p}_1 + \vec{p}_2$$

$$\frac{1}{\mu} = \frac{1}{m_1} + \frac{1}{m_2} \qquad P = \frac{m_2\vec{P}_1 - m_1\vec{P}_2}{M_0} \qquad M_0 = m_1 + m_2 \qquad (3)$$

still utilizing Barut's rotations [13] we obtain after some calculation

$$H = \frac{1}{2M_0}P^2 + \frac{1}{2\mu}p^2 - \vec{p}\cdot\frac{\vec{a}\times\vec{r}}{r^3} - \frac{\vec{P}\cdot\vec{b}\times\vec{r}}{r^3} + \frac{A}{r^4} + \frac{e_1 e_2}{r} - M_1 \cdot M_2\, S_{12}(\vec{r}) \qquad (4)$$

where

$$\vec{a} = \frac{e_1}{m_1}\cdot\vec{M}_2 + \frac{e_2}{m_2}\vec{M}_1\ ,$$

$$\vec{b} = \frac{e_1}{m_1 + m_2}\vec{M}_2 - \frac{e_2}{m_1 + m_2}\vec{M}_1\ ,$$

$$A = \frac{e_1^2}{m_2}M_2^2 + \frac{e_2^2}{m_2}M_1^2\ .$$

In the center of mass frame ($\vec{P} = 0$) we have

$$\mathrm{H}_{\mathrm{relative}} = \frac{1}{2\mu}p^2 - \vec{p}\cdot\frac{\vec{a}\times\vec{r}}{r^3} + \frac{A}{r^4} + \frac{e_1 e_2}{r} - M_1 \cdot M_2 \cdot S_{12}(\vec{r}) \qquad (5)$$

Using $\qquad -\vec{p}\cdot(\vec{a}\times\vec{r}) = \vec{p}\cdot(\vec{r}\times\vec{a}) = (\vec{p}\times\vec{r})\cdot\vec{a} = -\vec{a}\cdot(\vec{r}\times\vec{p}) = -\vec{a}$

we see that the second term corresponds to a charge-dipole potential, and the last term to a dipole-dipole potential.

In the special case $m_2 >> m_1$, $M_1 = 0$ hence $\vec{a} = \frac{e_1}{m_1} M_2$, $\vec{b} = 0$, $A = \frac{e_1^2}{m_1} M_2^2$, we have the simpler

Hamiltonian $$H_{relative} = \frac{1}{2\mu} p^2 + \frac{e_1 e_2}{r} - \frac{e_1 M_2}{m_1} \frac{\vec{\sigma} \vec{L}}{r^3} + \frac{e_1^2 M_2^2}{m_1} \cdot \frac{1}{r^4} \qquad (6)$$

We now try to solve exactly the eigenvalue problem $H\Psi = E\Psi$ with H given in equation (6). For simplicity we take the spin of the particle 2 to be 1/2.

As we shall see, following de Broglie [7], they are given by the relation

$$\frac{M^2 \hbar^2}{m_1 r^3} + \frac{\delta V(r)}{\delta r} = 0 \qquad (7)$$

where r denotes their radius and M an integer quantum number, multiplied by r^5 yields the relation:

$$\left(\frac{m^2 \hbar^2}{m_1} + B \right) r^2 = A r^3 + C r + D \qquad (8)$$

which can be written in the form $r^3 + a_2 r^2 + a_1 r + a_0 = 0$ (9)

Introducing $Q = (1/3) a_1 + (1/g) a_2^2$ and $R = (1/6) (a_1 a_2 - 3 a_0) - (1/27) 0_2^3$ we see that
-- with $Q^2 + R^2 > 0$ there is one real root and a pair of complex conjugate roots
-- with $Q^2 + R^2 = 0$ all roots are real and at least two are equal
-- with $Q^2 + R^2 < 0$ all roots are real.

Of course each real root denotes an infinite set (with m=1,2,...) of Bohr orbits. Introducing the two auxiliary quantities $S_1 = [R + (Q^3 + R^2)^{1/2}]^{1/3}$ and $S_2 = [R - (Q^3 + R^2)^{1/2}]^{1/3}$ one gets for these roots (which define three sets of Bohr orbits) the expressions

$$\begin{cases} r_1 = (S_1 + S_2) - \frac{a_2}{3} = f_1(m) \\ r_2 = -\frac{1}{2}(S_1 + S_2) - \frac{a_2}{3} + \frac{i\sqrt{3}}{2}(S_1 - S_2) = f_2(m) \\ r_3 = -\frac{1}{2}(S_1 + S_2) - \frac{a_2}{3} - \frac{i\sqrt{3}}{2}(S_1 - S_2) = f_3(m) \end{cases} \qquad (10)$$

which satisfy three constraints, i.e.:

$$\begin{cases} r_1 + r_2 + r_3 = -a_2 \\ r_1 r_2 + r_1 r_3 + r_2 r_3 = a_1 \\ r_1 r_2 r_3 = -a_0 \end{cases} \qquad (11)$$

According to the distance r one sees immediately
-- that when $A/r > (½) \cdot B/r^2 + (⅓) \cdot C/r^3 + (¼) \cdot D/r^4$ i.e. $Ar^3 > Br^2 + Cr + D$
one has a set of radii which varies like m^2 i.e. which corresponds to Bohrs initial orbits when $\theta = \pi/2$.

-- that when $C/3r^3 > A/r + (½) \cdot B/r^2$ i.e. $Cr > Ar^3 + D$ then $r \simeq C\, m_1 / m^2 \hbar^2$.

This set varies like $1/m^2$ and corresponds to a set of "tight" orbits never discussed by Bohr.
-- that when $(¼) \cdot D/r^4 > (⅓) \cdot C/r^3 + (½) \cdot B/r^2 + A/r$
then $r \simeq (D\, m_1 /m^2 \hbar^2)^{½} = (D\, m_1)^{½}/m\hbar$ a set which also yields a new set of "tight" Bohr orbits unknown in the literature.

Since a detailed analysis of the corresponding new Bohr energy levels is in preparation (and will shortly be published) we will now limit ourselves to the following remarks. The existence of these new "deep" Bohr levels depend, of course, on the relative spin (and spin-orbit) orientations, i.e. they can only be excited in special physical situations where they are determined by their surroundings. This appears now to be the case when Hydrogen-Deuterium, etc. are imbedded in dense media.

When one utilizes D_2 or other types of fusion material, the creation of excess heat by the tight D_2^+ states is generally accompanied by some real fusion processes: since an electron (when located by ions) behaves (within the deeper potential due to spin-spin and spin-orbit forces) as if it had acquired a heavier "effective" mass [4]. Indeed smaller Bohr orbits facilitate tunneling through the Coulomb barrier. Moreover, "heavier" electrons also explain some types of observed regular collective motions (i.e. cluster formations) which can contain triangular, tetrahedral, cubic ... configurations which move collectively and have been observed to have strongly enhanced cross sections (by many orders of magnitude) with individual particles. This configuration naturally arises when the Ampère force cuts the current into beads in a capillary since the situation of the ions then resembles what happens to fast going cars which crash successively into each other during a slowdown (accident) on a modern highway.

This situation is very different from the usual quantum mechanical interpretation of chemical phenomena, i.e. of the normal states of H_2^+ and D_2^+ which are assumed (according to the Born-Oppenheimer approximation) to correspond to the rapid motion of the electron in the field of two almost fixed nuclei. If one first neglects the spin and considers two masses M (with charges z) rotating at a distance r from a mass (charge z) i.e.

Fig. 1

z		z
M r	m	r M

this gives the Hamiltonian $H = \frac{2P^2}{2M} + \alpha\left(\frac{2Zb}{r} + \frac{Z^2}{2r}\right)$ (12)

which yield when quantized by the usual Bohr-Sommerfeld method ($\int pdq = n\hbar$)
with ($\hbar = C = 1$); Energy levels $E_n = - (¼) \{M\, \alpha^2/n^2\}\, Z^2\, (2z + Z/2)^2$ i.e.

-- For the He atom this yields $E_0 = 6{,}12$ Ryd close to the observed value $\simeq 5{,}69$ Ryd.

-- For H_2^+ and D_2^+ the Bohr energy levels are approached by $E_n = -(9/16)\ (M\ \alpha^2/n^2)$

which correspond to ground states of 28.1 KeV for H_2^+ and D_2^+. The first stage of this model, i.e. the existence of excess heat in H or H_2O experiment (in the author's opinion) can be considered as already proven by a growing set of experiments [1,3]. These experiments show the existence of a non-fusion origin for presently observed excess heat and seems to exclude its interpretation in terms of virtual neutron exchange.

The second stage, i.e. the existence of new "tight" molecules such as H_2 or D_2, is in fact already suggested by the experiments of Mills et al. [6] which have detected by cryometry and mass spectrometry the existence of new tight states of H_2.

To quote the authors "an exothermic reaction is reported wherein the electrons of hydrogen atoms and deuterium atoms are stimulated to relax to quantized potential energy levels below that of the *ground state* via electrochemical reactants K^+ and K^+; Pd^2+ and Li^+, or Pd and O_2 of redox energy resonant with the energy hole which stimulates this transition. Calorimetry of pulsed current and continuous electrolysis of aqueous potassium carbonate (K^+/K^+ electrocatalytic couple) at a nickel cathode was performed. The excess power out of 41 watts exceeded the total input power given by the product of the electrolysis voltage and current by a factor greater than 8. The "ash" of the exothermic reaction is atoms having electrons of energy below the *ground state* which are predicted to form molecules. The predicted molecules were identified by lack of reactivity with oxygen by separation from molecular deuterium by cryofiltration, and by mass spectroscopic analysis [8].

The third stage, i.e. the prediction of H_2 or D_2 to explain excess heat at low energy input can also be considered as supported by the experiments of Miles, Bush et al. [10] which report ^{4}He (which they did not attempt to distinguish from D_2) and by the experiment of Yamaguchi and Nishioka [10] who have detected by mass spectroscopy (along with fusion "ashes" ^{3}He with an energy of 4-5-6 Mev and protons with an energy of 3Mev) ^{4}He accompanied (as it should in our model) by a heavier D_2 peak. Their input being dominant at low input. Further search for soft X-rays and also for the existence of H_2^+ in H or H_2O experiments would help to prove (or disprove) the proposed model.

Proof of the last stage, i.e. the possibility to add to the excess heat (generated by the new Bohr orbits) fusion energy generated by high energy input pulses is still in infancy [4] due to reluctance to accept the existence of the new phenomena.

REFERENCES

[1] Y.R. Kucherov et al., *PLA* 170 (1992) 265 and J. Dufour, *Fusion Technology*, vol 24 (1993), p 205.

[2] J.P. Vigier, Frontiers of Cold Fusion, Proc. of Third International Conference on Cold Fusion, Nagoya, Japan, Universal Acad. Press, H. Ikegami, Ed. (1993).

[3] For example see the contributions of Drs. McKubre, Takahashi, Kunimatsu and Storms in Frontiers of Cold Fusion, Universal Acad. Press Inc., Tokyo (1993) H. Ikegami, Ed.

[4] R. Antanasíjević, I. Lakicević, Z. Marić, D. Zević, and J.P. Vigier, *PLA* 180 (1993) 24.

[5] M. Fleischmann and S. Pons, see Proceedings ICCF4 in Hawaii (6-9 Dec. 1993).

[6] A. Barut, "Prediction of new tightly bound states of $H_2^+(D_2^+)$ and `cold fusion experiments'," private communication (1992).

[7] L. de Broglie, "Non-linear Wave Mechanics," Elsevier, Amsterdam (1960). See also A.O. Barut and M. Basic, *Ann. Found. L. de Broglie*, vol 15 (1990), p 67.

[8] R.L. Mills, W.R. Good and R. Shanbach, "Dihydrino Molecule Identification," *Fusion Technology* (in press).

[9] See A. Takahashi et al., Proc. 2d Como Conference on Cold Fusion, The Science of Cold Fusion, Ital. Physical Soc. publ. (1992).

[10] E. Yamaguchi and T. Nishioka in Frontiers of Cold Fusion (see ref. 3) and M. Miles, B. Bush et al. in The Science of Cold Fusion (see ref. 8).

INTERNAL CONVERSION MECHANISM IN COLD FUSION

Chuan-Zan Yu, Yi-Fang Chang
Department of Physics
Yunnan University, Kunming, 650091, China

ABSTRACT

By using the internal conversion mechanism inside the nucleus, a possible solution for cold fusion is discussed. When a target nucleus reacts with the pellet nucleus (P^+, D^+, or T^+, etc.), an internal conversion electron emitted from the target nucleus is absorbed by the pellet nucleus, which becomes a neutral nucleus, so the Coulomb barrier of the target nucleus can be passed through easily, then a nuclear reaction happens. Since the internal conversion coefficient $\alpha \propto Z^3$. It will be favorable to those heavy nuclei. The mechanism can solve the difficulty of the barrier penetration and a part of the fusion energy is transformed to the electromagnetic radiation. Further, some results may be detected by the experiments.

The analysis of numerous experiments [1,2] and the calorimetric studies of the Pd-D_2O and Pd-D systems [3,4] at ICCF4 have proved that nuclear reactions exist in cold fusion. But the physical mechanism of cold fusion waits still for further research. When n(D)/n(Pd) > 0.83, cold fusion may happen in a Pd-D system. The Hamiltonian function of the system is approximately

$$H = H_1 + H_2 + H_{int} \tag{1}$$

$$H_{int} = \sum_i Ze^2 / | r_i - R | , \tag{2}$$

where H_1 and H_2 are the Hamiltonian function of a target nucleus, whose charge is Z, and a pellet nucleus (P^+, D^+ or T^+), respectively.

The reaction between both nuclei is mainly the Coulomb force. It produces many photon transitions from infrared ray to X-ray. But, even if we have introduced the multistage nuclear reaction mechanism, the penetration factor at very low energy is small [5].

This paper is analogue with the internal conversion theory of nuclear physics, a possible mechanism of cold fusion is discussed. The transition probability formula of internal conversion electron is

$$W_{fI} = 2\pi \int | \langle F | H_{int} | I \rangle |^2 \rho \, dv , \tag{3}$$

where I and F are the wave functions on initial and final states, ρ is the density of energy levels of an initial state. It may be estimated by a formula

$$\rho(E) = 1/D(E) = Ce^{2\sqrt{aE}} , \tag{4}$$

Where E is excited energy, D is an interval of energy levels, C and a are two parameters. The equation

(3) is

$$W_{fI} = 2\pi c e^{2\sqrt{aE}} \int |<F| H_{int} | I>|^2 dv. \tag{5}$$

$$<F| H_{int} | I> = <\psi_f u_f | H_{int} | \psi_i u_i>$$

$$= \sum_{i=1}^{Z} \int d^3 R \int d^3 r_i \psi_f u_f \frac{1}{|R - r_i|} \psi_i u_i, \tag{6}$$

$$\frac{1}{|R - r_i|} = \sum_{L,M} \frac{4\pi}{2L+1} \frac{r_i^L}{R^{L+1}} Y_{LM}(\Theta, \psi) Y^*_{LM}(\Theta_i, \varphi_i), \tag{7}$$

and

$$\frac{1}{|R - r_i|} = \begin{cases} \Sigma \frac{r_i^L}{R^{L+1}} P_L, & (R > r_i \quad outside\ nucleus) \\ \Sigma \frac{R^L}{r_i^{L+1}} P_L & (R \le r_i \quad inside\ nucleus) \end{cases} \tag{8}$$

It is called the finite nucleus effect, which is important for heavy nucleus, whose Z is larger. The internal conversion electron is a mechanism which compete with the photon transition, therefore the integral inside nucleus contributes and the internal conversion electron is emitted from the nucleus, when the photon transition is forbidden and the integral outside nucleus is zero. Through the simplification from equation (5)

$$W_{fI} = A \sum_L \frac{K^{2L-3}}{[(2L+1)!!]^2} \sum_M |Q_{LM}|^2 \tag{9}$$

can be obtained, where K is wave function of the internal conversion electron, A is a total constant, $\Sigma |Q_{LM}|^2$ is reduced, transition probability of the photon transition, so the internal conversion coefficient is

$$\alpha = \frac{\omega_{fi}}{\omega_8} \simeq BZ^3 \frac{L}{L+1} \left(\frac{2mc^2}{E} \right)^{L+5/2} \tag{10}$$

which is directly proportional to Z^3, so it increases rapidly for the heavy nuclei. For example, the energy level density D(E) of Pd nuclei is larger, D(E) ≈ 1 - 100ev for A ≈ 100. A series of the photon transitions from infrared ray to X-ray may happen for the D-Pd system, E_r ~ 1-100ev. In this case, both nuclei are resisted by the Coulomb barrier, the nuclear reaction is difficult. But if the photon energy reaches a threshold value, for instance, E ≈ 130 KeV, which had been found by Jiang Tang He and Peter Hagelstein et al., an internal conversion electron is emitted from the Pd nucleus, and is combined with a deuteron to become a dineuteron n^2 [6], so there is no obstacle of Coulomb barrier to the target nucleus, the nuclear reaction may produce

$$Pd^{A} + D^{+} \rightarrow Ag^{A} + e^{-} + D^{+} \rightarrow Ag^{A} + n^{2} \rightarrow Ag^{(A+2)*}\ , \qquad (11)$$

so various nuclear reactions in the References [1,2] can happen. An excited nucleus $Ag^{(A+2)*}$ produces a symmetric bifission, e.g., V and Cr, etc., the fission release energy $E_f \sim 36 - 43$MeV, which is larger than the fission barrier, so the fission should happen instantaneously. If it is $Pd^{102} \rightarrow 2V^{51}$ + 20 MeV, the fission release energy is smaller than the fission barrier, the probability of the spontaneous fission is very small.

Since the fission release energy is very high, an excited energy per fragment is 15 - 20Mev, which can evaporate neutron or can release a pair electron e^{+} e^{-} or electron e^{-} of internal conversion, these phenomena will compete with the photon transition. Moreover, the neutron n may raise another fission. The electrons at high energy may produce bremsstrahlung, so a part of the energy will transform to an electromagnetic radiation. If $e^{+}e^{-}$ happens, the annihilation effect should appear for a process of the slowing-down of the positrons, then a characteristic radiation E_r = 511 KeV will be able to be detected by the experiment.

A D-D system is a boson. The multiple D-D systems possess the Bose-Einstein condensation. When two deuterons are very close to each other, the photon transition will appear. Further, if both nuclei combine, the binding energy of 23.8 MeV will be released, then the system will transit to a stable state. When the D-D system forms a compound nucleus, an internal conversion electron will be produced,

$$D^{+} + D^{+} \rightarrow D^{+} + e^{-} + He^{2} \rightarrow n^{2} + He^{2} \rightarrow He^{4*} \qquad (12)$$

The spin-parity of n^2 may be 0^+ or 1^+, one of He^2 is 0^+ or 1^+, so one of He^{4*} should be 0^+, 1^+ or 2^+. The binding energy emmited from an excited nucleus He^{4*} to ground state is ΔE = 23.8 MeV. The spin-parity for the ground state He^4 is 0^+. Because the photon transition cannot happen for $0^+ \rightarrow 0^+$ and $2^+ \rightarrow 0^+$, it is necessary that He^{4*} releases energy mainly through a competition between the internal conversion electrons $e^{+}e^{-}$ (or e^{-}) and multistage photon transitions. The electrons at high energy may produce bremsstrahlung, whose energy is lower than X-ray, so the greatest part of the energy will transform to electromagnetic radiation. Therefore, it should be much less for $D+D \rightarrow He^3 + n$(2.45 Mev) and $D+D \rightarrow T+P$(3.03 MeV), and which is consistent with the present experiments.

REFERENCES

[1] Chuan-Zan Yu, Yi-Fang Chang, ICCF4, T2.4; *Fusion Facts,* vol 5, no 7, (1994) p 26.

[2] Chuan-Zan Yu, Yi-Fang Chang, Hui-Lan Wang, ICCF4, T2.11; *Fusion Facts,* vol 5, no 7, (1994) p 25.

[3] M. Fleischmann, S. Pons et al., ICCF4, C1.1.

[4] M.C.H. McKubre et al. ICCF4, C1.5.

[5] Yi-Fang Chang, Chuan-Zan Yu, ICCF4, T2.8; *Fusion Facts,* vol 5, no 7, (1994) p 21.

[6] Fu Yang Jie et al., ICCF4, T3.5; *Fusion Facts,* vol 5, no 7, (1994) p 24.

INTRODUCTION TO COLD FUSION TUTORIAL PAPERS

This Cold Fusion Source Book is meant to be used by many persons who are not cold fusion experts. Therefore, we have invited some papers which are designed to acquaint the reader with some of the important features of electrochemistry. We have also included in this section a paper by Dr. Li describing five years of cold nuclear fusion research in China.

For those who desire to perform their own experiments, we strongly advise your careful consideration of other papers. For example, the paper by Dennis Cravens (Proceedings of the Fourth International Conference on Cold Fusion, Hawaii, Dec, 1993). In addition, the new publication ***"Cold Fusion"*** is expected to be a source of practical experimental information.

The staff at the Fusion Information Center (publishers of this book) can also be of help to cite appropriate sources of information. An extensive bibliography on computer diskette is designed to go with purchased copies of this volume. Also, serious researchers should subscribe to the monthly newsletter, *Fusion Facts* for a continuing source of latest information on developments in cold fusion.

ELECTROCHEMISTRY, TRITIUM AND TRANSMUTATION

J. O'M. Bockris and R. Sundaresan
Department of Chemistry
Texas A&M University
College Station, TX 77843

INTRODUCTION

It is known that nuclear phenomena can be brought about in the cold, e.g., in cells containing D_2O in contact with a palladium electrode, in molten salt cells which contain lithium hydride, in light water cells in contact with nickel electrodes, in cells involving arcs in hydrogen and deuterium, in cells involving high potential differences across a series of palladium electrodes separated by membranes and those involving nickel electrodes under the influence of high frequency radiations.

However, most of these nuclear reactions at low temperatures have been carried out under electrochemical confinement and for this reason a brief outline of these cells is given as a background here.

Two other topics are briefly reviewed: the first published synthesis of tritium from deuterium in the cold, and some aspects of transmutation under conditions which have temperatures in the region of 1000 degrees.

RELEVANT ASPECTS OF ELECTROCHEMISTRY

The Electrochemical Cell

The typical electrochemical cell is shown in Fig. 1. It is filled with, say lithium hydroxide dissolved in heavy water. There are three elements: One is the working electrode (WE) at the interface of which with respect to the solution the electrochemical events occur. Of lesser importance is the counter electrode (CE) which serves to complete the circuit between the working electrode, the power source, and the solution. There is also a reference electrode (RE) as shown in Fig. 1. The potential of the working electrode is measured with respect to that of the reference electrode by means of a high resistance voltmeter.

Most people think that when we refer to the "electrode potential", we are referring to the potential difference between the working electrode and the solution. In fact, "electrode potential" has a complex meaning [1].

The reference electrode is generally the thermodynamically reversible hydrogen electrode. In practice, one sets up a piece of platinum covered with an active form of electrodeposited platinum ("platinum black") at which the reaction $2H^+ + 2e \rightleftharpoons H_2$ occurs and is at equilibrium.

Thus, the so-called electrode potential consists of three potential differences. The first is the one which we would like to know, - and the one which controls the phenomena at the boundary of the working electrode and the solution. But, there is another potential, seldom mentioned, which occurs at the join between the working electrode (consisting, say, of silver) and the reference electrode where the material

is platinum. Here, a contact potential difference develops and contributes to the overall potential which comes into what we call the potential on the hydrogen scale. There is, of course, the third potential which occurs at the interface between the reference electrode and the surrounding solution. Of these three potentials, however, the one at the boundary of the working electrode and the solution is the most important.

Equilibrium and the Exchange Current Density

When the working electrode is in equilibrium (at the equilibrium potential, E°), the rate of electrons leaving the electrode for the solution is equal and opposite to that of electrons leaving the solution for the electrode. Thus there is a dynamic equilibrium. There is no net reaction and the net current is zero. The rate of this equilibrium reaction, in one direction, stated in terms of amps per square centimeter, is the "exchange current density" and it is represented by a symbol, i^0.

Overpotential

In order that a net electrode reaction takes place, the working electrode potential is to be displaced from the equilibrium value, E^0, (using an external power supply) either in the negative or in the positive direction. This displacement is called the "overpotential", η. When the potential is displaced in the negative direction, for example, the net reaction is one in which electrons leave the electrode for the solution and a `net' cathodic current flows. The relationship between this current and the overpotential is given by

$$i = i_0 e^{-\beta\eta F/RT}$$

Here the symbol F means the number of coulombs which reside upon gram ion of univalent ions, R is the gas constant and T is the absolute temperature. The symbol β refers to the "symmetry factor" [2] and the value to use for rough calculations is 0.5.

Suppose we have a negative overpotential of 0.5 V, and an exchange current density of 10^{-6} amps cm^{-2}, the current density is c. 10^{-2} amp cm^{-2}. If one changes the overpotential by about 0.1 volt, the current density or rate of reaction changes by about 10 times.

Fugacity

In discussions in the theory of cold fusion, one sometimes hears the term "fugacity."

Considering the pressure-volume relationship of a gas at high pressures, one of the relations which is often given is the equation due to Van der Waals [3]. It runs as follows:

$$\left(P + \frac{a}{V^2}\right)(V - b) = nRT$$

The term V in the equation is the total volume available to the gas and the term n allows for the volume of the gas molecules themselves. Here the pressure P is what one actually measures. But, the reason for the term $\frac{a}{V^2}$ is to allow for the fact that the measured pressure is less than the pressure which occurs inside the gas. When gas molecules strike a sensor, they experience non-isotropic forces, i.e., they are pulled back towards the gas and consequently the pressure registered is less than the pressure within the

fugacity. Fugacity enters electrochemistry and cold fusion in an important way.

Thus, the fugacity of deuterium gas inside a cavity within a palladium electrode is given by the equation [4]

$$f_{H_2} = e^{-\chi\eta F/RT}$$

The factor x varies according to the mechanism of the hydrogen evolution reaction. It can be as high as two or as low as one half.

Thus, the fugacity inside a cavity for η = -1.0 V and x = ½ is 10^8 Atm, a very high value, while the measured pressure will be ~ 10^4 Atm.

TRITIUM

The first formation of tritium to be described in a refereed publication was carried out by a graduate student, Nigel Packham, in the Department of Chemistry at Texas A&M University. In those days (April-May 1989), there was enormous excitement in the Electrochemistry Laboratory and the entire group of about eighteen people were working in shifts of about twelve hours each through the night and seven days per week.

We did not know the conditions for bringing about the nuclear reactions reported by Fleischmann and Pons, so we took the attitude that it would be better to try all kinds of different conditions. Thus, we used electrodes which were untreated, annealed, worked and fused. We cleaned the surface in various ways in addition to leaving it untreated.

We had as many as 18 cells working at the same time. Only a few of these cells were properly controlled electrochemical cells with reference electrode, etc. Many of them were simple test tube cells with a palladium wire cathode and a platinum or nickel anode wrapped around it.

We were trying to find the abnormal heat produced by the cells. However, we looked in addition for the formation of tritium because, obviously, if one has deuterium inside a cell under high fugacity, and a nuclear reaction occurs, one would expect to find tritium in the electrode and eventually in the solution.

Electrolyte samples were analyzed in the Department of Nuclear Engineering for tritium. We were at first disappointed, for, the readings showed only an increase which corresponded to that expected by the classical theory of electrolytic enrichment (for the separation factor of 2 between deuterium and tritium, this comes to an increase of about two times). One day, however, still in April, there was a sudden large increase in tritium counts. At the beginning of the experiment these were of the order of 100 but increased to between 10^4 and 10^5, 10^2 - 10^3 times above background!

During the next few months, Nigel Packham himself and then, latterly, Ramesh Kainthla and Omo Velev were able to find tritium in a total of 15 cells during 60 runs[5,6]. These experiments were made largely with palladium in D_2O solutions of LiOH 0.1 mole. However, there were some findings of tritium in titanium electrodes.

We often allowed the experiments to run for a very long time, up to eight weeks in some cases. Tritium was seldom found at less than 100 hours and the average time after which we found tritium was around

500 hours. One can easily see that most persons would have judged the experiment a failure long before this time.

The occurrence of tritium was sporadic. It occurred in bursts. These bursts would last for several hours and on one occasion about one month. [Thus, in a recent paper by Will and Cedzynska[7], so-called "reproducible" measurements of palladium are reported. However, it is made clear in this paper that the reproducibility obtained was by four measurements on exactly the same kind of palladium and when this palladium was changed to palladium of another origin (perhaps with a different surface structure) no tritium was obtained.]

We tried at first to associate the heat with the tritium and indeed in one run (cf. Fig. 2) it seemed there was some parallelism [6]. However, simple calculation showed that the amount of nuclear heat which would be associated with the tritium would only explain about 0.1% of it. This was the first hint that the tritium formation was a side show in the major heat producing reaction. It had importance historically because the finding of other nuclear debris (helium and transmuted metals) is more difficult to discover from the experimental point of view, that the existence of tritium at this early time and its confirmed finding later in many laboratories was the foundation belief in the existence of nuclear reactions under solid state confinement.

Work on tritium went on and, later, in 1992, Chien and Hodko [8] found both tritium and helium in the same electrode (cf. Fig. 3). Chien also found He^4 in his electrode. [Determination made by Nate Hoffman and Brian Oliver, at Rockwell International. This finding corresponded to that of Melvin Miles at China Lake who made the more difficult experiment of finding helium in the gas phase. It had importance in confirming that the tritium which had been produced was not from spot contamination of the palladium with tritium, for the helium formed under these conditions would have been ^3He and not ^4He.]

Hodko also found later [9], using a technique first originated by Szpak and Boss, that the tritium could be brought up to ~ 66% reproducible by using gold electrodes on which deuterium and palladium were simultaneously plated out. However, the amount of tritium then found was a few times above the electrolytic enrichment factor.

TRANSMUTATION

It is possible to regard the reactions which form tritium as D^+-D^+ collisions but the distance apart of the D's and in the Pd lattice is greater than that in D_2. It may be possible to interpret them better from a reaction of D with Li^6 or Pd.

To test the possibility of transmutation reactions with elements of higher atomic weight, several experiments have been tried out in our group. The first was due to the suggestion of J. Champion, who claimed that he had found in 1986 that the imposition of radio frequencies caused the emission of an anomalous heat. Such a phenomenon was witnessed by Kainthla and Velev in 1989 [10]. [This work is similar to independent work carried out by D. Letts [16, 17] and also D. Cravens [18]. They describe a procedure in which a palladium cathode, sufficiently charged with deuterium (D/Pd ~ 0.9), was subjected to RF fields of moderate (30 - 100 mW) power or magnetic fields of about 200 Gauss; excess heat was observed in a very short time.]

Champion suggested that, by manipulating the frequencies to match the magnetic moments of individual isotopes, he could provoke a nuclear change in ions dissolved in solution. Experiments of this kind were

tried in Texas A&M laboratories in 1992 (under the sponsorship of W. Telander in a project known as the Philadelphia Project) but failed. Champion also suggested heat pulsing and provided a technique of applying a rapid heat pulse to mixtures of mercurous or lead chloride with KNO_3 and carbon. Radioactivity was observed ($\tau_{½} \simeq 20$ hrs) and in some runs up to 300 ppm of precious metals were found. However, the results were not reproducible.

One of the claims to have provoked a nuclear transmutation reaction concerns conversion of carbon to iron and was recently tried out in my laboratory. The technique was simple. Two spectroscopically pure iron rods with sharpened points were immersed in super-pure water and an arc was struck between them. The carbon detritus which fell to the bottom of the cell was analyzed and was found to contain an amount of iron higher than that had been present initially (as impurity) in the carbon rods.

Table 1 gives the results of this work by Sundaresan and Bockris [11]. Similar results have been reported by others, too [12, 13].

A mechanism suggested by Sundaresan and Bockris is as follows.

$$2\ {}^{12}_{6}C + 2\ {}^{18}_{8}O \rightarrow\ {}^{56}_{26}Fe +\ {}^{4}_{2}He$$

Transmutation reactions under solid state confinement have been reported by K. Wolf [14]. It was found that a palladium electrode which had become saturated with deuterium by means of electrolysis contained a large number (more than one dozen) of new nuclei. Kucherov [15] observed that, following a glow discharge between palladium electrodes in D_2 atmosphere, many elements were formed in the palladium electrode, some amounting to as much as 0.1 atomic percent.

During 1992-1993, a host of other reports became available which referred to experiments in which the formation of new nuclei under circumstances similar to those described have surfaced. A table comprising some of these reports is given here (Table 2).

REFERENCES

[1] Modern Electrochemistry, J.O'M.Bockris and A.K.N. Reddy, Plenum/Rosetta, New York, 1977, Chap.7.

[2] Ibid., Chap.8.

[3] Physical Chemistry, P.W.Atkins, W.H.Freeman and Co., San Francisco, 1982, Chap. 1.

[4] J.O'M. Bockris, D. Hodko and Z. Minevski, Electrochemical Society Proceedings, Edited by D.A. Corrigan and S. Srinivasan, vol 92-5 (1992) p 223.

[5] N.J.C. Packham, K.L. Wolf, J.C. Wass, R.C. Kainthla and J.O'M. Bockris, *J. Electroanal. Chem.*, vol 270 (1989) p 451.

[6] G.H. Lin, R.C. Kainthla, N.J.C. Packham, O. Velev and J.O'M. Bockris, *Int. J.Hydrogen Energy*, vol 15 (1990) p 537.

[7] F.G. Will and K. Cedzynska, *J. Electroanal. Chem.*, vol 360 (1993) p 161.

[8] C.C. Chien, D. Hodko, Z. Minevski and J.O'M. Bockris, *J. Electroanal. Chem.*, vol 338 (1992) p 189.

[9] D. Hodko and J.O'M. Bockris, *J. Electroanal. Chem.*, vol 353 (1993) p 33.

[10] R.C. Kainthla and O. Velev, private communication to J.O'M.B.

[11] R. Sundaresan and J.O'M. Bockris, *Fusion Technology* (communicated).

[12] K. Nakamura, O. Horibe, I. Ogura, and M. Odagiri, *Chemistry Express* [Kinki Chemical Society, Japan], vol 8 (1993) p 344.

[13] V.B. Kartha et al., private communication on pre-publication results to R.S.

[14] Private communication to J.O'M.B.

[15] A.B. Karabut, Ya.R. Kucherov and I.B. Savvatimova, Proc. ICCF3, Oct.21-25, 1992, Nagoya, Japan p 165.

[16] J.O'M. Bockris, R. Sundaresan, D. Letts and Z. Minevski, Proc. ICCF4, Dec. 6-9, 1993, Maui, USA, Abstr.# C 1.4.

[17] D. Letts, ibid., Abstr. # C 4.2.

[18] D. Cravens, ibid., Abstr. # C 3.12.

Table 1. Values of Iron in the Carbon Detritus After Arcing

Experiment No	Wt of carbon detritus (mg)	Fe content (μg)	ppm Fe in carbon
1	269	45	167
2	116	---	---
3	167	---	---
4[x]	361	45	125
5[x]	103	15	146
6	231	---	---
7	192	11	57
8	183	5.5	30
9	163	13.5	80
10	143	---	---
11	138	---	---
12	130	5.5	42
13[x]	471	53	112
14[1]	477	196	410

[x]same rod

[1] This value is abnormally high; it is possible that an instrument malfunction might have caused the error.

Table 2. Some Attestation of Low Energy Nuclear Change in Condensed Media (December 1993)

Authors	Date	Reference	Epiterne
P.I. Dee Cambridge Un.	1934	Nature, 133, 564	Deuterium beam onto $(NH_3D)_2SO_4$ gave DT
Kushi	1976	Michio Kushi, Boston, East West Foundation, Vol 3, (1976)	C → Fe, arc in water
N.J.C. Packham et al. Texas A&M Un.	1989	J. Electroanalyt. Chem. 270 (1989), 451.	Tritium formed from D dissolved in Pd and at high fugacity
G. M. Miley et al. Un. of Chicago	1991	ICCF 2, paper No.?	Odd isotopic anomalites interpreted in terms of low energy nuclear reactions such as: ^{2}H + ^{238}U ^{239}U + ^{1}H.
Enyo & Natoya Hokkaido Un.	1992	ICCF, 4 Paper, N2.1	K Ca
K. Wolf, Texas A&M Un.	1992	Priv. Comm. T. Passal (EPRI), T. Claytor (Los Alamos)	3 Pd electrodes, after D_2 evolution showed γ and x-rays. Analysis showed many new elements, concentration $\sim 10^3$ atoms cc^{-1}. But not reproducible.
Kucherov, Lutch Institute, Moscow	1993	ICCF, Paper N3.7	Found new elements after glow discharge Pd in D_2 Na, In Ag Zr, Nb, Sn + 10 others. Many new materials
Stringham	1993	ICCF,4, paper C3.8	Sono-luminations of C-saturated Pd in solution He^4 + Cd^{114}
Ohmori & Enyo Hokkaido Un.	1993	ICCF, N 2.3	H_2 electrolysis on Au electrodes produces heat + Fe Fe has isotopic abundance significantly different from normal one
Sundaresan, Texas A&M Un.	1993	Submitted J. Fusion Technology	C Fe, arc in water

Kim & Yoon, Purdue Physics Dept., Zubarov, Hebrew Un., & Rabinowitz, EPRI	1993	ICCF 4 T.2.2	Coulomb barrier is transparent to protons and deuterons in resonance condition. Discusses possible nuclear reaction D + Pd He^4; D + Li and involvement ^{39}K and ^{40}Ca, in solid lattice
Chuan-Zan and Yi-Fang, Yunnan Un., Physics Dept., PRC	1993	ICCF.4 T 2.4	Outrightly transmutational. All anomalous heat is due to formation new elements in lattice. > 10 nuclear schemes and reaction sequences suggested. Should expect Ag, Si, Au and many other new nuclei in Pd with H and/or D
Bazhutov, et al., Erzion Center, Moscow	1993	ICCF.4 T 4.9	Outrightly transmutational. There is no cold fusion: only transmutation in the Pd lattice to form numerous new elements
Koretsky, Erzion Center, Moscow	1993	ICCF T 4.10	Treats production of stable isotopes in lattice. States production of gold from mercury-attractive prospect [Sic]
Koretskiy, Erzion Center, Moscow	1993	ICCF.4, Paper 7 4.1?	Discusses cold nuclear transmutation reactions in solid lattices. Suggests high speed centrifugation; seems to suggest has found enrichment of Ni-64; Mo-100; Te-130; Xe-136; W-184 and Os-192
F. Will et al. EPRI	1993	J. Electroanalyt. Chem. 360 (1993), 161.	Tritium formed reproducibly from D dissolved in Pd. Cites 14 papers in peer reviewed journals, report same. Reports extensive testing contamination hypothesis negative.

Singh et al. Bhabha Atomic Research	1993	Priv. Comm. from BARC Center. Ms. available	C Fe arc in water
Nakamura Jr. of Tokyo	1993	Chemistry Express, 8, 341	C Fe arc in water
Bush & Eagleton Pomona Polytechnic	1993	ICCF 4, paper No. 2.2	Ca from K, Sr from Rb (Isotopic distribution radically different from normal)
Dash Jr. of Oregon	1993	ICCF 4 paper N 2.1	Light water electrolysis Ag and Au appearing in Pt
Dufour, Shell Oil Co. Research (Paris)	1993	ICCF,4 Paper N1.6	Predicts creation of new metals from Pd D reactions. Finds 4 new metals
Miles & Bush, China Lake, Navy Station	1993	ICCF,4, paper C.2,9	All steel equipment prevents leaks from air. He⁴ in gas is 1/3rd that necessary account heat on D + D $He^4 + \gamma$
Srinivasan et al., Bhabha Atomic Research, India	1993	ICCF,4 c. 3.8	Obtained heat and tritium from light water cells
Romodanov et al., Lutch Institute, Moscow	1993	ICCF,4 Paper N.3	Reproducible tritium from glow discharge
Hagelstein, MIT	1993	ICCF,4 Paper T.1.1	Theory of neutron transfer reactions and lattice induced low energy nuclear changes
Li, Physics Dept., Beijing Un.	1993	ICCF,4 T 2.1	In low energy nuclear charge in solids, his theory show no γ radiation (sic). Main expectation is β (sic)

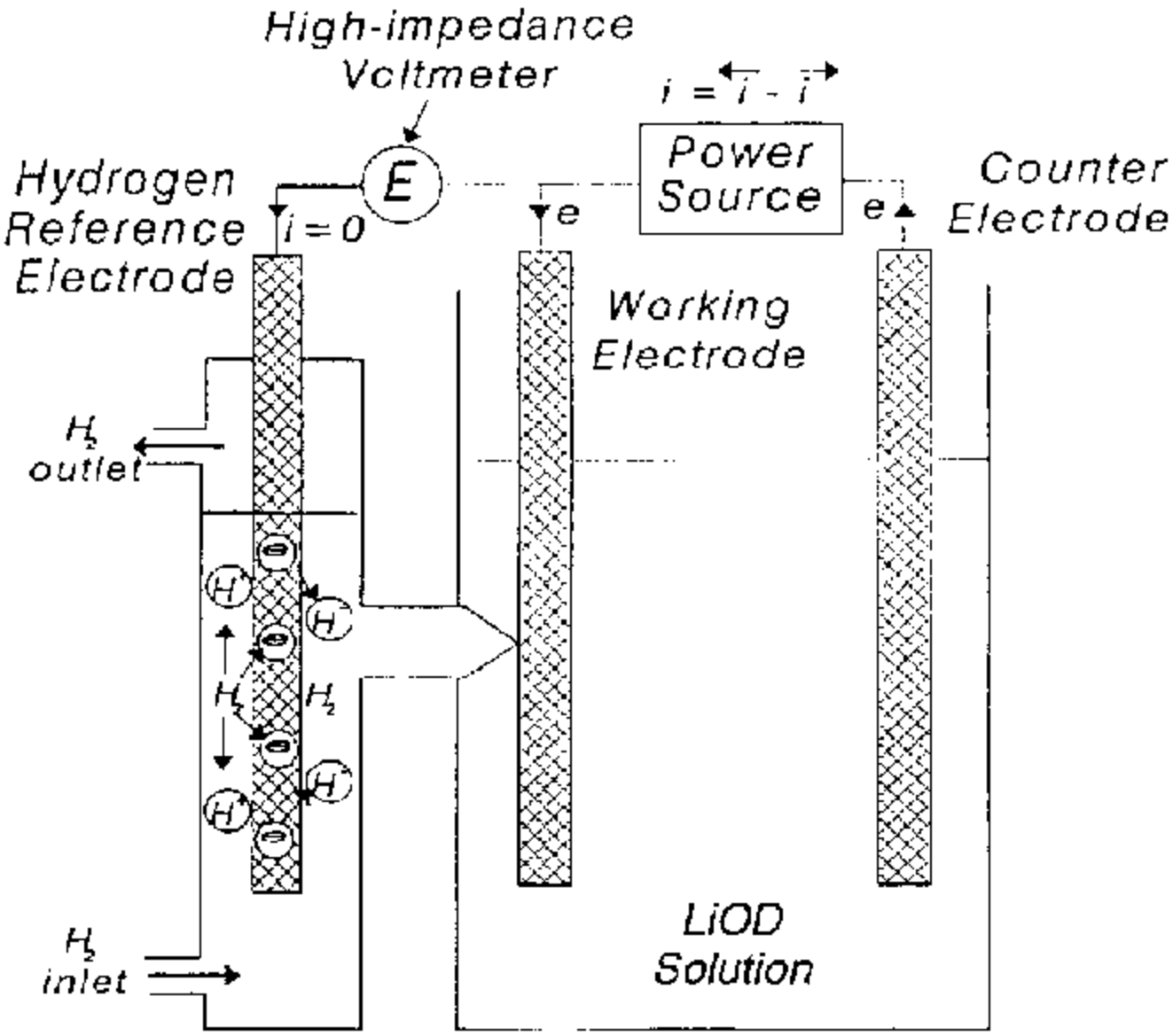

Fig. 1. Electrolysis Cell

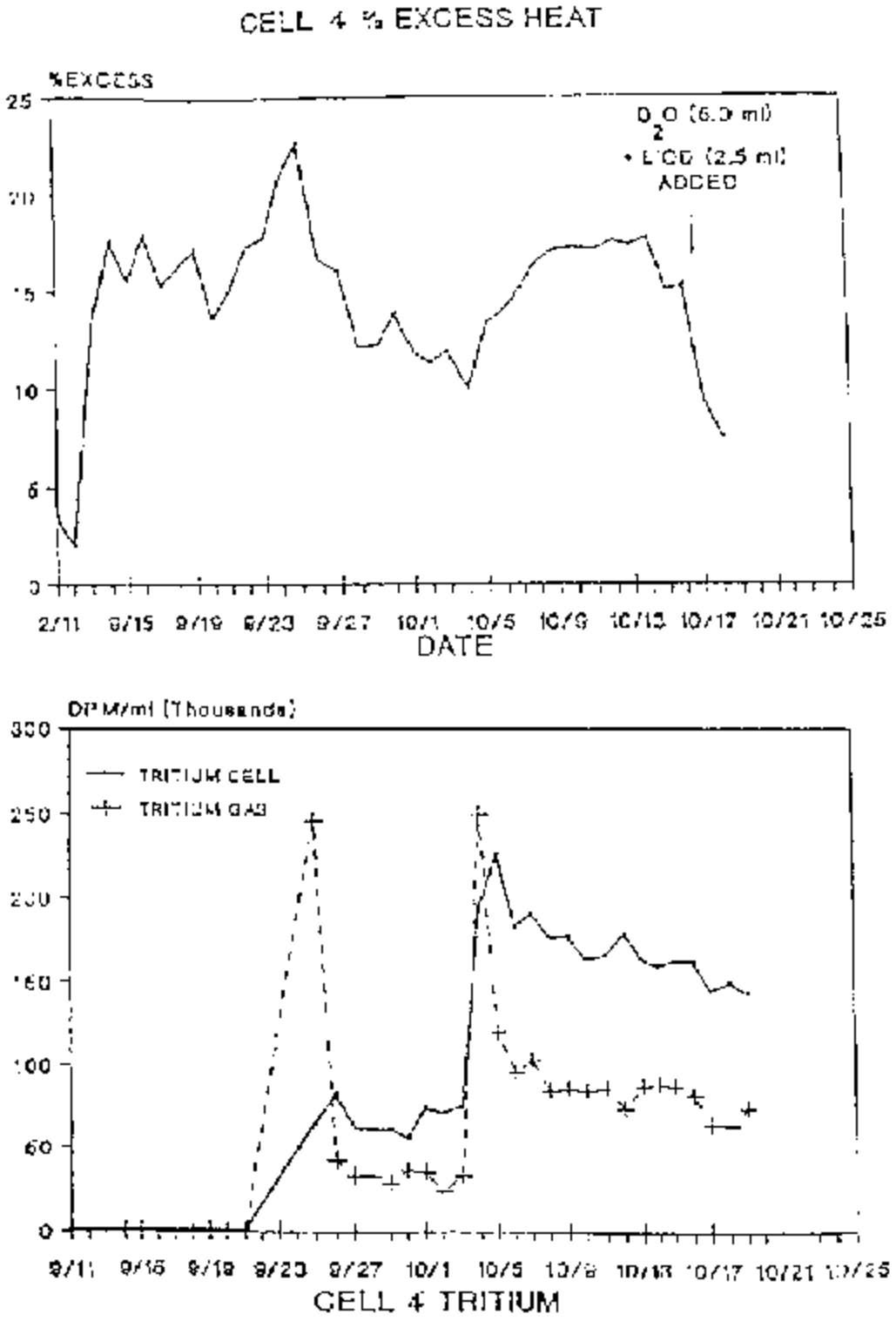

Fig. 2 The Heat Measurements and Tritium Activity Levels Showing a Possible Correlation Between the Two [Ref. 6]

3a

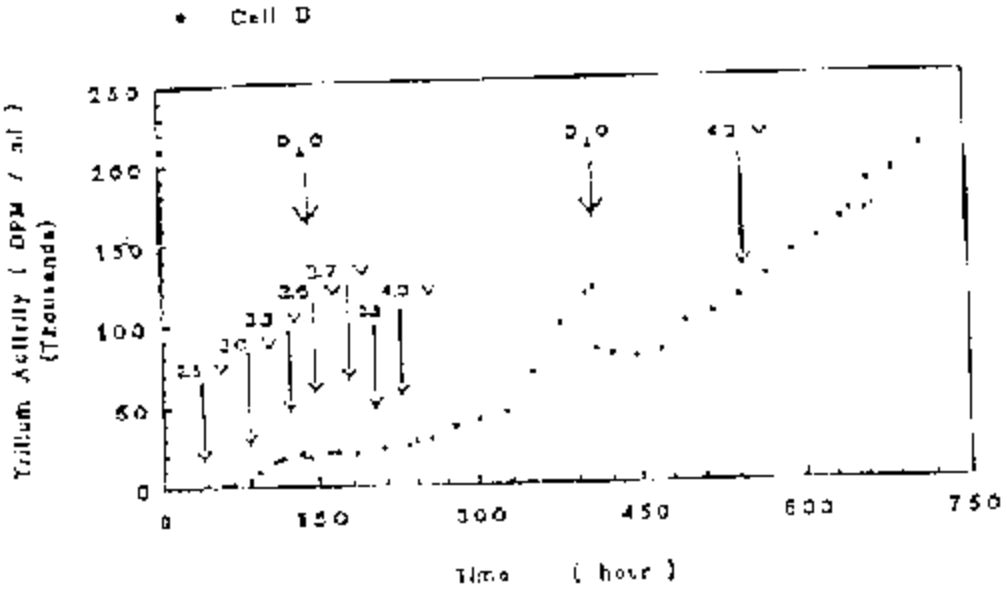
Cell B
Tritium Activity (DPM / ml)
(Thousands)
250
200
150
100
50
0
0
150
300
450
600
750
Time (hour)
2.5 V
3.0 V
3.3 V
3.6 V
3.7 V
4.0 V
3.8 V
4.2 V

3b

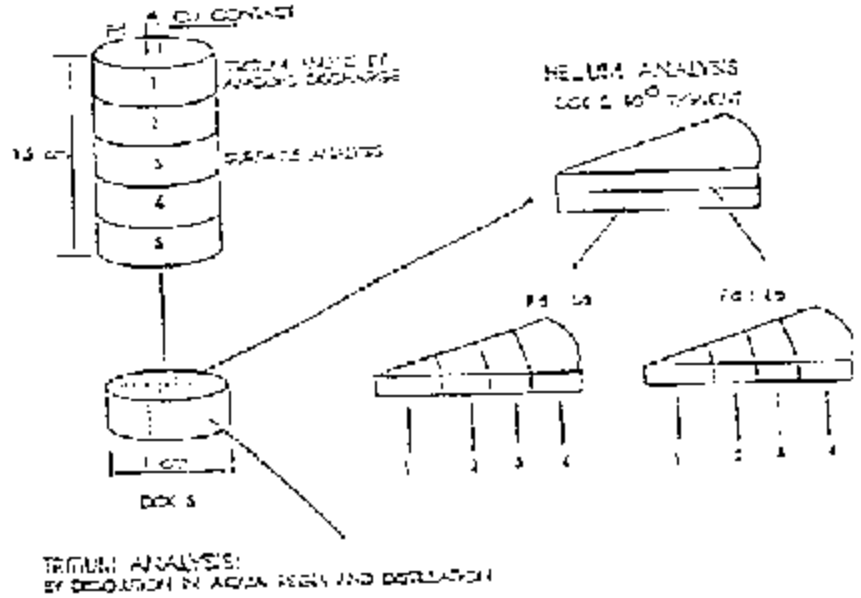
NEUTRON ANALYSIS
TRITIUM ANALYSIS
BY DEGASSING IN ACIDIC RESIN AND DISTILLATION

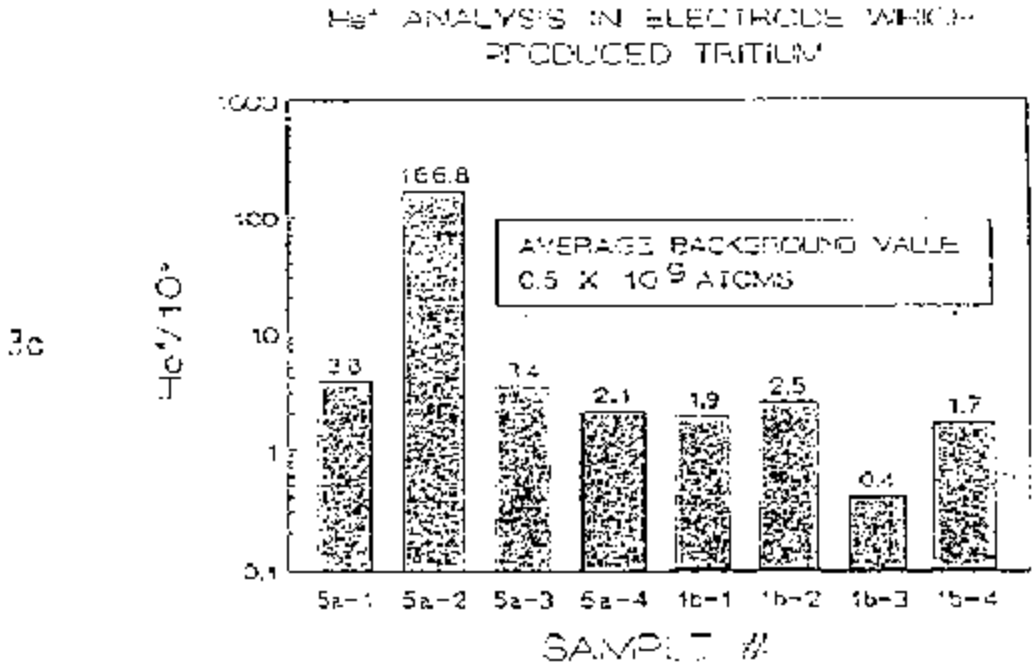

Fig.3 Helium Analysis of the Electrode Which Produced Tritium : a) Tritium

EXPERIMENTAL DETAILS FOR LIGHT WATER COLD FUSION RESEARCH AT CAL. POLY.- POMONA

Robert D. Eagleton
Physics Department, California State Polytechnic University* and
ENECO, Inc. (Formerly FEAT, Inc.)**

ABSTRACT

This paper presents a detailed description of the construction and operation of the two types of electrolytic cells employed in the experimental light water cold fusion research of R. Bush and R. Eagleton at California State Polytechnic University - Pomona.

INTRODUCTION

Electrolytic cells of the Fleischmann and Pons[1] type using light water with nickel cathodes and alkali carbonates were first employed at Cal. Poly - Pomona in August of 1991 following the announcement of excess heat production in light water by Mills and Kneizys[2]. Cell design and protocol was partially driven by considerations based upon the theoretical work of R. Bush[3]. Since that time a total of 27 light water cells have been run with alkali carbonate and alkali hydroxide electrolytes using two different cell and calorimeter configurations. These configurations and other details are described in this paper. The experimental results obtained with these cells are not discussed in this paper but are presented elsewhere[4,5,6,7,8].

CELL AND CALORIMETER DESIGN

The two types of cells used in our light water work are actually third and fourth generation cell designs which evolved from earlier work with heavy water. Consequently these cell types are designated as C and D respectively. They are illustrated in figures 1 and 2. Cells of type C were first used with heavy water in July of 1990 and continued to be used until January 1993. During that period 17 light water cells and 36 heavy water cells were run. Type D cells were phased in commencing February of 1993 and used for all cells constructed from that time until the present. To date ten light water cells have been operated using the type D configuration. Table I gives a summary of the light water cells that have been run to date.

The principal features which are common to both cell designs are as follows:

(1) They are all closed cells. This is achieved by use of a platinum black recombiner which is enclosed in the air space above the electrolyte. The recombiner is fabricated by bonding platinum black to a nickel screen mesh and coating one side of the mesh with a non-wetting agent (Teflon). The recombiner for all cells of type D and some of type C were enclosed within a nickel foil baffle that had extensions on either sides which served to return the recombination heat back into the electrolyte. This baffle also served to protect the recombiner from becoming contaminated with electrolyte residue. The recombiner for type C cells that was not placed in the baffle arrangement was instead affixed to the bottom side of the stopper and was unshielded. The cell is vented to the atmosphere via an oil bubbler which serves two purposes: (a) to maintain near ambient pressures, and (b) to isolate the cell from the external environment. A

balloon attached to the open end of the bubbler is used to monitor a cell for recombiner malfunctions. Of the light water cells run to date no recombiner malfunctions have been experienced. (2) Magnetic stirring is used to permit more uniform electrolyte temperatures. Tests have shown that these stirrers have no measurable effect on the electrolyte temperatures. (3) All surfaces except for electrodes and the nickel heat sinks are coated with Teflon. The neoprene stoppers are covered with form fitting Teflon tape and the cells were either pyrex coated with Teflon (type C) or made of Teflon bottles (type D). A special bonding agent is required to prevent the Teflon from becoming unbonded from the pyrex upon repeated thermal cycling. It is anticipated that the nickel heat sinks exposed to the electrolyte should pose no problems since they are shielded electrolytically by the nickel cathodes. (4) The electrodes are as follows: Platinum (AESAR 99.95%) wire anodes were 1 mm diameter and lengths of about 18 cm folded into five equal segments, nickel fibrex cathodes were formed into open ended cylinders having the platinum anode located along their central axis. Figures 3 and 4 are electron micrographs of a typical piece of 80/20 nickel fibrex mesh. Shown in these micrographs are nickel powder (20%) bonded to nickel fibers (80%) where the fibers are about 20 microns in diameter (Fig. 4). Also it should be noted that the nickel fibers are not fabricated from drawn nickel wires but are made from sintered nickel powder. These fibers are formed by extruding a slurry of nickel powder mixed in a plasticizer through a small orifice. After the plasticizer sets, the fibers are sintered in a hydrogen environment so that only porous nickel remains after the heat treatment. (5) Electrolytes were made of chemicals obtained from AESAR/Johnson Matthey and nanopure water (17 Mohm-cm) from a Barnstead filtering system. All electrolytes were 0.57 molar solutions. (6) A port for extracting electrolyte samples consists of a capped 1 mm diameter Teflon tube which passes through the neoprene stopper and into the electrolyte. (7) The electrolyte temperature is monitored by use of two 26 gauge type-K thermocouples. These are threaded into opposite ends of a 1 mm diameter Teflon tube that loops through the neoprene stopper to just below the cathode and above the magnetic stirrer. This tube is filled with mineral oil to permit more efficient thermal contact of thermocouples with the electrolyte. As shown in figures 1 and 2 these thermocouples are placed at different depths in the electrolyte. We find that these thermocouples read very nearly the same temperature provided the magnetic stirrer is operative. However, in the event of a stirrer malfunction the thermocouple readings may differ by as much as two or three degrees Celsius.

Features that differ for the two cells types are as follows:

Cell Type C - As illustrated in Figure 1, this is a double wall pyrex vessel which provides for a water jacket enclosing the electrolytic cell except for the top which is capped with a Teflon covered neoprene stopper. The inlet and outlet coolant temperatures were monitored with type K thermocouples. The pyrex cell was completely enclosed with a one inch thick layer of styrofoam.

Calibration for these cells was performed in one of two ways: (1) Either a nichrome reference heater was used or (2) the cell was calibrated by running anodically. When a nichrome reference heater was used it was placed in a close fitting Teflon tube that looped down into the electrolyte. The nichrome heating element was attached to electrical leads so as to have it completely immersed within the electrolyte. The cell calibration procedure is as follows: (1) The temperature of the coolant flowing through the water jacket was regulated so as to maintain the cell contents at a constant temperature. A typical value for the cell operation temperature was about 39°C. At this temperature the cells could be calibrated from 0 to 20 watts while using the laboratory as the heat sink for the cell bath. Table II gives typical calibration data for this type of cell. Note that the standard deviation in the calibration temperatures is less than 0.1°C. The cell calibration data points are obtained by plotting the steady state thermal power output (P_{out}) from the cell as a function of the average temperature decrease (∂T) across the cell walls. This temperature decrease is found by taking the difference between the average of the two cell thermocouples

readings and the average of the inlet and outlet thermocouple readings. (For steady state calibration conditions the electrical power input to the cell is equal to the thermal power output.) This plot of P_{out} versus ∂T was fit by either a linear or a third order polynomial. Figure 5 shows a typical calibration curve that was obtained for cell 62. The excess power (P_{ex}) was determined by subtracting the electrical power delivered to the cell from the steady state thermal power coming out of the cell as calculated from the fit that yielded the smallest value for P_{ex}.

Cell Type D - Cells of this type are illustrated in Figure 2. They are constructed from Teflon bottles and are designed to be immersed directly within the coolant water bath. The bath water was temperature regulated as well as stirred. The calibration procedure for these cells are essentially the same as that for type C cells with the exception that the temperature decrease across the cell walls were obtained by subtracting the bath temperature from the average of the two cell thermocouple readings. Table III gives a typical set of calibration data for this type of cell.

Data Acquisition System

All temperatures, currents, and voltages were monitored and logged using a Macintosh IIx computer equipped with National Instrument's LabView software. For type C cells four type K thermocouples were used: one at the bath inlet port, one at the bath outlet port, and two within the electrolyte. In the case of type D cells there was one type K thermocouple within the bath and two within the electrolyte. The thermocouple sampling rate is 1000/minute with the temperature averaged each minute. The thermocouple voltages were converted to temperature readings (°C) by use of AD595AQ/9217 integrated circuit chips. This system permitted steady state temperature measurements with standard deviations of about 0.05°C. Corrections for thermocouple temperature offsets were made within the software. Cell currents and voltages were logged from Fluke 45 dual display multimeters equipped with IEEE interface. Figure 6 shows a front panel view of the virtual instrument used for cell monitoring and control of data logging. Since our cells are calibrated for only steady state operation at a specified temperature, we make use of this virtual strip chart recorder to determine when the requisite conditions are achieved before logging data. Table IV gives a typical spread sheet of data logged for a cell which produced excess heat. Not shown but recorded with this spread sheet were the following: room temperature, multiplexer reference junction temperature, time mark and date mark. The data acquisition rate for both Table IV and Figure 5 was for one minute intervals. In Table IV it should be noted that the fractional uncertainty in P_{ex} about 2% for the 23 minute time interval shown there. However, all values of P_{ex} which we report are corrected for any differences found after recalibration.

ACKNOWLEDGMENTS

The following institutions are to be acknowledged for their support that has made this research possible: Southern California Edison, ENECO (Formerly FEAT of Salt Lake City, Utah). Roger Bush, son of R. Bush, is thanked for the software design of the virtual instrumentation employed in the data acquisition system.

REFERENCES

[1] M. Fleischmann and S. Pons, "Electrolytically Induced Nuclear Fusion of Deuterium", *J. Electroanal. Chem.*, vol 261, p 301 (1989).

[2] R. Mills and K. Kneizys, "Excess Heat Production by the Electrolysis of an Aqueous Potassium

Carbonate Electrolyte and the Implications of Cold Fusion", *Fusion Technol.*, vol 20, p 65 (1991).

[3] R. Bush, "A Light Water Excess Heat Reaction Suggests that `Cold Fusion' May Be `Alkali-Hydrogen Fusion'", *Fusion Technol.*, vol 22, p 301 (1992).

[4] R. Bush and R. Eagleton, "Experiments Supporting the Transmission Resonance Model for Cold Fusion in Light Water: I. Correlation of Isotopic and Elemental Evidence with Excess Heat," Proceedings of the 3rd International Conference on Cold Fusion, Nagoya, Japan, p 405 (1993).

[5] R. Bush and R. Eagleton, "Experiments Supporting the Transmission Resonance Model for Cold Fusion in Light Water: II. Correlation of X-Ray Emission with Excess Power," Proceedings of the 3rd International Conference on Cold Fusion, Nagoya, Japan, p 409 (1993).

[6] R. Bush and R. Eagleton, "Calorimetric Studies for Several Light Water Electrolytic Cells with Nickel Fibrex Cathodes and Electrolytes with Alkali Salts of Potassium, Rubidium, and Cesium," paper at 4th International Conference on Cold Fusion (1993), (Submitted to the Proceedings).

[7] R. Bush and R. Eagleton, "Evidence for Electrolytically Induced Radioactivity and Transmutation of Rubidium to Strontium Correlated with the Light Water Excess Heat Produced with Rubidium Salt Electrolytes and Nickel Mesh Cathode," paper presented at 4th International Conference on Cold Fusion (1993), (submitted to the Proceedings).

[8] R. Bush, "Evidence for an Electrolytically Induced Shift in the Abundance Ratio of Sr86 and Sr88," paper at International Cold Fusion and Energy Conference, Minsk, Belarus, May 1994 (submitted to the Proceedings).

*3801 West Temple Avenue, Pomona, CA 91768.
**University of Utah Research Park, 391-B Chipeta Way, Salt Lake City, Utah 84108.

Cell #	Cathode	Electrolyte	Cell Type
38	Ni Fibrex	0.57M K_2CO_3 in 50cc H_2O	C
41	Ni Fibrex	0.57M K_2CO_3 in 50cc H_2O	C
44	Ni Fibrex	0.57M K_2CO_3 in 50cc H_2O	C
45	Ni Fibrex	0.57M K_2CO_3 in 50cc H_2O	C
47	Ni Fibrex	0.57M K_2CO_3 in 50cc H_2O	C
48	Ni Fibrex	0.57M Na_2CO_3 in 50cc H_2O	C
49	Ni Fibrex	0.57M Rb_2CO_3 in 50cc H_2O	C
50	Ni Fibrex	0.57M Rb_2CO_3 in 50cc H_2O	C
51	Ni Fibrex	0.57M Na_2CO_3 in 50cc H_2O	C
52	Ni Fibrex	0.57M Na_2CO_3 in 50cc H_2O	C
53	Ni Fibrex	0.57M Rb_2CO_3 in 50cc H_2O	C
54	Ni Fibrex	0.57M RbOH in 50cc H_2O	C
55	Ni Fibrex	0.57M Rb_2CO_3 in 50cc H_2O	C
56	Ni Fibrex	0.57M RbOH in 45cc H_2O+2cc D_2O	C
57	Ni Fibrex	0.57M Rb_2CO_3 in 50cc H_2O	C
61	Ni Fibrex	0.57M K_2CO_3 in 200cc H_2O	C
62	Ni Fibrex	0.57M LiOH in 50cc H_2O	C
63	Ni Fibrex	0.57M K_2CO_3 in 62cc H_2O	D
64	Ni Fibrex	0.57M K_2CO_3 in 62cc dedeuterated H_2O	D
65	99.9975 Ni wire	0.57M K_2CO_3 in 60cc H_2O	D
66	99.9975 Ni wire	0.57M K_2CO_3 in 60cc H_2O	D
67	Ni Fibrex	0.57M K_2CO_3 in 70cc H_2O	D
68	Ni Fibrex+10%Cu	0.57M K_2CO_3 in 70cc H_2O	D
69	Ni Fibrex	0.57M Rb2CO3 in 65cc H2O	D
70	Ni Fibrex	0.57M Cs2CO3 in 65cc H2O	D
71	Ni Fibrex+10%Cu	0.57M Rb2CO3 in 65cc H2O	D
72	Ni Fibrex+10%Cu	0.57M Cs2CO3 in 65cc H2O	D

Table I: Details of Cell Type, Cathodes, and Electrolytes for all Light Water Cells Run as of 2/94.

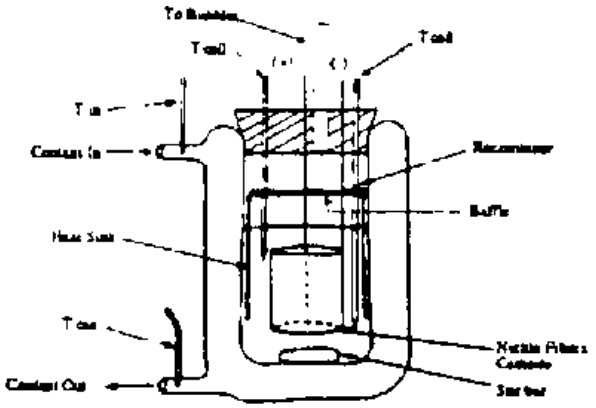

FIGURE 1. Third generation cell design: Cell type "C".

PRINCIPAL FEATURES

- CLOSED CELL OPERATION
- MECHANICALLY STIRRED ELECTROLYTE
- RECOMBINER BAFFLE & HEAT SINK
- TEFLON COATED PYREX CELL
- PLATINUM ANODE
- NICKEL FIBREX CATHODE
- NANOPURE H_2O BASE ELECTROLYTE
- CONSTANT COOLANT FLOW RATE
- CONSTANT CURRENT AND TEMPERATURE OPERATION

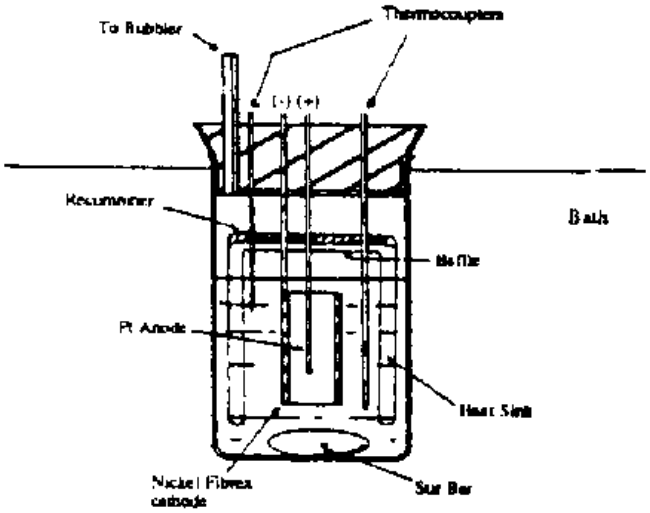

FIGURE 2. Fourth generation cell design: Cell type "D".

PRINCIPAL FEATURES

- CLOSED CELL OPERATION
- MECHANICALLY STIRRED ELECTROLYTE
- RECOMBINER BAFFLE & HEAT SINK
- TEFLON CELL
- PLATINUM ANODE
- NICKEL FIBREX CATHODE
- NANOPURE H_2O BASE ELECTROLYTE
- CELL IMMERSED IN BATH
- CONSTANT CURRENT AND TEMPERATURE OPERATION

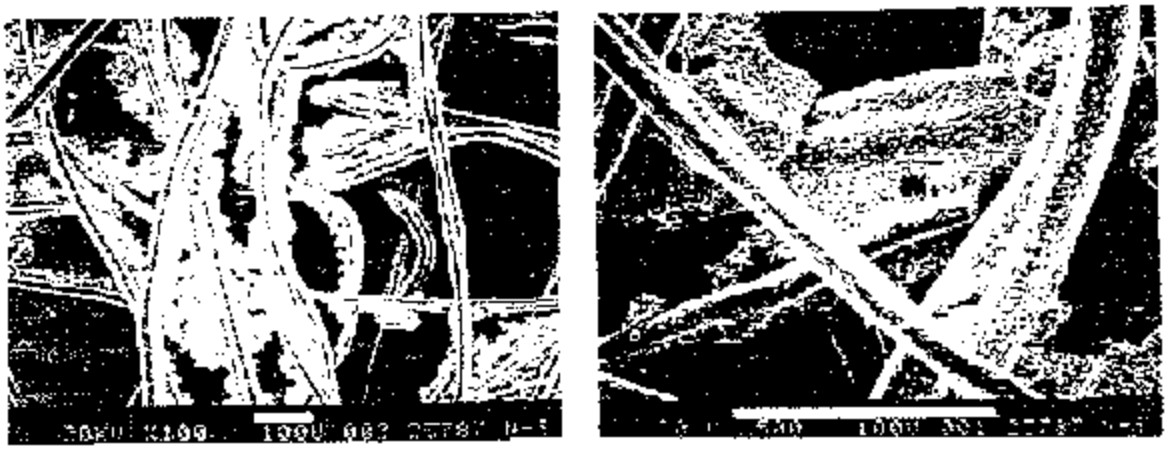

Figure 3. SEM photomicrographs of nickel fibrex cathode material having 80% nickel fiber and 20% nickel powder for magnification of 100x and 500x.

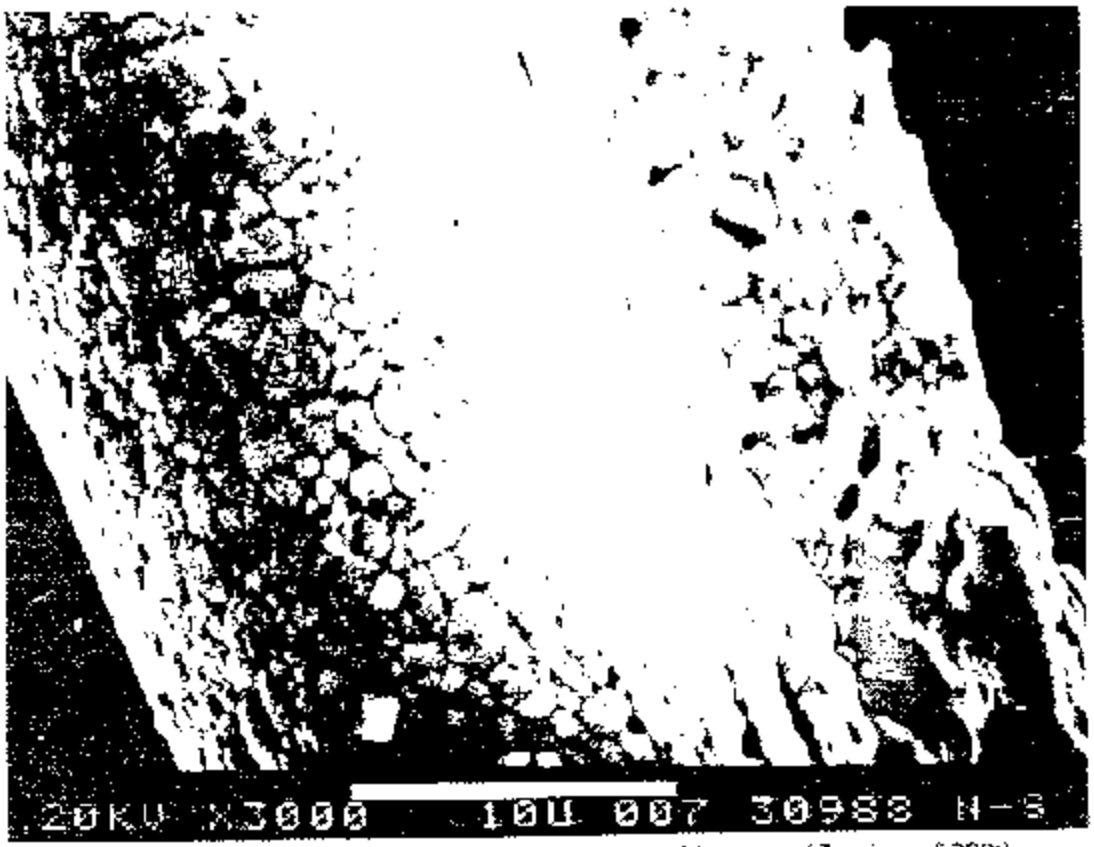

Figure 4. SEM photomicrograph of a single nickel fiber with a magnification of 3000x displaying its granular structure.

Tcal	TLD	Tcave	Tout	Tin	Tcase	VF	Vout		Pin	Time Mark
39.023	39.011	39.011	32.448	31.237	31.341	7.174	9.740	1.507	14.675	1:48:09 PM
39.023	39.045	39.034	32.454	31.209	31.309	7.225	9.731	1.506	14.640	1:48:24 PM
38.962	38.985	38.963	32.385	31.197	31.291	7.172	9.730	1.507	14.663	1:48:39 PM
39.130	38.967	39.049	32.432	31.144	31.263	7.266	9.726	1.507	14.655	1:48:54 PM
39.112	38.791	38.951	32.403	31.265	31.354	7.155	9.741	1.507	14.703	1:49:09 PM
38.967	38.931	38.876	32.424	31.175	31.295	7.175	9.761	1.507	14.710	1:49:24 PM
39.064	38.997	38.986	32.432	31.122	31.277	7.218	9.736	1.507	14.675	1:49:39 PM
38.985	38.940	38.972	32.442	31.139	31.276	7.189	9.751	1.507	14.712	1:49:54 PM
39.052	39.069	39.011	32.379	31.201	31.286	7.225	9.715	1.507	14.647	1:50:10 PM
39.112	39.049	39.040	32.417	31.172	31.295	7.249	9.675	1.508	14.571	1:51:40 PM
39.070	38.905	38.991	32.405	31.228	31.318	7.175	9.730	1.506	14.609	1:51:56 PM
39.121	38.939	39.030	32.424	31.185	31.304	7.225	9.715	1.508	14.631	1:52:11 PM
39.158	38.975	39.066	32.395	31.183	31.288	7.209	9.672	1.507	14.575	1:52:26 PM
39.139	38.826	39.024	32.439	31.189	31.312	7.212	9.746	1.508	14.683	1:52:41 PM
39.141	38.958	39.050	32.398	31.178	31.297	7.261	9.647	1.507	14.538	1:52:57 PM
39.093	38.993	39.043	32.432	31.188	31.309	7.234	9.674	1.508	14.589	1:53:12 PM
38.973	38.930	38.952	32.443	31.187	31.316	7.147	9.716	1.506	14.620	1:53:27 PM
39.123	39.029	39.076	32.429	31.150	31.299	7.207	9.699	1.508	14.607	1:53:42 PM
39.132	38.940	39.032	32.424	31.191	31.333	7.183	9.705	1.507	14.622	1:53:57 PM
39.121	39.012	39.039	32.444	31.213	31.328	7.241	9.743	1.508	14.673	1:54:12 PM
39.087	39.084	39.075	32.430	31.208	31.317	7.158	9.722	1.508	14.641	1:54:27 PM
39.081	38.984	39.028	32.414	31.214	31.314	7.173	9.710	1.507	14.633	1:54:42 PM
39.037	38.941	38.989	32.417	31.183	31.300	7.189	9.715	1.507	14.635	Averages
0.058	0.065	0.049	0.024	0.026	0.018	0.047	0.032	0.000	0.049	Std Dev

Table II: Calibration data for P_{in} = 14.6 watts for cell 62 at T_{cell} = 39C.

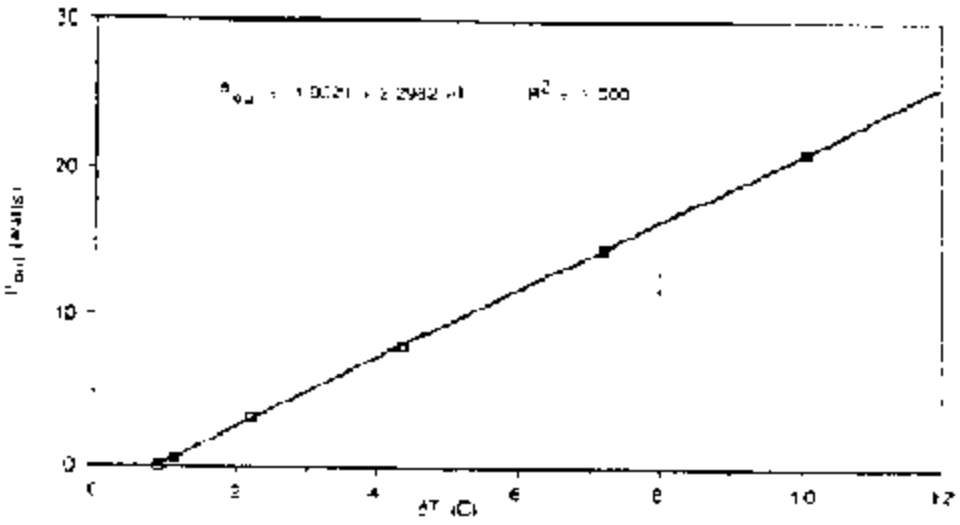

Figure 5. Calibration curve for cell 62 at a cell temperature of 39C

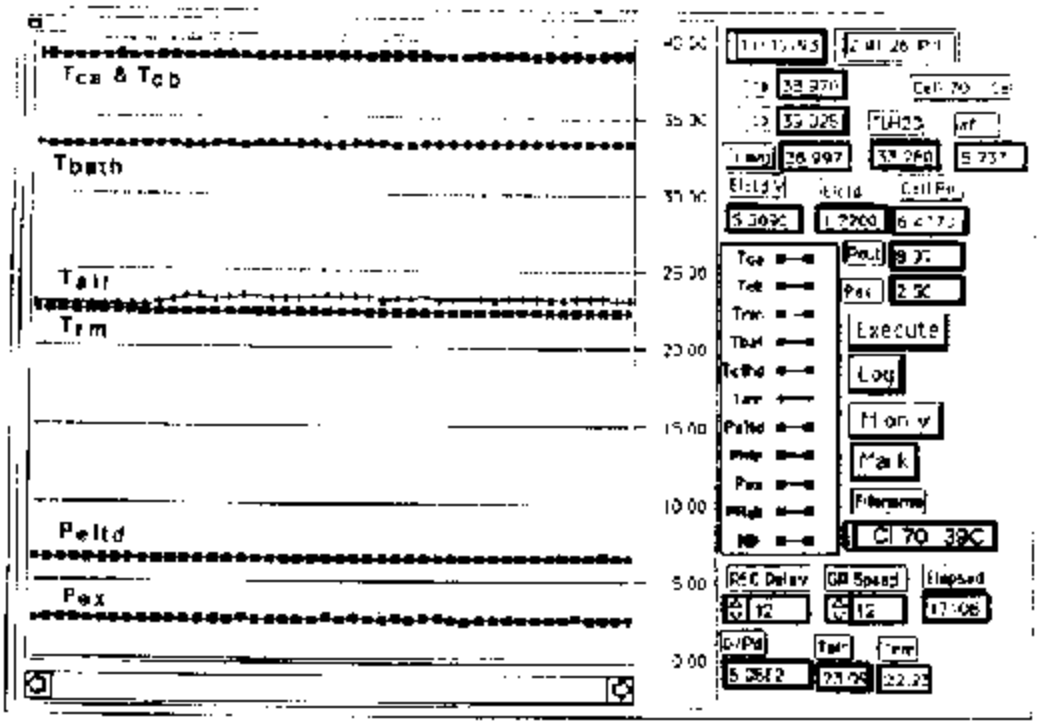

Figure 6. Front panel of virtual strip chart recorder for cell 70.

Tca	Tcd	Tavg	TdH20	dT	IE(1)	VE(1)	PinE(1)	
38.652	38.770	38.711	32.825	5.886	-2.100	-4.559	9.574	
38.689	38.761	38.725	32.852	5.873	-2.100	-4.585	9.628	
38.658	38.755	38.707	32.842	5.864	-2.100	-4.594	9.647	
38.648	38.761	38.705	32.850	5.874	-2.100	-4.556	9.568	
38.751	38.792	38.772	32.813	5.964	-2.100	-4.571	9.599	
38.761	38.792	38.777	32.813	5.964	-2.100	-4.571	9.599	
38.735	38.752	38.744	32.810	5.953	-2.100	-4.571	9.599	
38.658	38.749	38.709	32.805	5.903	-2.100	-4.580	9.618	
38.810	38.824	38.817	32.827	5.990	-2.100	-4.557	9.570	
38.729	38.772	38.751	32.853	5.896	-2.100	-4.564	9.584	
38.709	38.787	38.748	32.841	5.907	-2.100	-4.573	9.603	
38.750	38.806	38.793	32.830	5.963	-2.100	-4.564	9.584	
38.747	38.785	38.766	32.822	5.944	-2.100	-4.574	9.605	
38.747	38.785	38.766	32.822	5.944	-2.100	-4.571	9.599	
38.745	38.776	38.761	32.819	5.941	-2.100	-4.564	9.584	
38.841	38.826	38.834	32.803	6.030	-2.100	-4.560	9.576	
38.751	38.795	38.773	32.817	5.956	-2.100	-4.567	9.591	
38.731	38.782	38.756	32.825	5.931	-2.100	-4.569	9.596	Averages
0.055	0.023	0.038	0.015	0.046	0.000	0.010	0.021	Std Dev

Table III: Calibration data for P_{in} = 9.59 watts for cell 70 at 39C.

Tca	Tcd	Tavg	TdH20	dT	IE(1)	VE(1)	PinE(1)	Pout	Pex	
38.962	39.053	39.008	33.229	5.779	1.220	5.312	6.481	9.040	2.559	
38.940	39.053	38.997	33.233	5.763	1.220	5.352	6.529	9.015	2.486	
38.981	39.087	39.034	33.239	5.795	1.220	5.324	6.495	9.066	2.571	
38.979	39.009	38.994	33.257	5.737	1.220	5.318	6.488	8.974	2.486	
38.965	39.089	39.027	33.247	5.780	1.220	5.319	6.489	9.043	2.554	
38.950	39.079	39.015	33.228	5.786	1.220	5.271	6.431	9.052	2.622	
38.950	39.079	39.015	33.228	5.786	1.220	5.329	6.503	9.052	2.551	
38.947	39.130	39.039	33.241	5.798	1.220	5.304	6.471	9.070	2.599	
38.982	39.022	39.002	33.242	5.760	1.220	5.265	6.423	9.011	2.587	
39.008	39.026	39.017	33.269	5.747	1.220	5.305	6.472	8.990	2.518	
38.940	38.991	38.966	33.268	5.697	1.220	5.313	6.482	8.910	2.428	
38.956	39.074	39.015	33.254	5.761	1.220	5.312	6.481	9.012	2.532	
38.943	39.072	39.008	33.241	5.767	1.220	5.307	6.475	9.021	2.547	
38.941	39.053	38.997	33.242	5.755	1.220	5.308	6.476	9.002	2.527	
38.941	39.053	38.997	33.242	5.755	1.220	5.332	6.505	9.002	2.497	
38.945	39.028	38.987	33.270	5.716	1.220	5.303	6.470	8.940	2.470	
38.957	39.047	39.002	33.253	5.749	1.220	5.335	6.509	8.992	2.483	
38.975	39.039	39.007	33.245	5.762	1.220	5.296	6.461	9.013	2.552	
38.973	39.085	39.029	33.241	5.788	1.220	5.315	6.484	9.055	2.571	
39.002	39.029	39.016	33.250	5.765	1.220	5.334	6.507	9.018	2.511	
38.953	39.067	39.010	33.257	5.754	1.220	5.358	6.537	9.000	2.463	
38.978	39.055	39.017	33.249	5.768	1.220	5.307	6.475	9.022	2.548	
38.978	39.055	39.017	33.249	5.768	1.220	5.305	6.470	9.022	2.553	
38.963	39.055	39.009	33.247	5.762	1.220	5.314	6.483	9.014	2.531	Averages
0.020	0.031	0.016	0.012	0.024	0.000	0.021	0.026	0.038	0.047	Std Dev

Table IV: Excess power data for cell 70 at 39C.

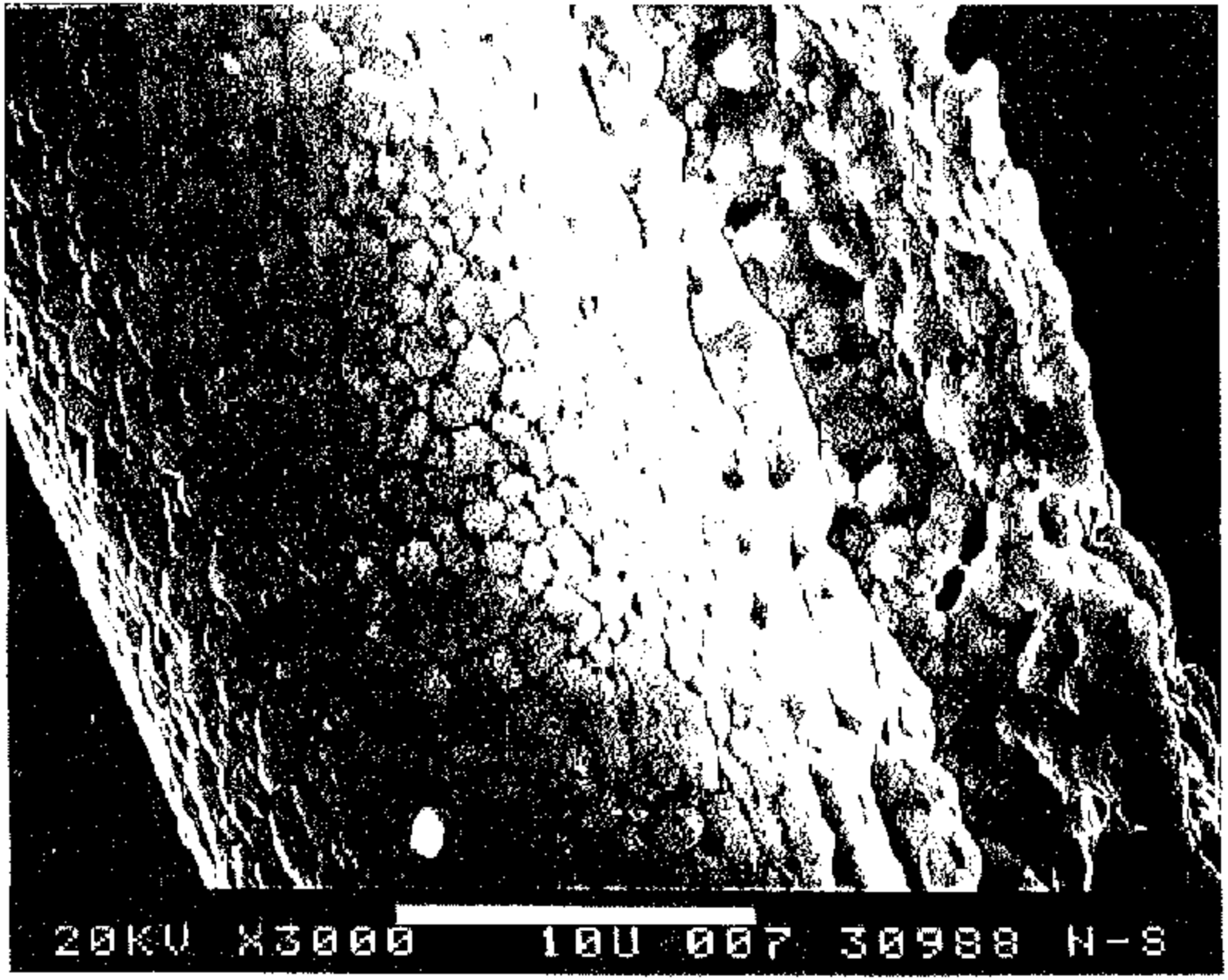
20KV X3000 10U 007 30988 N-S

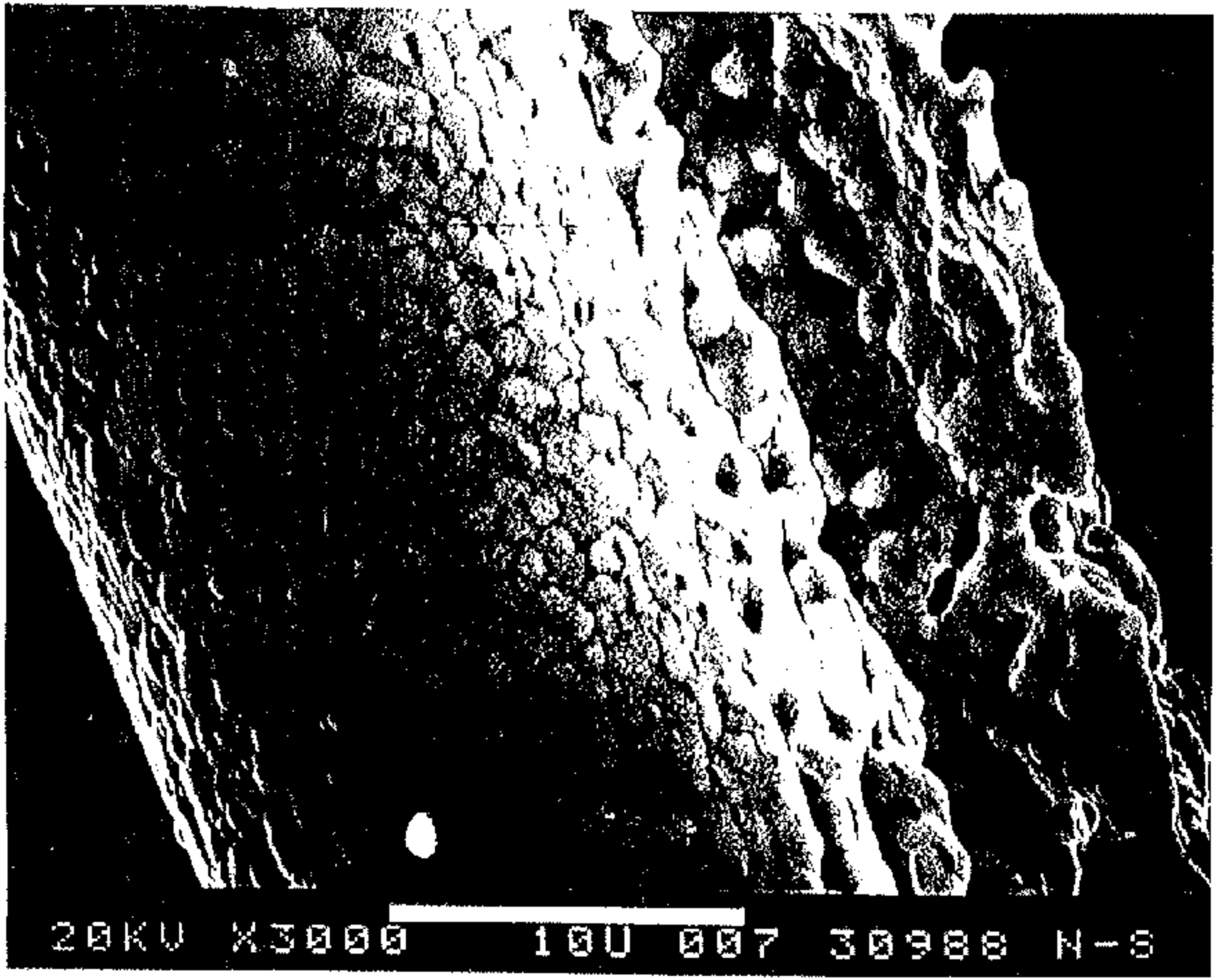
20KU X3000 10U 007 30988 N-S

SEARCHING FOR TRUTH WITH HIGH EXPECTATIONS

--5 Year Studies on Cold Fusion in China --

Xing Zhong Li
Department of Physics, Tsinghua University
Beijing 100084, China

ABSTRACT

The "cold fusion" research in China is reviewed for the past five years. Emphasis is focused on the attempt to set up the Chinese-based reproducible experiments and the study on the key parameter which is supposed to control the reproducibility. Theoretical effort in understanding these phenomena is described as well.

INTRODUCTION

The situation of "cold fusion" in China is similar to that in Russia. Since communication was somehow delayed, we started the "cold fusion" research based on our own understanding and the resources available to us[1-14].

After 5 years of studies on "cold fusion", more people in China think that there must be something behind it, and it is worthwhile to seek the truth for the fundamental physics, and for the possible future energy.

Research in China has been conducted in both theory and experiments with more emphasis on experiments. The experiments are in two categories: (1) Attempt to set up a Chinese-based experiment; (2) Study the key parameters which might control the reproducibility of the experiments.

We have three efforts to set up the Chinese-based experiments: (1) The electrical discharge in deuterium gas with palladium electrode; (2) Gas loading experiments with detectors to search the precursor and the energy carrier for the anomalous phenomena in D/Pd systems; (3) Excess heat measurements in D/Pd and D/Ti systems.

Based on international academic exchange, the loading ratio of deuterium in palladium was selected as a key parameter to study. We designed several systems to study the various treatments which might affect the terminal loading ratio and the loading speed. Some factors have been identified which may enhance the loading ratio to pass the resistance peak, and over the threshold (i.e. D/Pd~0.84).

Theory is important, although it is still in an immature stage. Wherever the experiments continued in these 5 hard years, there must be a plausible "theory" to stimulate the investigators. The penetration of the Coulomb barrier has been a persistent subject over 5 years. Bohm's theory has been developed in three aspects: (1) The direction of WKB connection formula, which has been a controversy for more than twenty years; (2) A simplified formalism for WKB method which is particularly useful for a chain of potential barriers and wells; (3) A new explanation of the penetration of potential barrier in quantum mechanics. The recent calculation shows that the split of the Coulomb barrier may be necessary, and some experiments have been suggested to test this idea.

We have started three new sets of experiments:
(1) The electrolysis of pressurized heavy water to study the "excess heat" in high temperature condition, based on our experience with pressurized light water fission reactors. (2) The enhancement of spontaneous fission in uranium due to hydrogen loading. (3) The positron annihilation studies of the surface layer of the palladium sheet during the hydrogen loading.

Electrical Discharge in Deuterium Gas

Five years ago, when the fax copies from the US were disseminated in China, a lot of experiments were tried to reproduce the electrolysis or the gas-loading results. Some of the Chinese scientists decided to do something else.[1-4] The electrical discharge in a deuterium gas tube was one of these pioneer works. Xiong[1] et al. at the Southwestern Institute of Nuclear Physics and Chemistry reported the first observation of neutron bursts in an electrical discharge tube with a palladium cathode and a tungsten anode. The neutron yield was $\sim 10^6$ per burst. It was too high to convince enough people to continue this experiment in that Lab. However, an elder scientist (Long, H.Q.[3,4]) at the Sichuan Institute of Material Technology continued this electrical discharge experiment under difficult conditions. After three years of silent research, it was found that the "anomalous neutron emission" was reproducible as long as three prerequisites were satisfied i.e. (1) a thin film of palladium was formed on the surface of discharge bulb; (2) the deuterium gas was flowing through the discharge bulb at a low pressure(5~17 Pa.); (3) the A.C. voltage between two electrodes was in certain range (6000~17000 V.).

The neutron emission was reproducible and verified by an activation method which was free of electromagnetic disturbance, and there was no neutron emission in the control run with hydrogen or helium gas. The neutron emission was considered "anomalous" because an unexpected peak was observed in the neutron energy spectrum. The ordinary D-D neutrons were supposed to peak at 2.45 MeV; however, a high energy component appeared with energy greater than 5 MeV. A careful study on this anomalous neutron emission revealed that this "neutron peak" was indeed caused by the overlap of intensive X-ray radiation.[5,6]

However, it is still a puzzle why the low energy radiation is so intensive at this discharge condition. Scientists at the Institute of High Energy Physics [7] were stimulated by this puzzle to redo their early experiment. In 1989, they detected an anomalous low energy radiation with no neutron emission. They stopped their experiment, because four years ago the overwhelming point of view was that neutron emission was the necessary feature of anomalous phenomena. Now more people believe that the neutron is not necessary, but the energy carrier must exist somehow to explain the excess heat. So they returned to their early data again. They have found that in fact there were several peaks in the low energy radiation (< 900 keV). These peaks corresponded to the characteristic lines of spectrum for electrodes: a peak at 425+40 keV which corresponds to the nuclear de-excitation process: $^{108}Pd^* \rightarrow {}^{108}Pd + \gamma$ (E_γ = 425 keV), and a peak at 870±50 keV which corresponds to $^{56}Fe^* \rightarrow {}^{56}Fe + \gamma$ (E_γ = 854 keV).

The electrical voltage between the electrodes of the discharge tube was 10 kV, which was too low to excite the nuclides for γ-ray emission. There should be some energetic charged particles with several MeV. So this was an indication of nuclear reaction products. The A.C. voltage was in a pulse shape, and the instruments for detection of neutron and γ-ray were set to work only in the intermission period when the pulse was over; hence, it was supposed that there was no electromagnetic disturbance. One might suspect that some induced high voltage could accelerate the deuterons to produce the ordinary D-D fusion reactions, but the neutron detector did not register any neutrons above the background level. Hence it is

suggested that there were two stages of reactions: the first stage was the anomalous D+D reaction which produced only proton (3MeV) and tritium without the neutron branches; the second stage was the Coulomb excitation induced by 3 MeV protons. Then the de-excitation gave the characteristic gamma ray.

Calculations show that the gamma yield is about 10^{-6} per 3 MeV proton absorbed in palladium, and this result can be probably explained by the decay of excited Pd* and Fe*. Since tungsten electrode was used also, there should be a de-excitation process: $^{184}W^* \rightarrow {}^{184}W + \gamma$ ($E\gamma$=110 keV). If the low energy spectrum could get rid of the noise, one should have seen the 110 keV gamma-ray as well. Recently an unexpected peak has been seen around 130 keV, which could not be attributed to any Coulomb excitation process. Fortunately, Professor Hagelstein is just looking for a peak around 129.5 keV to explain his neutron transfer reaction.

Gas Loading Experiment

Another early experiment in China was to identify the precursor and the energy carrier for the anomalous nuclear phenomena[8,9]. We proposed that the necessary product of any nuclear process is the energetic charged particle; the neutron is not a necessary product for any nuclear process. The CR-39 plastic track detector was used in a "freeze and thaw cycle" or D/Pd system to detect the energetic charged particles. The CR-39 detector is particularly suitable for this process, because it can be sealed in a high pressure container with direct contact to the palladium surface and is free of any electronic noise. It has the highest sensitivity among all the detectors available to us. It is possible to avoid any cosmic interference by the pre-etching method, and the air-borne radiation background can be deduced by control run with hydrogen. We saw the energetic charged particle in the early experiments with the Russian palladium imported in the early 60's. However, the signal was greatly reduced in the later experiments using other palladium samples or the titanium samples.

In order to reproduce the early experiments, a systematic study[10,11] on the loading ratio (D/Pd) in gas loading experiments was started in 1991 after a visit to Stanford Research Institute. It is clear that the reproducibility depends on the loading process. The annealing in the vacuum, and the multiple-step loading have been identified as two important factors which may affect the terminal loading ratio. Table 1 and Table 2 in Ref. 11 summarize the gas-loading experiments with palladium in hydrogen and in deuterium. It is possible to reach the loading ratio of D/Pd >0.84 by annealing in the vacuum, and multiple-step loading under 30 atm.

Excess Heat Experiments

Calorimetric experimentation is difficult and requires more funds and time, so it is done in only a few laboratories in China. The Institute of Chemistry, Academy of Science, keeps a small group using microcalorimetry[12]; and the Institute of Atomic and Molecular Science at High Temperature and High Pressure, Chengdu University of Science and Technology keeps doing electrolysis of heavy water with titanium cathode and platinum anode[13]. They measured the temperature inside the Ti-rod, and observed the extraordinary ascent of temperature five times among seven experiments. Although the explanation of extraordinary ascent of temperature is unclear yet, they found that if a mixture of H_2O and D_2O was used as the electrolyte, then no extraordinary ascent of temperature was observed. The extraordinary ascent of temperature was about 1.5~24°C dependent on the size of the Ti-rod. The SIMS (secondary ion mass spectrum) analysis showed strangely that the Ti-rod sample above the water level absorbed much more hydrogen than deuterium if there was some H_2O in the electrolyte. However, the Ti-rod sample beneath the water level absorbed both deuterium and hydrogen. The

hardness and the metallurgical structure of the Ti-rod were monitored before and after electrolysis.

Theory -- Precursor and Energy Carrier

It is too early to extract any definite theoretical model from these experiments. However, it is essential to have some kind of "plausible" theory to stimulate the effort in experiments. Five years ago when the neutron was taken as the characteristic symbol of the anomaly in D/Pd systems, we proposed that the energetic charged particles might be the necessary signal for any anomalous nuclear reaction. This idea led to a series of studies using CR-39 (plastic track detector). When the sporadic bursts made the experiment unpredictable, we suggested that there had to be some precursors before the anomaly appeared. This idea led to careful studies about the electromagnetic radiation using thermal luminescence detectors.[8,9] When international academic exchange revealed that the excess heat might not be accompanied with nuclear signals, or the amount of excess heat might not be compatible with the weak nuclear signal, we considered that a two-step model[14] might be necessary to reconcile the two facts: (1) More experiments confirmed that there was some excess heat in the closed system[15], and in the open system[16]; (2) The nuclear signals (helium-4[17] or tritium[18]) seemed always very weak, and were compatible only with low level energy release. The two-step model requires a strong electron screening effect to reduce the Coulomb barrier and release enough energy to explain the experiments. Although it is still premature to imagine some theoretical model for this kind of screening, it is possible to deduce some corollaries from this two-step model, which can be tested by experiment. For example, the screening means a region of high electron density which may be detected by positron annihilation technique; the penetration of the Coulomb barrier by resonance tunneling must help both the fusion and fission, which might affect the spontaneous fission of the fissile elements. Both of these experiments are currently under way in China. We have to identify what are the precursors, and what are the energy carriers in this D/Pd system.

The other aspect of theoretical work is just to develop the theory itself to make it compatible with the need to explain the experiments. For example, the WKB method is commonly used in quantum mechanics for calculating barrier penetration. However, the resonance tunneling needs special attention to the direction of the arrow of the WKB connection formula. Even in Bohm's discussion of resonance tunneling, the problem of the direction of the arrow is barely mentioned. The famous Russian theoretical physicist L.D.Landau said quite differently in the 1960's and 1980's[19]. This is still controversial in the textbooks on quantum mechanics today. We investigate this problem, and find that the existing WKB connection formula can be used only in one direction. In order to use the WKB connection formula in resonance tunneling, it should be modified to include some additional parameters. However, the conclusion is that the resonance tunneling is still possible with a little correction. On the other hand, the physical explanation of resonance tunneling is still an open question. Usually, it is explained by a steady state calculation; however, it is essentially a non-steady state phenomenon. A careful study is necessary through both theory and experiments[20].

Another example is the uncertainty principle. If the electron cloud shrinks to form a strong screening effect, an energy level lower than usual ground level is always assumed. The Mills model[21] or the solutions of the relativistic Schrodinger equation and Dirac equation[22] are invoked to find this energy level, but the uncertainty principle is not compatible with it. A multiple body problem in the crystal lattice should be investigated.

CONCLUDING REMARKS

After five years of searching with high expectations, we are still working very hard. As long as the experiments are getting stronger in confirmation, we will keep searching for the truth.

ACKNOWLEDGMENTS

This work is supported by the State Commission of Science and Technology and the Natural Science Foundation in China. The author would like to thank the Hawaii Natural Energy Institute at the University of Hawaii - Manoa for partial support of his sabbatical.

REFERENCES

[1] R.H. Xiong et al., "Anomalous Neutron Emission from the Discharge Tube with Palladium Electrode and Deuterium Gas," presented at the Symposium on Cold Fusion in China, Beijing, China, (May, 1990).

[2] S.Y. Duan et al., "Fusion Neutron Emission Induced by Injection of Deuterium into Titanium Target in a Mirror Plasma," in The Science of Cold Fusion, edited by T. Bressani et al., Italian Physical Society, Bologna, pp 139-143 (1991).

[3] H.Q. Long et al., "The Anomalous Nuclear Effects Inducing by the Dynamic Pressure Gas Discharge in a Deuterium/Palladium System," in Frontiers of Cold Fusion, edited by H. Ikegami, Universal Academy Press, Tokyo, 1993, pp 455-459.

[4] H.Q. Long et al., "Anomalous Effects in Deuterium/Metal Systems." in Frontiers of Cold Fusion, edited by H. Ikegami, Universal Academy Press, Tokyo, 1993, pp 447-454.

[5] H.Q. Long et al., "New Experiment Results of Anomalous Nuclear Effects in Deuterium/Metal Systems," presented at ICCF4 at Maui, Dec. 6-9, 1993.

[6] Z.Q. Ma, X.Z. Li et al., "The Analysis of the Neutron Emission from the Glow Discharge in Deuterium Gas Tube," presented at ICCF4 at Maui, Dec. 6-9, 1993.

[7] J.T. He et al., "A Study on Anomalous Nuclear Fusion Reaction by Using HV Pulse Discharge," presented at ICCF4 at Maui, Dec. 6-9, 1993.

[8] X.Z. Li et al., "The Precursor of 'Cold Fusion' Phenomenon in Deuterium/Solid Systems," in Anomalous Nuclear Effects in Deuterium/Solid Systems, AlP Conference Proceedings 228, edited by S.E. Jones, 1991, pp 419-429.

[9] S.Y. Dong, X.Z. Li et al., "Precursors to 'Cold Fusion' Phenomenon and the Detection of Energetic Charged Particles in Deuterium/Solid System," *Fusion Technology*, vol 20, p 330 (1991).

[10] D.W. Mo, X.Z. Li et al., "Real Time Measurements of the Energetic Charged Particles and the Loading Ratio (D/Pd)," in Frontiers of Cold Fusion, edited by H. Ikegami, Universal Academy Press, Tokyo, 1993, pp 535-538.

[11] G.S. Huang, X.Z. Li et al., "The Measurements and the Control of the Loading Ratio of Deuterium in Palladium," presented at ICCF4 at Maui, Dec. 6-9, 1993.

[12] Z.L. Zhang et al., "Calorimetric Measurements of the Electrolysis of Heavy Water at Palladium Cathode," presented at ICCF4 at Maui, Dec. 6-9, 1993.

[13] Q.F.Zhang et al., "The Excess Heat Experiments on Cold Fusion in Titanium Lattice," presented at ICCF4 at Maui, Dec. 6-9, 1993.

[14] X.Z. Li et al., "The 3-Dimensional Resonance Tunneling in Chemically Assisted Nuclear Fission and Fusion Reactions," presented at ICCF4 at Maui, Dec. 6-9, 1993.

[15] M.C.H. McKubre et al., "Excess Power Observations in Electrochemical Studies of the D/Pd System; the Influence of Loading," in Frontiers of Cold Fusion, edited by H. Ikegami, Universal Academy Press, Tokyo, 1993, pp 5-19.

[16] M. Fleischmann and S. Pons, "Calorimetry of the Pd-D2O System: from Simplicity via Complications to Simplicity," *Physics Letters A*, vol 176, p 118 (1993).

[17] M.H. Miles and B.F. Bush, "Heat and Helium Measurements in Deuterated Palladium," presented at ICCF4 at Maui, Dec. 6-9, 1993.

[18] F.G. Will, K. Cedzynska et al., "Tritium Generation in Palladium Cathodes with High Deuterium Loading during Heavy Water Electrolysis," presented at ICCF4 at Maui, Dec. 6-9, 1993.

[19] L.D. Landau and E.M. Lifshitz, Quantum Mechanics, 2nd edition, Pergamon, Oxford, Addison-Wesley, 1965, pp 15-17.

[20] D.K. Roy, Quantum Mechanical Tunnelling and Its Applications, Singapore, World Scientific, 1986, pp 1-79.

[21] R.L. Mills et al., "DiHydrino Molecule Identification," private communication (1993).

[22] J.A. Maly et al., "Electron Transitions on Deep Dirac Levels I," *Fusion Technology*, vol 24, p 307 (1993).

A BRIEF SURVEY OF USEFUL INFORMATION ABOUT HYDROGEN IN METALS

R.A. Oriani
Department of Chemical Engineering and Materials Science
University of Minnesota
Minneapolis, MN 55455 USA

INTRODUCTION

Because cold fusion phenomena are notoriously erratic, and the parameters necessary to obtain reproducible and consistent results are poorly understood, it is important to be aware of what is known about the state of hydrogen in metals and of the dynamics of its entry into and release from a metal. This short paper cannot do more than indicate some of the important areas; the interested reader can obtain more information by reading the references [1-3].

EQUILIBRIUM ASPECTS

Hydrogen dissolved in metals at low concentrations exhibits a linear relation between the concentration and the half power of the pressure, p, of the molecular gas. This is proof that hydrogen dissociates when it enters the metal. Much experimental information and theoretical considerations demonstrate that in transition metals the electron accompanying the proton of the dissociated hydrogen enters the s and d-bands of the host metal changing the density of states at the Fermi surface and causing shifts of the energy bands. The Fermi electrons concentrate about the proton, closely screening the positive charge and producing what is effectively a neutral atom [4]. These electronic reactions produce both short-range and long-range interactions between the dissolved hydrogen species.

Hydrogen occupies interstitial sites in the metal lattice, as shown by neutron diffraction in many cases. In so doing the hydrogen "atom" forces the nearest-neighbor metal atoms farther apart from each other, causing an increase of volume of the nearest-neighbor shell of atoms. The free surface of the metal specimen sweeps out to produce a larger volume increase than the volume increase of the inner shell of nearest-neighbor atoms. This is the physical reason for the increase of the lattice parameter of the metal upon absorption of hydrogen. At equilibrium a uniform distribution of dissolved hydrogen in a metal causes zero hydrostatic stress in the lattice, although each hydrogen atom is individually under a hydrostatic stress. There is no force or pressure tending to push the hydrogen atoms together into one interstitial site.

In palladium the interstitial sites having octahedral symmetry, of which there is one site per Pd atom, are the lower-energy sites so that these are preferentially occupied by hydrogen. Unlike the case with substitutional solid solutions, adding an interstitial solute atom to a metal does not increase the number of lattice sites for that solute species. The consequence is that interstitial solutes obey Fermi-Dirac statistics, and it follows that an infinitely large thermodynamic activity would result from a complete filling of all octahedral sites in a lattice. Therefore, as the molecular gas fugacity is increased in an attempt to fill all octahedral sites in palladium with hydrogen, a "spill-over" necessarily occurs into the higher-energy class of interstitial sites, namely, those of tetrahedral symmetry.

Because hydrogen changes the local and the global electronic structure of the host metal, one may expect that hydrogen changes the cohesive forces between metal atoms. Several theoretical

investigations [5] show that the cohesive interactions are in fact decreased in many transition metals including palladium. The consequence is that the effort required to cause brittle cracking of a metal is decreased by hydrogen [6]. In general, the mechanical response to applied stresses is variously affected by hydrogen in complex ways.

Dissolved hydrogen interacts attractively or repulsively with chemical and with structural singularities in the lattice. The interactions with the former, i.e., impurity atoms, are best treated from an electronic point of view. The same is true for structural imperfections when the hydrogen is exactly at the imperfection. However, at distances such that linear elasticity theory can be applied, and the stress field produced by the imperfection can be calculated, the thermodynamics of stressed bodies [7] can be used. For example, a dislocation, whether of edge, screw, or mixed type, has a stress field, as does a particle of a second phase within a matrix. The thermodynamics shows that a stress field that has a positive (i.e., tensile) hydrostatic component of stress, σh, decreases the chemical potential of an interstitial solute, whereas a negative hydrostatic component of stress increases the chemical potential of the solute. Therefore, at equilibrium, i.e., uniform chemical potential everywhere, dissolved hydrogen exhibits a higher concentration on the tensile side of an edge dislocation and a lower concentration on the compressive side. In cases where σh is zero, squared terms in the stress become significant and cause an increase in the chemical potential. Shear stresses also affect the chemical potential so that the shear stress field about a pure screw dislocation lowers the chemical potential of dissolved hydrogen. The relations between solute chemical potential and mechanical stress are valid whether the stress is internally generated, as by dislocations, second phase particles, grain boundaries, stacking faults, etc., or by externally imposed mechanical forces upon the solid body.

The appearance of one solid phase within another solid phase usually involves a change of density, and therefore stress fields are generated in the two phases which change the equilibrium compositions of the co-existing phases from those characteristic of stress-free phases. Thus, as hydrogen increases in concentration in palladium and the high-concentration phase, termed the ß-phase, is generated, the larger specific volume of the growing ß-phase causes compressive stresses upon it and a complex state of stress in the environing α-phase. Because at room temperature the Pd atoms do not diffuse and only the hydrogen atoms can move, a coherence between the α and ß lattices is maintained across the interface when the ß-particle is small. The coherent equilibrium involves equilibrium concentrations different from those obtained when the coherency is destroyed by the nuclear ion of interfacial dislocations. Thereby arises the difference between coherent and incoherent metal-hydrogen phase diagrams, and also the kinetic phenomena of hysteresis in hydrogen absorption and evolution into and from palladium.

KINETIC CONSIDERATIONS

Hydrogen has a very large mobility in transition metals especially in Pd, α-Fe, V and Nb. Its diffusivity is proportional to the product of the mobility and a thermodynamic parameter, $d \ln a / d \ln x$, where a is the thermodynamic activity and x the concentration of the hydrogen. This term can become significant at high concentrations, and in the neighborhood of the critical concentration and temperature of a miscibility gap system (of which Pd-H is an example) the thermodynamic term becomes very small.

Another reason for a decrease of the diffusivity of hydrogen in metals is the attractive interaction with chemical and structural defects. This is the so-called trapping phenomenon [8,9] which is very important at low hydrogen concentrations. Thus, dislocations in a metal will slow down the diffusion

of hydrogen when the dislocations are static. However, if the dislocations are caused to move by applied, or by internally generated shear stresses, hydrogen can be transported with the moving dislocations by virtue of the attractive interaction discussed above.

Diffusive fluxes of hydrogen are proportional to the gradient of the chemical potential of the dissolved hydrogen. Since mechanical stress affects the chemical potential, it is clear that gradients of state of stress can produce diffusive fluxes even in the absence of concentration gradients, and stress gradients can be as important, or more so, than concentration gradients for inducing diffusion of hydrogen. Temperature gradients and gradients of electrical potential can also produce fluxes of hydrogen. Lack of space prohibits discussion of these phenomena, except to assert that deductions about the state of ionicity of the dissolved hydrogen cannot be drawn from measurements of the motion of dissolved hydrogen in an electric field because of the existence of momentum transfer between electrons and electron holes and the dissolved hydrogen [10, 11].

The absorption of hydrogen into the lattice of a metal from the molecular gas must be preceded by adsorption of the molecule upon the surface, dissociation into adsorbed atoms, surface diffusion of the adsorbed atoms, and jumping of these atoms into the sub-surface region. Each of these steps is strongly affected by the atomic-scale topography of the surface and by the quantity and distribution of impurity species and any one of these steps may be kinetically controlling. If hydrogen is presented to the metal surface by electrochemical deposition or by means of a partially dissociated and/or ionized hydrogen gas, the dissociation step is avoided. In all cases the adsorbed species may encounter each other, recombine and return to the cell electrolyte as hydrogen molecules. Hence the transition of adsorbed atoms into the lattice is limited by the kinetics of the recombination reaction. To mitigate this limitation, recombination inhibitors ("poisons") may be added to the environing phase; the exact mechanisms by which these agents act are complex and not fully understood.

Further penetration from the sub-surface plane of the lattice is controlled by diffusion whose boundary condition is the sub-surface concentration, c_o, of hydrogen. This kinetically controlled concentration may be conceptually related to the input fugacity, f_i, of the source of the hydrogen: f_i equals the fugacity, f_e of molecular hydrogen gas, that at equilibrium would produce c_o in a metal at the given temperature. Sieverts law, $c_o = c = s f_e^{½}$ relates f and the hydrogen concentration, c, in the metal at equilibrium. For a gas of molecular hydrogen, there is a correlation between f_e and the gas pressure, p. However, f_i is a kinetically determined quantity without any relation to environing pressure. It is incorrect to believe that a hydrogen-charging system characterized by large f_i (because large c_o values are produced) subjects that metal lattice to a hydrostatic pressure given by the relation between p and f_e.

The input of hydrogen into the sub-surface layer expands that layer, as discussed in a previous section. Since that layer is coherent with the underlying metal which at the moment does not contain hydrogen and is therefore not expanded, a very large compressive stress is produced below the input surface; its magnitude decreases with increasing distance into the metal, and the stress becomes tensile further in. The distribution of both of the normal and the shear stresses is a function of the time of diffusion, but the largest values occur just below the input surface when the value c_o is generated there [12,13].

Because the shear stresses produced are in general very large, dislocations are generated. Some of these dislocations form entangled arrays near the input surface which increase the hardness of the metal and decrease the in-diffusion of hydrogen by trapping the atoms. Other dislocations are caused to glide, by the shear stresses, deeper into the specimen, carrying trapped hydrogen with them and

forming pile-ups at grain boundaries or being annihilated at grain and interphase boundaries. The merging of dislocations into grain boundaries causes the grain boundary to change its atomic configuration and rotation of the grains to occur with respect to each other [13]. Rotation of grains at the specimen surface can produce localized surface elevations and depressions, and emergence of edge dislocations can produce slip lines and serrations on the surface. Because of the dependence of f_i upon the atomic topography of the input surface, different metal grains achieve different c_o values and because dislocation dynamics are complicated functions of grain boundary configuration and of the orientation of the grain lattice with respect to the stress field, adjoining grains achieve different hydrogen contents at any one instant of time [13]. This phenomenon produces additional mechanical stresses between grains. This, as well as dislocation pile-ups at grain boundaries can produce microcavities the growth of which can produce linkage of the cavities and ultimately separation between grains [14]. Such separations, or cracks, fill with molecular gas at a pressure consistent with Sieverts law for the local hydrogen concentration. If the cracks communicate with the external surface of the specimen they provide channels for the loss of hydrogen from that region of the specimen [15].

REFERENCES

[1] R.A. Oriani, to be published in the Proceedings 4th International Conf. on Cold Fusion.

[2] Hydrogen in Metals, G. Alefeld and J. Volkl, eds., Springer-Verlag, Berlin, vols. 1 and 2, 1978.

[3] Metals-Hydrogen Systems, R. Kirchheim, E. Fromm, E. Wicke, eds., Vetlag, Munchen, 1989.

[4] E. Wicke and H. Brodowsky, in Ref. 2, vol. II, p. 73.

[5] M.S. Daw and M.I. Baskes, *Phys. Rev. B*, vol 29, p 6443 (1984); T. McMullen, M.J. Stott, and E. Zaremba, *Phys. Rev. B*, vol 35, p 1076 (1987).

[6] R.A. Oriani, *Ann. Rev. Mater. Sci*. vol 8, p 327 (1978).

[7] J.C.M. Li, R.A. Oriani, L.S. Darken, *Z. Physik. Chem.* (N.F.) vol 49, p 271 (1966).

[8] A.M. McNabb and P.K. Foster, *Trans. Metall. Soc*. AIME vol 227, p 618 (1963).

[9] R.A. Oriani, *Acta Metall*. vol 18, p 147 (1970).

[10] R.A. Oriani and O.D. González, *Trans. Met. Soc*. AIME vol 239, p 1041 (1967).

[11] H. Wipf, in Ref. 2, vol II, p 273.

[12] J.C.M. Li, *Metall. Trans. A*, vol 9A, p 1353 (1978).

[13] M.E. Armacanqui and R.A. Oriani, *Mater. Sci. Eng*. vol 91, p 13 (1987).

[14] T. Matsumoto, *Fusion Technology*, vol 19, p 567 (1991).

[15] E. Storms and C. Talcott-Storms, *Fusion Technology*, vol 20, p 246 (1991).

METHODS REQUIRED FOR THE PRODUCTION OF EXCESS ENERGY USING THE ELECTROLYSIS OF PALLADIUM IN D_2O BASED ELECTROLYTE

by
Edmund Storms
Member ENECO Science Advisory Board

INTRODUCTION

As first proposed by Drs. Pons and Fleischmann [1], excess energy can be created by electrolyzing palladium as the cathode in D_2O using an electrolyte containing 0.1-1.0 M LiOD. Reproducibility of this amazing result can now be greatly improved by following procedures described in this paper. A variety of other environments and materials have been found to produce the effect but these will not be discussed here.

Nuclear reactions can be initiated in a special condition of matter (SCM) that is formed from β-PdD having a sufficiently high deuterium content combined with several other factors. These factors include the presence of still unknown impurities in the palladium and the application of various forms of energy. Apparently, an activation energy exists for the formation of the SCM and this energy is lowered by a suitable deuterium and impurity concentration. This barrier is overcome by the application of some externally generated energy. The closer the chemical conditions are to the ideal condition, the less external energy is required to initiate SCM formation. Once the SCM forms, it is more stable than is ß-PdD thereby suggesting the existence of an activation energy for decomposition as well.

Heat production is not consistently associated with γ-ray, X-ray, neutron or radioactive isotope production. However, all of these products of nuclear reactions have been seen many times both with and without significant heat production while using the electrolytic technique. While these easily detected products do not prove that the excess energy is being produced by a nuclear process, they do demonstrate that various unexpected nuclear reactions can be made to occur in this environment. The most likely source of significant heat production appears to be the formation of ^4He [2,3,4].

CRITICAL DEUTERIUM CONTENT

The first requirement is to achieve the necessary deuterium content at the surface of the palladium. An average content greater than $PdD_{0.84}$ is required to support the larger value at the surface. The average concentration is created by competition between gain at the surface produced from electrolysis and loss of deuterium as gas from microcracks within the palladium. Gain of deuterium is improved by using a sufficiently high electrolytic current density and thin layers of certain impurities on the surface. The loss rate is reduced by using crack-free, high-strength palladium. Such palladium is rare and difficult to obtain with consistent properties.

1. Uptake Rate

The rate of deuterium uptake is determined by the current density and chemical conditions at the surface. A minimum current density of 150 mA/cm^2 appears to be required [5,6,7,8,9,10]. However, much higher current densities are occasionally found necessary to initiate heat production. This current should be uniformly distributed over the entire surface of the sample. Once excess heat production starts, the higher the applied current density above the onset value, the greater the excess power with a nearly linear

relationship between the two quantities. A D/Pd ratio above ≈ 0.84 for the average deuterium content is frequently observed when excess power production first starts [7,6,11,12]. Values above $PdD_{1.0}$ are occasionally achieved. The actual deuterium content of the SCM is still unknown.

In addition to a sufficiently high current density, the presence of certain impurities on the palladium surface is important to improve deuterium retention. These impurities can come from the anode, the electrolyte, or the container. Several of these beneficial impurities include aluminum and silicon [6], which result if Pyrex glass is used as the container. Aluminum (2-20 ppm) added after the palladium has achieved its maximum deuterium content is sometimes found useful in initiating excess heat production [6,10]. Thiourea has also been used with success [13]. Absence of certain surface impurities such as copper, lead, or silver (from solder) is also important. However, thin films of gold (≈ 7000 Å) on the palladium surface have been found to increase the limiting D/Pd ratio [14]. The benefit of lithium and platinum, two impurities normally observed on and within the surface region, is still unknown. Because of electrodeposition from the electrolyte and electromigration within the palladium, the chemical composition of the surface is a complex function of time, integrated current, temperature, and purity of the palladium. Therefore, the chemical composition of the SCM is unknown and is probably significantly different from the bulk material.

Heavy-water sometimes contains impurities that will inhibit the effect. Therefore, the D_2O should be distilled or purified before use. In addition, heavy-water easily picks up normal water from the atmosphere. Excess heat production is significantly reduced when the normal water content is only slightly increased.

2. Necessary Characteristic of Palladium

The nature of the palladium is the second part of the requirement. Most palladium forms microcracks and dislocations when it is converted to the hydride [15,16]. Only very unusual palladium is found to be relatively crack-free after hydriding. A quantitative measurement of the volume resulting from crack formation can be used to evaluate particular batches of palladium prior to heat measurements [17]. Crack volume in excess of 2% of the total volume after forming ß-PdD frequently makes the material inactive [18] while a smaller excess volume can result in a higher success rate. In addition, successful palladium can be seen to absorb almost 100% of the deuterium delivered to the surface until the composition reaches about $PdD_{0.6}$. During this stage, very few bubbles are formed on the surface. Further electrolysis of a potentially active cathode results in a stable average composition above $PdD_{0.85}$. If excess energy is to be produced by the sample, it will appear after several hundred additional hours of electrolysis at currents above the onset current density. During this time, uniform bubble formation should be observed across the entire surface. A successful cathode also shows higher overvoltage than does bad material [19,20]. Crack formation can be reduced if the initial loading rate and temperature are kept low. Initial current densities below 20 mA/cm^2 are suggested. Once a composition above $PdD_{0.7}$ is achieved, the current density and temperature may be increased.

Improved success has been claimed when the palladium has been polished [21] or when it has been cold-worked to achieve an unusually large hardness [22, 23]. Annealing in vacuum seems to have no significant effect while success may be improved after oxidizing in air between 500° and 800°C. Thin films (5-20 µm) of palladium formed on a silver substrate by electrodeposition or an alloy of 0.9 Pd and 0.1 Ag have also been found to give higher success rates.

Successful palladium has been found to produce excess energy even after it has been deloaded and reloaded, after it has been kept in liquid nitrogen before being reelectrolyzed, and when heated as hot as 100°C [24,25,21] during electrolysis. Bad palladium may occasionally work for brief periods at low

power production levels, but it can not be relied on to produce significant results regardless of treatment.

INITIATING CONDITIONS

Application of nonequilibrium conditions can initiate the "excess heat" effect. Very successful results have been reported after using pulsed (1 μsec) high voltages with a resulting high current (up to 100 A) [22], current switched between two extreme values [18,21,26], and MHz frequencies of particular values at the mW level [27,19].

Excess heat production also increases as the temperature is increased [10]. Indeed, significant heat has been produced at 100°C after electrolysis stopped when the electrolyte boiled off [24]. Therefore, increasing the temperature after excess heat has been produced can increase the magnitude of the effect. Even in the absence of externally applied energy, bubble formation creates micro regions of current and voltage variations that may produce the required frequencies and local heating. This energy source alone appears to initiate the effect once other necessary conditions have been achieved within the palladium. However, because the best conditions are seldom achieved over the entire surface, the application of additional energy is beneficial.

CONCLUSION

Three major factors are important to achieving excess power using palladium plus deuterium. These are: an average D/Pd ratio above 0.84, the presence of certain unknown impurities in the surface region of the palladium cathode, and the application of externally generated energy. When a proper mixture of these independent factors is achieved, a transformation takes place in the palladium deuteride. Various nuclear reactions can be initiated in the resulting SCM depending on several unknown variables. This SCM is more stable at high temperatures than is normal ß-PdD. It is unlikely that the SCM is simply another phase in the Pd-D system.

REFERENCES

[1] M. Fleischmann and S. Pons, "Electrochemically Induced Nuclear Fusion of Deuterium," *J. Electroanal. Chem.*, vol 261, (1989) p 301.

[2] M.H. Miles and B.F. Bush, "Heat and Helium Measurements in Deuterated Palladium," Fourth International Conference on Cold Fusion, Lahaina, Maui, Dec. 6-9, 1993. See also: M.H. Miles et al., *J. Electroanal. Chem.*, vol 346 (1993) p 99, and M.H. Miles and B.F. Bush, in Frontiers of Cold Fusion (H. Ikegami, ed), Universal Academy Press, Tokyo, 1993, p 189.

[3] D. Gozzi, G. Balducci, R. Caputo, P.L. Cignini, G. Gigli, M. Tomellini, "Helium-4 Quantitative Measurements in the Gas Phase of Cold Fusion Electrochemical Cells," Fourth International Conference on Cold Fusion, Lahaina, Maui, Dec. 6-9, 1993.

[4] R.S. Stringham, "Cavitation Induced Micro-Fusion," Fourth International Conference on Cold Fusion, Lahaina, Maui, Dec. 6-9, 1993.

[5] R.G. Kainthla et al., "Sporadic Observation of the Fleischmann-Pons Effect," *Electrochim. Acta.*, vol 34, 1989, p 1315.

[6] M.C.H. McKubre, S. Crouch-Baker, A.M. Riley, S.L Smedley and F.L. Tanzella, "Excess Power Observations in Electrochemical Studies of the D/Pd System; the Influence of Loading," Proceedings of the Third International Conference on Cold Fusion, October 21-25, 1992, Nagoya, Japan, Frontiers of Cold Fusion (H. Ikegami, ed), Universal Academy Press Inc., Tokyo, Japan, p 5.

[7] K. Kunimatsu, N. Hasegawa, A. Kubota, N. Imai, M. Ishikawa, K. Akita and Y. Tsuchida, "Deuterium Loading Ratio and Excess Heat Generation during Electrolysis of Heavy Water by a Palladium Cathode in a Closed Cell Using a Partially Immersed Fuel Cell Anode," Proceedings of the Third International Conference on Cold Fusion, October 21-25, 1992, Nagoya, Japan, Frontiers of Cold Fusion (H. Ikegami, ed), Universal Academy Press, Inc., Tokyo, Japan, p 31.

[8] S. Hasegawa, K. Kunimatsu, T. Ohi, and T. Terasawa, "Observation of Excess Heat during Electrolysis of 1M LiOD in a Fuel Cell Type Closed Cell," Proceedings of the Third International Conference on Cold Fusion, October 21-25 , 1992, Nagoya, Japan, Frontiers of Cold Fusion (H. Ikegami, ed), Universal Academy Press, Inc., Tokyo, Japan, p 377.

[9] T. Mizuno, T. Akimoto, and K. Azumi, "Cold Fusion Reaction Products and Behavior of Deuterium Absorption in Pd Electrode," Proceedings of the Third International Conference on Cold Fusion, October 21-25, 1992. Nagoya, Japan, Frontiers of Cold Fusion (K. Ikegami, ed), Universal Academy Press, Inc., Tokyo, Japan, p 373.

[10] E. Storms, "Some Characteristics of Heat Production Using the `Cold Fusion' Effect," Fourth International Conference on Cold Fusion, Lahaina, Maui, Dec. 6-9, 1993.

[11] N. Hasegawa, K. Kunimatsu, T. Ohi, and T. Terasawa, "Observation of Excess Heat during Electrolysis of 1M LiOD in a Fuel Cell Type Closed Cell," Proceedings of the Third International Conference on Cold Fusion, October 21-25, 1992, Nagoya, Japan, Frontiers of Cold Fusion (H. Ikegami, ed), Universal Academy Press, Inc., Tokyo, Japan, p 377.

[12] T. Mizuno, T. Akimoto, and K. Azumi, "Cold Fusion Reaction Products and Behavior of Deuterium Absorption in Pd Electrode," Proceedings of the Third International Conference on Cold Fusion, October 21-25, 1992, Nagoya, Japan, Frontiers of Cold Fusion (H. Ikegami, ed), Universal Academy Press. Inc., Tokyo, Japan, p 373.

[13] N. Hasegawa, N. Hayakawa, Y. Yamamoto, and K. Kunimatsu, "Observation of Excess Heat During Electrolysis of 1M LiOD in a Fuel Cell Type Closed Cell," Fourth International Conference on Cold Fusion, Lahaina, Maui, Dec. 5-9, 1993.

[14] A. Kubota, K. Karo, and K. Kunimatsu, "Electrolytic Deuterium Absorption by Pd Cathode with Sputtered Gold Field," Fourth International Conference on Cold Fusion, Lahaina, Maui, Dec. 6-9, 1993.

[15] Robert Huggins, "Some Materials Aspects of the Electrochemical Insertion of Hydrogen and Deuterium into Metals," Fourth International Conference on Cold Fusion, Lahaina, Maui, Dec. 6-9, 1993.

[16] R.A. Oriani, "Physical and Metallurgical Aspects of Entry of Hydrogen into Metals," Fourth International Conference on Cold Fusion, Lahaina, Maui, Dec. 6-9, 1993.

[17] E. Storms and C. Talcott-Storms, "The Effect of Hydriding on the Physical Structure of Palladium and on the Release of Contained Tritium," *Fusion Tech.,* vol 20 (1991), p 246.

[18] E. Storms, "Measurement of Excess Heat from a Pons-Fleischmann Type Electrolytic Cell," Proceedings of the Third International Conference on Cold Fusion, October 21-25, 1992, Nagoya, Japan, Frontiers of Cold Fusion (H. Ikegami, ed), Universal Academy Press, Inc., Tokyo, Japan, p 21.

[19] J.O'M. Bockris, R. Sundaresan, D. Letts and Z.S. Minevski, "Triggering and Structural Changes in Cold Fusion Electrodes," Fourth International Conference on Cold Fusion, Lahaina, Maui, Dec. 6-9, 1993.

[20] M. Okamoto, Y. Yoshinga and T. Kusunoki, "Excess Heat Generation, the Over Voltage Deviation and the Neutron Emission in D_2O-LiOD-Pd Systems," Fourth International Conference on Cold Fusion, Lahaina, Maui, Dec. 5-9, 1993.

[21] D. Cravens, "Factors Effecting the Success Rate of Heat Generation in CF Cells," Fourth International Conference on Cold Fusion, Lahaina, Maui, Dec. 6-9, 1993.

[22] F. Celani, A. Spallone, P. Tripodi, A. Nuvoli, A. Petrocchi, D. Di Gioacchino, M. Boutet, P. Marini, and V. Di Stefano, "High Power μs Pulsed Electrolysis for Large Deuterium Loading on Pd Plates," Fourth International Conference on Cold Fusion, Lahaina, Maui, Dec. 6-9, 1993.

[23] M. Schreiber, T.M. Gur, G. Lucier, J.A. Ferrante, J. Chao, and R.A. Huggins, "Recent Measurements of Excess Energy Production in Electrochemical Cells Containing Heavy Water and Palladium," Proc. 1st Annual Conf. Cold Fusion, Salt Lake City, UT, March 28-31, 1990, p. 44. See also: Proc. Cold Fusion Symp., 8th World Hydrogen Energy Conf., Honolulu, HI, July 22-27, 1990, p 71.

[24] S. Pons and M. Fleischmann, "Heat After Death," Fourth International Conference on Cold Fusion, Lahaina, Maui, Dec. 6-9, 1993.

[25] M.C. McKubre, B. Bush, S. Crouch-Baker, A. Hauser, N. Jevtic, T. Passell, S. Smedley, F. Tanzella, M. Williams, and S. Wang, "Calorimetry Studies of the D/Pd System," Fourth International Conference on Cold Fusion, Lahaina, Maui, Dec. 5-9, 1993.

[26] A. Takahashi, A. Mega, T. Takeuchi, H. Miyamaru and T. Iida, "Anomalous Excess Heat by D_2O/Pd Cell under L-H Mode Electrolysis," Proceedings of the Third International Conference on Cold Fusion, October 21-25, 1992, Nagoya, Japan, Frontiers of Cold Fusion (H. Ikegami. ed), Universal Academy Press, Inc., Tokyo, Japan, p. 79.

[27] Dennis Letts, "Triggering Exothermic/Endothermic Effects in Deuterated Palladium," Fourth International Conference on Cold Fusion, Lahaina, Maui, Dec. 6-9, 1993.

GENERALIZED ISOTOPIC FUEL LOADING EQUATIONS

MITCHELL R. SWARTZ
©JET Technology, Weston, MA 02193 USA

ABSTRACT

The quasi-one-dimensional (**Q1D**) model [1] of isotopic fuel loading, including the coupling to a material [2], has offered insights into electrodes and materials filled by an isotopic fuel. Past examinations [1,2,3] have discussed both competitive gas-evolving reactions at the surfaces of the electrode, the impact of the ratio of the applied electric field energy to thermal energy [k_B*T], and other factors which appear decisive in controlling the loading. Following the demonstration of sonic-induced loading, and cold fusion reactions [4] and complexities at the metal-double layer junction [5] the derived fusion flux equation linking the deuteron loading flux from the region external to the material to potential reactions at that site must be extended to include any ordering force including those derived from sonic fields.

There may be implications upon calculations of the activities and fugacities [6,7] following aqueous loadings [8] and derivations of distributions of deuterium in the palladium [9] and the solution [1,10]. Our present calculations attempt to account for induced drift by the applied electric field [11], electric field distributions altered with complex conduction and polarization phenomena [12,13,14], secondary space charge polarization, propagation of solvated deuterons, deuterons in clathrates, and L-,D-deuteron defects with their ferroelectric inscription in the heavy water [11,13], and the formation of low dielectric constant bubbles [14]. The double layer between the solution and the metal is created both by the cathode fall of ions and other polarization reactions [6,7,11] and is significant. At this double-layer boundary intermolecular deuteron transfer from the solution to octahedral sites within the palladium may control the loading [11]. Within the metal, the deuteron diffusion [1,3,9] involves optical and acoustic phonon spectra [3], material defects, grain boundary dislocations, "zeolite"-like diffusion [9] and fissures.

INTRODUCTION

Classical calculations of the activities of an ionic electrolyte [1,2] adjacent to a metal electrode have been applied to cold fusion reactions following loading of isotopic fuel into a metal [3], and have been used to derive the distributions of deuterium in the palladium [4] and in the solution [5,6]. However, one premise is that the systems are at equilibrium which may not be true [7]. Therefore, a quasi-one-dimensional (**Q1D**) model for an electrode filled by the isotopic fuel was formulated [5]. The **Q1D** model offers insight into the processes because it indicates how both competitive gas evolving reactions at the metal electrode surface and the ratio of the applied electric field energy to thermal energy [k_B*T] are decisive in controlling the loading of the metal by the deuterium [5]. We now extend that model and correct the derived fusion equation [8] which links the deuteron loading flux from the solution into the metal for potential reactions at that site.

DEVELOPMENT OF THE MODEL

Fig. 1 shows the four regions of the electrochemical cold fusion cell. Within the heavy water solution, most deuterons are tightly bound to oxygen atoms. The power source generates the applied electric field intensity. The induced drift by the applied electric field is shown schematically in the figure; which does not mean that the deuterons actually are free to travel in such a simple fashion [9]. The electric field

distribution is altered as the solution and system each respond with complex conduction and polarization phenomena [10,11,12]. Ionic drift, secondary space charge polarization, propagation of solvated deuterons, deuterons in clathrates, and L-,D-deuteron defects with their ferroelectric inscription in the heavy water [9,11], and the formation low dielectric constant bubbles abutting the cathode are the minimum expected [12]. The double layer between the solution and the metal is created both by the cathode fall of ions and other polarization reactions [1,2,9].

In the absence of significant convection, the flux (J_i) of any i_{th} species (here deuterons) results from both diffusion down concentration gradients and electrophoretic drift [5,7,10].

$$J_D = - B_D * \frac{d[D+(z,t)]}{dz} - \mu_D * [D^+(z,t)] * \frac{d\Phi}{dz} \quad (1)$$

Three components of the deuteron flux (J_i) must be considered at the cathode. The first flux component is the entry of deuterons into the bulk of palladium (J_e). The second flux component is the loss of deuterons secondary to gas evolution (J_g). The third flux component is caused by those deuterons lost to any putative fusion reactions, and is represented as J_{fus}. J_{fus} is assumed to be 0 in the bulk solution. The mathematical solution for the time rate of change of the deuterium in any given volume is determined by these fluxes and Gauss' Theorem [5].

Deuteron entry to the cathode is electron limited with all entry occurring at the cathode-double layer interface. At this boundary intermolecular deuteron transfer from the solution to octahedral sites within the palladium may control the loading [9]. Within the metal, the deuteron diffusion has been considered by several models [5,4,13]. Optical and acoustic phonon spectral [13], material defects, grain boundary dislocations, "zeolite"-like diffusion [4] and fissures, all may influence the deeper loading of the metal.

CRITICAL LOADING FLUX

The **Q1D** model links the deuteron flux from the solution into the pericathodic volume, and includes deuteron flow into the metal, deuterons involved in gas evolution, and deuterons consumed in any potential fusion reactions.

$$\frac{d[D^+(z,t)]}{dt} = \left[B_D * \frac{d^2(D^+)}{dz^2}\right] + \left[\mu_D * (D^+) * \frac{d^2\Phi}{dz^2}\right] + \left[\mu_D * \frac{d\Phi}{dz} * \frac{d(D^+)}{dz}\right] + \left[\frac{d(D^+)}{dz} * \frac{dB_D}{dz}\right]$$
$$+ (D^+) * \frac{d\Phi}{dz} * \frac{d\mu_D}{dz} - \frac{d[\Sigma J_i]}{dz} \quad (2)$$

The mathematical solution of equation 2 is determined both by the boundary conditions and by conservation of mass. There is assumed conservation of deuterons with the exception of a loss (J_{fus}) to all putative fusion reactions, extremely small compared to either most loading rates or gas evolving reactions[5]. As discussed previously [5], examination of the solution indicates that the deuteron loading rate into the electrode is critically linked to gas evolution and is also first order on [μ_D * E].

$$\kappa_e = (\mu_D * E) - (\kappa_g + \kappa_{fus}) \quad (3)$$

This loading rate equation relates deuteron availability (secondary to the applied electric field) to the losses of deuterons to both gas evolution and the fusion reactions. One simple but important corollary

is that the evolution of D_2 gas and deuteron loading to the palladium cathode are mutually exclusive for any given applied electric field.

Quantity of Deuterons Contributing (Ψ_{fus})

In a successful cold fusion system J_{fus} is not zero. Therefore, the non-dimensional parameter, Ψ_{fus}, is defined as the fractional amount of intrapalladial deuterons which actually contribute to the desired reactions. When the filling of the palladium with deuterium is complete, J_e would be on the order of J_f [5]. This fusion rate equation can be examined for its relation to thermal processes by substitution using further non-dimensional parameters and the Einstein relation.

$$\frac{B_D}{\mu_D} = \frac{k_B * T}{q} \tag{4}$$

The Loading Ratio ($\Lambda_{Pd,D}$)

The non-dimensional parameter $\Lambda_{Pd,D}$, is defined as the ratio of the two largest and most important pericathodic fluxes; the loading flux (J_e) to the gas evolution (J_g). It is very much a function of the isotope and the material, hence the paired subscript.

$$\Lambda_{Pd,D} = J_e / J_g \tag{5}$$

Thus if $\Lambda_{Pd,D}$ is .01, most of the current is going to gas electrolysis, whereas $\Lambda_{Pd,D} = 100$ would indicate more efficient loading. Substitution of the transolution voltage, and $\Lambda_{Pd,D}$ as the loading factor, and the Einstein relation yields equation 6.

$$J_{fus} = \frac{[2\Lambda_{Pd,D}]}{[2\Lambda_{Pd,D} + 1]} * \frac{[B_D * <D_i>]}{L_c} * \frac{1}{[1 - \exp\left(\frac{q * V}{k_B * T}\right)]} * \frac{[q * V]^2}{[k_B * T]^2} * \Psi_{fus} \tag{6}$$

This fusion flux equation (equation 7) contains five terms after separation of variables. The first term results from gas evolution. The second term is composed of geometric and material factors. The next two terms reflect the applied electric field intensity and k_BT and are dominated by the ratio of the applied electrical energy which are organizing the deuterons to the energy causing their random thermal disorganization. The final term is the fraction of deuterons which actually partake in any potential fusion process(es). Ψ_{fus} is the fractional amount of intrapalladial deuterons which actually contribute to the desired reactions. Introducing ζ, the electric order/thermal disorder ratio, then simplifies this fusion flux equation.

$$J_{fus} = \frac{[B_D * <D_i>]}{[L_c * [1 + (2\Lambda_{Pd,D})^{-1}]]} * \frac{[\zeta^2]}{[1 - \exp[-\zeta]]} * \Psi_{fus} \tag{7}$$

This relationship is demonstrated in Fig. 2 and Fig. 3 which show the impact. In figure 2, for simplicity, J_{fus} is assumed to be 0. The loading flux of deuterons into the palladium at the cathode surface (J_e) is shown as a function of the electric field intensity, for various rates of gas [D_2] evolution rates (J_g). The series of parametric curves indicates how the loading rates are sensitively dependent both upon the electric field energy as well as the competing gas evolving reactions. Examination of equation 7 indicates that

although $\Lambda_{Pd,D}$ has major effects for every ζ, however, that importance requires a level of $\Lambda_{Pd,D}$ approx. > 1 to plateau its importance as is shown in Fig. 3.

The critical term previously did reflect the applied electric field intensity and k_BT and are dominated by the ratio of the applied electrical energy (or generally, other organizing energy) which are organizing the deuterons to the energy causing their random thermal disorganization. The final term is the fraction of deuterons which actually partake in any potential fusion process(es). We now expand the analysis with ξ which is the generalized order/thermal disorder ratio. Θ is the term interrelating the build up of the isotopic fuel to the desired final pathways.

$$J_{fus} = \frac{[B * <D_i>]}{[L_c * [1 + (2\Lambda_{Pd,D})^{-1}]]} * \frac{[\xi]^2}{[1 - \exp[-\xi]]} * \Psi_{fus} * \Theta$$

Ψ_{fus} is the fractional amount of intrapalladial deuterons which actually contribute to the desired reactions. $\Lambda_{Pd,D}$ the loading flux ratio.

Summary

The quasi-one-dimensional (**Q1D**) model of isotopic fuel loading has been modified using three non-dimensional factors, $\Lambda_{Pd,D}$ the loading flux ratio, Ψ_{fus} the fractional amount of intrapalladial deuterons which actually contribute to the desired reactions, and ξ the generalized order/thermal disorder ratio.

Acknowledgements

The author thanks Profs. P. Hagelstein, M. Zahn, and Drs. S. Baer and Roger Stringham, Gayle Verner and especially Hal Fox for their helpful comments, suggestions, and support with the development of this model for this text.

TABLE OF VARIABLES

B_D	diffusivity of deuterons [cm^2/sec]	q	electric charge
$[D^+]$	deuteron concentration	T	absolute temperature (Kelvin)
$<D_i>$	initial deuteron concentration [t=0]	V	voltage = - Φ the potential
E	electric field intensity	κ_f	first order deuteron fusion rate
F	the Faraday	κ_g	deuteron gas evolution rate
I	electrical current	κ_e	first order deuteron entry rate
J_e	flux of deuterons entering Pd cathode	$\Lambda_{Pd,D}$	flux loading/gas evolution ratio
J_g	flux of deuterons evolving to gas	μ_D	electrophoretic mobility
J_f	flux of deuterons in fusion reaction(s)	η_D	electrical transference ratio
k_B	Boltzmann constant	Ψ_{fus}	fraction of deuterons involved
L	length	ζ	electric order/thermal ratio

REFERENCES

[1] M. R. Swartz, "Quasi-One-Dimensional Model of Electrochemical Loading of Isotopic Fuel into a Metal", *Fusion Technology*, vol 22, no 2, Sept. 1992, pp 296-300.
[2] M. Swartz, "Isotopic Fuel Loading and Other Reactions within an Electrode", ICCF-4 (1993).
[3] M. R. Swartz, "Catastrophic Active Medium Hypothesis of Cold Fusion", ICCF-4 (1993).
[4] R. Stringham "Cavitation Induced Micro-Fusion", ICCF-4 (1993).
[5] R. Oriani, "Physical and Metallurgical Aspects of the Entry of Hydrogen into Metals", ICCF-4 (1993).

[6] J. O'M Bockris, A. K. N. Reddy, Modern Electrochemistry, Plenum Press (1970).
[7] H. H. Uhlig, Corrosion and Corrosion Control, Wiley (1971).
[8] M. Fleischmann, S. Pons, "Electrochemically Induced Nuclear Fusion of Deuterium", *J. Electroanal. Chem*., vol 261, p 301 (1989).
[9] S. Szpak, C.J. Gabriel, J.J. Smith, R.J. Nowak, "Electrochemical Charging of Pd Rods," *J. Electroanal. Chem*., vol 309, (1991) pp 273-292.
[10] M. Viitanen, "A Mathematical Model for Metal Hydride Electrodes," *J. Electrochem. Soc*., vol 140, no 4 (1993), pp 936-942.
[11] M. R. Swartz, "Double Layer Transfer of Deuterons into Metals", in preparation.
[12] J. R. Melcher, Continuum Electromechanics, MIT Press, Cambridge (1981).
[13] A. Von Hippel, D.B. Knoll, W.B. Westphal, "Transfer of Protons Through 'Pure' Ice I_h Single Crystals," *J. Chem. Phys*., vol 54, p 134 (also p 145), (1971).
[14] A. Von Hippel, ed., Dielectric Materials and Applications, MIT Press (1954).

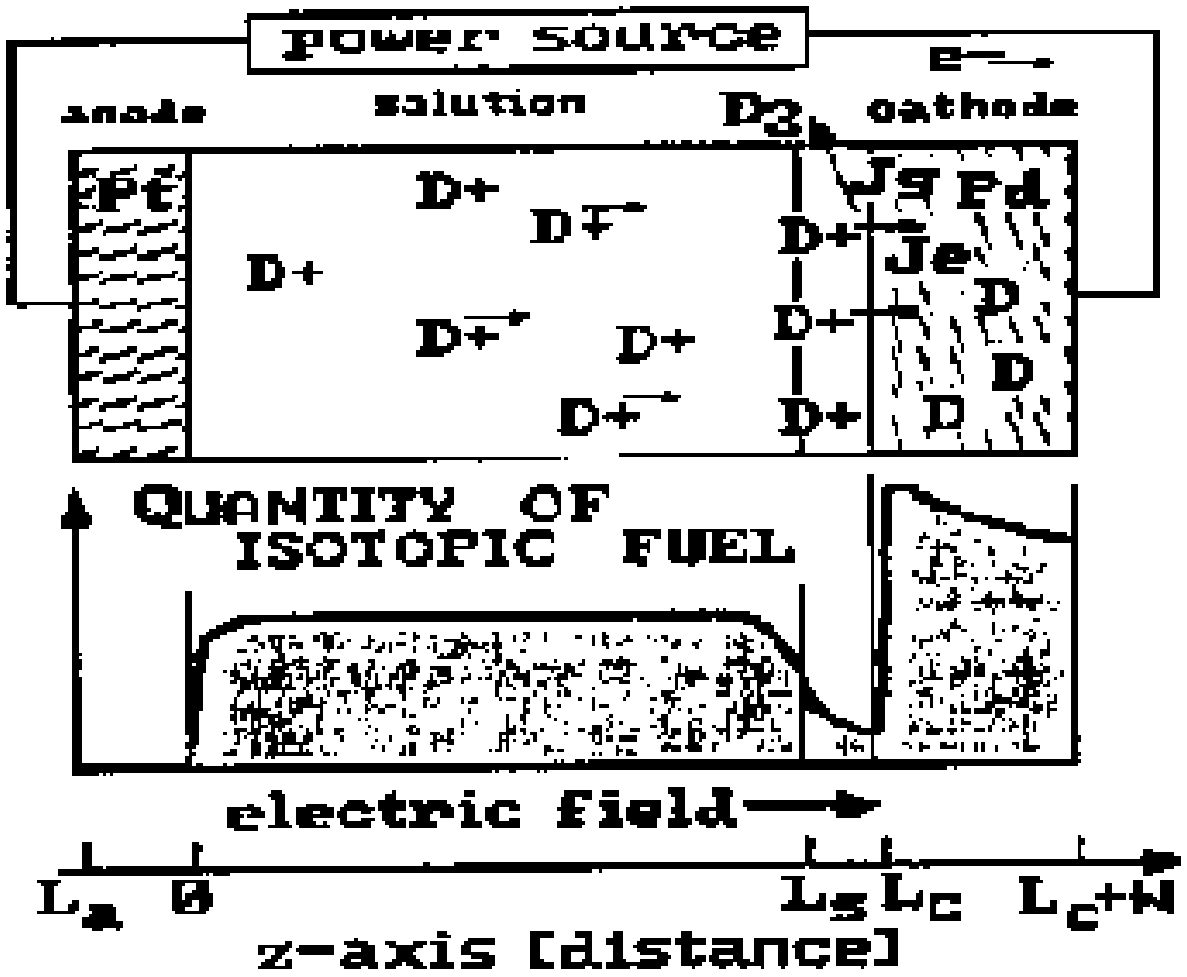

FIGURE 1 - THE Q1D MODEL OF ISOTOPIC FUEL LOADING

The applied electric field influences the spatial distribution of deuterons in aqueous solution. There are four compartments considered outside of the material (palladium electrode in this case) to be loaded with the isotopic fuel. The first is the anode. The induced drift in the second compartment (heavy water) by the initial applied electric field is schematically shown. There is a double layer region, the "width" of which is greatly exaggerated in the figure. The last compartment is the gas volume outside of the material.

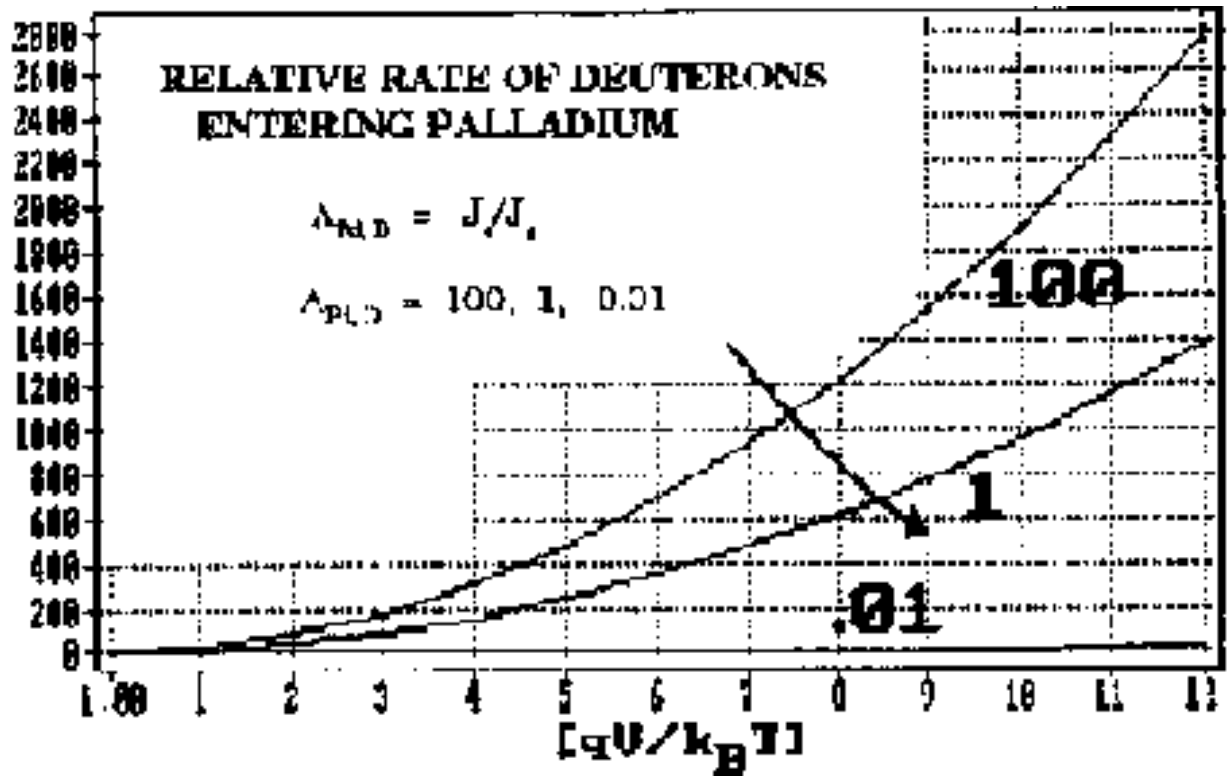

FIGURE 2 - LOADING RATE OF PALLADIUM
The relative values for the loading flux (J_e) is shown as a function of the electric field intensity, parametrically for various rates of gas [D_2] evolution rates at the cathode (characterized as J_g). In this example, J_{fus} is zero. The curve is shown as a function of ζ, the electric order/thermal disorder ratio.

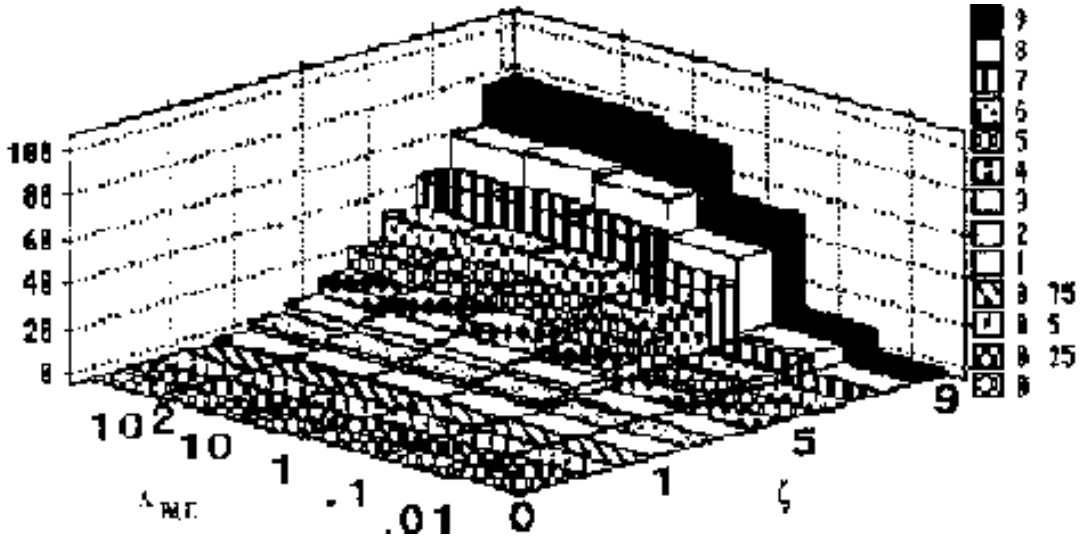

Figure 3 - Parametric Examination of Q1D Fusion Flux
This 3-D parametric graph represents an examination of the fusion flux equation based upon ζ and $\Lambda_{Pd,D}$ (see eq. 7).

EXPERIMENTAL EVIDENCE FOR "COLD FUSION"

Over 300 papers have been published or presented at conferences that provide experimental data in support of the original announcement by Pons and Fleischmann. In addition, many other papers have been written to report on new "cold fusion" phenomena, some of which have greatly surprised even Pons and Fleischmann.

Some of these papers report on "transmutation." For some scientists, the use of the term **transmutation** is unacceptable. The logic behind this rejection of the term is unclear. **Most nuclear reactions involve change from one element to another. Nuclear reactions involve changes to the nuclei either by fusion or by fission.** Experimental **cold nuclear fusion** is a record of elemental changes.

If one carefully examines all of the possible nuclear reactions that are allowed by the Conservation of Charge, allowed beta processes, Conservation of Baryon Number, etc., there are 338 such possible nuclear reactions **which DO NOT emit neutrons.**
There are very few possible (allowed) nuclear reactions that emit neutrons. One of the well-known branching ratios of d + d fusion is that **under gas plasma conditions**, about 50% of the time neutrons are produced. The experimental fact that few neutrons are produced in the variety of cold nuclear fusion experiments has been used by the pathological skeptics as evidence that cold fusion is not real. In fact, this is about the only basis they have for their sustained avoidance of the many positive indications of nuclear reactions.

The following papers provide an array of experimental evidence that supports the claims for a variety of nuclear reactions that appear to occur in many cold fusion experiments. However, healthy skepticism should be exercised. There may be new phenomena involved in these experiments that produce excess heat without producing nuclear reactions. Specifically, two new phenomena **could explain some of the observed experimental findings:** these are (1) the possibility of a collapse of the hydrogen atom below its ground state (as first proposed by Mills, and discussed in this volume by Vigier), and (2) the ability of high-density charge clusters to produce excess energy as taught by Ken Shoulders (U.S. patent 5,018,180) and Harold E. Puthoff. High density charge clusters can be produced under appropriate conditions whenever electric discharges, arcing, or sparking occur.

ON THE POSSIBILITY OF D-D FUSION STIMULATION BY A HIGH-CURRENT ARC DISCHARGE IN GAS-FILLED METAL

V.P. Afanaseyev, G.A. Dyuzhev, A.A. Logatchev, B.I. Tsirkel', S.M. Shkolnik.
A.F. Ioffe Physical-Technical Institute, RAS
Polytechnicheskaya 26, St. Petersburg, 194021, Russia.

N.M. Kazarinov, L.M. Solin.
V.G. Khlopin Radium Institute
Shvernik Avenue 28, St. Petersburg, 194021, Russia.

INTRODUCTION

Beginning in 1989 there appeared many publications on the study of the so-called "cold nuclear fusion" (CNF). Some of the reported results affirm the existence of the CNF phenomena, while others deny it. Distinctive peculiarities of the experiments where the CNF has been observed include poor reproducibility, a sporadic character of the corresponding signals and the observation only under the non-equilibrium conditions in the metal-deuterium system. A generally accepted view on the CNF mechanism up to the present is absent. One widespread hypothesis is the assumption of an "accelerating" or "accelerating-fracture" mechanism, which actually suggests not a "cold" (as in μ-catalysis) but a "microscopically hot" fusion [1,2]. Of interest is the quest for the ways in which CNF initiation can be reproduced to observe the same reactions proceeding under definite conditions. In [3] the initiation of the nuclear reaction was carried out by impact destruction of a monocrystal LiD. In the present study we tried to initiate the CNF by means of a high-current low-voltage pulse arc discharge in a vacuum with palladium or titanium cathodes loaded with deuterium.

The vacuum arc is a low-voltage (U = 20-30 volts) discharge in electrode material vapors. The so-called cathode spots (CS) are formed on the cathode of the vacuum arc. CS are bright luminescent regions of small dimensions, through which there occurs a shorting of the current between the integrally cold metal and plasma. CS on the de-gassed clean metal electrodes are studied in detail [4]. The spot size is tens of microns, the current density $j \approx 10^7$ A/cm^2. The metal surface temperature in the spot is estimated to be several thousands of degrees. A CS exists on the electrode during $\approx 10^{-6}$ s, dying away afterwards. The current, going through one spot is $I_r \leq 10^2$ A. Thus in a discharge with a current $I \geq 10^3$ A several tens of spots are functioning simultaneously on the cathode surface; during the pulse time with a duration of e.g. $\tau \approx 10^{-3}$ s the cathode spots must die away several hundred times and form again on other parts of the surface. The CS are sources of hypersonic jets of the highly ionized plasma.

An arc discharge is also realized on the gas-filled cathodes, its integral characteristics are somewhat different from those of the discharge on a degassed clean metal [5]. The cathode processes in the discharges with gas-filled electrodes are at present poorly studied, but there is evidence to consider that the spot properties, which are the most significant for us, are preserved. These properties include a high current density, short life-time, and a high temperature of the surface.

The above described CS properties render promising the attempts to initiate the CNF by means of an arc discharge with deuterium-filled electrodes. In fact, during the burning of the arc discharge tens of localized thermal sources with a high $\approx 10^8$ W/cm^2 energy flux density to the electrode (volt-equivalent of the cathode ≤ 10 V), as if wandering over the cathode, cause a rapid local heating of near-surface metal regions (which have a characteristic size of $l \approx rs \approx 10^{-3}$ cm) till the temperature nears the melting point

(the current spreading region is implied). The temperature gradient on the metal turns out to be correspondingly > 10^6 K/cm. In the metal-deuterium system a strong local non-equilibrium is created. The high current density leads to an appearance of a strong friction forced between the implanted deuterium nuclei and the electron flux. In the spot formation stage ($\tau \leq 10^{-8}$s) the electron current density and consequently the energy flux density is 1 to 2 orders of magnitude higher. In addition, on the cathode surface in the region directly adjoining the spot, there flows a current of metal and deuterium ions, whose density may reach $j_{ik} \approx 10^5$ A/cm^2, and the ion energy $E_{ik} \approx 10$eV. The deuterium ions, having such energy, may effectively implant themselves in the near surface metal layer. At the anode surface the ion current flows essentially more uniformly, its density is significantly lower $j_{ia} \approx 10^2$ A/cm^2, but the ion energy is $E_{in} \approx 10^2$eV.

The absence of generally accepted theory on the CNF-mechanism does not allow the identification of the enumerated factors which may turn out to be essential for the CNF initiation. It may be presumed e.g. that the local overheating of the surface, caused by the pulsed voltage, will produce a formation of microfractures and thereby induce fusion [1]. It may be thought that the arc effect on the deuterium-filled metal will locally increase the possibility of exciting two deuterium nuclei in one octahedral cavity, which may lead (according to the presumption expressed in [6]) to cause a fusion reaction.

EXPERIMENTAL SET-UP AND TECHNIQUE

In the experiment an attempt was made to record the neutrons, emitted from a gas-filled electrode, if the reaction D + D → ^{3}He+n is produced. The experimental set-up is shown in Fig. 1. The discharge was initiated in a vacuum chamber constructed of stainless steel (100 mm diameter, 180 mm long). The anode was a Cu cylinder 20 mm diameter (in this experiment the gas-filled anode was not used). The contact gap d =8 to 10 mm. The cathodes were of two types:

1. A Cu cylinder 20 mm diameter, with one end coated with 57.4 mg Ti layer (h ≈ 50μ), containing either 22.8 cm^3 of deuterium at normal conditions (which corresponds approximately to about 1 atom of D per atom of Ti), or 2.8 mg Ti (h ≈ 2.5μ), containing 0.92 cm^3 of deuterium.

2. A cylinder of stainless steel with a thin Pd disk welded on it, l = 0.5 mm thick. Directly before the measurement began, the Pd was filled with D during the electrolysis D_2O with an admixture of a water-free salt K_2CO_3, or an alkali CsOD in an open ditch with a current I ≈ 100-300 mA. The electrolysis duration was either 1.5 to 2 hours or 22-24 hours.

The discharge was triggered by a current break in the auxiliary circuit. For creating the discharge a square-wave voltage pulse generator was used, V=90 V, duration $\tau \approx$ 0-5 ms. The voltage generator provided a stable output $\pm$ 2% at a current I ≤ 2kA. The current was controlled by a ballast resistor. In the present study current pulses (I ≈ 1 kA, $\tau \approx$ 1 ms) were used. The details of this part of the experiment are described in [7]. For the purpose of diminishing electrical interferences, the high-current circuit was made coaxially, including the inside of the vacuum chamber (Fig. 1). In order to measure the discharge radiation in the anode cylinder along the axis, a 1.5 mm diameter hole was drilled, and an optical fiber was introduced (a quartz monofiber of 0.8 mm diameter), with the end sealed into the anode to avoid the fiber being coated by cathode erosion products [8]. The measurements were carried out in the single pulse regime. A strong gas-release during the pulse made it necessary to provide continuous mechanical pumping (p ≈ 10^{-2} Torr).

The vacuum chamber was inserted into an all-wave 4π neutron counter. The counter was calibrated using a standard neutron source ^{244}Cm. The efficiency of neutron recording with an energy of E ≈ 2.5 MeV was

$\alpha \approx$ 11-13%.

Before sinking the vacuum chamber into the counter, it is placed inside a special copper screen shaped like a bottle. The neck is used for ignition and high-current supply cables as well as vacuum hose through which the optical fiber is placed. A special press provided reliable contact between the screen neck and the exterior copper sheeting of the counter. In this way we succeeded in making an effective screening of the recording equipment from the interferences, arising during the arcing process. The interferences at the arc ignition and extinction were so strong, that they were registered as false signals. Therefore, activation of the recording devices was begun about 100 μs after the arc ignition, and the strobing duration was selected to complete the strobing pulse ≈100 μs before the end of the discharge pulse. Note that the technique used by us (the coaxial input, the screen, a special organization of the chains, synchronizing the recording facilities) permitted to suppress the interferences, generated by the discharge when using the gas-filled cathode. The vacuum arc on the de-gassed metal is such a strong interference source, that the measures taken by us (as will be seen further on) turned out to be not sufficiently effective.

During the experiment with the help of oscilloscope C9-8 the current and the arc discharge voltage were controlled. The discharge plasma radiation and the measurements from the counting block were also recorded. The radiation was recorded by a multichannel optical analyzer, joined to the exit split of the monochromator MDR-3, to the entrance split of which the light conductor was attached. Both a spectrum plot $4760 \leq \lambda \leq 4960$A, involving line D_{β}, as well as the spectrum plots, involving the most sensitive spectral lines TiII and PdII were recorded. A calibration of the optic analyzer was made using a spectral lamp filled with deuterium. The measurements were carried out by the alternation of two kinds of regimes: a "working" one (during the high voltage pulse) and an "idle" regime (the high voltage is turned off).

EXPERIMENTAL RESULTS

The experiments carried out by us can be arranged into 3 series.

1. Experiments with a Ti-cathode.
2. Experiments with a Pd-cathode, preliminary exposed to electrolysis for 22 to 24 hours.
3. The same with the electrolysis duration of 1.5 to 2 hours.

Unlike the vacuum arc with degassed electrode, where the arcing is followed by strong high-frequency voltage oscillations, in all three experimental series using gas-filled electrodes during the first ten pulses the arc was burning with a low noise level. Accordingly, the interference level was kept low (small counts during the idle regime). Some peculiarities in the intensity radiation of the spectral line of the discharge plasma gas components were observed in this initial measurement period using low-noise arcs. The dependence of radiation intensity J_D on the pulse number was non-linear; in some experiments it had a clearly pronounced maximum. Beginning from the pulse numbers 20-25 the J_D was monotonically dropping, and in the voltage oscillograms the noise level was increased. Apparently there was a decrease in the cathode gas saturation.

The characteristic results for the first series (the thickness of the Ti layer is $h = 50\mu$) are presented in Fig. 2. Note the initial plot of the curve ($N \leq 20$). We did not succeed in finding a satisfactory explanation of the dependence $J_D = J_D(N)$ in this section. Any significant differences in the counter indications in a "working" and "idle" regime could not be found. A similar result was received also on the cathode with a thin ($h=2.5\ \mu$) Ti layer. The received results taking into account the efficacy of the counter record indicate that the neutron flux out of the examined sample at any rate did not exceed 10^4 neutron/s.

A discouraging result has also been received in the second series. However, such an issue of the experiment in this case is probably quite natural. From Fig. 3 (curve 1) it can be seen that the spectral line observed by us near $\lambda = 4860$ A is not symmetrical and represents a superposition of H_β and D_β. Apparently after long-duration electrolysis (near 20 hours) in an open channel there occurs a replacement of deuterium, dissolved in Pd during the initial electrolysis stage by the hydrogen. It would not seem to be surprising, because the Pd-hydrides reveal an inverse isotopic effect, but it is not clear what the source is for the large quantity of hydrogen that appears in the solution. In the present work we did not intend to study this effect, but only reduced the duration of the electrolysis. The electrolysis duration was limited to 1.5 - 2 hours with the purpose of transferring a quantity of D-ions to the cathode, which by 2-3 times exceeded the minimal necessary quantity to fill the cathode with "one-to-one" ratio of deuterium to metal atoms.

The results received in one of the experiments in the third measurement series, obtained with a fresh cathode, are presented in Fig. 4. In this series the spectral line observed by us is quite symmetrical, and the position of its maximum corresponds to $\lambda = 4860$ A (D_β, Fig. 3, curve 2). The characteristic results for this series is the existence of the maximum in dependence $J_D = J_D$ (N), although it was not measured in all experiments as clearly as in the experiment whose results are given in Fig. 4. In this experiment the average count in the "working" regime exceeds the counts in the "idle" regime (averaging was made after first 21 pulses till the appearance of noises in the discharge).

DISCUSSION

It may be thought that we succeeded in realizing by means of an arc discharge the stimulation of the D-D fusion in the Pd filled with the deuterium. The neutron flux out of the sample may be estimated as 10^4 neutrons per second. Assuming that the reaction may be realized in the near surface layer $l \approx 10^{-3}$cm, the volumetric density of the neutron flux is: $q \approx 10^7$ neutron/s/cm^3. Assuming that the deuterium content in the sample corresponds to the β-phase ($c \approx 0.6$), one may estimate that Λ - the counting rate related to a pair of deuterium nuclei is: $\Lambda \approx 10^{-16}$s^{-1} per deuteron pair, which exceeds the so-called "Jones level" by 7-8 orders of magnitude [1,9]. Supposing that the reaction could proceed in the whole sample volume, then $\Lambda \approx 10^{-18}$s^{-1} per deuteron pair.

The experiments carried out by us have several drawbacks, the most serious of which, in our opinion, are as follows:

1. We did not control the deuterium content in the sample. The electrolysis was carried out blindly.

2. The Pd-plate, of which the cathode was made, did not have any certificate of purity. The metallographic analysis was not made either before or after the experiment.

3. The two Pd-cathodes were used more than once (before the second use the deuterium filled cathode was annealed in the air) although after the first use their surfaces were covered with erosion traces (CS autographs). The surfaces of the cathodes were remelted (the results presented in Fig. 4 belong to the fresh sample).

4. No attempts were made to record the formation of tritium in the sample, whose appearance is possible from the CNF occurring in the $D + D \rightarrow T$ channel.

5. A pure Cu, but not gas-filled electrode, was used as anode.

CONCLUSIONS

The absence of financial support forced us to break off this study. Therefore, we did not check the reproducibility of the results. The experiments were fulfilled in spring 1990, and we did not publish them because we hopped to continue this work and to receive definite results. Since we consider that the results received in this study show good prospects for CNF production by using our method we decided to publish the results of our work. We hope that we will be able to resume the study. We hope that by improving some of the drawbacks of this work future experimenters will have a tool for a reliable replication of CNF, consequently it will make the study of these phenomena easier.

REFERENCES

[1] (In Russian)
[2] (In Russian)
[3] (In Russian)
[4] (In Russian)
[5] (In Russian)
[6] (In Russian)
[7] S.M. Shkolnik, "The Plasma Parameters in the Interelectrode Gap of the Vacuum Arc," *IEEE Trans. Plas. Sci.*, 1985, vol ps-13, no 5, pp 336-338.
[8] V.P. Afanaseyev, A.A. Logatchev, N.K. Mitrofanov, S.M. Shkolnik, "Spectroscopy Measurements of High Resolution in High-current Vacuum Arc," Proc. XIV ISDEIV, Santa Fe, NM, September 1990, pp 187-191.
[9] S.E. Jones, E.P. Palmer, J.B. Czirr et al., "Observation of Cold Nuclear Fusion in Condensed Matter," *Nature*, 1989, vol 338, pp 737-740.

Fig. 1. Experimental set-up.

1. cathode; 2. gas-filled metal; 3. anode (Cu); 4. glass insulator; 5. current feed cylinder (Cu); 6. vacuum chamber (stainless steel); 7. inner screen (Cu); 8. detectors; 9. polyethylene; 10. external screen (Cu); 11. quartz fiber; PG - pulse generator, C9-8 - digital store oscilloscope, MDR-3 - monochromator, PM - photo multiplier.

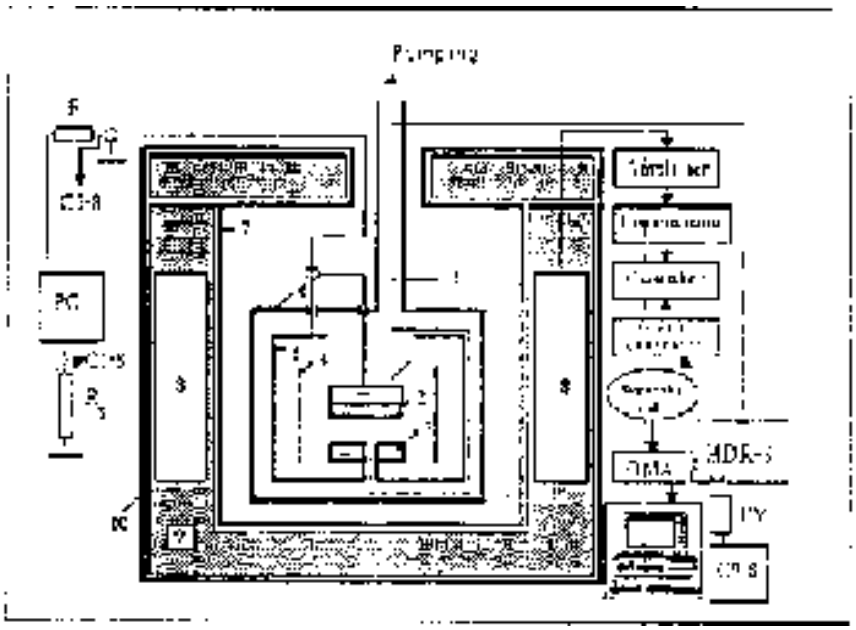

Fig. 2.

* - "working" regime
o - "idle" regime

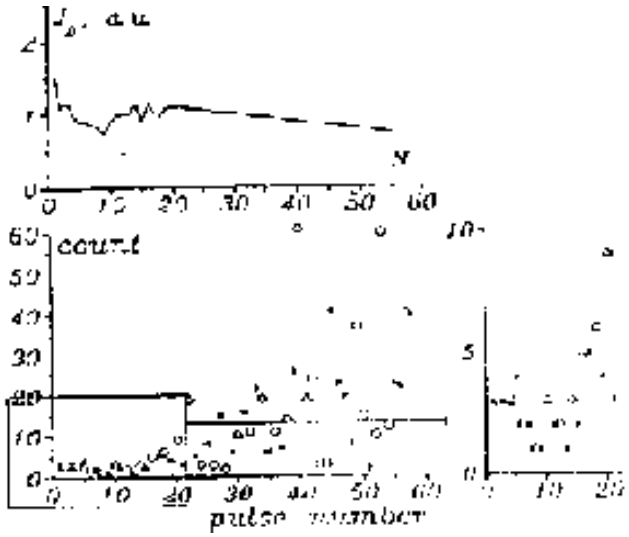

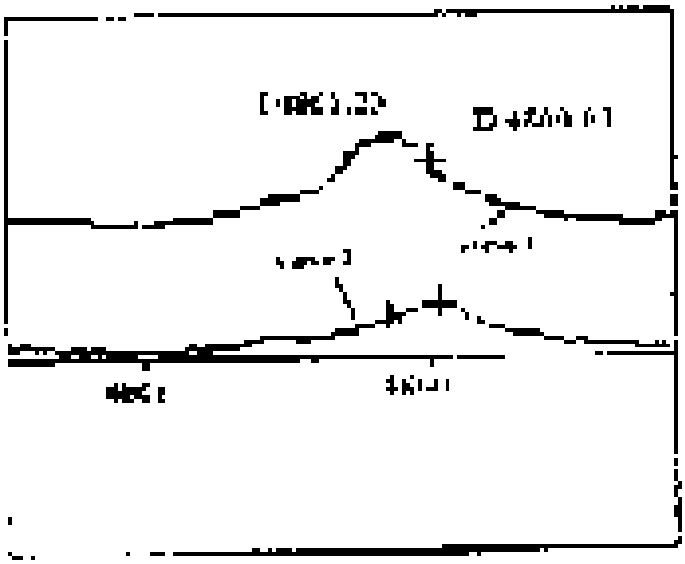

Fig. 3.

Dβ spectral line profile
1. electrolysis 22 h
2. electrolysis 2 h

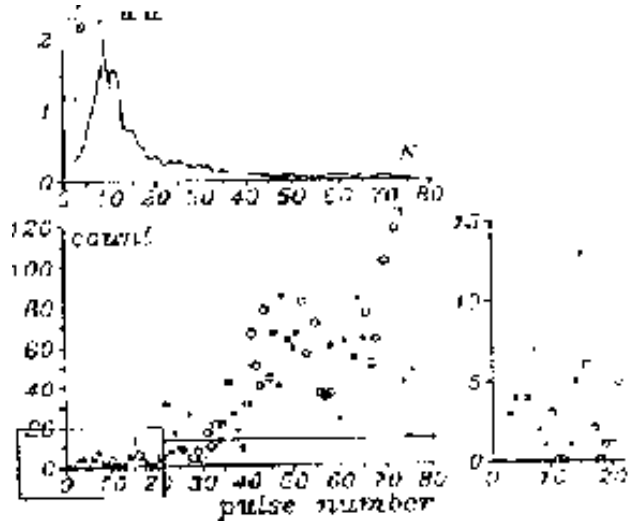

Fig. 4.

* - "working" regime.
o - "idle" regime.

ENERGY AMPLIFIER WITH MULTILAYER THIN FILM ELECTRODES

G.H. Miley, E.G. Batyrbekov[1]. H. Hora[2], J.U. Patel[3],
J.W. Tompkins[4], R.K. Zich[5]

Fusion Studies Laboratory
University of Illinois
100 NEL, 103 South Goodwin Avenue
Urbana, IL 61801-2984 U.S.A.

ABSTRACT

The application of the "swimming electron layer" theory [1-4] to the design of multilayer thin film electrodes is discussed. A key advantage of this approach is that the enhanced reaction rate at interfaces between select metals is predicted to produce a high power density throughout the volume of the multilayers. Initial experimental studies of heat production by electrolysis, using a multilayer thin-film cathode specially designed on the basis of this theory, are presented.

INTRODUCTION

The excess heat during heavy or light water electrolysis using Pd cathode with LiOD (LiOH) electrolyte has been reported by several groups [5]. To date, heat production equal to as much as ten times the input energy has been reported from some of these experiments [6]. Many theoretical explanations have been offered to explain these exciting experimental results. Most of these theories explain the reaction as a quantum mechanical tunneling effect in the presence of a solid lattice. This does not, however, explain the high reaction rates observed in the experiments which are thought to involve surface or intersurface effects [7]. Thus the "swimming electron layer" theory was developed to address that issue [1-2]. This model is based on the effect of surface tension on an exotic plasma at metallic interfaces, resulting in enhanced reaction rates.

In the present research, we have concentrated on the experimental investigation of excess heat production phenomena, using a unique multilayer electrode design that is predicted to increase reaction rates by increasing the electrode interface area and by using select metals with large Fermi-energy-level differences. Initial experimental studies of heat production by electrolysis, using a multilayer thin-film cathode specially designed on the basis of the "swimming electron layer" theory is described.

"SWIMMING ELECTRON LAYERS" THEORY

Several experiments reported by other workers have indicated that cold fusion is a surface-related exothermic phenomena. The "swimming electron layer" theory is consistent with this observation and suggests the use of multilayer thin foils in order to induce reactions throughout the volume of an electrode. This approach would in turn allow direct scaling to high power levels in minimum size cells.

Multilayer electrodes suggested by this model will have closely spaced interfaces at which cold fusion would occur to provide a high power output. Related experiments using coated electrodes have been reported by Arata and Zhang [7], where as multiple large volume Pd/Si layers have been studied by T. Claytor [8]. Both experiments were quite successful and thus provide encouragement for the multilayer

film concept.

The metal pairs used in the present experiments for fabricating multilayer electrodes are selected so that the metals do not diffuse into each other, maintaining well-defined interfaces. Differences in Fermi levels adjust at the interfaces creating an electron layer that is most effective in shielding the positive charges of fusing deuterons. The dynamic shielding effect of the electron layer may further be enhanced if the electrode is connected to the negative terminal of a power source that floods the conduction bands of metals with electrons. Thus, when one uses an AC power source or ramps the current from a DC source during the electrolysis, a dynamical non equilibrium condition is created. This effect is related to the enhanced reaction rate observed by others using oscillating or ramped voltages [7,8].

The basis process is viewed as involving colliding thermal deuterons in a double potential layer region developed at the internal interfaces of the multilayer electrodes. At the low speeds involved, the D^+ nuclei will be polarized (see Figure 1). The shielding of the positive charge in this state by swimming electron layer allows a very close approach, where the nuclear forces become effective to form a compound nucleus in an excited state [1].

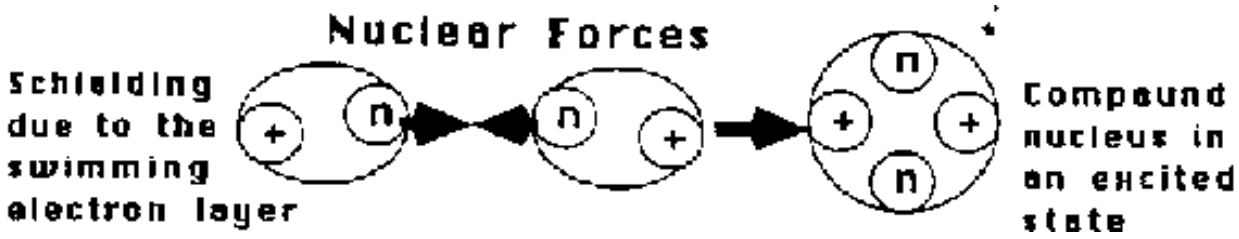

Figure 1. Cold fusion of D^+ shielded by swimming electron layer.

3. EXPERIMENTAL INVESTIGATION.

The experiments were carried out by observing the temperature increase and gas production compared to input power. The experiment employed a calorimeter technique, which used paired identical electrolytic cells. These cells were identical except that one utilized the multilayer cathode, while the second used a plain stainless steel (copper) plate of the same size. The multilayer cathode is made from a stainless steel plate (copper), 25 mm x 25 mm x 3 mm thick, coated with alternating layers of Ti and Pd, deposited by a unique e-beam evaporation method specifically developed for this purpose. The cathode has six layers of Ti, alternating with five layers of Pd per side (having a total thickness of 100 Å) sandwiched around the stainless steel core.

The electrolyte cell design is shown in Figure 2. Each cell represents 250-ml vacuum jacked dewars closed by 5-cm thick tapered rubber stopper. Glass boxes (60x40x20 mm) with a system of electrodes and 0.1 - 0.57 molarity LiOH electrolyte solution were placed into both dewars. The glass box is used for decreasing the amount of electrolytes and as a result increasing the thermal sensitivity of this apparatus. The space between dewar's wall and the glass box was filled with distilled water to increase the heat system's capacity.

Both cells were connected on parallel to the same power supply, in order to provide a matched power deposition. Midway during the experimental run, as an added control, the electrodes were interchanged between the cells.

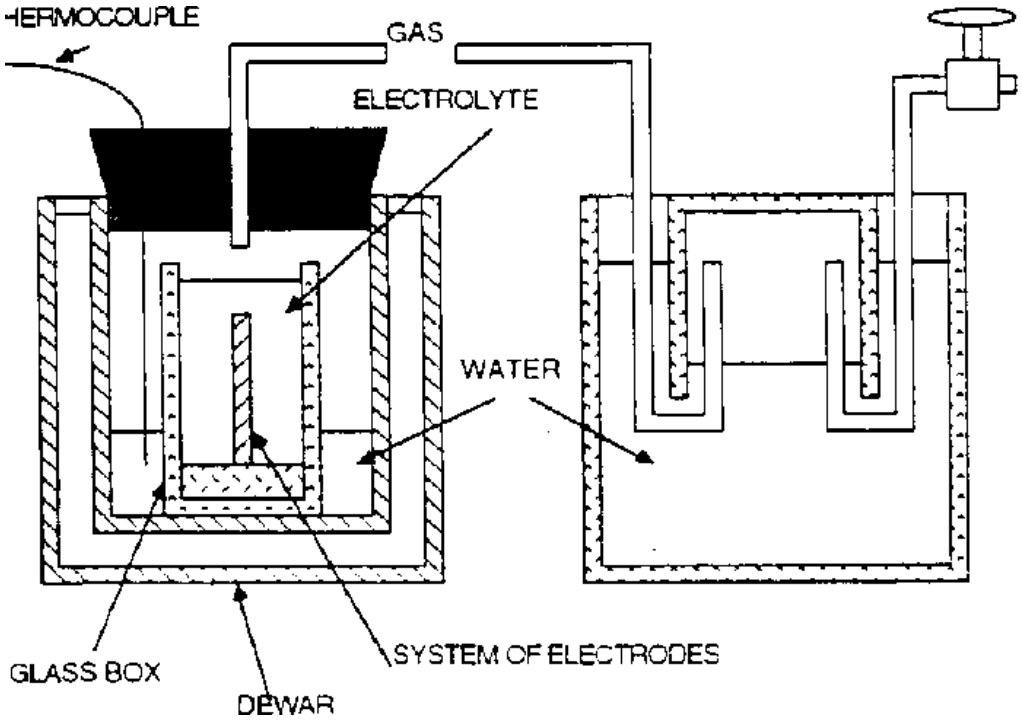

Figure 2. The electrolyte cell design.

The temperature of the multilayer-cathode cell was consistently 1.5 ± 0.5 °C higher than that of reference cell, but for short periods limited by damage flaking of the thin films on the electrode surface. This corresponds to ~2 kW/cm^3 energy production in the thin-film interface region, assuming reaction occurs, as predicted, over a region extending an electron-Debye length from the interface. The total volume average power, if applicable, would be several orders of magnitude lower than the interface value.

These results must be viewed as very preliminary, since the experimental runs have been limited by early flaking of thin layers, probably due to differential expansion of the layers during intense heating. Also, this preliminary calorimeter technique involves some assumptions that need further study. Some advantages and disadvantages of conventional calorimetric methods have been eliminated in this design, which provides a closed system and allows simultaneous measurement of both gas and heat production.

A new electrode design, with several improvements to increase film stability, has been developed for future experiments. This design and results using it will be presented.

CONCLUSION

The approach proposed here is unique in describing cold fusion as an interface phenomenon, consistent with both the "swimming electron layer" theory and with experimental results that indicate reactions mainly occur at electrode surfaces. Techniques have been developed to fabricate multilayer thin film electrodes, and preliminary experiments indicate a high power density throughout the film volume. If a stable film design can be found, this approach could be a promising one for an energy amplifier.

REFERENCES

1. H. Hora, J.C. Kelly, J.U. Patel, M.A. Prelas, G.H. Miley, and J.W. Tompkins, "Screening in Cold Fusion Derived from D-D Reactions," *Phys. Lett. A,*, vol 175, p 138 (1993).

2. H. Hora, G.H. Miley et al., "Surface Models for Cold Fusion and the Possibility of Multilayered Cells for Energy Production," Proceedings, 8th World Hydrogen Energy Conference. Cold Fusion Symposium, Hawaii Natural Energy Institute, U. of Hawaii, p 169 (1990).

3. G.H. Miley, H. Hora, J. Javedani et al., "Multi-Layer Thin Film Electrodes for Cold Fusion," Proceedings of the Third International Conference on Cold Fusion, Nagoya, Japan, October 21-25, p 54 (1992).

4. G.H. Miley, E.G. Batyrbekov, J.U. Patel et al., "Heat Production with Multilayer Thin-Film Electrodes," Proceedings of the Fourth International Conference on Cold Fusion, Lahaina, Hawaii, December 6-9, C 3.1 (1993).

5. Will be included in the Proceedings of the Fourth International Conference on Cold Fusion, December 1993, Lahaina, Hawaii.

6. E. Storms, "Review of Experimental Observations About the Cold Fusion Effects," *Fusion Technology,* vol 20, p 433 (1991).

7. Y. Arata and Y.-C. Zhang, "Reproducible "Cold" Fusion Reaction Using a Complex Cathode," Fusion Technology, vol 22, p 287 (1992).

8. T. Claytor, D.G. Tuggle and H.O. Menlove, "Tritium Generation and Neutron Measurements in Pd-Si under High Deuterium Gas Pressure". Proceedings of the Second Annual Conference on Cold Fusion, Villa Olmo, Como, Italy, June 29-July 4, p 34 (1991).

PRACTICAL ASPECTS OF HEAT AND HELIUM MEASUREMENTS IN DEUTERATED PALLADIUM

B.F. Bush* and M.H. Miles
Chemistry Division, Research Department
Naval Air Warfare Center, Weapons Division
China Lake, CA 93555-6001, USA

ABSTRACT

Metal flasks were used to collect electrolysis gas samples in Pd/D2O + LiOD and Pd/H_2O + LiOH experiments in order to minimize effects due to helium diffusion through glass. For five control experiments yielding no excess power, the mean value for the background helium concentrations in our system was 4.4 ± 0.6 ppb (parts per billion) or 5.1 ± 0.7 X 10^{13} ^{4}He/500mL. For five experiments producing excess power, the measured helium concentration was higher than the background level in each case. Three different laboratories have been used for measurements of the helium concentrations in various electrolysis gas samples from our experiments during the past three years. The helium measurements from all three laboratories yield helium production rates of 10^{11}-10^{12} ^{4}He/s*W.

INTRODUCTION

Our previous results present a correlation between the measured excess power and helium production in D_2O-LiOD electrolysis cells using palladium cathodes. [1] The measured rate of 4He production (10^{11}-10^{12} ^{4}He/s*W) is the correct magnitude for typical deuteron fusion reactions that yield helium as a product. [2] Because helium is present in the atmosphere (5.22 ppm), it is essential that atmospheric contamination be prevented. It is indeed a very challenging experimental problem to clearly establish the production of ^{4}He from Pd/D_2O electrolysis cells. This situation is compounded by difficulties in obtaining large excess power effects in these experiments.

Table I presents the theoretical relationship between the excess power and helium production assuming ^{2}H + ^{2}H → ^{4}He + 23.8 MeV as the major fusion reaction with the energy being deposited within the calorimeter. At low levels of excess power, the uncertainties in measurements of the helium and the excess power are rather large. When the excess power exceeds 0.2 W, however, it could be possible to correlate the rate of ^{4}He production with proposed fusion reaction pathways. It should be noted that for any given excess power, the helium concentration in the electrolysis gas stream will be inversely proportional to the current. For example, an experiment producing 0.500 W of excess power when I = 250 mA would theoretically yield 112 ppb of ^{4}He in the electrolysis gas stream.

EXPERIMENTAL

The electrolysis cells initially contained 16 cm^3 of 0.1 M LiOD + D_2O (99.9% Cambridge Isotope Laboratories) or 0.1 M LiOH + H_2O. The design of the electrolysis cells and calorimeters were similar to previous reports. [1-4] The major difference was that electrolysis gas samples were collected in stainless steel, all metal flasks rather than the 500 mL Pyrex glass flasks used in previous experi-ments [1-3]. Four identical metal flasks (numbered 1-4) and four similar calorimetric cells (A, B, C, D) were used in this study. The helium concentrations in the metal flasks were measured by a Department of the Interior (DOI) laboratory (Helium Field Operations, Amarillo, Texas). The standard deviation (σ) for the

measurement of the helium concentration was generally about ±1 ppb, meaning that there is a 67% confidence that the true concentration is within 1 ppb of the stated value and 95% confidence at 2σ ie. ± 2 ppb.

Most of the palladium rod cathodes investigated in this study were obtained from Johnson Matthey. The Pd-Ag alloy cathode (4mm x 1.6 cm) was loaned to us by Dr. Shinji Nezu of IMRA Japan. The palladium sheet cathode (1.0 mm x 3.2 mm x 1.6 cm) was cut from a sample loaned to us by Tanaka Metals (Japan). Two palladium rod cathodes (1mm x 1.5 cm and 2 mm x 1.2 cm) were produced by Johnson Matthey (UK) using the "original recipe" and were loaned to us by Dr. Haven E. Bergeson of the University of Utah.

The flasks were made by welding discs onto the ends of sections of stainless steel pipe and high temperature silver soldering two 0.25 inch stainless steel tubes into the side of the pipe. Nupro brand model SS-4-BK-TW valves were soft soldered to the tubes using Sn-Ag 96%-4% solder and stainless steel soldering flux. The valves were modified by replacing the standard bellows gasket with a copper gasket to effect a metal seal, while the normal Kel-F valve seat was retained in preference to a metal seat, to preclude seat galling induced mass transport leaks. To effect an all metal envelope, the valves were fitted with Cajon VCR fittings soft soldered in place and sealed with a nickel gasket and cap fitting for storage and shipping; the volume between the valve seat and VCR cap seal was flushed out with boil-off nitrogen as it was sealed, to preclude helium diffusing through the Kel-F valve seat.

Metal sample flasks are fragile and must be handled, packaged and shipped with care. The soft solder is easily broken using the leverage available from the valve knob and tubes. For best results, the flasks are routinely baked out at ≈100°C for four hours while dynamically evacuated to 5μ vacuum, and stored filled with boil-off nitrogen to avoid contamination by residual helium that might otherwise be trapped in any pores present in the flask metal.

RESULTS

Helium measurements in D_2O and H_2O control experiments are presented in Table II. Stainless steel metal flasks were used to collect the electrolysis gas samples in order to minimize atmospheric contamination due to helium diffusion.[2] The helium concentrations in Table II support a detection limit of approximately 10^{13} ^{4}He/500mL in these experiments as reported previously.[2] The measured helium concentrations in these control experiments yield a mean value of 4.4 ± 0.6 ppb or 5.1 ± 0.7 x 10^{13} ^{4}He/500mL.

For experiments producing excess power, five helium measurements using these same metal flasks have been completed. These experiments are shown in Table III and yield a mean value of 1.4 ± 0.7 x 10^{11} ^{4}He/s*W after correcting for background levels of helium measured in control studies (Table II), ie. 45 Mev per ^{4}He atom. This value is the correct magnitude for typical deuteron fusion reactions that yield ^{4}He as a product[2]. It is interesting to note from Table III that the two palladium rods produced by Johnson Matthey using the "original recipe" yielded excess power. The palladium sheet from Tanaka Metals also produced excess power. The excess power density is greater than 1 W/cm^3 Pd for each of these three cathodes. However, the excess power levels measured during the collection of the gas samples in these new experiments were only 0.1 W or less, hence experimental errors are rather large (Table I). Further experiments using metal flasks are needed that involve equal numbers of control cells and cells producing large excess power effects. This should provide additional statistical evidence regarding helium production in Pd/D_2O electrolysis cells.

Table II shows that no measurable differences occur in background levels of ^{4}He over a time period

exceeding four months. Nearly identical ^{4}He concentrations are obtained for the electrolysis cell C gas sample collected on 24 February 1993 and then again in a different experiment on 7 July 1993. Furthermore, Table II illustrates that the particular metal flask used produces no significant difference in the ^{4}He result. The lowest ^{4}He concentration (3.4 ± 1.1 ppb) was obtained using metal flask #4. However, the highest ^{4}He concentration (9.7 ± 1.1 ppb) was obtained using this same metal flask in an experiment producing excess power (Table III).

Discussion

The strategy of the experimental work was to preclude atmospheric contamination by a system of overlapping and redundant precautionary measures. Cell, gas lines and D_2O were flushed with nitrogen, and then the electrolysis off-gas itself was allowed to flush the entire system and the flask (usually over night). Because of the self flushing feature of open cell operation, contamination by in-diffusion of helium reached a steady state value, allowing a reasonable background correction.

By contrast, closed cell operation would have collected the sum of all contamination sources. Thus, a closed cell experiment requires the use of all-metal apparatus with all metal seals and high vacuum electrical feedthroughs, lest the ingress of atmospheric helium cause the concentration to equilibrate to that of air, followed then by the egress of any helium produced in the experiment to maintain the equilibrium helium concentration. Given impermeable sealing, quantitation of the closed cell build-up experiment for energy versus helium would require that the sum of all energy produced be measured.

Thus, open cell operation provides a much more tractable and reliable experimental method than the closed cell build-up experiment, for the purpose of heat versus helium correlation. The open cell method when upgraded to an impermeably sealed apparatus provides for direct quantification, within instrumental resolution.

The likely source of the measured helium concentration in the control experiments (Table II) is the diffusion of atmospheric helium through the glass in the system and through the thick-walled rubber tubing that connects the electrochemical cell, collecting flask, and oil bubbler [3]. The contribution of atmospheric helium that diffuses through the glass in a system can be calculated by the equation

$$q = KP/d \qquad (1)$$

as discussed previously [1,2]. For Pyrex glass with surface area of 300 cm^2 and thickness (d) of 1.8 mm, Equation 1 yields 2 X 10^{11} ^{4}He/500mL when I = 500 mA (500 mL of $D_2 + O_2$ gas is generated in 4870 seconds at 23 °C and 700 torr). This amount of ^{4}He is more than two orders of magnitude smaller than the measured helium levels in the control experiments (Table II). Thus diffusion of atmospheric helium through the thick-walled rubber tubing is the major source of helium in our control experiments. This conclusion is supported by measured diffusion rates of helium through rubber tubing [5].

The background helium concentration of 4.4 ± 0.6 ppb or 5.1 ± 0.7 x 10^{13} ^{4}He/500 mL places our helium production rate at 10^{11}-10^{12} ^{4}He/s*W as reported previously [2,6]. Furthermore, this background level of helium in our system explains why the effect of atmospheric helium diffusing into our glass flasks during storage and shipment was not observable in experiments involving the analysis of our electrolysis gas samples at the University of Texas [1-3]. The experimental rate of atmospheric helium diffusion into our Pyrex glass flasks when filled with H_2 or $D_2 + O_2$ is 1.96 ± 0.34 x 10^{12} ^{4}He atoms/day as measured by Rockwell International[2]. Based on this result, it would require 26 days before the atmospheric diffusion of helium into our glass flasks would equal the minimum helium detection limit for those studies[1-3]

In our initial study, wherein the glass flask samples were analyzed at the University of Texas[1-3] ^{4}He was found in 8 out of 8 experiments generating significant excess power, while no ^{4}He was found in 6 out of 6 control experiments not generating excess power; no ^{3}He was detected. In a later study the helium diffusion rate for typical glass sample flasks was determined, and showed that our earlier findings were in fact quite reasonable; and further, that the quantity of helium produced was of the right order of magnitude to indicate a nuclear fusion reaction [6]. In the study described here, we approach direct identification of nuclear fusion as the heat producing process, by quantitative helium analysis
(see Table III).

ACKNOWLEDGMENTS

We thank Tanaka Metals for the loan of the palladium sheet samples, Dr. Shinji Nezu for the loan of Pd-Ag rod, and Dr. Haven E. Bergeson for the loan of two palladium rods. We thank David L. Miles for the computer analysis and display of the experimental data. We thank Mary Garasu and the Joint Training Partnership Act Summer Youth Training Program for her experimental and computer assistance. We also thank John Fontenot for material essential to the completion of this work.

REFERENCES

[1] M.H. Miles, R.A. Hollins, B.F. Bush, J.J. Lagowski, and R.E. Miles, "Correlation of Excess Power and Helium Production During D_2O and H_2O Electrolysis Using Palladium Cathodes," *J. Electroanal. Chem.*, vol 346, 1993, pp 99-117.
[2] M.H. Miles and B.F. Bush in Frontiers of Cold Fusion, H. Ikegami, Editor, Tokyo, Japan: Universal Academy Press, 1993, pp 271-278.
[3] B.F. Bush, J.J. Lagowski, M.H. Miles, and G.S. Ostrom, "Helium Production During the Electrolysis of D_2O in Cold Fusion Experiments," *J. Electroanal. Chem*., vol 304, 1991, pp 271-278.
[4] M.H. Miles, K.H. Park, and D.E. Stilwell, "Electrochemical Calorimetric Evidence for Cold Fusion in the Palladium-Deuterium System," *J. Electroanal. Chem*., vol 296, 1990, pp 241-254.
[5] T. Davidson, U.S. Department of the Interior, Bureau of Mines, Helium Field Operations, Amarillo, Texas, personal communication.
[6] M.H. Miles, B.F. Bush, and J.J. Lagowski, "Anomalous Effects Involving Excess Power, Radiation, and Helium Production During D_2O Electrolysis Using Palladium Cathodes," *Fusion Technology* (accepted for publication).

Table I. Theoretical Relationship Between Excess Power and Helium Production. Magnitude of Expected Experimental Errors.

Px (W)	^{4}He[a] (ppb)	^{4}He (atoms/500mL)	^{4}He Error[b] (%)	Colorimetric[c] Error (%)
0.050	5.6	6.38×10^{13}	18.0	40
0.100	11.2	1.28×10^{14}	8.9	20
0.200	22.4	2.55×10^{14}	4.5	10
0.500	56.0	6.38×10^{14}	1.8	4
1.000	112.0	1.28×10^{15}	0.9	2

[a] For I = 500 mA assuming $^2H + {}^2H \rightarrow {}^4He + 23.8$ MeV is the fusion reaction.
[b] ±1 ppb.
[c] ±0.020 W.

Table II. Helium Measurements in Control Experiments Using Metal Flasks. No excess power was measured.

Electrode	Flask / cell (date)	^{4}He[a] (ppb)	^{4}He (atoms/500mL)
Pd Rod[b] (4mm x 1.6 cm)	1/C (2/24/93)	4.8 ± 1.1	5.5×10^{13}
PdAg Rod[b] (4mm x 1.6 cm)	2/D (2/24/93)	4.6 ± 1.1	5.2×10^{13}
Pd Rod[b] (4mm x 1.6 cm)	3/C (2/28/93)	4.9 ± 1.1	5.6×10^{13}
PdAg Rod[b] (4mm x 1.6 cm)	4/D (2/28/93)	3.4 ± 1.1	3.9×10^{13}
Pd Rod[c] (1mm x 1.5 cm)	3/C (7/7/93)	4.5 ± 1.5	5.1×10^{13}
(Mean)		(4.4 ± 0.6)	($5.1 \pm 0.7 \times 10^{13}$)

[a] Helium analysis by U.S. Bureau of Mines, Amarillo, Texas.
[b] D_2O + LiOD (I = 500 mA).
[c] H_2O + LiOH (I = 500 mA).

Table III. Helium Measurements Using Metal Flasks. Experiments Producing Excess Power.

Electrode	Flask / Cell (date)	^{4}He[a] (ppb)	P_x (W)	^{4}He/s*W[b]	MeV/^{4}He
Pd Sheet[c] (1.0mm x 3.2 mm x 1.6cm)	3/A (5/21/93)	9.0 ± 1.1	0.055	1.6×10^{11}	39
Pd Rod[c] (1mm x 2.0cm)	4/B (5/21/93)	9.7 ± 1.1	0.040	2.5×10^{11}	25
Pd Rod[c] (1mm x 1.5cm)	1/C (5/30/93)	7.4 ± 1.1	0.040	1.4×10^{11}	45
Pd Rod[c] (2mm x 1.2cm)	2/D (5/30/93)	6.7 ± 1.1	0.060	7.0×10^{10}	89
Pd Rod[d] (4mm x 2.3cm)	1/A (7/7/93)	5.4 ± 1.5	0.030	7.5×10^{10}	83

[a] Helium analysis by U.S. Bureau of Mines, Amarillo, Texas.
[b] Corrected for background helium level of 5.1×10^{13} ^{4}He/500 mL.
[c] D_2O + LiOD (I = 400 mA).
[d] D_2O + LiOD (I = 500 mA).

"EVIDENCE FOR AN ELECTROLYTICALLY INDUCED SHIFT IN THE ABUNDANCE RATIO OF SR-88 TO SR-86"

by R.T. Bush
Physics Department, California State Polytechnic University*
& ENECO** (Formerly FEAT)

ABSTRACT

Compelling preliminary strong evidence is presented for an electrolytically induced shift in the ratio of Sr-88 to Sr-86. Since the natural abundance ratio of these two isotopes is constant, this shift would, if corroborated, constitute a unique signature of cold nuclear reactions.

INTRODUCTION

Since the natural abundance ratio of Sr-88 to Sr-86 is a constant, it is of some interest that compelling preliminary evidence [3,5,7,10] strongly suggests the achievement of electrolytically stimulated shifts in the ratio of these isotopes amounting to many standard deviations as determined from mass spectrometric analyses. Such shifts, if confirmed, constitute a unique "signature" of cold nuclear reactions in the condensed matter environment of the cathode. Mass spectrometric evidence (SIMS and ICPMS with the latter preceded by an ion-exchange column separation of strontium and rubidium) provide strong preliminary evidence for the electrolytically stimulated production of the strontium isotopes Sr-86 and Sr-88 resulting in a shift in the natural abundance ratio. The two electrolytic cells employed nickel mesh cathodes and light water based 0.57 M rubidium salt electrolytes. The fact that the SIMS analysis yielded a ratio of Sr-88 to Sr-86 approximately equal to the natural abundance ratio of Rb-87 to Rb-85 provides support also for the author's CAF Hypothesis [3] ("Cold Alkali Fusion"), which seeks to unify the heavy water [1] and light water [2] excess heat effects. The author's LANT Hypothesis [6] ("Lattice Assisted Nuclear Transmutation"), which is a generalization of CAF, also receives support from the calorimetric and mass spectrometric results.

CELL DESIGN and CALORIMETRY

Cell and calorimeter design for the two cells of interest have been previously presented in references [3, 7, and 10]. In addition, R. Eagleton [13], the author's research colleague, has submitted a detailed recitation of these for all the light water cells of our research collaboration. [See paper by R. Eagleton in this publication.] (These cells were constructed by Eagleton, but designed by the two of us with essential design features driven by considerations based upon the author's theoretical work. Essentially all of the data has been gathered by the author with Eagleton playing the key role in maintaining the equipment. Data analysis and theoretical work in understanding the data is carried out by the author with Eagleton playing an important part as a sounding board for the theoretical interpretations.) [See Eagleton's paper for description of the cells.]

SIMS Analysis (Post-run Cathode of Cell 53)

The post-run cathode material for cell 53 evidences strong signals at mass numbers 86 and 88 of the SIMS mass spectrograph (Fig.1) compared to that for the pre-run cathode material (Fig. 2). (Analyses of pre-run and post-run electrolyte samples via mass spectrometry for both cell 53 and 56 has limited strontium concentrations to less than approximately 5 ppb in the electrolyte samples of about 50 ml

volume.) Fig. 3 and Fig. 4 contain the mass spectrographs, respectively, for the following respective cases: Post-run cathode material (cell 53) 100-200 amu and pre-run cathode material (cell 53) 100-200 amu. Appendix S provides a table of data from the original lab report. See also reference [10]. The text of Appendix A can be obtained by writing to the author. (SIMS tests were performed by a well-known U.S. National Laboratory which prefers to remain anonymous at this time.)

A key fact from the author's CAF Hypothesis is the fact that the ratio of the line height for mass number 88 to that for 86 (Fig. 1) is approximately the same as that for the ratio of the rubidium signals for masses 87 and 85. According to CAF these rubidium isotopes are the parents of the strontium isotopes by way of the addition of a proton in a cold nuclear reaction which differs greatly from thermonuclear reactions. An alternative interpretation is that the signals at mass numbers 88 and 86 (Fig. 1) are actually associated with rubidium hydride, has been rejected for two reasons: (1) the mass signal for rubidium oxide, a much more stable compound than RbH, in the post-run spectrum (Fig. 3) is lower than that for the putative RbH. (2) The ICPMS mass spectrometric analysis has verified the production of a significant shift in the ratio of Sr-88 to Sr-86, as discussed in the following section.

ICPMS Analysis Following an Ion-Exchange Column Separation

The analysis of the pre- and post-run cathode materials for cell 53 and cell 56, the latter used rubidium hydroxide (0.57 M) instead of rubidium carbonate in the light water based electrolyte and generated about five times as much excess heat as cell 53 [3,7,10]. The analyses [3,7,10] consisted of ICPMS ("Inductively Coupled Plasma Mass Spectrometry) mass spectrometry preceded by an ion-exchange column separation of the divalent strontium from the monovalent rubidium. The analyses shows that this separation provided enough enrichment of the strontium relative to the rubidium to guarantee a meaningful ICPMS measurement of the ratio of Sr-88 to Sr-86.

The mass spectrograms of Fig. 1 and Fig. 2 were carried out by SIMS analysis, respectively, for the postrun cathode material and for the prerun cathode. (Earlier measurements established an upper limit on strontium in the post-run electrolyte (cell 53) of 5 ppb.) Note the following from Fig. 2 (Prerun):

Fig. 2 (Prerun): Mass 86: Signal height of 3.6 cm corresponds to 190 counts.

Nickel 58: 10.O cm signal height: 1,250,000 counts.

Fig. 1 (Postrun): Note that signal height discrimination is greater than that for Fig. 2. (Fig. 2 had a 50 V offset, and Fig. 1 a 125 V offset. Thus, in comparing signal heights are corrected using the ratios of the Nickel signals from both (ratio = 40.3):

Mass 86:3.25 signal height: 36 counts
Mass 88:2.6 cm signal height: 16 counts

Corrected counts from Fig. 1 to compare with those in Fig.2:

Mass 86:36 x 40.32 = 1,452 counts
Mass 88:16 x 40.32 = 645

Ratio of Sr-86 to Sr-88: (Corrected for background in Fig.2): = (1,452-190)/(645-150) = 2.55. (1)

Note: the natural abundance ratio of Sr-86 to Sr-88 is approximately: = 0.12. (2)

Thus, we have an isotopic abundance ratio shift by a factor of 2.55/0.12 = 21. (3)

Note: the natural abundance ratio of Rb-85 and Rb-86 is about = 2.59. (4)

Nota Bene: The ratio in (1) so closely matches (4) which is strong support for Bush's hypothesis that

the strontium arises from the rubidium via the addition of a proton at the surface of the nickel.

Using the analytical data, for cell 53, the ratio of Sr-88 to Sr-86 is **3.504 ± 0.002**, which is lower than the ratio for the standard and the pre-run cathode materials by about 716 standard deviations. Similarly, for cell 56 the ratio of Sr-88 to Sr-86 for the post-run cathode material is approximately **2.731 ± 0.003**, which is about 826 standard deviations below the ratio for the pre-run cathode materials. Note that the fact that this ratio is lower than that for cell 53 is consistent with the fact that cell 56 gave much more excess heat than did 53 and the CAF Hypothesis according to which excess heat is associated with the amount of nuclear product. Therefore, there is compelling preliminary experimental support for electrolytically stimulated transmutation and the author's CAF Hypothesis [3,5,7,10]. **It is important to note that contamination of the cell by material containing strontium would not produce a spurious shift in the isotope ratio.** For that reason, this isotope shift result is much stronger evidence than an elemental shift such as the claimed production of calcium [3,4] in the case of a light water based potassium carbonate electrolyte for which the contamination issue is paramount because of the ubiquitous presence of calcium in the general environment. This shift in a ratio that is otherwise constant in nature, assuming that it can be corroborated, appears to be an unique signature of cold nuclear reactions [3,5,7,10].

The LANT ("Lattice Assisted Nuclear Transmutation") Hypothesis

The author's LANT Hypothesis [6] ("Lattice Assisted Nuclear Transmutation") is a generalization of the author's CAF Hypothesis. Applied to the isotopes of hydrogen, LANT essentially states that a hypothetical cold nuclear reaction made possible by the lattice structure of a metal (such as nickel or palladium) in which a proton, deuteron, or triton is added to another nucleus is possible if the sum of the rest-mass energies of the reactants is greater than that of the products. (Of course, in addition to mass-energy conservation, no Laws of Physics should be violated.) The difference (surplus) in rest-mass energy is assumed to show up initially as phonons and the kinetic energies of the products. Because the reactions are cold, it is a good approximation to ignore the kinetic energies of the reactants.) Due to various degradation processes, essentially all of the surplus energy would quickly degrade to what is referred to as "excess heat" in connection with the heavy water [1] and light water [2] excess heat effects.

According to the LANT model [6], the Sr atoms formed in the lattice would themselves become targets for the lattice assisted addition of a proton. The Table of Fig. 5 entitled "Isotope Production via Cold Nucleosynthesis: Rubidium Series" [6,7,10] contains isotopes for which evidence of production in connection with the operation of cell 53 is provided by a comparison of the post-run and pre-run SIMS spectrographs of Fig. 1 through Fig. 4. Note from the Table that the total excess heat theoretically produced in connection with the isotopes synthesized is **$(3.8 \pm 0.4) \times 10^{19}$ MeV**, whereas the actual excess heat determined for cell 53 via calorimetry was about **$(4.0 \pm 0.8) \times 10^{19}$ MeV**. This computation provides strong initial support for the LANT.

THE COULOMB BARRIER: Can there be Sufficient Tunneling for Genuine Cold Fusion?

It is the author's opinion that the cold nuclear reactions constitute genuine cold fusion in which the width of the Coulomb barrier is sufficiently narrowed due to shielding by electrons to stimulate sufficient quantum mechanical tunneling to achieve the fusion rates inferred from experimental excess powers. Of course, this begs the question of how the electrons are enabled to increase their proximity to the positively charged particles to achieve the shielding. Two proposals to explain this effect were previously suggested: (1) In an earlier paper [3] it was recalled that s-state electrons can exist for a small fraction of the time inside a proton (light water case) or a deuteron (heavy water case) during

which time there is a much-narrowed Coulomb barrier experienced by a second charged particle colliding with the combination. The difference between an ordinary deuterium or hydrogen gas (or mixture) sealed in a glass jar and a deuteron (proton) "gas" sealed in a solid (e.g. palladium or nickel) by an electric field, or gas pressurization, will simply be a consequence of the greater opportunities for electrons in the solid to achieve s-state status vis-a-vis the deuterons (protons). Thus, one might conceive of a situation in the solid where a single electron in a zero angular momentum state passes periodically through an entire line of deuterons (protons) charge-neutralizing each in turn as it passes through. (2) Electron collapse into a sufficiently reduced-radius orbit because of a limitation on the energy density of the zero point electromagnetic field achieved in the condensed matter environment. Thus, Puthoff [12], building upon the pioneering work of Boyer [11], has shown that the ground state of hydrogen is actually a dynamical state of equilibrium in which the accelerating electron absorbs as much energy from the background zero-point field as it radiates away. This mechanism provides the basis for the author's recent mode [8,9], the ECFM ("Electron Catalyzed Fusion Model"), to attempt to unify heavy- and light-water cold fusion. This is one of the first cold fusion models to consider the zero-point energy field, and the first to fit actual data on excess power versus loading.

CONCLUSIONS

Compelling mass-spectrometric evidence using SIMS and ICPMS (preceded by ion-exchange column separations of strontium and rubidium), although of a preliminary nature, in the form of a significant shift in the ratio of Sr-88 to Sr-86 relative to their natural abundance ratio supports the author's CAF and LANT hypotheses of cold nuclear reactions associated with a condensed matter environment. Additional work is under way to check these preliminary results.

ACKNOWLEDGMENTS

H. Fox, Editor, *Fusion Facts*, is thanked for his encouragement and interest in the Cal Poly research. ENECO, formerly FEAT, is thanked for its financial support and encouragement. M. Hovanec of West Coast Analytical Service, Inc. (Santa Fe Springs, CA) is greatly appreciated for the independent, and first rate, mass spectrometry (ICPMS) preceded by an ion-exchange column separation.

REFERENCES

[1] M. Fleischmann and S. Pons, "Electrochemically Induced Nuclear Fusion of Deuterium," *J. Electroanal. Chem.*, vol 261, p 301 (1989).

[2] R. Mills and K. Kneizys, "Excess Heat Production by the Electrolysis of an Aqueous Potassium Carbonate Electrolyte and the Implications for Cold Fusion", *Fusion Technol.*, vol 19, (1991).

[3] R. Bush, "A Light Water Excess Heat Reaction Suggests that `Cold Fusion' May Be `Alkali-Hydrogen Fusion'", *Fusion Technol.*, vol 22, p 301 (1992).

[4] R. Notoya and M. Enyo, "Excess Heat Production in Electrolysis of Potassium Carbonate Solution with Nickel Electrodes", Proc. of the Third Intl. Conf. on Cold Fusion, vol 421 (1993).

[5] R. Bush, "Will the Light Water Excess Heat Effect Lead to a Unification with Cold Fusion?", *Twenty First Century Science and Technology*, Fall 1993, p 75.

[6] R. Bush, "Towards a Nuclear Physics of Condensed Matter", accepted for *Fusion Technol*., under

revision.

[7] R. Bush and R. Eagleton, "The Transmission Resonance Model for Cold Fusion in Light Water: I. Correlation of Isotopic and Elemental Evidence with Excess Power", Proc. 3-ICCF, p 409 (1993).

[8] R. Bush, "An Electron-Catalyzed Fusion Model (ECFM) Suggests a Unification of Heavy- and Light Water Cold Fusion Phenomena", manuscript submitted for publication to *Fusion Technology*.

[9] R. Bush, "A Unifying Model for Cold Fusion", submitted to the Proceedings of the ICCF-4.

[10] R. Bush and R. Eagleton, "Evidence for Electrolytically Induced Radioactivity and Transmutation of Rubidium to Strontium Correlated with the Light Water Excess Heat Produced with Rubidium Salt Electrolytes and Nickel Mesh Cathode", submitted to the Proceedings of the 4-ICCF.

[11] T. Boyer, *Phys. Rev. D*, vol 11, p 809 (1975).

[12] H. Puthoff, "Ground State of Hydrogen as a Zero-Point-Fluctuation Determined State", *Phys. Rev. D*, vol 35, p 3266 (1987).

[13] R. Eagleton, "Experimental Details for Light Water Cold Fusion Research at Cal Poly (Pomona)", submitted for the Proceedings of the Minsk Conference (1994).

*3801 West Temple Avenue, Pomona, CA 91768.
**University of Utah Research Park, 391-B Chipeta Way, Salt Lake City, Utah 84108.

NOTE: A complete copy of the West Coast Analytical Service, Inc. report is available form the author.

Table 1

Date	Sample ID	Sr 86	Sr 88	Total Strontium
4- 8-93	0.01ppm Sr Std	10.48	89.52	10ppb
4- 9-93	0.01ppm Sr Std	10.48	89.52	10ppb
4-13-93	0.01ppm Sr Std	10.56	89.44	10ppb
4-14-93	0.01ppm Sr Std	10.53	89.47	10ppb
		10.51±0.04	89.49±0.04	

Date	Sample ID	Sr 86	Sr 88	
4-13-93	100ppm Rb/0.01ppm Sr	10.47	89.53	10ppb
4-15-93	100ppm Rb/0.01ppm Sr	10.55	89.45	10ppb
		10.51±0.06	89.49±0.06	

Date	Sample ID	Sr 86	Sr 88	
4- 8-93	A#53	ND	ND	ND
4- 9-93	A#53	22.2	77.8	1400ppb
4-15-93	A#53	12.05	87.95	NC

Date	Sample ID	Sr 86	Sr 88	
4- 8-93	#56PR	22.3	77.7	NC
4- 9-93	#56PR	26.8	73.2	1500ppb

NC - not calculated

Figure 2. Cathode post-run mass spectrogram.

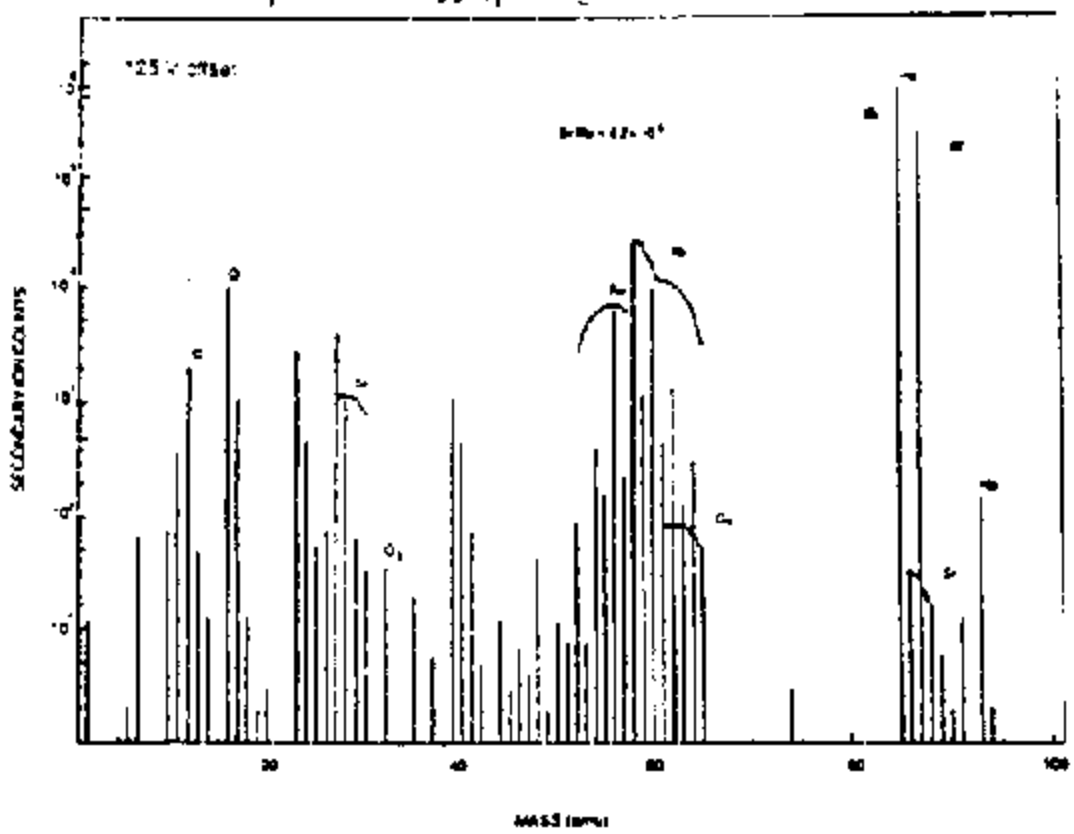

Figure 3. Cathode pre-run mass spectrogram

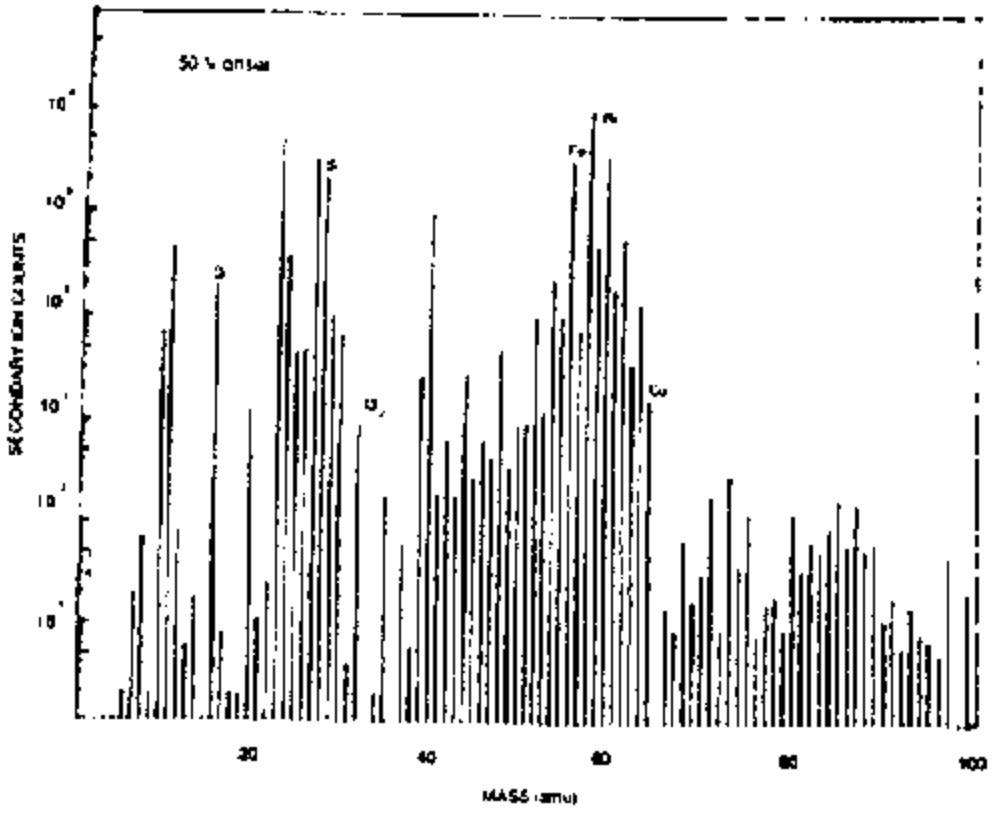

Figure 3. Cathode post-run mass spectrogram

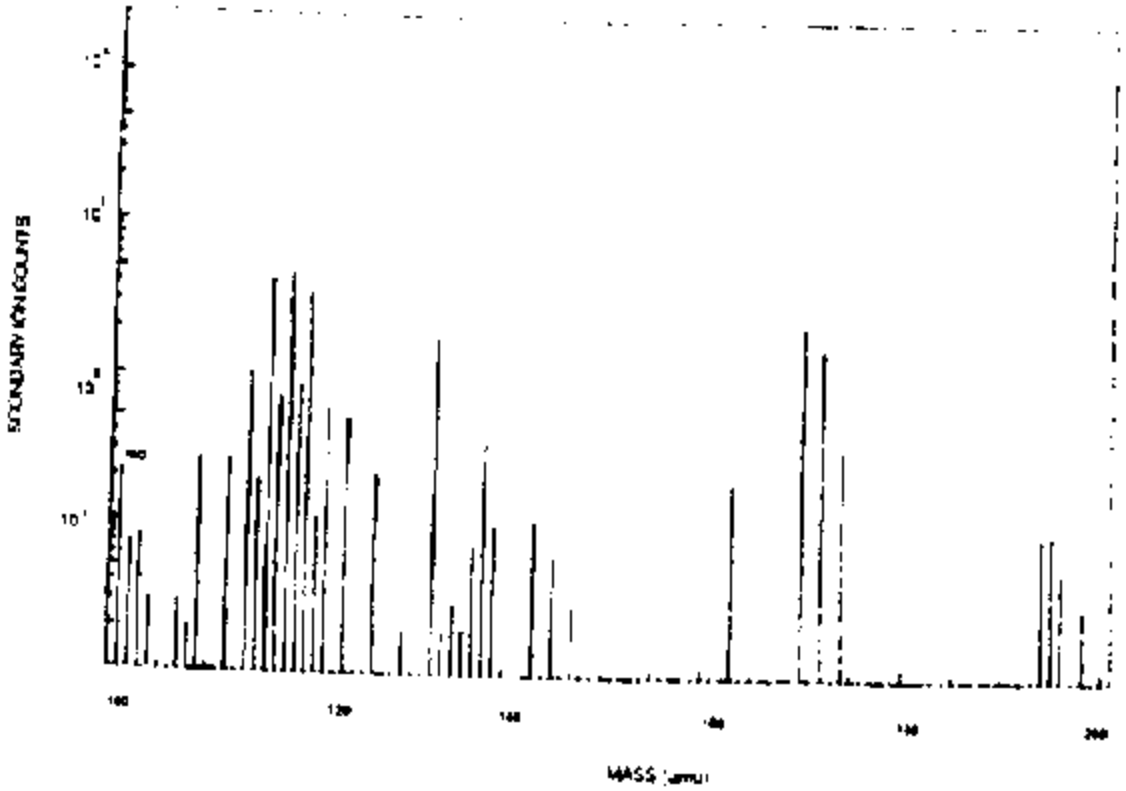

Figure 4. Cathode pre-run mass spectrogram

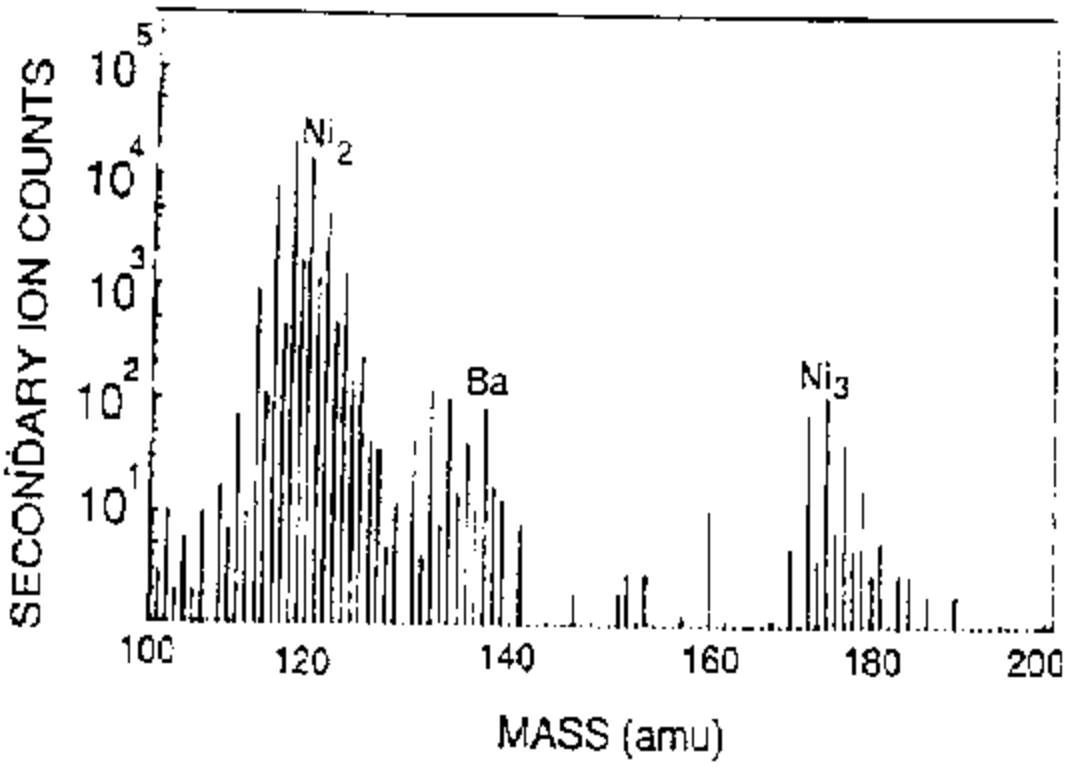

Figure 5

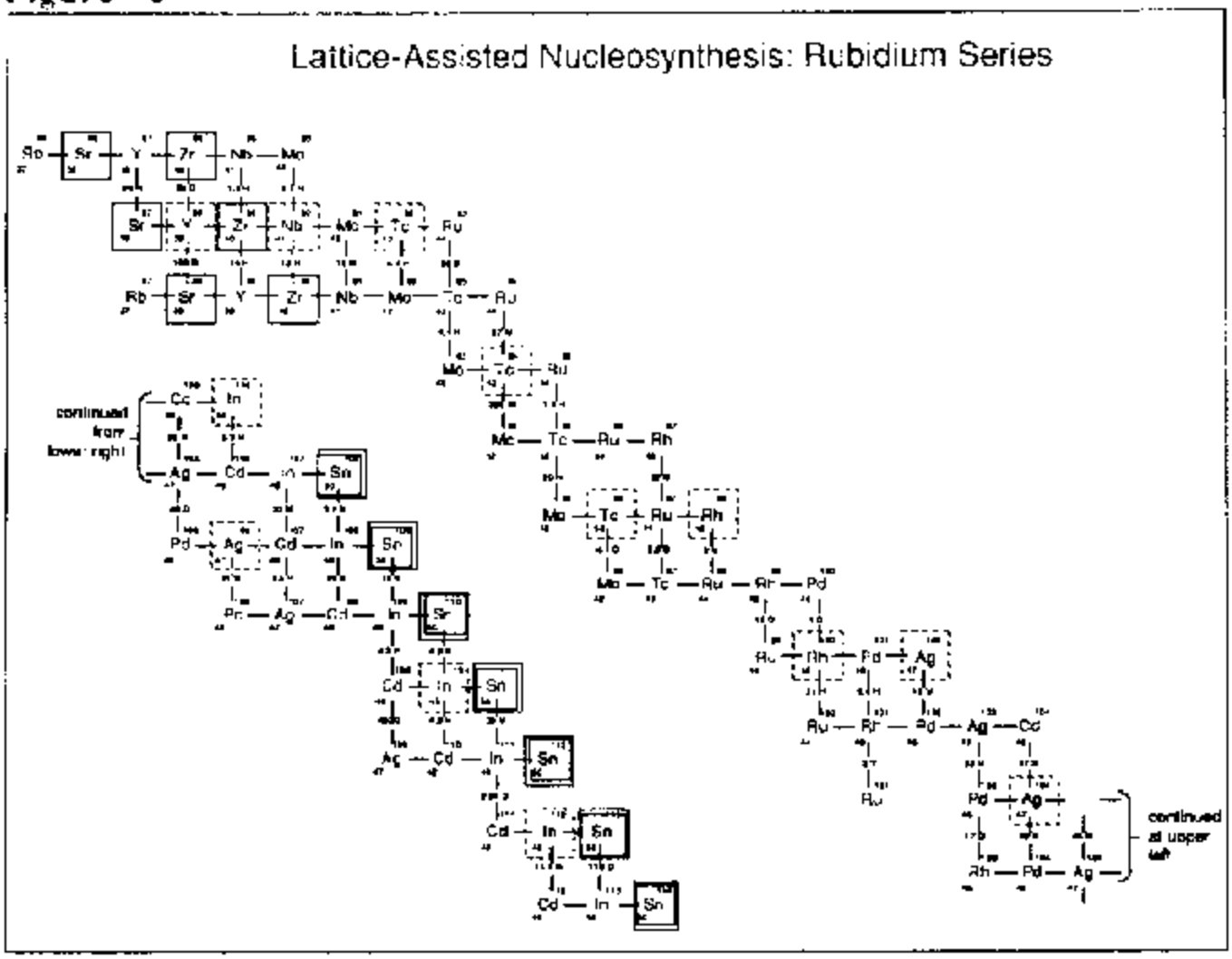
Lattice-Assisted Nucleosynthesis: Rubidium Series
continued from lower right
continued at upper left

Figure 6

Isotope Production via Cold Nucleosynthesis: Rubidium Series
(Cell 53)

Mass Number (A)	Nuclides Synthesized	Net number of Nuclei Synthesized x 10^{16}	Total Energy Released (MeV x 10^{17})
86	$_{38}Sr^{86}$	1.34	1.29
87	$_{38}Sr^{87}$	19.25	33.30
88	$_{38}Sr^{88}$, $_{39}Y^{88}$(108D), $_{40}Zr^{88}$(88D)	0.52	0.55
89	$_{39}Y^{89}$	1.66	4.6
90	$_{40}Zr^{90}$	0.28	1.1
91	$_{41}Nb^{91}$	3.00	12.1
92	$_{42}Mo^{92}$	(small)	(small)
93	$_{42}Mo^{93}$	27.03	148.10
94	$_{42}Mo^{94}$	0.23	1.43
95	$_{42}Mo^{95}$	(small)	(small)
96	$_{44}Ru^{96}$, $_{43}Tc^{96}$(4.35D)	(small)	(small)
97	$_{43}Tc^{97}$, $_{44}Ru^{97}$(2.9D)	(small)	(small)
98	$_{44}Ru^{98}$	(small)	(small)
99	$_{44}Ru^{99}$, $_{45}Rh^{99}$(16.1D)	(small)	(small)
100	$_{45}Rh^{100}$, $_{46}Pd^{100}$(4D)	0.30	3.90
101	$_{44}Ru^{101}$, $_{45}Rh^{101}$(3y)	3.70	41.30
102	$_{45}Rh^{102}$, $_{46}Pd^{102}$	1.21	14.50
103	$_{45}Rh^{103}$, $_{46}Pd^{103}$(17D)	1.40	17.80
104	$_{46}Pd^{104}$	0.54	7.30
105	$_{46}Pd^{105}$, $_{47}Ag^{105}$(40D)	(small)	(small)
106	$_{46}Pd^{106}$, $_{48}Cd^{106}$	(small)	(small)
107	$_{47}Ag^{107}$	0.54	7.30
108	$_{48}Cd^{108}$	0.23	3.90
109	$_{47}Ag^{109}$, $_{48}Cd^{109}$(453D)	2.25	39.70
110	$_{48}Cd^{110}$	(small)	(small)
111	$_{48}Cd^{111}$, $_{49}In^{111}$(2.8D)	(small)	(small)
112	$_{50}Sn^{112}$	2.25	44.60
	Sums:	65.73 x 10^{16}	**384.17 x 10^{16} MeV**

Estimating a ten percent error, then, the total energy to produce the above based upon the LANT Model is approximately **(3.8 ± 0.4) x 10^{19} MeV** versus the total excess heat determined from calorimetry for Cell 53 of **(4.0 ± 0.8) x 10^{19} MeV**.

D/PD LOADING RATIO UP TO 1.2:1 BY HIGH POWER μS PULSED ELECTROLYSIS IN PD PLATES.

F. Celani, A. Spallone, P. Tripodi, A. Petrocchi,
D. Di Gioacchino, M. Boutet

INFN, Laboratori Nazionali di Frascati,
via E.Fermi, 00044 Frascati (Italy).

P. Marini, V. Di Stefano

SKITEK, IRI, Pomezia (Italy) (*)

ABSTRACT

We tested metallurgically different Pd plates made with cold working procedures. We focused on the Deuterium absorption for these plates during pulsed electrolysis. We used high peak current intensity (up to 100 A) with very short (1 μs) pulse duration, up to 20 KHz of repetition rate. The peak power of each pulse can be as large as 50 KW. The LiOD 0.3 M/I D_2O solution has at Pt net as anode.
Very high D/Pd ratio (up to about 1.2:1) have been reached and the Deuterium absorption behavior versus time is strongly dependent on the metallurgy of the plates. Even surface preparation of the plates seems to play a role in the absorption phenomena.

Metallurgical and electrical parameters like hardness, over-voltage and absorption rate can give useful indications about the absorption of the Deuterium into the plate: they behave like cross-correlated parameters.

1. The Experimental Set-Up

The adopted electrolytical system was already described in the previous ICCF3 Conference at Nagoya (Japan)[1] and, very recently, at ICCF4 Conference (Maui, USA)[2] about the latest, significative, experimental improvements performed.

In short, it is a flow calorimeter composed by a cylindric polyethylene vessel containing a double turned copper coil used for cooling and input-output energy computing (fig. 1). The ordinary water, passing through the coil, cools the solution. Seven temperature sensors are properly located in order to measure the produced heat and to cross-check the proper calorimeter operation. The Pt wire net was turned around a teflon sample-holder in a proper geometrical shape in order to smooth the non-uniform electric field at the edges of the plate. In this way we reduced the effect of the Deuterium discharge at the edges of the plate due to the strong electric field gradients. A reference electrode, just a Pt wire, was located in front of the two sides of Pd plate (3 mm far); the wired Pt anode (1 mm diameter) net is 1 cm far from the cathode; the electrolytic solution is LiOD 0.3 M/I D_2O. An electrovalve was inserted along the outgoing gas pipe just to define a close volume (about 150 cc) to store the gas coming from the electrolysis. We determine this volume measuring both the gas pressure developed during the electrolysis and the electric charge flowed through the electrodes: we used the gas law and the Faraday equation. In this way we are able to calculate the quantity of moles of D_2 absorbed from the Pd, measuring the missing pressure. We usually operate leaving close the electrovalve until the gas pressure reaches a definite value (50 mbar), further on we open this valve allowing the gas to flow away. A proper circuitry was made to control this cyclic operation.

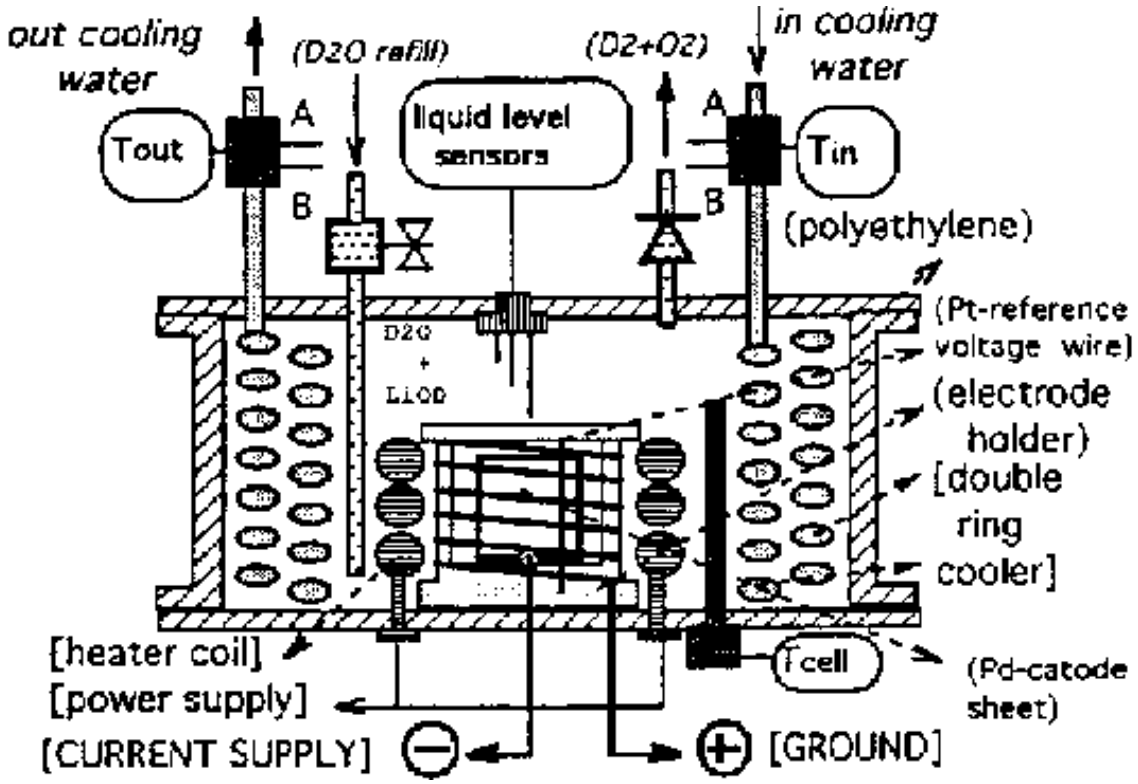

A specific circuitry was made to generate very sharp high peak current pulses (rise time <300 ns at 100 A peak values). A circuit measures the flowing electric charge and the power absorbed from the cell in each single pulse. Another circuit (out-of-phase) measures both the voltage of the cathode and the voltage of the Pt wire floating electrode (RHE), which is put in the solution close to the cathode (3 mm). These voltages are properly used to determine the over-voltage parameter too. The out-of-phase voltage measurements are performed after a delay (30 μs) from the end of the power pulse, when the Pd/Pt system is electrically decoupled from all circuitry by 2 ultra-fast power recovery diodes (40HFL80S05) properly connected in series.

2. The Deuterium Absorption Measurements

We performed same absorption blank runs using an Au plate in order to obtain reference measurements to compare with the Pd plates one. We tested three cold-worked Pd sheets (25x25x1 mm) named: T05 (TANAKA K.K.) and I65, I63C (IMRA MATERIAL). The TANAKA plate (very high hardness value: 300 Hv) was prepared with proper impurities (2780 ppm) enclosed during the melting preparation: the high hardness value reached is due to the doping (under patent). The 2 IMRA plates (140 Hv) had the same cold-worked treatments (same batch) and no impurities were added. The I63C was warmed to about 750°C for 10 minutes 2 times (after cooling to room temperature in about 20 minutes) in a oxidizing atmosphere to reduce the cold-worked hardness to the original value of pure Pd just melted (about 50 Hv). After this treatment we observed a dark-blue thin film covering the surface: this film (probably PdO) was quite hard and even resistant to 65% concentrated HNO_3 acid attack.

All the tests were performed under the following operating conditions: pulse peak current 16 A, pulse width 0.5 μs, pulse repetition rate 5 KHz, peak current density 1.3 A/cm^2. These conditions are equivalent

to an electrolytical mean current of about 64 mA (i.e. only 5mA/cm2).

In figure 2 it is shown the absorption rate (in Mole/s · cm^2) of the plates T05, I65 and I63C. It provides information about the quantity of Deuterium flowing through the Pd-surface per time unit and surface unit. In this figure we can put in evidence strong differences comparing the T05 and I63C (the very hard plate and hard modified surface) plates with the I65 one (softer plate): i.e. the hard plates show a relevant shoulder on the shape. This shoulder seems to indicate that, in the α+ß phase, the Deuterium diffusion coefficient is higher and about constant in respect to the expected one, like the I65 plate. The I63C (modified surface) plate shows that the absorption rate, very high at the beginning of the charging up, decreases faster than the other plates and we can suppose that the modified surface is not stable enough during the whole electrolysis (Oxygen reduction at PdO surface due to D?). The absorption rate decreases during the ß phase, zeroing when the D/Pd concentration reaches its maximum value equal to 1.2:1 with I63C, 1.02:1 with T05 and 0.96 with I65 (fig. 3).

The D/Pd concentration has been evaluated accumulating the absorbed Deuterium moles over time. The absorption efficiency (defined as the ratio of the quantity of absorbed Deuterium to the Deuterium developed during the electrolysis) reaches its maximum value (about 71%) in the α phase. The plate (I63C), providing the highest absorption rate and loading efficiency, reaches also the highest (1.2:1) D/Pd ratio.

In figure 4 it is shown the over-voltage* (i.e. normalized to the charge flow, V/C, see following), due to deuterium loading, versus the charge flow itself. We define the over-voltage as the difference between the cathodic potential and the reference electrode previously described. We recall that these voltages are measured during a fixed time (10μs) after a fixed delay (30 μs) from the end of each power pulse (out of phase measurement). All electric potentials are measured in respect to the Pt net electrode which is connected to the electric circuit ground. During the electrolysis the Deuterium gas, developed at the cathode, surrounds the reference electrode and we can assume it as equivalent to a R.H.E. (Reversible Hydrogen Electrode). In the over-voltage calculation we take into account the fact that the peak-up electrode surrounded by the D_2 gas is not a platinized Pt, but just a pure Pt: this difference is reported by the literature to be 0.09 V for H_2 gas; we consider this value appropriate for our calculations.

We would like to note that the over-voltage* reported in figure (4) is computed subtracting, at the same experimental conditions:

a) the Tafel component, due to the current density;
b) the Li contribution at the total apparent overvoltage.

The last subtraction was allowed through blank experiments with the Au plate: we assume that, along the whole time of the electrolysis, there is not appreciable deuterium absorption at Au plate but only Li deposition and that the amount of Li deposited is the same in the cases of experiments with Au or Pd.

All the overvoltage considered are normalized with the charge flown and properly corrected for cell temperature variations, if any. We found that the "normalized" overvoltage* increases surface D/Pd ratio according to the metallurgy of the plates: hardest plates show largest values of overvoltage.

Conclusions

Independently from the metallurgy of the Pd electrodes, we developed a high peak current pulse technique able to load deuterium into Pd plates at values as large as, at least, 0.96:1 and 1.2:1 maximum.

The metallurgy of the plates affects the absorption rate "shape" parameter. The hardness parameter is increased by cold working from a value of 50 Hv (ordinary Pd) to about 140 Hv in two of the samples used (IMRA plates); some impurities were intentionally added to another Pd plate in order to increase this value up to 300 Hv (TANAKA plates).

A heavy warming (750°C), in an oxidizing atmosphere, at the surface of one of the two 140 Hv plates was able, along a measurable experimental time, to increase the surface hardness giving noticeable effects both on Deuterium absorption shape and absolute value stored.

It seems that high values of hardness increase the D/Pd charging ratio into the plates studied. The absorption rate shape is related to the surface metallurgy of the plates: we can hypothesize that very high D/Pd ratios (larger than the "mean" value computed) are reached at thin layers of the plate surface. We think that the short-time high-current pulses can enhance this useful effect.

The over-voltage parameter gives useful indications about the Pd plate surface status during the Deuterium absorption. An important role can play the ionic Li on the surface, in particular way when the Pd plate reaches high D/Pd values.

Some tests are in progress in order both to enhance and make steady the positive effects of "surface changing" by proper surface poisoning.

Acknowledgements

We are indebted to Dr. K. Mori and Dr. M. Nakamura (TANAKA K.K.) because of their effort, in a joint experiment, to develop and characterize the new 300 Hv Pd plates (under patent). We are grateful to Y. Oyabe and S. Nezu (IMRA MATERIAL) because both provided us with pure Pd plates (of different metallurgical properties) and gave useful suggestions and comments in order to fully characterize the new "surface modified" Pd plate. We thank Dr. A. Mancini (ORIM S.r.l.) for providing us with some ultrapure Pd plates for cross-reference studies.

References

1. F.Celani, A.Spallone, P. Tripodi, A. Nuvoli, Frontiers of Cold Fusion, Edited by H.Ikegami, p. 93 (1992), Frontier Science Series n.4, Univ. Acad. Press, Tokyo (Japan).

2. F.Celani, A.Spallone, P. Tripodi et al., "High Power μs Pulsed Electrolysis for Large Deuterium Loading on Pd Plates," presented at ICCF4 Conference, Dec. 6-9, 1993 Maui (USA). Publishing in Frontier Science Series n.5, Ed. by EPRI, Palo Alto, California (USA)

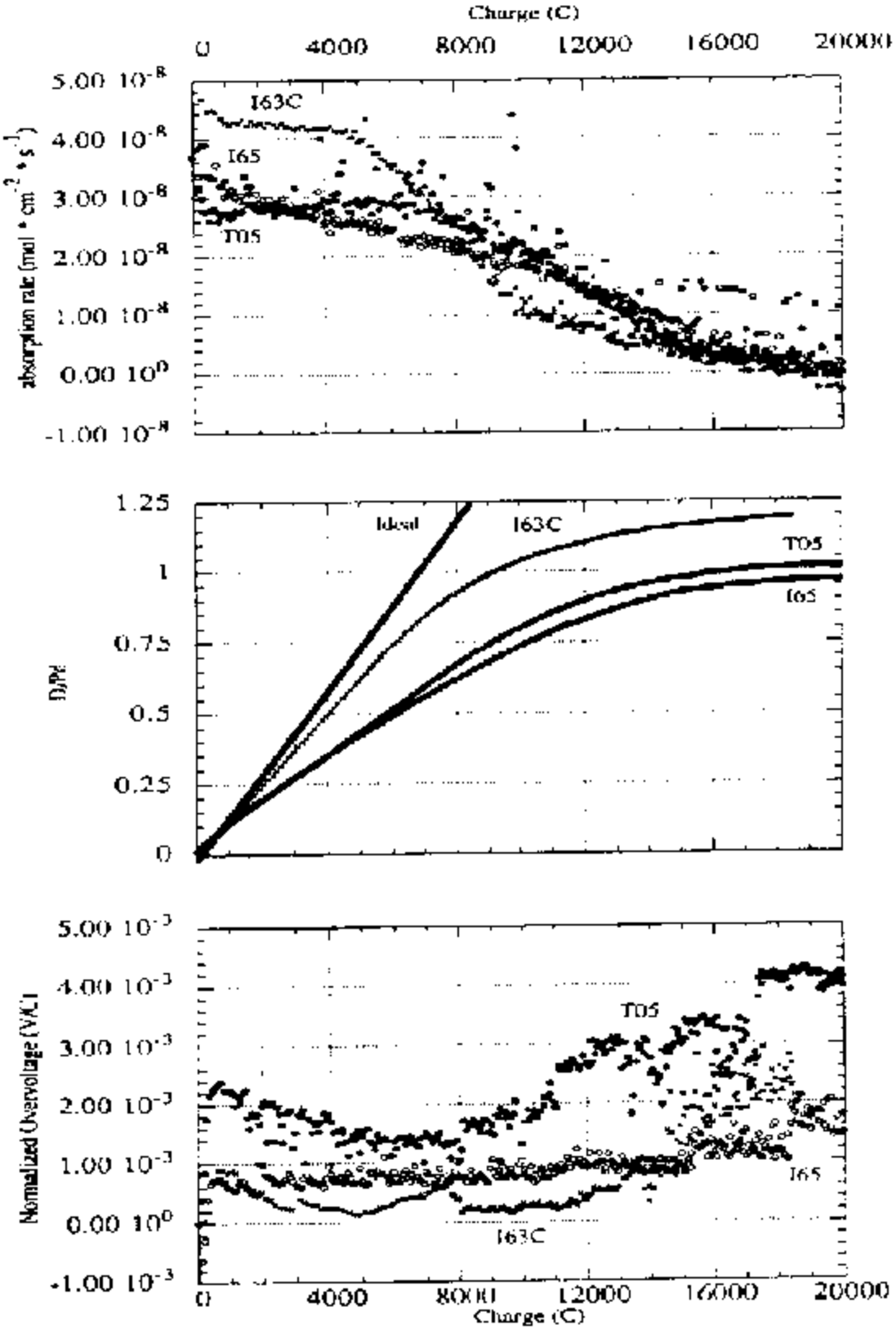

Fig. 2- The absorption rate during the first charging up.
Fig. 3- The D/Pd ratio reached by the plates.
Fig. 4- The normalized overvoltage* parameter indicates the D role.

CHANGES IN SURFACE TOPOGRAPHY AND MICROCOMPOSITION OF A PALLADIUM CATHODE CAUSED BY ELECTROLYSIS IN ACIDIFIED LIGHT WATER

J. Dash and G. Noble
Department of Physics
Portland State University
P.O. Box 751
Portland, Oregon 97207-0751

and

D. Diman
Carleton College
Northfield, Minnesota 55077

ABSTRACT

A thin palladium cathode became bent and torn during electrolysis in acidified light water. Localized changes in composition were observed, including the occurrence of chlorine and possibly silver. Transmutation by neutron absorption may have caused the formation of silver.

Introduction

It has been shown that electrolysis with a palladium cathode in an electrolyte containing a mixture of sulfuric acid and either light water or heavy water results in greatly altered surface topography [1,2,3], excess heat [2,3] and unexpected elements which could have been produced by absorption of neutrons [3]. For example, silver was observed in high concentrations at microscopic surface aspirates on the 0.060 mm thick palladium cathode after electrolysis in the heavy water electrolyte [3]. But silver was not detected when larger areas which included the surface aspirates were analyzed. Thus, the internal processes which result in surface aspirates and high concentrations of unexpected elements are highly localized.

We report here the results of analysis of a 0.060 mm thick palladium cathode after electrolysis in a light water electrolyte.

Experimental Methods and Results

Platinum foil (99.9% Pt) was used for the anodes and palladium foil (99.9% Pd) was used for the cathodes. The palladium foil was produced by cold rolling from the initial 0.5 mm thickness to 0.06 mm. The electrolyte consisted of 0.06 mol fraction H_2SO_4 (analytical reagent) in deionized H_2O for the light water cell and 0.06 mol fraction H_2SO_4 in D_2O (99.9% D_2) for the heavy water cell. The cells were connected in series, and electrolysis was performed for five hours at a current density of about 0.67 A/cm^2. Excess gases from electrolysis escaped through the tops of the cells. Excess heat production of about 0.1 watt was observed for the heavy water cell, compared with the light water cell [3].

After electrolysis, the palladium cathode from the light water cell was cleaned ultrasonically in deionized water. It was then examined with a scanning electron microscope (SEM) and analyzed

chemically with an attached energy dispersive spectrometer (EDS).

Fig. 1a shows the upper portion of the palladium cathode which was not immersed in the electrolyte during electrolysis. This is almost as smooth and flat as the original cold rolled palladium before electrolysis. In contrast to this, Fig. 1b shows the distorted and torn lower portion of the palladium cathode which was immersed in the electrolyte during electrolysis.

Using the EDS, spectra were taken from the square areas indicated on Fig. 1a and 1b, using identical experimental conditions. These are shown in Fig. 2. Superimposed on these spectra are vertical bars which indicate the positions and expected relative intensities of six palladium L peaks. The two most intense L peaks are $L\alpha_1$ at 2.84 KeV with relative intensity 100% and $L\beta_1$ at 2.99 KeV with relative intensity 42%. Actual relative intensity of $L\beta_1$ to $L\alpha_1$ in Fig. 2a is 50% and in Fig. 2b it is 54%. Similar results were obtained by analysis of the remainder of the electrode areas shown in Fig. 1a and 1b. Thus, the ratio of the Pd $L\beta_1$ intensity to the Pd $L\alpha_1$ intensity is slightly greater in the electrolyzed portion of the palladium cathode (Fig. 1b) than in the unelectrolyzed portion (Fig. 1a). Changes in this ratio can be caused by factors such as differences in absorption [4]. Overlap with emission lines from another element could also produce changes in this ratio. For example, silver $L\alpha_1$, the strongest silver L line [4], occurs at 2.98 KeV. If silver were present in the palladium, it would increase the intensity of Pd $L\beta_1$ without appreciably changing the intensity of Pd $L\alpha_1$. Thus, the presence of silver would increase the ratio of Pd $L\beta_1$ to Pd $L\alpha_1$.

The spectrum in Fig. 2b, which came from the electrolyzed portion of the palladium cathode, has a strong platinum peak. This results from slow dissolution of the platinum anode and subsequent electroplating of Pt on the palladium cathode. The platinum peak is not present in the Fig. 2a spectrum from unelectrolyzed palladium.

The arrow at the bottom left of Fig. 1b indicates an area which is enlarged in Fig. 3a, and enlarged further in Fig. 3b. An EDS spectrum from the feature which protrudes from the surface in Fig. 3b is shown in Fig. 3c. An EDS spectrum from the square area indicated in the lower right-hand corner of Fig. 3b is shown in Fig. 3d.

The protruding feature shown in Fig. 3a and in more detail in Fig. 3b appears to have erupted out of the surface of the palladium cathode. The surroundings are smooth and flat. The protrusion also differs in composition from the surroundings, as indicated by the intense chlorine peak between the platinum and palladium peaks in Fig. 3c and the absence of this peak in Fig. 3d. These is also a weak potassium peak to the right of the palladium peak in the spectrum of the protrusion, but there is no potassium peak in the spectrum from the right of the protrusion (Fig. 3d).

Three more spectra were taken from other positions on the protrusion in addition to that shown in Fig. 3b. Although the relative intensities differed from one position to another, the same elements (Pt, Cl, Pd, and K) were detected in all four spectra.

At about 50μm from the lower edge of the palladium cathode shown in Fig. 3a, the surface topography changes from uniform gray to a dark, mottled appearance, as shown in Fig. 4a. A spectrum from the spot indicated on Fig. 4a is shown in Fig. 4b. This shows the presence of palladium, but there is no peak for platinum such as that in Fig. 3d which was obtained from the uniform gray area on the lower right of Fig. 3b. In the spectrum of Fig. 4b the ratio of Pd $L\beta_1$ to Pd $L\alpha_1$ is 0.61, or about 0.1 greater than this ratio in all of the spectra shown above, from either the unelectrolyzed or the electrolyzed portions of the palladium cathode.

The upper portion of Fig. 4a has a fairly uniform, light gray appearance, similar to the region on the lower right of Fig. 3b which contains a large amount of platinum (Fig. 3d). It may be that the platinum peeled off of the lower edge during ultrasonic cleaning of the electrode. The current density was highest at the lower edge, and the electroplated platinum may have been dendritic and loosely adherent.

The mottled structure near the lower edge of the electrode in Fig. 4a is shown at higher magnification in Fig. 5a. The contrast in this photograph is most likely due to topographic differences. Light gray areas are probably higher in elevation than the interspersed dark, sub-micron diameter areas.

The composition of the area within the square indicated above the center in Fig. 5a is given by the spectrum in Fig. 5b. This is similar to the spectrum in Fig. 4b in that platinum is not present. The ratio of the palladium $L\beta_1$ peak height to the $L\alpha_1$ peak height is 0.75, which is 0.15 greater than the same ratio in Fig. 4b and about 0.25 greater than this ratio in all the spectra taken at distances more than 50μm above the lower edge of the cathode.

Discussion of Results

The above results illustrate the drastic changes in surface morphology of a palladium cathode which occur during electrolysis with an electrolyte containing H_2O and H_2SO_4 and a platinum anode. The violent interaction of hydrogen with palladium caused inhomogeneous distortion and tearing. Analysis of a surface protrusion revealed the presence of chlorine (probably as a compound) on the protrusion but not on the adjacent area of the palladium cathode. The source of chlorine is not known.

The morphology of the lower edge of the cathode, where current density most likely was highest during electrolysis, shows a large number of sub-micron sized surface pits. Analysis shows a large change in ratio of x-ray fluorescence peaks of palladium. The ratio of Pd $L\beta_1$ at 2.99 KeV to Pd $L\alpha_1$ at 2.84 KeV changed from about 0.50 for the upper part of the palladium cathode to 0.75 for the lower edge. It is known that changes in this ratio can be caused by changes in absorption by the sample [4]. But it is not clear why the absorption from a region near the edge should change in such a way as to cause the observed change in intensity ratio. It seems more likely that the change in intensity ratio was caused by the presence of silver which produces an $L\alpha_1$ peak at 2.98 KeV. If this is the correct explanation, then the region in Fig. 5a from which the spectrum in Fig. 5b was obtained contains about 20% Ag. This is much less than was found in localized areas of a similar palladium cathode electrolyzed in heavy water [3].

If silver is present, then it either diffused from within the palladium, was electroplated, or was produced by transmutation caused by neutrons produced during nuclear fusion of hydrogen or deuterium. The results show that platinum electroplates onto the palladium, but that the platinum probably peeled off of the lower edge during ultrasonic cleaning after electrolysis due to poor adherence of the electroplated layer. Therefore, if silver had been electroplated, it probably would have peeled off with the platinum. The likelihood that silver would diffuse from the interior and concentrate at selected sites on the surface seems extremely remote because silver and palladium are miscible in all phases [5].

We previously concluded that a nuclear fusion reaction may have resulted in silver deposits on a palladium cathode electrolyzed in an electrolyte containing D_2O and H_2SO_4 [3]. It seems most probable that the enhanced x-ray intensity at 3 KeV in Figs. 4b and 5b may also be due to transmutation caused by neutrons from a fusion reaction. If a neutron is captured by Pd^{108}, an abundant isotope, it becomes Pd^{109}, which rapidly decays to Ag^{109}, a stable isotope [6].

References

1. D.S. Silver, J. Dash, and P.S. Keefe. "Surface Topography of a Palladium Cathode After Electrolysis in Heavy Water, *Fusion Technology*, vol 24, p 423 (1993).

2. J. Dash, P.S. Keefe, E. Nicholas, and D.S. Silver, "Comparison of Light and Heavy Water Electrolysis with Palladium Cathodes," Proceedings AESF 80th Annual Conference, Orlando, Florida (June 1993), p 755.

3. J. Dash, G. Noble, and D. Diman, "Surface Morphology and Microcomposition of Palladium Cathodes After Electrolysis in Acidified Light and Heavy Water: Correlation with Excess Heat," Proceedings of 4th International Conference on Cold Fusion, Lahaina, Hawaii (December 1993).

4. G.G. Johnson, Jr., and E.W. White, "X-ray Emission Wavelengths and KeV Tables for Nondifferential Analysis," ASTM Data Series DS 46 (ASTM, Philadelphia, 1970).

5. I. Karakaya and W.T. Thompson, Binary Alloy Phase Diagrams, vol 1 (T. B. Massalski, ed.-in-chief.) Metals Park, Ohio: ASM, 1986, pp 55-56.

6. Handbook of Chemistry and Physics, 41st ed., Cleveland: Chemical Rubber Publishing Co., 1959/60, pp 470-471.

a

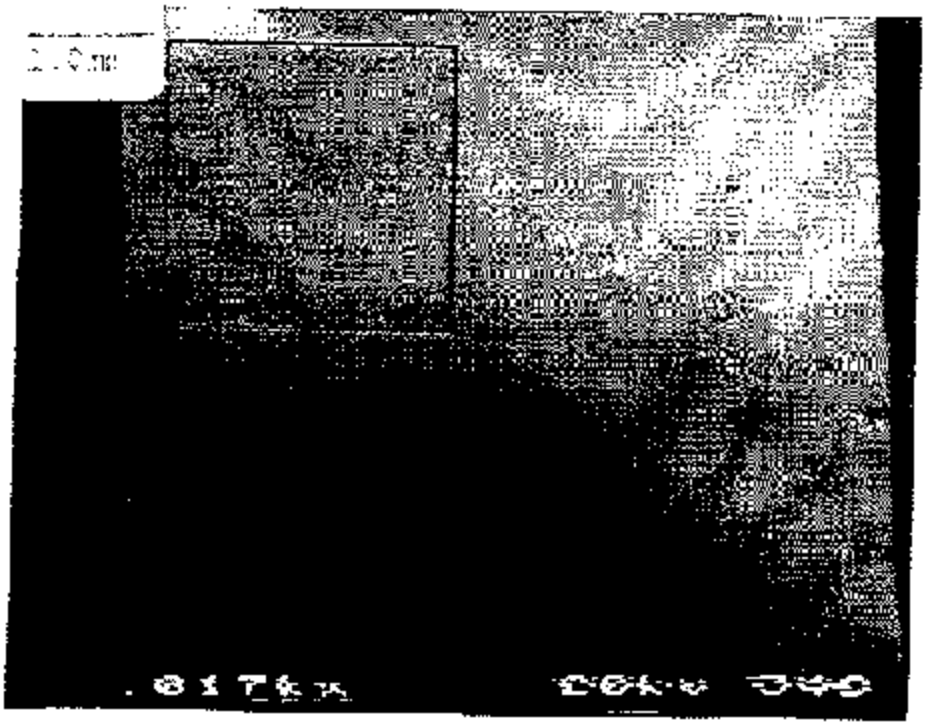

b

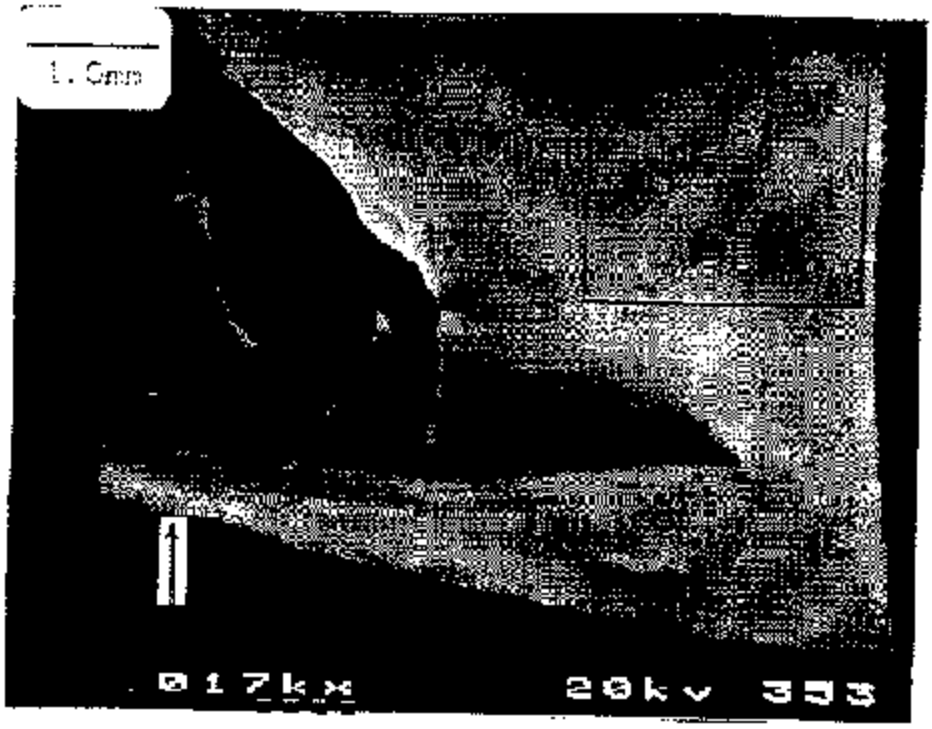

Fig. 1. Palladium cathode after electrolysis in acidified light water. (a) **Portion of the cathode above the electrolyte.** (b) **Portion of the cathode immersed in the electrolyte, concave side (facing anode).**

a

b

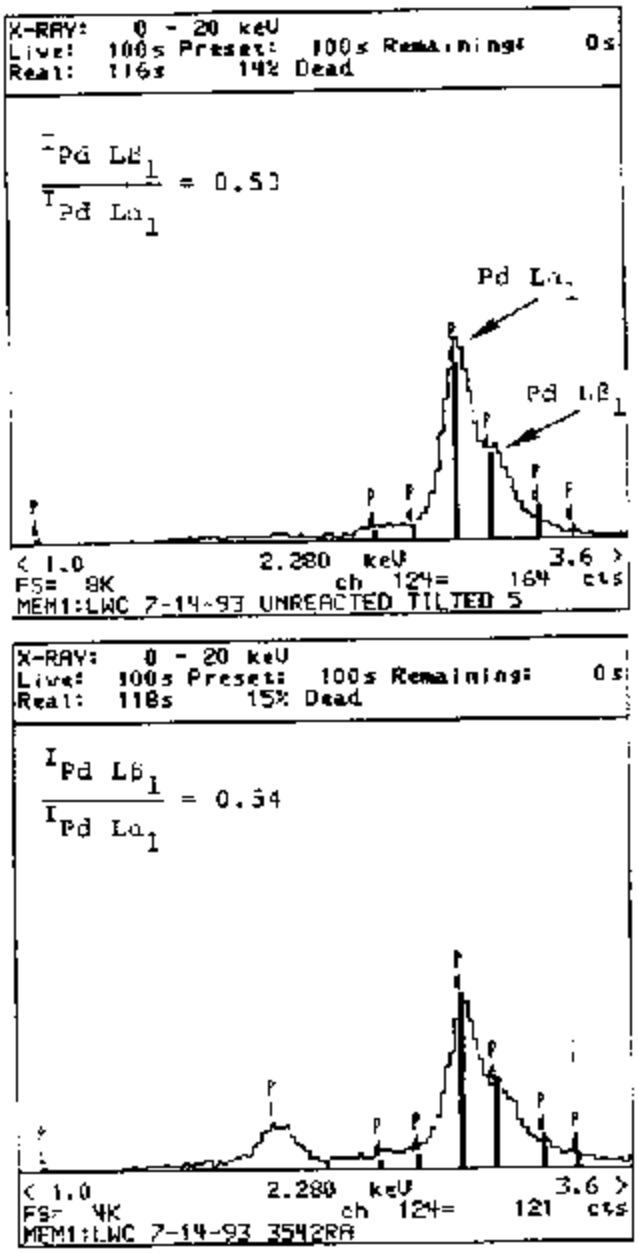

Fig. 2. EDS spectra from a palladium cathode after electrolysis in acidified light water. (a) Spectrum from the square area in Fig. 1a. The positions of Pd $L\alpha_1$ and Pd β_1 are indicated. (b) Spectrum from the square area indicated in Fig. 1b. The ratio $I_{Pd\ L\beta_1}/I_{Pd\ L\alpha_1}$ is indicated for each.

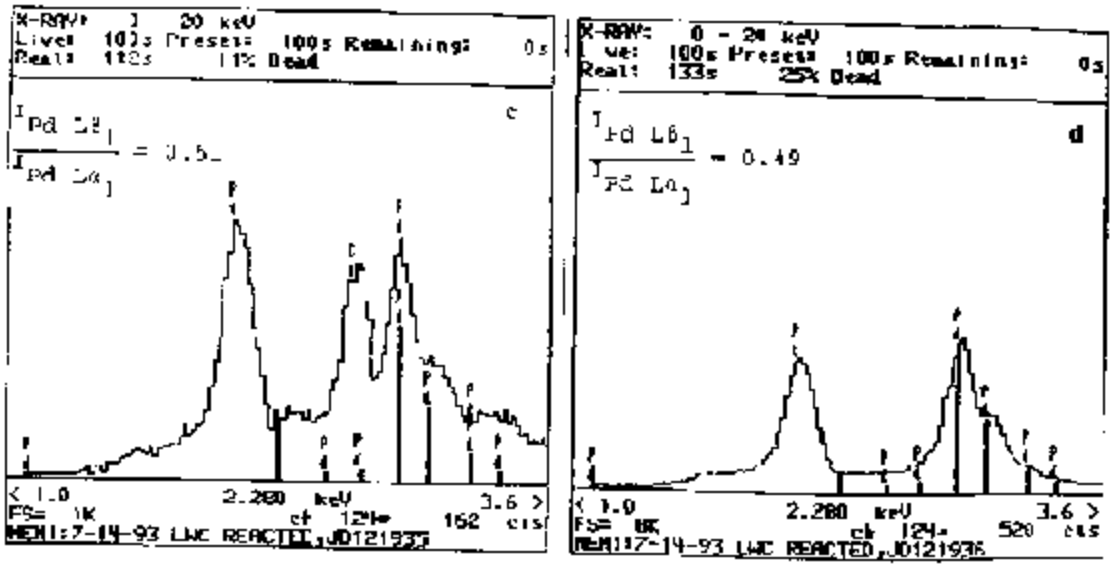

Fig. 3. (a) Enlargement of area near arrow in Fig. 1b. (b) Enlargement to show details of the protrusion near the center of Fig. 3a. (c) EDS spectrum from position 1 on the protrusion in Fig. 3b. (d) EDS spectrum from the square area shown on the lower right of Fig. 3d.

a

b

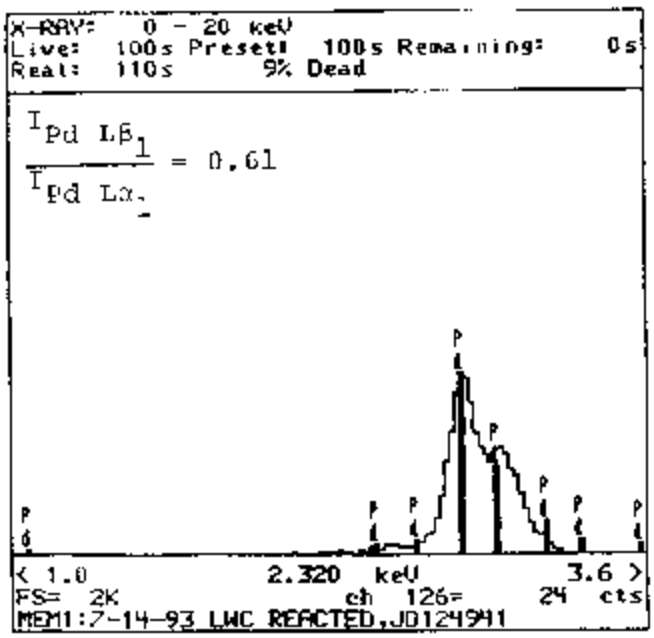

Fig. 4. (a) Enlargement of lower edge of palladium cathode to show changes in surface topography. (b) EDS spectrum from spot shown in Fig. 4a. Note that there is no platinum peak in this spectrum.

a

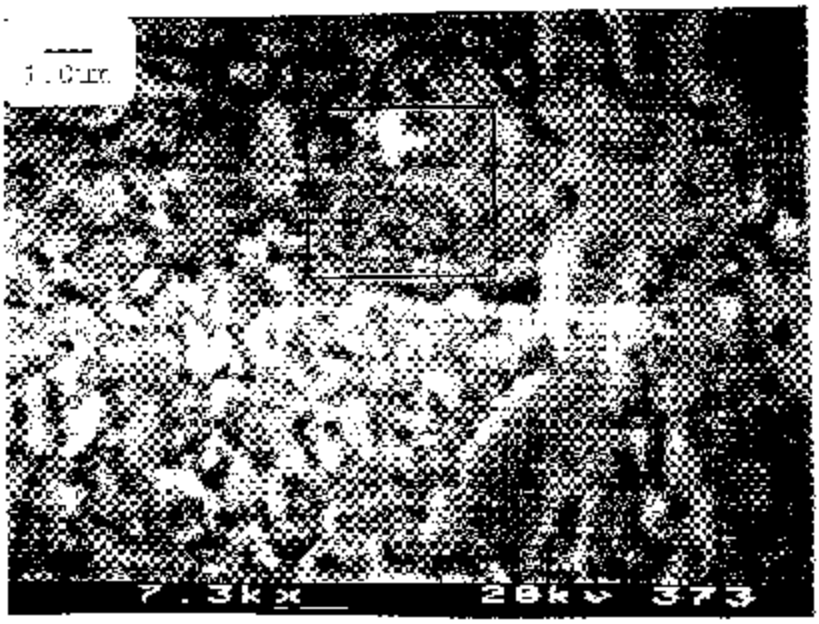

b

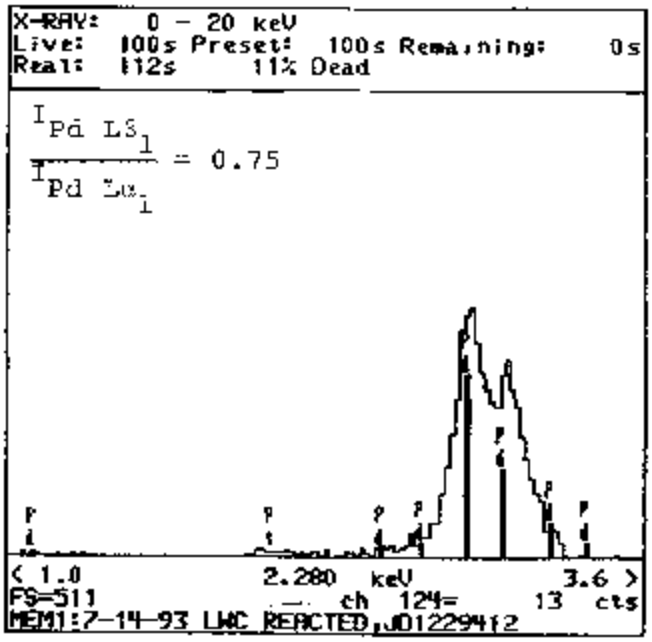

Fig. 5. (a) Enlargement of area a few microns from the lower edge of the Pd cathode. (b) EDS spectrum from square area indicated on Fig. 5a. Note that there is no platinum peak.

COLD FUSION BY SPARKING IN HYDROGEN ISOTOPES

by
J.Dufour
SRSA/CNAM 292 Rue St Martin
75003 Paris FRANCE

J.Foos and J.P. Millot
CNAM 292 Rue St Martin
75003 Paris FRANCE

INTRODUCTION

The idea of transmuting hydrogen isotopes into heavier species (helium), at room temperature, with the aid of palladium acting as a kind of catalyst can be traced back as early as 1926.[1,2] In 1989, a rebirth was given to the concept.[3,4] By electrolyzing heavy water with a palladium cathode, Jones, Fleischmann and Pons claimed to obtain significant energy production, in excess of the electrical energy introduced into the apparatus to carry out the electrolysis. This excess energy was tentatively explained by nuclear fusion reactions of the deuterium present in the cathode, reactions justified by the observation of the emission of neutrons, with an energy corresponding to the known reaction channels of deuterium hot fusion. The amount of neutrons measured was nevertheless many orders of magnitude lower to what would be expected to explain the energy generation observed.

Since 1989, a great number of various approaches were explored, implying contacting hydrogen isotopes and palladium (or metallic hydride forming metals such as nickel) : liquid state electrolysis, pressure variation of hydrogen isotopes in contact with palladium, low pressure electrical discharges in hydrogen isotopes with palladium cathode, sparks in hydrogen isotopes, solid state electrolysis, with protonic conductors ....

For the time being, no firm correlation has been established between the excess of energy measured and the possible nuclear ashes, which are often detected at levels close to the detection limits of the methods used (^{4}He, ^{3}H, neutrons, high energy radiations, isotopic changes in the host metal ...). In the present state of the art, we thus define cold fusion as being the abnormal thermal effects that are observed when an hydrogen isotope is contacted with a metallic hydride forming metal, under various physical or chemical conditions. The object of the work which we are carrying out, is to try to firm up the above mentioned correlations. For that, we are aiming at obtaining excess of energy in the order of tens of watts on periods of several weeks, to measure the amount of possible nuclear ashes well above the detection limits of the methods used. We shall give in this paper an overview of the results already obtained and indications on the improved calorimetric system which is now under construction.

Concept used and main results

Among the various methods available to contact hydrogen isotopes with metallic hydride forming metals, we have chosen to contact hydrogen isotopes in the gaseous phase (H_2 or D_2) at a pressure round the atmospheric pressure, with dissymetrical electrodes, at least one of them being made of a metallic hydride forming metal. A transient electrical discharge (sparks or ozonizer discharge) is struck between the two electrodes through the gaseous hydrogen isotope.

Precise and repeated energy balances show that excess energy is generated in the system, in a fully reproducible way. The amount measured on a steady state basis (several days), excludes chemical or physical explanations or at least classical ones. This excess energy is observed with both hydrogen and deuterium and with various metals (stainless steel was tested and gave a positive response).

On the basis of electrical energy input to the reactor, energy breakeven has been obtained (taking into account an efficiency of 50 % for electricity generation). Excess energy up to 2.5 W has been measured.

With the calorimetric set-up we have been using until now and which will be described below, we cannot exclude a systematic error that could explain the excess energy we measure. We are thus starting the operation of a new calorimetric system that will exclude such errors. We shall describe in this note the results obtained with the first calorimetric set-up (system I), which measures powers by measuring heat fluxes and the main characteristics of the new one (system II).

Experimental

The calorimetric set-up used until now (system I), has been previously described in detail[5]. We thus give here only the main features of it.

The reaction is carried out in a pyrex reactor as represented in fig.1. The sparks are generated by using a car ignition system, comprising an electronic ignitor, which is powered by a DC current, low voltage (14 V) generator and generates high voltage pulses by discharging a capacitor through a coil. The 3 parts of the set-up (car ignition system, coil and reactor) are each placed in a calorimeter, as shown in fig.2.

The electrical supply of the system is represented on fig.3., which also shows the 4 elements of the energy balance of the system :

- electrical power input P(E), measured at the outlet of the DC generator
- thermal power generated by the ignitor T_I.
- thermal power generated by the coil T_C.
- thermal power generated by the reactor T_R.

The entire installation is housed in an insulated portable cabin, placed in the shade. The internal temperature of the cabin is kept at a mean value of 21°C, by the regulating action of a ventilation fan and an electrical radiator. The three power meters are installed in such a way that they receive no direct heat (or cold) from any source (sun, radiator, ventilation).

Strategy used for the power balance of the system

Any excess power produced in the system will show up as a positive difference between the thermal power output and the electrical power input :

$$P(F) = T_I + T_C + T_R - P(E)$$

In contrast, P(F) should be zero when no excess power is produced (with fluctuations around zero due to the noise in the measurements).

To identify such an excess of power P(F), the strategy was as follow :

1. Establish the calibration curves of the three power meters.
2. Measure precisely the electrical power input P(E).

3. Use the three calibration curves obtained and the electrical power input to establish the power balance of three types of experiments :

- Reference experiments.
- Active experiments.
- Control experiments.

These types of experiments will be defined below.

The detailed protocol used to measure the elements of the power balance has been described [5] together with the precautions taken to avoid possible systematic errors. The possible influence on the results of electromagnetic interference, of contact resistances used in the electrical network, of the position of the thermometers in the power meters, of the background temperature variations, and of the way the system is heated have been evaluated.

Experiments run and results

The following types of experiments have been run. Their results are summarized in figure 4 :

a. Reference experiments in which heat is generated in the reactor by replacing the sparks by a resistance, heat being also generated in the coil and the ignitor through calibrating resistances. In this series, P(F) should fluctuate round zero, yielding the base line of the system. 40 of these experiments were run (26 reference type 1 where use is made of an additional resistance to heat the ignitor and the coil, and 14 reference type 2 where use is made of the internal resistance of the coil and the ignitor for heating). Reference type 1 experiments are indicated by Ref.1 on figure 4, and Reference type 2 by Ref.2.

b. Active experiments were then assessed against this baseline. In active experiments the reactor contains a hydrogen isotope, in contact with at least one metallic hydride forming metal, and a discharge is struck through it. Two types of active experiments were assessed:

- sparks through hydrogen isotopes between two metallic electrodes. 21 of these experiments were run, and indicated by Act.Spa. on figure 4.
- ozonizer discharge through hydrogen isotopes between one metallic electrode and one dielectric barrier (pyrex). 22 of these experiments were run according to an experimental set-up which has been described[6]. These experiments are indicated by Act.Ozo. on figure 4.

c. Control experiments of two types were finally run :

- sparking through nitrogen or argon between two metallic electrodes (Con.N2Ar on figure 4). 3 of these experiments were run.
- ozonizer discharge through hydrogen isotopes, between two dielectric barriers (pyrex). In this type of experiments the discharge is of the same type as in active experiments (the gas is an hydrogen isotope) but is never in contact with a metal (Con.Ozo. on figure 4). 6 of these experiments were run.

Fig. 4 is an overview of the results of the 92 experiments run. The excess power P(F) measured is plotted against the chronological sequence of the experiments (the measurements were made during a period of 18 months). The excess power measured fall clearly into 2 different categories :

- Reference and control experiments form a category with mean value 0.03 W and standard deviation 0.54 W.
- Active experiments form a second category, with mean value 1.6 W and standard deviation 0.44 W.

From these figures, the difference between the 2 categories is statistically highly significant. Provided no systematic error can explain this difference, it can be concluded that striking a discharge (spark or

ozonizer) through an hydrogen isotope gives an excess power production, when the hydrogen isotope is in contact with at least one metallic hydride forming metal. This excess power production have been observed to last up to 216 hours, is fully reproducible and begins within 2 days after starting an experiment (we cannot give any indications on the first two days of an experiment, due to the thermal inertia of the calorimetric system).

A number of possible systematic errors have been examined as mentioned above. None of them was found able to explain the results we obtain. Of special interest are the control experiments that seem to exclude a systematic error on the way the reactor is heated (resistance or electrical discharge).

Most of the experiments have been run with the combination deuterium/palladium. A few (8) have been run with the combination hydrogen/palladium or deuterium/stainless steel. The results obtained fall within the category of the active experiments. Due to their small number, it is impossible to give a precise evaluation of the excess power they have generated.

CONCLUSION

Striking a discharge (spark or ozonizer type) through an hydrogen isotope in contact with at least one metallic hydride forming metal, yields, in the set-up we have used, an excess power production that is fully reproducible and stable over long periods. No systematic error has been found that could explain the statistically significant excess power production we have measured.

One possible explanation of this phenomena is an hypothetical class of nuclear reactions, based on the virtual neutron concept. [5,6]

To completely exclude the possibility that a systematic error can explain our results, we have designed and are starting a new calorimetric system (system II), where only one calorimeter is used (adiabatic and flow type calorimeter).

A search for nuclear ashes is also being carried out. [6]

We hope this effort will shed more light on cold fusion.

REFERENCES

1. F. Paneth and K. Peters, "Uber die Verwandlung von waterstoff in Helium," Naturwissenschaften, vol 14, p 958 (1926).

2. J.Tandberg, "Method for Producing Helium," Swedish patent application (1927).

3. S.E Jones et al., "Observation of Cold Nuclear Fusion in Condensed Matter," Nature, vol 338, p 739 (1989).

4. M. Fleischmann and S. Pons, "Electrochemically Induced Nuclear Fusion of Deuterium," *J. Electroanal. Chem.*, vol 261, p 301 (1989)

5. J.Dufour, "Cold Fusion by Sparking in Hydrogen Isotopes," *Fusion Tech*. vol 24, p 205 (1993)

6. J.Dufour et al., "A Strategy to Prove the Reality of Cold Fusion," preprint 4th ICCF, Hawaii, Dec. 1993.

ELEMENT-PHASE TRANSITIONS WITH THE COLD NUCLEAR SYNTHESIS (CNS) TYPE REACTIONS IN METALLIC ALLOYS OF GLASS-FORMING SYSTEMS

A.M.Durachenko, E.Ya.Malinochka

Lenin All-Russian Electrotechnical Institute
111250, Moscow, Krasnokhazarmennaya, 12

In spite of great interest in the mechanisms of CNS (cold nuclear systems) and its ecological and material science application aspects, the information up to now about such reactions in metallic systems, beside deuterides, is contradictory. The present research is devoted to the analysis of the results of experiments, the foundation conditions and mechanisms of CNS reactions by the examples of metallic alloys of glass-forming systems. The choice of objects under investigation is connected with their nonergodic behavior in all interval of their existence. The last is the necessary condition for the observation of the CNS-reactions when there are strict volume and kinetic limitations on the phase-transition processes.

The investigation of the CNS reactions was carried out by using the glass-forming metallic alloys of "metal-metalloid" system Fe-Ni-P-C and "metal-metal" Cu-Zr system. The essential levels of volume and kinetic limitations, and the corresponding degree of non-equilibrium in phase transition were achieved by electro-impulse compactation of power samples with heating under pressure up to 10JPa. The method of experiment is close to that described in [1].

The X-ray diffraction analysis of samples was done by DRON-2,0 (Cu K420); the election microdifraction (by powdered method) -by [Russian word]-100K (U=70kV); the cross-section surface investigation of the samples and X-ray spectrum microanalysis were done by scanning electron microscope JSM-35, with the spectrometre of the KEVEX-5100 type; the quantitative X-ray spectrum microanalysis and Auger-electron spectroscopy (XSMA and AES) were done by NB-100; the secondary-ion mass spectrometry (SIMS) by Cameca IMS-4F; the chemical analysis of the initial rod and powder were done by atomic-absorption spectrometer; and the registration of the presence of transition radiation was done by [Russian word]-70 apparatus.

For the initial powder samples composition Fe(70)Ni(10)P(13)C(7) after impulse treatment the presence of at least two (2) hexagonal closely conjugated lattices was revealed by X-ray diffraction, and one of them was identified as WC-lattice. Aliquot increase of lattice parameters, fixed by X-ray diffraction, shows the evidence of scaling (reproduction of the same structure on more and more increasing scales.)

Faceted crystals of WC on the surfaces of impulse-treated samples are seen without any optical magnification (Fig. 1a). By XSMA and AES methods (Fig. 1b) the element content of faceted crystals and matrix were determined. They are as follows: W(6)Fe(40)Ni(40)C(14) - matrix; Fe(2,25)Ni(2,25)W(46,5)C(50) - inclusions. Caverns of gas bubbles exiting are distinctly seen on the faceted surfaces. The results of SIMS (Fig. 2a) confirm the results of XSMA, AES and chemical analysis. The lines of all isotopes of elements fixed are present (with the changing of intensity of isotope lines Fe and Ni on mass spectrum of treated samples as compared with initial). Strong lines of hydrogen are (H) also present on the mass-spectrum of the treated samples. The groups of lines corresponding to the isotopes with masses 2Fe(56), Fe(56)Ni(58) must be noted. The line shifting of KLL-series Fe (2.5-1.5 eV) to the high-energy side, the appearence of the additional transition lines with the energies of 776 eV and 585.7 eV; the additional transition lines relative intensity is more than 5 times; the splitting of several peaks; the shifting carbon KLL series at 3.9 eV to the high-energy side in matrix - all this is evidence for the existence of strong-bounded molecular complexes in the treated

samples. It must be pointed out that the amount of WC in the samples after the treatment is exactly the same as (Me)(3)P in the initial ones, and phosphorus is absent in the treated samples. Taking into consideration the balance of elements, it is possible to present the reaction:

$$\frac{199}{(Me(3)P)} \rightarrow (WC)^{199} + H^{1} \quad \text{with variation of isotope masses.}$$

The X-ray diffractional analysis of the impulse treated samples made of amorphous powder with the initial composition of Cu(60)Zr(40) shows the preservation of the amorphous structure after the treatment. The qualitative XSMA of the samples cross-sections from the depth of 1000 Å revealed Co, Sm, Fe and slight amounts of Cu and Zr. SIMS (primary ion beam 05 ± 0.6 keV) results confirm these data (Fig. 2b). There are also lines of ions of light elements with M/Z ratio from 1 to 12.

The quantitative Auger-spectrum analysis samples cross-sections gives the data (the whole surface): 19 at.% Sm, 42 at.% Co, 2 at.% Fe, 10 at.% Cu, slight amounts of B, about 23 at.% O_2 in oxides and about 4 at.% C in carbides (according to the form of spectrum lines). It must be noted that there are variations of element's content in different regions.

The shifting of KLL Co series for 1.5 - 2 eV, MLL Sm series for 3 - 4.9 eV to the high-energy side; 2.5 times line broadening of Sm in comparison with pure element may be interpreted as a residual excitation. Based on these data the main reaction may be written:

$$Cu_2^{63,65} \; Zr^{90,91,92,94} \rightarrow Co^{59} \; Sm + X,$$

were X are light elements with masses from 1 to 12.

As a result of convection processes in the melt and in correlation phase transition (called vitrification) [2] in alloys under investigation the hierarchy of structural topological subsystems is formed in them according to the scaling rule. The sizes of non-uniformities stretch from several hundreds to about ten Å [3,4]. Each topological subsystem contains its own dynamic soliton subsystem. A number of subsystems depends on the method of fabrication as well as on the alloy composition. The smallest scale structural subsystems may by considered polyhedral chains, and each of these polyhedrons may be considered as a quasi-molecular complex. It must be pointed out, that when spinning the formation of subsystems hierarchy may be described by soliton solutions of KDV - equation, which possess the properties of Toda lattices (hierarchy of lattices placed one into another).

The conduction of the current impulse of sufficient magnitude leads to the high-power soliton envelope formations and all soliton modes of all subsystems appear to be in the own modes of such soliton envelopes. Due to this fact, the resonance connection of subsystems with a high coefficient of transmitting is possible (if to take into account high-frequency oscillating soliton "tails"). The superposition of the soliton envelope with the coherent phase transition front in the quasi-molecular complex determines "energy depth" of the last transformation. When analysing the transition process, the quasi-molecular complex in the range of crucial effects is considered as an ensemble of dynamic structures, which demonstrates a particular number of variations in the ensemble in transition to a new steady state. The results of the numerical modeling of discret Ginsburg-Landau equation, for example, may illustrate the behaviour of such a system.

The consecutive excitation of intrinsic degrees of freedom in quasi-molecule - it means the appearence of pulsing precession of electron orbits under variable electromagnetic field of soliton envelope influence. The range of crucial effects may be described on the basis of an improved Bohr's atomic model. In this improved model, orbital currents interact with constants different from those of classical electrodynamics [5], and they are considered as parameters of stability in stationary solutions of self-oscillation system's

equation of motion.

The transition to the unsteady state result in "overcommutating" of orbital currents in the same way as "blow out" effects proceed in a plasma trap. The effects are accompanied by radiating high-frequency continuous spectrum. Such processes of orbit "overcommutating" are analogous to phase transitions of the second type, which proceed without entropy change, and when expanded to nuclear shells, one can explain the absence of barriers and entropy changes in CNS-reactions.

REFERENCES

[1] Durachenko A.M., Elagin V.N., Danilchuk A.A., Patent SU 1801059A3, Bull. N9, 1993 (in Russian).
[2] Gotze W., "Liquid-Glass Transition," M., *Nauka*, 1992 (in Russian).
[3] Novicov J.J., Timofeev V.N., Sofronova R.M., Thes. of sympos. "Electron Microscopy and Electronography in Investigation of Creation, Structure and Properties of Condensed Matter," M., 1983, p 4.
[4] Borbey Sh., Nartova T.T., Tarasova O.B., Thes. of II all-Union conf. "Physicochemistry of Amorphous (glass) Metallic Alloys", M., *Nauka*, 1989, p.183 (in Russian).
[5] Nadycto B.A., Doklady ANSSSR, 1991, vol 316, N6, p 1389 (in Russian).

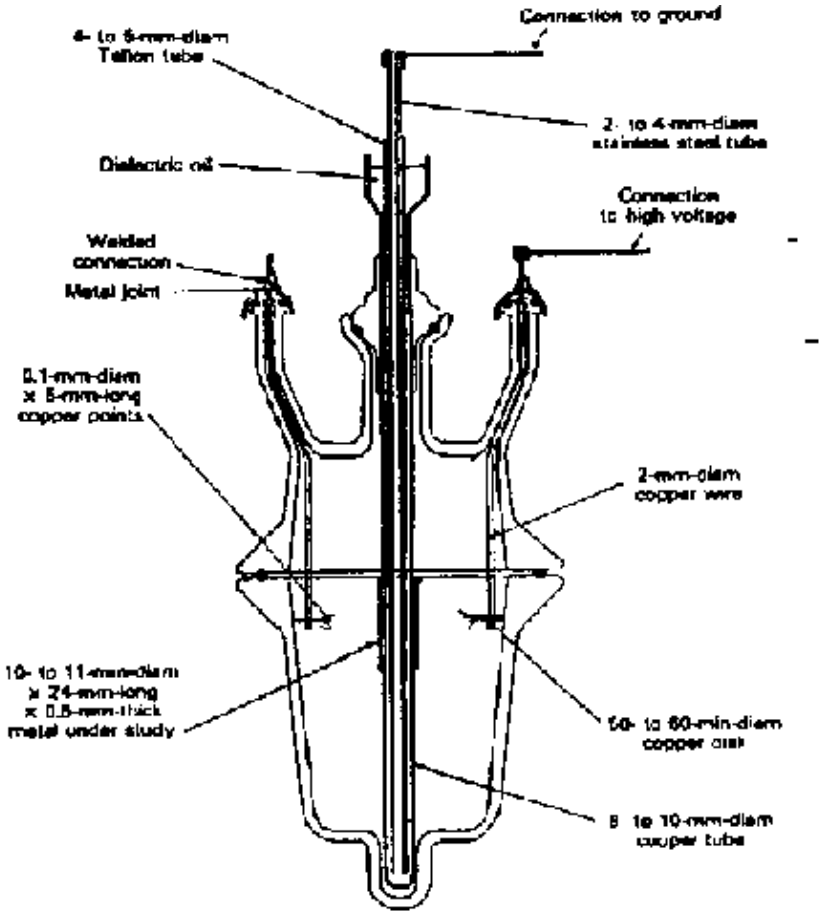

Fig. 1. Reactor.

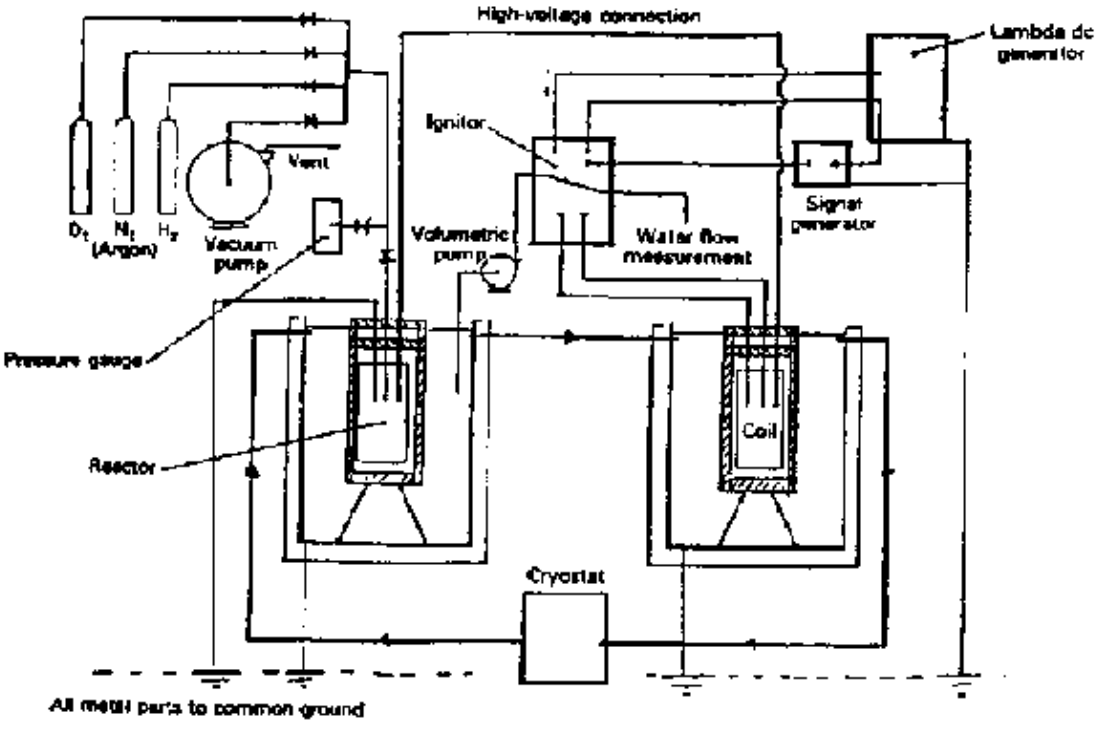

Fig. 2. Overall setup.

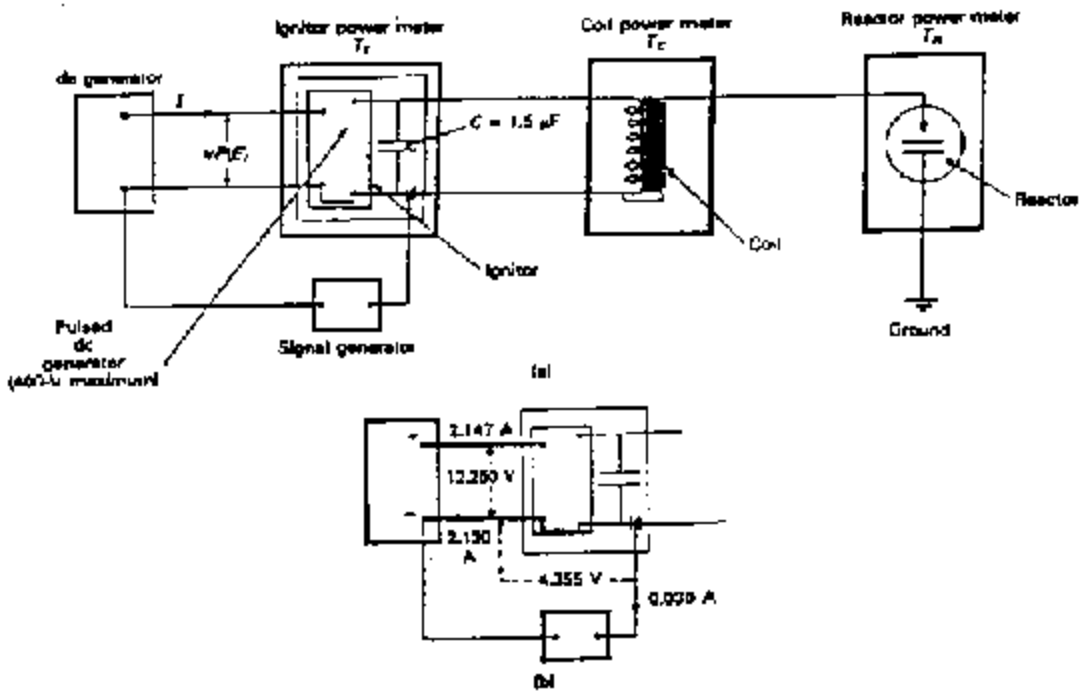

Fig. 3. Electrical supply and power balance.

Fig. 4. Excess power in all experiments
as a FUNCTION of EXPERIMENTS SEQUENCE

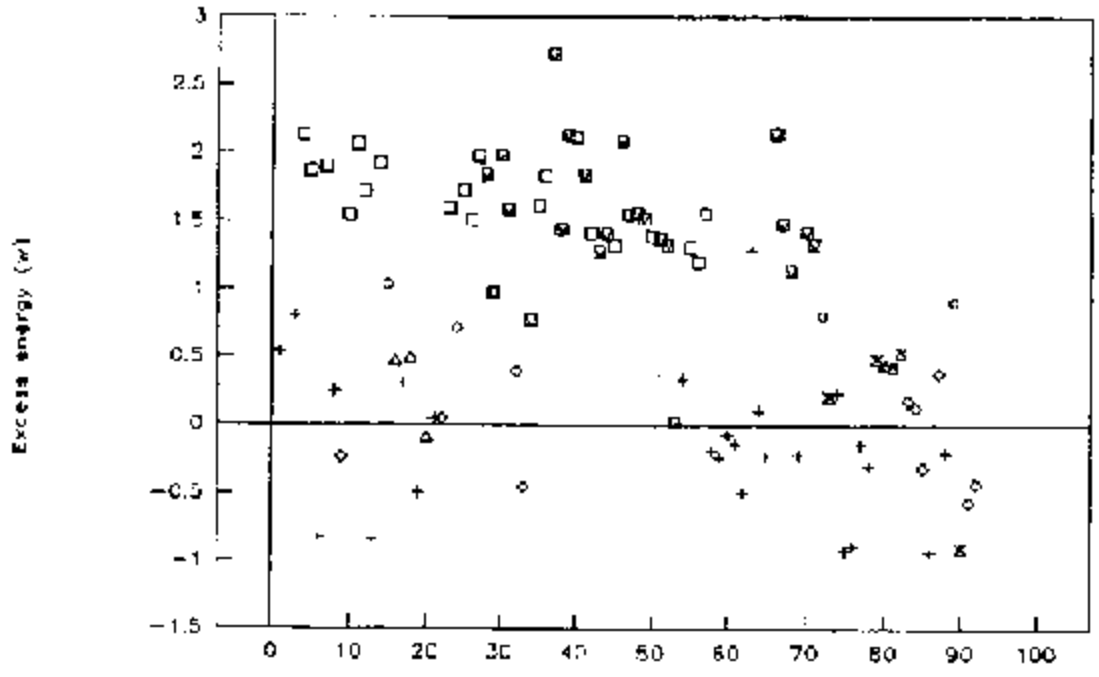

Fig.1. Sample surface (initial alloy FeNiPC) with faceted crystalline inclusion WC (x 500) (a); Auger-spectrum. whole view, central cross-section (b).

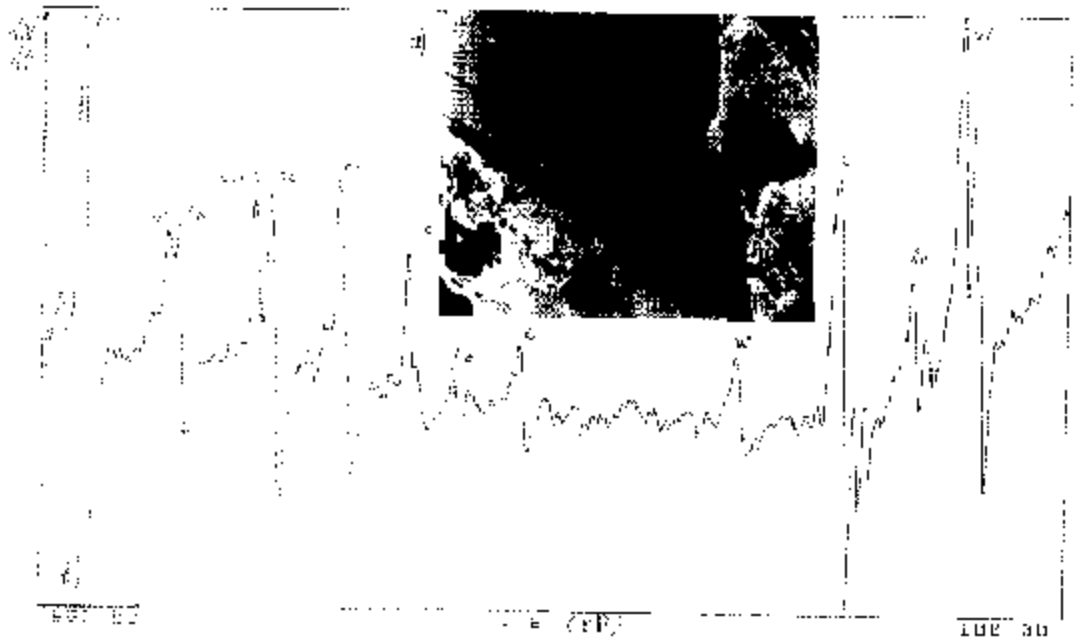

Fig.2. Mass-specrums of secondary ions of treated samples: FeNiPC - initial composition (a), Cu-Zr - initial composition (b).

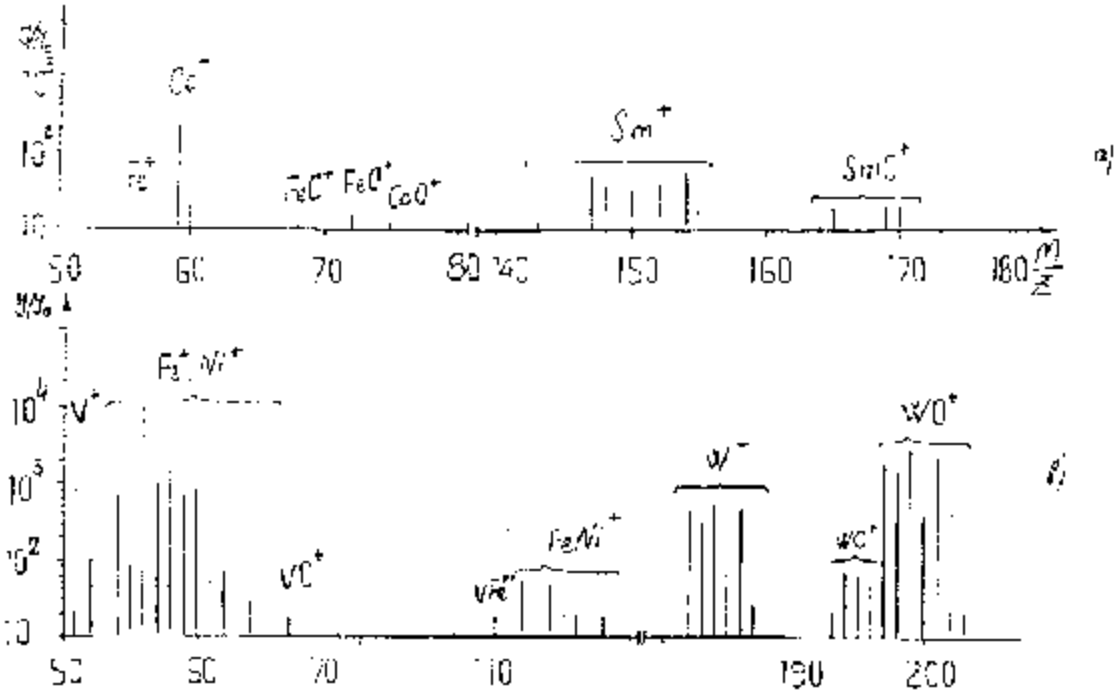

THE INVESTIGATION OF THE MECHANISM OF ENERGY ACCUMULATION IN LONG-LIVING LIGHTNING OBJECTS, FOUND AFTER A POWERFUL IMPULSE ENERGY RELEASE IN WATER.

Golubnichiy P.I., Gromenko V.M., Krutov Yu.M., Lysenko N.I.
East-Ukrainian State University.
20a, kvartal Molodiozny, Lugansk, Ukraine, 348034

ABSTRACT

The long-living lightning objects (LLO), formed after an electric discharge in water, were reported by the authors recently [1,2]. In the process of researching the spectra of LLO and of the discharge plasma emission, the optical properties of the objects, their dynamics, their interaction with obstacles, the physical fields, and other related phenomena were studied. The whole set of obtained data indicates that the formation of LLO was unknown before our report of this phenomenon. This phenomenon couldn't be explained by such effects as luminescence of the electrode's material, combustion (reactions between hydrogen and oxygen), a cluster of ideal or non-ideal plasma or an association of exited molecules and atoms.

INTRODUCTION

The main difficulty we have is to develop an explanation of the shape and energetics of the objects. LLO, which are formed of the products of discharge plasma, have a shape which is very close to a sphere. The LLO's do not lose this shape under considerable mechanical interactions. The matter comprising the LLO objects has the ability to accumulate energy [from some source] which is spent on emission with power of the order of 0.1 Wt/cm3. In some cases, the LLO's emission is followed by a process, which could be identified as a burst.

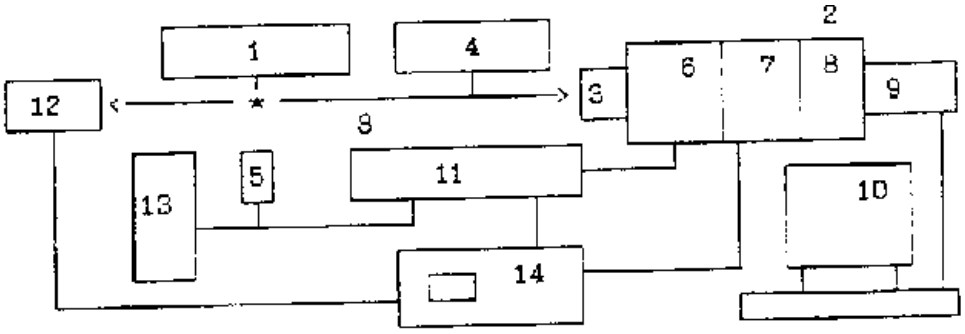

Fig.1
1-generator of high-voltage impulses, 2-EOC, 3-objective, 4-monochromator, 5-device of phasing, 6-time-analysing EOT, 7,8-brightness amplifiers, 9-CCD digital camera, 10-IBM PC/AT, 11-controller, 12-photomultiplier, 13-source of the standard spectrum, 14-oscillograph.

The present work is about the experiments, due to which the data on the formation and energetics of LLO were obtained. A schematic diagram of the experimental device is presented on Fig. 1. The initiation of plasma in water requires a generator to produce high-voltage impulses. This generator was built from the scheme of Arkad'ev-Marx. The breakdown voltage used is about 60 kV, stored energy to produce about 30 Joules. The time of energy release is about 6 microsec. The processes, which follow the discharges, were recorded by using an electron-optical camera (EOC), which was made on the base of time-analyzing electron-optical transducer (EOT) of the PIM-103 type and by using brightness amplifiers PMU-2B and PM-031. The EOC was used in the frame-by-frame mode and also in the chronography mode. In the first case we had an opportunity to use up to 9 frames. An exposition of each frame, including intervals [between frames] could be set independently of one another in 50 ns to 100 mcs [micro-seconds] increments. In the

second mode the EOC provides a time-analysis of one-dimension picture (spectra of emission, for example). The time of chronography could be changed from 50 ns to 100 mcs. There was also a feature to delay the start of shooting after the initiating impulse. The minimum time of delay was 30 ns, the maximum was 0.1 s. Amplification of brightness of the EOC image could be changed over a wide region and could reach 10^6 Wt/Wt [sic] on the wavelength of 0.42 mcm, depending on the type of the photocathode used in the time-analyzing EOT.

It was possible to record video-information on film and on the laboratory IBM PC/AT personal computer. In the first case the recording was conducted by using contact with the screen of the brightness-amplifier PMU-28. (PM-031 was not used). Data input to the personal computer was accomplished using "no-film" video-information device. The information was read from the device with a help of cooled CCD matrix. There was a need to connect the solid-body device of no-film record with the EOC. For diminished images from the PM-031, we used this brightness amplifier. The PM-031 used a screen with maximum of emission at wavelength 630 nm. Processing of the video information was accomplished using a package of computer programs, making it possible to scale and to pseudocolor the image received and also helped to measure the relative density of emission at every point of the image and to point out the regions with equal density. When working with recording and analyzing the spectra of this complexity, we were able to automatically partition the time intervals by wavelengths. The wavelengths of lines of emission or absorption were found and real spectral density of emissions from the object were determined (using the comparison with a spectra of a standard source).

Control of the EOC's work was accomplished with the help of dual-beam oscilloscope (C8-14 type.) Signals indicating the functions of the camera were transmitted on one of photo-multiplier channels (thereby registering emission accompanying the studied process).

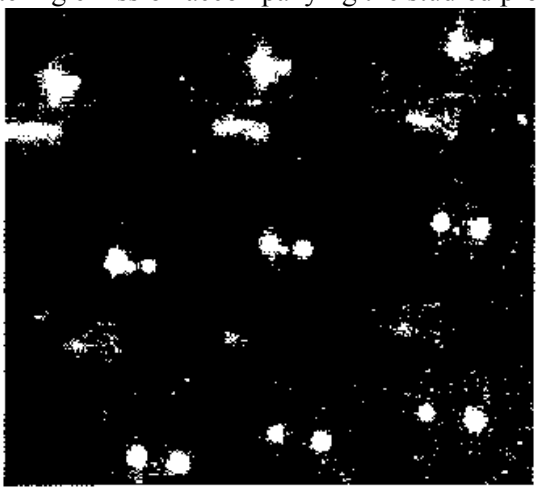

Fig. 2

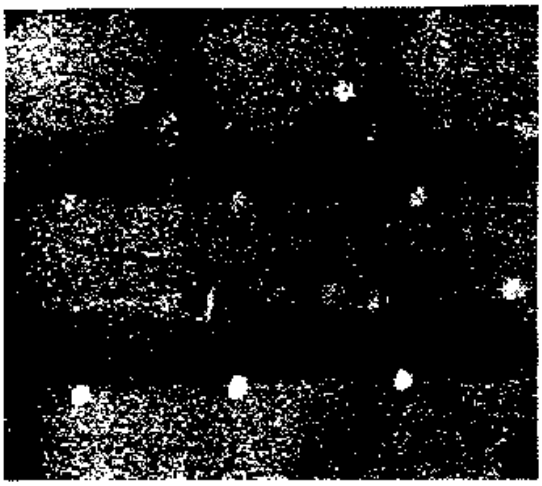

Fig. 3

Fig. 2 Fig. 3

LLO were found for the first time inside a pulsating cavern, formed in water after a powerful energy release [1,2]. Later there was found the way to eject discharge plasma out of the water into the atmosphere [3,4]. Using the same conditions of energy release, LLO discharges into the atmosphere had, on the average, 5 times greater dimensions (up to 0.5 cm) and duration (time of luminescence) of up to 0.1 s. Fig. 2 presents the results of frame-by-frame recording of the process of LLO formation out of an irregular luminescent cloud. This cloud was ejected to the atmosphere after the discharge in water (the recording was done using the illumination of the LLO). The plasma was ejected upwards out of the water. The time lag from the start of recording to the end of the energy release was 500 mcs. The time of exposure was 10mcs, and the interval between two frames was 10^{-4} s. The order of frames was from left to right, from top to bottom. The maximum dimensions of an LLO was approximately 3 mm. One can see on the image that two LLO are gradually forming from the cloud (one big and one small cluster - see images 5 and 6). The smaller cluster disappears quickly, however the larger cluster exists until the end of the recording sequence.

On the first frame one can already see a formed LLO, which expands later, reaching its maximum on frame 6 together with the cloud [as the cloud appears to reach its maximum brightness. The densitometry of the negative shows the density of the radiation flux from the LLO, which was formed from this cloud. The process which was registered on Fig. 2 resembles condensation. The formation of the LLO was found also at a time when there was an influence of low temperature on the ejected products. In this experiment a copper plate, cooled to the boiling point of liquid nitrogen, was placed in the way of ejected plasma flying out of the field the camera. It was found, that the already formed LLO clusters disappear on their way to this cooled surface. That is, the LLOs cease to shine. On the other hand, there were found some cases of shining objects forming on this cooled surface. These surfaces objects were evidently formed from the products of discharge, which had traveled to the surface. The dynamics of such a process is presented in Fig.3. Shooting was delayed for 1 ms. The speed of recording was the same as before. The side light was positioned and used for determination of the location on the cooled surface and of the jet position with respect to the camera, thus showing the space between them. On each frame of Fig. 3, this space is seen as a poorly shining square, the "jet" is coming out of the camera from below. Products of disintegration are moving up from the bottom. A start of formation of an LLO object [on the chilled plate] is seen in frame 3 (Fig. 3, upper right) as a slight nonuniformity in the upper left portion of frame 3. Fig. 3 shows on frames 4, 5, 6, & 7 the increase in brightness of this object. On frame 7 one sees a well-formed LLO. The same processes were observed under the illumination of the objects own light (without the use of the side-light).

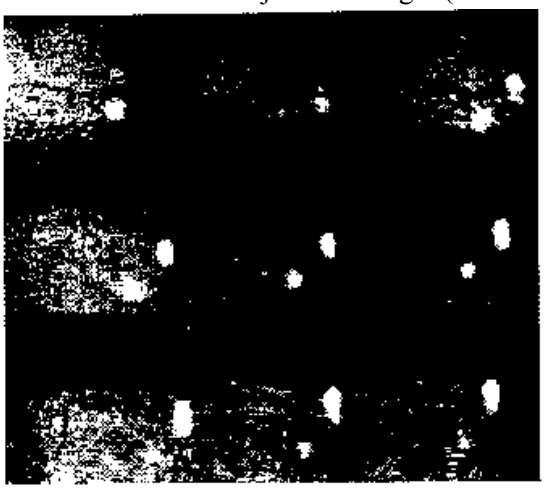

Fig. 4

Fig. 5

Fig. 4

Fig. 5

Another interesting case of low temperatures influence on LLO is presented in Fig. 4. The delay of recording was 500 mcs, and the frame interval of recording the same. On this image the elongation of the LLO's toward the side of the cooled surface can be observed. The analysis of the photograph shows that this elongation is connected with building-up of the LLO's shining matter from the low temperature side. The rate of growth is comparable to the speed of movement of the objects (of the order of 10 m/s). On the photograph one can see another LLO, which grows and diminishes during the recording of Fig. 4.

The influence of high temperatures on these shining objects is shown in Fig.5. The recording was made using the emitted light from the "shining objects." The speed of recording and the order of the frames was the same. The number of frames was 6. In this experiment a plane two-fold metal spiral was used instead of the cooled surface. The metal spiral was heated by an electric current. The diameter of the Ni/Cr alloy wire was 0.1 mm, with the step of winding = 1 mm. The temperature of heated wire mesh was measured using a pyrometer and equaled 1000°K for the upper layer and 800°K for the lower layer. The distance between layers was 4 mm. The LLOs could freely pass through both layers of wire. Some filters were during the recording. These filters were used to block out an intense infra-red emission from the two wires. The upper layer of the spiral is seen on each frame (Fig. 5). The lower wire is indicated on Fig. 5 with an arrow. One can clearly see that LLO lose their spherical shape when they come up to the zone of heating. They disappear completely near the lower layer of the spiral. Any darkening in this case is out of question. In the space between two layers the LLO appears once more. They disappear again when they cross the second layer. The LLO's disappearance is observed at a time of its crossing the heated spiral in 40% of the cases observed. Sometimes the shining objects appear once more, though they are much smaller in dimensions.

All these observations emphasize the dependence of the processes of LLO luminescence on the temperature and on the presence of a strong interparticle interaction within the LLO's matter. This interaction can modify some processes, which are analogous to phase transitions accompanied by heating. This heating may explain LLO's luminescence at a time of its formation on cooled surface. Temperature is sustained by heating, which is a result of condensation.

In [1,2] the authors propose a cluster nature for the LLO. Still, all these experiments shown above contradict this hypothesis. All parameters of charged water clusters are known [5]. At the time of their heating up to 1000°K the covers of the LLOs must destruct, thus causing a sharp growth in the speed of recombination and, as a consequence, the rapid release of energy. In all of the experiments using heating, there were no phenomena which were considered to be the result of this process (flash of light, ejection of the substance, and so on). The explanation of the nature of the LLO's is difficult using the concept of clusters of non-ideal plasma. This plasma, having appeared at discharge, could not disintegrate and condense once more, because all properties of the non-ideal plasma are explained by collective interaction of charged particles. All the more reason that one cannot explain the formation of a clot of non-ideal plasma on a cooled surface by the condensation on this surface by products of disintegration and just recombined discharge plasma. In addition, one can hardly explain the fact of LLO's penetration from the cavity to water [1,2] and the fact that the LLOs maintain their spherical form even when their speed in air is higher than 50 m/s (using a model of non-ideal or cluster plasma.)

CONCLUSION

All the foregoing enables the authors to put forward the hypothesis that LLO's matter consists of previously unknown combination of oxygen and hydrogen, which has a store of energy that exceeds thermodynamic equilibrium energy. This hypothesis is confirmed by the results of spectral investigation. After 20 mcs after the end of energy release there was found, in the spectrum of emission of disintegrating water plasma, registered a group of lines lying in wavebands: 792-798 nm, and 741-744 nm. This group of lines is observed for a period of 100 mcs and cannot be identified as spectral lines of hydrogen, oxygen, water or the OH-group. The formation of these lines always preceded the formation of LLO.

The fact that these are not associated with hydrogen, oxygen, or water unequivocally supports the author's conclusions.

A meta-stable combination having a store of energy can appear from the stage of disintegration of plasma from exited atoms or molecules. Much more probable is the formation of combinations with meta-stable atoms because of their long lifetimes. In addition to the above-mentioned group of lines, there were found lines of emission of hydrogen and oxygen in the emission spectrum of the disintegrating plasma. These lines appear 5 mcs after the end of the observed energy release and are registered for about 5-10 mcs. One of this group of lines with wavelengths: 7771,94; 7774,39 Å [6] is an evidence of meta-stable atoms of oxygen formations on this stage. These atoms are in a 3S state and their line of emission is 180 mcs [7]. It is quite logical to suppose that meta-stable atoms of hydrogen are also formed under these conditions. They are in the 2S-state and have a duration of 10^{-1} sec. The upper electron levels of these exited atoms are similar to the valence levels of atoms of alkali metals. That is why there are some reactions between these exited atoms of oxygen, hydrogen and molecules of water. These reactions are like those which happen in certain types of lasers [8] between exited atoms of inert gases and halogen gases.

Such excited complexes can have energy of the order of a few electron-volts. Their duration could be long enough. For example, this could happen because of a potential barrier, which hampers the rebuilding of electron layers of excited complexes into electron layers of stable excited molecules. Each such complex, by our estimate, has a store of energy, which considerably (more than 10 times) exceeds the energy released by a chemical reaction.

It is perfectly clear that matter, consisting of such high-energy complexes, is an example of an ecologically clean fuel, because the final products after its use are nothing but ordinary water. In addition, one can state (with a large probability of being correct) that such a substance (i.e. an previously unknown high-energy combination based on O and H) is highly effective and, in general, a different natural phenomena. This phenomena is accompanied by a powerful energy release from any origin in water-saturated structures (including Earth's crust, atmosphere, ocean and so on). One such manifestations is the phenomenon of ball lightning and long-living lightning objects in the atmosphere. The interest is such phenomena has grown sharply recently. To prove this statement we must remind the reader of a number of international scientific conferences and symposiums on the above-mentioned problems that have been held (e.g. in Japan, Hungary, USA, Austria) in 1988-1993.

REFERENCES

[1] Golubnichiy P.I., Gromenko V.M., Krutov Yu.M., "Long-living lightning objects inside the pulsating cavern, initiated by the powerful energy emission in water," Dokl. AN SSSR, 1990. -V.311. N2. P.356-360.

[2] Golubnichiy P.I., Gromenko V.M., Krutov Yu.M., "Formation of long-living lightning objects after the collapse of dense low temperature water plasma," -Zhurnal Techn.Fiziki. 1990.- V.60. N.1.P.183-186.

[3] Golubnichiy P.I., Gromenko V.M., Krutov Yu.M., "Formation and dynamics of long-living lightning objects -- Lightning ball, summary report". -Moscow: Inst. Vysokih Temp. 1991. N2. P.73-75.

[4] Golubnichiy P.I., Gromenko V.M., Krutov Yu.M., "Dynamics of long-living lightning objects throw-out, initiated by the powerful spark energy emission in water.--High-velocity photography, photonics and metrology of fast-occuring processes. Summary of reports at the 15th All-Union conference," -Moscow: VNIIOFI, 1991. P.113.

[5] Kebarle P., Searles S., Zolla A. et al. - J.Amer. Chem. Soc., 1967,89 N25, P.6393.

[6] Golubnichiy P.I.,Gromenko V.M.,Krutov Yu.M.,Lisenko N.I., "Investigation of an influence of thermal fields on long-living lightning objects.--High-speed photography, photonics and metrology of fast-occurring processes. Abstracts of the 16-th sci. conf." - Mos. VNIIOFI, 1993. P.72.

[7] Radich A.A., Smirnov B.M., Parameters of atoms and molecules. Reference book, Moscow, Energoizdat.1986.

[8] Gudzenko L.I., Yakovlenko S.I. Plasma lasers. -M. Atomizdat. 1978,P.256.

DETECTION OF CHARACTERISTIC GAMMA RAYS FROM ELECTRODES IN PD-D SYSTEM BY HV DISCHARGE

Jingtang He, Yingping Zhang, Guoxiao Ren
Guoyi Zhu, Xiaoli Dong
Duanbao Chen, Hongguang Han
Institute of High Energy Physics, Academia Sinica
P.O. Box 918, Beijing 100039, P.R. of China

Long Wang, Sunsheng Yi
Institute of Physics, Academia Sinica
Beijing 100080, P.R. of China

Shangxian Jin
Graduate School, Academia Sinica
Beijing 100039, P.R. of China

ABSTRACT

Evidence is presented to show the different characteristic gamma rays from electrodes in Pd-D system, by HV discharge. It might be explained as the elements of electrodes excited by high energy charged particles originated during HV discharge de-exciting radiations.

During HV pulses no neutron signal was detected.

In addition, neither neutron signals nor gamma signals were detected in the intervals between the HV pulses.

INTRODUCTION

Since M. Fleischmann, B.S. Pons [1,2] and S.E. Jones et al. [3] reported in 1989 that nuclear fusion of deuterium (D_2) occurred at room temperature in Pd or Ti cathodes during the electrolysis of heavy water (D_2O), considerable efforts have been made to investigate so -called `cold fusion' by many laboratories in the world. These experiments include several types: Electrolysis of heavy water; cold-hot cycles of deuterated palladium between liquid nitrogen temperature and room temperature; processing deuterated palladium by mechanical treatment and gas discharging of deuterated palladium [4,5] etc. However the results are in conflict with each other [6].

As is well known, there exists three reaction modes in D-D fusion:

(1) $D + D \rightarrow n(2.45MeV) + {}^3He(0.82MeV)$
(2) $D + D \rightarrow P(3.02MeV) = T(1.0MeV)$
(3) $D + D \rightarrow {}^4He + \gamma + 23.85\ MeV$

From the knowledge of thermonuclear fusion, the reaction probability of mode 3 is extremely low, mode 1 and 2 have nearly the same probability. If we define

$$R = \frac{\text{(reaction rate of mode 2)}}{\text{(reaction rate of mode 1)}}$$

For normal D-D fusion $R \approx 1$.

The neutrons originated from the reactions can come out front the discharge chamber and can be detected by neutron detectors, but the charged particles originated from the reactions, P,T,^{3}He and ^{4}He cannot be directly detected because their low energies are insufficient to penetrate the chamber envelope. The charged particles would collide with the material of the reactor, such as the Pd cathode, exciting the Pd nuclei. When the excited Pd de-excites, a characteristic gamma ray would be originated, for example:

$$^{108}Pd^{*} \rightarrow {}^{108}Pd + \gamma\ (425KeV)$$

In order to investigate the anomalous nuclear effects, we have designed and performed a new type of experiment by using high voltage discharge. We simultaneously, during the HV period and during periods of no HV, provided detectors for both neutrons and gamma rays.

EXPERIMENT

The arrangement of the experimental set up is shown in Fig. 1. The main parts include a discharge chamber, HV pulse generator, gamma counters and neutron counters.

*γ counter

The scintillator is a Nal(Ti) with diameter of 4 cm and thickness of 4 cm. It was coupled directly with PMT(GDB-44F) via silicon oil. The spectrum of gamma counter for ^{22}Na is shown in Fig. 2. The energy resolution of the γ counter is 11% for 1270KeV. The efficiency of the γ counter is about 2.6 X 10^{-3} for 1270 KeV.

* Neutron counter

The diagram of neutron counter is shown in Fig. 3. In the front there is a 17cm X 17cm plastic scintillator with thickness of 5 cm, then a Φ 10cm ^{6}Li glass scintillator with thickness of 0.3cm. ^{6}Li glass was directly coupled on to PMT(GDB-l00) by silicon oil.

When ^{6}Li absorbed a slow neutron, ^{6}Li(n,α)T reaction will take place, then the glass can produce light by α and T emissions. The light is viewed by PMT and a neutron signal comes out which will be recorded by MCA.

The slow neutron spectrum of ^{252}Cf neutron source with intensity of about 3000/4 π· view is shown in Fig. 4. The FWHM (full width, half magnitude) of the peak is 25%. The efficiency of the neutron detector is about 3 X 10^{-3}.

First the chamber was pumped to 2.7 X 10^{-2} torr, and then fill with 1 atm deuterium gas. The D_2 was absorbed for some time by the electrode Pd. Switching on 10KV HV, the pulse generator produced pulses of 10KV in amplitude, 150μs in width and 10Hz in rate. At this time, sparks appeared in the chamber.

The gate A was triggered by the rising of the HV pulse and opened until the HV pulse terminated (see Fig. 1). The signal of gate A triggered MCAs A_1 and A_2. A_1 and A_2 recorded simultaneously gammas and neutrons coming out from the discharging chamber during the discharging.

There is a gate B in the interval between HV pulses. The gate B is triggered by the falling of the HV pulse and opened until another HV pulse rising. The width of gate B is about 0.1 sec. The signal B triggered MCAs B_1 and B_2. B_1 and B_2 recorded simultaneously the gammas and neutrons which came from the chamber.

RESULT

Results are summarized as follows:

1. The spectra of both gammas and neutrons outside the period of HV pulse detected by system B are consistent with background spectra recorded with no HV within statistical error.

2. During HV discharging, the neutron signals are comparable with background.

However, there are extra gamma rays. Figure 5(a) is the gamma ray spectrum detected by MCA A_1 in 8h. Figure 5(b) is the background spectrum in 4h. From Fig. 5(a), we subtracted the background for 8h to obtain Fig.5(C). In Fig.5(C) it is very clear that there exist two peaks. According to the calibration curve of system A_1, one peak is at 425±40KeV, another is at 870±50KeV. Because the electrodes are made of Pd, Fe and also W, the spectrum of gamma rays might be relevant to the following nuclear deexcitation processes:

$$^{108}Pd^* \rightarrow {}^{108}Pd + \gamma\ (E_\gamma = 425KeV)$$
$$^{56}Fe^* \rightarrow {}^{56}Fe + \gamma\ (E_\gamma = 854KeV)$$
$$^{184}W^* \rightarrow {}^{184}W + \gamma\ (E_\gamma = 110KeV)$$

However, the energy of γ originated from $^{184}W^*$ is too low to be seen against noise.

Pd was used as cathode, and Cu as anode discharging in deuterium for another data run. We made two background runs: first, Pd was used as cathode and Cu as anode but air was used instead of deuterium for discharge, second, Cu was used both as cathode and anode discharge in deuterium. In addition, we made another calibration run. Fig.6 is the net gamma ray spectrum after background subtraction. There are another two peaks of gamma ray. The energies of the two rays are at 430 Kev and 990 Kev respectively. It might be explained as $^{108}Pd^*$ and $^{83}Cu^*$ excited by high energy charged particles de-exciting radiations.

Since the HV is only 10KV, the electron/deuteron with energy of 10KeV can excite only atoms, but not nuclei. So, the high energy gamma ray could be produced only from nuclear Coulomb excitation by charged particles with high energies [7]. The gamma yields are about 10^{-6} per 3.0 HeV proton absorbed in palladium [8]. Our result can probably be explained by the exciting Pd, Fe and Cu in the products from the reaction mode 2. From the present experiment, we would conclude that in HV pulse discharging experiment we only detected the characteristic gamma ray without neutrons. It seems that the reaction rate of mode 2 is much higher than mode 1 in the low energy D-D fusion under palladium environment.

Taking the acceptance into account, from our experimental results, we can deduce: $R > 10^9$.

ACKNOWLEDGEMENT

Authors would thank Prof. Xiaowei Tang for his encouraging and support from time to time. We wish to thank our many colleagues at IHEP and Institute of Physics for affording us many equipments and helpful discussions.

REFERENCES

[1] M. Fleischmann, B.S. Pons and M. Hawkins, *J.Electroanal.Chem*., vol 261, (1989) p 301.

[2] B.S. Pons and M. Fleischmann, *Fusion Technol.*, vol 17, (1990) p 669.

[3] S.E. Jones et al., *Nature*, vol 338, (1989) p 737.

[4] F. Celani et al., Report *Il Nuovo Cimento* Conf. Varenna, 15-16 Sept. 1989.

[5] E. Yamaguchi et al., *Japan. J. Appl, Phys*., vol 29, (1990) p L666.

[6] R.W. Kuhne, *Phys. Lett. A*, vol 155, (1991) p 1666.

[7] K. Alder et al., *Rev.Mod. Phys*., vol 28, (1956) p 432.

[8] David C. Bailey, UTPT-89-15.

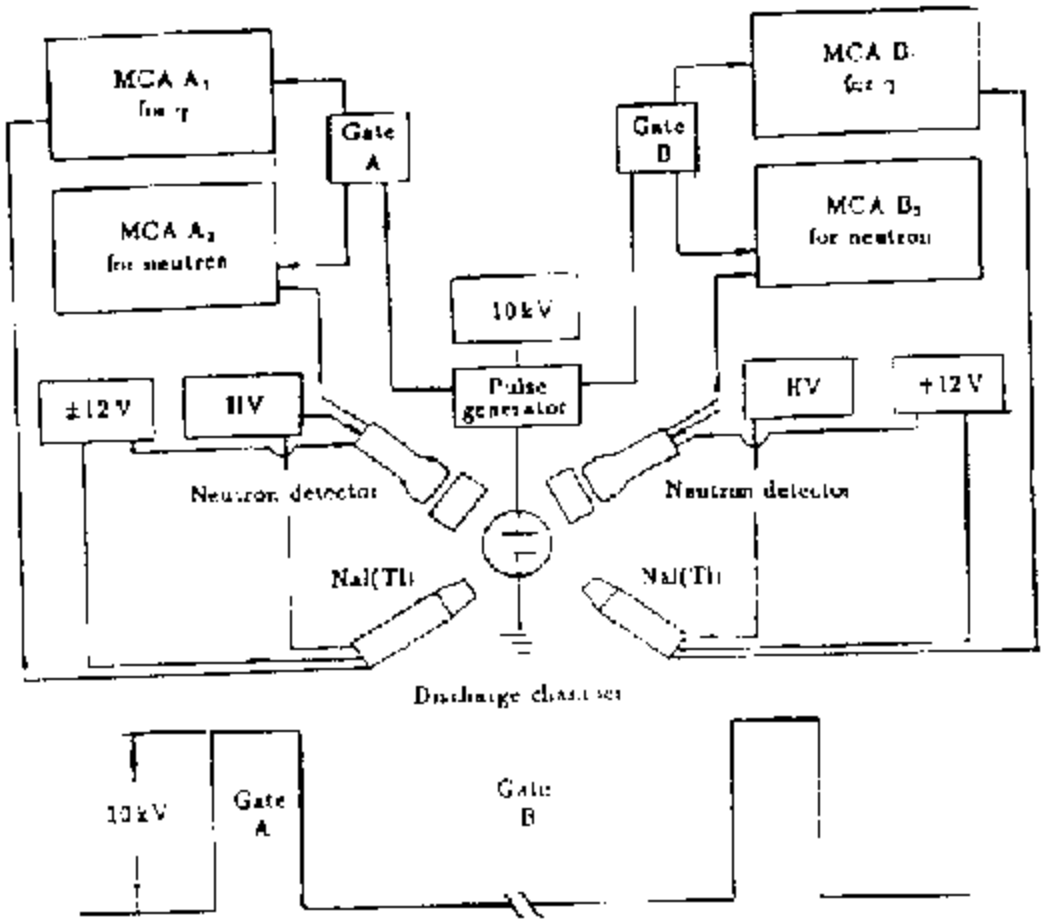

Fig. 1. Schematic diagram of the experimental arrangement and electronic system.

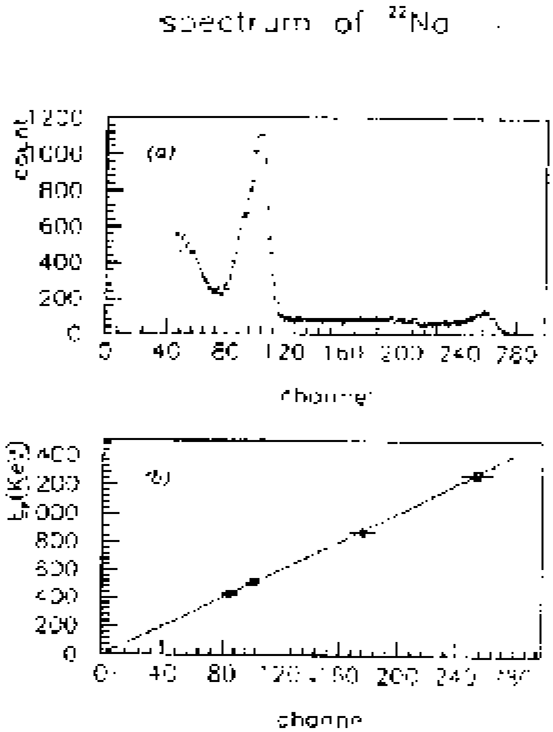

Fig.2 Calibration of NaI [illegible]
a) Spectrum of source [illegible]
b) Calibration curve

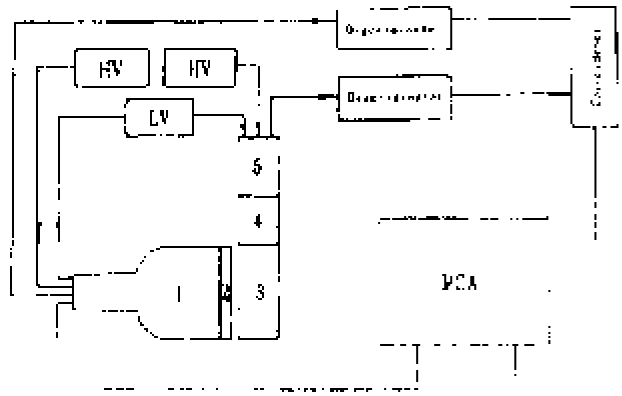

Fig.3 Neutron detector system
1—GDB- 00P [illegible] 2—φ 100×3 [illegible]
3—5cm [illegible] of plastic [illegible]
4—[illegible] 5—56 AVP Pb

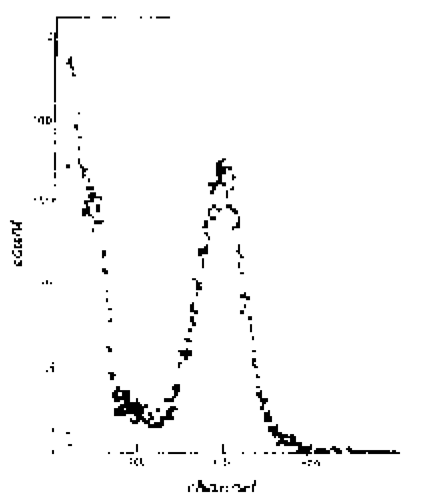

Fig. 4 Slow neutron and [illegible] ray spectrum from lithium glass detector

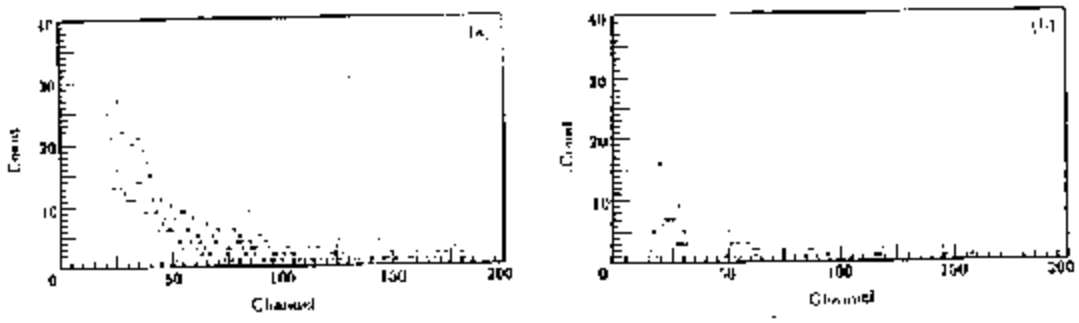

Fig. 5. The gamma rays spectrum.
a) Spectrum during HV pulse for 8 h.
b) Background for 4 h

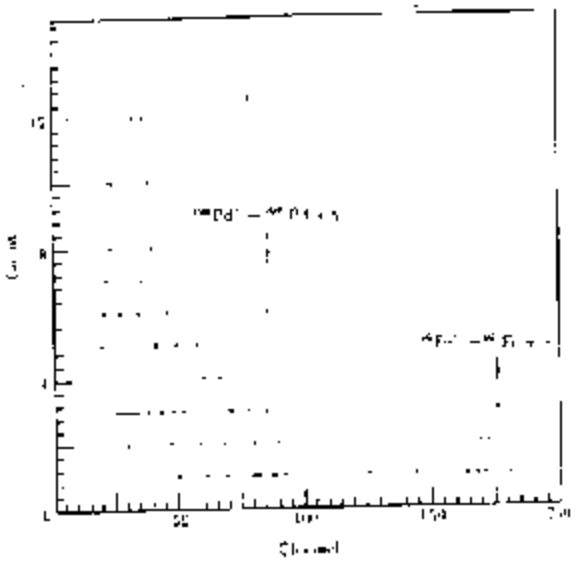

Fig. 6 (c). The net spectrum of gamma ray.

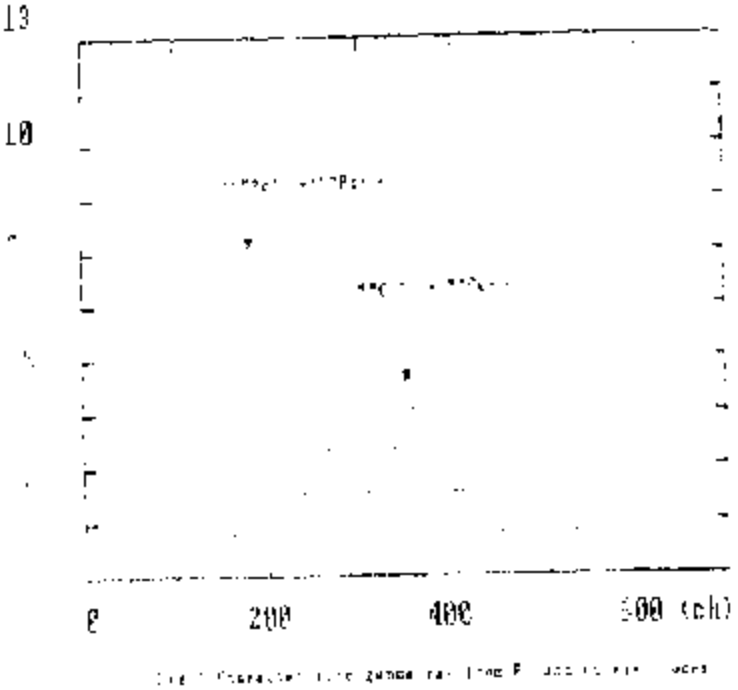

MOLTEN SALT TECHNIQUES FOR EXCESS HEAT PRODUCTION AND THE LOADING ISSUE

Bor Yann Liaw
Hawaii Natural Energy Institute
School of Ocean and Earth Science and Technology
University of Hawaii at Manoa
2540 Dole Street, Holmes Hall 246
Honolulu, HI 96822, USA

ABSTRACT

An interesting molten salt technique for elevated-temperature excess heat production has recently been reported, promising great potential for commercial applications. This technique shows improved efficiency due to a high-temperature operation, high-grade heat production and fast kinetics in metal-hydrogen reactions. This paper gives an overview of our work in molten salt electrolysis experiments using Ti and Pd as anodes in deuteride melts, in which substantial excess heat was found. This paper also presents some preliminary results using Ni and steel as anodes for electrolysis in hydride melts. Because the deuterium loading in Pd is considered a critical parameter for excess heat production, this paper will discuss this aspect and extend to elevated-temperature conditions.

THE MOLTEN SALT TECHNIQUES

Deuteride-Based Systems

Since the announcement of the Fleischmann-Pons effect in 1989, a team led by Liebert and Liaw has been working on a project using the molten salt techniques to verify such an effect. Earlier experiments in 1989 involved the electrolysis of Ti and Pd anodes in LiD-containing melts [1,2], in which commercially available Al alloys were used as the cathode. Operating at about 400°C, these molten salt cells produced excess power, ranging from 30% in the Ti-D system to more than 600% in the Pd-D system. No excess power or heat has ever been measured in analogous experiments using LiH-containing melts. However, replication of the excess heat effect in the Pd-D system has been difficult due to several problems, including chloride formations involving various electrodes and lead materials under a starving LiH(D) condition in the melts and severe cracking and disintegration from uncontrollable sample preparations and uneven charging conditions associated with the Pd electrodes.

Molten salt techniques provide an interesting alternative to the aqueous electrolysis methods for excess heat production, although the degree of control of these techniques need to be improved. Typical molten salt electrolytes used in our experiments are eutectic LiCl-KCl melts saturated with excess LiH(D). This electrolyte system has a melting point of 350°C and has a very high ionic conductivity of the order of 1 Ω^{-1} cm^{-1}, higher than any other proton-based conductors at these temperatures. The presence of LiH(D) in the melts introduces a very reducing environment, in which most transition metal oxides become unstable. This unique property provides an effective method of removing metal surface oxides in situ, resulting in "hydrogen-transparent" metal surfaces which facilitate the metal-hydrogen reactions. This technique is particularly useful for transition metals such as Ti, Zr, V, Ta, and their alloys, whose potential for excess heat production might be attractive due to their high solubility of hydrogen and deuterium.

The molten salt techniques are based on the electrolysis of LiH(D) through hydrogen-transparent surfaces to charge H or D into metal anodes and produce excess heat with enhanced kinetics and efficiency. Several interesting results were found in our successful excess-heat-producing Pd-D experiments:

- The excess power level, of the order of 9-25 W, was 6-15 times, or 600-1,500%, larger than the input electrochemical power (≈0.6-1.7 W, depending on current density) with no consideration of thermoneutral potentials. The excess power was a linear function of current density. The excess heat was of the order of 6-7 MJ mol^{-1} D_2, significantly larger than any known chemical reaction enthalpies. Fig. 1 shows the input and output power excursion profiles at different current densities in this particular experiment.

- The total excess heat was of the order of 5 MJ, at a rate of about 9-25 W for 4 days. This magnitude of excess power is difficult to be explained by any storage mechanisms, contaminations or other artifacts.

- Four specimens from the spent Pd electrode have been analyzed by high-precision mass spectroscopy to quantify their residual He-4 content. All of them have shown enhanced He-4 content above the level of the background or a control Pd blank [3]. Although the amount of excess He-4 was not commensurate with the magnitude of excess heat, the increased He-4 content was a surprise to us since a similar H-based experiment showed an opposite result. Fig. 2 shows the He-4 enhancement in the Pd specimens versus those of the background and the virgin electrode used as a control.

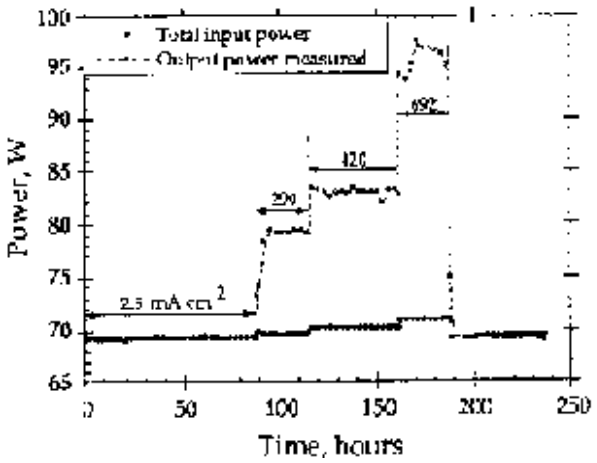

Figure 1. The power excursion curves of the inputs and ouputs during a charging experiment using a Pd anode and an Al alloy cathode in a D-melt. Charging current densities are indicated. For detailed experimental parameters, please refer to refs. 1 and 2.

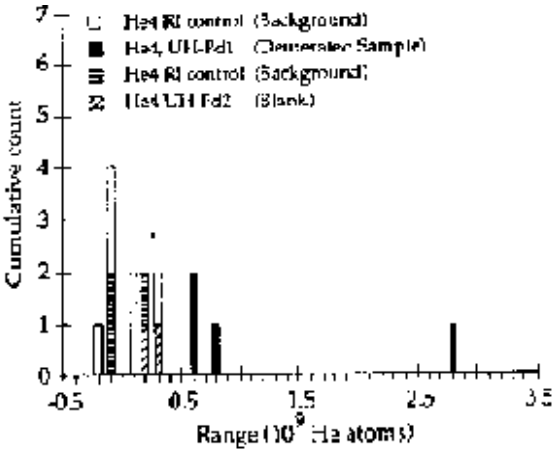

Figure 2. He-4 analysis results of the spent Pd anode and a control sample. All four specimens of the anode show increased He-4 content, although the amount was not commensurate with the excess heat measured.

Electrochemical Characterization

Because of the irreproducibility of the molten salt techniques, substantial effort has been made to study the electrochemical behavior of the electrodes in the molten salt system. Cyclic voltammetry technique and polarization studies [4,5] were conducted in the H-containing melts using various anode materials, including Pd, W, Mo, Al and Ni. These studies have led to the understanding of the effect from impurities such as Si, which acts as an inhibitor to the hydrogen evolution reaction. The results also indicate the LiH concentration can alter electrochemical behaviors and reaction paths. When LiH concentration is low, increased chloride activity can promote the metal chloride formation that corrodes

the electrode and the lead, leading to the failure of cell operation. It is important to control the type of impurity present in the melt and its concentration to facilitate the Pd-hydride formation, thus enhancing the loading.

Hydride-Based Systems

These electrochemical studies also led to a more recent calorimetric investigation of the Ni-H system in the molten salt [6], in which excess power was measured, similar to those reported by several groups using carbonate-electrolyte light-water electrolysis and Ni cathodes at ambient temperature. Preliminary results showed that some low level of excess power was measured during the galvanostatic charging process with different current densities. The excess power (≈0.5 W) was of the order of 30-100% of the input power. If we take the thermoneutral potential from various possible cell reactions into consideration, the gain of the excess power was even higher, of the order of several hundred per cent. Although the Ni-H experiments seem quite reproducible, the magnitude of the excess power however is low, unlike the Pd-D results. The origin of the excess power in this Ni-H case is unknown and may be caused by side reactions or other artifacts, which need to be investigated further. However, in a similar electrolysis using steel as the anode, it showed no excess power.

THE LOADING ISSUE

It has been demonstrated in low-temperature heavy-water electrolysis experiments [7,8] that a threshold loading ratio of about 0.84 is essential for excess heat production. In all molten salt experiments so far, we have not been able to report the loading ratio related to the calorimetric measurements. It is inherently difficult in our elevated-temperature experiments, particularly in situ, to measure the loading ratio. The resistivity ratio (R/R°) and gas volumetric techniques are two methods often used to measure the loading ratio in ambient-temperature experiments. The gas volumetric technique has recently been adopted by Okamoto and Nezu [9] at the IMRA Material R&D, Japan, to measure the loading ratio of H in Pd in the molten salt environments.

They reported a very shallow loading, similar to what would be expected from the equilibrium phase diagram, in their Pd samples from electrochemical charging. Their cyclic voltammetry results, however, showed a series of anodic and cathodic peaks, quite different from what we have reported [3,4], indicating a very complicated environment in their electrolyte systems. According to the phase diagram reported by Levine and Weale [10] and the overpotentials often measured in our cells (≈0.6-1.0 V), we can estimate the fugacity of the Pd anode to be about 10^{10}-10^{15} atm. The relationship of pressure and fugacity reported by Baranowski and Wisniewski [11] can then be used to extrapolate the loading ratio during an effective charging. A range of D/Pd>0.7 is thus obtained, which is quite different from those reported by Okamoto and Nezu.

The gas volumetric technique is less sensitive than the R/R° technique for time-dependent loading measurements in a dynamic charging situation. Nevertheless, reliable data between the R/R° and the loading ratio at elevated temperatures have not been established experimentally. The R/R° technique is difficult to be used in the molten salt environment due to the lack of a suitable insulating material in order to confine the cell geometry. In addition, the high conductivity of the melt makes the parasitic resistance of the electrolyte comparable to that of the electrode hence increases the difficulty of an accurate measurement. Despite these problems, the loading ratio is still an important parameter to be characterized for better control of the excess heat effect.

The issue of the threshold loading for observing anomalous excess heat effect is an interesting open question for both ambient and elevated temperatures. Although the necessity of such a threshold loading at elevated temperatures has not yet been demonstrated or verified experimentally, there is a consensus in this field that such a threshold loading should exist.

The underlying mechanism dictating how the threshold loading control the excess heat effect has not been revealed yet. The meaning of R/R° and its relationship to this threshold loading have not been discussed in great details, either. On the other hand, experimental evidence shows that R/R° could vary with the state of the electrode to some extent associated with the electrode preparation, heat treatment, history, and other metallurgical and material aspects such as microstructure and morphology, defect type and concentration, magnification and interaction of defects, stress state and distribution, etc. However, how well are these factors related to the origin of the excess heat should provide important clues to our understanding of the excess heat phenomenon. To seek such links, we have to carefully investigate these factors and their effect on the loading issue.

The threshold loading of D/Pd=0.84 at room temperature did not coincide with the crystallographically-ideal, saturated composition of D/Pd=1, of which deuterium will occupy all the octahedral sites in the lattice. This threshold loading did not coincide with the maximum of the R/R° curve at D/Pd≈0.72, either. More recently, the possibility of a new γ-hydride phase was proposed. The structure of this phase has not been reported yet. It could be associated with tetrahedral-site occupancy. It could also be associated with a lattice distortion in which octahedral sites were distorted into a different symmetry due to partial site occupancy of deuterium. It could also come from a disordered-ordered lattice transition with preferred site occupancy. If the structure is anisotropic, it could exhibit a Jahn-Teller effect. This phase, if it exists, should be considered metastable, to only occur under certain extreme, non-equilibrium conditions.

In the case of elevated temperatures such as 400°C, according to the phase diagram of the Pd-H(D) system, it is difficult to conceive how a loading ratio of over 0.8 can be achieved through gas loading unless an extremely high hydrogen pressure was applied. The pressure-concentration-temperature (p-c-T) curves of the system indicate that the H(D) concentration in Pd decreases with temperature under an isobaric condition. The equilibrium H(D) concentration in Pd is rather low (<0.1) at low ambient pressures (<30 atm) and high operating temperatures such as 400°C. On the other hand, electrolysis is a dynamic situation which could be significantly different from the equilibrium condition. It is generally believed that electrochemically charging can achieve conditions beyond those from gas loading. If we believe the threshold loading is related to excess heat production through some crystal structure changes and/or defect interactions, it would be beneficial to consider the loading from a thermodynamic point of view to reveal more insightful aspects of the defect chemistry involved.

It is well known that crystal defect structure and interaction strongly affect the p-c-T characteristics. Wagner [12] has shown, from thermodynamic principles, the significance of the curvature of the p-c-T curves, or, in electrochemical sense, the coulometric titration curves in terms of stoichiometry of a solid compound, which is readily attainable from the following analysis:

Consider the compound $PdH_{\beta+\delta}$ involving H atoms in interstitial sites (H_i) of the Pd lattice and their vacancies (V_H) as the essential point defects, as described by a Frenkel disorder model. The excess H is the difference between the mole fractions of H_i and V_H,

$$\delta = X(H_i) - X(V_H), \tag{1}$$

where $X(H_i)$ equals the loading ratio, and PdH_β is presumably the stoichiometric composition of the hydride phase at a particular temperature. When the defect concentrations are low, interaction among defects may be neglected. We can then assume that

$$X(H_i) \approx a_H, \text{ and} \tag{2}$$

$$X(V_H) \approx a_H^{-1} \tag{3}$$

For the stoichiometric composition PdH_β, where $\delta = 0$,

$$X^\circ(H_i) = X^\circ(V_H). \quad (4)$$

We can rewrite

$$X(H_i) = X^\circ(H_i)(a_H/a^\circ_H), \text{ and} \quad (5)$$

$$X(V_H) = X^\circ(H_i)(a_H/a^\circ_H)^{-1}. \quad (6)$$

Substituting (5) and (6) in (1), we obtain

$$\delta = X^\circ(H_i)[(a_H/a^\circ_H) - (a_H/a^\circ_H)^{-1}] = 2X^\circ(H_i)\sinh[\ln(a_H/a^\circ_H)]. \quad (7)$$

A plot of $\ln(a_H/a^\circ_H)$ versus δ yields an antisymmetric curve with an inflection point at the ideal stoichiometric composition. We can thus determine the stoichiometric point for a solid phase at the inflection point of the coulometric titration curve. This behavior applies to the p-c-T curves of the Pd-H system at high temperatures above the 300°C critical point, and, indeed, distinct inflection points are identifiable. Thus, at 400°C, the stoichiometric point is at about H/Pd≈0.38, according to the p-c-T curves reported by Levine and Weale [10].

Below the critical point, where the α-ß miscibility gap presents, the p-c-T curve in the ß-phase region is concave above the phase boundary (H/Pd>0.59 at 25°C) [13]. Neutron diffraction measurement, however, indicated that the hydrogen occupies the octahedral sites in Pd, thus leading to the belief that, at saturation, H/Pd=1 is the stoichiometric composition of the ß-phase. There is no indication if the p-c-T curve turns convex and an inflection point exists that represents the stoichiometry as described above. Therefore, it seems that the defect chemistry may be different at low and high temperatures. Despite the difference, how the defect chemistry relates to the maximum (H/Pd≈0.72) of the R/R° versus loading ratio curve and the threshold loading (D/Pd=0.84) for the anomalous excess heat effect is an intriguing subject for future studies.

CONCLUSION

The molten salt technique is a unique approach to excess heat production at elevated temperatures, promising high grade heat and improved efficiency. Both the Pd-D and Ni-H systems were investigated, and excess power was observed, although the origin of these anomalies were not identified. The electrochemical behavior of the molten salt system is complicated by the presence of impurities. Control of the electrode material property and the impurities are critical for reproducibility. Although demonstration of a threshold loading to the excess heat effect in elevated-temperature electrolysis is lacking, the importance of this parameter is speculated. We are interested in investigating the temperature-dependent relationships among the stoichiometric composition of the hydride phase, the loading of the maximum R/R° value and the threshold loading of the excess heat effect. The correlation of these three loading values with the underlying defect chemistry may reveal some important crystal structure variations and associated defect interactions that may be related to the excess heat phenomenon.

ACKNOWLEDGEMENT

This work has been supported by the University of Hawaii, U. S. Office of Naval Research, and Fusion Resources, Inc./ENECO. I would also like to acknowledge the contributions from my colleagues, Professor Bruce E. Liebert, Dr. Robert A. Huggins, Dr. Debra R. Rolison, Dr. Robert J. Nowak, Dr. Talbot Chubb, and many others.

REFERENCES

[1] B. Y. Liaw et al., in the Proceedings of the Symposium on "Cold Fusion," the 8th World Hydrogen Energy Conference, Honolulu/Waikoloa, Hawaii, July 22-27, 1990, p 49.
[2] B. Y. Liaw et al., *J. Electroanal. Chem*., vol 319 (1991), p 161.
[3] B. Y. Liaw et al., *Fusion Tech*., vol 23 (1993), p 92.
[4] B. Y. Liaw and B. E. Liebert, Proc. of the 8th Internat. Symp. on "Molten Salts," ed. R. J. Gale, G. Blomgren and H. Hojima, Electrochem. Soc., PV 92-16, p 1.
[5] B. Y. Liaw and Y. Ding, to be published in *Solid State Ionics*.
[6] B. Y. Liaw and Y. Ding, to be published in Proc. ICCF-4, Maui, Hawaii, Dec. 6-9, 1993.
[7] M. C. H. McKubre et al., in Frontiers of Cold Fusion, ed. H. Ikegami, Universal Academy Press, Inc., Tokyo, p 5.
[8] K. Kunimatsu et al., in Frontiers of Cold Fusion, ed. H. Ikegami, Universal Academy Press, Inc., Tokyo, p 31.
[9] H. Okamoto and S. Nezu, to be published in Proc. ICCF-4, Maui, Hawaii, Dec. 6-9, 1993.
[10] P. L. Levine and K. E. Weale, *J. Chem. Soc. Faraday Trans*., vol 56 (1960), p 357.
[11] B. Baranowski and R. Wisniewski, *Phys. Stat. Sol*., vol 35 (1969), p 593.
[12] C. Wagner, in Progress in Solid State Chemistry, Vol. 6, ed. Reiss and McCaldin, Pergamon Press, Oxford, 1971, p 1.
[13] J. R. Lacher, *Proc. Roy. Soc*., vol 161 (1937), p 525.

THE X-RAY EMISSION FROM ELEMENTS OF FIRST PERIOD AND COLD FUSION

Ren-bao Lu

Beijing Institute of Applied Physics
and Computational Mathematics
Beijing 100088, P.R. CHINA

Keywords: photoelectric effect, X-ray, bremsstrahlung, cold fusion, bound state

ABSTRACT

The elements of first period and their isotopes can produce A+-ion when they are electrolyzed or ionized or under the action of photoelectric effect. If these A+-ions run into the range of Bohr orbit radius of the A-atom or He^+, under the electromagnetic interaction they can form the bound states A^+-e-A^+, A^+-e-He^{++}, He^{++}-e-He^{++},..., and then emit X-rays from bremsstrahlung. The probable distance between the cations is nearly 10^{-12}cm at this time. For the particles among which the nuclear attractive force exists, cold fusion can happen from the strong interaction and the electromagnetic interaction. For example, D^+-T, D^+-D, T^+-D, D^+-$^3He^+$, ..., and so on. As an example, considering D^+-D we have

$$V(x) = -\frac{1+\xi}{2(1-\xi)}\frac{e^2}{x} \qquad 0 \le \xi \le 1 \ ,$$

$$\Psi = 2k^{3/2} x e^{-kx} \ ,$$

$$k = \frac{1+\xi}{2(1-\xi)}\left(\frac{\mu}{\mu e}\right)\frac{\mu e}{h^2}e^2$$

$$E = -\frac{1}{4}\left(\frac{1+\xi}{1-\xi}\right)2\frac{\mu}{\mu e}E_1$$

Where μ is the converted mass. μe is the mass of electron, E_1 is the energy of the basic state of hydrogen. When $\xi = 3/8$ we have E = -30.17keV and $k = 0.38*10^{12}cm^{-1}$. Then the following results can be obtained:

R_o (10^{-13}cm)	kR_o	W	W^{-1}
1.0	0.038	$6.91x10^{-5}$	$1.45x10^4$
0.5	0.019	$8.89x10^{-6}$	$1.13x10^5$
0.25	0.0095	$1.127x10^{-7}$	$0.89x10^6$

If the energy of X-ray is 30kev, the energy of a 30kev, the energy of the fusion is 3.5Mev, the range of nuclear force is 0.5fm - 0.25fm, then the ratio of the energy of bound state to the energy of fusion is nearly 10^3 - 10^4. Thus it can be concluded that the excess heat comes mainly from the energy release of bound state. It does not come from the energy of nuclear fusion.
When cold fusion happens from D^+ - D, the reactions of first order are

$$D^+ + D \rightarrow \begin{matrix} n + {}^3He - e \\ D + T - e \\ \alpha + \gamma - e \end{matrix}$$

where `- e' means an electron is captured. The reactions of second order are

$$D^+ + {}^3He^+ \rightarrow \alpha + p - e$$

$$D^+ + T \text{ (or } T^+ + D) \rightarrow \alpha + n - e$$

Moreover, there are (n, γ), the absorption and excitation of X-ray, ..., and so on. All of these complicated processes of reaction make the experiment analysis difficult.

Of course, the nuclear reaction may not happen among the particles, e.g. the polywater is formed from H^+ and H. [5,6]. Since the proton of polywater is connected by the electronic bond, it may be more suitable to use the name `water of electronic-chain.' Possibly, its construction is

$$e \quad \begin{matrix} H & O & H \\ H & O & H \end{matrix} \quad e \qquad \text{or } H - e - H - O - H - e - H$$

It was found that when the negative electrode of Pd is used to electrolyze the heavy water, D/Pd must be larger than 0.84 for the appearance of anomalous effects. This means that there are an average of 3.36 D-atoms in a Pd crystal cell. Several D-atoms in a Pd crystal cell is the condition for D^+ -D to satisfy the demand of Bohr orbit radius.

For the experiments in which cold fusion happens (e.g. use Pd negative electrode to electrolyze the heavy water, the D/metal system of glow discharge,...), the essential fact is that D^+ -D forms a bound state and emits X- ray, meanwhile, there is a probability of 10^{-5} - 10^{-6} that nuclear fusions will occur.

REFERENCES

[1] M. Fleischmann, S. Pons et al., *J. Electroanal. Chem*., vol 261, p 301 (1989).

[2] D.L. Wang et al., "On the Neutron, γ and X-ray of the Gas Which Glows Discharge," *Chinese J. Atomic and Molecular Physics*, (1993.7).

[3] R.B. Lu, "The X-ray Emitted from a Class of Gases Which Glows Discharge and the Possible Mechanism of D-D and D-T Nuclear Fusion Under Normal Temperature," to appear in *Chinese J. High Power and Particle Beams*, 1994.

[4] Y. Kucherov, A. Karabut and I. Savvatimova, "Calorimetric and Nuclear Products Measurements at Glow Discharge in Deuterium, ICCF 4, Notebook 2, N1.1, 1993.

[5] B.V. Geryagin, N.V. Churayev, *Priroda*, no. 4 P/6-22 (1968)

[6] E.R. Lippincott et al., *Science*, vol 164, no 3887, p 1482 (1969).

EXTRAORDINARY TRACES ON NUCLEAR EMULSIONS OBSERVED DURING ELECTRICAL DISCHARGE IN WATER

Takaaki Matsumoto

Department of Nuclear Engineering
Hokkaido University
Sapporo 060, JAPAN

ABSTRACT

Experiments of cold fusion were performed using electrical discharge in water. AC shots of up to 100 V were applied to wire electrodes of palladium, platinum and nickel in ordinary water mixed with potassium carbonate. The reactions were observed by nuclear emulsions and a system utilizing a microtelescope and a VTR (video tape recorder). It was shown that cold fusion reactions were easily induced on the surface of the metal. Strange traces indicating cold fusion reactions were recorded on the nuclear emulsions.

INTRODUCTION

The Nattoh Model [1] proposes that cold fusion reactions occur when a hydrogen cluster is compressed into a tiny particle. In the compressed state, internuclear distances are so short that various kinds of fusion-like reactions can take place: (1) a new two-body fusion reaction that predominantly contributes to heat production and mainly produces helium-4 instead of helium-3,
(2) multibody fusion reactions that contribute to the production of new elements and (3) in the most significant case, the production of tiny black holes and white holes. The compression process can be significantly enhanced by electrical discharge that induces additional electrons into the hydrogen clusters [2].

This paper describes cold fusion experiments using electrical discharge in water. The reactions were observed by a system utilizing a microtelescope and VTR and nuclear emulsions.

EXPERIMENT

Two kinds of cold fusion experiments were performed using electrical discharge: cold fusion directly induced by electrical discharge and implosive cold fusion induced by the explosions of the cold fusion reactions. Both experiments were made by applying AC shots (50 Hz and up to about 100 V) to wire electrodes in water.

The electrolyte solution consisted of ordinary water mixed with 0.6 Mol/l potassium carbonate. Wires of palladium, platinum and nickel were used for the electrodes. Two kinds of electrode arrangements were employed for the direct discharging cold fusion: vertical and parallel. In the former, a pin of the platinum wire (0.3 mm dia. x 2 mm long) was vertically located about 2 or 3 mm distance from the wire of palladium (0.5 - 2.0 mm dia. x about 25 mm long). In the latter, two wires of palladium, nickel and platinum (0.3 - 2.0 mm dia. x about 25 mm long) were located parallel to one another with a gap of 2 - 3 mm. For the implosive cold fusion that needs to concentrate on the electrical field, on the other hand, a helical electrode of nickel (0.5 dia.) was placed around a pin electrode of palladium (0.5 dia. x about 3 mm long). The diameter of the helical electrode was about 10 mm. The electrical discharge was

employed with pulsed AC up to 100 V (20 - 80 msec ON and 1 - 15 sec OFF). The phase was fixed such that the voltage at the anode started to increase positively.

Reactions were directly observed with a system utilizing a microtelescope and VTR, that were located outside the bottom (acrylite plate of 2 mm thick) of a cylindrical glass cell. The cell was located such that the bottom was vertical. Pictures from the microtelescope (10 - 100 times amplification) were recorded on the VTR. Important pictures were then picked up stepwise with a color copier.

Reaction products of cold fusion were recorded using nuclear emulsions, that were similar to that previously used [3]. Although it takes a long time to search for traces on the nuclear emulsions, they are very sensitive and the traces contain a lot of credible information that can contribute to identify the reaction products. The nuclear emulsions (made by Fuji Film Inc.; MA-7B) of 100 μm thick were coated on both sides of an acrylite plate of 1 mm thick x 50 mm x 50 mm. The nuclear emulsions coated on the acrylite plates were partly provided by Fuji Film Inc. Some nuclear emulsions were coated in our laboratory in order to reduce background traces. The nuclear emulsions were irradiated by natural radiation so they should be used as soon as possible after the coating, at least within a month. After irradiation, the nuclear emulsions were treated in solutions that are available for usual processing of films. Since the nuclear emulsions were thick, the processing time was long: 25 min in a developing solution, 15 min in a stopping solution and 150 min in a fixing solution, respectively. Traces on the nuclear emulsions were searched by a microscope (500 times amplification) that provided a transmission and reflection lights. The former was used when the traces were located inside the nuclear emulsions. The latter was useful not only for traces recorded on the surface but also for distinguishing noise. To distinguish the noise traces, reference nuclear emulsions were located about 5 m from the cell in the same room.

RESULTS: (a) Direct Discharging Cold Fusion

Fig. 1 shows a sequence of pictures taken by the VTR system of the discharge in the vertical arrangement. The time step was 33 msec. An explosion was induced on the surface of the palladium pin (0.5 mm dia. x 3 mm long) and left it hot. A couple of wave fronts that were reflected by the AC cycle could be clearly seen in the pictures, and particles with high energy seem to have been emitted. The observation of the nuclear emulsions showed that the explosion was a cold fusion reaction and that the pin electrode was heated to a red temperature by the released energy. The VTR system also recorded explosive reactions induced in the parallel arrangement. Here it is clearly shown that explosive reactions took place on the surface of the wire.

Several extraordinary traces were recorded on the nuclear emulsions located outside the acrylite window. The first is a star that emitted a lot of fragments, shown in Fig. 2. Similar traces were also observed in a previous experiment [4]. A star can be created inside the nuclear emulsion by a multibody fission reaction of a heavy nucleus such as silver, that becomes a highly excited compound nucleus by capturing a multiple-neutron emitted from the cell.

The second is the observation on explosive traces that can be generated by the gravity-decay of multi-neutrons. Similar traces were also observed in the previous experiments [l]. This trace is one of the most credible pieces of experimental evidence indicating that cold fusion has taken place. When the hydrogen-cluster is compressed to induce a cold fusion reaction, hydrogen atoms that are not directly involved in a fusion reaction should scatter. Those traces could be clearly seen. Simultaneous plural reactions might take place in the compressed hydrogen-cluster. Fortunately, pictures indicating such reactions were taken by chance with mismade nuclear emulsions that were thinner.

The third phenomena are strange combined rings that were first observed in this experiment. The rings

can be clearly distinguished from the previous explosive traces because they were recorded only on the surface and had combined with each other. The diameter of the combined rings is different in each event but similar within the same event. The events were densely concentrated between the first and second nuclear emulsions.

(b) Implosive Cold Fusion

Implosive cold fusion experiments were attempted by applying AC shots to a helical wire within which a strong electrical field was concentrated to the tip of the pin electrode. A sequence of two explosions occurred. The first explosion was directly induced by the discharge. The second explosion was not induced by the electrical discharge, but by the first cold fusion reactions. This was caused by the duration of the discharge which was 80 msec, and the second explosion occurred after 100 msec. After the explosions, fine black materials remained.

DISCUSSIONS

In this paper, two kinds of cold fusion experiments were attempted. In the direct discharge experiment, AC shots of up to 100 V were applied to wire electrodes that were located parallel to one another and vertically. We could actually see the cold fusion reactions on the surface of the metal by the VTR system. This means that the hydrogen charging into the metal is not always needed for inducing cold fusion as the Nattoh model predicted. The traces on the nuclear emulsions showed the production of stars and the gravity-decays of multiple-neutrons. All of those traces were already obtained in previous experiments [l].

The strange traces of the combined rings, first observed in this experiment, suggest the production of tiny black holes. The tiny black holes that were produced in the cell dropped down to the space between the first and second nuclear emulsions. They seem to have continued hopping there and remained as the combined rings.

Secondly, implosive cold fusion was successfully attempted. It can be expected to release higher energy.

REFERENCES

[1] T. Matsumoto, "Mechanisms of Cold Fusion: Comprehensive Explanations by the Nattoh Model," Submitted to *Fusion Technology* in March and distributed at the Hawaii conf. in December (1993).
[2] T. Matsumoto, "Experiments of One-Point Cold Fusion," *Fusion Technology*, vol 24, p 332 (1993).
[3] T. Matsumoto, "Observation of New Particles Emitted on Cold Fusion," *Fusion Technology*, vol 18, p 356 (1990).
[4] T. Matsumoto, "Observation of Stars Produced during Cold Fusion," *Fusion Technology*, vol 22, p 518 (1992).

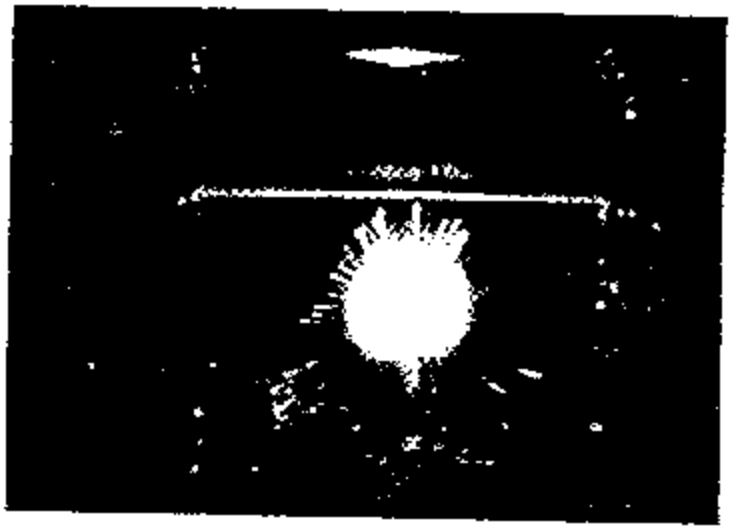

(a)

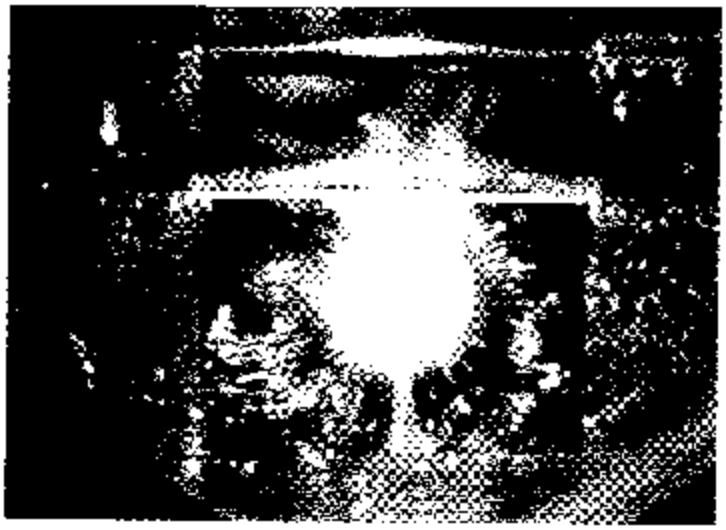

(b)

(c)

5 mm

Fig. 1: Explosion in the vertical arrangement

Fig. 2: Cold fusion star

DETECTION OF IRON ATOMS ON GOLD ELECTRODES USED FOR ELECTROLYSIS OF NEUTRAL AND ALKALINE H_2O AND D_2O SOLUTIONS

Tadayoshi Ohmori and Michio Enyo

Catalysis Research Center,
Hokkaido University, Kita 11 Nishi 10,
Kitaku, Sapporo, 060 Japan

ABSTRACT

Detection of any products possibly produced during the excess heat evolution by electrolysis was attempted on Au electrodes, in parallel with the excess heat observations. The electrolytes used were K_2CO_3, Na_2CO_3, Na_2SO_4, KOH and NaOH. The electrolysis was performed for 7 days with a constant current of 1 A. The electrode surface was then analyzed by means of AES spectroscopy. In every solutions a notable amount of Fe atoms were detected, being in the range of 1.1 to 9.9 x 10^{16} atoms. These values are much larger than those contained as impurities in the reagents used (ca. 7 x 10^{14} atoms for Na_2SO_4) or possibly originated from the cell materials. The mean excess heat observed was in the range of 187 to 723 mW. The amounts of Fe atoms observed were approximately proportional to the total amounts of the excess energy observed during the electrolysis. These results suggest that the iron formation reaction may be responsible for the excess heat evolution.

INTRODUCTION

The identification of any product caused by the cold fusion reaction is essential to conclude whether this reaction really exists or not. Several authors have reported that T or Ca atoms were detected in the electrolysis in Ni/K_2CO_3/ H_2O systems [1-2].

In addition, the latter author claimed detection of Sr in Ni/$RbCO_3$/ H_2O system [3]. These results suggest that various types of nuclear fusion reactions might be taking place in the electrolysis in various metal/electrolyte systems.

In the previous work we have observed evaluation of the excess heat ranging from 0.2 to 0.9 W during the electrolysis with Sn, Au, Ni and Ag electrodes in various alkali metal salts (K_2CO_3, Na_2SO_4, etc.) / H_2O systems [4-5]. It may then be conceivable that any nuclear fusion reaction products, apart from neutron, He and T, are formed at the electrode.

In this study, we tried to detect such products on Au electrode after the electrolysis in alkali-metal sulfates, carbonates and hydroxides / H_2O and D_2O systems using AES spectroscopy.

EXPERIMENTAL

The electrolytic cell used was a flat-bottomed cylinder made of quartz glass (ca. 23 cm^2 x 15 cm, Fe < 0.3 ppm, nominal) with a 5 cm-thick silicone rubber stopper holding a test electrode, a counter electrode, a thermocouple, and a quartz glass inlet tube for hydrogen gas. The cell was placed in an air thermostat

whose temperature was regulated at 21 ± 1 °C; the variation was periodical with 10 cycles/h. The precision of the solution temperature measurement was 0.03 °C. The working electrode used is a Au sheet (5 cm^2 area, 0.1 mm thick, 99.99% purity, Fe <1 ppm), whose surface was scraped with edge of a cleaned glass fragment and then washed with acetone, methyl alcohol and MQ water. The true surface area determined from the double layer capacitance [6] was 10.0 cm^2. The counter electrode was a 1 x 7cm, 80-mesh platinum net (99.98% purity, Fe <16 ppm). The working and counter electrodes were placed near the bottom of the cell to minimize the temperature gradient in the electrolytic solution by stirring with H_2 and O_2 bubbles evolved from these electrodes. The electrolysis cell was cleaned carefully with hot mixed acid (1:1 H_2SO_4 + HNO_3) and then rinsed with MQ water ultrasonically and finally rinsing for ca. 10 times with MQ water before conducting the electrolysis. The electrolytic solutions used were 0.5 M K_2CO_3, Na_2CO_3, Na_2SO_4, KOH and NaOH which are prepared from Merck suprapure grade chemicals. Heavy water was also obtained from Merck (99.8% purity) which was doubly distilled under vacuum. The volume of electrolytic solution used was 100 ml.

An electric heater used for measuring the calibration curve between solution temperature and input power was a 0.3 mmϕ diam., 1.6Ω nichrome spiral, connected to copper wires at both ends, which was inserted into a Pyrex-glass tube (6 mm diam., 15 cm long) containing silicone oil and set in the middle position of the cell. During the measurement, the solution was stirred by H_2 with the same flow rate as the rate of the evolution of H_2 and O_2 gases during the electrolysis.

The electrolysis was conducted galvanostatically for 7 days with a constant current of 1 A, and the variations of the applied cell voltage and the solution temperature growth were monitored by penrecorders.

RESULTS AND DISCUSSION

Excess heat

Fig. 1 shows a typical calibration curve between input power of the electrolysis cell and solution temperature. As seen, a very reproducible linear relationship was obtained up to 20 °C. The cell constant k calculated from the gradient was 3.25 ± 0.04 °C/W. The rates of excess heat evolution R_{ex} in H_2O and in D_2O solutions were determined from the solution temperature growth AT, cell voltage E and the polarization current I by the following equation [6], respectively.

$$R_{ex} = \Delta T/k - (E - 1.48)I \quad (1)$$

$$R_{ex} = \Delta T/k - (E - 1.54)I \quad (2)$$

where the values of 1.48 and 1.54 are the thermoneutral potentials for H_2O and D_2O decomposition reactions, respectively.

Fig. 2 shows typical variations of the solution temperature with polarization time obtained in Na_2SO_4/H_2O and Na_2CO_3/H_2O systems. The variations of the cell voltage were also shown in this figure. As seen, the increase of the solution temperature in Na_2SO_4 was larger than in Na_2CO_3 although the cell voltages were nearly the same with each other. The difference was essentially unchanged during the whole period of polarization. This result indicates that noticeable amount of excess heat is produced in the $Au/Na_2SO_4/H_2O$ system.

The excess heat obtained in various solutions was listed in Table 1. The maximum excess heat observed was 914 mW (in K_2CO_3/D_2O), which corresponded to 17.2% of the input power (EI 1.481). The mean excess heat evolved during 7 days of polarization in 11 kinds of electrolyte systems was in the range of 204 to 723 mW, the amounts of which seemed to be rather independent of the nature of electrolytes. These values of excess heat well reproduced the results reported previously in

Au/K_2CO_3, Na_2CO_3 and Li_2SO_4/H_2O systems [4-5].

The results of the excess heat measurement on Au and Pt electrodes in H_2SO_4/H_2O solutions are listed in Table II. The excess heat was negative, but very close to 0.0 in every case; it can be regarded that no excess heat was evolved. No observation of excess heat in electrolysis in H_2SO_4 solutions without exception supports reliability of our measurements of excess heat.

The total excess heat evolved during 7 days of polarization ranged between 130 and 437 KJ in the electrolyte systems shown in Table I. This means that at least several moles of reaction products should be produced during the electrolysis if the excess heat is caused by any conventional chemical reactions. However, no such large amounts of the reaction products were obtained except for H_2 and O_2, suggesting that some nuclear fusion reaction might be responsible for the excess heat.

The reaction products

Fig. 3 shows AES spectra from the Au electrode surface after 7 days of polarization in Na_2SO_4/H_2O system. In the spectrum on the top-surface (no Ar^+ ion bombardment), Fe and O signals were observed other than Au ones. On carrying out Ar^+ ion bombardment, the intensity of Fe and O signals decreased while that of Au signals increased, and the former signals disappeared completely after 2 minutes of bombardment. Fig. 4 shows similar AES spectra obtained on the Au electrode used in Na_2SO_4/D_2O system. The Fe and O signals were again observed in this case, whose intensity was somewhat larger than those in Na_2SO_4/H_2O system. Such Fe and O signals were observed in every electrolyte systems used, while no signals other than Fe, O and Au were detected. As seen from Fig. 3 and Fig. 4, the O signal is present together with the Fe signals and the ratio of the signal intensity of these species is not much different in every spectra observed. This suggests that these O atoms are present only on Fe atoms. Perhaps, they are contained originally in Ar gas as impurity and bound with surface Fe atoms during the Ar^+ ion bombardment. Therefore, the atomic contents of O on Au surfaces estimated from O signals can be replaced by those of Fe, assuming that O atoms bind with Fe atoms with the ratio of 1:1, so that the contents of Fe can be estimated by summing up the number of Fe and O atoms.

It is interesting to see the distribution of Fe atoms in the layers close to the electrode surface and to estimate the total amounts of Fe atoms. The number of iron atoms, N_{Fe}, sputtered from the surface by Ar^+ ion bombardment was estimated by the following equation [6].

$$N_{Fe} = f_{Fe} \text{ X } N_{Ar+} = \frac{f_{Fe} \cdot I_{Ar+} \cdot t}{1.6 \cdot 10^{-19}} \qquad (3)$$

where N_{Ar+} is number of Ar^+ ion bombarded per unit surface area, I_{Ar+} is its current density, f_{Fe} is the sputtering yield for Fe, and t is a duration of the bombardment. In this case I_{Ar+} was 21 $\mu A/cm_2$ and f_{Fe} was estimated at 2.4 [7]. The number of layers sputtered was estimated roughly by dividing N_{Fe} with 10^{15}.

The distributions of Fe atoms in the layers close to the surface, as calculated on the basis of the results in Fig. 3 and Fig. 4, are shown in Fig. 5. The content of Fe atoms in the top layer of the surface amounts to 78 and 44 at.% in Na_2SO_4/D_2O and Na_2SO_4/H_2O solutions, respectively. The Fe atoms distributed down to several ten layers. Similar results were obtained in other electrolyte systems. The total numbers of Fe atoms formed on Au electrodes in each electrolyte system, ranging between 1.1×10^{16} and 9.9×10^{16} atoms, are listed in Table III together with the mean excess heat. These values correspond to 1 - 10 layers of Fe atoms. The total amounts of Fe atoms against the mean excess heat in every electrolyte systems are plotted in Fig. 6. Although the data obtained were rather scattered, it is seen that the total

amounts of Fe atoms is likely to be proportional to the mean excess heat. This result may suggest that the Fe is produced along with the excess heat evolution.

The possibility of the Fe atoms coming from impurities in chemical reagents or impurities of cell materials are considered unlikely because of the following reasons; (i) the number of Fe atoms from the reagent impurity is believed to be at most 7 x 10^{14} atoms, e.g., in 100 ml of 0.5 M Na_2SO_4 (Merck suprapure grade agent) solution, and (ii) the number of Fe atoms from the quartz material by its dissolution during 7 days of electrolysis should amount only 10^{11} atoms. Hence, the amount of Fe atoms actually formed on Au electrode is roughly 2 orders of magnitude larger than the values estimated above. Even if all the Fe atoms as impurities were deposited on the Au electrode it cannot give the Fe signals shown in Fig. 3 and Fig. 4.

Further, nearly the same amounts of Pb, Cd, Cu, Co, Ni, Mn, Ti and Zn as that of Fe are contained as impurities in Na_2SO_4, but no signal other than Au, O and Fe was detected in AES spectra.

From the considerations presented above, we believe that there is a high possibility that the formation of Fe atoms is caused by a nuclear fusion reaction. However, no reaction scheme may be suggested at the present stage. It may only be mentioned that O, H and/or D atoms might be taking part in the present case, judging from the independence of the Fe atom production upon alkali-metal ions.

REFERENCES

[1] M. Srinivasan, A. Shyam, T.K. Sankaranarayanan, M.B. Bajpai, H. Ramamurthy, U.K. Mukherjee, M.S. Krishnan, M.G. Nayar and Y.P. Naik. Presented at 3rd Annual Conf. Cold Fusion, Nagoya, Japan, October 21 - 25 (1992).

[2] R.T. Bush, *Fusion Technol.*, vol 21, p 163 (1992).

[3] R.T. Bush and R. Eagleton, presented at 4th Annual Conf. Cold Fusion, Lahaina Hawaii, December 6 - 9 (1993).

[4] T. Ohmori and M. Enyo, presented at 3rd Annual Conf. Cold Fusion, Nagoya, Japan, October 21 - 25 (1992).

[5] T. Ohmori and M. Enyo, *Fusion Technol*., vol 24, p 293 (1994).

[6] T. Ohmori, *Electroanal. Chem.*, vol 157, p 159 (1983).

[7] A. Takeuchi, K. Tanaka, I. Toyoshima and K. Miyahara, *J. Catal.* vol 40, p 94 (1975).

[8] M. Kaminsky, Atomic and Ionic Impact Phenomena on Metal Surfaces, Springer-Verlag, Berlin, 1965.

FIGURE CAPTIONS

Fig. 1

Calibration curve between solution temperature and input power.

Fig. 2

Variations of input potential and solution temperature with polarization time: (1) and (1') Na_2SO_4/H_2O; (2) and (2') Na_2SO_4/D_2O.

Fig. 3

AES spectra of the Au electrode surface after electrolysis in Na_2SO_4/H_2O system.

Fig. 4
AES spectra of the Au electrode surface after electrolysis in Na_2SO_4/D_2O system.

Fig. 5

Distribution of Fe atoms on the Au electrode in the layers close to its surface: (1) Na_2SO_4/H_2O; (2) Na_2SO_4/D_2O.

Fig. 6

Plots of the total amounts of Fe atoms against the mean excess heat:

(○) (●) Na_2SO_4; (◇) Na_2CO_3; (□) (■) K_2CO_3; (▽) NaOH; (△) (▲) KOH.
Open mark, H_2O solutions; filled mark, D_2O solutions.

TABLE I

Amount of excess heat in various electrolyte systems

system	E (V) %	R_{ex},mean (mW)	R_{ex},max (mW)	efficiency
Na_2SO_4/H_2O	4.88	215	300	4.4
Na_2SO_4/H_2O	5.09	535	849	10.5
Na_2SO_4/H_2O	5.07	723	805	14.5
K_2CO_3/H_2O	4.95	281	417	5.7
K_2CO_3/H_2O	5.10	461	573	9.0
Na_2CO_3/H_2O	5.20	204	285	3.9
$NaOH/H_2O$	4.82	391	470	8.1
KOH/H_2O	4.51	526	815	11.7
Na_2SO_4/D_2O	5.15	523	770	10.2
K_2CO_3/D_2O	5.29	689	914	13.0
KOH/D_2O	5.11	187	280	3.7

TABLE II

Amount of excess heat in 0.5 M H_2SO_4/H_2O systems

electrode	E (V)	ATex (°C)	Rex (mW)
Au	3.10	-0.03	-9
Au	3.10	-0.04	-12
Au	2.83	-0.03	-9
Pt	2.95	-0.10	-30

TABLE III

Amount of Fe atoms and mean excess heat in various electrolyte systems

system	NFe (atom)	R_{ex},mean (mW)
Na_2SO_4/H_2O	3.0×10^{16}	215
Na_2SO_4/H_2O	3.1×10^{16}	723
K_2CO_3/H_2O	3.1×10^{16}	281
K_2CO_3/H_2O	1.8×10^{16}	461
Na_2CO_3/H_2O	1.5×10^{16}	204
$NaOH/H_2O$	1.1×10^{16}	391
KOH/H_2O	6.5×10^{16}	526
Na_2SO_4/D_2O	9.9×10^{16}	523
K_2CO_3/D_2O	3.8×10^{16}	689
KOH/D_2O	1.5×10^{16}	187

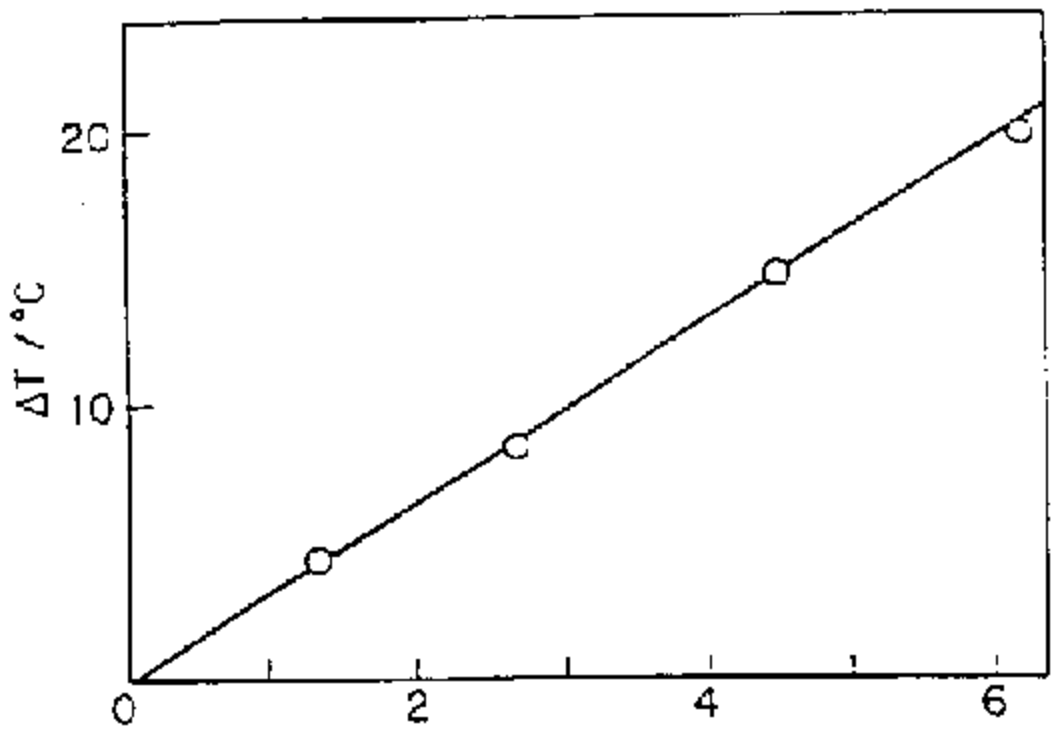

Figure 1

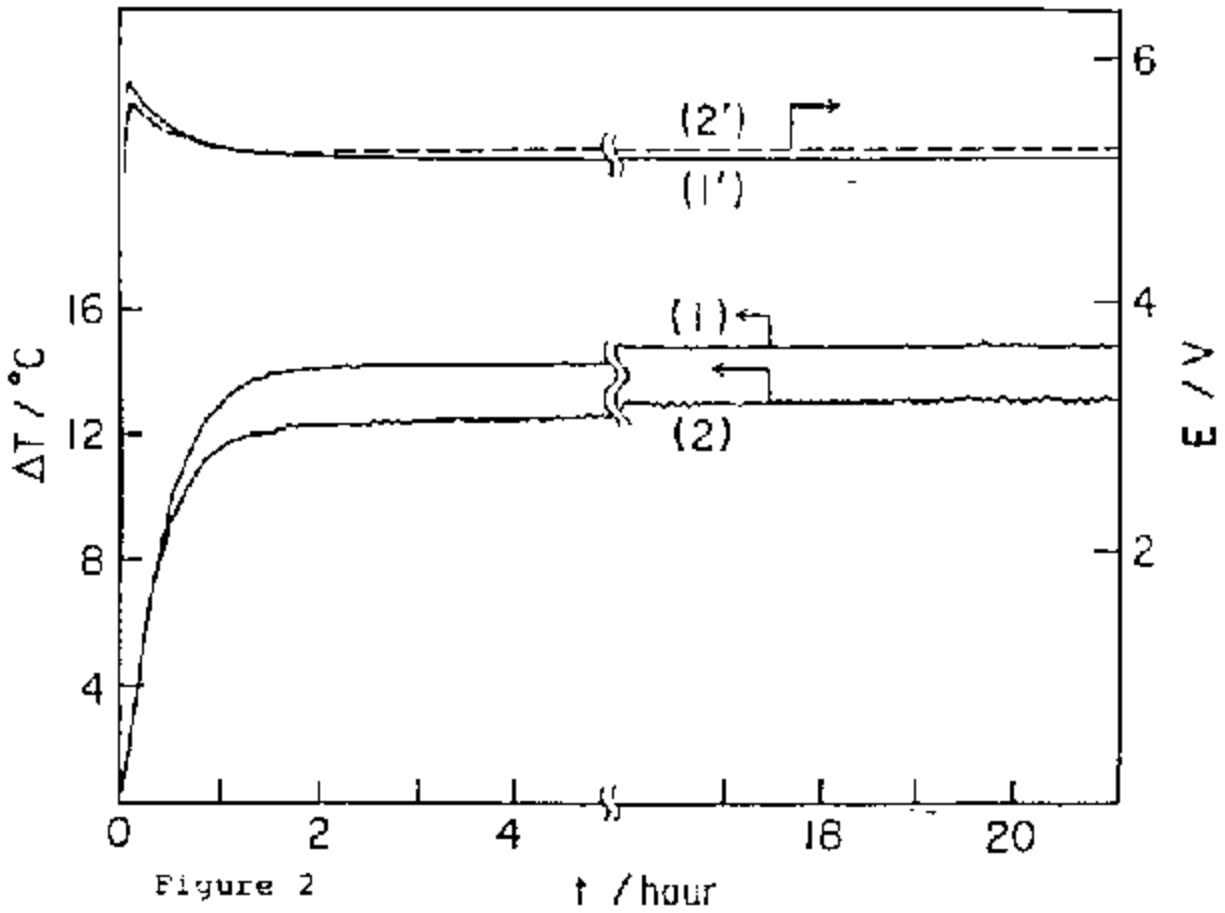

Figure 2

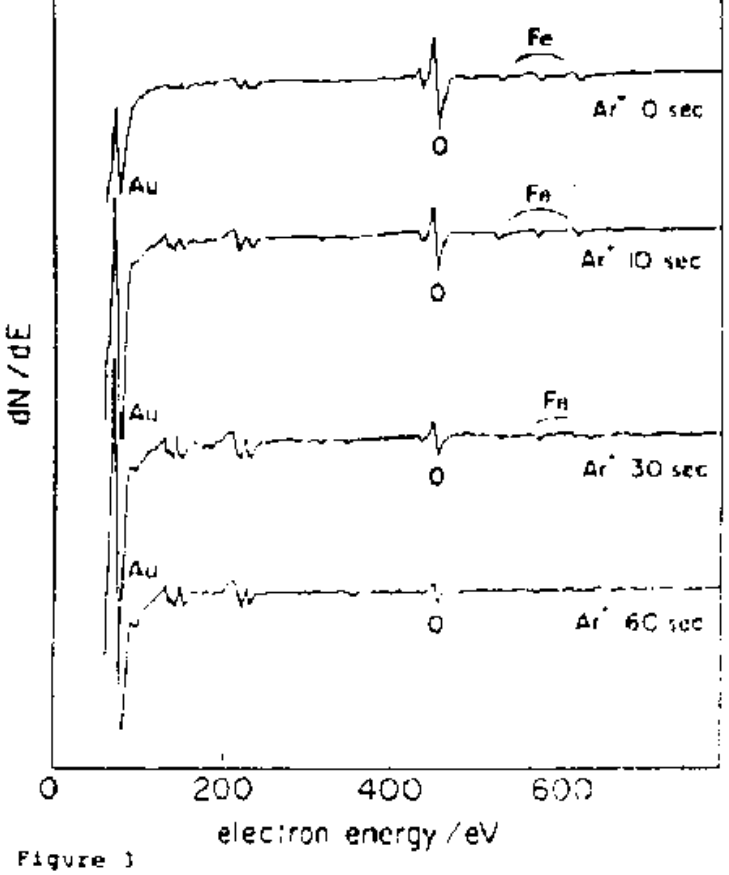

Figure 3

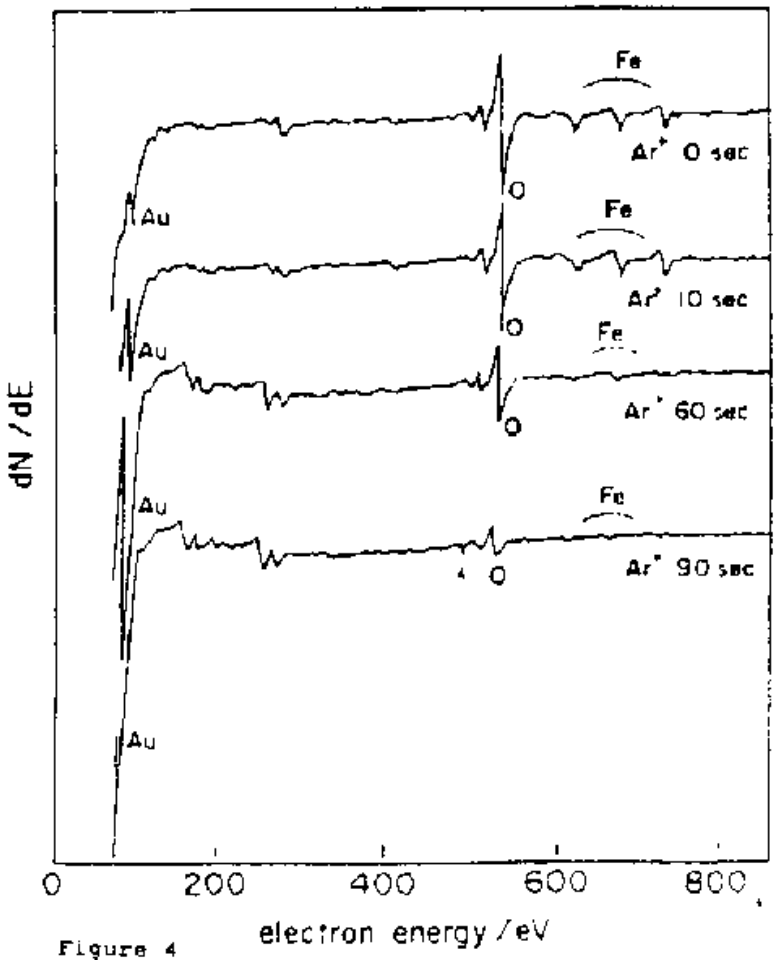

Figure 4

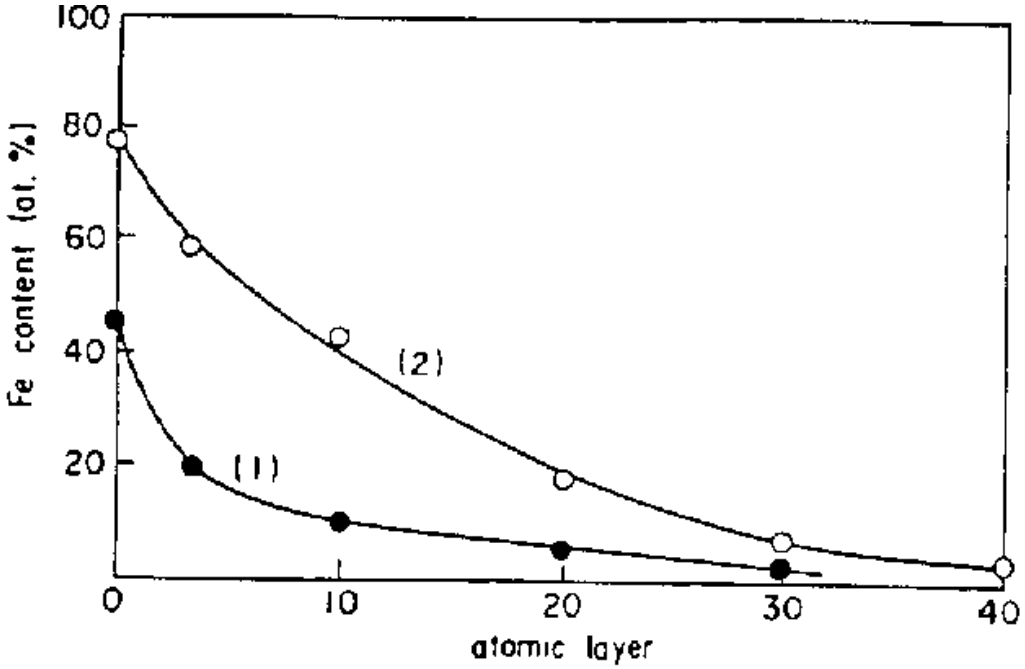

Figure 5

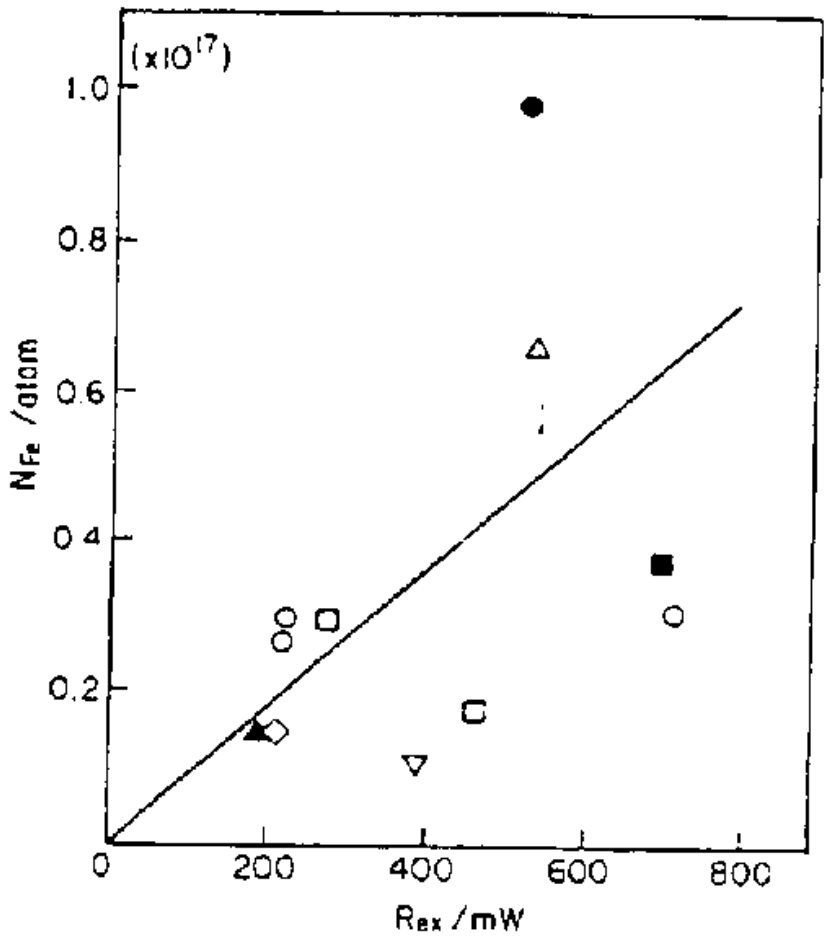

Figure 6

REPRODUCIBILITY OF TRITIUM GENERATION FROM NUCLEAR REACTIONS IN CONDENSED MEDIA

V.A. Romodanov, V.I. Savin, V.V. Elksnin
of SRI of SPA LUTCH
142100 Podolsk, Moscow Region, Zhelenodorozhnaya 24,

Ya.B. Skuratnik
of SRPCI named after Karpov, Obukha 10, Moscow

ABSTRACT

In this work, based on the proposed model, the results of practical activity in the nuclear reactions in condensed media (NRCM) field are given. We also specify the requirements for these reactions and for the selection of the materials to be used for the purpose of obtaining good reproducible results on tritium generation. In addition, we discuss the limits of the main parameters of the ion bombardment by using a glow discharge as an example.

INTRODUCTION

The nuclear reactions in condensed media (NRCM) have been studied more in breadth rather than in depth. As a result, at present reliable results of investigations of practically all types do not much exceed the background. The powerful glow discharge system, that we have used for the similar NRCM investigation, have allowed us to obtain reliable data on tritium and neutron generation and element transmutation [1]. One of the main features of our glow discharge system is the use of higher plasma-generating gas pressures which makes it relatively easy to obtain high flux densities for the deuterium ions bombarding the target sample (cathode).

EXPERIMENTAL PROCEDURE

The design of the plasma-discharge unit and the experimental procedure on tritium detection is similar to that described in [1]. Plates, pipes having the wall of 0.2-5.0 mm thick, and rods having 2-20mm in diameter were used as samples. The samples were mainly made of tungsten and niobium.

DISCHARGE PARAMETER EFFECT ON TRITIUM GENERATION

ION ENERGY. According to the estimated calculations (Table 1, [1]) the optimal interaction energy depends on the matrix material. This energy is about 30 eV for the deuterium medium and reaches 5 keV for heavy elements of Mendeleyev's periodic table. The lower energy range is verified by Fig. 1 [1] and Table 2 in this article. In Table 2 one can see that, when operating in the near-threshold energy range, the tritium generation efficiency (the nuclear interaction coefficient) decreased by about an order of magnitude as a result of some ion energy decrease, in spite of the fact that the current density has increased by a factor of 30. Perhaps, the rapid decrease in the tritium generation efficiency when the ion energy exceeds the model predictions (Fig. 1, [1]) is connected with the fact that according to the experimental conditions the energy increase is accompanied with a density decrease.

Table 1. **NRCM** Efficiency versus Discharge Parameters

Material	Discharge Parameters					Nuclear interaction coefficient, atom.ion^{-1}	Tritium flux. aton.s^{-1}
	Voltage, V	Current density, A.cm^{-2}	Temperature, K	Pressure, 10^3 Pa	Time, h		
1	2	3	4	5	6	7	8
Nb	1560	0.05	1070	20	22	$5.3\cdot10^{-13}$	$2.6\cdot10^{6}$
Nb	1900	0.10	1270	30	23	$5.0\cdot10^{-13}$	$2.7\cdot10^{6}$
Nb	760	0.10	1170	12	162	$3.8\cdot10^{-13}$	$1.0\cdot10^{7}$
Nb	1800	0.20	1670	40	8	$2.5\cdot10^{-12}$	$1.7\cdot10^{7}$
Nb	2100	0.30	1770	50	6	$3.1\cdot10^{-12}$	$2.6\cdot10^{7}$
Nb	1080	2.00	1670	20	6	$7.1\cdot10^{-11}$	$0.8\cdot10^{9}$
Nb	1000	2.00	1670	40	8	$1.2\cdot10^{-10}$	$0.9\cdot10^{9}$
Nb[1)]	820	10.00	1170	20	60	$6.8\cdot10^{-11}$	$1.7\cdot10^{9}$
W[111]	640	0.08	1470	10	20	$6.4\cdot10^{-14}$	$0.7\cdot10^{6}$
W[111]	640	0.08	1270	10	18	$7.3\cdot10^{-14}$	$0.7\cdot10^{6}$
W[2)]	1550	0.20	900	30	44	$1.1\cdot10^{-13}$	$1.5\cdot10^{6}$
W	1200	0.30	1670	40	42	$2.8\cdot10^{-13}$	$4.2\cdot10^{6}$
W	1080	1.00	3500	50	7	$4.8\cdot10^{-12}$	$4.5\cdot10^{7}$
W	800	1.50	3600	65	6	$8.1\cdot10^{-12}$	$8.4\cdot10^{7}$
W[1)]	720	10.00	1500	21	115	$9.1\cdot10^{-12}$	$2.5\cdot10^{6}$
W	800	1.00	1670	20	8	$3.0\cdot10^{-11}$	$2.5\cdot10^{8}$
W	1150	8.00	1670	40	20	$2.5\cdot10^{-11}$	$1.7\cdot10^{8}$

1) - Discharge in the magnetic field
2) - Pulsed discharge

ION FLUX. The nuclear interaction coefficient versus the current density at a slight deviation of the rest of the parameters can be determined from Table 1. The current density increase in the discharge can be optionally accompanied by the NRCM efficiency increase if it results in decreasing the energy of the deuterium ions bombarding the target. In particular, this effect is observed under higher pressures in the near-threshold energy range (See Table 2). According to Table 1, one can consider the current density about 500 Amp.m-2 to be the lower limit to detect the NRCM reliably.

Table 2. **NRCM** Efficiency versus Discharge Parameters at Higher Pressure.

Material	Discharge Parameters: Voltage, V	Current density, $A.cm^{-2}$	Temperature, K	Pressure, 10^3 Pa	Time, h	Nuclear interaction coefficient, $atom.ion^{-1}$	Tritium flux. $aton.s^{-1}$
1	2	3	4	5	6	7	8
W	900	0.2	1070	20	22	$9.4 \cdot 10^{-13}$	$1.1 \cdot 10^{7}$
W[1)]	1300	0.6	1170	40	46	$3.2 \cdot 10^{-13}$	$4.0 \cdot 10^{6}$
W[1)]	2540	2.0	1170	80	115	$1.0 \cdot 10^{-13}$	$1.5 \cdot 10^{6}$
W[1)]	1380	6.0	1170	120	52	$1.6 \cdot 10^{-13}$	$2.5 \cdot 10^{6}$

1) - pulsed discharge

PRESSURE. The plasma-generating gas pressure has an effect on the hydrogen solubility and the mean energy of the ions bombarding the surface. The pressure increase results in increasing the hydrogen concentration in the target and decreasing the mean ion energy. The normal current density in the discharge is proportional to ~ P2 under normal and abnormal conditions that are close-to-normal. Therefore, it is difficult to obtain the required hydrogen atom concentration in the matrix and to provide a sufficient current density under the specific pressure optimum. And under higher pressures the increase in the current density and concentration cannot compensate for the NRCM efficiency decrease by reducing the energy of the ions bombarding the target (Fig. 1). In Fig. 1, one can see that the pressure optimum for molybdenum, tantalum, and tungsten according to the maximum value of the nuclear interaction coefficients is within (20 to 40) x 1000 Pa. For niobium, the optimum is most probably shifted down to (10 to 30) x 1000 Pa.

TARGET TEMPERATURE. As the target is bombarded by the deuterium ions having a minimum energy of tens of electron volts (hundreds of thousands of Kelvins), the target temperature should have a slight direct effect on the NRCM efficiency. However, the temperature has a direct effect on the hydrogen concentration in the target. Therefore, for the hydride-generating materials (niobium, zirconium, palladium, etc.) temperature increases should result in a tritium generation decrease and for the nonhydride-generating materials (nickel, molybdenum, tungsten, etc.) - in tritium increase. The nonhydride-generating materials have the optimal temperature about 0.5 Tmelt (1300-1800°K for molybdenum and tungsten), because temperature increase is accompanied by the exponential thermionic emission increase. The hydride-generating materials also have the optimal temperature.

TARGET MATERIAL AND SURFACE STATE. According to our model [1] two deuterons of Coulomb potential are efficiently shielded by the excited atoms of the target matrix, most probably as a result of some additionally released electrons, which (the deuterons) can generate as quasi-plasma. For example, see reference [2]. Therefore, one can come to two important conclusions. First, the heavy elements will have a higher shielding efficiency because their atoms have more electrons at a lower binding energy except for K-cladding. Secondly, the NRCM area won't exceed the value of the projected ion run path in the condensed media; about (10-1) nm for the energies of about 1 keV. In this case different surface

compositions with lighter elements, e.g. carbides, nitrides or oxides, will considerably cover the NRCM efficiency both by decreasing the hydrogen solubility in the near-surface layer and by reducing the efficiency of Coulomb potential shielding. It is verified by the experiment that where the reverse deuterium countercurrent flows though the wall of the tight sample the foreign material film formation was inhibited at the surface facing the plasma (Table 3).

Table 3. **NRCM** Efficiency versus Deuterium Flux Through the Sample Wall.

Material	Discharge Parameters					Nuclear interaction coefficient, atom.ion^{-1}	Tritium flux. aton.s^{-1}
	Voltage, V	Current density, A.cm^{-2}	Temperature, K	Pressure, 10^3 Pa	Time, h		
1	2	3	4	5	6	7	8
Zirconium	Steady state	820	1070	15	6	$1.7 \cdot 10^{-12}$	$1.1 \cdot 10^{7}$
Zirconium	Deuterium *)	950	1270	30	5	$1.4 \cdot 10^{-11}$	$1.4 \cdot 10^{8}$

*) countercurrent flow, $\Delta P = 60 \cdot 10^3$ Pa

CONCLUSIONS

For the simplest reproducibility of the above-mentioned results one can use the glow discharge of direct current at a deuterium pressure of about 20 x 1000 Pa. One can use either rods having 5-10 mm in diameter or plates 0.2-1.0 mm thick made of molybdenum, tungsten, or niobium as a target sample (cathode). The sample temperature should be kept within 1100-1500°K at the expense of the glow discharge power. In this case forced cooling isn't required. The discharge voltage within 600-1000 V can be additionally controlled by the distance between anode and cathode. Current also depends on the sample dimensions and cooling degree. The value of 1-5 A will be sufficient. We think that if one follows these recommendations, the tritium will be generated at a level of 1,000,000-10,000,000 atoms per second when the efficiency is at least 10 - 14 atoms per ion. Following the above recommendation we have made over 60 experiments during the last year. In all the experiments the tritium fluxes were at a level of 10^{-6} to 10^{-7} atoms per ion, when the nuclear interaction coefficients were at least 10^{-14} atoms per ion for such target materials as niobium, molybdenum, and tungsten.

REFERENCES

[1] V. Romodanov, V. Savin, Ya. Skuratnik and Yu. Timofeyev, "Nuclear Fusion in Condensed Matter," Frontiers of Cold Fusion. Proceedings of the Third International Conference on Cold Fusion. October 21-25, 1992, Nagoya, Japan. Ed. by. H. Ikegami. Universal Academy Press Inc., Tokyo, Japan, 1993, pp 217-229.

[2] H. Hora, J.C. Kelly, J.U. Patel et al., "Screening in Cold Fusion Derived from D-D Reactions," *Physics Letters A*, 1993, vol 175, no 2, pp 138-143.

EXCESS HEAT AND TRITIUM MEASUREMENTS IN Ni-H2O ELECTROLYTIC CELLS

M. Srinivasan@, P. Adi Babu† , M. B. Bajpai*, D. S. Gupta*,
U. K. Mukherjee†, H. Ramamurthy†, T. K. Sankarnarainan*,
A. Sinha@, A. Shyam@

@Neutron Physics Division, *Chemical Engineering Division,
†Process Instrumentation Systems Division
Bhabha Atomic Research Centre
Trombay, Bombay 400085, India

BRIEF DESCRIPTION OF THE CELLS AND CALORIMETRIC TECHNIQUE

A large number of open cell electrolysis experiments of the Mills and Kneizys [1] [and the Bush-Eagleton 16-18] type have been carried out in light water solutions of 0.6M K_2CO_3, 0.1M Li_2CO_3 (natural and enriched in Li^6) and 0.6M Na_2CO_3 using Ni as cathode and Pt as anode, at the Bhabha Atomic Research Centre in Bombay. The cells were fabricated of double walled glass dewars with either vacuum or air between the inner and outer glass vessels. In the more recent experiments there was no silver coating in the dewar, rendering the cells transparent. A variety of nickel samples were tested as cathodes: some were solid nickel foils; others were in the form of porous sheets sintered from fine nickel powder; some cathodes were produced by electrodepositing nickel onto a stainless steel rod and later peeling it off; yet others were in the form of a mesh made of Ni fibres (procured from National-Standard Co., USA as used by Bush and Eagleton [16-18]). While most of the experiments deployed planar geometry for the electrode assembly, a few cells used cylindrical geometry. In some cells a mixture of H_2O and D_2O was used. No external stirrer was employed. However during the electrolysis runs, the vigorous bubbling caused by the escaping H_2 and O_2 gases served to mix the solution well and reduce temperature gradients. Typically a bank of five operating cells and one dummy cell was run at a time. Experiments with a given bank lasted for two to six weeks each. Two type-T copper-constantan thermocouples, either bare or encased in a stainless steel or glass tubing were deployed in each cell for temperature measurements. The difference (ΔT) in average temperature at steady state between the operating cell (T_c) and that of the reference cell (T_{ref}) was taken as a measure of the heat generation in the cell. The accuracy of the differential temperature measurements is estimated to be better than ± 0.5C. The cells were calibrated using resistance heaters. For each cell ΔT was measured at steady state for different input joule powers. The maximum input joule power [(V-1.482) * I] varied from 1.0 to 6.5W depending on the cell design and calibration constant. Cell currents varied from $I \approx 0.1A$ to 1.5A.

Calorimetric measurements have so far been carried out in over 70 cells, since January '92. Results as of October '92 were reported [2] at ICCF-3 in Nagoya and those of the further studies (up to August '93) were presented [3] at ICCF-4 in Maui. A few similar open cell measurements have also been carried out by one of the authors (MS) at SRI International in Menlo Park, [4] California, during the winter of 93-94 employing very sensitive RTDs for the temperature measurements.

As a general observation it was noted that for the results to be reliable, the ambient air and reference cell temperature variations/fluctuations should be much smaller than the ΔT given by (T_c - T_{ref}) being measured. Likewise, the difference in reading between the two temperature sensors of a cell, which is a measure of temperature gradients in the cell, should be << ΔT being measured. It was observed that even minor changes in electrode assembly design, or the height-to-diameter ratio of the solution region of the

cell (this influences the pattern of convection currents), the presence of structural components, if any, which may impede convection induced mixing, etc. can result in unacceptably large (T_1 - T_2) values, giving rise to poor reliability of the ΔT measurements. This aspect was given due attention in cell design as there was no separate mechanical stirrer in our cells.

SUMMARY OF CALORIMETRIC RESULTS

A summary of the main findings of the calorimetric studies is given below:

(1) Of the 70 or so cells investigated to date roughly half have shown "detectable" amounts of "excess power", typically $\leq$ 1.0W with respect to the quantity (V - 1.482) * I. However, the fact that there were indeed many cells which did not indicate any "excess power" and wherein the electrolysis points fell neatly on the calibration line gives us confidence in the validity of the calorimetric technique employed. In the BARC measurements the lower limit of detectable excess power was $\approx$ 0.2W, whereas in the experiments conducted by MS at SRI International, apparent excess power values down to 30mW could be measured because of the use of very sensitive RTDs for temperature measurements. On the other hand the maximum excess power observed at SRI was only $\approx$ 0.2W; possible reasons for this are being examined.

(2) The "excess power" expressed as a fraction of the input joule power varied between 10% and 110%. In most cases the percent "excess power" diminished with increasing input power.

(3) In the majority of the cells investigated, the absolute "excess power" was almost constant above a threshold value of input power which varied from 0.15W to $\approx$ 0.6W. In the more recent desilvered flask experiments at BARC the electrolysis runs did not scan the region below about 1.0 to 1.5W; hence we do not know where the threshold for "excess power" was in these runs. In these new cells the electrolysis data points fell on a line nearly parallel to the calibration line.

(4) Neither a Ni-Ni cell nor a Pt-Pt cell has ever indicated any "excess power" in our experiments so far.

(5) In most cases, if any "excess power" was present, it was detectable on the very first day of commencement of electrolysis. If the electrolysis was interrupted for a day or two for a heater calibration run and resumed subsequently, the "excess power" reappeared once again. The "excess power" episodes (with interruptions for heater calibration runs) have been observed for up to 6 weeks.

(6) In some cells if no "excess power" was observable within the first few days, subjecting the Ni electrode to high current anodic stripping (electrolysis with reversed voltage at a current of $\approx$ 1 to 2 amps for a period of 10 to 24 hours) resulted in appearance of some "excess power", lasting for days to weeks thereafter.

(7) Likewise in other cells not showing "excess power", taking the electrode assembly out and having it cleaned for a few hours in an ultrasonic cleaning bath (under distilled water) had a similar beneficial effect. However, unfortunately for us, these procedures did not always succeed in switching on a "dead" cell.

(8) One of the remarkable observations was the role of certain additives on the "excess heat" phenomenon. For example when the PVC sheathed copper-constantan thermocouples with bare junction exposed to the electrolyte which were used for temperature measurements were replaced by similar thermocouples encased in stainless steel tubes, none of the cells showed "excess heat". But the moment we went back to the bare copper-constantan thermocouples or used glass encapsulated TCs, the "excess

heat" reappeared. We conclude that stainless steel is a "poison" (or inhibitor) and copper a promoter for the "excess heat" phenomenon, whatever its nature may be.

In this context it is significant to point out that the "success rate" of observing "excess heat" which was over 90% in our Nagoya paper [2] dropped to about 50% in the results reported at Maui. [3] The former cells used copper-constantan thermocouples with their bare hot junction dipping directly into the electrolytic solution while the latter cells employed glass encapsulated TCs. (It was verified by using mercury in glass thermometers that the temperature measurements of the bare thermocouples was genuine and not due to some electrochemical artifact).

The beneficial effect of adding small quantities of copper was pointed out by R. Bush of the California State Polytechnic University, Pomona at the Maui meeting. Addition of trace amounts of copper in the form of cupric nitrate crystals into his electrolyte, significantly improved the excess heat margin in their Ni-H_2O cells. After the Maui meeting Bush's suggestion of adding copper directly into the electrolyte was tested during January '94 in two K_2CO_3 cells at BARC. In both these cells there was a dramatic increase in the "excess power" margin from about 10% level to ≈ 50% level after copper was added in the form of cut wire pieces. One of these cells (with Fibrex t.m. Ni cathode) has shown an excess power margin of 2W at an input electrolytic joule power of 4W. Similar copper addition tests in several cells carried out by MS at SRI however did not show any improvement in raising "excess power" levels.

(9) Some cells which showed "excess power" in the BARC experiments used a parallel plate electrode arrangement with a Pt foil anode on one side of the Ni foil cathode (interelectrode gap ≈ 8 mm) instead of the normal Pt wire anode wound around a central Ni cathode. Similarly "sandwich" type electrode assemblies wherein a planar Ni electrode is sandwiched between a pair of perforated teflon plates and bound tightly by means of a Pt wire anode coil have also shown "excess heat" in several cells.

(10) Finally, a remark may be in order regarding the use of anodic operation of the nickel electrode for purposes of cell calibration. We often find that the ΔT points in such runs fall below the heater calibration curve. However, in several other runs these "reverse electrolysis" points fall close to or on the heater calibration line. The reason for this behavior has not yet been understood.

TRITIUM MEASUREMENTS

At the Nagoya meeting we reported [2] that more than 50% of the cells analyzed showed tritium at levels of ≥ 10 Bq/ml. Observation of tritium even when the electrolyte did not contain any D_2O (other than natural abundance) was a surprising new finding which has been met with considerable skepticism. We ourselves would have had less faith in these results were it not for the fact that at least one cell (Cell # OM-3 with 54% Li^6 enrichmetn and with Li_2CO_3 solution in H_2O) which was sampled, distilled and counted every few days showed a steadily increasing tritium activity reaching a maximum value of 225 Bq/ml, at the end of about a month (See Figure 8 of our Nagoya paper [2]). The tritium results reported at Nagoya were from the analysis carried out at the Isotope Division of BARC which handles tritium samples of varying strengths received from other research groups of BARC also. There is therefore scope for suspicion that cross contamination could have occurred during distillation/counting of samples there. This is one of the reasons why we reported tritium results only above a rather high value of 10 Bq/ml, at that time. The background count rate in the scintillation counting set up used therein was ≈ 48 cpm which corresponds to ≈ 3 Bq/ml, since counting efficiency was ≈ 28%.

In order to avoid any likelihood of cross contamination, we acquired (in May '93) a new low noise liquid scintillation counting set up, exclusively for the analysis of our electrolysis samples. This equipment has been installed in a laboratory where no other tritium or radioactivity is handled. This unit has a background count rate of ≈ 27 cpm equivalent to a tritium activity of ≈ 2 Bq/ml (or 120 dpm/ml). This

new set up is found to be capable of detecting tritium levels in the electrolyte down to 0.5 Bq/ml (≈ 30 dpm/ml). The tritium results reported [3] at ICCF-4 in December '93 were obtained using this new set up. Prior to loading any cell with electrolyte it was ensured, to begin with, that the electrolytic solution does not contain any tritium contamination. The main findings (during May-August, '93) regarding tritium production in Ni-H_2O cells, as reported at the Maui meeting, are as follows:

(a) 10 out of 23 (roughly 40%) of the Ni-H_2O cells analyzed showed tritium.

(b) No preference is seen for T-production, with respect to electrolyte type, H_2O vs. D_2O, natural vs. enriched Li, or type of Ni cathode material.

(c) The maximum amount of tritium measured in the post Nagoya experiments is only ≈ 200 dpm/ml (≈ 3.5 Bq/ml).

(d) Electrolytic enrichment of the tritium isotope cannot account for the tritium observed by us, since the currents were < 1.5 amp, temperatures of cell operation above ambient, and addition of make up water was carried out frequently.

(e) Surprisingly the tritium activity of the electrolyte in several cells was found to vary in a sawtooth fashion. Close scrutiny of the sampling/distilling and counting techniques, in conjunction with several auxiliary measurements, strongly suggests that the tritium level in the electrolytic solution actually increased and decreased, and that it was not a measurement artifact or experimental error. While a sudden sharp increase of tritium activity can be understood as a production (or burst) phase, the decreasing phase lasting for tens of days at times, cannot be accounted for easily. We are thus forced to conclude that there is a strong as yet unidentified mechanism cleansing the electrolyte of tritium periodically. It could be an electrochemical adsorption/desorption phenomenon on the nickel cathode surface.

DISCUSSION AND CONCLUSIONS

Excess power measurements in open Ni-H_2O cells have also been carried out by at least five other groups so far, namely Noninski [5], Notoya [6,7], Ohmori and Enyo [8,9], Criddle [10,11], and Bazhutov et al. [12] besides the originators of this concept, namely Mills et al. [1,13]. There has however been persistent criticism/suspicion that the "excess heat" in open cells could be due to recombination effects. At BARC, early on, we did carry out Faraday efficiency measurements in some cells by measuring the volume of electrolytic gases evolved and found it to be > 95% but since our excess heat margins were up to 70% or even 100% at times, we concluded that recombination effects cannot account for the excess power reported by us. Until now we have not carried out any Faraday efficiency measurements simultaneously with calorimetry to confirm that Faraday efficiency is close to 100% in a heat producing cell. Also the fact that we have never measured excess power over and above V*I in any of our open cells has led to suggestions that recombination/leakage current effects need to be addressed by us.

Recently J. E. Jones et al. [14] of Brigham Young University, Provo, Utah and Zvi Shkedi et al. [15] of Bose Corporation, Massachusetts, have reported measuring Faraday efficiency simultaneously with calorimetry and claim that the apparent excess power in their open Ni-H_2O cells can be accounted for by recombination effects. Of these, the Jones experiment was carried out at such low currents (0.96 mA to 8.08 mA) and power levels (< 11 mW) that they are not perhaps particularly relevant to the higher current regimes (> 100 mA) of most other open cell experiments. At very low currents there are competing electrochemical phenomena which come into play and which need to be considered to interpret Faraday efficiency measurements. However the Bose experiments were at a current of 0.35 amps (cell voltage ≈ 3V). They measured the mass of water reformed in a separate test tube containing Pt catalyst, into which

the electrolytic gases were directed. Since the amount of water reformed was less (by ≈ 30% to 40%) than that expected on the basis of coulombs passed (≈ 1 ml of water is expected from 3 Ah of charge passed), by precisely the quantity that could account for the excess power (30% to 40%) measured in their open cells, they conclude that the apparent excess power in their cells could be accounted for by recombination or leakage current effects within the cells. However, it is instructive to note at this point, that Mills et al. find that in their Ni-H_2O cells with K_2CO_3 solution which generate excess power, while the Faraday efficiency measured from gas production was close to 100% (see Table III of Ref. 13), "The combustion of the gases . . . . . was incomplete" (see p. 118 of Ref. 13), supposedly due to formation of "dihydrino molecules", which do not combine with oxygen.

The crucial test in open cells therefore appears to be to perform simultaneously calorimetry, measurement of masses of water lost due to electrolysis and water reformed catalytically in an adjacent vessel. There are three possible outcomes: If recombination were the source of excess power, mass of water lost would be equal to the mass of water reformed but both will be less than the Faraday value. On the other hand if the excess power were of nuclear origin, mass of water lost from cell will be equal to that reformed and both will correspond to the Faraday value. In contrast if Mill's dihydrino molecule formation theory were valid, mass of water lost will correspond to the Faraday value but mass of water reformed will be much less in the case of a heat producing cell. It would be advantageous to also measure the rate of evolution of electrolytic gases in order to have an independent check on the Faraday efficiency. Such experiments are currently underway at SRI International with a view to resolving some of these issues.

The other approach is to carry out closed cell experiments, although Mills et al. seem to indicate that according to their theory of compact hydrogen atom formation, excess heat will not be observable in closed cells. On the other hand, if the excess heat is nuclear in origin as Robert Bush has suggested, closed cell experiments should indicate excess heat unambiguously. Further the excess heat should probably not depend on whether carbonate or hydroxide is used or whether the alkali salt is of Na, K, Rb or C_s. Bush and Eagleton [16] are perhaps the only group to date to have carried out extensive calorimetric studies in Ni-H_2O systems using closed cells. They have experimented with over 30 cells during the period August '91 to February '94 [17]. Bush was the first to propose and present experimental evidence to suggest that the light water excess heat effect is of nuclear origin. An elegant overview of the Cal Poly work [18] traces the historical evolution of Bush's concept that the excess heat in these light water cells is due to nuclear transmutation reactions involving a proton (from H_2O) and an alkali metal atom of the electrolyte such as K, Rb or Cs. So far Notoya and Enyo [6] are the only other group who have provided experimental support to Bush's theory that in a K_2CO_3 cell Ca is being formed from potassium.

The other evidence indicating that some nuclear phenomenon is indeed occurring in these cells is the detection of tritium in the electrolyte by the BARC group. As discussed earlier in this paper, Notoya [7] has since also presented evidence that tritium is formed in some of their Ni-H_2O cells. Interestingly however neither Bush and Eagleton [17] nor Bazhutov et al. [12] detected any tritium in their cells in spite of careful analysis of the electrolyte samples. The open cell experiments conducted by MS at SRI have also not shown any tritium to date. [Readers should consider the concept of the tritium desert mentioned by R.T. Bush. See papers by both R.T. Bush and Eagleton in this volume. Ed.]

In conclusion, it thus appears that further carefully planned experiments are warranted in both open and closed cells to definitively settle the issue of the origin of the apparent excess power in Ni-H_2O cells. The question of tritium production also needs to be independently verified.

REFERENCES

1. Mills, R. L. and Kneizys, K., *Fusion Technol.*, vol 20, p 65 (1991).
2. Srinivasan, M. et al., Frontiers of Cold Fusion, Universal Academy Press, Inc., Tokyo, pp. 123-128 (1993).
3. Ramamurthy, H. et al., Paper # C 3.8 presented at ICCF-4, Maui, (Hawaii), December 6-9, 1993.
4. Srinivasan, M. et al., Internal Note, SRI International, Menlo Park, California, March 1994.
5. Noninski, V., *Fusion Technol*., vol 21, p 163 (1992).
6. Notoya, R. and Enyo, M., Frontiers of Cold Fusion, Universal Academy Press, Inc., Tokyo pp 421-426 (1993).
7. Notoya, R., Paper # N 2.1 presented at ICCF-4, Maui (Hawaii), December 6-9, 1993.
8. Ohmori, T. and Enyo, M., *Fusion Technol*., vol 24, pp 293-295 (1993).
9. Ohmori, T. and Enyo, M., Paper # N 2.3 presented at ICCF-4, Maui, (Hawaii), December 6-9, 1993.
10. Criddle, E. E., Frontiers of Cold Fusion, Universal Academy Press, Inc., Tokyo, pp 417-420 (1993).
11. Criddle, E. E., Paper # M 2.9 presented at ICCF-4, Maui, (Hawaii), December 6-9, 1993.
12. Bazhutov, Yu. N. et al., Paper # C 4.3 presented at ICCF-4, Maui, (Hawaii), December 6-9, 1993.
13. Mills, R. L. et al., *Fusion Technol*., vol 25, pp 103-119 (1994).
14. Jones, J. E. et al., Brigham Young University, Provo, Utah, Preprint, 14th October, 1993.
15. Shkedi, Z. et al., Preprint dated March '94 (to be published).
16. Bush, R. and Eagleton, R., Paper # C 3.6 presented at ICCF-4, Maui, (Hawaii), December 6-9, 1993.
17. Bush, R. and Eagleton, R., Summary Report of Work Done at Cal Poly During January 1990 through July 1993, (unpublished).
18. Bush, R., *21st Century Science and Technology*, Fall 1993, pp 75-79.

UPGRADE OF THE FERMI APPARATUS WITH DETECTION AND IDENTIFICATION OF PROTONS IN THE 3 MeV ENERGY REGION.

F.F. Kayumov, B.N. Lomonosov, G.I. Merzon,
D.I. Minasyan, V.A. Tsarev
P.N. Lebedev Physical Institute, Russian Academy of Science,
Leninsky Prospekt 53, Moscow - Russia; Dipart. di Fisica Università di Roma III
at Univers. "La Sapienza", Roma; INFN Roma 1 - Italy

A. Asmone, M. Corradi, F. Ferrarotto,
B. Stella
INFN Roma 1 and Dipart. di Fisica Univ. Roma III,
Università "La Sapienza," P.A. Moro 2, 00185 Roma - Italy

F. Celani, A. Spallone, P. Tripodi
Lab. Naz. INFN - Via E. Fermi 40-00044 Frascati (Roma) - Italy

ABSTRACT

The FERMI apparatus is mainly a neutron moderator-detector developed for cold fusion research, situated in the Gran Sasso INFN underground laboratory. It has 40%-8% detection efficiency for neutrons in the range 1 keV-20 MeV (25% at 2.5 MeV), low background, pulse shape acquisition and good time resolution for neutron bursts; it also allows us to perform a good reconstruction of the average original neutron energy. Gamma rays are revealed mostly by a complementary low background NaI detector with a 26% solid angle coverage. The performances are controlled by a full MC simulation, experimentally tested.

The samples are put in the central axial gap. Aside, close to the sample (a specially designed electrolyzer with a thin Pd cathode/wall), two MWPC's and a CsI scintillator provide charged particles detection, dE/dx and E measurement, with identification of protons (hadrons) in the region of 3 MeV. The performances are tested with α particles, giving ~10% FWHM for each of two MWPC and 20% for the scintillation counter (25% and 15% respectively are expected for protons). A three-fold coincidence with very low background drives the data acquisition for charged hadrons.

INTRODUCTION

The FERMI apparatus is described elsewhere [1] and has been summarized in the abstract of this paper. Previous research activities of the FERMI collaboration are listed in [2]. Here we will only describe the upgrading with a multiple detector specially designed for protons of the dd→pT fusion reaction.

THE PROTON SYSTEM

The charged particles detectors (Fig. 1) consist of two multiwire proportional chambers (MWPC), filled by 95% He + 5% CH_4, and a CsI scintillating counter. Protons (or other hadrons) coming from a palladium foil, through a cellular brass collimator of 5 mm thickness (cells diameter being 2.7 mm drilled with 3 mm steps), pass through MWPC's (each being 9 mm thick) and stop in the CsI crystal (1 mm thick). In this way the pulse height of the two MWPC give the dE/dx of the particles and the CsI photomultiplyer provides their residual energy.

A permanent calibration of the system is provided by a ^{241}Am α particle source (of $\approx 10^{-1}$ per minute intensity) placed outside the detector. Alpha particles pass into detector through 7 μm mylar window (or 4-6 μm aluminum) in the same plane of the Pd foil, and through a collimating hole (3 mm diameter, 14 mm length) drilled in the Al body of the MWPC with declination angle of 45 degrees.

Threefold coincidence trigger (WC1*WC2*CsI) reduces the proton-like background records down to <0.04 per hour (no protons for 24 hours observation).

A typical plot of energy losses in MWPCs versus energies measured in CsI for alpha particles is shown in Fig. 2 (in arbitrary units). For 5.5 MeV initial energy of α's, they are expected to have ≈2.2 MeV at the entrance of CsI.

A calibration (with a slightly different gas) was performed by use of alpha particles from a ^{238}Pu source of $\approx 10^{-2}$ per second intensity. In this way the resolution was found to be ≈10% FWHM for each of two MWPC and 20% for scintillation counter (25% and 15% respectively are expected for protons in the same energy region). In addition to alpha particles from source, we have observed with the present gas the weak proton flow of 1 per hour intensity when alpha particles pass through mylar window (Fig. 3). This proton flow is to be referred mainly to elastic scattering of alpha particles on hydrogen in mylar ($C_5H_4O_2$), as we have demonstrated by doubling the thickness of the mylar window. It provides a handy proton source for calibration, with approximately the same end energy of the spectrum as one expected from cold fusion, but for obvious background reasons it cannot be used for permanent calibration when searching for cold fusion protons. We will use an aluminum window instead, available at the same time in another hole of the detector.

In the last conditions the proton background is found to be ≈1/day, if we exclude background contributions (the few points in the corner of Fig. 3 are due to noise from pulse generator and have been subtracted off line). Without an alpha source the α particle background is found to be ≈1/hour in the outside laboratory.

The special electrolyzer is made of teflon (Fig. 4). Outside surface of Pd sample (of 100 μm thickness or less) is covered by silver (of 1-5 μm thickness) to prevent deuterium leakage from the sample. Electrolyzer and proton detector are coupled so that emitted protons leave the sample and immediately pass into detector without crossing any material excluding silver coating.

MWPC occurs to be very sensitive to hydrogen leakage: its signal amplitude sharply depends on the fractional hydrogen content in the gas mixture. Several coatings were investigated to find the appropriate one (surface coated by mercury amalgama, poisoned by iodine, coated by vacuum evaporation of 800 Angstrom gold and others).

Time dependencies of mean MWPC signal amplitude from alpha particle source are shown in Fig. 5 for three samples: a) the one covered by ≈5 μm silver; b) pure palladium sample; c) the one covered by palladium oxide.

Deuterium loading of the palladium sample is performed by use of current pulse generator analogous to the one presented in this book by Celani et al. Electrolyte used is 0.3 M LiOD solution in heavy water. Current pulse amplitude goes from 15 A up to 100 A on 5 KHz frequency.

Electrolyte level is controlled by capacity sensor and peristaltic pump. Capacity sensor consists of two teflon wires, immersed into electrolyzer, the electric capacity depending on electrolyte level. The electrolyte level control (computerized) is available with ±1 mm accuracy and automatically drives the peristaltic pump.

CONCLUSIONS

The proton system is still being developed. A first experiment will be running at the time of the conference. Once assembled together with the existing detector, the full FERMI system will have the possibility to detect multiple correlations of neutrons, gammas, protons, alpha particles, tritium, thermal effects and deuterium loading. Search for ^{4}He could be possible in the future.

REFERENCES

[1] B. Stella et al., "The FERMI Apparatus," Proceedings of the Rome Workshop on the Status of Cold Fusion in Italy, Univ. di Roma III, 14-16 Feb. 1993, pp 25-41. (Dip. di Fisica, P.A. Moro 2, 00185 Roma)

B. Stella et al., "The FERMI Apparatus: a high efficiency, low background neutron and gamma detector for cold fusion experiments," Submitted to *Nuclear Instruments and Methods A*.

[2] B. Stella et al., "Evidence for Stimulated Emission of Neutrons in Deuterated Palladium," Frontiers of Cold Fusion (ed. H. Ikegami, Universal Academy Press, 1993, p 437), Proceedings of ICCF3, Nagoya, Japan, 21-15 Oct. 1992.

M. Alessio et al., "Measurement of Tritium, Neutrons, and Gamma Rays Produced in an Electrolytic Pd-D Experiment," Proceedings of the Rome Workshop on the Status of Cold Fusion in Italy, Univ. di Roma III, 14-16 Feb. 1993, (ed. by B. Stella) pp 93-109.

M. Corradi et al., "Excess of Neutrons Coming out of Deuterated Palladium Samples Irradiated by Prevalent Thermal Neutrons," ibid. pp 110-125.

ALTERNATIVE ENERGY SYSTEMS AND SUPPORTING TECHNOLOGY

The following papers report on a variety of topics: alternative energy systems, technology in support of new energy systems, and sonoluminescense. Recently, Julian Schwinger suggested that sonoluminescence is caused by a bubble of vapor being compressed by Casimir forces and thereby **extracting energy from the Zero-Point Energy** that fills all space.

Zero-point energy may also be the source of energy for the excess heat apparently produced by Griggs in his specially-designed Hydrosonic pump. The explanation advanced by this editor is that cavitation bubbles can also be compressed by Casimir forces as explained by Schwinger and result in the production of anomalous heat.

Tewari tells us about another enhanced energy device which obtains anomalous amounts of energy. The explanation again is that this rotating device may be tapping the energy of space. For those who are skeptical about extracting energy from the environment around us, it is suggested that they read the papers of Boyer, Wheeler, and especially the papers of Harold E. Puthoff.

We also welcome the reports of devices that will advance the conversion of thermal to electrical or mechanical energy in the papers that follow.

SEMICONDUCTOR THERMAL-MECHANICAL ENERGY CONVERTER

L.P. Bulat, V.S. Zakordonets
Ternopil Mechanical Engineering Institute
Ruska St. 56, Ternopil 282001, Ukraine

ABSTRACT

Among unusual autonomous systems for conversion of energy, the most interesting is the conversion of low potential thermal energy into mechanical energy. That is why such sources of energy are practically inexhaustible and ecologically clean.

DISCUSSION

References [1,2] describe thermoelectric motors (TEM) where an interactional principle of thermoelectric currents appearing in a conductor is used. The conductor can revolve on its axis in a magnetic field. However, because of low efficiency and some imperfection in construction, this kind of motors is not used. As comparative analysis has shown, the best prospect from the energetic point of view could be converters which make use of the advantages of short-circuited [3,4] thermoelectric generators (under small differences of temperatures 0T).

We propose that a short-circuited thermoelectric converter of thermal energy into mechanical one can be produced [5]. See Fig. 1. In cylindrical frame (stator) on the conducting axis in a magnetic field (not in the figure) there is a ferromagnetic disk (rotor). Electric current is generated by thermoelectric battery. The electric current goes to the axis (see the arrow and *i* on the drawing) from the current conducting busbar and through the liquid metal contact to rotor and spreads around the rotor radially. Owing to Ampère's forces, the rotor will pivot around its axis.

The motor work in stationary regime as can be described with the help of Maxwell's equation [6] and the generalized law of electrical conductivity [3] See equations (1), (2) where $\vec{E}$, $\vec{B}$, and $\vec{j}$ are the electric field, magnetic and current density respectively, σ, α are coefficient of electrical conductivity and the Seebeck coefficient.

$$rot\ \vec{E} = -\frac{d\vec{B}}{dt}, \tag{1}$$

$$\vec{j} = \sigma\ \vec{E} - \sigma\alpha\ \nabla T, \tag{2}$$

Using the expressions (1) and (2) and integrating around the circuit a-b-c-d (Fig. 1) to compute the mechanical power of the converter we obtain equation (3)

$$P = \frac{(\alpha_{pn}\,\Delta T)}{r_{pn}\,(1+\rho)}\,S(1-S), \tag{3}$$

where $\rho = r_0/r_{pn}$, α_{pn} and r_{pn} are Seebeck coefficient and the electrical resistance p-n thermocouple, r_0 is a summary result of rotor resistance, liquid metal contact, and current conducting busbar; $S = (n_{max}$ -

n) /n_{max} is sliding, n is rotor rotation frequency, n_{max} is rotor rotation frequency under idling.

Maximum power of converter is obtained when S = 1/2 and it is given by equation

$$P_{\max} = \frac{(\alpha_{pn} \Delta T)}{4 r_{pn} (1 + \rho)} . \tag{4}$$

Using (4) for the electromagnetic moment one can obtain

$$M = \frac{1}{2\pi} \frac{\alpha_{pn} \Delta T \Phi}{r_{pn} (1 + \rho)} S, \tag{5}$$

where Φ is the magnetic flow going through rotor of the motor.

Obviously, the maximum moment (5) is reached under regime of short circuit, where S = I. For rotation frequency of rotor we have the fundamental expression

$$n = \frac{\alpha_{pn} \Delta T}{\Phi} (1 - S), \tag{6}.$$

This expression reaches maximum value under idling (where S = 0).

Using a calculation method for the efficiency of thermoelectric generators [4] for efficiency of converter we get

$$\eta = \frac{\Delta T}{T_1} \frac{S(1 - S)}{(z_c T_1)^{-1} + S + S^2 (\Delta T / 2T_1)} , \tag{7}$$

where $z_d = z_n (1 + \rho)^{-1}$: is a thermoelectric figure of merit of the p-n couple [3] $z_m = \alpha_{pn}^2 / [(æ_p / \sigma_p)^{1/2} + (æ_n / \sigma_n)^{1/2}]^2$. T_1 - is hot junction temperature.

The maximum efficiency of the motor is reached when $S = S_0$ and is given by

$$\eta_{\max} = \frac{\Delta T}{T_1} \frac{1 - 2S_0}{1 - S_0 + S_0 T_2 / T_1} , \tag{8}$$

where T_2 is the cold junction temperature,

$$S_0 = \frac{1}{(z_d T_a + 1)^{1/2} + 1} . \qquad T_a = \frac{T_1 + T_2}{2} . \tag{9}$$

We have come to the conclusion that using typical thermoelectric materials based upon Bi-Sb-Te-Se working under a mid-range temperature of about T =300°K and under temperature difference of about 0T = 20°K, the efficiency of converter is only several percent. It is approximately five times less than the thermodynamic efficiency of an ideal reversible engine under the same temperatures. The efficiency of converter will increase with and increase in the temperature difference and, of course, if the thermoelectric

characteristics of materials can be improved.

In addition to power application in autonomous systems, this suggested converter can be used for making autonomous counter measurements of thermal energy.

REFERENCES

[1] F. Peters, Thermoelemente und Thermosoulen, Halle, 1908, 184s
[2] B.S. Pozdnyakov, E.A. Koptekov, Thermoelectric Energy Production. Moscow, 1974, 264 pp.
[3] L.I. Anatychuk, Thermoelements and Thermoelectric Devices, Kiyev, 1979, 768 pp.
[4] A.S. Okhotin et al., Thermoelectric Generators. Moscow, 1976, 320 pp.
[5] V.S. Zakordonets V.S. Author's certificate of USSR No 1670723 (1991).
[6] I.P. Kopylov, Electrical machines. Moscow, 1986, 360 pp.

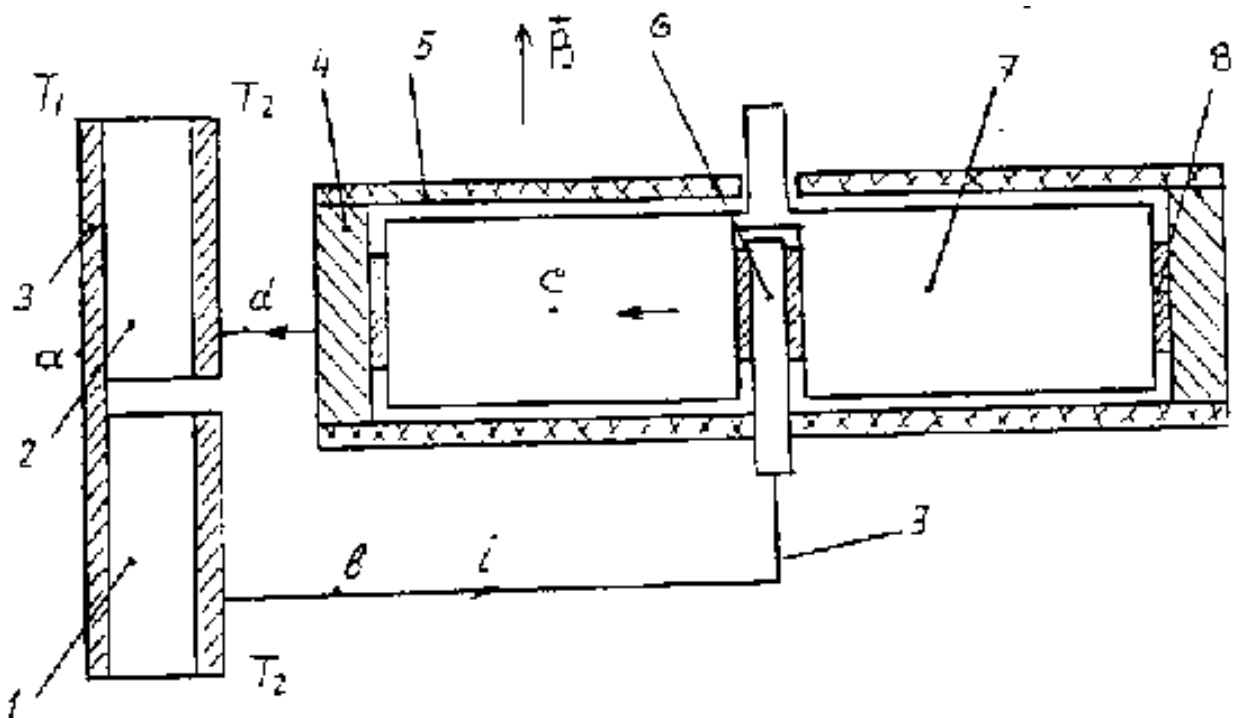

Fig. 1. Scheme of thermal-machanical energy converter.
1 - Thermoelement branch p-type; 2 - thermoelement branch n-type; 3 - Current conducting busbar;
4 - stator; 5 - insulator; 6 - axis; 7 - rotor; 8 - liquid metal contact.

THE DESCRIPTION OF SELF-OSCILLATION PROCESSES OF ENERGY TRANSFER-CONVERSION AS A LINEAR APPROXIMATION

A.V. Bulyga
Institute of Physico-Chemical Problems, Belarussian State University
Leningradskaya 14, Minsk 220080, Belarus.

A.G. Shashkov
Luikov Heat and Mass Transfer Institute, Belarus Academy of Science
P. Brovki 15, Minsk, 220728, Belarus.

ABSTRACT

It is pointed out that the partial direct energy conversion transported by heat conduction in heavily non-equilibrium systems which are characterized by the unattainability of local thermodynamic equilibrium in them is possible. The methods of description of this complex process with the help of the bounds of the applicable law and the expediency of their combined use are emphasized. With heat conduction in non-equilibrium systems taken as an example, one can show the possibility of adequate substitution of the nonlinear heat transfer equation with a limited velocity for a linear differential equation of a higher order. This equation is based on a wider use of dynamic laws which gives the opportunity to describe the complex processes of energy transfer-conversion with the help of a simpler theory.

INTRODUCTION

Development of a new energy source, including those based on the cold nuclear fusion phenomenon, is closely connected with solution of the problem of energy transfer, in particular, by heat conduction, accompanied by energy dissipation. Apparently heat conduction processes are most logically investigated in the book [1] devoted to heat propagation with a finite rate. However, with highly intensive transfer processes in non-static systems in which local thermodynamic equilibrium becomes unfeasible [2], energy is transferred not only as heat but as some other forms, for example, as a mechanical displacement work or electric current. These transfer-conversion processes are typical of direct energy conversion into the work of random types. This conversion is possible, for example, with the help of thermionic converters [3,4]. In these cases modern energy transfer and conversion theories are based on the idea that statistical laws (SL), determining ambiguous causal relationships in structurally complex many-particle systems play the main role. As for dynamic laws (DL) which can, together with the given initial conditions, correctly predict all subsequent states of global non-equilibrium systems, they are given a secondary part.

Indeed, though DL are comparatively simple and easily understood to be physically interpreted, it is evident that to also interpret SL is impossible mainly because it is difficult to adequately take into account the fact that in open structurally complex systems there come into being qualitatively new states and the tendencies for their development. That is why when describing complex phenomena in macroscopic, multi-particle systems one can consider DL to be only approximate. On the other hand, the non-ambiguity of DL affirms their heuristic value. In connection with this, the methods of solving complex problems of energy transfer and conversion which are based on the use both of SL and DL prove to be most effective. Depending on the character and specific aims of the problems being solved, the boundaries between SL and DL can be markedly different.

PURPOSE

The purpose of this paper is to try to show the possibility of formulating linear differential equations for description of the self-oscillating process of energy transfer-conversion in heavily non-equilibrium systems of neutral and charged particles. The realization of such a possibility depends on the use mobility of the boundaries between SL and DL, at which nonlinear effects responsible for self-oscillations are taken into consideration by increasing the order of the differential equations. The best known example of the combined use of SL and DL is the method of solution of the Boltzmann integro-differential equation [5]

$$\frac{\partial f}{\partial \tau} = - \frac{\vec{p}}{m_0} \vec{\nabla}_r f - \vec{F}^* \vec{\nabla}_p f + \left(\frac{\partial f}{\partial \tau} \right)_{col}, \qquad (1)$$

by its linearization and presentation in the relation form

$$\frac{\partial f}{\partial \tau} = - \frac{\vec{p}}{m_0} \vec{\nabla}_r f - \vec{F}^* \vec{\nabla}_p f + \left(\frac{f - f_0}{r} \right) \qquad (2)$$

where f_0, f are equilibrium and non-equilibrium distribution functions; m_0, $\vec{p}$, $\vec{F}^*$ are the unmovable [sic] particles mass, their momentum and external force respectively; $(\partial f/\partial \tau)_{col}$ is the collision integral non-linearly related to $f' f'_1 - f f_1$, where f', f'_1 are the distribution functions after mutual collision of the particles, τ_r is the relaxation time characterizing the velocity of the non-equilibrium system coming back into equilibrium state after the force $\vec{F}^*$ stops acting on it.

In this case the substitution of non-linear equation (1) by model linearized equation (2) can be considered not only as one of the ways of the simplification of the problem at the cost of the loss of some important information contained in this equation, for example, the possibility of the description of non-elastic collision of particles. In reality the field of applications of [2] can be defined and substantially expanded, regardless of equation (1), if the distribution function f and especially the parameters are provided with new values, made suitable for the character of the phenomena studied and taking into account the practice of analyzing and solving equation (1). This approach to the solution of this equation is well known; however, the approach, used in [6], cannot be excluded. Its author considers the solution of Boltzmann's model equation in his statement and interpretation to be accurate.

When formulating Boltzmann's model equations, it is important to try to use DL as much as possible because they substantially expand the range of applicability of equations, based on CL, and simplify their physical interpretation. Therefore, it is not a coincidence that it is the law of energy degradation but not Boltzmann/s H-theorem that is widely used to explain an experimental fact. This fact, as a basic assumption acting as a dynamic principle, in the development of irreversible theories, in synergetics, and in a recent Prigogine's publication -- see monograph [7]. In any case there are no reasons to neglect the heuristic role of DL, when developing new theories for the description of complex phenomena even if one can successfully use the methods of statistic physics.

Unlike paper [6] in which Boltzmann's model equation is solved by Lorentz diffusion approximation [5], in which the parameter τ_r is taken as the mean time τ_L between the particles collision, $\tau_r \equiv \tau_L$. In [3,4] this parameter is defined with the help of DL and in a more complicated way depending on a concrete statement of the problem. This method makes it possible to obtain more precise results for a specific problem solution and make them more valuable from the information point of view. For example, the

intensity and qualitative peculiarities of energy transfer processes during the period of time $\tau \gg \tau_L$ (which is much longer than the mean time of the particles path τ_L under conditions of stationary heat conductivity in non-static systems of neutral particles) depends not only on the kinetic energy exchange between the adjacent L-subsystems, measuring the mean-free-path length (L) of particles in the period of time $\tau_\epsilon > \tau_L$, but also on the dynamic exchange of particle momentum in the period of time $\tau_p < \tau_\epsilon$ and also on the diffusion exchange of the particles themselves in the period of time τ_L, where $\tau_L < \tau_p < \tau_\epsilon$.

The hierarchy of the periods of time, which is expressed by the latter inequality (which can be easily substantiated with the help of DL in the presence of interaction of neutral particles in the L-subsystems) is the cause of the self-oscillation in them during the period of time τ_{pr}. This period is equal in its value to the relaxation time τ_ϵ of the slowest process responsible for the temperature formation. However, it is due to the complex multichannel energy transfer process in L-subsystems occurring in the direction of temperature decrease and realizing not only in the form of the heat Q_L to the time τ_ϵ, and not only in the form of the heat Q_L to the time τ_ϵ, but also in the form A_L, for the time $\tau_A \rightarrow (\tau_A (\tau_L, \tau_p)$ approx. $< \tau_\epsilon)$ what in the L-subsystems self-oscillations arise and local thermodynamic equilibrium (LTE) in the non-static system is, in principle, unattainable. It follows from this that the energy transfer therein only as heat is impossible and one must consider there is a complex process of energy transfer-conversion, which can be only approximated by the equilibrium temperature T. The exact integral mean temperature at period $\tau_{pr} \sim \tau_\epsilon$ of non-static system is found in reactions of the form [3,4].

$$\frac{d\,t}{d\tau} = -\frac{t - T}{\tau_\epsilon}, \quad t = \int_{\tau}^{\tau + \tau_\epsilon} t(\tau)\,0 \tag{3}$$

where $t(\tau)$ is the temperature depending on the time; $T = t_{(\tau_\epsilon \rightarrow 0,\ L \rightarrow 0)}$ is the equilibrium temperature, it is strongly dependent on the co-ordinates used (or not used).

The statement of unattainability of LTE in non-static systems, discussed above, was used in [3,4] for formulation and solution of the generalized equation of energy transfer-conversion

$$\frac{\partial t}{\partial \tau} + \tau_\epsilon \frac{\partial^2 t}{\partial \tau^2} = a \left(\frac{\partial^2 t}{\partial X^2} + L \frac{\partial^3 t}{\partial X^3} \right) \tag{4}$$

This equation describes the process approximately as completely as the non-linear heat conductivity equation in paper [8].

$$\frac{\partial T}{\partial \tau} \quad a \frac{\partial}{\partial X} T^n \frac{\partial T}{\partial X}, \quad n \lessgtr 1 \tag{5}$$

and has the advantage of linearity. This advantage was achieved at the cost of the order increase of the differential equation. This approach essentially keeps the information which can be obtained from a non-linear equation and allows one to solve such problems with the help of the well-developed methods of linear analysis.

The important element of the method based on the unattainability of LTE within the limits of equation (4) is the conclusion that the finite value of the relaxation time τ_ϵ, approximately equals the period of self-oscillation in L-subsystems. This coincides with one of the necessary conditions of the mixing formulated by N.S. Krylov [9]. It was done with the help of the analysis of probability processes when substantiating

the logical bases of statistical physics. Moreover, the preliminary analysis proved the expediency of the additional study of feasibility of LTE, not only as a necessary, but also as a sufficient condition of the systems mixing according to N.S. Krylov.

Thus, the method taking into account both a statistical and dynamic conformity in L-subsystems of non-static system of charged particles, can be considered to be prospective. Such systems with the *a priori* assumed the inequality of the relaxation times $\tau_L \neq \tau_p \neq \tau_\epsilon$ in their L-subsystems can tend to self-oscillations which is a consequence of unattainability of LTE or local electrodynamic stability in them. Practical application of the results can be especially useful for mere logical solution of traditional problems of vacuum and semiconductors electronics, including the problem of thermoelectronic energy conversion. Apart from the above problems, we may mention the following:

1. The determination of the hierarchy of the relaxation time values τ_L, τ_p and τ_ϵ in non-static systems of charges particles;

2. The formulation of a set of linear differential equations for the description of a multichannel process of energy transfer-conversion in such systems;

3. The presentation of the process of energy transfer-conversion on non-static systems of neutral and charged particles as a simple model of a self-organization process of non-equilibrium systems.

FUTURE PLANS

In the future the proposed method is supposed to be applied to the solution of the problem of high temperature superconductivity and to try to substantiate the possibility or impossibility of the practical application of a cold nuclear fusion in energetics. It is supposed to use the method, proposed by de Broglie [10, 11] and developed by his followers - Bohm [10, 12], Vigier [10, 13], Lochak [14] and others. The essence of this method lies in the taking into account of complex natural phenomena on the sub-quantum level of matter. This, in turn, demands a more precise definition of modern ideas about the concept of a "particle" and a "field".

REFERENCES

[1] A.G. Shashkov, V.A. Bubnov, S.Yu. Yanovski, "Wave Phenomena of Heat Conductivity: System and Structural Approach," Minsk, 1993 (in Russian).
[2] A.V. Bulyga, *Sibirski Fizico-technicheski Jurnal*, vol 1, (1992) p 129.
[3] A.V. Bulyga, *Dokladyy Akad. Nauk BSSR*, 1990, no #, p 224.
[4] A.V. Bulyga, *Irreversible Thermodynamics*, Ed. A.I. Lopushanskaya, Moscow, *Nauka* (1992), p 39, in Russian.
[5] A.M. Vasil'ev, Introduction to Statistic Physics, Collected Translations, Moscow, 1980, in Russian.
[6] G.D. Mahan, *Phys. Rev. B* no 5, (1991) p 3945.
[7] M.I. Prigogine, "From Being to Becoming: Time and Complexity in the Physical Sciences," W.H. Freeman and Company, 1980.
[8] Ya.B. Zeldowich, A.S. Kompaneets, in Collect. Dedicated to the Seventieth Birthday of Acad. A.F. Ioffe, Moscow, 1959, p 91 (in Russian).
[9] N.S. Krylov, "Books on Substantiation of Statistical Physics," Moscow, 1950 (in Russian).
[10] Problems of Causality in Quantum Mechanics, Collected Translations, Moscow, 1956 (in Russian).
[11] L. de Broglie, "Les Incertitudes d'Heisenberg et l'Interpretation Probabilistique de la Méchanique Ondulatoire," Bordas, Paris, 1982 (translated into Russian, Moscow, 1986).

[12] D. Bohm, "Causality and Chance in Modern Physics," London, 1957.
[13] J.P. Vigier, *Vopr Filos.* no 6, (1956) p 91.
[14] J. Andrade e Silva, G. Lochak, "Fields, Particles, Quanta," Moscow, 1972 (in Russian).

THE UPPER BOUND OF HOT-SPOT TEMPERATURES INDUCED BY SUPERSONIC FIELD

Kenji Fukushima
Physics Department, Joetsu University of Education
Yamahashiki, Joetsu, Niigata 943 Japan

Tadahiro Yamamoto
Department of Physics, Tokyo Metropolitan University
Minami-osawa, Hachioji, Tokyo 192-03, Japan

ABSTRACT

The phenomenon of sonoluminescence has attracted an intense attention of researchers in a variety of fields of science and technology. Recently direct measurements of temperatures of a hot spot, which was created in a liquid exposed to a supersonic field, were carried out and very large values, for example $T \approx 6eV$, were obtained.

It seems thereby to be an urgent, interesting scientific problem to determine the upper bound of temperatures and densities realizable in the hot spot, particularly in connection with the possibility of so called cold fusion.

In this paper we calculate the maximum of hot-spot temperature allowable for a particular set of parameters, by use of the bubble dynamics which has been developed for sixty years.

1. Introduction

Let us start with a brief description of the phenomenon of sonoluminescence. A supersonic field applied to a liquid is known to yield vapor and/or gas-filled cavities in the liquid, which then starts to oscillate almost in phase with the applied supersonic pressure field. In the contraction phase the content of the cavity is greatly, adiabatically compressed so that the temperature is highly raised and atoms or molecules in it are excited to eventually irradiate photons.

Recently Flint and Suslick [1] succeeded in directly measuring the temperature of hot spots in a silicon oil by analyzing the luminescence spectra from C_2 molecules and obtained the value

$$T = 5{,}075 \pm 156K.$$

After a year Hiller, Putterman and Barber [2] raised the upper bound to

$$T \approx 6eV$$

by fitting the spectra of the luminescence from an air bubble in water to those of black body radiation.

The aim of this work is to calculate the maximum value of hot-spot temperatures which is allowable for a suitably chosen set of parameters.

2. Fundamental equation

The sonoluminescence has a long history of research of about sixty years and constitutes a well established branch of science and technology. We now have a lot of review works, by which one may easily get familiar with the theories and experiments on sonoluminescence. For example, see References [3] and [4].

For simplicity, we at first ignore the compressibility and bulk viscosity of a liquid and assume the spatial uniformity of a gas content, i.e., we are here considering a gas-filled cavity. Furthermore we neglect the thermal irradiation and mass diffusion from or to the cavity. The spherical symmetry of the cavity is also assumed throughout the present paper.

Let a cavity with radius R_o be initially in equilibrium with a liquid of hydrostatic pressure P_o and temperature T_o and a supersonic field

$$P^e(t) = -P_A \sin \omega_A t \tag{1}$$

be applied to the liquid at t=0. By use of the conservation laws of mass and momentum for the liquid, we can get the dynamical equation of motion

$$R\ddot{R} + \frac{3}{2}\dot{R}^2 = -\frac{1}{\varrho R}\left(P(R,t) - P(\infty,t)\right) \tag{2}$$

for the radius R of the cavity, [3,4] where P(R,t) and P(∞,t) are pressures in the liquid at the wall and at a remote point from the cavity, respectively. The former should be in equilibrium with the pressure of the gas content, i.e.,

$$P(R,t) = \left(P_0 + \frac{2\sigma}{R_0}\right)\left(\frac{R_0}{R}\right)^{3\kappa} - \frac{2\sigma}{R} - \frac{4\mu\dot{R}}{R}, \tag{3}$$

where ϱ, σ and μ are, respectively, the density, surface tension and viscosity coefficient of the liquid. In the above the equation of state of an ideal gas is assumed for definiteness. The generalization to a van der Waals gas is straightforward. The κ is the polytropic index, which verifies between the specific heat ratio γ and unity; adiabatic and isothermal limits, respectively. On the other hand

$$P(\infty,t) = P_0 + P^e(t) \tag{4}$$

3. Maximum of hot-spot temperatures

In this section we try to solve the equation (2). It has been well known that there are two types of solutions, i.e., a stable solution and transient one, depending on values of parameters, P_A and w_A, the amplitude and frequency of the applied supersonic field. For the purpose of obtaining high hot-spot temperatures, transient cavities are preferable. In the present paper, however, we do not optimize parameters P_A and w_A for that purpose. Instead we try to get the solution for a particular point of the parameter space which lies in the transient region and then examine the response of the solution to the variation of the initial radius R_o.

Let the point of the parameter space be

$$P_A = 4\text{bar and } \omega_A = 15\text{kHz}. \tag{5}$$

The solution corresponding to (5) is examined in detail by Walton [4]. Namely in the first three quarters of a period of the supersonic field the cavity abnormally expands mainly due to the inertia of the surrounding liquid, in spite of the fact that $P(\infty,t)$ which decreased from zero to $P_o - P_A$ turns to increase up to around $P_o + P_A$. Let the maximum value of the radius be R_{max}. In the last quarter of a period the cavity collapses very rapidly towards the minimum radius R_{min}, where the gas achieves the maximum temperature T_{max}.

The expansion phase is describable by numerically solving (2). Fig. 1 depicts R_{max} against R_o. There is no appreciable difference between an ideal gas and a van der Waals one. In calculating Fig.l the isothermal process ($\kappa = 1$) is assumed since the expansion takes place slowly.

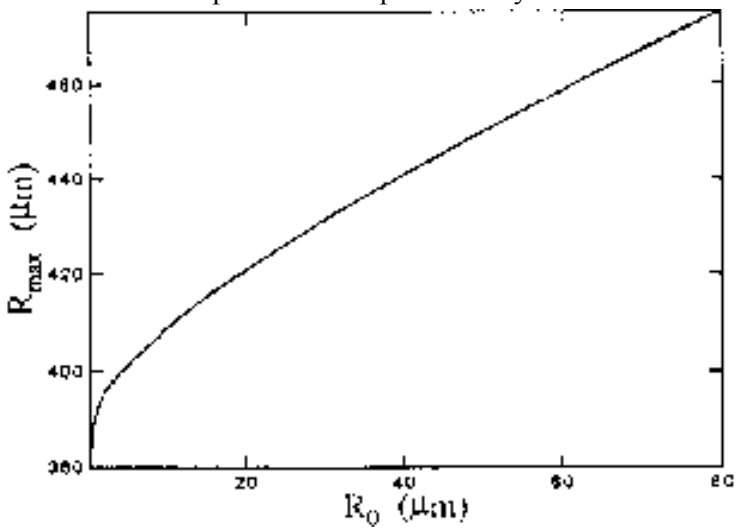

Fig. 1. The maximum radius R_{max} vs. the initial radius R_0. There is no appreciable difference between an ideal gas and a van der Waals one for R_{max}. The values of parameters are shown in (5).

Next turn to the contraction phase. It turns out to be a very tough job to numerically calculate the collapse process because it occurs in a very short time.

So let us try to analytically solve (2) by use of the fact that the collapse takes place around

$$P(\infty,t) \approx P_m \equiv P_0 + P_A,$$

as Walton [4] did. Multiplying $R^2\dot{R}$ and integrating over t from the time when R reaches the maximum value R_{max}, (2) may reduce to

$$\dot{R}^2 = \frac{2}{3\rho}\left[\frac{Q}{1-\gamma}\left(\left(\frac{R_m}{R}\right)^{3\gamma} - \left(\frac{R_m}{R}\right)^3\right) - \frac{3\sigma}{R}\left(1 - \left(\frac{R_m}{R}\right)^2\right) - P_m\left(1 - \left(\frac{R_m}{R}\right)^3\right)\right] ,$$

where the adiabatic process (kappa = gamma) is assumed since the contraction occurs very rapidly and Q is the pressure when $R=R_{max}$.

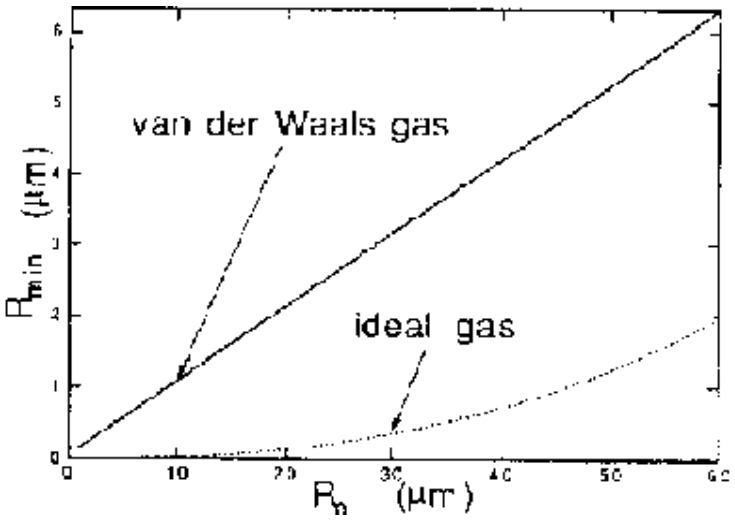

Fig. 2. The minimum radius R_{min} vs. R_0. The broken line and solid one correspond to an ideal gas and a van der Waals one (D_2), respectively.

The minimum value R_{min} is obtainable by equating $\dot{R}$ to zero in (6) and it may follow that

$$Z \equiv \left(\frac{R_{\max}}{R_{\min}} \right)^3 \approx \left(\frac{(\gamma - 1) P_m}{Q} \right)^{\frac{1}{\gamma - 1}} \tag{6}$$

The maximum temperature and pressure are achieved when $R=R_{MIN}$ and may result in

$$T_{\max} = T_0 Z^{\gamma - 1} \approx \frac{(\gamma - 1) P_m}{Q}$$

$$P_{\max} = Q Z^{\gamma} \approx Q \left(\frac{(\gamma - 1) P_m}{Q} \right)^{\frac{\gamma}{\gamma - 1}} \tag{7}$$

Figs. 2 and 3 depict R_{min} and T_{max} against R_0, where we have used values of R_{max} calculated in Fig. l. The dashed and solid lines in Fig. 2 correspond to an ideal gas and a van der Waals one (D_2), respectively. No appreciable difference is recognized between both kinds of gas in Fig. 3.

As seen from Fig. 3, it is remarkable that for cavities which have radii of a few microns the maximum temperatures reached are high enough for nuclear fusion to take place.

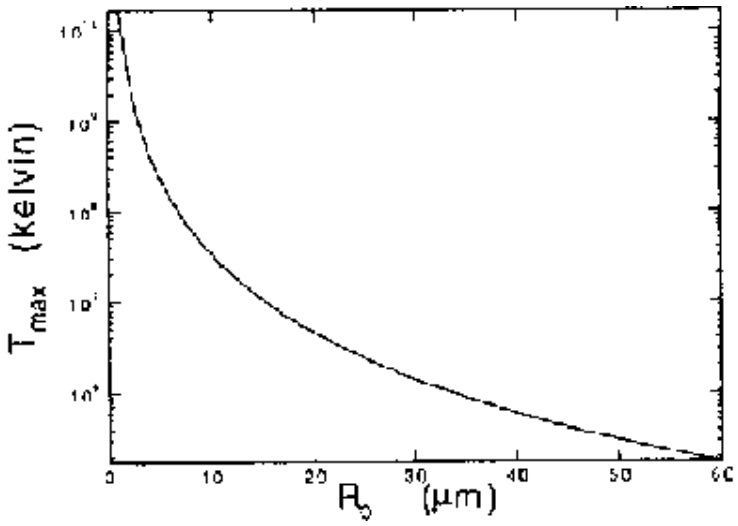

Fig. 3. The maximum temperature T_{max} vs. R_0. Both types of gas yield no appreciable difference for T_{max}.

DISCUSSIONS

As mentioned in Section 2, we have made a lot of simplifications to calculate the maximum temperature. Among them the assumption of the incompressibility seems crucial, since the speed of wall of the cavity exceeds the sound velocity of water in the collapse process. This fact means the invalidity of the incompressibility assumption.

Furthermore we neglected the diffusion of mass, which is usually ignored in the application of the bubble dynamics because the speed of wall is very large as compared to the diffusion velocity and then the effect is negligible in a few periods of the oscillation. The linear response theory however, would not be valid for such extreme condition that is realizable for cavities with initial radii of order of micron. We have to take account of the thermal radiation too.

Lastly the phase transition from a gas phase to a plasma phase and the instability of a spherical cavity should be taken into account.

After all, to obtain quantitatively acceptable results, we have to examine the above-mentioned in detail and then seek for the optimum condition for the realization of the upper bound of hot-spot temperatures. The present work, therefore, constitutes a preliminary step of the whole task and detailed calculations will appear in another place.

REFERENCES

[1] E.B. Flint and K.S. Suslick, *Science*, vol 253 (1991), p 1397.
[2] R. Hiller, S.J. Putterman, *Phys. Rev. Letts*., vol 69 (1992), p 1182.
[3] E.A. Neppiras, *Physics Reports*, vol 61 (1980), p 159.
[4] A.J. Walton and G.T. Reynolds, *Advances in Physics*, vol 33 (1984), p 595.
[5] K. Fukushima, Frontiers of Cold Fusion, edited by H. Ikegami (Universal Academy Press, Tokyo, 1992), pp 609-612.

CALORIMETRIC STUDY OF EXCESS HEAT PRODUCTION WITHIN THE HYDROSONIC PUMP SYSTEM USING LIGHT WATER

James L. Griggs
Hydro Dynamics Inc.
611 Grassdale Road
Cartersville, Georgia 30120
404-386-2649 Fax 404-386-8139

ABSTRACT

The Hydrosonic pump is a device that has shown "excess heat" in steady state running conditions continually for a number of years. The basic premise of the pump is that when shock waves are generated in a fluid, a small amount of energy would be given off in the form of heat. The pump has been specifically designed to create millions of controlled shock waves per minute, which in turn generates an acoustical wave in the range of 36K Hertz.

The pump's excess output varies as input parameters are intentionally varied and the phenomenon can be controlled.

In this paper three different experiments will be presented to show the pump in its different stages of production.

1. An experiment where all the input supply water provided to the systems will be converted to a gas (steam).
2. An experiment where the output from the pump is a combination of gas and liquid.
3. An experiment where a liquid state is maintained throughout the entire experiment.

A complete overview of the pump and its related system will be given with a complete description of the experimental procedure. The calorimetry for the experiments will be a combination of computer generated and human data collection and reported in detail.

A BRIEF INTRODUCTION TO THE HYDROSONIC PUMP AND "EXCESS ENERGY" PHENOMENON TESTING

HISTORY OF THE PUMP

The Hydrosonic Pump was invented by Jim Griggs, an electrical engineer, who has specialized in the field of energy conservation. Jim is a member of the Association of Energy Engineers and a member of the National Society of Professional Engineers. He has received numerous awards in the field of energy conservation and has been a consultant to several national companies.

The first production model of the Hydrosonic Pump was completed in 1989. Hydro Dynamics was incorporated in 1990, and the first patent was issued in February of 1993, with a number of U.S. and international patents pending.

OPERATIONAL PRINCIPLES

Although called a "pump", the Hydrosonic pump is not a pump in the conventional sense of the word. While fluid will move through the Hydrosonic Pump unassisted to a minor extent, it requires a conventional circulation pump to achieve satisfactory results in most applications. It is called a pump for marketing reasons. Company management preferred not to associate the Hydrosonic Pump with the negative connotations arising from the term "steam boiler"

The Hydrosonic Pump uses shock waves to generate sufficient energy to produce hot water (fluids) or steam. Physics books state that when water or other liquids flowing in a restriction are suddenly stopped, pressure of approximately 63.4 PSI is created for each foot of extinguished velocity. This pressure wave then travels back up the conduit to the reservoir or other source of the liquid, and cycles are established and repeated. Normally, the waves dissipate in a short period of time. The term used to describe this wave and cycle effect is commonly called "water hammer". It is also stated in textbooks that as the shock waves pass through the liquid, a portion of the energy is converted into heat energy and is dissipated into the mass. The thermodynamic aspects of this effect were considered small and of no significant harm or value. However, this is where the Hydrosonic Pump achieves its objective.

The pump was designed to accomplish a more energy efficient and environmentally safe way of producing hot water and steam. The basic premises of operation are as follow: Water (basically any aqueous solution or fluid) is injected through an opening and is moved across a spinning rotor which is powered by an external source. The rotor is designed as a sphere with numerous cavities drilled in a specific pattern around the surface. This patented design causes several things to occur. There is a shearing stress created as the water first enters the chamber and a small amount of heat energy is created and released into the water. Because the water enters the chamber under a specified amount of pressure, additional heat is generated and absorbed into the water. The shearing stress (dynamic viscosity) increases as the water continues its movement across the rotor to the outlet port. As the water moves across the rotor surface it is being drawn into the numerous dead end openings because of the centrifugal force created by the moving rotor. Millions of shock waves are generated thereby producing heat.

As the shock waves are produced a standing wave effect is established and a resonance is set up within the water. As the rotor continues to spin these waves are intensified and resonances of 25 kilo hertz and higher (frequencies vary with rotor size and design) are produced continuously.

It also appears that tiny air bubbles are formed at some point in the process and the formation and eventual collapse of those bubbles may aid the heat transfer process.

As the heated water leaves the outlet side of the Hydrosonic Pump, it will leave as a combination of steam and condensate, or hot water (liquid). The temperature at which it exits and the state (liquid or gas) in which it exits depends on rotor speeds, hole designs, tolerances between the rotor and housing, water flow rate into the Hydrosonic Pump, and several other design items. An exhaust pressure is also created at this point which can be varied to satisfy the end user's process requirements.

"ENERGY PHENOMENON"

Testing completed to date by both the Company and independent agencies indicates that the Hydrosonic Pump has a significant energy efficiency advantage over conventional boiler(s) or heat transfer processes. Numerous tests conducted by the Company as well as independent third parties continue to reveal an as yet unexplained phenomenon occurring within the patented process relating to energy input and output. Shortly after the Hydrosonic Pump is operational, the "measurable energy" required to operate the Hydrosonic Pump is less than the measured energy output of the Pump. Present during such tests have been representatives from large utility companies as well as independent engineers and consultants. Two

of these recent tests will be presented in this paper.

The initial reaction from the "experts" when reviewing these results is almost always the same--impossible! On the surface, these results would seem to violate the second law of thermodynamics; however, the Company believes that because of ultrasonic fields and other unknown forces possibly affecting fluids flowing through the Hydrosonic Pump, it is possible that an energy source is being tapped that has to date not been identified. We at Hydro Dynamics believe that further testing will prove that such an additional source does exist and, most importantly, will identify the source.

TESTING

When the idea for using shock waves to produce heat was conceived, it was thought that such a process might be highly efficient and environmentally clean. The possibility that COP's greater than one could be achieved became apparent immediately, but because this contradicted the laws of thermodynamics the results were viewed with skepticism. However, the phenomenon has continued to persist throughout the years and is still evident in the tests that will be discussed.

It should be noted that these test results on the Hydrosonic System show efficiencies with ratios greater than 1:1. The tests being presented follow a procedure we have recently been requested to use. We perform other tests with different procedures, routinely, in a continuing effort to find the best combination of energy efficiency, reduced capital cost, ease of maintenance, etc., for our market place. We believe that these tests, along with all the others performed for the past three years, may not be representative of the best possible results that can be obtained from the Pump from purely an energy efficiency standpoint.

When Hydro Dynamic Inc. was formed, the working prototypes at that time were bulky and could possibly require considerable maintenance and repairs. It was not unusual to get efficiency ratios of 2:1. It was believed at that time that the Pump should be basically simple to operate and "maintenance free". The housing and bearing configuration was completely redesigned with that concept in mind and, in so doing, reduced the Pump efficiency.

It was thought at this time that the reduced efficiency would not affect the company's specialty marketing effort, which emphasized other features of the Pump. However, because there has been extreme interest in the "energy phenomenon" and the manner in which the Hydrosonic Pump achieves it, the company began production of a pump with a design similar to the original prototype for energy testing purposes only. This pump was completed and testing began in late December 1993.

At this point it has been shown that, with or without the "excess energy" phenomenon, there are numerous applications for the Pump. The Company is continuing its intensified research and development efforts and welcome any suggestions by phone, mail, or personal visits to our operations in Cartersville, Georgia.

FORCED STEAM BARREL TEST 1 and 2

On January 6, 1994 two tests were conducted at the offices of Hydro Dynamics Inc. to determine the efficiency of a Hydrosonic Pump system producing steam. The coefficient of performance (COP) is the basic parameter used to compare the performance of heating systems, and is defined in the Handbook of Energy Engineers, The Fairmont Press, 1989, page 249, as follows:

"COP = RATE OF NET HEAT REMOVAL - divided by -TOTAL ENERGY INPUT"

$$\frac{\text{energy out}}{\text{energy in}}$$

The test was conducted by Jim Griggs, Kelly Hudson, Phillip Griggs and Marvin Dawkins, with the assistance of Jed Rothwell, author and co founder of Cold Fusion Research Advocates, and Dr. Eugene Mallove. Dr. Mallove is the former Chief Science Writer for MIT news office, a noted author holding advanced degrees in astronautical engineering and environmental science, and is presently Editor in Chief of "Cold Fusion" magazine, according to the following procedures:

Before the test begins, a 55 gallon open steel drum weighing 30.5 lbs. empty is placed on a factory weight scale. It is filled with 350 lbs of tap water and temperature and weight are recorded.

Water is fed to the Hydrosonic pump from a 16 gallon feed water tank. A large clear plastic bucket mounted at the top of the tank serves as a hopper. It is marked in two scales: tenth-gallon up to one gallon; and pounds up to 8 lbs. (One U.S. gallon weighs 8.33 lbs.). Care is taken and water is added in 8 lb increments to the hopper making it easy to record the flow and total water added.

Water from the feedwater tank is forced through the Hydrosonic pump by a small auxiliary pump. The flow rate is regulated and displayed with a flowmeter.

The pump is turned on and allowed to reach a steady state of operation with steam being exhausted through a valve to the atmosphere. At the beginning of the test the steam is re-routed into the drum of water through a secondary valve and electrical input power is recorded.

The test was continued for a specific period of time with continual temperature and energy input measurements being recorded.

The results were as follows:

TEST 1

Starting mass and temperature of water in the drum: 350 lbs, 53 degrees F.
Ending mass and temperature in steel drum: 381 lbs, 103 degrees
Water temperature Delta T: 50 degrees F.

Energy added to water: 50 degrees x 381 lbs. = 19050 BTU's = 5.58 KWH
Electrical input power recorded: 4.80 KWH

C.O.P. computation--

	Input KWH	C.O.P.
Apparent	4.80	117%
Adjustment for power factor (apparent-true) and motor efficiency (82.5%)	3.33	168%

TEST 2

Starting mass and temperature of water in steel drum: 350 lbs, 53 degrees F.
Ending mass and temperature in steel drum: 392 lbs, 122 degrees F.
Water temperature Delta T: 69 degrees F.

Energy added to water: 69 degrees F x 392 lbs. = 27048 BTU's = 7.92 KWH
Electrical input power recorded: 7.26 KWH
(test 2 was ran for 10 minutes longer than test 1)

C.O.P. computation--

	Input KWH	C.O.P.
Apparent	7.26	109%
Adjustment for power (apparent-true) and motor efficiency (82.5%)	5.03	157%

Conclusion: excess heat energy was detected at levels far beyond any reasonable limits for error from the instrumentation used in the test.

FORCED STEAM BARREL TEST 3

On February 15,1994, Mr. Ron Dubose on behalf of ENECO visited our plant to participate in two additional tests of the Hydrosonic Pump. Mr. Dubose is a P.E. in mechanical engineering and President of Emprise Corporation in Marietta, Georgia. Emprise Corporation specializes in the design, construction and installation of testing facilities throughout the world.

The same test procedure was followed as in the two previous tests conducted earlier in the report, with the following results:

TEST 3

Starting mass and temperature of water in the drum: 325 lbs, 48 degrees F.
Ending mass and temperature in steel drum: 412 lbs, 124 degrees F.
Water temperature Delta T: 76 degrees F.

Energy added to water: 76 degrees x 412 lbs. = 31312 BTU's = 9.17 KWH
Electrical input power recorded: 8.39 KWH

C.O.P. computation--

	Input KWH	C.O.P.
Apparent	8.39	109%
Adjusted for power factor (apparent-true) and motor efficiency (82.5%)	6.23	147%

Conclusion: once again excess heat was recorded in excess of possible instrumentational error. Mr. Dubose stated in his report to ENECO dated February 16, 1994, "I could find no fault with the test technique or instrumentation. Some factors such as heat sink losses were neglected that would improve measured pump performance if they could be included. "

As stated earlier, we at Hydro Dynamics Inc., do feel that this phenomenon is real and that at some

point in the near future it will be fully explained.

To quote from the great physicist, Albert Einstein, "All the laws of physics are absolute, not in the sense of being unalterable by the progress of research but in the sense I have already noted--they are consistent throughout the universe."

The two tests that have been examined in this paper were conducted under the strictest control conditions available to the researchers. Manufacturers' specifications as to the accuracy of all test equipment has been supplied in appendix B, and based on the company's interpretation of these specifications, instrumentation error cannot possibly explain away the large amounts of excess heat energy produced by the Hydrosonic Pump.

During the past three years the tests performed at Hydro Dynamics continue to indicate COP's greater than one. We believe additional research in this area must continue.

AUTHOR'S NOTE

Hydro Dynamics Inc. as a company and I myself personally invite any input in the form of recommendation, possible explanations, and criticism as to our process or testing techniques. We realize that we do not have the final answer, but the question remains open, what is the source of the "excess?" We invite anyone to our facility at anytime for a demonstration, or an attempt to prove us wrong.

DESIGN CONSIDERATIONS FOR SUPER-CONDUCTING MAGNET N-MACHINE JPI-II

by

Shiuji Inomata, Ph.D.*
and Yoshiyuki Mita, M.S. **

ABSTRACT

The successful confirmation of the so-called incremental over-unity phenomena in the JPI-I N-machine (Inomata and Mita, 1993) has led the authors to design the system over-unity machine JPI-II, which is composed of a super-conducting magnet N-machine, and a super-conducting magnet Faraday motor. This combination on the same axle, after being started by the outside electrical power source, is expected to feed some 30 to 40 KW AC power. This power is in addition to the required cooling energy of the vaporized coolant which is essentially negligible if sufficient heat insulation is provided for the super-conducting coils. The N-machine theory, the experimental data (JPI-I) and the design details of the super-conducting magnet N-machine, JPI-II, will be described in this paper.

INTRODUCTION

Recently, there has been increasing interest in the N-machine "space power generator", because it has the possibility of producing electrical energy with significantly less mechanical power input. Furthermore, the possibility of system over-unity operation could be envisaged. The constructed JPI-I machine is a small Neodymium magnet twin N-machine. Having carried out several experimental measurements, we had confirmed the so-called incremental over-unity or local violation of energy conservation law. That is, in case of one experiment, at 6000 rpm, the electrical power extracted from vacuum is 5.81 watt, and the increased electrical power to the drive motor, in that time, is 3.24 watt. Therefore, we have 2.57 watt surplus of energy. The experimental results had been presented at Japan Psychotronics Institute (JPI) monthly meeting on 27 March, 1993, Tokyo. On the other hand, the back-torque was found rather big. This suggests that improvements are necessary.

Nevertheless, we have found very surprising phenomena, in which electrical current increases nonlinearly as rotational speed increases. It is as if copper-carbon brushes were cooled down more than 100°C. This decreasing resistance phenomenon has occurred in the copper-carbon brush materials around the rotating magnets disc with high speed. This phenomenon might be one of the most important evidence of shadow energy extraction from the vacuum. Inomata's vacuum theory (Inomata, 1987) requires the reexamination of Dirac's vacuum theory. The absolute vacuum is considered as a balanced sea of both positive and negative "shadow energy" Both positive and negative shadow energy are described by shadow Dirac equation. We consider that the sea of shadow charge corresponds to non-material ether.

Furthermore, we can obtain probability density flows between real world and shadow (imaginary) world, which coincide with what the consciousness-electrical charge, complex matter, complex energy triangle claims. Because matter is energy in conventional physics, so the energy extraction becomes legitimate in this paradigm of new science.

In this paper we describe the design of a New N-machine (JPI-II) aiming at system over-unity, which uses super-conducting coils for the construction. It is shown that there exists the possibility of system over-unity operation by showing the detailed design and estimating output-power.

THEORETICAL CONSIDERATIONS

According to the Dirac's vacuum theory, a vacuum consists of a sea of electrons in negative energy levels. We consider here that this viewpoint of a vacuum should be abandoned.

From our new paradigm viewpoint, the absolute vacuum is considered as a sea of non-material ether which transcends space-time. We consider that the ether consists of a balanced sea of both positive and negative "shadow" energy of infinite magnitude. This corresponds to the stationary ether, which H.A. Lorentz assumed in his theory. In this theoretical considerations, the CGS system will be used.

We shall consider the S reference frame, which is a stationary frame for the observers and the ether, and the S′ frame, which is moving with constant velocity relative to the S. For simplicity, we shall consider the S′ to be moving with speed v along x (or x') axis relative to S. We think that the Maxwell equations of the same forms are satisfied in the reference frames S and S'

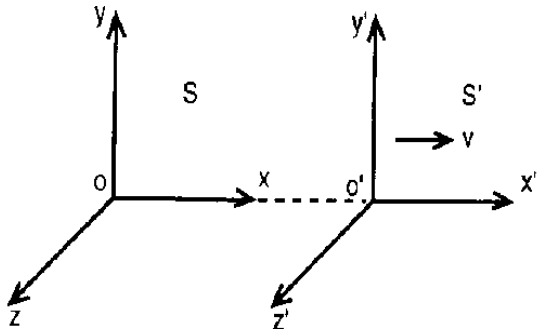

Figure 1. Coordinate Reference Frames S and S′

We can obtain the transformation formulae for E and H. We will do this only for the particular Lorentz transformation described by Equation (1).

$$\begin{aligned} E'_x &= E_x & H'_x &= H_x \\ E'_y &= \gamma\,(E_y - \beta H_z) & H'_y &= \gamma\,(H_y + \beta E_z) \\ E'_z &= \gamma\,(E_z + \beta H_y) & H'_z &= \gamma\,(H_z - \beta E_y) \end{aligned} \qquad (1)$$

(where $\gamma = 1/(1 - v^2/c^2)^{1/2}$, $\beta = v/c$)

If v is far smaller than c, we can obtain the relations $\gamma \fallingdotseq 1$, $\beta \ll 1$. Moreover when there exists only H field perpendicular to the moving direction, we can obtain the transformation formulae of Electromagnetic Field described by (2).

$$\begin{aligned} E'_x &= 0 & H'_x &= 0 \\ E'_y &= -\beta H_z & H'_y &= H_y \\ E'_z &= \beta H_y & H'_z &= H_z \end{aligned} \qquad (2)$$

$$E' = \beta \times H \quad (3) \qquad H' = H \quad (4)$$

These results clearly show that the electric and magnetic field vectors E and H are really non-independent existence. The resolution into electric and magnetic components is due to the motion relative to the observer and the ether. Moreover, if there exists a completely uniform magnetic field, there is no meaning of distinction between H and H′ field. However, in S′ moving frame, electric

field E′ appears due to H field in S′ frame. In the paradigm of the absolutism EM, E′ is thought to be created by the H field moving in the stationary frame.

From (3), we can obtain the EMF for N-machine. Thus, we consider a plane conducting disk with magnets of radius r rotating with constant angular speed ω. The uniform H field is perpendicular to the plane of the disk.

$$E'_r = (v/c) \times H = (\omega/c)H_z r \quad (5)$$
(where $v \perp H$, $v = (\omega \times r)$)

In the paradigm of relativistic EM, E′ (x,t) only exists in the mind of an observer of S frame. On the contrary, in the paradigm of the absolutism EM, E′ (x,t) is thought to be "real", irrespective of the existence of an observer (Inomata, 1991). This expression is the same as the Faraday generator. If the rotation is reversed, the equation changes the sign.

The potential difference between the center and the periphery of a copper disk become as below. R is the radius of a copper disk.

$$V'(EMF) = \int_0^R E'_r dr = (\omega/c)H_z \int_0^R r dr = (\frac{1}{2})(\omega/c)H_z R^2 \quad (6)$$

Thus, the quantity of the potential difference are equal to the case of Faraday generator. The exact place where EMF is created is in a copper disk, and is not in a conducting wire, as relativistic EM (Einstein theory) predicts. H.A. Lorentz's theory which presupposes the stationary ether can supply the correct answer.

In Oriental philosophy, beside the cosmological view of "what is form that is emptiness, what is emptiness that is form", the idea of "real and imaginary, Yin and Yang" is also considered to be very important. Thus, in existing vacuum, if any amount of positive shadow energy exists, exactly the same amount of negative shadow energy should exist and they should offset each other. From new paradigm viewpoint, the vacuum is considered as a sea of non-material energy which transcends space-time. Mathematically, this concept is described by complexified Dirac equation [real and imaginary (shadow) equations] using natural unit.

Dirac equation

$$i \cdot \frac{\partial \psi}{\partial t} = (-i\,\alpha \cdot \nabla + \beta\, m)\,\psi \quad (7)$$

Shadow Dirac equation

$$- \frac{\partial \psi}{\partial t} = (-i\,\alpha \cdot \nabla + \beta\, m)\,\psi \quad (8)$$

where ψ is a wavefunction. We can obtain probability density flows from an imaginary Dirac equation. Inomata's theory goes beyond the contemporary conventional statement which relates mass and energy (Einstein; $E=Mc^2$), conservation of energy and charge. This theory introduces complexfied mass, energy, charge and develops mathematical relationships for each one and their relatedness.

Here we would like to discuss the interdependency of real and shadow (imaginary) world. In general, Schrodinger equation in quantum mechanics is obtained from the conventional relation between energy and momentum, $E=p^2/2m$. After replacing by the operators; $E \rightarrow i \cdot \partial/\partial t$, $p \rightarrow -i \cdot \nabla$, Schrodinger equation becomes

$$i \cdot \frac{\partial}{\partial t}\psi = -\frac{1}{2m}\nabla^2 \psi = H\psi \quad (9)$$

where H is called Hamiltonian. When the eigenfunction of Equation (9) changes with time as $\psi(x,t) = \psi_0(x)e^{-iEt}$, it becomes $H\psi = E\psi$. On the other hand, to the relation which is $E = p^2/2m$ multiplied by i, and replacing by the operators, then we obtain

$$-\frac{\partial}{\partial t}\psi = -i\frac{1}{2m}\nabla^2\psi = iH\psi \tag{10}$$

and we obtain $iH\psi = iE\psi$. This is "shadow Schrodinger equations". Generally speaking, it may be possible to regard $iH\psi = iE\psi$ as the quantum system to express vacuum as "void". But as iE indicates only positive shadow energy, it does not match the Yin and Yang property of shadow energy which we require. P.A.M. Dirac supposed the following linear equation for both $\partial/\partial t$ and ∇ to obtain positive and finite probability density $\rho \geq 0$.

$$i\cdot\frac{\partial\psi}{\partial t} = (-i\,\alpha\cdot\nabla + \beta\, m)\,\psi\,(x,t) \tag{11}$$

Dirac required that Equation (11) fulfills real Klein-Gordon's equation.

$$-\frac{\partial^2\psi}{\partial t^2} = (-\nabla^2 + m^2)\,\psi \tag{12}$$

From this, Dirac's equation allows not only positive but also negative energy. The free solution of Dirac's equation is obtained in the form of $\psi = \omega\, e^{-ip\cdot x}$ when ψ is a column with 4 components and ω is a spinor with 4 components. Where, $p\cdot x = p_\mu x^\mu = Et - p\cdot x$. Since the details of mathematical treatments is explained in the literature (Inomata, 1987), we limit ourselves to state here that two values are allowed for E, as follows,

$$E = \pm (m^2 + p^2)^{1/2} \tag{13}$$

On the other hand, how does the probability of Dirac's equation flow? Here, the flow of probability can be obtained in relation with the following probability density.

$$\rho = \psi^*(x,t)\,\psi\,(x,t) \tag{14}$$

In Dirac's equation, the probability density of four dimensional wave function is definite and positive, and this is where it is different from Klein-Gordon's equation. Here we try to obtain shadow Dirac's equation. For this, we start from the following equation. That is:

$$-\frac{\partial\psi}{\partial t} = (-i\,\alpha\cdot\nabla + \beta\, m)\,\psi \tag{15}$$

After theoretical treatments, regarding a certain value of p, we obtain the same results as shadow Klein-Gordon's equation:

$$E = \pm i(m^2+p^2)^{1/2} \tag{16}$$

This means we can obtain the sea of positive and negative shadow energies. Now let's look for the flow of probability density of shadow Dirac's equation. After mathematical treatments, we can show

that there is a flow of probability density from the state of shadow energy. Thus, we can obtain the probability density:

$$\rho = \exp \{\pm 2(m^2 + p^2)^{½} t\} + c_{\pm} \tag{17}$$

where $c_{\pm}$ is an integration constant. When shadow energy level is positive, we select $c_{+} = -1$,

$$\rho = \exp \{+2(m^2+p^2)^{½} t\} - 1 \tag{18}$$

and it indicates the probability density flow from shadow energy level to real energy level, thus, inflow of particles. However, this equation has no meaning when $\rho>1$. On the other hand, when shadow energy level is negative, selecting $c_{-} = 0$, we obtain

$$\rho = \exp \{-2(m^2+p^2)^{½} t\} \tag{19}$$

and this indicates probability density flow from real world to shadow world, thus, outflow of particles.

By transferring from shadow Klein-Gordon's equation to shadow Dirac's equation, we could obtain the basic equations of micro-world which coincides with real and imaginary world as being interdependent and correlated, but not conventionally connected.

Thus, shadow Dirac's equation gives manifestation of vacuum as "void", which is lacking in contemporary physics. Now we want to discuss the problem of pair creation and pair annihilation of electron and its antiparticle, i.e. positron, using real Dirac's equation and shadow Dirac's equation simultaneously. In this case, we have two kinds of energy levels (in case p=0). Thus: (1) continuous state of positive ($E \geq + m_0$), negative ($E \leq -m_0$) real energy, (2) continuous state of positive ($E \geq +im_0$), negative ($E \leq -im_0$) shadow energy. If we suppose that negative real energy exists as Dirac did, we have to unreasonably equate negative infinite energy to zero energy and to equate infinite negative charge with zero charge. So we discard this level. And we suppose that shadow negative and positive energy levels exist. When these levels are occupied, it is clear that they bring no effect which can be observed externally as positive and negative shadow energy levels offset with each other exactly.

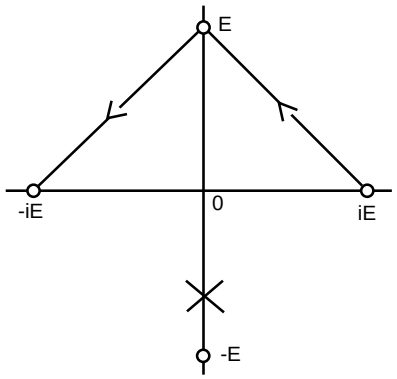

Figure 2. Complexified Energy Level

Now we suppose complexified energy level as indicated in Fig. 2. As it became clear through this section, positive shadow energy level acts in creation of probability density (particles), and negative shadow energy acts in annihilation of probability density (particles). It is known experimentally that 2m of energy (photon) is required for pair creation of electron and positron. We rewrite 2m as follows:

$$2m = m + m - im + im \tag{20}$$

That means, to transfer one electron from shadow positive energy level to real positive energy level, complexified energy m - im is required. At the same time, from the law of charge conservation, the hole indicates positive charge, m supplies mass and im repairs the hole made in the sea of shadow energy (see Fig. 2). On the other hand, it is known that 2m photon is freed in case of pair annihilation of electron and positron. In this case, too, 2m is rewritten as Equation (20). An electron annihilates after freeing m + im complexified energy. At the same time, positive charge of positron disappears, and its mass is freed as energy m. On the other hand, -im is freed, and the equilibrium of positive shadow energy level and positive energy level is restored. What we explained so far is for the case when the law of usual energy conservation is maintained. However, as we analyzed in this chapter, there is a possibility of creation and annihilation of particles in line with "the super law of energy conservation" according to the consciousness-matter-energy triangle. The creation and annihilation of particles as matter, at the same time, indicates a possibility of energy creation and annihilation from vacuum as "void".

This preliminary study on vacuum indicates that the concept of "void" in Oriental philosophy is also correct scientifically. Now we are confident that the universe is formed from non-material primary substance, which may be described as the shadow charge (Chi or prana in Oriental philosophy) that gives birth to all things.

Now, we modify Newton's laws regarding two complexified masses, $M = M_1 + iM_2$ and $m = m_1 + iM_2$. That is, using CGS system,

$$f_1 = \frac{GMm}{r^2} r^0 = -\frac{G(M_1 + iM_2)(m_1 + im_2)}{r^2} r^0 = \frac{(iG^{1/2} M_1 - G^{1/2} M_2)(iG^{1/2} m_1 - G^{1/2} m_2)}{r^2} r^0 \tag{21}$$

where G is Newton's constant, r^0 is the unit vector to indicate the direction of r and i is the imaginary unit. When we compare this with the equation of Coulomb force referring to complexified charge $Q = Q_1 + iQ_2$, $q = q_1 + iq_2$, using esu system;

$$f_2 = \frac{Qq}{r^2} r^0 = \frac{(Q_1 + iQ_2)(q_1 + iq_2)}{r^2} r^0 \tag{22}$$

the conditions to equate f_1 and f_2 for one branch are the following equations.

$$Q_1 = -G^{1/2}M_2 , q_1 = -G^{1/2}m_2 \tag{23}$$
$$iQ_2 = iG^{1/2}M_1 , iq2 = iG^{1/2}m_1 \tag{24}$$

when (23),(24) are fulfilled, f_1 and f_2 become equivalent, and it becomes more consistent, if we take Newton's constant G as real number from psychotronics viewpoint. The meaning of (23),(24) is that the real part of the complexified gravitational mass functions as shadow charge and that its imaginary part functions as real charge. The origin of positive and negative charge is, then, imaginary part of negative and positive gravitational mass. The origin of positive gravitational mass is imaginary part of positive charge. Furthermore, we consider that gravitational mass and energy have only positive property. Thus, the imaginary part of charge is only positive. In real and imaginary part, we can obtain mass and energy relations by Einstein's famous formula ($E=mc^2$). We have reached the conversion formulae of complex charge, complex mass, complex energy triangle. These conversion formulae and relationships are summarized as following in Figure 3.

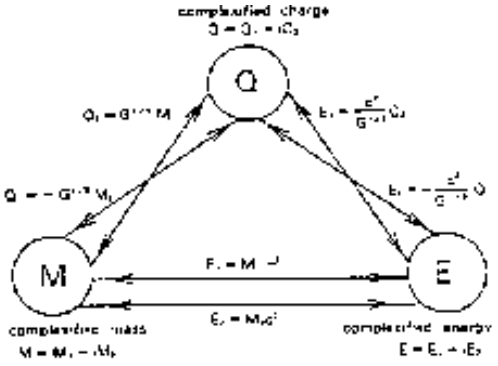

Figure 3. Conversion Formulae of Complex Charge, Mass and Energy Triangle

Figure 3.

Conversion Formulae of Complex Charge, Mass and Energy Triangle

In this triangle, every element, that is, charge, energy and mass, are complexified. The imaginary elements compose the imaginary world or shadow world. The real elements compose the real world, which we perceive. From our new paradigm viewpoint, we can understand the real and imaginary worlds as being interdependent and correlated, but not conventionally connected. Although there exist separate conservation laws of energy and charge in contemporary physics, we should recognize the violation of conservation laws for energy and charge in the real world, if we consider the shadow world. In the N-machine experiments, the electrical output energy is from the vacuum itself. This phenomenon indicates the conversion law from imaginary charge to real energy,

$$E_1 = \frac{c^2}{G^{1/2}} Q_2. \tag{25}$$

We believe that the imaginary charge corresponds to "Chi" or "Prana" in Oriental philosophy. We consider that the positive and negative states of imaginary energy corresponds to "Yin and Yang" in Oriental philosophy.

We also believe that the most fundamental element in universe is imaginary charge, which we call "panpsychic consciousness." Here, we have considered that imaginary charge is described by shadow Dirac neutrino equation.

$$-\frac{\partial \psi}{\partial t} = -i\alpha \cdot \nabla \psi \tag{26}$$

Thus, we believe that the basic oneness of yhe universe is not only the central characteristic of the mystical experience, but is also one of the most important revelations of modern science and technology. The result of the paradigm shifts are shown in the Appendix: New versus Old Paradigms.

Here, we would like to discuss the integration of fundamental forces in nature, that is, gravitational, electromagnetic, strong and weak forces. It is widely known that at present physicists are studying this type of problem under the title of so-called "gauge theory" in relation to cosmology. However, this gauge theory misses the point how these four basic forces are interrelated in the universe in which we are existing. We consider that it is very significant to seek these mutual relationships in the

universe in which we are living. In these paradigm shifts, we can obtain the integrated theory. The core theory is the complexified EM theory, and this theory is an integrated theory of EM force and gravity.

EXPERIMENTAL RESULTS

An illustration of the JPI-I machine is shown in Fig. 3. This machine is a two-rotor series machine and the driving force is supplied by a DC motor. The details of the JPI-I are given in Table 1. This test machine was fabricated by using four 9.0cm permanent magnets; two on each side of copper disks, four copper-carbon brushes are used. These brushes are mounted in aluminum blocks (Fig. 5). The rotation of the DC motor was transmitted to the N-machine by 1 to 2 ratio belt and pulley system.

The N-machine equivalent circuits for the measurements are shown in Fig. 6. According to the theory, an open circuit voltage (EMF) is linearly proportional to the magnet area, the strength of the magnet and the angular velocity. Using MKSA system,

$$V(EMF) = \frac{1}{2} \cdot \omega \cdot B \cdot (r_1^2 - r_2^2) \tag{27}$$

where ω is the angular velocity of a disk. B is the magnetic field perpendicular to the disk and r is the radius of the disk. The effective strength of the magnetic field is supposed to be 0.4 Tesla, according to the experimental date of the JPI-I machine. Furthermore, we have confirmed that the EMF has been produced in a magnets-copper disk, not in an electric conducting wire from the disk edge (Fig. 7). Moreover, we think that the magnetic shield to the conducting wire from the disk edge was especially very important to minimize the back torque. Yokogawa Electric shunt resistance (1mΩ) was used for accurate current measurements. The maximum capacity of this shunt resistance is 100 Amp. Furthermore, it is known that an N-machine behaves exactly as a regulated voltage source does. Thus, when tested at a fixed speed, the EMF remains the same no matter how much current is drawn from a generator (Valone, 1991).

Now, we present the experimental results. The measurements were carried out on 14 February and 7 March, 1993. The measurement data are shown in Table 2,3. The following measurements were carried out under the conditions shown in Fig. 6 unless otherwise specified. The experimental results are shown in Fig. 8, Fig. 9, Fig. 10, Fig. 11, Fig. 12, and Fig. 13. Next, we made the experiments to clarify the shadow energy extraction from the vacuum. We carried out the measurements about two different circuits, thus, open circuit and closed circuit modes. As Table 4 shows, we have made the comparison between the N-machine output power and the power increment of motor DC supply at same rotational speed. According to the energy conservation law, the N-machine output power should be less than the incremental power of the drive motor. In our N-machine measurement, even if the efficiency of the drive motor were 100%, one of four cases apparently shows incremental over-unity. However, we consider that the efficiency of the drive motor is less than 80% in these high rotational velocity range. Therefore, we conclude that all cases have shown the incremental over-unity phenomena.

Summarizing the measurement results of the JPI-I , we have obtained the following results and phenomena. (1) Linearly increasing EMF proportional to the rotational velocity. (2) Nonlinearly increasing load current as the rotational velocity increases. (3) The decreasing electrical resistance phenomenon in the copper-carbon brush materials around the rotating magnets disk in high rotational velocity range. (4) The confirmation of the incremental over-unity or local violation of energy conservation law in high rotational velocity range.

From our experimental results and experiences, we consider that there are three major improvement items for constructing a system over-unity machine. Those are: (1) a producing stronger magnetic flux density, (2) an expansion of rotor disk diameter and effective area, (3) a magnetic shielding to the conducting wires to extract current from the disk edge.

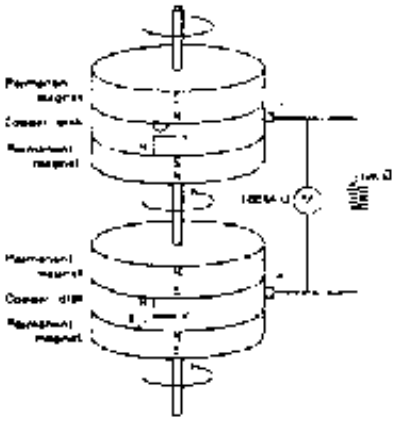

Figure 4. An Illustration of JP1-I Machine

Table 1. JPI-I Machine Data

type	
brush	copper carbon
	copper

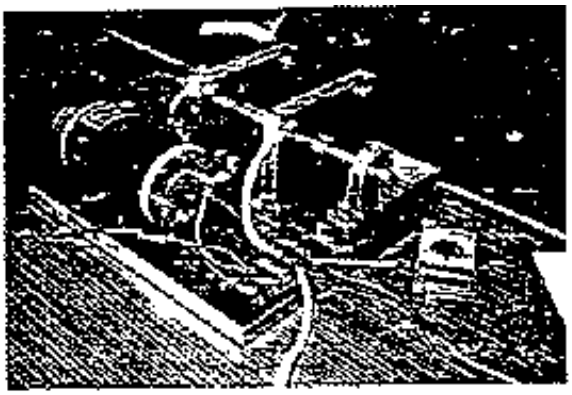

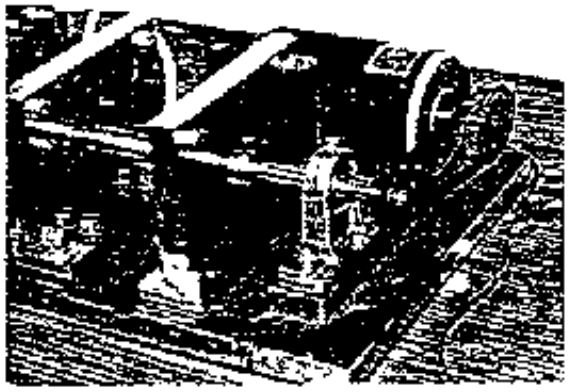

Figure 5. JPI-I Machine

Design Specifications of JPI-II

Based on the knowledge obtained from the design, manufacture, and experiments with JPI-I machine, this machine (JPI-II) has been designed to be a system over-unity machine or a self-rotating electrical generator.

For this purpose, full utilization of super-conducting magnets and technology is planned. In the N-machine - Faraday motor combination, such a situation is realized, if the electrical energy created from the vacuum is bigger than the energy needed for no-load rotation of the N-machine plus the loss in the Faraday motor (Inomata, 1991). Moreover, the energy needed for reliquidization of vaporized coolant will be negligible, if sufficient heat insulation is provided for the N-machine-Faraday motor combination.

We begin our discussion of basic design specifications of JPI-II, based on the experimental data obtained from the JPI-I. The conceptual figure of JPI-II is shown in Fig. 14 and the specifications of JPI-II are shown in Table 5.

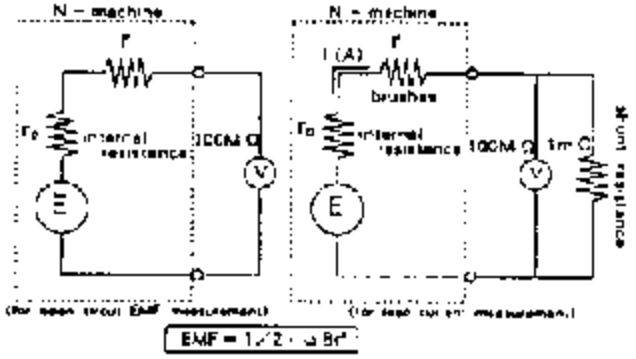

Figure 6. N-Machine Equivalent Circuits for The Measurement

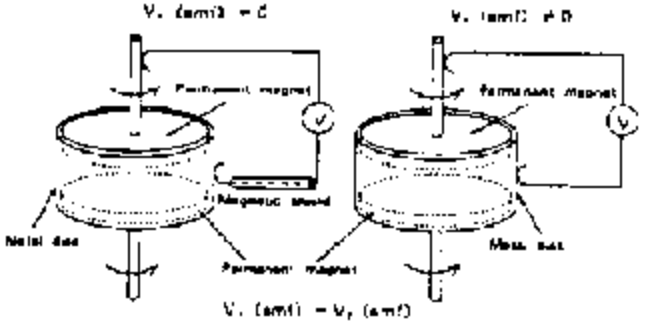

Figure 7. The Experiments to Confirm The Place of EMF

Table 2. The Measurement Data of JPI-I

300	14.8	0.8	0.02	11.1	4.5	8.0	38.0
1000	37.3	0.7	0.03	13.3	4.4	8.1	37.7
1500	54.9	0.5	0.05	18.8	6.8	8.4	54.8
2000	74.5	1.5	0.11	48.5	8.1	8.8	71.8
2500	93.1	2.2	0.20	40.8	8.6	9.2	88.2
3000	113.8	2.9	0.38	38.2	12.8	8.7	110.4
3500	128.0	4.0	0.58	51.5	13.6	8.6	118.8
4000	144.8	5.1	0.78	28.5	18.4	8.6	132.8
4500	162.5	6.3	1.00	15.7	17.0	10.4	175.8
5000	181.2	12.5	2.27	23.8	19.0	11.4	208.0
5500	202.6	8.5	1.53	41.1	21.0	11.2	236.2
6000	220.0	26.5	5.83	7.3	23.0	11.6	264.8
6500	242.0	40.0	8.68	5.1	28.0	12.4	330.2

Table 3. The Measurement Data of JPI-I

500	8.3	1.1	0.4	18.6	3.8	8.4	32.2
000	21.8	1.8	0.1	18.5	4.8	8.6	39.8
1500	82.0	2.3	0.1	24.3	5.4	8.4	66.3
2000	82.0	3.8	0.3	34.3	6.3	9.4	78.2
2500	10.0	1.7	0.2	51.9	10.2	8.8	87.8
3000	110.0	1.6	0.3	36.2	12.6	9.8	117.8
3500	138.0	1.0	0.8	68.6	13.8	8.8	136.8
4000	145.0	2.8	0.4	54.6	15.6	10.1	151.9
4500	60.5	0.8	1.0	13.8	17.4	10.8	177.6
5000	160.0	18.6	3.3	8.7	19.1	10.6	207.5
5500	188.2	21.6	4.2	8.8	20.6	11.1	230.0
6000	216.0	34.6	8.3	7.8	22.6	11.0	255.4
6500	130.0	20.5	7.0	8.8	24.8	12.2	301.4
5500	180.0	38.0	8.8	6.8	25.8	11.0	334.1

Warm-up run (about 30 min.) is necessary for load current measurement.

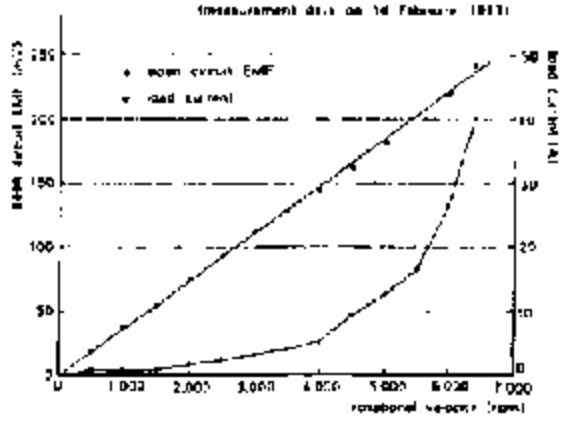

Figure 8. Open Circuit EMF and Load Current

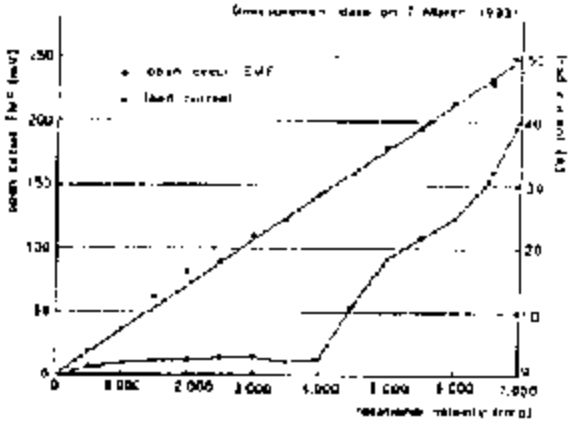

Figure 11. Open Circuit EMF and Load Current

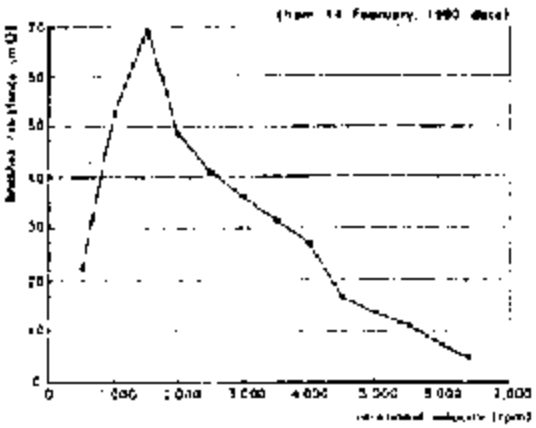

Figure 9. The Measurement of Brush Resistance

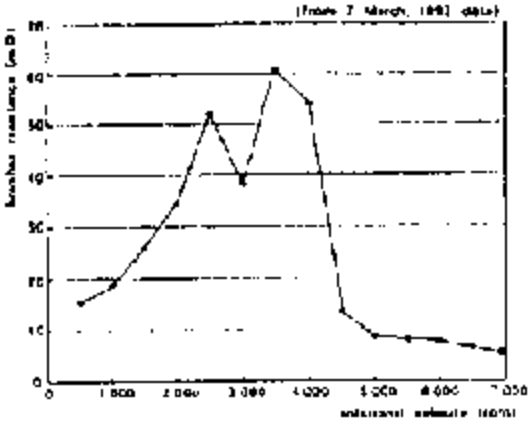

Figure 12. The Measurement of Brush Resistance

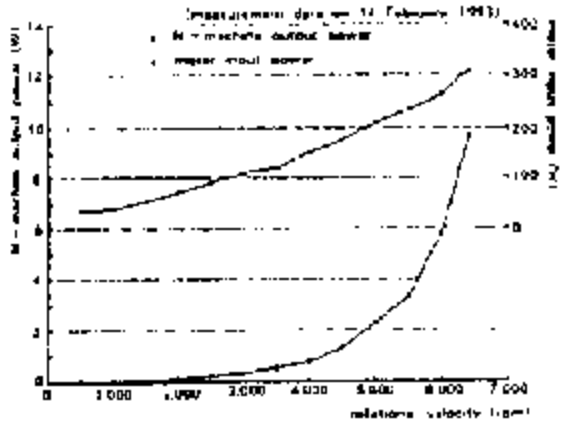

Figure 10. The Measurement of Electrical Power

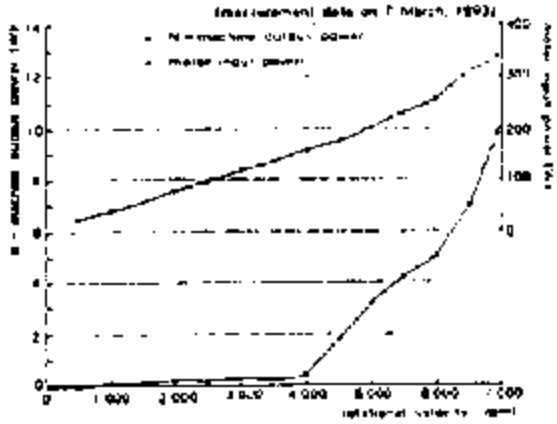

Figure 13. The Measurement of Electrical Power

Table 4. The Measurement of Back Torque

(measurement data on 7 March, 1993)

rotational velocity (rpm)	N-Machine open circuit mode			N-Machine close circuit mode		
	N-Machine	drive motor power supply		N-Machine	drive motor power supply	
	open EMF(mV)	voltage (V)	current (A)	load cur. (A)	voltage (V)	current (A)
6302	215	22. 2	11. 8	27. 0	22. 1	12 0
7032	256	26. 1	12. 7	41. 2	26. 1	13 1
7100	258	26. 1	12. 4	33. 7	26. 0	12. 8
6000	215	21. 9	11 6	21. 0	21. 9	11 8

rotational (rpm)	N-Machine output power (W)	power increment of motor supply (W)	
		the efficiency of the DC drive motor	
		100%	80%
6302	5 8	3 2	2. 6
7032	10 5	10 4	8. 3
7100	8 6	9 2	5. 5
6000	4 5	4. 4	3. 5

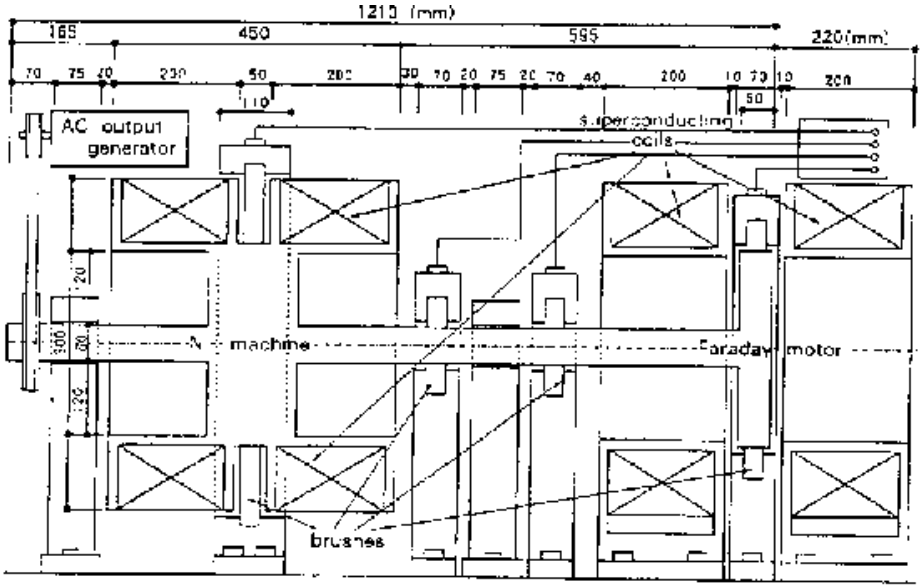

Figure 14. Conceptual Figure Of JPL-I Test Machine

DC power supply: A DC power supply of low voltage and large current is used to energize the super-conducting coils and for starting the machine.

The vacuum electrical power vs. rotational velocity were estimated for two cases (30cm and 50cm diameter, 4 Tesla magnet) in Table 6, 7 and Fig. 15. Moreover, we estimated the expected torque of Faraday motor for 30cm diameter case (Table 8). We estimate that the self-sustaining condition would be met in 5,000 (rpm) in this case.

DC power supply: A DC power supply of low voltage and large current is used to energize the super-conducting coils and for starting the machine.

The vacuum electrical power vs. rotational velocity were estimated for two cases (30cm and 50cm diameter, 4 Tesla magnet) in Table 6, 7 and Fig. 15. Moreover, we estimated the expected torque of Faraday motor for 30cm diameter case (Table 8). We estimate that the self-sustaining condition would be met in 5,000 (rpm) in this case.

Conditions for output power estimation:
Open EMF : V = (1/2) ω B (r_2^2-r_1^2) (V)
Magnetic flux density : B = 4.0 (T)
Load resistance : R = 1 (mΩ)
(using MKSA unit system)

Table 5. Specifications of JPI-Ⅱ

Type	single rotor type
Diameter	300 (mm)
Rotor material	copper
Magnetic field	generated by super-conducting coil
Magnetic flux density	4 (T) (average density on the copper disk)
Maximum rotational velocity	8,000 (rpm)
Maximum output power · EMF · current	 40 (V) 7,000 (A)
Brushes · material · cross section	copper-carbon 30×55 (mm) (periphery of disk : six picecs) (periphery of axis : two picces)
DC power supply · maximum voltage · maximum current	 50 (V) 7,000 (A)
Electrical generator	AC generator

On the other hand, recent astronomical findings indicate that our earth travels with speed 600 km/sec relative to the Lorentz ether. As rotational motion is "absolute", N-machine theory is valid for the experiments on the earth as confirmed by our experiments.

Table 6. Estimated Electrical Output Power

Rotation disk diameter : 30 (cm)
(r_1(inner radius) = 3 (cm) : r_2(outer radius) = 15(cm))

rotation velocity (rpm)	V (V) (open EMF)	I (A) (load current)	W (kw) (output power)
3000	13.57	365.1	4.95
4000	18.10	649.6	11.76
5000	22.62	1559.6	35.28
6000	27.14	3269.9	88.72

Table 7. Estimated Electrical Output Power

Rotation disk diameter : 50 (cm)
(r_1(inner radius) = 3 (cm) : r_2(outer radius) = 25(cm))

rotation velocity (rpm)	V (V) (open EMF)	I (A) (load current)	W (kw) (output power)
3000	20.42	549.4	11.22
4000	27.23	977.2	26.61
5000	34.03	2346.2	79.84
6000	40.84	4919.4	200.91

Conclusions

In view of the experimental results and theoretical considerations which were obtained and described above, we have concluded that the N-machine provides a basis for "space power generation", in that under certain conditions the extraction of electrical output energy is not reflected as a corresponding mechanical load to the driving source. The complaint of small EMF of JPI-I is not the case for a

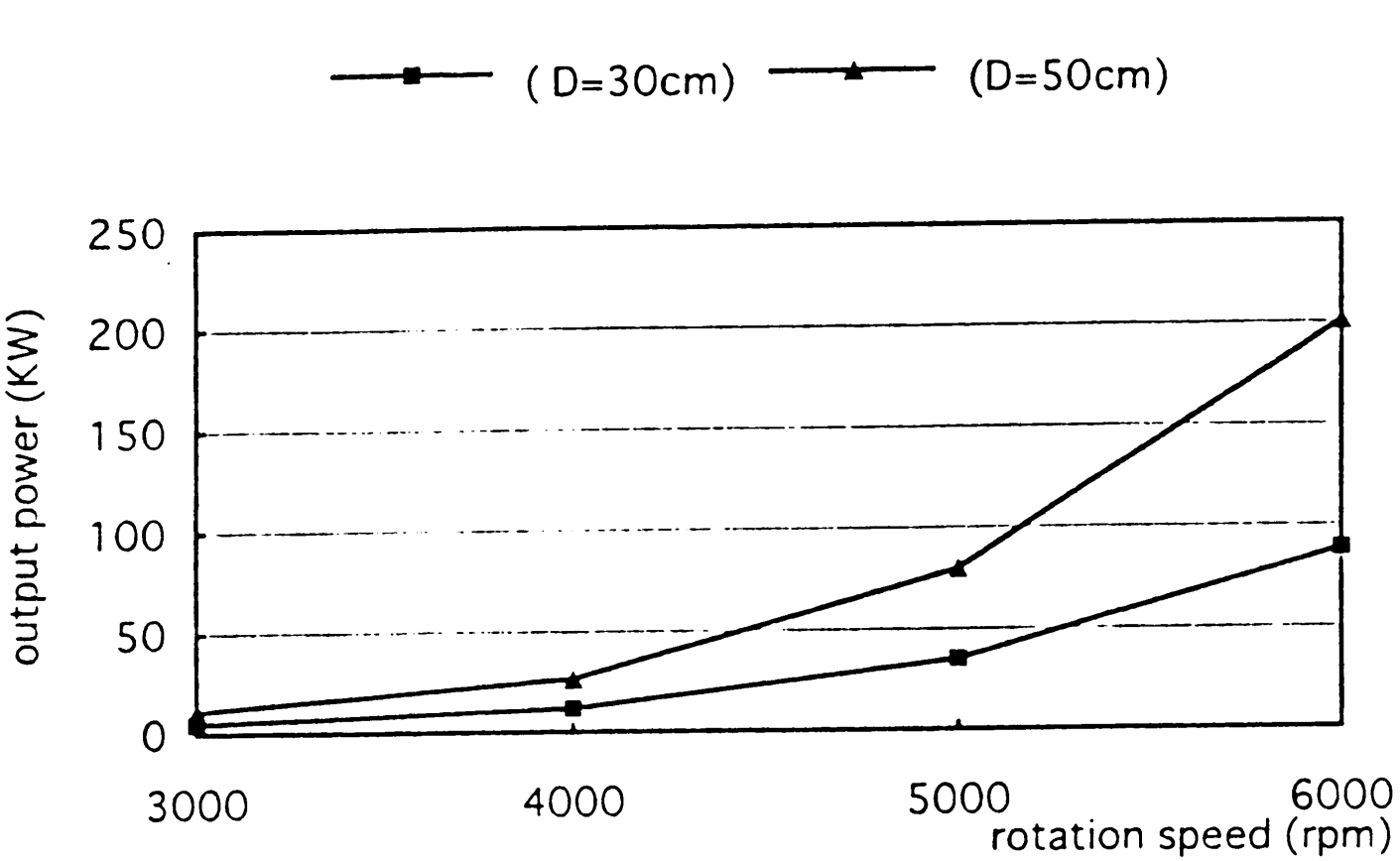

Figure 15. Estimated Electrical Output Power

Table 8. Estimated Faraday Motor Torque

Conditions : B = 4.0 (T) : magnetic flux density
r_1 = 0.03 (m) : inner radius
r_2 = 0.15 (m) : outer radius

rotation velocity (rpm)	supply current (A)	estimated torque (N · m)
3000	365.1	15.8
4000	649.6	28.1
5000	1559.6	67.4
6000	3269.9	141.3

bigger and stronger magnet N-machine, which utilizes not only neodymium magnets, but also super-conducting magnets.

All these experimental and theoretical developments strongly indicated that the simple mechanistic picture of basic building blocks of nature had to be abandoned. Furthermore, we are confident that this new paradigm and its application may bring the technological breakthrough for solving the energy crisis and the environmental holocaust.

Acknowledgements

We first acknowledge Mr. H. Yamashita, former MITI vice-minister, and MITI officials for their interest in this research. We would like to thank Mr. K.Kazama, president, Kazama Giken Kaihatsu Co., for manufacturing the JPI- I and the measurement team of Electric Power Development Corp. for the cooperation. We also acknowledge Mr. D.A. Kelly, Space Energy Association U.S.A., and Mr. Toby Grotz, Institute for New Energy, for encouragement to our research.

REFERENCES

[1] Inomata, S., Paradigm of New Science-Principia for The 21st Century. Gijutsu Shuppan Pub. Co., 1987, Tokyo.

[2] Inomata, S., "NEW PARADIGM AND N-MACHINE", Proceedings of the 26th IECEC, vol 4, 1991, pp 331-335.

[3] Inomata, S., and Mita, Y., "Small Neodymium Magnet Twin N-machine", Proceedings of the 28th IECEC, vol 2, 1993, pp 2.347 - 2.352.

[4] Mita, Y., "The 28th IECEC report for NT session" Journal of PSI Research Committee, The Univ. of Electro-Communications, Tokyo, no. 3, 1993, pp 6-18.

[5] Valone, T., "The One-Piece Faraday Generator: Research Results," Proceedings of the 26th IECEC, vol 4, 1991, pp 473-478.

Appendix : New versus Old Paradigms

Old paradigms	New paradigms
Newton's mechanics	Newton's Mechanics
1st law: law of inertia 2nd law: equation of motion $\frac{d\vec{P}}{dt}=\vec{F}$ ($\vec{P}=m\vec{v}$, m, inertial mass) 3rd law: law of action and reaction Gravitation $f=\frac{GM_1M_2}{r^2}$	1st law: law of inertia 2nd law: equation of motion $\frac{d\vec{P}}{dt}=\vec{F}$ ($\vec{P}=m\vec{v}$, m, inertial mass) 3rd law: law of action and reaction Above laws are effective only if there is no gravitational function Gravitation $f=\frac{Q_1Q_2}{r^2}$ $Q_1=iG^{\frac{1}{2}}M_1$ $Q_2=iG^{\frac{1}{2}}M_2$
Electromagnetic equations (CGS unit in vacuum)	Electromagnetic-gravitational equation (CGS unit in vacuum)
$\nabla\cdot E=4\pi\rho_e$, $\nabla\times E=-\frac{1}{c}\frac{\partial H}{\partial t}$ $\nabla\cdot H=0$, $\nabla\times H=\frac{1}{c}\frac{\partial E}{\partial t}+\frac{4\pi}{c}J_e$	$E=E_1+iE_2$, $H=H_1+iH_2$ $\nabla\cdot E_1=4\pi\rho_e$, $\nabla\times E_1=-\frac{1}{c}\frac{\partial H_1}{\partial t}$ $\nabla\cdot H_1=0$, $\nabla\times H_1=\frac{1}{c}\frac{\partial E_1}{\partial t}+\frac{4\pi}{c}J_e$ The above equations indicate electromagnetic field
	$\nabla\cdot(iH_2)=4\pi\rho_m$ $\nabla\times(iH_2)=\frac{1}{c}\frac{\partial(iE_2)}{\partial t}$ $\nabla\cdot(iE_2)=0$ $\nabla\times(iE_2)=-\frac{1}{c}\frac{\partial(iH_2)}{\partial t}+\frac{4\pi}{c}J_m$ The above equations indicate gravitational field
General representation $\square\phi=4\pi\rho$ $\square A=-\frac{4\pi}{c}J$ $\square=\nabla^2-\frac{1}{c^2}\frac{\partial^2}{\partial t^2}$ Lorentz condition $\nabla\cdot A+\frac{1}{c}\frac{\partial\phi}{\partial t}=0$	General representation $\square\phi=4\pi\rho$ $\phi=\phi_e+i\phi_m$ $\square A=-\frac{4\pi}{c}J$ $\rho=\rho_e+i\rho_m$ $\square=\nabla^2-\frac{1}{c^2}\frac{\partial^2}{\partial t^2}$ $A=A_e+iA_m$ Complex Lorentz condition $\nabla\cdot A+\frac{1}{c}\frac{\partial\phi}{\partial t}=0$
Integration theory of electromagnetism and gravity	Integration theory of electromagnetism and gravity
none	$\square\phi=-4\pi\rho$ $\square A=-\frac{4\pi}{c}J$ $\square=\nabla^2-\frac{1}{c^2}\frac{\partial^2}{\partial t^2}$ $\rho=\rho_e+G^{\frac{1}{2}}M_1+i(\rho_m+G^{\frac{1}{2}}M_2)$ $J=J_e+iJ_m$ $M=M_1+iM_2$ complex mass.
Thermo-dynamics	Complex thermo-dynamics
	Complex temperature $T=T_1+iT_2$ Complex heat quantity $Q=Q_1+iQ_2$

Old paradigms	New paradigms
Entropy $\Delta S=\frac{\Delta Q}{T}$	Entropy $\Delta S=\Delta S_1+i\Delta S_2$ $\Delta S_1=\frac{\Delta Q_1}{T_1}$ $\Delta S_2=\frac{\Delta Q_2}{T_2}$
Quantum mechanics/elementary particle theory	Quantum mechanics/elementary particle theory
Schrödinger equation $i\frac{\partial}{\partial t}\phi=H\phi$	Schrödinger equation $i\frac{\partial}{\partial t}\phi=H\phi$ Shadow Schrödinger equation $-i\frac{\partial}{\partial t}\phi=H\phi$
Klein-Gordon equation $-\frac{\partial^2\phi}{\partial t^2}=(-\nabla^2+m^2)\phi$	Klein-Gordon equation $-\frac{\partial^2\phi}{\partial t^2}=(-\nabla^2+m^2)\phi$ Shadow Klein-Gordon equation $\frac{\partial^2\phi}{\partial t^2}=(-\nabla^2+m^2)\phi$
Dirac equation $i\frac{\partial\phi}{\partial t}=(-i\alpha\cdot\nabla+\beta m)\phi$ Dirac neutrino $i\frac{\partial\phi}{\partial t}=-i\alpha\cdot\nabla\phi$ (natural unit)	Dirac equation $i\frac{\partial\phi}{\partial t}=(-i\alpha\cdot\nabla+\beta m)\phi$ Shadow Dirac equation $-i\frac{\partial\phi}{\partial t}=(-i\alpha\cdot\nabla+\beta m)\phi$ Shadow Dirac neutrino $-i\frac{\partial\phi}{\partial t}=-i\alpha\cdot\nabla\phi$ (natural unit)
Yukawa equation $\square\phi_1-\mu^2\phi_1=0$ (strong interaction)	Yukawa equation $\square\phi_1-\mu^2\phi_1=0$ (strong interaction)
(CGS unit)	Shadow Yukawa equation $\square\phi_2-\beta^2\phi_2=0$ (Weak interaction) (CGS unit)
Space-time	Space-time
[illegible]	[illegible]
Conversion formula: mutual mass and energy	Conversion formula: conversion among mass and energy
$E=Mc^2$ 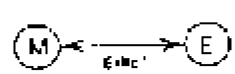 	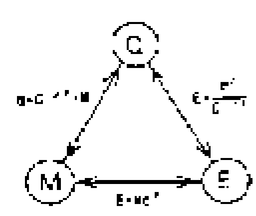
	[illegible] the meaning of symbols please confer with the text

SONOLUMINESCENCE, COLD FUSION, AND BLUE WATER LASERS

Thomas V. Prevenslik

Consultant, Tokyo, Japan

The blue light observed in sonoluminescence experiments with water is explained, in this model, by Rayleigh scattered ambient UV light reflected in a blue Raman line of water. The ambient UV light incident on the spherical liquid geometry is concentrated to a high intensity and reflected in a Raman line that appears to the observer as blue light. The spherical liquid geometry functions as a spherical UV lens that concentrates ambient UV light at the center of the water compression field. By providing an external spherical UV laser cavity driver concentric to the spherical liquid lens, the concept of a cold fusion blue water laser is developed where the laser driver is pulsed with the acoustic field to fuse the deuterium in heavy water molecules. Therefore (according to this model) the blue water laser is a cold fusion device because the liquid structure required in concentrating the UV light would only operate below about 50 C, say in an application as a residential heater, even though the local hot fusion reaction is actually producing the heat.

Sonoluminescence (SL) is described [1] as a non-equilibrium phenomenon in which the energy in a sound wave becomes highly concentrated so as to generate synchronous repetitive flashes of blue light in liquid water at room temperature. With regard to cold fusion, SL as a significant mechanism of energy focusing in combination with a heavy D-O-D water target [2] is important because it would offer the prospect of a mechanism of fusing deuterium at room temperature.

In the standard model [3] for SL, bubble collapse energy is delivered to a number of molecules and the molecules are excited to emit blue light upon recombination. However, it is possible that the blue light observed in SL is nothing more than concentrated Rayleigh scattered light reflected in the blue Raman line of water. The Raman effect is the phenomenon of light scattering from the material medium whereby the light undergoes a frequency change in contrast to Rayleigh scattering where a frequency change does not occur.

The SL explanation given here is that the low intensity ambient UV light scattered inside the spherical water geometry is concentrated at the center of the compression field and reflected to the observer as a visible blue Raman line of water. This SL explanation is referred hereinafter as the Light Scattering (LS) model.

In contrast, the standard SL model contends the blue light is generated in the water. Since the ambient UV light is not visible, the appearance of blue light alone may have led the observers [1] to conclude that the blue light was being emitted from the water consistent with the standard SL model when, according to the LS model, the blue light is reflected ambient UV light.

In the standard SL model, light absorption for hydrogen takes place on the order of 10 ns. However, the data [1] shows that duration of the blue light < 100 ps. The LS model response based on Rayleigh and Raman scattering does not involve light absorption and takes place within the period of vibration. For blue light the response is < 1 fs, and may explain why the flashes cannot be resolved with the

fastest photomultiplier tubes available.

Raman emission data [4] of water for various frequencies of exciting mercury light shows that for blue light to be emitted in a prominent Raman at 470 nm, the Rayleigh scattered incident UV line is required to be about 405 nm. The Raman lines are caused by totally symmetric O-H vibrations of the water molecule. The LS model contends that the 470 nm blue light observed during SL in water is actually a Raman line corresponding to incident UV light at 405 nm.

The standard SL model finds difficulty in explaining the data [1] which reports a 3.3 ev photon energy at a frequency of 8.0^{14} Hz which corresponds to a wavelength of 375 nm, but the observer sees a blue light at 470 nm. The LS model contends that in addition to reflected blue light, ambient UV light may also be also reflected to produce a UV spectrum of Raman emission, and the 375 nm wavelength is the spectrum average. This lowering may be due to a prominent Raman line at 350 nm in water that corresponds to a 313 nm UV exciting line [4].

With regard to verification of the LS model, polarization measurements of the reflected blue light in the SL experiment [1] should be made. Since Raman emissions from water are highly polarized, the LS model predicts that the intensity of the blue light as viewed through the polarizer will be significantly diminished. If so, not only is the correctness of the LS model verified, but more importantly, the spherical liquid lens formed in the compression field of the water offers a controllable mechanism for the concentration of the ambient UV light.

The concept of the cold fusion blue water laser finds basis in the observation of the significant concentration of ambient UV light by the spherical water lens during SL and is illustrated in Fig. 1. A surrounding UV laser cavity congruent to the spherical compression field lined with mercury lamps emitting UV radiation in the 300 to 400 nm range is flashed in sync with the SL acoustic frequency. Diametrically opposite inlet and outlet openings in the spherical arrangement may be made without affecting the isotropic irradiation of the water molecules to provide a through flow of heavy water to transfer the fusion energy to a heat sink. During blue water laser operation using heavy water, the water molecules at the center of the spherical compression field may be ionized to high temperatures causing the fusion of deuterium in the molecules and a possible fusion energy release. The fusion plasma may be contaminated by the oxygen in the water molecule itself, but this may not be a problem because the very large concentration of UV energy may accommodate the radiation loss and still achieve local fusion temperatures for deuterium. In this arrangement, the blue water laser may find application as a residential heater by increasing ambient water temperature to about 50 C without a loss of the spherical liquid lens structure.

The cold fusion blue water laser is similar to the Inertially Confined Fusion Reactor (ICFR) hot fusion concept [5] where fabricated D-T fuel pellets are ignited at fusion temperatures by imploding the fuel pellets through laser ablation of the exterior pellet surface. The ICFR requires the fuel pellet to be repetitively fabricated and precisely positioned at the center of the reactor prior to ignition. Further, the ICFR requires high energy MJ lasers because the minimal pellet size is limited by the fabrication and positioning process. However, the blue water laser is a far simpler concept because the water molecules at the center of the compression field function as the pellet and are continually replenished in repetitive ignitions. Since the fusing deuterium water molecules are very small quantities of fuel, the required UV laser energy for ignition is similarly a very small fraction of the ICFR laser energy, and therefore the blue water laser would make possible ignition of the neutron free D-D reaction, instead of opting for the lower energy D-T reaction with attendant radioactivity problems. Instead of the large size of laser drivers common with the ICFR, the mercury lamp arrangement is a simple and compact laser driver, and therefore miniature blue water lasers providing a limitless supply of low

temperature water < 50 C for residential home heating may be envisioned.

REFERENCES

[1] B.P. Barber and S.J. Putterman, "Observations of Synchronous Picosecond Sonoluminescence." Letters to *Nature*, vol 352, pp 318-320, (1991).

[2] K. Fukushima, "Is Sono-Fusion to be a Possible Mechanism for Cold Fusion?" Frontiers of Cold Fusion, Universal Academy Press, pp 609-612, 1993.

[3] A.J. Walton and G.T. Reynolds, "Sonoluminescence", *Advances in Physics*, vol 33, no 6, pp 595-660 (1984).

[4] C.A. Parker, "Raman Spectra in Spectrofluorimetry," *Analyst*, vol 84, pp 446-453 (1959).

[5] J.A. Maniscalco, W.R. Meir, and M.J. Monsler, "Design Studies of a Laser Fusion Power Plant", Proceedings of a Technical Committee and Workshop on Fusion Reactor Design, Madison, Wisconsin USA, pp 299-315, 1977.

Editor's Note: This model for sonoluminescence may or may not be correct. Readers should also read the following paper wherein Nobel-prize winner J. Schwinger suggests that sonoluminescence taps space energy (zero-point energy): Julian Schwinger (UCLA, Los Angeles), "Casimir Light: the Source," *Proc. Natl. Acad. Sci. USA*, vol 90, March 1993, pp 2105-2106.

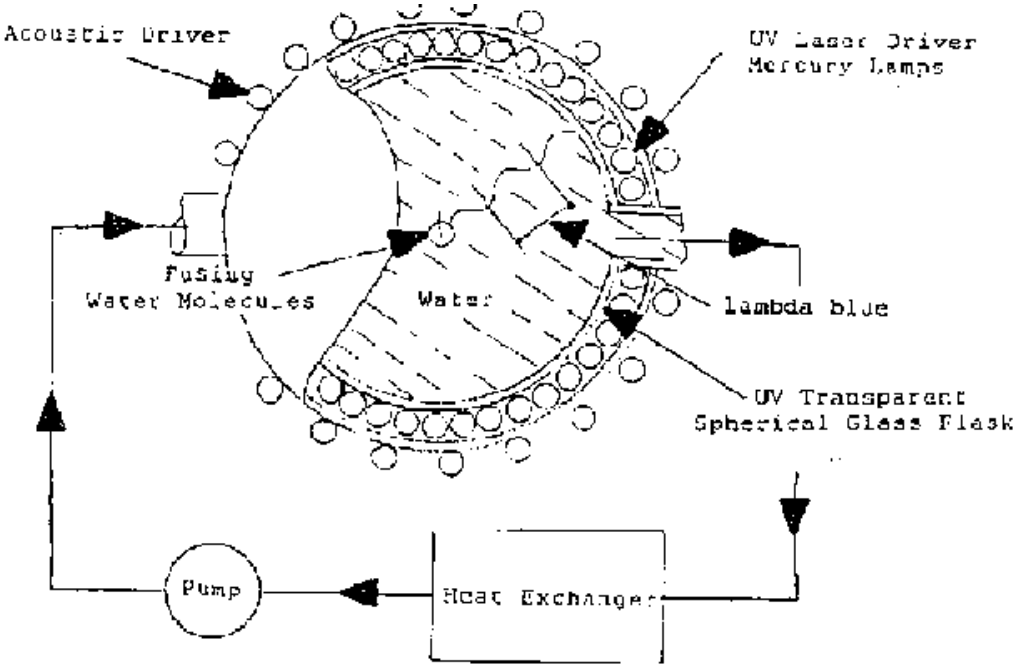

Fig. 1 Cold Fusion Blue Water Laser Concept

Fig. 1 Cold Fusion Blue Water Laser Concept

INVENTORS

Are you looking for a proven team who will help protect and develop your cold fusion invention?

MANUFACTURERS

Do you need information on cold fusion inventions and processes that are available for commercialization?

ENECO can help.

We are an intellectual property clearinghouse serving the interests of both cold fusion inventors and commercial developers throughout the world. Our staff is actively pursuing allowance of U.S. and international patents in most areas of cold fusion effects.

Call us to discuss our development and licensing programs: (801) 583-2000

ENECO

COLD FUSION SOURCE BOOK

Edited by Hal Fox

We are pleased to present this technical source material on cold fusion to the world. To a large extent this publication represents a five-year culmination of activities in the new science of cold fusion. This new science was first announced to the world in a press conference called by the University of Utah on March 23, 1989.

Few scientific announcements have caused as much initial interest as the announcement of the discovery of cold fusion. Historically, cold fusion has joined the several advances in science that have been strongly resisted by many in the scientific community and then grudgingly accepted. Cold nuclear fusion can now be created and controlled by a variety of methods. Some of these methods will become the commercial prototypes for your future energy systems.

We are pleased to publish this important contribution to the ultimate success of a new science that will help solve some of this world's most pressing problems.

The editor, Hal Fox, is also editor of *Fusion Facts* and of *New Energy News.* His book **Cold Fusion Impact in the Enhanced Energy Age** has been translated into Russian and Spanish and will soon be available in German.

Fusion Information Center, Inc.
P.O. Box 58639, Salt Lake City, UT 84158
Voice (801) 583-6232 FAX (801) 583-2963

Suggested Retail Price: $99.95 with bibliography diskette.
Diskette is updated quarterly. Contains over 1500 references from the extensive professional literature on cold fusion.

Cold Fusion Source Book

Hal Fox, Editor

FIC 1994